ACTA CHIMICA

ACADEMIAE SCIENTIARUM HUNGARICAE

ADIUVANTIBUS

V. BRUCKNER, GY. DEÁK, K. POLINSZKY,
E. PUNGOR, G. SCHAY, Z. G. SZABÓ

REDIGIT

B. LENGYEL

TOMUS 74 FASCICULUS 1

AKADÉMIAI KIADÓ, BUDAPEST

1972

ACTA CHIM. (BUDAPEST) ACASA 2 74 (1) 1—120 (1972)

ACTA CHIMICA

A MAGYAR TUDOMÁNYOS AKADÉMIA KÉMIAI TUDOMÁNYOK OSZTÁLYÁNAK IDEGEN NYELVŰ KÖZLEMÉNYEI

SZERKESZTI

LENGYEL BÉLA

TECHNIKAI SZERKESZTŐK

DEÁK GYULA és HARASZTHY-PAPP MELINDA

Az Acta Chimica német, angol, francia és orosz nyelven közöl értekezéseket a kémiai tudományok köréből.

Az Acta Chimica változó terjedelmű füzetekben jelenik meg, egy-egy kötet négy füzetből áll. Évente átlag négy kötet jelenik meg.

A közlésre szánt kéziratok a szerkesztőség címére (Budapest 112/91 Műegyetem) küldendők.

Ugyanerre a címre küldendő minden szerkesztőségi levelezés. A szerkesztőség kéziratokat nem ad vissza.

Megrendelhető a belföld számára az „Akadémiai Kiadó"-nál (Budapest V., Alkotmány utca 21. Bankszámla 05-915-111-46), a külföld számára pedig a „Kultúra" Könyv- és Hírlap Külkereskedelmi Vállalatnál (Budapest I., Fő utca 32. Bankszámla: 43-790-057-181) vagy annak külföldi képviseleteinél és bizományosainál.

Die Acta Chimica veröffentlichen Abhandlungen aus dem Bereiche der chemischen Wissenschaften in deutscher, englischer, französischer und russischer Sprache.

Die Acta Chimica erscheinen in Heften wechselnden Umfanges. Vier Hefte bilden einen Band. Jährlich erscheinen 4 Bände.

Die zur Veröffentlichung bestimmten Manuskripte sind an folgende Adresse zu senden:

Acta Chimica
Budapest 112/91 Műegyetem

An die gleiche Anschrift ist auch jede für die Redaktion bestimmte Korrespondenz zu richten. Abonnementspreis pro Band: $ 16.00.

Bestellbar bei dem Buch- und Zeitungs-Außenhandels-Unternehmen »*Kultúra*« (Budapest I., Fő utca 32. Bankkonto No. 43-790-057-181) oder bei seinen Auslandsvertretungen und Kommissionären.

ACTA CHIMICA

ACADEMIAE SCIENTIARUM HUNGARICAE

ADIUVANTIBUS

V. BRUCKNER, GY. DEÁK, K. POLINSZKY,
E. PUNGOR, G. SCHAY, Z. G. SZABÓ

REDIGIT

B. LENGYEL

TOMUS 74

AKADÉMIAI KIADÓ, BUDAPEST

1972

ACTA CHIMICA

TOMUS 74

Fasciculus 1: 1972
Fasciculus 2: 1972
Fasciculus 3: 1972
Fasciculus 4: 1972

INDEX

Azizov, Sh. S. s. Tasmukhamedov, S. A.

Báder, I. s. Berecz, E.

Badran, A. H. s. Sakla, A. B.

Bakos, J. s. Dévay, J.

Bánsági, T. s. Solymosi, F.

Beke, Gy. s. Nagy, M.

Berecz, E. and Báder, I.: Comparative Study of the Variations in the Properties of Binary Solutions on Temperature Change or on Addition of a Third Component, and its Application to the Viscosity of Metal Chloride–HCl–H_2O Systems 213

Bernáth, G., Göndös, Gy., Márai, P. and Gera, L.: Stereochemical Studies, XI. Studies on Cyclic 2-Hydroxycarboxylic Acids, II. Synthesis of *Cis*- and *Trans*-2-Hydroxycyclopentanecarboxylic Acid and *Cis*- and *Trans*-2-Hydroxycycloheptanecarboxylic Acid 471

Bernáth, G., Láng, K. L., Göndös, Gy., Márai, P. and Kovács, K.: Stereochemical Studies, XII. Cyclic Aminoalcohols and Related Compounds, VI. N → O Acyl Migration in N-Benzoyl Derivatives of *Cis*- and *Trans*-2-Aminomethylcyclopentanol and *Cis*- and *Trans*-2-Hydroxymethylcyclopentylamine 479

Bhattacharya, P. K., s. Panchal, B. R.

Bognár, R. s. Makleit, S.

Bruckner, V.: László (Ladislaus) Vargha† 1

Burger, M. s. Kőrös, E.

Csűrös, Z., Sallay, P. and Deák, Gy.: Synthesis of 2,4,6-Triarylpyrylium Fluoroborates from Aromatic Aldehydes and Arylmethyl Ketones, III. The Claiser-Schmidt Condensation 357

Czárán, E. and Schnabel, K. H.: Die Dispersität des Platins in Platin-Alumosilikat-Trägerkatalysatoren in Abhängigkeit von den Eigenschaften des Trägers. (Investigation of the Distribution and Dispersity of Platinum in Platinum-Alumosilicate Carrier Catalysts Under the Conditions of Industrial Production) ... 445

Deák, Gy. s. Csűrös, Z.

Dévay, J., Janászik, F., Mészáros, L. and Horkay, F.: Electrochemical Method for the Investigation of the Corrosion Resistance of Paint Coatings 199

Dévay, J., Lengyel, B. Jr., Sayed Sabet Abd El Rehim and Bakos, J.: Study of the A. C. Corrosion of Nickel by Linear Polarization 193

Dévay J., Mészáros, L. and Garai, T.: Third Harmonic Component of the Electrode Current Due to a Sinusoidal A. C. Voltage in the Case of Diffusion and Transfer Polarization 205

Do Ngoc Lien s. Kiss, L.

Dudar, E. s. Náray-Szabó, G.

Egri, J., Halmos, J. and Rákóczi, J.: Synthesis of Substituted 4-Hydroxyquinoline-3-carboxylic Esters, II. Preparation of 6,7-Diisobutoxy-4-hydroxyquinoline-3-carboxylic Acid from the Nitrile and Its Esterification 345

Egri, J., Halmos, J. and Rákóczi, J.: Synthesis of Substituted 4-Hydroxyquinoline-3-carboxylic Esters, III. A One-step Process Starting from Substituted Phenylimino Esters 351

FARKAS, J. s. KISS, L.

FARKAS, L., WOLFNER, A. and OLECHNOWICZ-STEPIEN, V.: The Synthesis of Calycosin and Calycosin-7-β-D-glucoside 367

FEJES, P. s. VARGA, K.

FODOR-CSÁNYI, P.: An Interpretation of the Behaviour of Scintillation Systems by the Spectral Properties of the Components 179

FÓTHI, A. s. KISS, L.

FRAKNÓY-KŐRÖS, V. s. VÉRTES, A.

FÜSSY, É. s. KŐRÖS, E.

GALIBA, I. s. SZABÓ, Z. G.

GARAI ,T. s. DÉVAY, J.

GARZÓ, G. s. LENGYEL, B.

GÁL, D. s. SZABÓ, Z. G.

GELENCSÉR, P. A. s. VÉRTES, A.

GERA, L. s. BERNÁTH, G.

GERGELY, A. and SÓVÁGÓ, I.: Thermodynamic Data of Transition Metal Complexes with D-Glucosaminic Acid 273

GÖNDÖS, Gy. s. BERNÁTH, G.

HALMOS, J. s. EGRI, J.

HENSEKE, G. s. WILDENHAIN, W.

HOBINKA, I. s. KARÁCSONYI, R.

HORKAY, F. s. DÉVAY, J.

HORVÁTH, G. s. NÁRAY-SZABÓ, G.

HORVÁTH-PARDAVI, M. s. LÁZÁR, K.

INZELT, Gy. s. NAGY, M.

JANÁSZIK, F. s. DÉVAY, J.

KAPOSI, O. s. KARÁCSONYI, R.

KARABAYEV, A. Sh. s. TASMUKHAMEDOV, S. A.

KARÁCSONYI, R., KAPOSI, O., RIEDEL, M., HOBINKA, I. and PODMANICZKY, I.: A Study of the Positive Ion Emission of Molybdenum by Means of a Time-of-flight Mass-spectrometer 169

KISS, Á. I. and SZŐKE, J.: Theoretical Investigation of the Electronic Spectra of Mono-substituted Benzene Derivatives 59

KISS, L., FARKAS, J. and FÓTHI, A.: Untersuchung der Ionisation von Metallen und der Neutralisation von Metallionen mit der rotierenden Ring-Scheibenelektrode, IX. (Investigation of the Ionisation of Metals and of the Neutralisation of Metal Ions on the Rotary Ring-and-Discelectrode, IX) 123

KISS, L., LAKATOS-VARSÁNYI, M. and DO NGOC LIEN: Anodic Behaviour of Iron in Formamide Solutions 135

KLIVÉNYI, F., STÁJER, G., SZABÓ, E. A., PINTYE, J. and VINKLER, E.: Aromatic Sulfenyl Chlorides, V. Reaction of Sulfenyl Chloride with N^2-Aryldithiocarbazates, O-Alkyl-Thiocarbazates and O-Aryl Substituted Phenylthiocarbamates 87

KOVÁCS, K. s. BERNÁTH, G.

KŐRÖS, E., ORBÁN, M., BURGER, M., VÖRÖS, K. and FÜSSY, É.: Iodine Exchange Between Molecular Iodine and Some Iodomethylcarbonyl Compounds in Benzene . 387

LACZKÓ, B. s. RUFF, I.

LAKATOS-VARSÁNYI, M. s. KISS, L.

LARIN, P. P. s. TASMUKHAMEDOV, S. S.

LÁNG, K. L. s. BERNÁTH, G.

LÁZÁR, K., HORVÁTH-PARDAVI, M. and VÉRTES, A.: Magnetic Properties of the Binuclear Ion $[Fe_2(OH)_2(H_2O)_8]^{4+}$ 163

LENGYEL, B. Jr. s. DÉVAY, J.

LENGYEL, B., SZÉKELY, T. and GARZÓ, G.: Study of Degradation in Dimethylsiloxane

Containing Polymers by Dynamic Thermogravimetry and Pyrolysis Gas Chromatography 253

LÉVAY, B.: New Method for the Determination of Stability Constants of Molecular Complexes from Selfdiffusion Data 143

LÉVAY, B. s. VÉRTES, A.

MAKLEIT, S., RADICS, L., BOGNÁR, R., MILE, T. and OLÁH, É.: Conversions of Tosyl and Mesyl Derivatives of the Morphine Group, X. 14-Hydroxymorphine Derivatives, I. Azido and Amino Compounds 99

MAKLEIT, S., RADICS, L., BOGNÁR, R. and MILE, T.: Conversions of Tosyl and Mesyl Derivatives of the Morphine Group, XI. 14-Hydroxymorphine Derivatives, II. Halogen Compounds 111

MÁRAI, P. s. BERNÁTH, G.

MÉSZÁROS, L. s. DÉVAY, J.

MIHÁLYI, L. s. SZABÓ, K.

MIKA, J. s. SZABÓ, K.

MILE, T. s. MAKLEIT, S.

MINK, Gy. s. MÓGER, D.

MINK, Gy. s. NAGY, F.

MÓGER, D., MINK, Gy. and NAGY, F.: Study of the Catalytic Hydrogenation (Deuteration) of Cyclohexene on a Platinum Catalyst. Aging of the Catalyst During the Reaction 27

MÓGER, D. s. NAGY, F.

NAGY, F., MINK, Gy. and MÓGER, D.: Selective Poisoning of Pt Catalysts by CO_2 Chemisorption, I. Reaction of CO_2 with Adsorbed Hydrogen 225

NAGY, F. s. MÓGER, D.

NAGY, F. s. VÉRTES, Gy.

NAGY, M., WOLFRAM, E., INZELT, Gy. and BEKE, Gy.: Effect of the Structure of Liquid Mixtures on the Equilibria of Polymer Gel–Aliphatic-Alcohol–Water Systems .. 233

NÁRAY-SZABÓ, G., DUDAR, E. and HORVÁTH, G.: Quantum Chemical Interpretation of the Spectroscopic Data of Pharmacologically Active Homopyrimidazole Derivatives 281

NYILASI, J. s. ORSÓS, P.

OLÁH, É. s. MAKLEIT, S.

OLECHNOWITZ-STEPIEN, V. s. FARKAS, L.

ORBÁN, M. s. KŐRÖS, E.

ORSÓS, P. and NYILASI, J.: Contributions to the Analysis of Osmium Compounds 267

PANCHAL, B. R. and BHATTACHARYA, P. K.: Study of Metal Exchange in Some π-Bonded Complexes, II. 399

PARAK, F. s. VÉRTES, A.

PETHŐ, Á.: Distributions in Time and Space, Respectively, in Fixed Bed Multistage Exchange Processes of Linear Kinetics (Short Communication) 71

PINTYE, J. s. KLIVÉNYI, F.

PODMANICZKY, I. s. KARÁCSONYI, R.

RADICS, L. s. MAKLEIT, S.

RANOGAJEC-KOMOR, M. s. VÉRTES, A.

RÁKÓCZI, J. s. EGRI, J.

RECENSIONES 115, 383, 499

RIEDEL, M. s. KARÁCSONYI, R.

RUFF, I. and LACZKÓ, B.: Fermi Statistical Treatment of Acid–Base Processes, II. Distribution and Acidity of Individual Proton Hydrates in Concentrated Aqueous Solutions of Perchloric Acid 335

SAKLA A. B., BADRAN, A. H. and SAYED, N. A.: Thermoelectric Microdetermination of Molecular Weights of Organic Compounds in Homogeneous Binary Solvent Systems Using Thermistors 51

SALLAY, P. s. CSŰRÖS, Z.

SAYED SABET ABD EL REHIM s. DÉVAY, J.

SAYED, N. A. s. SAKLA, A. B.

SCHNABEL. K. H. s. CZÁRÁN, E.

SIMIONESCU, Cr. et VASILIU, S.: Recherches dans le domaine des polyphénylacétylénes de polycondensation (II) 461

SOHÁR, P. s. VARSÁNYI, Gy.

SOLYMOSI, F. and BÁNSÁGI, T.: Stabilities of Ammonium Halates in the Solid Phase. Study of the Effects of Aging and Various Additives on the Thermal Decomposition of Ammonium Chlorate 35

SÓVÁGÓ, I. s. GERGELY, A.

STÁJER, G. s. KLIVÉNYI, F.

SUBA, M. s. VÉRTES, A.

SZABÓ, E. A. s. KLIVÉNYI, F.

SZABÓ, K., MIHÁLYI, L. and MIKA, J.: Effect of Mercury Impurities on the Hydrogen Overvoltage on Gallium Electrodes 185

SZABÓ, Z. G., GALIBA, I. and GÁL, D.: Study of the Oxidation of *n*-Heptane 239

SZEKERKE, M. and SZENDE, B.: The Synthesis of Methyl- and Dimethyl-Substituted Amino Acid Hydrazides, as Potential Cytotoxic Agents 371

SZENDE, B. s. SZEKERKE, M.

SZÉKELY, T. s. LENGYEL, B.

SZŐKE, J. s. KISS, Á. I.

ТАШМУХАМЕДОВ, А., ЛАРИН, П. П., КАРАБАЕВ, А. Ш., АЗИЗОВ, Ш. А., ТИЛЛАЕВ, Р. С., УСМАНОВ, Х. У.: Исследование физуко-химических свойств привитых сополимеров поливинилового спирта с поливинилпиридином ..... (TASMUKHAMEDOV, S. A., LARIN, P. P., KARABAYEV, A. Sh., AZIZOV, Sh. A., TILLAYEV, R. S. and USMANOV, Kh. U.: Physico-Chemical Properties of Poly (vinyl Alcohol)–Poly(vinylpyridine) Graft Copolymers) 453

TILLAYEV, R. S. s. TASMUKHAMEDOV, S. A.

USMANOV, Kh. U. s. TASMUKHAMEDOV, S. A.

VARGA, K. and FEJES, P.: Study of the Rate of Sorption on a Single Spherical Adsorbent Particle, III. Experimental Conformation of the Rate Equation 417

VARSÁNYI, Gy. and SOHÁR, P.: Infrared Spectra of 1,2,3,5-Tetrasubstituted Benzene Derivatives, I. 315

VASILIU, S. s. SIMIONESCU, Cr.

VÉRTES, A. and PARAK, F.: Relationship Between the Spin Relaxation and Certain Chemical Properties of Paramagnetic Iron(III)Salt Solutions 293

VÉRTES, A., FRAKNÓY-KŐRÖS, V., LÉVAY, B., GELENCSÉR, P. A. and RANOGAJEC-KOMOR, M.: Investigation of the Antimony Content of Calcium Halophosphate Luminescent Powders by Mössbauer Spectroscopy 151

VÉRTES, A. and SUBA, M.: Study of the Electron-Exchange Reaction Between Iron(II) and Iron(III) in Formamide 439

VÉRTES, A., RANOGAJEC-KOMOR, M. and SUBA, M.: Investigation of the Hydrolysis of Antimony Chloride by Mössbauer Spectroscopy 159

VÉRTES, A. s. LÁZÁR, K.

VÉRTES, Gy. and NAGY, F.: Oxidation on the Nickel Hydroxide Electrode, VI. Mechanism of the Oxidation of Primary Alcohols 405

VINKLER, E. s. KLIVÉNYI, F.

VÖRÖS, K. s. KŐRÖS, E.

WILDENHAIN, W. und HENSEKE, G.: Acide Inhaltsstoffe der Torffulvosäurefraktion. (Acidic Substances of Turfulvonic Acid Fraction) 79

WOLFRAM, E. s. NAGY, F.

Acta Chimica Academiae Scientiarum Hungaricae, Tomus 74 (1), pp. 1—25 (1972)

LÁSZLÓ (LADISLAUS) VARGHA

(1903—1971)

Am 1. Juli 1971 verschied L. VARGHA, ord. Mitglied der Ungarischen Akademie der Wissenschaften, Direktor des Instituts für Arzneimittelforschung, gewesener Professor der organischen Chemie an der Ungarischen Bólyai-Universität zu Kolozsvár (Cluj, Rumänien). Durch seinen Tod erlitt die organisch-chemische und pharmazeutisch-chemische Forschung in Ungarn einen großen Verlust.

L. VARGHA wurde am 25. Januar 1903 in Berhida (Komitat Veszprém) geboren. Sein Vater (Kálmán V.) war reformierter Pastor, seine Mutter (geb. Vilma OSWALD) verlor er schon in seinem Kindesalter. Seine Mittelschulstudien absolvierte er im altehrwürdigen reformierten Kollegium zu Pápa. Nach vorzüglich bestandener Reifeprüfung bezog er die Philosophische Fakultät der Universität Budapest, wo er sich vorwiegend mit naturwissenschaftlichen Studien beschäftigte. Damals war keiner der drei Lehrstühle für Chemie mit einem Organiker besetzt, doch beschäftigte sich glücklicherweise Privatdozent und Oberassistent E. PACSU (später Professor der organischen Chemie an der Universität Princeton, N. J., USA) mit organisch-chemischer Forschung und nahm L. VARGHA in sein Labor auf, wo er dann später — nach Absolvierung der von E. PACSU vorgezeichneten organisch-chemischen Grundstudien — an seiner Dissertation, die sich mit der Untersuchung der partiellen Verseifung von Diacyl-protocatechualdehyden befaßte, arbeitete.

Als Abschluß seiner Universitätsstudien bestand er 1926 das Doktorexamen aus Chemie als Hauptfach, Physik und Geologie als Nebenfächer, mit der Qualifikation »summa cum laude«. Nachher arbeitete er ein Jahr lang als Privatassistent neben Prof. G. ZEMPLÉN an der Technischen Universität Budapest, danach als ungarischer Staatsstipendiat zwei Jahre am chemischen Institut der Universität Berlin neben a. o. Prof. H. OHLE und schließlich weitere zwei Jahre als Privatassistent neben a. o. Prof. A. SCHÖNBERG am organisch-chemischen Institut der Technischen Hochschule Berlin-Charlottenburg. Mit SCHÖNBERG hatte er Untersuchungen über organische Schwefelverbindungen durchgeführt, von OHLE erhielt er Anregung, auf dem Gebiet der Kohlenhydrate zu arbeiten. Die in Berlin verbrachten vier Jahre waren

für ihn recht fruchtbringend; dies bezeugen 10 Publikationen [2—11]*, die größtenteils in den Berichten d. D. Chem. Gesellschaft erschienen sind.

Nach vierjährigem Aufenthalt in Berlin kehrte VARGHA nach Ungarn zurück. Zunächst war es ihm nur möglich, im Besitze von Gelegenheitsstipendien, die jedoch sehr bescheiden waren und nur für je ein Jahr erteilt wurden, seine Forschungstätigkeit fortzusetzen. Er arbeitete ein Jahr neben Prof. A. SZENT-GYÖRGYI am Medizinisch-chemischen Institut der Universität Szeged, dann ein Jahr am Biologischen Forschungsinstitut zu Tihany, darauf wiederum in Szeged, diesmal zwei Jahre am Organisch-chemischen Institut der Universität und schließlich ein Jahr am Physiologischen Institut der Universität Budapest. Obzwar in diesen Jahren seine Dotation nur knapp für einen sehr bescheidenen Lebensunterhalt ausreichte, und ihm keine jüngeren Mitarbeiter oder technischen Hilfskräfte zur Verfügung standen, gelang es ihm doch, gute Ergebnisse auf dem Gebiet der Kohlenhydratchemie selbständig durchgeführter Forschungen aufzuweisen. Dies wurde auch von der Naturwissenschaftlichen Fakultät der Universität Szeged anerkannt, als sie ihm 1935 aus dem Spezialgebiet »Chemie der Kohlenhydrate« die »venia legendi« erteilte. Kurz darauf erhielt er ein Angebot der Pharmazeutisch-chemischen Fabrik G. Richter Budapest, ein Forschungslaboratorium zu organisieren und dessen Leitung zu übernehmen. Er nahm dieses Angebot an, obwohl er sich dessen bewußt war, daß er seine beliebte Grundforschung auf dem Gebiet der Kohlenhydrate aufgeben wird müssen. So zu entscheiden war jedoch damals für ihn nicht bloß eine Existenzfrage, sondern diesen Entschluß zu fassen bewog ihn auch die Aussicht auf eine bessere, durch junge Mitarbeiter unterstützte Möglichkeit einer gleichfalls viel Interessantes mit sich bringenden Forschungsarbeit auf verschiedenen Gebieten der organischen Chemie. Hier kam er in engste Berührung mit Aufgaben der Arzneimittelforschung und bekam zugleich einen Einblick in so manche Probleme der pharmazeutisch-chemischen Industrie Ungarns. Bei dieser Gelegenheit bekräftigte sich seine ältere Überzeugung, daß eine erfolgreiche pharmazeutisch-chemische Forschung ohne organisch-chemische Grundforschung kaum möglich ist.

Nun ergab sich für VARGHA im Herbst 1940 wiederum die Möglichkeit, organisch-chemische Grundforschung nach Belieben durchzuführen, indem er zum Professor der organischen Chemie an die von Szeged nach Kolozsvár (jetzt: Cluj, Rumänien) rückgeführte Franz Josef Universität ernannt wurde. Da galt es zunächst, das Universitätsinstitut für organische Chemie und damit den Unterricht zu organisieren, junge Mitarbeiter in die organisch-chemische Forschung einzuführen. Kaum war dies geschafft, mußte er kurz nach Kriegsende — wegen des Imperiumwechsels — das nach seiner Direktive eingerichtete Institut wiederum verlassen und ein neues Institut an der von der rumänischen

* Die in Klammern gesetzten arabischen Zahlen beziehen sich auf die betreffenden Publikationen, deren Verzeichnis anhängend mitgeteilt ist.

Regierung neu gegründeten Ungarischen Bólyai-Universität organisieren. Gleichzeitig wurde er vertragsgemäß — als ungarischer Staatsbürger — als Professor für organische Chemie angestellt. Im Herbst 1950 wurde der Vertrag nicht mehr erneuert, so daß VARGHA nach Budapest zurückkehrte und am neu gegründeten Ungarischen Institut für Arzneimittelforschung die Leitung einer Sektion übernahm; 1957 wurde er zum Direktor des Instituts ernannt und behielt diesen Posten bis zu seinem Lebensende. Als er hier zu arbeiten begann, hatte das Institut nur eine provisorische Unterkunft, doch wurde in einigen Jahren — nicht zuletzt auf seine Anregung — ein großangelegter Neubau mit modern ausgestatteten Laboratorien errichtet. Bei der Organisierung des Neubaus konnte er sich schon auf eine Anzahl tüchtiger Mitarbeiter stützen, die er — Dank seiner guten Urteilskraft — in diese Arbeit einbezogen hatte.

In Anerkennung seiner Forschungsergebnisse wurde er von der Ungarischen Akademie der Wissenschaften 1951 zum korrespondierenden, 1964 zum ordentlichen Mitglied gewählt; 1958 erhielt er den Kossuth-Preis; ob seiner Verdienste als Direktor des Forschungsinstituts wurden ihm dreimal (1961, 1963, 1965) hohe Regierungsauszeichnungen verliehen. Es ist ein Zeichen internationaler Anerkennung seiner Forschungsergebnisse, daß er zum Mitglied des Redaktionskomitees der 1964 gegründeten internationalen Zeitschrift »Carbohydrate Research« gewählt wurde.

Die Forschungstätigkeit von L. VARGHA bezeugen fast 100 Publikationen, weiterhin zahlreiche Arzneisynthesen, die in Patentschriften festgelegt sind. Seine Forschungen erstreckten sich auf mehrere Gebiete der organischen Chemie, am meisten interessierte ihn jedoch die Kohlenhydratchemie und seine auf diesem Gebiet erreichten Forschungsergebnisse verschafften ihm schon in seinen jungen Jahren einen guten Ruf. Seine knapp gefaßten Publikationen lassen seine scharfe Urteilskraft, tüchtige Kenntnis der einschlägigen Fachliteratur und den vorzüglichen Experimentator erkennen. In späteren Etappen seiner Laufbahn konnte er es nur schwer hinnehmen, daß ihm die schwere Last der vielen, zeitraubenden Verwaltungsarbeit — und in seinen letzten Jahren sein labiler Gesundheitszustand — das persönliche Mitwirken in der Laborarbeit nicht mehr ermöglichte.

Von den ersten Forschungsergebnissen, die er noch in Gemeinschaft mit H. OHLE erzielt hat [2—8], verdient besonders die Synthese der 1,2-O-Isopropyliden-6-O-tosyl-D-glucofuranose **(I)** und aus dieser die Herstellung des 5,6-Anhydroderivats **II** durch Einwirkung von Natriummethylat Erwähnung. Dadurch war eine neue und einfache Methode zur Herstellung von Zuckerepoxyden geschaffen worden, die seitdem oft Anwendung gefunden hat. Aus dem Epoxyd **II** konnte durch Einwirkung von Lauge einerseits das D-Glucosederivat **III**, andererseits — infolge einer bei der Aufspaltung des Epoxydringes am Asymmetriezentrum 5 erfolgenden Inversion — das 1,2-Isopropyliden-Derivat der seltenen D-Idose erfaßt werden. Es wurde die Sprengung des Drei-

ringes auch mit einem Überschuß von Natriummethylat bewirkt, in der Hoffnung, auf dem Wege **II** → **V** → **VI** zur 5-O-Methyl-D-glucofuranose **(VI)** gelangen zu können. Spätere Untersuchungen haben jedoch eine *trans*-Öffnung des Ringes bewiesen, somit dürfte also anstatt der 5-O-Methyl-D-glucofuranose **(VI)** das isomere D-Idose-Derivat **VIa** entstanden sein.

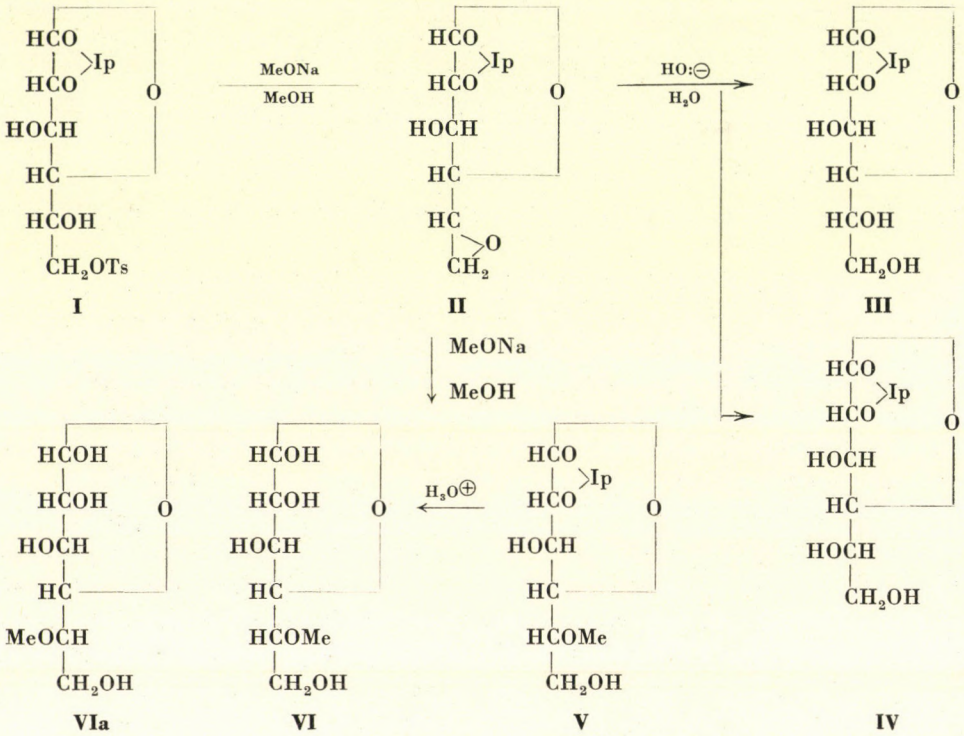

Die Herstellung der sehr interessanten 5-O-Methyl-D-glucose ist VARGHA — wie weiter unten gezeigt wird — später auf anderem Wege doch gelungen.

Von den in Gemeinschaft mit A. SCHÖNBERG publizierten Arbeiten [6—11] ist besonders die zu Thiolestern führende thermische Isomerisierung von Thionestern der Thiokohlensäure zu erwähnen, die einen guten Weg zur Umwandlung der Phenole zu Thiophenolen eröffnet hat:

$$S{=}CCl_2 + 2ArOH \xrightarrow{\text{Pyridin}} S{=}C(OAr)_2 \xrightarrow{280°C} O{=}C\begin{matrix}\diagup SAr \\ \diagdown OAr\end{matrix} \longrightarrow$$

$$\xrightarrow[H_2O]{HO:\ominus} ArOH + ArSH \xrightarrow{H_2O_2} 1/2Ar{-}S{-}S{-}Ar \xrightarrow{\text{Red.}} ArSH$$

Seine ganz selbständigen Untersuchungen, die er zunächst am Medizinisch-chemischen Institut der Universität Szeged begann, führten alsbald zu einem wichtigen Ergebnis. Zu dieser Zeit hatte SZENT-GYÖRGYI zum erstenmal aus dem Preßsaft von Paprikaschoten in auffallend großer Menge die von ihm einige Jahre früher aus tierischer Nebennierenrinde mit großer Mühe in bescheidener Menge bereits isolierten »Hexuronsäure« abgeschieden. Er hatte vermutet, daß die auch in Pflanzen vorkommende und stark reduzierende Substanz mit dem seit langem gesuchten Vitamin C identisch sein dürfte, umsomehr, als aus Tierversuchen bekannt war, daß die Vitamin-C-Wirkung verschiedener Früchte bzw. der aus ihnen gewonnenen Preßsäfte und Extrakte mit ihrem Reduktionsvermögen in saurer Lösung parallel ansteigt. Die Richtigkeit seiner Vermutung konnte zwar mit dem Tierversuch (Meerschweinchen) bestätigt werden, wurde jedoch auch noch von einigen Experten der Vitaminforschung in Frage gestellt, da laut des kurativen bzw. präventiven Tests der tägliche Bedarf viel größer war (1 mg/l kg Körpergewicht) als von anderen isolierten Vitaminen, deren Einheitlichkeit damals noch nicht einmal gewährleistet war. Deshalb schien es nicht ausgeschlossen zu sein, daß die Vitamin-C-Wirkung nicht der Hexuronsäure selbst, sondern nur einer, ihr in minimaler Menge anhaftenden Begleitsubstanz zuzuschreiben ist, die sich durch einfache Kristallisierung nicht entfernen läßt. Da stellte VARGHA aus Hexuronsäure ein gleichfalls gut kristallisierendes Isopropylidenderivat her, aus dem sich die Hexuronsäure sehr leicht regenerieren ließ [14]. Die auf diese Weise »gereinigte« Substanz zeigte nun im Tierversuch auch in quantitativer Hinsicht dieselbe biologische Wirkung wie vor dem doppelten Umsatz, dem sie unterworfen wurde. Letzten Endes gaben folgende experimentellen Befunde von VARGHA gute Anhaltsprodukte zur Strukturermittlung des später L-Ascorbinsäure genannten Vitamins C: (a) Isopropyliden-ascorbinsäure ist — wie die Ascorbinsäure selbst — eine saure, stark reduzierende Verbindung, die in wäßriger Lösung bereits beim kurzen Aufbewahren wieder in Ascorbinsäure und Aceton zerfällt; (b) die Ascorbinsäure enthält eine tritylierbare primäre Hydroxylgruppe [15].

Während seiner einjährigen Tätigkeit am Biologischen Forschungsinstitut zu Tihany hat VARGHA ein interessantes und einfaches Verfahren zur Herstellung der 1,2-O-Isopropyliden-α-D-glucofuranose ausgearbeitet, das nicht auf einer partiellen Hydrolyse der Di-isopropyliden-D-glucose beruht, sondern aus der Methanolyse des aus D-Glucose durch gleichzeitige Einwirkung von Borsäure und Aceton herstellbaren 1,2-O-Isopropyliden-3,5-borsäureesters der D-Glucose besteht [16]. Diese Methode hatte er später auch zur Synthese des 1,2-O-Isopropyliden-D-mannits herangezogen [17]. Mit dieser Arbeit haben eigentlich seine vielseitigen Untersuchungen über Zuckeralkohole begonnen, denen er besonders später große Aufmerksamkeit widmete. Es gelang ihm, die Struktur des seit langem beschriebenen Benzal-sorbits zu ermitteln [22],

diese Erkenntnis zur Synthese der früher nur schwer zugänglichen L-Xylose zu verwerten **(VII → VIII → IX)** und letztere zugleich zur L-Xyloketose zu isomerisieren. Die L-Xyloketose wurde von LEVENE und LAFORGE aus Harn isoliert und identifiziert, aber ihre Synthese erst von VARGHA durchgeführt.

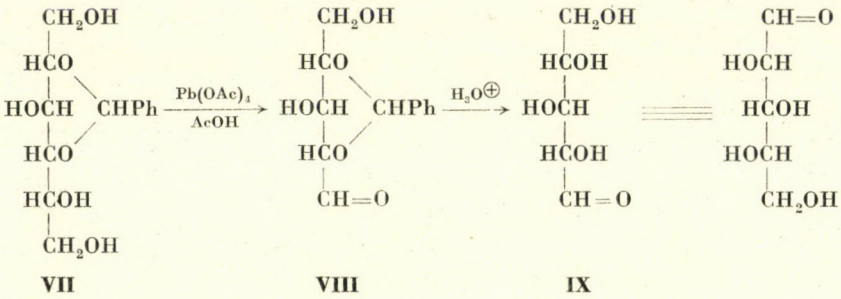

VII **VIII** **IX**

Nennenswert ist auch die aus der 1,2-O-Isopropyliden-3-O-tosyl-6-benzoyl-α-D-glucofuranose **(X)** ausgehende Synthese der seit langem angestrebten 5-O-Methyl-D-glucose **(XIII)** über Derivate **XI** und **XII** [24]:

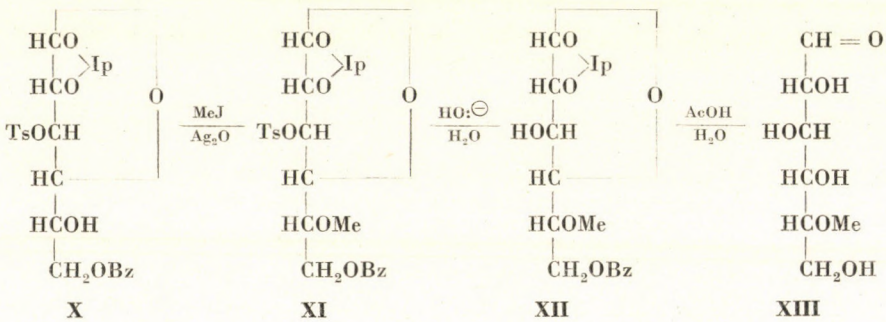

X **XI** **XII** **XIII**

Hierbei wird man besonders auf die Präzision dieser Arbeit aufmerksam, ferner auch auf den Befund, daß im öligen Endprodukt die 5-O-Methyl-D-glucose vorwiegend in der *al*-Form **(XIII)** vorliegt, woraus der Schluß gezogen werden kann, daß in der D-Glucofuranose der Ring sehr labil ist.

Mit der letzterwähnten, im August 1936 verfaßten Publikation wurden VARGHAS kohlenhydratchemische Untersuchungen vorläufig unterbrochen, da er seine Tätigkeit im Forschungslabor der Pharmazeutisch-chemischen Fabrik G. Richter begann. Von den hier durchgeführten bzw. in Angriff genommenen Arbeiten [25—28, 30] ist vor allem die interessante Synthese des *trans*-1,2-Diäthyl-1,2-di-(*p*-hydroxyphenyl)-äthylens **(XVIIIb)** zu erwähnen. Bekanntlich wurde dieses Kunstprodukt mit auffallend starker östrogener Wirkung zum erstenmal von DODDS und ROBINSON 1937 beschrieben und kurz darauf (1938) eine aus Anisaldehyd startende Synthese ausgearbeitet. Noch im selben

Jahre hatte VARGHA eine viel einfachere und ausgiebigere Synthese durchgeführt (Patentanmeldung vom 30.3.1938) und zugleich anstatt der Hydroxyle andere Substituenten enthaltende Analoga hergestellt, um den Effekt der Substituenten auf die biologische Wirkung studieren zu können. Als Ausgangssubstanz wurde Propiophenon bzw. sein *p*-substituiertes Derivat **(XIV)** herangezogen, das laut der Reaktionsreihe **XIV → XV → XVI → XVII → XVIII** zum gewünschten *trans*-Äthylenderivat umgesetzt werden konnte:

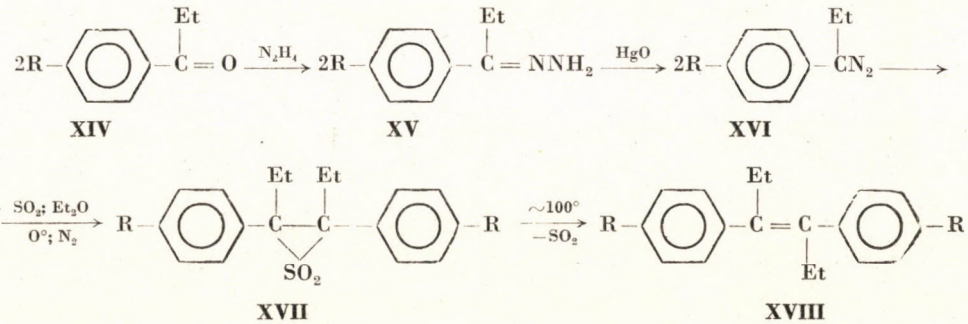

a: R=OMe; **b**: R=OH; **c**: R=Br; **d**: R=NH_2; **e**: R=H

Auf diese Weise ließ sich aus **XIVa** das *trans*-Stilbenderivat **XVIIIa** gewinnen, das mit alkoholischer Kalilauge zu **XVIIIb** (»Stilböstrol«) demethyliert werden konnte. Aus dem Keton **XIVc** wurde nicht nur das Derivat **XVIIIc**, sondern auch die isomere *cis*-Verbindung gewonnen; beide ließen sich dann durch Ammonolyse in die **XVIIId** *trans*-Verbindung überführen. Schließlich wurde noch aus Propiophenon **(XIVe)** selbst die unsubstituierte Grundsubstanz **XVIIIe** hergestellt. Die pharmakologische Untersuchung all dieser Äthylenderivate hat ergeben, daß zur Entfaltung einer östrogenen Wirkung die phenolischen Hydroxyle unentbehrlich sind.

Während seiner Professur in Kolozsvár hat VARGHA wiederum kohlenhydratchemische Untersuchungen in Gang gesetzt, aber gleichzeitig einen regen Kontakt mit der pharmazeutisch-chemischen Industrie aufrechterhalten. Zuerst galt es, früher zwangsweise unterbrochene Untersuchungen über Benzalsorbit [21, 22] fortzusetzen, d. h. die mit verdünnter Säure bewirkte Hydrolyse des früher aus 2,4-O-Benzal-1,6-O-tosyl-D-glucit **(XIX)** durch partielle Detosylierung (Natriummethylat, Methanol) gewonnenen Tosyl-2,4-O-benzal-5,6-anhydro-D-glucits **(XX)** zu studieren [29]. Es hat sich ergeben, daß diese Reaktion nicht zu einem 1-O-Tosyl-hexit (erwartungsgemäß zum 1-O-Tosyl-D-glucit und/oder -L-idit) führt, sondern zu einem 1-O-Tosyl-X,X'-anhydrohexit, in welchem eine primäre und zwei sekundäre, *trans*-ständige vicinale Hydroxyle nachweisbar sind. Dies entspräche dem 1-O-Tosylat des 2,5-Anhydro-L-idits **(XXIa)** und auch des 2,5-Anhydro-D-glucits **(XXIIa)**. Von den

beiden Möglichkeiten ließ sich **XXIIa** ausschließen, da das aus dem Monotosylat herstellbare Ditosylat bei der Oxydierung mit Bleitetraacetat einen optisch aktiven Dialdehyd lieferte, der nur aus den 1,6-Di-O-tosyl-2,5-anhydro-L-idit **(XXIb)** entstehen konnte, da ja das entsprechende D-Glucitderivat **(XXIIb)** einen optisch inaktiven Dialdehyd liefern sollte.*

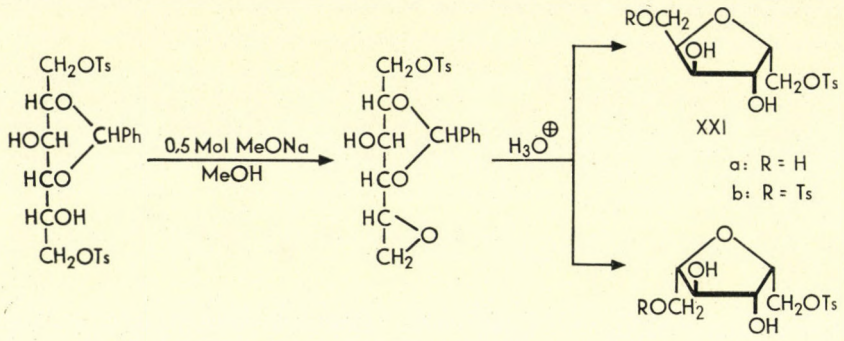

XIX **XX** **XXII**

Die Isomerisierung bzw. Epimerisierung der Zucker und Zuckeralkohole [39] war des öfteren Gegenstand seiner Untersuchungen, auch schon deshalb, weil ja der leichteste Weg der Epimerisierung über Epoxyde führt und zur Herstellung der letzteren eben OHLE und VARGHA eine verallgemeinerungsfähige Methode entwickelt haben [6]. Dadurch wurde seine Aufmerksamkeit schon auf O-Tosyl- und später auch auf O-Mesyl-derivate der Zucker und Zuckeralkohole gerichtet. Als ein interessantes Ergebnis derartiger Arbeiten sei die ausgiebige und verhältnismäßig einfache Herstellung der L-Idose aus D-Glucose hervorgehoben, die folgenden Weg einschlug: die Tosylgruppen der aus D-Glucose leicht zugänglichen 1,2-O-Isopropyliden-5,6-di-O-tosyl-α-D-glucofuranose **(XXIII)** lassen sich gegen Acetylgruppen vertauschen, wobei am Asymmetriezentrum 5 eine Inversion erfolgt. Das so gebildete Triacetat **(XXIV)** liefert nach der alkalischen und dieser folgenden sauren Hydrolyse L-Idose **(XXV)**. Chromatographische Untersuchungen zeigten, daß das als Sirup anfallende Endprodukt einheitlich ist und somit reine L-Idose **(XXV)** darstellt. Es ist jedoch schon nach einwöchigem Aufbewahren neben L-Idose auch L-Sorbose nachweisbar und nach drei Monaten läßt sich aus dem allmählich trüber gewordenen Gemisch mit einer Ausbeute von rund 60% kristallisierte L-Sorbose **(XXVI)** absondern. Die L-Idose (die laut Reaktionen des Gemisches vorwiegend in ihrer *al*-Form vorliegt) ist somit recht unbeständig und macht es verständlich, daß in der Natur weder L- noch D-Idose vorkommt. Die Umlagerung der L-Idose zur

* Die Formeln XXI und XXII sind aus der Originalmitteilung [29] entnommen worden, obzwar sie nicht die im Text richtig erwähnten 2,5-Anhydro-hexite, sondern aus Versehen ihre Antipoden darstellen.

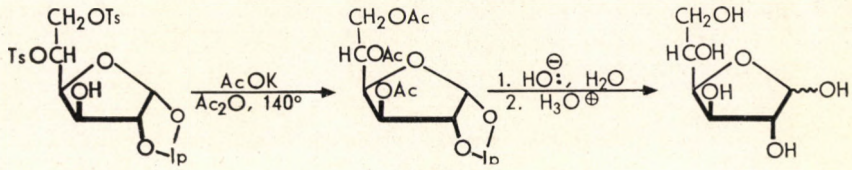

XXIII XXIV XXV

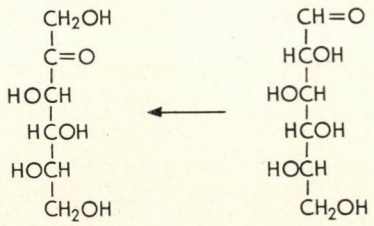

XXVI XXV

L-Sorbose ließ sich übrigens auf stereochemische Gründe zurückzuführen [41].

Die oben geschilderte Arbeit ist Gegenstand der ersten Mitteilung, die VARGHA aus dem Institut für Arzneimittelforschung publizierte, doch in kurzer Zeit folgten ihr zahlreiche Publikationen über ähnliche Arbeiten, die erkennen lassen, daß sich in diesem Institut ein neues Zentrum und eine neue Schule kohlenhydratchemischer Forschung in Ungarn ausgebildet hat, wodurch sich junge Chemiker in dieses Gebiet gut einarbeiten konnten. Die Anregung zu derartigen Forschungen gab VARGHAS Idee, daß Cytostatica, mit denen man die Bekämpfung des Krebses und der Leukämie angestrebt hat, vorwiegend Derivate zellfremder Verbindungen darstellen, und eben dies könnte als eine Ursache dessen angenommen werden, daß diese Verbindungen nicht selektiv nur auf Krebszellen wirken, sondern auch normale Zellen schädigen und deshalb äußerst toxisch sind. Dieser Gedanke ist das Leitmotiv einer zusammenfassenden Mitteilung [66], die er in Gemeinschaft mit sechs Mitarbeitern 1961 publizierte. Sie faßt die Ergebnisse zehn Jahre langer Forschungen zusammen, deren Zielsetzung die Synthese cytoaktive Gruppen enthaltender Derivate von Zuckern und Zuckeralkoholen war [47—49, 55, 56, 59—65]. Die Untersuchungen in dieser Richtung wurden auch noch nach 1961 fortgesetzt und ihre Ergebnisse in weiteren Publikationen [71—78, 81, 82, 84, 86—88, 93—96] niedergelegt. Diese Arbeiten enthalten eine Fülle von neuen Erkenntnissen auf dem Gebiet der Kohlenhydratchemie und haben oft den Charakter einer typischen Grundforschung, da ja die pharmazeutisch-chemische Zielforschung — wie dies auch VARGHA stets betonte — mit der organisch-chemi-

schen Grundforschung engstens verknüpft ist. In der Tat widerspiegeln zahlreiche Arbeiten, die im Institut für Arzneimittelforschung durchgeführt worden sind, diese Auffassung, der es auch zu verdanken ist, daß mehrere in dieser Gemeinschaft arbeitende Chemiker in die Reihe der besten ungarischen Organiker emporgestiegen sind und zum guten Ruf des Institutes vieles beigetragen haben.

Von den cytoaktiven Verbindungen fiel die Aufmerksamkeit VARGHAS vor allem auf die biologischen Alkylierungsmittel, deren Prototyp der sogenannte Stickstoffsenf **(XXVII)** darstellt, doch gehören hierher ihrer Wirkungsart gemäß auch 2,4,6-Tri-äthylenimino-1,3,5-triazin **(XXVIII)** und 1,4-Dimesyloxy-butan **(XXIX)**.

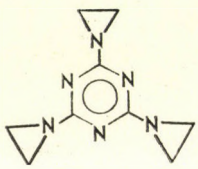

$CH_3N(CH_2CH_2Cl)_2$ $CH_3SO_2O(CH_2)_4OSO_2CH_3$

XXVII **XXVIII** **XXIX**

Es war schon bekannt, daß viele Analoga von **XXVII**, die anstatt der Methylgruppe andere Gruppen enthalten, die Cytoaktivität der Verbindung **XXVII** nicht übertreffen und gleichfalls sehr toxisch sind. Nun vermutete VARGHA, daß cytoaktive (z. B. »alkylierende«) Gruppen, die nicht zellfremden Trägermolekülen, sondern z. B. Zuckern oder Zuckeralkoholen angegliedert sind, eine mehr selektiv auf Krebsgewebe gerichtete Wirkung und demzufolge eine geringere Toxizität haben könnten, und dies besonders dann, wenn es sich um Moleküle asymmetrischen Baus handeln würde, da ja zwischen der biologischen Wirkung und der Chiralität asymmetrischer Moleküle ein gewisser Zusammenhang zu erwarten ist. Dieser Überlegung gemäß wurde zunächst aus 1,2-5,6-Dianhydro-3,4-O-isopropyliden-D-mannit **(XXX)** durch Einwirkung von Äthylenimin die Verbindung **XXXI**, dann aus dieser mittels konzentrierter Salzsäure das Bishydrochlorid des 1,6-Didesoxy-1,6-di-β-chloräthylamino-D-mannits **(XXXII)** hergestellt. Letztere Verbindung erwies sich als ein starkes Cytostaticum auffallend niedriger Toxizität und wurde alsbald in die klinische Praxis (unter dem Handelsnamen »Degranol«) eingeführt.

Dieses Ergebnis hat nun folgende Erkenntnis mit sich gebracht: a) die Entfaltung einer cytostatischen Wirkung ist nicht unbedingt daran gebunden, daß die beiden »alkylierenden« Gruppen an ein und demselben Stickstoffatom haften müssen; b) die cytostatische Wirkung scheint auch von der Anwesenheit von Hydroxylgruppen bedingt zu sein, da das zum Vergleich hergestellte Hydrochlorid des 1,6-Di-β-chloräthylamino-hexans ganz wirkungslos ist.

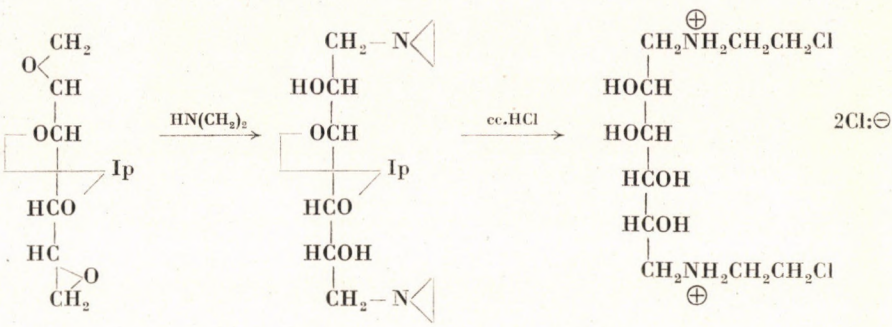

XXX **XXXI** **XXXII**

Dieser Befund regte zu weiteren Untersuchungen an, die das Ziel hatten, den Einfluß des Trägermoleküls auf den therapeutischen Index der Cytostatica weiter zu studieren. Dieser Zielsetzung entsprechend wurden zuerst — zwecks Ermittlung des Zusammenhanges der biologischen Wirkung mit der Chiralität der Asymmetriezentren — die mit dem Degranol **(XXXII)** analogen Derivate des L-Mannits, D-Glucits, Dulcits und L-Idits aufgebaut. Ihre pharmakologische Testung hat ergeben, daß die Konfiguration der Asymmetriezentren ausschlaggebend ist, und daß das D-Mannitderivat **XXXII** den weitaus günstigsten therapeutischen Index aufweist. Zugleich wurden auch Analoga der Verbindung **XXXII** hergestellt, die anstatt der Chloratome andere Halogene enthielten; ihre Prüfung zeigte, daß das analoge Bromderivat einen noch günstigeren therapeutischen Index aufweist als Verbindung **XXXII**. Dies ist ein Hinweis darauf, daß die in vivo Wirkung der biologischen Alkylierungsmittel in der Tat so zu deuten ist, daß sich ihre beiden substituierten Alkylgruppen an nukleophile Zentren von Proteinen (Enzymen) und Nucleinsäuren binden und dadurch Kettenvernetzungen verursachen.

Aus entsprechenden Aldonsäurelactonen hergestellte β-Chloräthylamide, ferner die aus Zuckersäure- und D-Mannozuckersäure-dilacton hergestellten Di-β-chloräthylamide erwiesen sich als biologisch inaktiv. Die Erfahrenheit auf dem Gebiet der Kohlenhydratchemie und eine gute Erfindungsgabe bezeugt die Herstellung einiger Zuckerderivate, die als nähere Analoga des Stickstoffsenfes **(XXVII)** zu betrachten sind. Hierzu gehören: N,N-Di-β-chloräthyl-D-glucosamin und sein L-Antipode, 5-Desoxy-5-(di-β-chloräthyl)-amino-äthyl-D-ribofuranosid, 1-Desoxy-1-(di-β-chloräthyl)-amino-2,3-isopropyliden-L-sorbofuranose und 1-Desoxy-1-(di-β-chloräthyl)-amino-3,4-isopropyliden-L-sorbofuranose bzw. ihre Salze. All diese Verbindungen zeigten zwar eine ausgeprägte, schwache cytostatische Wirkung, erwiesen sich jedoch als sehr toxisch.

Schließlich haben unter den biologischen Alkylierungsmitteln auch

Dimesylate die Aufmerksamkeit von VARGHA erregt, nachdem bekannt wurde, daß das Dimesylat des 1,4-Butandiols **(XXIX)** eine cytostatisch wirkende Verbindung darstellt, die später auch in der klinischen Praxis zur Behandlung der myeloiden Leukämie (unter dem geschützten Namen »Myleran«) Anwendung fand. Es war somit zu erwarten, daß man durch Änderung der Kettenlänge und Einbau von alkoholischen Hydroxylen, weiterhin durch Variierung der Konfiguration von Asymmetriezentren zu α,ω-Dimesylaten von schärferer Selektivität ihrer cytostatischen Wirkung, verbunden mit einer niedrigen Toxizität, wird gelangen können. Diese Vermutung gab Anlaß zur Synthese des 1,6-Di-O-mesyl-D-mannits (das unter den Namen »Mannogranol« therapeutisch verwendet wird) und seines L-Antipoden, des 1,2-5,6-Tetramesyl-D-Mannits (das unter dem Namen »Zytostop« in die Therapie gleichfalls eingeführt worden ist), der 1,6-Di-O-mesyl-L-sorbose, der 1,6-Di-O-mesyl-D-fructose und 1,4-Di-O-mesyl-*meso*-erythrits. Von diesen hatten wiederum die Derivate des D-Mannits die günstigste therapeutische Wirkung und dies weist wiederum auf die Wichtigkeit der Kettenlänge und der Konfiguration der Asymmetriezentren hin. — In Kenntnis des cytostatisch wirkenden Antibioticums, des Azaserins, wurden aus entsprechenden Aldonsäure- und Zuckersäurechloriden durch Einwirkung von Diazomethan 1-Desoxy-1-diazo-D-glucoheptulose und 1,8-Bis-diazo-2,7-dioxo-3,4,5,6-galactotetrahydroxy-octan aufgebaut, doch zeigten diese Verbindungen nur eine schwache cytostatische Wirkung.

Noch im Laufe der oben erörterten Untersuchungen wendete VARGHA seine Aufmerksamkeit einer prinzipiell anderen Möglichkeit der Krebstherapie zu, nämlich der Anwendung gewisser Purin- und Pyrimidinderivate als Antimetabolite. In der ersten diesbezüglichen Mitteilung [73] wird die Synthese der 2-Desoxy-2-chlor-D-ribose **(XXXVI)** und des analogen D-Arabinose-Derivats **(XXXV)** beschrieben. Auf diese Verbindungen fiel deshalb die Wahl, weil in beiden die 5- und 3-ständigen Hydroxyle im Organismus vermutlich phosphoryliert und dadurch in Nucleinsäuren eingebaut werden können, umsomehr, als auch die Konfiguration des Asymmetriezentrums 3 entsprechend ist. Als Ausgangssubstanz diente in beiden Fällen leicht zugängliches Diacetyl-D-arabinal **(XXXIII)**, aus welchem durch Chloraddition das Mischprodukt **XXXIV** erhältlich war und dieses dann nach einer zweistufigen Hydrolyse die erwünschten, in kristalliner Form trennbaren Endprodukte lieferte, deren Konstitution streng bewiesen wurde:

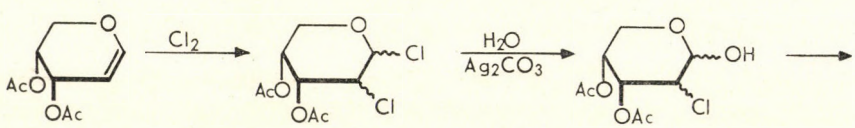

XXXIII **XXXIV**

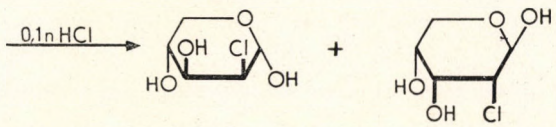

XXXV **XXXVI**

Das Dichlorderivat **XXXIV** konnte auch zur Herstellung der wichtigen 2-Desoxy-D-ribose **(XXXIX)** herangezogen werden, wobei folgender Weg eingeschlagen wurde: Derivat **XXXIV** ließ sich in Gegenwart von Silbercarbonat mit Methanol zu einem Gemisch von stereoisomeren Methylglykosiden **(XXXVII)** umsetzen, aus welchem das D-Arabinose-Derivat **XXXVIII** in kristalliner, einheitlicher Form abgesondert werden konnte. Die in alkoholischem Medium in Anwesenheit von Raney-Nickel bewirkte Hydrogenolyse und darauf eingesetzte Hydrolyse mit 2%iger Benzoesäure lieferte 2-Desoxy-D-ribose **(XXXIX)** [73]:

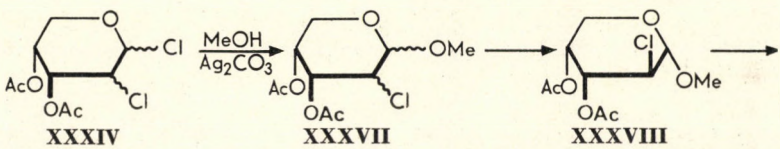

XXXIV **XXXVII** **XXXVIII**

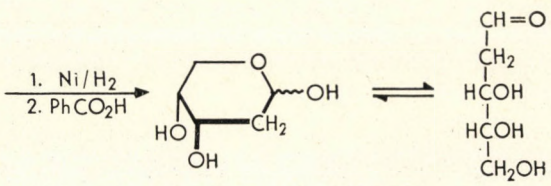

XXXIX

Diese, biologisch so wichtige Aldopentose wurde von anderen Forschern bereits 1949 gleichfalls aus Diacetyl-D-arabinal **(XXXIII)** hergestellt, jedoch durch Anwendung des alten FISCHERschen Verfahrens (d. h. Wasseraddition in saurem Medium), wobei nur eine Ausbeute von 10% erreicht werden konnte, während sie bei der oben erörterten Synthese 65% betrug. Eine Vereinfachung der aus Diacetyl-D-arabinal **(XXXIII)** ausgehenden Synthese, die zugleich eine weitere Steigerung der Ausbeute ermöglichte, bestand aus folgendem Verfahren: aus dem Diacetat **XXXIII** ließ sich durch Anlagerung von Chlorwasserstoff in Benzol 2-Desoxy-acetochlor-D-ribopyranose **(XL)** und hieraus ein Methylglykosid **(XLI)** gewinnen, das nach einer ZEMPLÉNschen Desacetylierung und darauffolgenden schonenden Säurehydrolyse 2-Desoxy-D-ribose **(XXXIX)** lieferte. Auf diese Art konnte das Endprodukt in Form ihres kristallinen Anilids mit 80%iger Ausbeute gewonnen werden [74]:

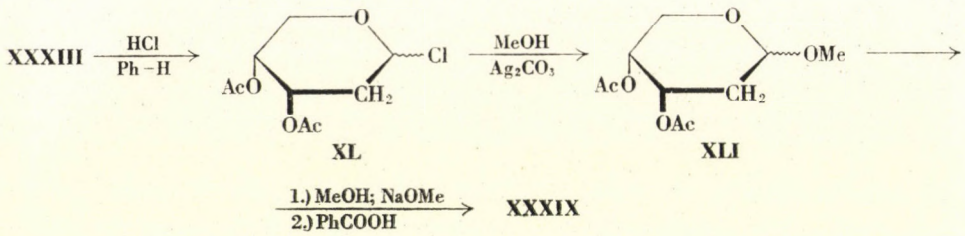

Ein Versuch, die kristalline, gut definierte 2-Desoxy-2-chlor-D-arabinose mit Adenin zum 2'-Desoxy-2'-chlor-2'-epi-adenosin zu koppeln, mißlang zuerst, obzwar die zur N-Glykosidbildung geeignete 1,2-Didesoxy-1,2-dichlor-3,5-O-diacetyl-D-arabofuranose **(XLII)** aus der entsprechenden Pyranose hergestellt werden konnte. Da jedoch der N-Glykosylierung Adenin in Form des Natriumsalzes des 2,8-Dichloradenins unterworfen wurde, und nach erfolgter Kupplung die aromatisch gebundenen Chloratome selektiv nicht entfernt werden konnten, sondern im Laufe einer reduktiven Eliminierung alle drei Chloratome gegen Wasserstoff ausgetauscht worden sind, bildeten sich als Endprodukte 2'-Desoxy-α- und -β-D-ribofuranosyl-adenin **(XLIII** und **XLIV)**, in sich selbst auch ein interessantes Ergebnis:

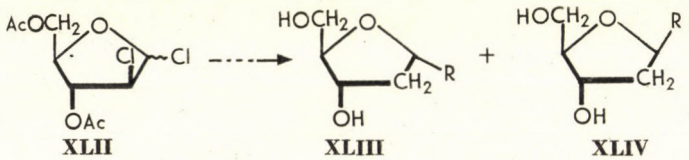

Das erwünschte 9-(2'-Desoxy-2'-chlor-α-D-arabofuranosyl)-adenin und sein β-Anomer ließ sich schließlich durch Kupplung des 6-Benzoylamino-9-chlormercuri-purins mit dem Derivat **XLII** und darauffolgende Desacylierung nach ZEMPLÉN gewinnen [81]. Beide Verbindungen zeigten zwar nur eine schwache tumorhemmende Wirkung, doch lohnte sich ihr Aufbau hauptsächlich wegen der interessanten Beobachtungen, die im Laufe ihrer Synthese gemacht werden konnten.

Die Versuche, gewisse Derivate von Zuckern und Zuckeralkoholen zu synthetisieren, führten oft zu überraschenden Ergebnissen, doch haben VARGHA und Mitarbeiter die Konstitution unerwartet gebildeter Verbindungen meisterhaft geklärt und mehr als einmal falsche Angaben der Fachliteratur richtiggestellt (vgl. z. B. [84]). Wenngleich gewisse Derivate der Zucker und Zuckeralkohole, wie z. B. ihre mit Phosphorsäure-(di-β-chloräthyl)-amid gebildeten cyclischen Ester [86], oder Diepoxyde [87], weiterhin Diepithio-Derivate [88, 89] als Therapeutica überhaupt nicht in Frage kommen konnten, hat ihre Synthese und ihr Konstitutionsbeweis die Kohlenhydratchemie doch mit wichtigen Kenntnissen bereichert.

Von den weit ausgedehnten Untersuchungen, die das Ziel hatten, geeignete, in der Therapie verwertbare Cytostatica zu synthetisieren, seien noch einige positive Resultate herausgegriffen. So wurde z. B. aus D- und L-Mannit 2,3-4,5-Dianhydro-1,6-di-O-mesyl-L- bzw. -D-Idit [94], 1,6-Didesoxy-1,6-dibrom-2,3-4,5-dianhydro-L-idit [95], das 1,6-Dibrom-, 1-Brom-6-chlor- und 1-Brom-6-jod-Derivat des 1,6-Didesoxy-D-mannits und 1-Desoxy-1-brom-6-O-mesyl-D-mannit [96] aufgebaut. (Von diesen findet 1,6-Didesoxy-1,6-dibrom-D-mannit unter dem Namen »Myelobromol« klinische Anwendung.) Die Synthese all dieser Verbindungen hatte viel Interessantes an sich und die Strukturermittlung so mancher intermediärer Verbindungen bezeugt eine gute Invention. Dabei konnten aus den Unterschieden, die zwischen den biologischen Wirkungen all dieser Verbindungen zu beobachten waren, gut brauchbare Einzelheiten über den Zusammenhang der cytostatischen Wirkung und des Molekülbaus festgestellt werden.

Nun sind auch Untersuchungen nennenswert, die VARGHA auf dem Gebiet der Furanverbindungen durchgeführt hat [33—38, 52—54, 58, 79, 80, 97, 98]. Diese wurden noch in Kolozsvár begonnen und hatten ursprünglich das Ziel, das noch unbekannte 2-Amino-furan herzustellen um seine biologische Wirkung studieren zu können. Es wurde also versucht, durch Umsetzen des 2-Aceto-furanoxim-tosylats **(XLV)** im Sinne der Neberschen Reaktion **(XLV → → XLVI → XLVII)** das toluolsulfonsaure Salz des 2-Amino-furans herzustellen:

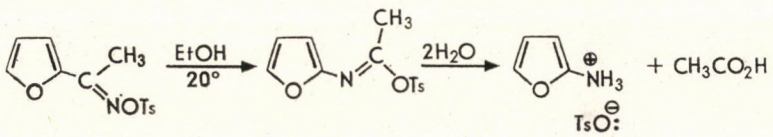

XLV **XLVI** **XLVII**

Die Reaktion verlief jedoch in einer ganz anderen Richtung, da anstatt des erwarteten Produktes **(XLVII)** Ammonium-toluolsulfonat und ein stickstofffreies, luftempfindliches, i. V. ohne Zersetzung destillierbares Öl entstand, das laut seiner Elementaranalyse, seinem Molekulargewicht und mehreren seiner chemischen Reaktionen das Diäthylacetal eines Hexen-dion-als **(XLVIIIa)** zu sein schien; wurde beim Umsatz Methanol anstatt Äthanol angewandt, so schien das entsprechende Dimethylacetal **(XLVIIIb)** gebildet worden zu sein. Die Bruttoreaktion hatte man folgend formuliert:

$$\textbf{XLV} + 2\,ROH + H_2O \longrightarrow TsONH_4 + CH_3COCOCH{=}CH - CH(OR)_2$$

XLVIII; a: R = Et; **b:** R = Me

Da in saurem Medium beide Produkte **(XLVIIIa, XLVIIIb)** mit Wasserstoffhyperoxyd oxydiert u. a. Maleinsäure lieferten, fiel die Wahl von den möglichen Äthylenisomeren auf die *cis*-Verbindung. Die Säurehydrolyse des ungesättigten

Acetals konnte nicht ohne tiefgehende Zersetzung bewirkt werden, deshalb wurde das gesättigte Derivat **XLIX** diesem Eingriff unterworfen, wobei jedoch anstatt des Diketo-hexanals **L** infolge einer gleich einsetzenden intramolekularen Kondensation Brenzcatechin **(LI)** entstand und dies schien wiederum für die Richtigkeit der Formel **XLVIII** zu sprechen:

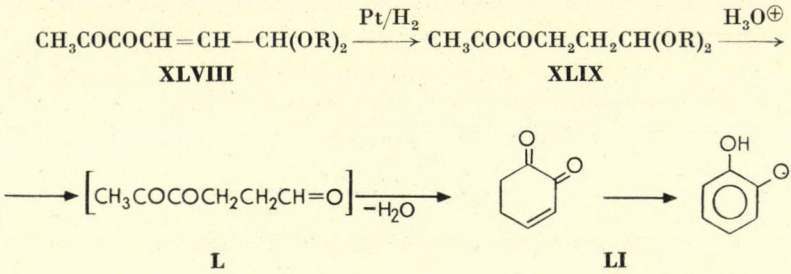

XLVIII **XLIX** **L** **LI**

Da hier ein genetischer Zusammenhang des Acetofurans mit Brenzcatechin *in vitro* demonstriert ist, ist man geneigt, auch auf einen biogenetischen Zusammenhang natürlicher Aromaten und Furanderivate (z. B. Furanosen) zu denken.

Obzwar die Herstellung des 2-Amino-furans aus dem Oxim-tosylat **XLV** mißlang, schien die beobachtete andersartige Umsetzung so interessant zu sein, daß die Untersuchungen auch auf Oxim-tosylate anderer Furylketone erstreckt wurden. Dies waren die Tosylate des 2-Aceto-cumaron-oxims, des 2-Propio-furan-oxims und des 2-Benzoyl-furan-oxims. Diese Verbindungen zeigten schon in mehrere Richtungen verlaufende Reaktionen. So bildeten sich z. B. aus dem 2-Aceto-cumaron-oxim-tosylat **(LII)** auf Einwirkung von Methanol oder Äthanol außer Ammonium-*p*-toluolsulfonat ein öliges, i. V. destillierbares und zwei kristalline Produkte. Das eine Kristallprodukt erwies sich als (das damals noch unbekannt gewesene) 2-Methyl-3-hydroxy-chromon **(LIII)**, dem anderen wurde mit Vorbehalt die Struktur eines 3-Keto-chromanon-acetols **(LIV)** zugeschrieben.

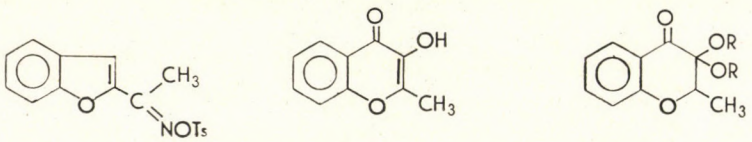

LII **LIII** **LIV**

Die Bildung mehrerer Umsetzungsprodukte hat die Aufmerksamkeit auf die Raumstruktur dieser Oxim-tosylate gerichtet, da es ja naheliegend war, daß die Alkoholyse geometrischer Isomere in zwei verschiedenen Richtungen verlaufen könnte. Deshalb wurden sehr gründliche Untersuchungen in Gang gesetzt, die vor allem das Ziel hatten, *syn*- und *anti*-Isomere dieser Oxim-

tosylate herzustellen und genau zu identifizieren. Diesem Bestreben entsprechend gelang es *syn-* und *anti*-Isomere sechs verschiedener, eine 2-Furyl- bzw. 2-Benzofuryl-Gruppe enthaltender Ketoxime herzustellen und zu identifizieren [52]. Zugleich wurde manch irrtümliche Angabe der Fachliteratur korrigiert und bewiesen, daß einige bereits beschriebene Ketoxime Gemische der *syn-* und *anti*-Isomeren darstellen. Der Umsatz der sterisch einheitlichen Oxim-tosylate hat nun ergeben, daß die Richtung der Reaktion — wie vermutet wurde — tatsächlich von der Raumstruktur abhängt: *syn*-Furyl-2-alkyl-ketoxim-tosylate **(LV)** werden von kaltem Äthanol oder Methanol nicht verändert, während *syn*-Furyl-2-aryl-ketoxim-tosylate **(LVI)** unter diesen Bedingungen eine BECKMANNsche Umlagerung erleiden, hingegen werden die bereits erwähnten ungesättigten Acetale nur aus *anti*-Furyl-ketoxim-tosylaten **(LVII)** gebildet; eine Ausnahme bildet nur das *anti*-5-Methyl-furyl-2-methyl-ketoxim-tosylat **(LVIII)**, das infolge einer BECKMANNschen Umlagerung eine zur Lävulinsäure führende Reaktion erleidet.

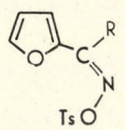

LV R=Alkyl
LVI R=Aryl

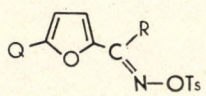

LVII Q=H
LVIII Q=CH_3

VARGHA und Mitarbeiter diskutierten keinen Mechanismus dieser Reaktionen, umsomehr nicht, da die vermutete Struktur **XLVIII** des ungesättigten Acetals bloß durch einige Reaktionen und das Ergebnis seines oxydativen Abbaus unterstützt werden konnte, einen synthetischen Strukturbeweis zu liefern gelang jedoch nicht. Doch später (1957) wurde von DUNLOP und PETERS, und kurz darauf (1958) von MEINLAND ein Mechanismus dieser merkwürdigen Reaktion erwogen. Beide, von einander nicht sehr wesentlich unterschiedlichen Mechanismen schienen plausibel zu sein und es ließ sich mit ihnen auch die unterschiedliche Reaktionsart der *syn-* und *anti*-Verbindungen annehmbar deuten. Vor kurzem (1967) haben jedoch GREEN und LEWIS die Umsetzung der *anti*-Oxim-tosylate **(LVII)** mit Alkohol reproduziert und die gewonnenen ungesättigten Acetale IR-, UV- und NMR-spektroskopischen Untersuchungen unterworfen. Aus den Ergebnissen ließ sich der Schluß ziehen, daß die ungesättigten Acetale nicht offenkettig, sondern Derivate des 2,5-Dihydro-furans sind. So stellt z. B. das aus dem Tosylat des *anti*-2-Aceto-furan-oxims **(LVII;** $R=CH_3$) auf Einwirkung von Methanol entstandene Produkt ein Gemisch der stereoisomeren Acetale **LIXa** und **LIXb** dar, die sich chromatographisch auch trennen lassen.



LIXa



LIX

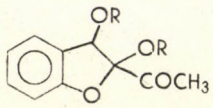

LX

Übrigens ist die Struktur in vollem Einklang mit den chemischen Reaktionen, die auch die Struktur **XLVIII** zu unterstützen schienen.

Fraglich blieb die Struktur des einen, aus dem Oxim-tosylat des 2-Aceto-cumarons gewonnenen Umsetzungsproduktes, dem mit Vorbehalt die Formel **LIV** zugeschrieben wurde. In der letzten Mitteilung von VARGHA und Mitarbeitern [98] wurde nun auch dieses Problem gelöst, und zwar mit Hilfe von IR-, NMR- und Massen-spektroskopischen Untersuchungen konnte das fragliche Produkt als das Cumaran-derivat **LX** erkannt werden. Auf Grund der bewiesenen Strukturen wurde zugleich der Mechanismus der Alkoholyse von den *anti*-Oxim-tosylaten **LII** und **LVII** erörtert, womit es sich erklären ließ, daß das *anti*-Oxim-tosylat **LII** mit wenig Wasser enthaltendem Alkohol einerseits zum 2-Methyl-3-hydroxy-chromon **(LIII)**, andererseits zum Cumaran-Derivat **LX** umgesetzt wird. Aus letzterem Produkt konnte übrigens chromatographisch eine *cis*- und eine *trans*-Komponente abgetrennt werden. Es ließ sich zugleich die zu den stereoisomeren 2,5-Dihydro-furan-Derivaten **LIX** führende Methanolyse des *anti*-2-Aceto-furan-oxim-tosylats **(LVII**; R=CH_3) gut deuten. All diese Reaktionen werden durch eine nucleophile Addition des Alkohols eingeleitet, die — gleichzeitig mit der Ablösung des Toluolsulfonat-anions — am Kohlenstoffatom 5 (bzw. im Falle des 2-Aceto-cumaron-oxim-tosylats am Kohlenstoffatom 3) erfolgt. Der nucleophile Angriff des Alkohols ist nur dann erfolgreich, wenn die Tosyloxy-Gruppe zum Furanring in *anti*-Position ist, denn nur in diesem Fall ist eine Koplanarität sterisch möglich und somit eine mit der Ablösung des Tosyloxy-anions parallel verlaufende Verschiebung der positiven Ladung in Position 5 bzw. 3. Im letzteren Falle verhindert das stabile π-Sextett eine Ladungsverschiebung bis zum Kohlenstoffatom 5 des Furangerüstes.

Die Umsetzungsreaktion der Furyl-ketoxim-tosylate kam schließlich doch in gewisse Beziehung mit pharmazeutisch-chemischen Untersuchungen. In Kenntnis der coronardilatatorischen Wirkung, die dem Khellin, einem pflanzlichen Naturstoff mit einem Furano-chromonring, eigen ist, haben 1951 SCHMUTZ und Mitarbeiter zahlreiche einfachere Chromonderivate, darunter auch das von VARGHA und Mitarbeitern erstmals aus dem Tosylat **LII** gewonnene 2-Methyl-3-hydroxy-chromon **(LIII)**, synthetisiert und auf ihre biologische Wirkung geprüft, wobei gefunden wurde, daß manche dieser einfacheren Verbindungen die Wirkung des Khellins nicht nur erreichen, sondern sogar übertreffen. Da das Khellin selbst zwei Methoxyl-Gruppen enthält, wurden am

Institut für Arzneimittelforschung mehrere Dimethoxy-2-methyl-chromone und Dimethoxy-chromon-2-carbonsäureester aufgebaut und auf ihre Wirkung geprüft [40]. Dabei wurde gefunden, daß diese Verbindungen 5—6mal aktiver sind als das nur umständlich isolierbare bzw. synthetisierbare Khellin.

Interessant wurden schließlich die am Ring mit Methoxyl-, Methylendioxy- und Hydroxyl-Gruppen substituierten Derivate von Benzoylamiden, deren Synthese und pharmakologische Testung deshalb vorgenommen wurde, weil in Alkaloiden starker physiologischer Wirkung derartige Gruppen oft vorkommen. Nun wurden rund 50, größtenteils neue Verbindungen diesen Typs aufgebaut und auf ihre Wirkung geprüft [69, 70]. Von derartigen Verbindungen zeigte 2,3,4-Trimethoxy-benzoyl-morpholin **(LXI)** nebst sehr geringer Toxizität eine gute tranquillierende Wirkung [69, 70] und wurde unter den Namen »Trioxazin« in die ärztliche Praxis eingeführt. Dieser Befund gab Anlaß zur Synthese weiterer Verbindungen ähnlichen Typs [91], besonders um ihre Wirkung auf das zentrale Nervensystem untersuchen zu können [92]. Von diesen zeigten einige Dibromderivate eine signifikante Antinicotinwirkung und ermöglichten es, die Abhängigkeit dieser Wirkung von der Molekülstruktur zu studieren. Dieser Verbindungsreihe gehört u. a. auch das krampfstillende 3,5-Dimethoxy-4-decylocy-benzoesäureamid (»Denegit«; **LXII**), das starke Schlafmittel 3,5-Dichlor-4-methoxy-benzoesäure-cyclopropylamid **(LXIII)** und das Hydrochlorid des 3,5-Dimethoxy-4-butyloxy-benzoesäure-β-pyrrolidinyl-äthylesters (»Vasopenton«; **LXIV**) an.

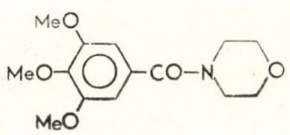

LXI

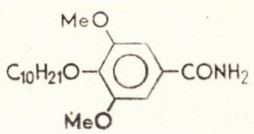

LXII

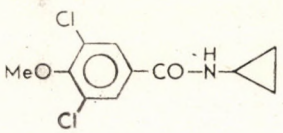

LXIII

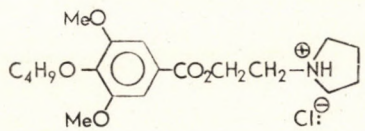

LXIV

Neben den Synthesen, die das Ziel hatten, neue Antituberculotica zu finden [42—44], ist auch die Modifizierung der Wibautschen Herstellung des 4-Äthyl-pyridins, das bekanntlich die Ausgangssubstanz bei der technischen Synthese des wichtigen Isonicotinsäure-hydrazids bildet, zu erwähnen. Die Modifizierung bestand einfach darin, daß der reduktive Umsatz des Pyridins mit Essigsäureanhydrid in Anwesenheit von Eisen anstatt Zink durchgeführt wurde, wodurch die Ausbeute auf das Doppelte gesteigert werden konnte.

Als Beispiel der Vielseitigkeit der organisch-chemischen Arbeiten von VARGHA dürfte die vereinfachte und verbesserte Isolierung der Hyodesoxycholsäure aus Schweinegalle und ihre Umwandlung zu 3β-Acetoxy-chol-5-ensäuremethylester hervorgehoben werden. Obzwar wegen der schwachen Ausbeute der Einsatz der letzteren Verbindung zur Herstellung von Steroidhormonen nicht lohnend wäre, ist diese Arbeit wegen ihrer interessanten stereochemischen Beziehungen doch erwähnenswert [46]. — Schließlich sei noch erwähnt, daß durch Acylierung von 6-Amino-penicillansäure eine Reihe von halbsynthetischen Penicillinen hergestellt worden sind, deren einige in die Therapie eingeführt wurden (z. B. »Pirazocillin«).

Als Vorstand des Instituts für Arzneimittelforschung hat VARGHA seiner festen Überzeugung in Wort und Tat des öfteren Ausdruck gegeben, daß nämlich die Arzneimittelforschung von der organisch-chemischen Grundforschung kräftig unterstützt werden muß, denn nur auf diese Weise ließe sich die Lebensfähigkeit und eine gesunde Entwicklung der ungarischen pharmazeutisch-chemischen Industrie sichern. Diese Überzeugung bewog ihn zur vielseitigen wissenschaftlichen Zusammenarbeit mit mehreren Universitätsinstituten. Es ist auch dieser Ansicht zu verdanken, daß sich im Institut für Arzneimittelforschung eine vielseitige und erfolgreiche Forschungstätigkeit auf organisch-chemischem Gebiet offenbart hat und mehrere junge Chemiker, die dort ihre Tätigkeit begonnen haben, zu anerkannten Forschern herangewachsen sind. Dies bezeugt auch der Umstand, daß einige von ihnen durch ihre am Institut geleistete Forschungsarbeit wissenschaftliche Grade erworben haben und sogar sechs von ihnen mit dem Kossuth- bzw. Staatspreis ausgezeichnet worden sind. Gebührend wurde dieses Institut 1967 als erstes von den unter der Obhut des Ungarischen Ministeriums für Schwerindustrie stehenden Forschungsinstituten mit dem Ehrentitel »Vorzügliches Forschungsinstitut« ausgezeichnet. — Den Erfolg, den VARGHAS Lehrtätigkeit während seiner zehnjährigen Professur in Kolozsvár erreicht hat, bezeugen seine gewesenen Schüler, die als Chemielehrer oder Chemiker in führende Posten erhoben worden sind.

Trotz der großen Inanspruchnahme, die die verantwortungsvolle Leitung des Instituts für Arzneimittelforschung mit sich brachte, hat VARGHA nicht nur an diesem Institut, sondern ganz allgemein für den Aufschwung der organisch-chemischen Forschung in unserem Lande sein Bestes getan. Als Mitglied der Ungarischen Akademie der Wissenschaften hatte er gelegentlich der Sitzungen der Chemischen Klasse, weiterhin des Komitees für Organische Chemie dieser Klasse, des Komitees für Arzneimittelforschung und schließlich als Präsident des Komitees für Kohlenhydratchemie des öfteren seine — manchmal auch scharf kritische aber immer von gutem Willen durchdrungene — Meinung geäußert. Als Präsident der Sektion für Organische Chemie des Vereins Ungarischer Chemiker war er als Vorstand des Organisationskomitees von

inländischen Kongressen immer bereitwilligst tätig. Er hat auf die Pflege internationaler Verbindungen stets großes Gewicht gelegt, wozu als solide Grundlage seine persönliche Bekanntschaft und manch freundschaftliches Verhältnis zu hervorragenden Forschern des Auslandes gedient haben.

In seinen letzten Lebensjahren hat sich sein Gesundheitszustand Jahr für Jahr verschlechtert. Doch sein zäher Schaffungsdrang, die Leidenschaft der wissenschaftlichen Forschung haben ihm die Fähigkeit gegeben, bis zum letzten Atemzuge weiter zu arbeiten und standzuhalten an seinem verantwortungsvollen Posten. Durch seinen Tod hat die organisch-chemische und pharmazeutisch-chemische Forschung in Ungarn eine der führenden Persönlichkeiten verloren. Nicht nur alle, die ihn persönlich kannten, sondern auf viel weitere Sicht die Ergebnisse seiner ideenreichen Forschungsarbeit werden sein Andenken treu bewahren.

V. BRUCKNER

PUBLIKATIONEN

1. E. PACSU, L. VARGHA: Über eine Acyl-Wanderung bei der teilweisen Verseifung acylierter Polyphenol-aldehyde. Ber. **59,** 2814—2824 (1926)
2. H. OHLE, L. VARGHA: Über die Aceton-Verbindungen der Zucker und ihre Umwandlungsprodukte (9. Mitteil.): Umwandlung der Monoaceton-glucose in 6-Aminoglucose. Ber. **61,** 1203—1208 (1928)
3. H. OHLE, L. VARGHA, H. ERLBACH: Über die Aceton-Verbindungen der Zucker und ihre Umwandlungsprodukte (11. Mitteil.): Umwandlung der Monoaceton-D-glucose in 3.6-Anhydro-D-glucose. Ber. **61,** 1211—1216 (1928)
4. H. OHLE, L. VARGHA: Über die Aceton-Verbindungen der Zucker und ihre Umwandlungsprodukte (10. Mitteil.): Eine neue *p*-Toluolsulfon-diaceton-glucose. Ber. **61,** 1208—1210 (1928)
5. H. OHLE, L. VARGHA: Über die Aceton-Verbindungen der Zucker und ihre Derivate, XIV. Mitteil.: Isodiaceton-glucose. Ber. **62,** 2425—2434 (1929)
6. H. OHLE, L. VARGHA: Über die Aceton-Verbindungen der Zucker und ihre Abkömmlinge, XV. Mitteil.: 5,6-Anhydromonoaceton-glucose und der 5-Methyläther der Gluco-furanose (Glucose-(1,4)-5-methyläther). Ber. **62,** 2435—2444 (1929)
7. A. SCHÖNBERG, L. VARGHA: Über die (thermische) Umlagerung von Thionkohlensäureestern in Thiol-kohlensäureester (16. Mitteil. über organische Schwefelverbindungen). Ber. **63,** 178—180 (1930)
8. A. SCHÖNBERG, L. VARGHA, W. PAUL: Über die thermische Umlagerung von Thion-kohlensäureestern in Thiol-kohlensäureester. II. Über die Bildung von Disulfiden aus Phenolen. Ann. Chem. **483,** 107—114 (1930)
9. A. SCHÖNBERG, L. VARGHA: Über die Einwirkung von Verbindungen der Diazomethan-Reihe auf Thionester. Über eine Synthese von Keten-mercaptolen, -acetalchloriden und -thioacetalchloriden. Diphenyl-diazomethan als »freies Radikal«. Ann. Chem. **483,** 176—189 (1930)
10. A. SCHÖNBERG, L. VARGHA: Über eine neuartige intramolekulare Atomverschiebung (Wanderung eines Cl-Atoms vom Kohlenstoff zum Schwefel). Tautomerie- und Desmotropie-Studien an Thion-carbonsäure-estern (19. Mitteil. über organische Schwefelverbindungen). Ber. **64,** 1390—1399 (1931)
11. A. SCHÖNBERG, L. VARGHA, H. KALTSCHMITT: Über die Ester-Ester-enol-Umlagerung und das dimere Diphenyl-thioketen. Ber. **64,** 2582—2584 (1931)
12. L. VARGHA: Über die »Antiglyoxalase« des Pankreasgewebes. Biochem. Z. **246,** 215—216 (1932)
13. I. BANGA, A. SZENT-GYÖRGYI, L. VARGHA: Über das Co-Ferment der Milchsäureoxydation. H. S. Z. Physiol. Chem. **240,** 228—235 (1932)
14. L. VARGHA: Monoacetone Hexuronic Acid. Nature **130,** 847 (1932)
15. L. VARGHA: Triphenylmethyl derivative of vitamin C. Nature **131,** 363 (1933)

16. L. VARGHA: Partielle Acetonierung der Zucker und Zuckeralkohole. I. Mitteil.: 1,2-Aceton-D-glucose-3,5-monoborsäureester (1,4). Ber. **66**, 704—707 (1933)
17. L. VARGHA: Partielle Acetonierung der Zucker und Zuckeralkohole. II. Mitteil.: 1.2-Monoaceton-D-mannit und neue partiell acylierte Derivate des D-Mannits. Ber. **66**, 1394—1399 (1933)
18. A. MÜLLER, L. VARGHA: Untersuchungen an partiell acylierten Zucker-Alkoholen. III. Mitteil.: Über die Toluol-sulfonierungs-Produkte des 1,6-Dibenzoyl-mannits. Ber. **66**, 1165—1168 (1933)
19. VARGHA L.: A Balaton és a Tihanyi Belső-tó vizének phosphor-tartalma. Magyar Biol. Kutatóint. Munkái **7**, 209—210 (1934)
20. L. VARGHA: Zur Kenntnis der Acylwanderung in der Zuckergruppe. Ber. **67**, 1223—1229 (1934)
21. L. VARGHA: Über die Konstitution des Monobenzal-D-sorbits. Eine Synthese der D-Xylose. Ber. **68**, 18—24 (1935)
22. L. VARGHA: Über die Konstitution des Monobenzal-D-sorbits. II. Mitteil.: *p*-Toluolsulfonyl- und Anhydro-Derivate des D-Sorbits. Ber. **68**, 1377—1384 (1935)
23. VARGHA L.: Vizsgálatok a cukoralkoholok köréből. Magy. Kém. Foly. **40**, 151—162 (1934)
24. L. VARGHA: Über den 5-Methyl-äther der Glucose. Ber. **69**, 2098—2102 (1936)
25. GEIGER E., VARGHA L.: Egy új higanydiuretikummal (dilurgen) végzett vizsgálatok. M. Orvosi Arch. **39**, Heft 5
26. VARGHA L.: A *p*-amino-benzol-sulfonamid dicarbonsavakkal alkotott fél-amidjairól. M. Biol. Kutatóint. Munkái **11**, 372—374 (1939)
27. VARGHA L.: A phenylhydrazin néhány új származékáról. M. Biol. Kutatóint. Munkái **14**, 441—444 (1942)
28. L. VARGHA, E. KOVÁCS: Untersuchungen über künstliche Wirkstoffe. I. Mitteil.: Eine neue Synthese von symmetrischen Dialkyl-diaryl-äthylen-Verbindungen. Ber. **75**, 794—802 (1942)
29. L. VARGHA, T. PUSKÁS: Untersuchungen über Zuckeralkohole. III. Mitteil.: Über 2,5-Anhydro-L-idit-Derivate. Ber. **76**, 859—863 (1943)
30. VARGHA L., GYŐRFFY ZS.: Új alkamin-származékok szintézise. Magy. Kém. Foly. **50**, 5—12 (1944)
31. G. IVÁNOVICS, L. VARGHA: Über die biologische Bedeutung und Synthese von Sulfosäure-Analoga der Pimelinsäure. Acta Bólyaiana, Fac. Sci. Nat. **1**, 123—131 (1947)
32. L. VARGHA, T. PUSKÁS, E. NAGY: Alcohols of the Sugar Group. IV. 2,5-Anhydro-L-iditol. J. Am. Chem. Soc. **70**, 261 (1948)
33. L. VARGHA, J. RAMONCZAI, P. BITE: Studies on Furan Compounds. I. Conversion of 2-Acetofuran to Hexen-2-dion-4,5-acetal-1 and Pyrocatechol. J. Am. Chem. Soc. **70**, 371 (1948)
34. L. VARGHA, J. RAMONCZAI, J. BÁTHORY: Studies on Furan Compounds. II. Conversion of 2-Aceto-benzofuran to 2-Methyl-3-hydroxychromone. J. Am. Chem. Soc. **71**, 2652—2655 (1949)
35. J. RAMONCZAI, L. VARGHA: Studies on Furan Compounds. III. A New Synthesis of Furyl Ketones. J. Am. Chem. Soc. **72**, 2737 (1950)
36. L. VARGHA, F. GÖNCZY: Studies on Furan Compounds. IV. Reactions of the *p*-Toluenesulfonyl Derivatives of Several Furylketoximes with Alcohols. J. Am. Chem. Soc. **72**, 2738—2740 (1950)
37. L. VARGHA, M. REMÉNYI: Selective Oxidations with Red Lead. J. Chem. Soc. **235**, 1068—1069 (1951)
38. VARGHA L.: Furil-ketonok átalakulásai. MTA Kém. Tud. Oszt. Közl. **1**, 63—71 (1952)
39. VARGHA L.: Polihidroxi-vegyületek epimerizációja. MTA Kém. Tud. Oszt. Közl. **3**, 95—104 (1953)
40. L. VARGHA, M. RADOS: Über die Synthese von neuen biologisch wirksamen Chromonderivaten. Acta Chim. Acad. Sci. Hung. **3**, 223—229 (1953)
41. L. VARGHA: Über die Substitution von Tosyloxy-Gruppen durch Acetoxy-Gruppen in Polyoxy-Verbindungen. Eine neue Darstellungsweise von l-Idose-Derivaten aus D-Glucose. Ber. **87**, 1351—1356 (1954)
42. L. TOLDY, T. NÓGRÁDI, L. VARGHA, G. IVÁNOVICS, I. KOCZKA: Untersuchungen über Antituberkulotika, I. Thiosemicarbazone, Hydrazide. Acta Chim. Acad. Sci. Hung. **4**, 303—313 (1954)
43. L. VARGHA, L. TOLDY, S. LENDVAY, I. KOCZKA, G. IVÁNOVICS: Untersuchungen über Antituberkulotika, II. *p*-Amino-salicylsäure-Derivate und Analoge. Acta Chim. Acad. Sci. Hung. **4**, 345—354 (1954)

44. T. NÓGRÁDY, L. VARGHA, G. IVÁNOVICS, I. KOCZKA: Untersuchungen über Antituberkulotika, III. 8-Oxychinolin-Derivate und Analoga. Acta Chim. Acad. Sci. Hung. **6**, 287—293 (1955)
45. L. VARGHA, T. HORVÁTH, T. NÓGRÁDI, L. GYERMEK: Über die Synthese und biologische Aktivität von einigen Diphenyl- und Indanderivaten. Acta Chim. Acad. Sci. Hung. **5**, 111—119 (1954)
46. L. VARGHA, M. RADOS, M. KRAUT: 3β-Oxy-Δ5-cholensäure und Δ5-Pregnen-3β-ol-20-on aus Hyodesoxycholsäure. Acta Chim. Acad. Sci. Hung. **8**, 303—308 (1955)
47. L. VARGHA: Über neue Zuckerderivate mit zytostatischer Wirksamkeit. Naturwiss. **42**, 582 (1955)
48. L. VARGHA, L. TOLDY, Ö. FEHÉR, S. LENDVAI: Synthesis of New Sugar Derivatives of Potential Antitumour Activity. Part I. Ethyleneimino- and 2-Chloroethylamino Derivatives. J. Chem. Soc. **151**, 805—809 (1957)
49. L. VARGHA, Ö. FEHÉR, S. LENDVAI: Synthesis of New Sugar Derivatives of Potential Antitumour Activity. Part II. Di-2-(chloroethyl)-D-glucosamine Hydrochloride. J. Chem. Soc. **152**, 810—812 (1957)
50. VARGHA L.: Citosztatikus hatású, új cukorszármazékok szintézise. Kém. Közl. **9**, 93—101 (1957)
51. T. HORVÁTH, L. TOLDY, L. VARGHA: Synthese des Isonicotinsäurehydrazids. Acta Chim. Acad. Sci. Hung. **14**, 197—201 (1958)
52. L. VARGHA, G. OCSKAY: Untersuchungen über Furan-Verbindungen, V. Tetrahedron **2**, 140—150 (1958)
53. L. VARGHA, G. OCSKAY: Untersuchungen über Furan-Verbindungen, VI. Stereospezifische Ringöffnungsreaktionen in der Furan-Reihe. Tetrahedron **2**, 151—158 (1958)
54. L. VARGHA, G. OCSKAY: Untersuchungen über Furan-Verbindungen, VII. Umwandlung von 2-Acyl-Benzofuran-Derivaten in Chromonol-Derivate. Tetrahedron **2**, 159—163 (1958)
55. M. KRAUT, L. TOLDY, E. KASZTREINER, O. FUCHS, L. VARGHA: Investigations in the Field of Antihistamines, I. Preparation of Substituted Acid Amides and their Reduction by Lithium Aluminium Hydride. Acta Chim. Acad. Sci. Hung. **15**, 19—25 (1958)
56. L. VARGHA, T. HORVÁTH: 1,6-Di-(2-Bromoethylamino)-1,6-Dideoxy-D-Mannitol Dihydrobromide: a New Cytostatic Agent. Nature **183**, 394—395 (1958)
57. L. VARGHA, J. KUSZMANN: 1,6-Dimethansulfonyl-D-mannit, eine neue tumoraffine Substanz. Naturwiss. **46**, 84 (1959)
58. L. VARGHA, GY. OCSKAY: Stereospecific Conversions in the Furyl-2-ketoxime Series. Acta Chim. Acad. Sci. Hung. **19**, 143—163 (1959)
59. L. TOLDY, L. VARGHA, I. TÓTH, J. BORSY: Über Untersuchungen von Promethazin, I. Acta Chim. Acad. Sci. Hung. **19**, 273—275 (1959)
60. L. VARGHA, L. TOLDY, E. KASZTREINER: Über die Synthese neuer Zuckerderivate mit potentieller cytostatischer Wirksamkeit, III. Über 2-Halogenäthylamino- und Äthyleniminoderivate von Zuckeralkoholen. Acta Chim. Acad. Sci. Hung. **19**, 295—306 (1959)
61. L. VARGHA, Ö. FEHÉR, S. LENDVAI: Über die Synthese neuer Zuckerderivate mit potentieller cytostatischer Wirksamkeit, IV. Über 2-Dichlordiäthylaminoderivate einiger Monosaccharide. Acta Chim. Acad. Sci. Hung. **19**, 307—314 (1959)
62. L. VARGHA, E. KASZTREINER: 1,2 : 5,6-Dianhydro-3.4-isopropyliden-D-sorbit und -L-idit. Neue Stickstoff-Derivate des D-Sorbits, D-Mannits und L-Idits. Ber. **92**, 2506—2515 (1959)
63. L. TOLDY, L. VARGHA: Über Benzal-Derivate des L-Idits. Ber. **92**, 2694—2700 (1959)
64. L. VARGHA, E. KASZTREINER: Untersuchungen über Diepoxyhexite. Bildung von 1,6-Anhydro-hexiten. Ber. **93**, 1608—1616 (1960)
65. L. VARGHA, Ö. FEHÉR, T. HORVÁTH, L. TOLDY, J. KUSZMANN: Über die Synthese neuer Zuckerderivate mit potentieller cytostatischer Wirksamkeit, V. ω,ω'-Dimethansulphonylderivate von Zuckeralkoholen und Ketosen. Acta Chim. Acad. Sci. Hung. **25**, 361—368 (1960)
66. VARGHA L., TOLDY L., FEHÉR Ö., HORVÁTH T., KASZTREINER E., KUSZMANN J., LENDVAI J.: Citosztatikus hatású cukorszármazékok. A Magyar Gyógyszerkutató Intézet tíz éves működése, S. 19—44. Műszaki Könyvkiadó, Budapest, 1961
67. E. KASZTREINER, L. VARGHA: Methadone Analogues Containing the Xanthene Skeleton, I. Preparation of the Starting Materials and 9-(β-dimethylaminoethyl)-9-propionylxanthene. Acta Chim. Acad. Sci. Hung. **32**, 473—477 (1962)
68. E. KASZTREINER, L. VARGHA: Methadone Analogues Containing the Xanthene Skeleton, II. Preparation of Isomeric 9-(N-morpholino)-propyl-9-propionylxanthenes. Acta Chim. Acad. Sci. Hung. **38**, 137—144 (1963)

69. L. VARGHA, E. KASZTREINER, J. BORSY, L. FARKAS, J. KUSZMANN, B. DUMBOVICH: Synthesis and Pharmacological Investigation of New Alkoxybenzamides, I. 3:4:5-Trimethoxy Benzamides. Biochem. Pharmacology **11,** 639—649 (1962)
70. E. KASZTREINER, J. BORSY, L. VARGHA: Synthesis and Pharmacological Investigation of New Alkoxybenzamides, II. Biochem. Pharmacology **11,** 651—667 (1962)
71. J. KUSZMANN, L. VARGHA: Über die Acetylierung der Arabinose. Rev. Chim. Acad. Roum. **7,** 1025—1031 (1962)
72. Ö. FEHÉR, L. VARGHA: Synthesis of New Sugar Derivatives of Potential Antitumour Activity, VI. 1,6-Di-(2-chloroethylamino)-1,6-dideoxy-L-sorbose Dimethanesulphonate. Acta Chim. Acad. Sci. Hung. **37,** 443—452 (1963)
73. L. VARGHA, J. KUSZMANN: Über die Synthese neuer Zuckerderivate mit potentieller cytostatischer Wirksamkeit, VII. 2-Chlor-2-desoxy-D-arabinose und -D-ribose. Eine neue Darstellungsweise der 2-Desoxy-D-ribose. Ber. **96,** 411—419 (1963)
74. L. VARGHA, J. KUSZMANN: Notiz über eine praktische Synthese der 2-Desoxy-D-ribose. Ber. **96,** 2016 (1963)
75. J. KUSZMANN, L. VARGHA: Über die Synthese neuer Zuckerderivate mit potentieller cytostatischer Wirksamkeit, VIII. Eine neue Synthese des 2-Desoxy-α- und 2-Desoxy-β-D-ribofuranosido-adenins. Ber. **96,** 2327—2333 (1963)
76. P. SOHÁR, L. VARGHA, E. KASZTREINER: Determination of Association Features, Configuration and Number of Ring Members in Anhydro Sugar Alcohols and their Partially Deuterated Derivatives by Means of the Infrared Spectra. Tetrahedron **20,** 647—653 (1964)
77. L. VARGHA, T. HORVÁTH: New Methanesulphonyl Sugar Alcohols and their Cytostatic Activity. Acta Union Internat. Contre le Cancer **20,** 76—81 (1964)
78. T. HORVÁTH, L. VARGHA: New Alkylsulfonic Acid Esters with Cytostatic Activity. Acta Union Internat. Contre le Cancer **20,** 71—75 (1964)
79. P. SOHÁR, GY. VARSÁNYI, L. VARGHA, GY. OCSKAY: Infrared Spectra of Furyl Methyl Ketoxime Isomers and of their Acyl Derivatives. Acta Chim. Acad. Sci. Hung. **40,** 431—443 (1964)
80. L. LÁNG, G. HORVÁTH, L. VARGHA, G. OCSKAY: Études spectroscopiques sur les dérives acylés des cétoximes isomères de la série furannique. Bull. Soc. Chim. France **1965,** 2724—2730
81. L. VARGHA, J. KUSZMANN: Über die Synthese neuer Zuckerderivative mit potentieller cytostatischer Wirksamkeit, IX. 9-(2'-Chlor-2'-desoxy-α-D-arabofuranosido)-adenin und sein β-anomeres. Ann. Chem. **684,** 231—235 (1965)
82. VARGHA L.: 2'-Halogén-2'-dezoxi-nukleozidok szintézise és átalakulásai. Kém. Közl. **24,** 173—179 (1965)
83. L. VARGHA: Alexander (Sándor) Müller (1903—1966). Acta Chim. Acad. Sci. Hung. **49,** 319—328 (1966)
84. Ö. FEHÉR, L. VARGHA: Synthesis of New Sorbose Derivatives. Acta Chim. Acad. Sci. Hung. **50,** 371—379 (1966)
85. E. KASZTREINER, L. VARGHA, J. BORSY: Derivatives of Alkoxybenzoic Acids, III. Basic Esters of 4-Alkoxy-3,5-dimethoxy- and 2-Alkoxy-3,4-dimethoxy-benzoic acids with Papaverine-like Spasmolytic Action. Acta Chim. Acad. Sci. Hung. **51,** 327—338 (1967)
86. J. KUSZMANN, L. VARGHA: Synthesis of New Sugar Derivatives having Potential Antitumour Activity. Part IX. Cyclic Phosphoric Acid Derivatives. Carbohydrate Research **3,** 38—46 (1966)
87. L. VARGHA, J. KUSZMANN: Synthesis of New Sugar Derivatives having Potential Antitumour Activity. Part XI. 2,5 : 3,6-Dianhydro-D-glucitol. Carbohydrate Research **8,** 157—163 (1968)
88. J. KUSZMANN, L. VARGHA: Synthesis of New Sugar Derivatives having Potential Antitumour Activity. Part XII. 1,2 : 5,6-Diepithio-L-iditol and Some Derivatives Thereof. Carbohydrate Research **11,** 165—171 (1969).
89. VARGHA L.: A Gyógyszerkutató Intézet működéséről. Magy. Kém. Lap. **1968,** 54—59
90. SZILÁGYI G., KASZTREINER E., MÉSZÁROS L., VARGHA L.: Az ánizssav észtereinek klórozása. Magy. Kém. Foly. **75,** 186—188 (1969)
91. SZILÁGYI G., KASZTREINER E., VARGHA L., BORSY J.: Központi idegrendszerre ható fenilecetsav- és fahéjsav-származékok. Acta Pharmaceutica Hung. **39,** 63—73 (1969)
92. G. SZILÁGYI, E. KASZTREINER, L. VARGHA, J. BORSY: Substituted Benzamidines Acting on the Central Nervous System. Acta Chim. Acad. Sci. Hung. **65,** 325—332 (1970)
93. J. KUSZMANN, L. VARGHA: Synthesis of New Sugar Derivatives Having Potential Antitumour Activity, XIII. Synthesis of 1,2 : 5,6-Diepithio-D-mannitol, -D-glucitol and Some of Their Derivatives. Acta Chim. Acad. Sci. Hung. **66,** 307—314 (1970)

94. T. HORVÁTH, L. VARGHA: Über die Synthese neuer Zuckerderivate mit potentieller cytostatischer Wirksamkeit. Teil XIV. 2,3:4,5-Dianhydro-1,6-di-O-(Methylsulfonyl)-D- und -L-iditol aus 1,2,5,6-Tetra-O-(Methylsulfonyl)-mannitol. Carbohydrate Research **16,** 253-259 (1971)
95. J. KUSZMANN, L. VARGHA: Synthesis of New Sugar Derivatives Having Potential Antitumour Activity. Part XV. 2,3:4,5-Dianhydro-1,6-dibromo-1,6-dideoxy-D-iditol and -galactitol. Carbohydrate Research **16,** 261—271 (1971)
96. J. KUSZMANN, L. VARGHA: Synthesis of New Sugar Derivatives Having Potential Antitumour Activity. Part XVI. Derivatives of D-mannitol which are Differently Substituted at C—1 and C—6. Carbohydrate Research **17,** 309—318 (1971)
97. P. SOHÁR, L. VARGHA, J. KUSZMANN: Association Structure of 3-Hydroxy-chromones. Acta Chim. Acad. Sci. Hung. **70,** 79—82 (1971)
98. L. VARGHA, J. KUSZMANN, P. SOHÁR, GY. HORVÁTH: Reinvestigation of the Rearrangement of 2-Acetylbenzofuran oxime *p*-Toluenesulfonate. J. Heterocyclic Chemistry **9,** 341—346 (1972)
99. G. SZILÁGYI, E. KASZTREINER, L. VARGHA, J. BORSY: Substituted Benzylamines Acting on the Central Nervous System. Acta Chim. Acad. Sci. Hung. **73,** 29—32 (1972)

Acta Chimica Academiae Scientiarum Hungaricae, Tomus 74 (1), pp. 27—34 (1972)

STUDY OF THE CATALYTIC HYDROGENATION (DEUTERATION) OF CYCLOHEXENE ON A PLATINUM CATALYST

AGING OF THE CATALYST DURING THE REACTION

D. MÓGER, GY. MINK and F. NAGY

(Central Research Institute for Chemistry of the Hungarian Academy of Sciences, Budapest)

Received July 20, 1970

The heterogeneous catalytic hydrogenation of cyclohexene was studied in a reactor in which fresh platinum catalyst was prepared during the reaction by means of continuous abrasion.

It was found that the cracking of the cyclohexene occurs simultaneously with its hydrogenation. As a result of the decomposition carbon deposits and CH (methyne) radicals, chemisorbed on the catalyst surface, are formed. It is assumed that the aging of the catalyst is caused primarily by the enrichment of these decomposition products, that is, by the decrease of the number of free active sites. The rate of cracking decreases more strongly with the decrease of the activity of the catalyst than does the rate of hydrogenation, and only in the case of fresh catalyst therefore do the two processes take place with commensurable rates.

Introduction

The decrease of the activity of metal hydrogenation catalysts during reaction has long been known, and is a much studied problem. Despite the numerous observations to be found in the literature with regard to the causes of the aging, this question, which is equally important both theoretically and practically, can still be considered as unsolved.

It was earlier shown [1] that if hydrogenation reaction cycles are carried out on a given catalyst at room temperature with initial pressure of 20 torr cyclohexene and 40 torr hydrogen, the activity of a fresh platinum catalyst decreases at first rapidly, and then the aging becomes more moderate.

Under the experimental conditions of [1] it seems probable that the decrease of the number of active sites is brought about by the strong chemisorption of the products of the side reactions. In the case of the cyclohexene–hydrogen system the possible side reactions are the dehydrogenation and cracking of the cyclohexene.

It is known that the cyclohexadiene and benzene formed by the dehydrogenation of cyclohexene are not catalyst poisons, for at room temperature in the presence of platinum catalyst each of them is readily hydrogenated. It appears more probable that the aging of the catalysts is caused by the chemisorption of the cracking products formed by the cleavage of the cyclohexene ring.

In the present paper we report some investigations connected with the above problem.

Experimental results

It is substantially easier to determine the cracking products of cyclohexene in the gas phase if the saturation is carried out with deuterium. The fate of the hydrogen released during the cracking reactions can easily be traced in this case with the use of a mass spectrometer.

Our first series of measurements was made with a mixture initially containing 20 torr cyclohexene and 40 torr deuterium at 30 °C in the presence of a platinum sponge catalyst obtained by reduction with formaldehyde. The already reported [2] closed-circulation reactor was selected for the study. The progress of the reaction was followed by means of the decrease of the pressure in the system. The samples taken from the gas space during the reactions were separeted by means of a gas chromatograph, and the distribution of the deuterium atoms in the cyclohexane ($C_6H_{12-v}D_v$) and cyclohexene ($C_6H_{10-x}D_x$) was determined on a mass spectrometer.

The sorption capacities of the catalysts used in the previous measurements [1] were 10^{-6}—10^{-7} mole, and the same time the amount of material used in each experiment was $1—5 \times 10^{-4}$ mole. In order for the cracking products to occur in measurable concentration in the gas space, the deuteration reactions were carried out in this series of measurements on catalysts consisting of much greater amounts of Pt sponge than previously.

The results of the measurements showed that the percentage ratio of the deuterated cyclohexane fractions formed in the reaction varies strongly during the conversion. This variation is particularly striking with regard to the $v = 0$ fraction.

Fig. 1 shows the variation of the percentage ratio of the $v = 0$ fraction of cyclohexane as a function of the conversion, in the cases of 0.7 g (curve 1) and 0.2 g (curve 2) catalyst. After this latter experiment the system was evacuated and a new measurement was carried out with a fresh reaction mixture; the result of this is shown in curve 3 of Fig. 1. It can be seen that in the case of curve 3 the percentage amount of the $v = 0$ cyclohexane is practically independent of the extent of the reaction, and with the progressing of the reaction curve 2 increasingly approaches curve 3.

In the case of the measurements relating to curves 1 and 2, water and carbon dioxide were found in the gas space, in amounts proportional to the quantity of catalyst. The given experimental results show that the surface of the Pt sponge catalyst is covered with oxygen.

In the experiments relating to curve 3, the analysis of the gas space showed that water and carbon dioxide did not form in this reaction.

The experimental results given in Fig. 1 can only be interpreted by accepting that the oxygen can be removed from the surface of the platinum catalyst not only by hydrogen but also by cyclohexene. The appearance of CO_2 in the

gas space, and the strong decrease of the percentage amount of the $v = 0$ cyclohexane with the progressing of the reaction confirm that a part of the cyclohexene adsorbed on the oxide surface is oxidized. The hydrogen atoms formed on the cleavage of the cyclohexene skeleton either react with the oxygen bound on the surface, or saturate the cyclohexene.

It is easy to see that, with the exception of film catalyst prepared in high vacuum, platinum catalysts applied come into contact with oxygen (air) in general before reaction. It may be presumed that their surface, or a part of it, is covered with oxide, and oxidation side reactions must therefore be reckoned with during the hydrogenation.

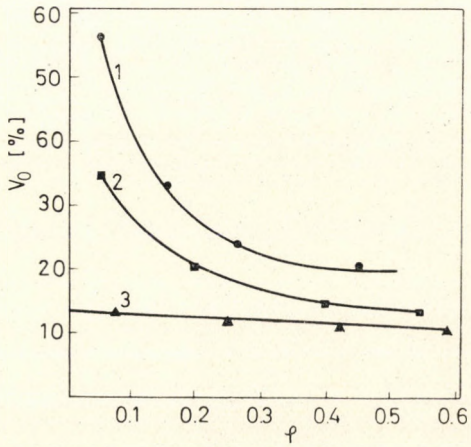

Fig. 1. Percentage change of the $v = 0$ fraction of cyclohexane as a function of the conversion

It follows from the above that the film catalysts prepared in high vacuum should primarily be considered for the study of the mechanism of aging of pure metallic platinum catalysts. It is known that the activity of the film catalysts depends strongly on their methods of preparation (temperature, the cleanness of the walls of the vessel, etc.). Even if the most careful preparative conditions are employed, the activities of the catalysts vary within an order of magnitude.

The disturbing factors in the solution of our original aim are not primarily those mentioned above, but the fact that the increase of the sorption capacity of the catalyst is practically unattainable.

Taking the above into account, on the principle of the dropping mercury electrode used in electrochemistry we constructed a closed reactor in which the surface of the platinum catalyst can be continuously renewed during the reaction.

The amount of the pure metallic catalyst in this reactor can be increased at will, and so a possibility is arisen for the study of the side reactions.

The operating principle of the reactor can be understood from Fig. 2.

The platinum band (1) stretched onto the disc (2) turns in a bed (4) filled with glass powder. An electric motor outside the reactor moves the drive rod (5) backwards and forwards across a rotary arm; the rod turns the ratchet wheel (3), together with the disc (2) fitted onto the same axle, one tooth at a time, and the catalyst surface is thus constantly abraded during the rotation. The packing (6) above the glass-filled bed prevents the entry of the abrading powder into the reactor space during the rotation of the disc. The tube membrane (7) soldered to the outside wall of the reactor and to the drive rod isolates the reactor from the surroundings.

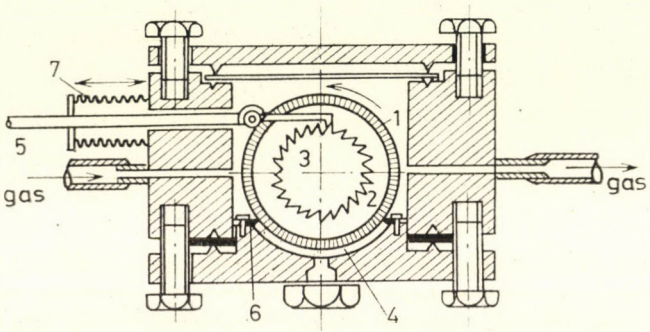

Fig. 2. Closed reactor suitable for the continuous abrasion of the Pt catalyst. 1 — Pt band, 2 — metal disc, 3 — ratchet wheel, 4 — abrading bed, 5 — drive rod, 6 — packing, 7 — elastic tube membrane

Experiments were carried out with this rotating catalyst at room temperature, using a mixture of 20 torr cyclohexene and 40 torr deuterium. In every measurement the initial rate of the reaction was nearly the same, and then began to increase gradually during the individual experiments. The reason for this is that the amount of platinum particles abraded off and left in the glass powder bed continually increases, and the imperfect seal permits these particles to take part in the hydrogenation reaction.

Since our aim was to study the side reactions occurring on the fresh catalysts, in Figs 3—5 we give the results of experiments in which (on the basis of the extrapolation of the reaction rate to the initial time) the estimated amount of cyclohexane formed on the rotating platinum disc was the same as or more than the amount of cyclohexane formed on the platinum particles in the abrading bed.

The hydrogen isotope composition in the gas space was studied, and it was found that an H—D exchange occurs: the originally 99.6% deuterium is diluted with HD and H_2 in the course of the reaction. This is shown in Fig. 3, where the light hydrogen content of the deuterium is plotted against the cyclohexane conversion.

In the same experiment the average deuterium content of the cyclohexane and cyclohexene during the conversion was also determined. This can be seen in Fig. 4.

($\Sigma\bar{D}$ in Fig. 4 is the number of deuterium atoms per mole of cyclohexane formed, which are incorporated into the cyclohexene or the cyclohexane. Accordingly, $\Sigma\bar{D}$ is defined by the equation:

$$\Sigma\bar{D} = \bar{v} + \frac{1-\varphi}{\varphi}\bar{x}$$

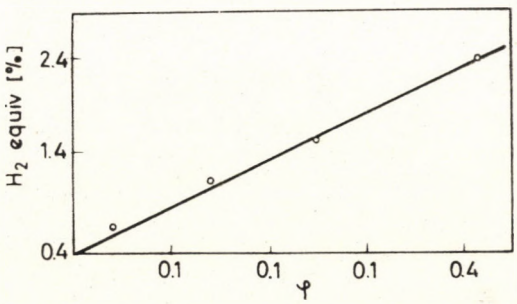

Fig. 3. Change of the hydrogen content of the deuterium with the conversion of the cyclo hexane in the case of the continuous abrading of the catalyst

where $\bar{x}$ is the average number of deuterium atoms in the cyclohexene, and $\bar{v}$ that in the cyclohexane, at a given conversion.) It is striking in the figure that in the examined conversion range $\Sigma\bar{D} < 2$. In accordance with the material balance, if only the hydrogenation reaction occurs, taking into account the fact that the pressure ratio in the cyclohexene–D_2 mixture is 1 : 2, then

$$\Sigma\bar{D} = \frac{2}{\varphi}\bar{a}_0 - \bar{a}\left(\frac{2}{\varphi} - 1\right)$$

where $\bar{a}_0$ and $\bar{a}$ are the average numbers of D atoms in the hydrogen–deuterium phase (average composition: $H_{2-\bar{a}}D_{\bar{a}}$; $0 \leq \bar{a} \leq 2$) at $\varphi = 0$ conversion and a given φ.

Since $\bar{a}_0 \approx 2$, it can be seen from such a relation that $\Sigma\bar{D} = 2$ if $\bar{a}_0 = \bar{a}$ (H—D exchange does not occur), or $\Sigma\bar{D} > 2$ if $\bar{a}_0 > \bar{a}$ (parallel with the deuteration H—D exchange also takes place). During reaction an H—D exchange takes place (Fig. 3), and accordingly it would be expected that $\Sigma\bar{D} > 2$. Hydrogen can be formed only via a reaction between the catalyst and the cyclohexene introduced into the system. In this case the other reaction product will be a hydrocarbon complex poor in hydrogen.

During a study of the self-hydrogenation of ethylene, SELWOOD [3] showed that the hydrogen-poor particles formed in the reaction, which are

chemisorbed on the metal catalyst, can be regenerated with hydrogen (deuterium) even if complete carbonization has previously occurred. For this reason, after 50% conversion the cyclohexane and cyclohexene in our system were

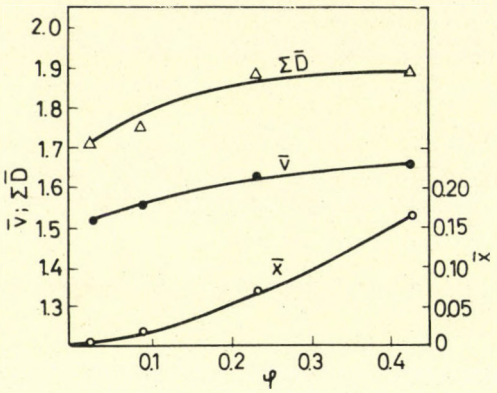

Fig. 4. Change of $\Sigma\bar{D}$ and of the average deuterium content ($\bar{v}$ and $\bar{x}$) of the cyclohexane and cyclohexene with the conversion in the case of the continuous abrading of the catalyst

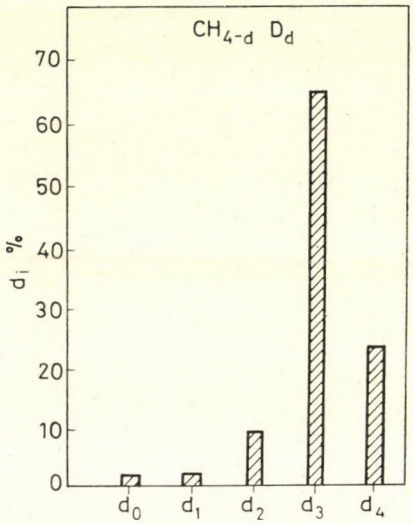

Fig. 5. Deuterium distribution in the methane formed on treating the spent catalyst with gaseous deuterium

frozen out with liquid air, and the deuterium was circulated in the reactor for several hours at an elevated reaction temperature (approx. 50 °C). Following this, samples were withdrawn from the gas space. Small amounts of methane were detected in these by gas chromatography. The isotope distribution in the methane was determined mass-spectrometrically, and is shown in Fig. 5.

The fact that the main fraction in the methane as a result of the action of the deuterium is CHD_3 indicates that CH radicals are formed in by far the greatest amount on the surface of the catalyst during the decomposition of the cyclohexene.

A deuteration experiment was next carried out in which, before the reaction, the catalyst was abraded for several minutes in the bed filled with

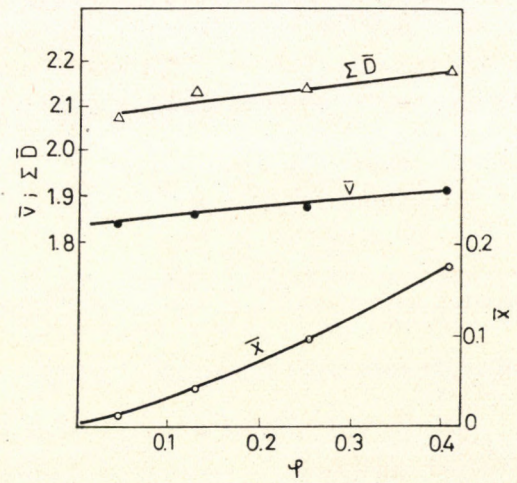

Fig. 6. Change of $\bar{v}$, $\bar{x}$ and $\Sigma\bar{D}$ with the conversion

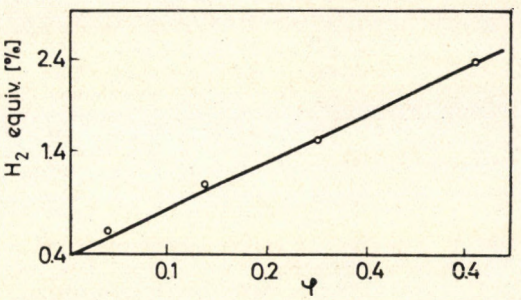

Fig. 7. Change of the hydrogen content of the deuterium with the cyclohexane conversion

fresh glass powder, but during the reaction the disc was not rotated. The changes of $\bar{v}'$, $\bar{x}$ and $\Sigma\bar{D}$ with the conversion were determined as before, and are shown in Fig. 6.

The hydrogen enrichment in the deuterium was also measured during the reaction, and this is given in Fig. 7 as a function of the conversion. The figures show that in the conversion range between 0 and 0.4, $\Sigma\bar{D} \sim$ ~ 2.1—2.2, and the hydrogen content of the deuterium, expressed in H_2 equivalents, increases to 2.3%.

The experimental results illustrated in Figs 2—7 can be summarized as follows.

Simultaneously with the hydrogenation (deuteration) of cyclohexene on a Pt sponge catalyst which has been in contact with the air, its oxidation also occurs. The water and carbon dioxide appearing in the gas phase indicate that the surface of the catalyst is covered with oxygen. Under such experimental conditions, therefore, an answer cannot be given to the question of whether the cleavage of the cyclohexene skeleton occurs on the pure metal too (after the removal of the oxygen). A clear positive answer to the question, however, is provided by the investigations carried out in the rotating disc reactor.

The experimental results to be seen in Figs 3—5 can only be interpreted if it is accepted that the cyclohexene skeleton is cloven on the catalyst surface. It was seen that an H–D exchange takes place in the direction of the gas phase (Fig. 3), and at the same time $\Sigma\bar{D} < 2$ (Fig. 4); this confirms that a light hydrogen 'source' operates in the system during reaction. This is possible only if the quotient H/C in the cracking products formed after the cleavage of the cyclohexene is <1.66.

It can be seen in Fig. 5 that methane primarily of isotopic composition CHD_3—CD_4 enters the gas phase from the catalyst treated with deuterium after the end of the deuteration reaction ($H/C < 1$). This finding confirms that CH radicals and C deposits are formed on the catalyst surface during the decomposition of cyclohexene.

It can be established from the experimental results given in Fig. 6 that during the period of the hydrogenation reaction hydrogen does not enter the system in the case of a reaction on an aged catalyst. This experiment supports the correctness of our earlier assumption that the cracking reactions must primarily be reckoned with in the case of fresh catalysts.

REFERENCES

1. MÓGER, D., MINK, GY., NAGY, F.: Magy. Kém. Foly. **74**, 318 (1968)
2. MÓGER, D., MINK, GY., NAGY, F.: Magy. Kém. Foly. **74**, 315 (1968)
3. SELWOOD, P. W.: J. Am. Chem. Soc. **83**, 2853 (1961)

Dezső MÓGER
György MINK
Ferenc NAGY
Budapest II., Pusztaszeri út 59—67.

Acta Chimica Academiae Scientiarum Hungaricae, Tomus 74 (1), pp. 35—49 (1972)

STABILITIES OF AMMONIUM HALATES IN THE SOLID PHASE

STUDY OF THE EFFECTS OF AGING AND VARIOUS ADDITIVES ON THE THERMAL DECOMPOSITION OF AMMONIUM CHLORATE

F. SOLYMOSI and T. BÁNSÁGI

(Gas Reaction Kinetics Research Group of the Hungarian Academy of Sciences, Szeged)

Received January 3, 1971

A study was made of the effects of aging, various gases and solid additives on the thermal stability of ammonium chlorate. The effects on the self-decomposition of the compound were also examined when it was stored under various conditions. Of the gases, the greatest effect was exhibited by ammonia; at low pressures it primarily changed the direction of the decomposition of the ammonium chlorate, while at higher concentrations it also decreased the extent of the decomposition. Of the different additives, the largest accelerating effects were exerted mainly by the acids.

The stability of the compound decreased on aging, and at the same time its tendency to explode increased. Detailed measurements were carried out on the solid residue, with special regard to the detection of the disproportionation of the chlorate.

In an earlier paper [1] we made a detailed study of the kinetics and mechanisms of the thermal decomposition and explosion of ammonium chlorate (AC). The slow decomposition of the AC began at 50 °C, and it exploded at 90 °C.

On the basis of the kinetic investigations and other observations too, we came to the conclusion that the decomposition of AC proceeds *via* a proton-transfer mechanism. This conclusion was supported by experiments carried out in a mass spectrograph, which indicated the formation of ammonia and chloric acid in the primary decomposition reaction [2]. The proton transfer mechanism has also been used by MACK *et al.* [3] to describe the decomposition of ammonium chlorate. During the kinetic investigations we also obtained much information with regard to the properties of the compound, and in particular its thermal behaviour, which was not reported in the paper dealing with the kinetics and mechanism of the decomposition. *These observations and experimental results, however, can be regarded as data useful in the recognition of the thermal stability of AC.* Accordingly, in the present paper we report and discuss the effects of various pretreatments and foreign additives on the stability of the compound and on the direction of its transformation.

Experimental

Materials

The AC was prepared in a similar way as previously [1], by the reaction

$$NH_4Cl + NaClO_3 = NH_4ClO_3 + NaCl$$

It was recrystallized from doubly distilled water, and kept in a refrigerator at —5 °C.

Method of measurement

The decomposition of AC was followed by the measurement of the decrease of weight of the sample, and the pressure of the gases formed. For this purpose a sensitive thermobalance was constructed, the details of which are reported here. The apparatus is in essence a development of the torsion balance described by SZABÓ and KIRÁLY [4]. Three changes were made:

(i) By the modification of the introduction of the reaction vessel and the sample the apparatus was suitable also for the study of the decomposition of solid materials.

(ii) The pressure of the gases formed could be measured simultaneously with the weight loss, with the aid of the cold-trap and the manometer system incorporated into the reaction vessel.

(iii) By the modification of the electrical part of the apparatus it was possible to increase the limits of the measurement (to 1—50 mg) and also the mA change corresponding to a weight loss of 1 mg.

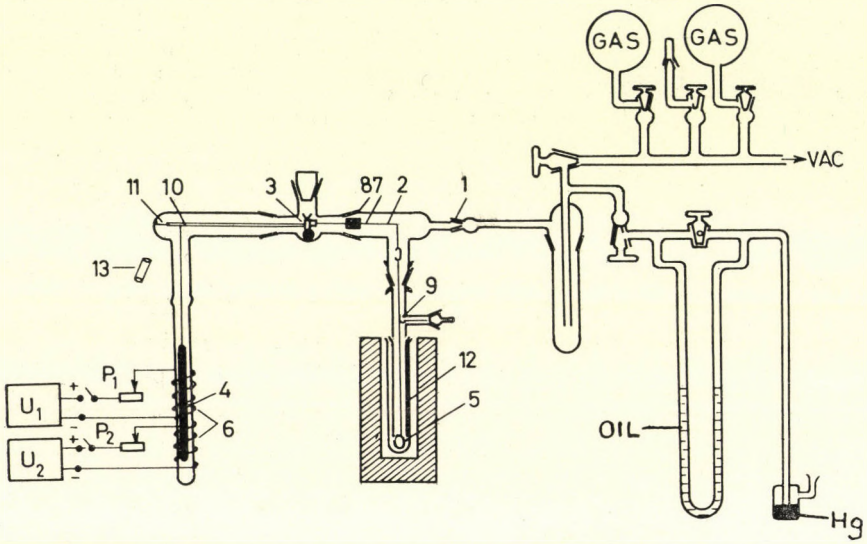

Fig. 1. Outline diagram of the thermobalance used in the studies

The apparatus is depicted in Figure 1.

The balance is connected to the evacuation apparatus and to the gas storage flasks *via* the ground-glass joint (1). The balance arms (2) are made of aluminium wire 20 cm long and 2 mm in diameter. The clamping screw (3) fixes the balance arms onto an 11 cm long "Melodia extra E" violin string situated perpendicularly to the plane of the drawing. A soft-iron rod (4) is suspended from one of the balance arms (10) and a small glass cup containing the sample (5) from the other. Two solenoids (6) are wound onto the glass tube enclosing the soft-iron rod. The role of these is to compensate for the torque created by the loss of weight of the decomposing material, and to re-establish the equilibrium state of the balance arm, referred to the hairline of the telescope, by the variation of the intensity of the current. U_1 and U_2 are stabilized D. C. sources, variable in the range 0—12 V, and P_1 and P_2 are multicoil potentiometers (with graduations from 0 to 999). If the solenoid is suitably dimensioned, the change of the current intensity is directly proportional to the weight change. The soft-iron rod (4) is counterbalanced by a small lead block (8) which can be moved along the screw thread (7). To assist in the accurate establishment of the equilibrium position, a very thin quartz needle is attached (11) to one side of the balance arm.

The substance to be examined is placed into a glass spoon (9) fitted with a joint, and after a vacuum of 10^{-4}—10^{-5} torr has been attained the spoon is turned so that the substance falls into the glass cup (5) in the reaction zone at the required temperature. A glass tube (12) ensures that the substance falls into the glass cup. By the adjustment of the currents of the solenoids, the quartz needle (11) on the balance arm is brought into coincidence with

the hairline of the telescope (13). In the case of the decomposition of a considerable proportion of the sample taken, that is if the percentage weight change is comparatively high, the source U_2 and the potentiometer P_2 are not used. When the substance falls into the cup the balance is equilibrated by the switching on of the source U_1 and with the aid of the potentiometer P_1. The weight loss arising during the decomposition is compensated for by the adjustment of P_1. If the percentage weight loss is small, both sources (U_1 and U_2) are switched on. The weight of the starting material is counterbalanced here too with the aid of the potentiometer P_1, whereas the weight change is followed only by the adjustment of P_2.

The balance was calibrated (mA-mg curve) also in vacuum with known weights in the glass cup. The current intensity was plotted as a function of the charge and a straight line was obtained. The correctness of the calibration was checked from time to time. The sensitivity the balance was ± 0.02 mg.

The explosion experiments were carried out in air at atmospheric pressure. The average particle-size of the AC was 80—100 μ. The tablets were prepared with a pressure of 2700 kg/cm^2. 50 mg material was generally used in each experiment.

The derivatographic studies were made in a Paulik—Paulik—Erdey derivatograph. The infrared spectra were recorded with a Unicam SP 200 instrument, using KBr pellets.

Results and discussion

1. *The effect of storage conditions on the stability of AC*

When the substance was stored at room temperature it had already suffered a weight loss of 1—2% on the second day. By the tenth day, already about 50% of the substance had been converted into gaseous products. When stored at —5 °C, only 5% of it had decomposed even on the tenth day. The composition of the substance changed in parallel with the decrease of weight. When 3 g of the doubly recrystallized, but not powdered substance was kept in an open vessel at room temperature, the chlorate content was practically unchanged for 4 days. After this, however, it gradually decreased, and after 21 days a chlorate content of only 60% was found. The ammonia content did not follow the change in the amount of chlorate, and always exceeded the amount equivalent to the chlorate. In agreement with the data of FAIRBROTHER [5], this is a result of the formation of ammonium nitrate. When the substance was stored in a similar way, but at —5 °C, the change of the composition was substantially less extensive. If the substance was powdered after its preparation, the rate of decomposition increased. A higher stability was found, on the other hand, if the ammonium chlorate was spread out in a thin layer in the vessel. Our experimental results are given in Table 1.

It was observed in our earlier experiments that the acidity of the substance changes with the progress of the decomposition: it first increases, and then decreases, but even after the reaction is completed it is considerably higher than that of the starting material. A similar change was also observed in the case of the substance stored at room temperature. The procedure during our measurements was to take 42 mg daily from the AC stored in a desiccator, to dissolve this in 15 ml distilled water, and to measure the pH of the solution

Table I

Self-decomposition of ammonium chlorate under various storage conditions

Number of days	Compound stored at room temp. in open vessel		Compound stored at room temp. in desiccator		Compound stored at −5 °C in open vessel		pH*
	Percentage decomposition	AC content in %	Percentage decomposition	AC content in %	Percentage decomposition	AC content in %	
1	0.00	99.53	0.00	99.47	0.00	99.55	6.65
2	0.13	99.42	0.22	99.23	0.00	99.49	6.6
3	1.88	99.28	1.91	99.01	0.13	99.38	6.5
4	4.64	99.27	4.47	98.00	0.43	99.33	6.13
5	6.85	99.1	5.92	97.9	1.30	99.32	4.93
6	9.76	98.81	7.42	97.50	3.05	99.31	4.23
7	18.39	98.45	12.15	96.3	3.57	99.30	3.87
8	26.89	98.06	17.75	95.00	3.79	99.17	3.61
9	34.77	96.9	22.89	93.6	4.36	98.95	3.44
10	43.7	95.62	29.00	92.51	5.15	98.14	3.33
11	53.88	93.00	35.61	88.78	5.62	98.10	3.26
12	61.38	91.5	38.92	87.0	6.32	—	3.14
13	72.28	91.18	42.12	84.32	7.06	97.08	3.07
14	72.82	86.3	44.44	81.4	7.93	94.51	3.00
15	74.73	83.0	47.19	77.6	8.32	92.94	2.95
16	75.60	78.97	49.86	74.36	8.72	90.12	2.92
18	77.0	69.98	53.70	61.69		87.48	2.86
19	77.50	67.0	54.16	59.0		85.2	2.86
21	78.6	59.61	58.50	50.13		80.73	2.84
22	79.19		59.14				2.83
24	79.5		62.5				2.93
26	79.96		64.96				2.95
27	80.2		65.05				3.00
31	81.3		67.5				3.34
33	81.88		68.16				

* The pH measurements were carried out on the material stored in the desiccator. About 40 mg was dissolved in doubly distilled water, and the pH of this solution was measured.

so obtained. In the initial section of the self-decomposition the pH of the solution scarcely altered, but a significant decrease occurred after the fourth day. On the twenty-second day a pH of 2.83 was measured, but from this time on the acidity of the material again decreased. The results of these experiments are also given in Table I.

2. *Effects of aging on the stability of AC and on the decomposition of the solid residue*

In the course of the study of the thermal decomposition of ammonium bromate it was observed that the decomposition of the substance which had been stored for 4 days differed fundamentally from that of the freshly prepared material [6]. The induction period for the decomposition of the older material was shorter, the reaction proceeded at a higher rate, and the autocatalytic reaction changed to one of a breakdown type.

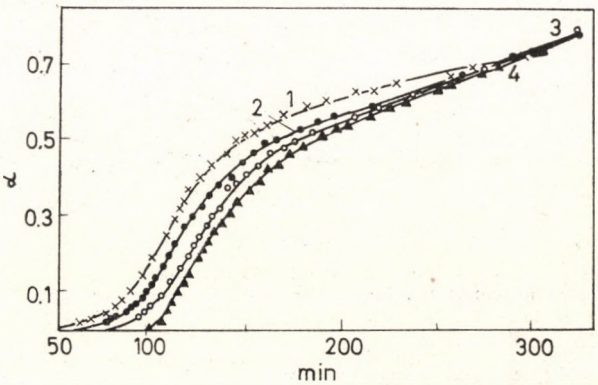

Fig. 2. Effect of aging on the decomposition of AC. Age of substance: (1) 26 days; (2) 9 days (3) 2 days; (4) fresh crystals. Temperature: 60 °C

In the case of AC, however, as can be seen from the curves in Fig. 2, with the increase of the age of the substance the induction period of the decomposition decreases, but the shapes of the decomposition curves and the rates of decomposition scarcely differ from each other.

A similar change was also observed in the course of the explosion of the substance. With the increase of its age, not only did the time preceding the explosion decrease, but so did also the lowest temperature of explosion of the AC. Whereas the fresh material and the few days old merely decomposed at 75 °C, the 30 and 44 day old materials exploded after 13 and 7 minutes, respectively (Fig. 3). The 24 day old material only decomposed at 70 °C, but the 34 day old material exploded after 17 minutes. The relevant data are given in Table II.

It was found in our earlier investigations that similarly to the decompositions of ammonium bromate and ammonium perchlorate the decomposition of the AC is not complete. About 10—15% of the original sample remained unchanged. The solid residue contained ammonium nitrate in addition to AC, with an average composition of 47.6% AC and 51.8% ammonium nitrate.

Larger amounts of the solid residue were collected together and its thermal stability was studied. It was observed that the substance obtained in

vacuum, after being stored in a desiccator for a few days, again decomposed at 65 °C. The decomposition was slower than that of the original substance, and was not complete in this case either. The decomposition began with maximum rate. (In a separate experiment it was shown that ammonium nitrate

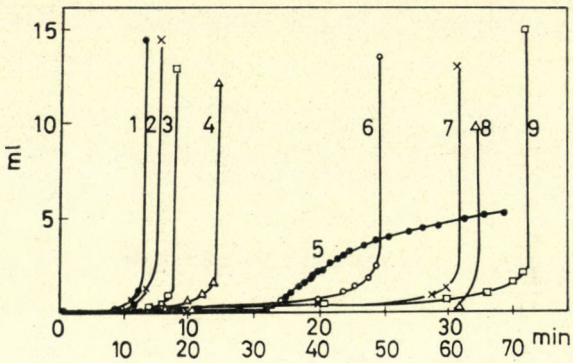

Fig. 3. Effect of aging on the explosion of AC. Age of substance: (1) 44 days; (2) 35 days (3) 33 days; (4) 30 days; (5) fresh crystals; (6) 24 days; (7) 10 days; (8) 8 days; (9) 5 days **Temperature:** 75 °C. The lower time scale refers to curve (5)

exerted practically no effect on the decomposition of AC.) The weight loss was 38.4%. The composition of the residue was 30.2% AC and 69.8% ammonium nitrate.

Table II

Effect of aging on the stability of ammonium chlorate

Temperature °C	Age of substance, days	Time elapsed until explosion, minutes
70	1	no explosion
70	5	no explosion
70	24	no explosion
70	34	17
70	37	15.3
70	44	15.1

3. *Effects of gases and foreign additives on the decomposition and explosion of AC*

It has already been mentioned in an earlier paper [1] that the prior addition of chloric acid to the AC accelerated its decomposition, whereas this was decelerated by the presence of ammonia. The effect of ammonia was investigated more thoroughly in the present work, and our experiments were also

extended to the study of the effects of the other gaseous products. Our results referring to the quantitative effects of ammonia are given in Fig. 4. The presence of even a small amount of ammonia (6.5 torr) increased the induction period of the decomposition and decreased its rate. A more significant inhibiting effect appeared at ammonia pressures above 100 torr. The percentage decomposition too decreased in the presence of ammonia. In the case of 648.2 torr ammonia the weight loss was only 29%. With regard to the fact that a solid product, ammonium nitrate, is also formed in the decomposition of AC, it appeared conceivable that the proportions of gaseous and solid prod-

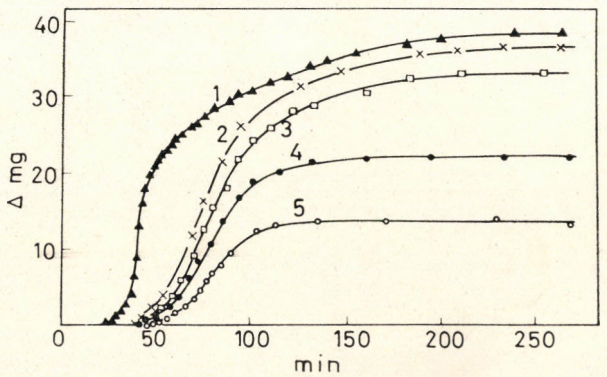

Fig. 4. Effect of ammonia on the decomposition of AC. Initial pressure of ammonia: (1) vacuum; (2) 6.5 torr; (3) 23.3 torr; (4) 101.8 torr; (5) 648.2 torr. Temperature: 70 °C. The ordinate shows the weight loss in mg

ucts would be modified in the presence of ammonia. As shown by the data of Table III, the analysis of the solid product confirmed this assumption.

In the presence of a small amount of ammonia the percentage transformation of the AC, in contrast with the weight loss, changed only to a slight extent, and the amount of ammonium nitrate increased. This latter continued to increase with the increase of the pressure of the ammonia, but at the same time the quantity of AC converted decreased considerably.

The other gaseous products, chlorine, nitrogen and dinitrogen oxide, exerted a substantially smaller effect on the decomposition of the AC (Fig. 5). Chlorine decreased the induction period of the decomposition, and increased its rate and extent to a small degree. The induction period also decreased on the action of nitrogen, and the shape of the curve was flatter than that of the curve measured in vacuum. A smaller inhibiting effect was exerted by the dinitrogen oxide, which also decreased the extent of the decomposition.

Chemical analysis of the solid residue showed that in the presence of gaseous dinitrogen oxide and nitrogen the amount of ammonium nitrate formed was a few % larger.

Table III

Decomposition of ammonium chlorate in the presence of various gases

Temperature °C	Gas atmos. torr	Sample mg	Residue mg	Weight loss %	AC found in residue mg	AN formed mg	AC transformed %	Percentage AC in residue %
65	vacuum	49.1	13.0	73.52	6.618	6.382	86.52	50.31
60	vacuum	49.8	12.5	74.89	6.8	5.7	86.34	54.4
70	vacuum	48.3	9.0	81.37	4.355	4.645	90.98	48.4
75	vacuum	100.7	17.6	82.52	8.64	8.96	91.42	49.1
80	vacuum	100.9	16.7	83.44	7.93	8.77	92.14	47.49
80	vacuum	100.8	17.7	82.44	8.81	8.89	91.25	49.8
70	6.5 NH_3	48.2	11.0	77.18	5.281	5.72	89.04	48.01
70	23.3 NH_3	48.5	14.5	70.11	7.003	7.5	85.56	48.3
70	101.8 NH_3	49.0	26.2	46.50	12.96	13.24	73.55	49.46
70	648.2 NH_3	48.3	34.1	29.4	17.02	17.08	64.76	49.91
65	100 N_2	49.4	14.7	70.24	6.8	7.9	86.23	46.3
70	20 N_2	47.8	8.1	83.05	3.53	4.57	92.61	43.61
70	100.2 N_2	49.1	8.7	82.28	3.65	5.05	92.56	41.91
60	400 N_2	47.55	13.1	72.45	6.039	7.061	87.29	46.1

AN = ammonium nitrate

Similarly to the effect of chloric acid, a significant accelerating action on the decomposition of AC was exhibited by perchloric acid, and even more so by nitric acid. Both acids also decreased the induction period of the explosion of the AC to a considerable extent. The results are given in Fig. 6.

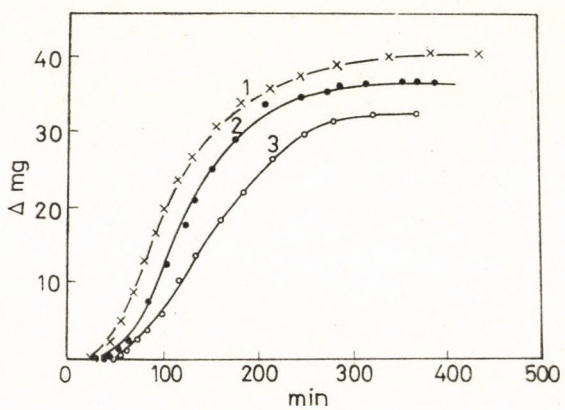

Fig. 5. Effects of various gases on the decomposition of AC. Initial pressure of gas: (1) 100 torr chlorine; (2) vacuum; (3) 100 torr dinitrogen oxide. Temperature: 65 °C. The ordinate shows the weight loss in mg

A detailed investigation was also made of the effects of various semiconductor oxides, copper(II) oxide, copper(I) oxide, chromium(III) oxide, nickel(II) oxide, cadmium oxide, titanium dioxide and zinc oxide on the stability of AC. It emerged from our earlier studies [7] that the metal oxides, particularly the p-conductors of an electron-acceptor type, are extremely effective catalysts of the decomposition and explosion of ammonium perchlorate.

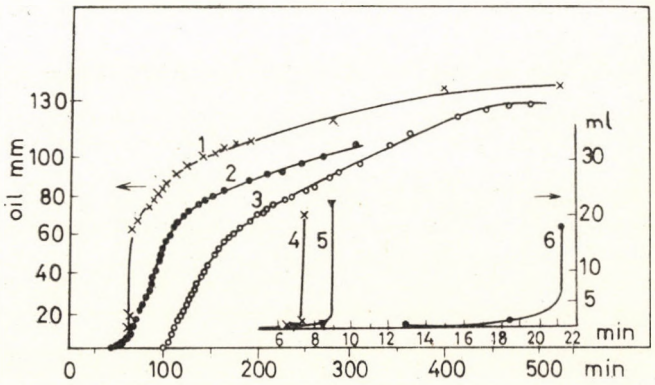

Fig. 6. Effects of acids on the stability of AC. (1) AC + 1 drop 0.65% HNO_3 solution; (2) AC + 1 drop 0.6% $HClO_4$ solution; (3) AC. Temperature: 60 °C. (4) AC + 1 drop 0.65% HNO_3 solution; (5) AC + 1 drop 0.6% $HClO_4$ solution. Temperature: 80.2 °C. The ordinate shows the volume of gases formed before and after the explosion, in ml

Table IV

Self-decomposition of ammonium chlorate in the presence of various oxides at 27 °C

Number of days	Pure substance		AC + CuO		AC + Fe_2O_3		AC + Cr_2O_3	
	weight loss %	AN content of AC %	weight loss %	AN content of AC %	weight loss %	AN content of AC %	weight loss %	AN content of AC %
1	0	0	0	0	0	0	0	0
2	7.7	5.3	10.3	6.2	10.3	5.9	9.9	6.7
3	20.4	12.2	26.3	20.8	25.9	16.7	25.5	16.7
6	38.6	27.1	45.2	39.4	44.0	32.3	41.3	33.0
7	44.1	30.7	47.5	46.1	46.6	34.2	43.4	33.4
9	47.2	38.3	51.8	50.8	52.3	43.7	48.5	40.7
10	48.6	41.0	53.3	57.2	54.2	48.8	50.4	40.9
13	53.0	48.2	57.0	57.0	59.7	48.5	55.0	49.1
17	54.8	53.5	59.1	67.6	63.0	51.8	57.0	55.3
20	56.3	55.3	60.7	66.8	65.0	53.8	58.3	55.9
34	60.1	76.7	68.5	80.1	70.8	63.0	65.3	74.8

AN = ammonium nitrate. The molar ratio AC : oxide = 10 : 1.

The effects of the oxides were also studied with regard to the self-decomposition of AC at 25 °C, and the rapid decomposition and explosion occurring at higher temperatures. A few of our results referring to the self-decomposition are reported in Table IV, where the changes in weight and composition of the AC in the presence of various oxides are given as a function of time. It may be stated that the self-decomposition of the AC is increased to only a slight extent by the oxides examined. A fairly slight catalytic effect was also observed at

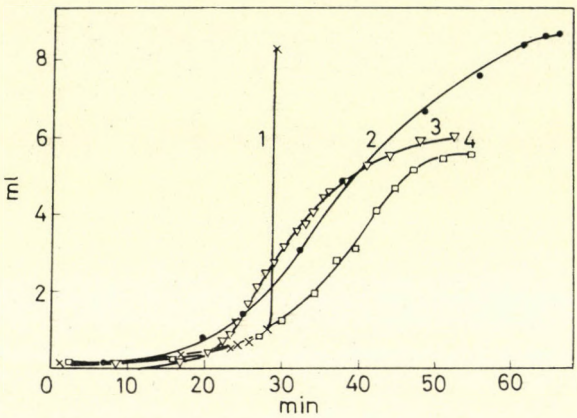

Fig. 7. Effects of oxides on the stability of AC. (1) AC + Cu_2O; (2) AC; (3) AC + TiO_2; (4) AC + ZnO. The molar ratio AC : oxide = 16 : 1. Temperature: 78 °C

higher temperatures. In the presence of copper(II) oxide the induction period preceding the explosion of AC at 90 °C decreased from 589 sec to 480 sec. The lowest temperature of explosion, on the other hand, remained unchanged. AC doped with chromium(III) oxide behaved similarly. In the presence of copper(I) oxide the induction period increased, but the lowest temperature of explosion decreased by about 14 °C. A light-green material readily soluble in water, remained after the explosion, and analysis proved this to be copper(II) chloride. On the effects of nickel(II) oxide and cadmium oxide the induction period preceding the explosion decreased. Doping with titanium dioxide and zinc oxide caused the temperature of explosion to increase. The effects of a few oxides are illustrated in Fig. 7.

4. *The effect of interruption on the decomposition of AC*

Following this, a study was made of how the course of the decomposition is affected by interruption for various times in the individual stages of the decomposition. The experiments were carried out in the following way. The progress of the reaction was followed by the measurement of the pressure of

the gases formed for various times, and the substance was then taken out of the hot zone and cooled to room temperature in vacuum. After standing for 15—20 minutes, the substance was again put into the hot zone, and the reaction was followed further. The results of the interruption measurements are shown in Fig. 8. The results indicate that the interruptions in the various stages of the decomposition influence the course of the decomposition of the AC either not at all, or to only a very small extent.

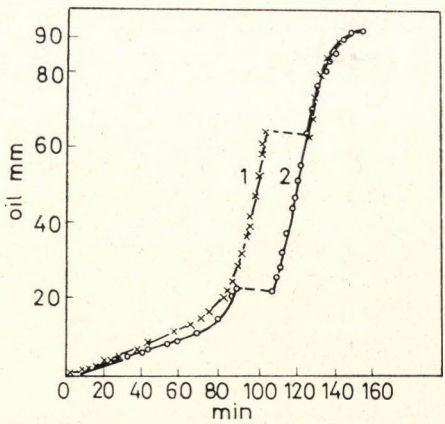

Fig. 8. Effect of interruptions on the course of the decomposition of AC. (1) Measurement interrupted in the 103rd minute; (2) Measurement interrupted in the 89th minute. Temperature: 65 °C

5. *The question of the disproportionation of AC*

It has long been known that besides decomposing, chlorates disproportionate with the formation of perchlorate and chloride. From the point of view of the chemistry of the chlorates, it appeared interesting to study whether in the case of AC the disproportionation reaction can in fact be completely excluded, or whether it proceeds to only an extremely small extent.

The infrared spectrum of the solid residue is reported in Fig. 9. For purposes of comparison, the spectra of pure AC, ammonium nitrate, ammonium perchlorate, and mixtures of these compounds are also given. It can be stated after comparison of these spectra that, in agreement with the chemical analysis, the residue from the decomposition of AC consisted of a mixture of ammonium nitrate and still undecomposed AC. The presence of the perchlorate ion could not be established. Our measurements indicated that the presence of about 5% ammonium perchlorate could be detected with the available apparatus, but the identification of 1% perchlorate was uncertain.

The detection of the perchlorate ion resulted in a similar negative result in the case of bipyridylcopper azide [8]. It should be noted that if 1% ammo-

nium perchlorate was added to the solid residue, the presence of the perchlorate ion was indicated by a characteristic yellowish colouration.

The residue was also thermally analyzed. The TG and DTA curves for the materials are shown in Fig. 10.

In order to reduce the violence of the explosion of the AC, it was mixed in a 1 : 1 weight ratio with aluminium oxide which had been ignited at 1100 °C. A weight decrease accompanied by an exothermal change appears at 105 °C

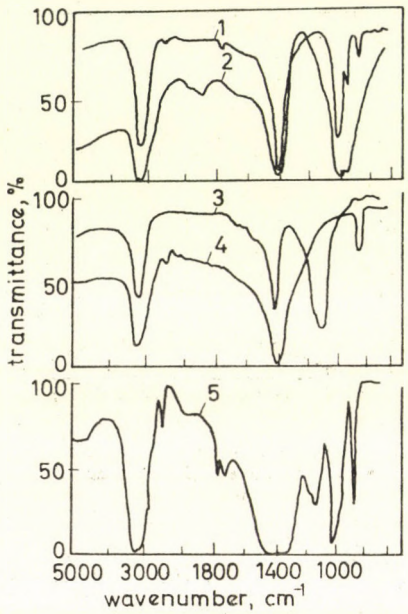

Fig. 9. Infrared spectra. (1) Solid residue of the decomposition; (2) AC; (3) NH_4ClO_4; (4) NH_4NO_3; (5) 50 weight % AC, 45 weight % NH_4NO_3; and 5 weight % NH_4ClO_4

on the TG curve for the pure substance; in this, 87% of the substance is converted to gaseous products. With the increase of the temperature a further small, slow change of weight occurs. Exothermal peaks are found on the DTA curve at 260 and 396 °C.

A derivatogram was also obtained, under similar conditions, for the solid residue of AC which had been decomposed at 75 °C in vacuum. The TG curve consists of two well-separated steps. The first begins at 135 °C, and the second at 276 °C. Both decomposition processes are accompanied by exothermal changes. An exothermal peak is also to be found on the DTA curve at 362 °C.

The weight change at 105 °C on the TG curve of the fresh substance, and the related exothermal peak, correspond to the decomposition of pure AC. The weight change at the higher temperature, however, is the decomposition of the material which does not decompose in the process at lower temperature.

This is also confirmed by experiments made with the residue of the decomposition of AC. The reaction beginning at 276 °C on the TG curve corresponds to the decomposition of the ammonium nitrate formed in the course of the transformation of the AC.

Although the infrared spectroscopic measurements and the chemical analyses did not support the presence of the perchlorate ion, the peak appearing above 360 °C on the DTA curves for AC and for its decomposition residue

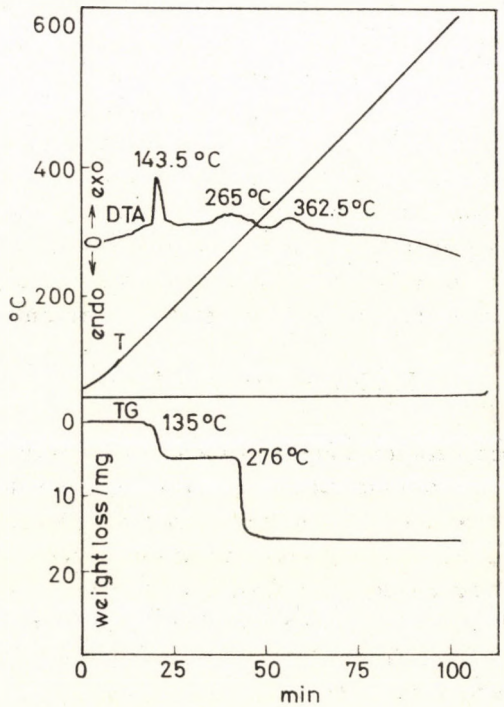

Fig. 10. Derivatogram of the solid residue of AC decomposed in vacuum at 75 °C. Sample: 16 mg; heating rate 6 °C/min

points to the presence of ammonium perchlorate. However, since the exothermic change is not accompanied by an observable weight change, it can be concluded that the perchlorate ion can only be present as an impurity in the material. In contrast with the alkali metal chlorates, therefore, AC disproportionates to only an extremely small extent, or not at all. In our view, the reasons for the different behaviour of the AC and for the non-occurrence of the disproportionation are the oxidizability of the cation and the different decomposition mechanism. The high instability of the substance is presumably connected with these factors. A result of the high instability, on the other hand, is the

fact that the tendency of the substance to decompose and to explode increases with the storage time and with its aging. When we reported on the kinetic characteristics of the decomposition we pointed out that the decomposition of AC is a process of an autocatalytic nature, and that the formation and growth of surface nuclei take place in the stages of latency and acceleration of the decomposition. Microscopic observations show that nucleus formation begins on the surface of the AC crystals 2—3 days after their preparation on standing at room temperature, and after 6—8 days at —5 °C. As a result of this, when the crystals are heated to a higher temperature the reaction accompanied by gas formation begins sooner and takes place more rapidly in the acceleration stage.

The behaviour of AC is surprising, in that its decomposition is affected by the various semiconductor oxides to only a small extent, or not at all. In contrast with this, the oxides studied exert large effects on the thermal stabilities of both ammonium perchlorate and the alkali metal chlorates. One reason for the non-appearance of the catalytic effect may be the low temperature of decomposition. In our view, however, a substantially more important role is played by the fact that the AC decomposes by a proton transfer reaction:

$$NH_4ClO_3 = NH_3 + HClO_3$$

and one of the decomposition products formed is also an unstable compound. The slowest step in the decomposition is the proton transfer reaction itself. The oxides are not capable of influencing the proton transfer process. On the other hand, they can accelerate the decomposition of chloric acid and the oxidation of ammonia. Nevertheless, the former of these reactions is so fast that it plays a very small part in the formation of the overall measured rate value. The oxides may exert a small effect on the oxidation of the ammonia, which according to the mechanism given is brought about by atomic oxygen and oxides of chlorine. In the case of ammonium perchlorate, in contrast, the oxide catalysts can take part in the low-temperature (200—240 °C) electron transfer reaction of the ammonium perchlorate by promoting the formation of the perchlorate radical, and can also exert a catalytic effect on the high-temperature decomposition of ammonium perchlorate by accelerating the decomposition of the perchloric acid formed in the dissociation process. At the temperature of the decomposition of ammonium perchlorate, perchloric acid is still a fairly stable compound.

It is a characteristic of the decompositions of ammonium halates that at low temperatures the decompositions are not complete. In all probability the phenomenon is related to the strong inhibiting effect of the ammonia. As a result of the rapid decomposition of the halic acid, the oxidation of ammonia is not complete and the ammonia adsorbed on the surface hinders the

dissociation of the AC. One of the interesting results of our experiments was the fact that in the presence of ammonia the amount of ammonium nitrate increases. It is highly probable that the accelerating effects of mineral acids previously mixed into the AC, or added to the substance in the course of the decomposition, result from the decrease of the inhibiting effect of the ammonia. The catalytic effect of gaseous chlorine too can be explained by its promotion of the oxidation of ammonia.

On the action of the other gases (nitrogen and dinitrogen oxide) the rate of evolution of gas decreased, whereas the amount of AC transformed increased. This behaviour can be explained in that the removal from the surface of the oxidizing products formed during the reaction is impeded in the presence of these gases, and hence the rate of oxidation of the ammonia increases and the formation of ammonium nitrate becomes more prominent.

REFERENCES

1. SOLYMOSI, F., BÁNSÁGI, T.: Combustion and Flame **13**, 262 (1969); Magy. Kém. Foly. **75**, 227 (1969)
2. SOLYMOSI, F., BÁNSÁGI, T., SAVINTSHEV, P., KARPENKO, A., BOLDYREV, V. V.: Kinetika i Kataliz., in press. Magy. Kém. Foly. **78**, 215 (1972)
3. GUILLORY, W. A., KING, M., MACK, J. L.: J. Phys. Chem. **73**, 4370 (1969)
4. SZABÓ, Z. G., KIRÁLY, D.: Acta Chim. Acad. Sci. Hung. **17**, 393 (1958)
5. FAIRBROTHER, F.: J. Am. Chem. Soc. **44**, 2419 (1922)
6. SOLYMOSI, F., BÁNSÁGI, T.: J. Phys. Chem. **74**, 15 (1970)
7. SOLYMOSI, F., RÉVÉSZ, L.: Z. anorg. allgem. Chem. **322**, 86 (1963); Kinetika i Kataliz. **488** (1963); SOLYMOSI, F., KRIX, E.: J. of Catalysis **1**, 468 (1962)
8. SENICE, P.: Anal. Chim. Acta **34**, 53 (1966)

Frigyes SOLYMOSI
Tamás BÁNSÁGI
Szeged, Rerrich tér, Hungary.

Acta Chimica Academiae Scientiarum Hungaricae, Tomus 74 (1), pp. 51–57 (1972)

THERMOELECTRIC MICRODETERMINATION OF MOLECULAR WEIGHTS OF ORGANIC COMPOUNDS IN HOMOGENEOUS BINARY SOLVENT SYSTEMS USING THERMISTORS

A. B. SAKLA, A. H. BADRAN and N. A. SAYED

(Microanalytical Unit, Department of Chemistry, Faculty of Science. Cairo University, Giza, Egypt)

Received May 3, 1971

Thermometric molecular weight determinations of organic compounds in homogeneous binary solvent systems using thermistors can be carried out with a relative error of less than 2%. The method can also be used as a simple and reliable procedure to determine the behaviour of a homogeneous binary mixture with respect to Raoult's law.

Introduction

Molecular weight determination provides a useful means of characterizing organic compounds. Many of the well known macro-procedures have been adapted to the micro scale.

The microscopic method of RAST [1] (depression of the freezing or melting point of the solvent) is adequate for general purposes but it has certain limitations. It cannot be used if the compound is coloured as the melting of the solvent cannot be observed, owing to the colour of the sample–solvent mixture. Also, the sample compound must have a sharp melting point and should not decompose near or at the melting point [2].

The ebullioscopic method (elevation of boiling point of the solvent) has also been proposed, but its disadvantage is concerned with measurement of the temperature change.

The main disadvantage of SIGNER's method [3] (isothermal distillation) is the time necessary for equilibrium to be established, which is a precondition of the calculations [4].

The thermoelectric method appears quite suitable from the viewpoint of both speed and accuracy. This method depends on the establishment and measurement of the steady state temperature difference between drops of the solvent and solution suspended in an atmosphere of the solvent at a fixed ambient temperature [5]. Thermistors are mainly used when only small temperature ranges are to be passed and a high resolution is required.

The aim of the present work is to apply the thermoelectric method to the determination of organic compounds with low molecular weights in homogeneous binary solvent systems, and to study the deviation of the binary systems from Raoult's low.

Experimental

Apparatus

The apparatus is similar to that developed by NEUMAYER [6]. The Knauer Universal Temperature Measuring Instrument [7] was used in this work. The instrument includes a Wheatstone bridge with a stabilized source for measuring the temperature difference. A fully transistorized chopper amplifier permits a significant increase in sensitivity.

Table I

	Molarity(1)	ΔR at 37 °C	Molarity(2)	ΔR at 37 °C	Molarity(3)	ΔR at 37 °C	Molarity(4)	ΔR at 37 °C
(a)	0.01066	31.5	0.00448	9.5	0.01081	16	0.01315	30
	0.01614	47.75	0.00898	21	0.01826	29.5	0.02052	42.5
	0.02389	70	0.01720	39	0.02750	44.25	0.03872	80
	0.02992	88	0.02550	53	0.03730	64.25	0.07432	152
	0.04394	128.5	0.04380	98	0.05229	84		
(b)	0.00947	14	0.00966	14.75	0.01423	78	0.00965	17
	0.02537	39.25	0.02400	36.5	0.02656	53.5	0.01489	28
	0.03067	47.5	0.03840	59	0.03494	69.5	0.0278	51
	0.04078	64.75	0.04830	74	0.04364	88	0.0494	91.5
	0.04436	69	0.06940	107	0.05870	113		
(c)	0.01069	18	0.00469	7	0.00691	13	0.00534	8.5
	0.01844	34	0.01110	21	0.01441	28.75	0.0143	28
	0.02139	38.25	0.01838	35.5	0.02444	48	0.0298	59
	0.03190	54.5	0.02349	44	0.03518	68.5	0.0510	101
	0.04012	72.25	0.03000	55	0.04023	78		
(d)	0.01649	26.75	0.00343	7	0.00656	11.75	0.0172	35
	0.01851	29.5	0.00865	16	0.01787	32.75	0.0275	56
	0.03411	55	0.01821	37.5	0.02430	45	0.0554	109
	0.03783	61.25	0.03461	60	0.03043	56.75	0.0772	152
	0.05147	82	0.02443	42	0.04290	81.5		
(e)	0.00969	13.75	0.00665	12				
	0.02352	36.25	0.01610	27				
	0.02653	41.25	0.01860	38				
	0.02906	45.5	0.03790	62				
	0.04337	70	0.05290	85				

Solvents

All solvents used were of M. A. R. quality. The homogeneous binary mixtures were:
(A) *n*-Hexane and *n*-heptane in the ratios of 1 : 1, 1 : 2 and 1 : 3; and chloroform and benzene in the ratios of 1 : 1; 1 : 2 and 1 : 3 (ideal system, [8]).
(B) Benzene and cyclohexane in the ratios of 1 : 1; 2 : 1 and 3 : 1 (positive deviation, [9]).
(C) Ethyl acetate and chloroform in the ratios of 1 : 1; 2 : 1 and 3 : 1 (negative deviation, [8b]).

Procedure

(i) Construction of the calibration curves of a reference substance.
Prepare accurately a series of solutions of a reference substance, *e.g.* *o*-nitrophenol, with different molarities ranging from 0.004 to 0.006 in the binary solvent system to be used with a given ratio. Pour the binary solvent into the chamber so that there is about 1 cm of excess solvent on the bottom of the chamber over that required to saturate the absorbent paper lining of the inside wall of the chamber. Rinse off both platinum wire coils covering the thermistors with the solvent (binary mixture) and adjust the resistance to zero reading. Rinse one of the coils with the solution and the other with the solvent and record the resistance difference (Δ, ohms) after a steady state has been reached (3—5 min). The procedure is repeated with the series of solutions of different compositions (Table I).
Plot the resistance difference (ΔR, ohms) against the molarity of solute at different temperatures, *e.g.* 25, 37 and 45 °C (Figs 1—4).
(ii) Dissolve an accurately weighed amount (5—20 mg) of the organic compound in 5 ml of the binary mixture with the same ratio as that used with the above calibration curve. Rinse one of the coils with the solvent and the other with the solution and record the resistance difference (ΔR, ohms) after a steady state has been reached. Using the calibration curves of the reference substance obtained in (i) above (Figs 1—4) determine the corresponding molarity of solute. Determine the molecular weight of the solute (M. W.) from the following equation:

$$\text{M. W. solute} = \frac{(\text{mg of solute}) \times 1000}{(\text{ml of solvent}) \times \text{molarity}}$$

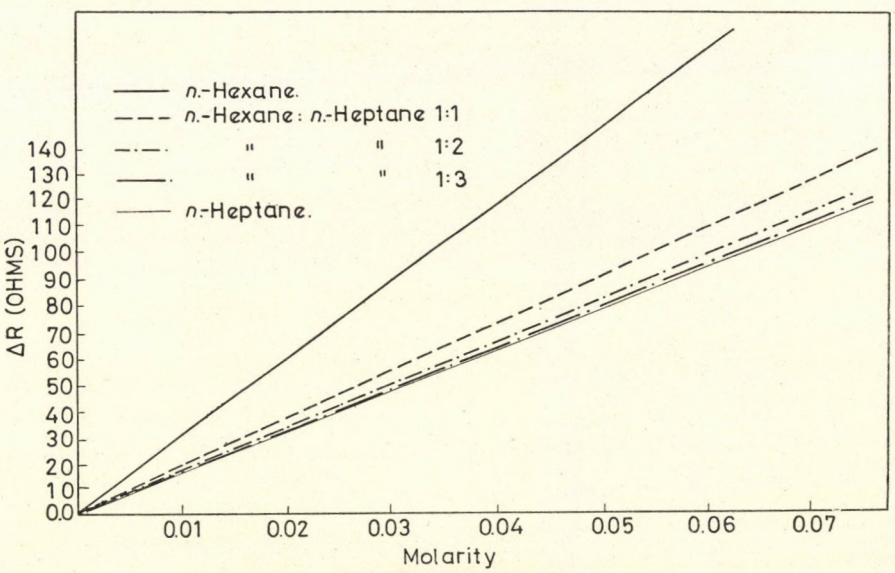

Fig. 1. Resistance difference (ΔR, ohms) *vs.* molarity for *o*-nitrophenol at 37 °C

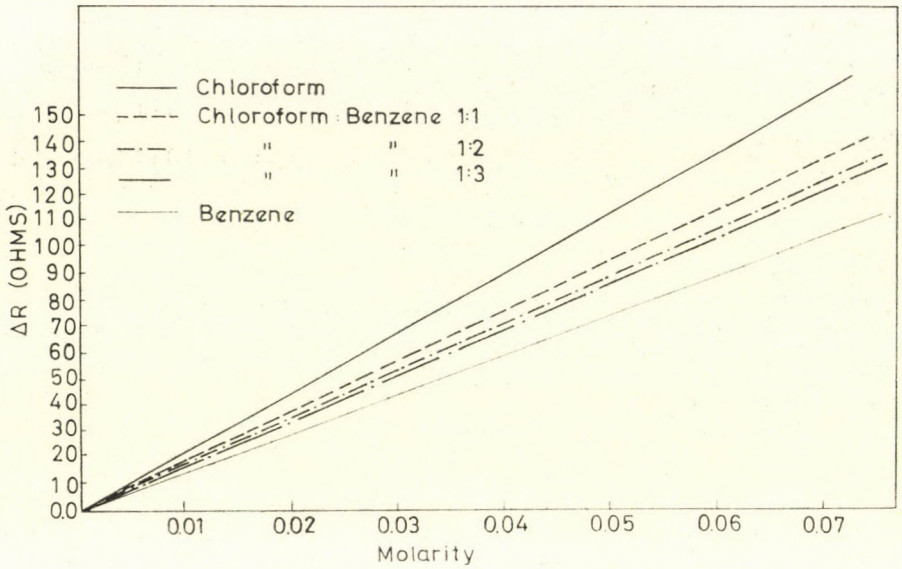

Fig. 2. Resistance difference (ΔR, ohms) *vs.* molarity for *o*-nitrophenol at 37 °C

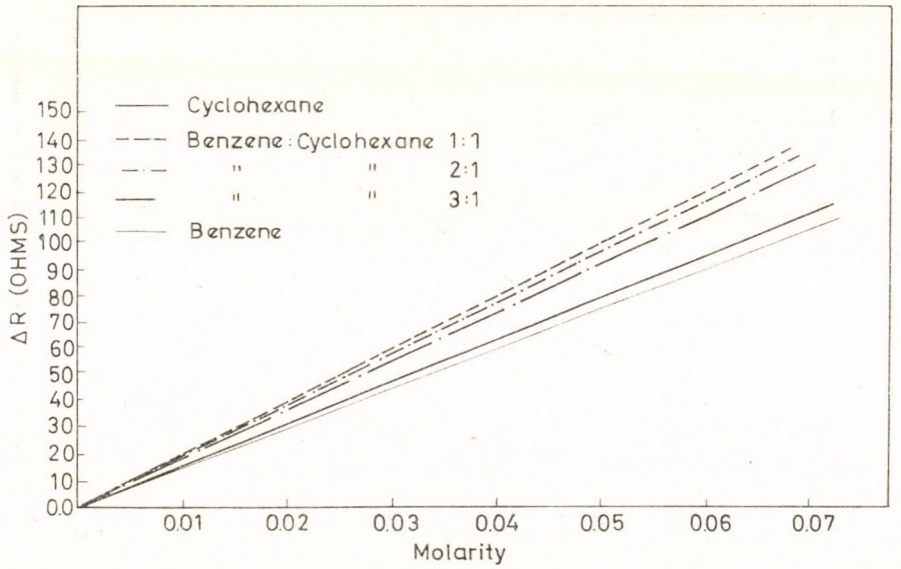

Fig. 3. Resistance difference (ΔR, ohms) *vs.* molarity for *o*-nitrophenol at 37 °C

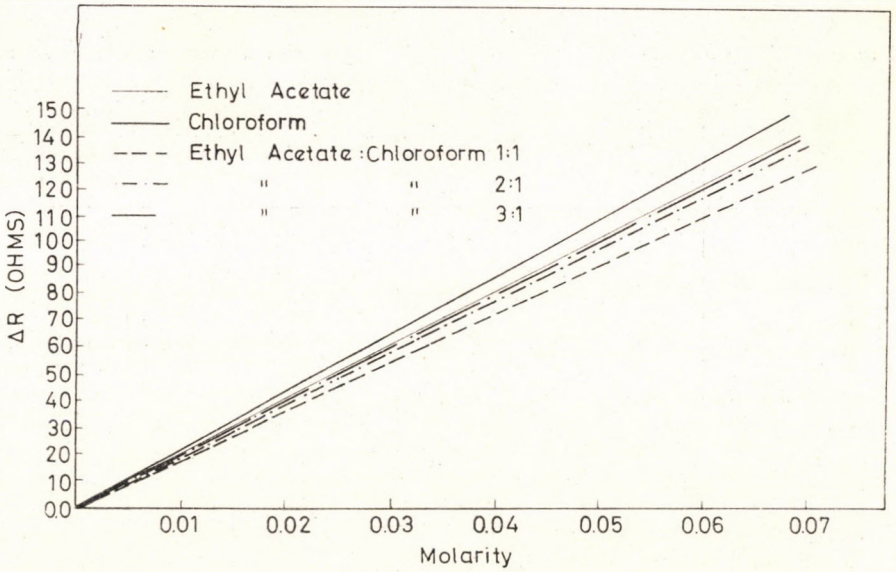

Fig. 4. Resistance difference (ΔR, ohms) *vs.* molarity for *o*-nitrophenol at 37 °C

Results and discussion

HILL [10] has described a thermoelectric method for measuring the difference in vapour pressure between two solutions, or between a solution and the pure solvent. The principle involved is simply that of a differential wet-bulb thermometer of high sensitivity. This principle has been used by MÜLLER *et al.* [11] to determine molecular weights with thermistors as the temperature sensing elements, and stainless steal cups filled with the solvent and solution. Modifications of the apparatus used [5, 6] allowed convenient and rapid determination of the molecular weights.

If a solution of an organic compound in a homogeneous binary solvent system is exposed to the vapour of the same mixture it assumes a temperature higher than that of the solvent mixture alone exposed to the same vapour. This temperature difference is due to vapour condensation onto the solution of the organic compound in the binary mixture. In the solvent mixture at the same temperature the rates of evaporation and condensation of vapour are equal (*cf.* HILL [10]). This principle can be applied to determine the molecular weight of organic compounds in homogeneous binary solvent systems (Table II). Sometimes it is necessary to use binary homogeneous mixtures in molecular weight determinations by the thermoelectric method with thermistors. to achieve complete dissolution of the organic compound.

Table II

Microdetermination of molecular weights of organic compounds in homogeneous binary mixtures

System	Compound	Wt. (mg/5 ml)	ΔR Ohms	Molarity	Molecular weight		
					theoretical	found	error (%)
(A) *Ideal system*	Azobenzene	8.597	17.5	0.00950	182.2	180.5	—0.93
(i) *n*-Hexane and *n*-heptane (1:1) at 37 °C	1-Chloro-2,4-dinitrobenzene	11.282	20.5	0.01100	202.6	205.1	+1.4
	Benzil	13.990	24.5	0.01325	210	211.1	+0.52
(ii) Chloroform and benzene (1:1) at 37 °C	Anthracene	9.142	20.0	0.01040	178.2	175.8	+0.5
	Phenacetin	7.760	16.0	0.00850	179.2	182.5	+1.6
	1-Chloro-2,4-dinitrobenzene	18.405	35.0	0.0185	202.6	198.9	—1.9
(B) *With positive deviation e. g.* benzene and cyclohexane (1:1) at 37 °C	Azobenzene	7.912	18.0	0.00875	182.2	180.8	—0.76
	Anthracene	11.842	27.0	0.01325	178.2	178.7	+0.28
(C) *With negative deviation e. g.* ethyl acetate and chloroform (1:1) at 37 °C	Anthracene	7.255	8	0.00403	178.2	180	+1.01
	1-Chloro-2,4-dinitrobenzene	15.230	14	0.00761	202.6	200.1	—0.987

The steady state temperature difference is reached within 3—5 minutes. The method is illustrated on the example of *o*-nitrophenol since, due to chelation, the *ortho*-compound behaves as a monomer [12].

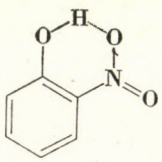

The sample size ranges from 5—20 mg in 5 ml of the binary solvent mixture. A relative error of less than 2% is obtained.

It is interesting to note that plots of the resistance difference (ΔR, ohms) for an organic compound in an ideal homogeneous binary mixture against the molarity of the solute lie between the corresponding curves for the same compound in the two components of the solvent mixture (Figs 1 and 2).

On the other hand, the plot of the resistance difference in homogeneous binary mixtures with a positive deviation lies above, whereas with a negative deviation below, the resistance difference *vs.* molarity curves of the solute in both pure components of the binary solvent mixture (Figs 3, 4).

This observation can be used as a simple and reliable procedure to determine the behaviour of a homogeneous binary mixture with respect to Raoult's law.

However, the possibility of decomposition, dissociation, reaction, polymerization, etc. should not be ignored during determination of the molecular weights of organic compounds, either in a single solvent or in homogeneous binary solvent systems. Details will be reported in due course.

REFERENCES

1. RAST, K.: Ber., **55***B*, 1051 (1922); Ber., **55***B*, 3727 (1922)
2. INGRAM, G.: Methods of Organic Elemental Microanalysis, 1st Ed., p. 479. Reinhold, New York, 1962
3. SIGNER, R.: Annalen, **478**, 246 (1930)
4. SPEYERMARK, A.: Quantitative Organic Microanalysis, 2nd Ed., p. 535. Academic Press, New York, 1961
5. WELCHER, F. J.: Standard Methods of Chemical Analysis, Volume II A, 6th Ed., p. 448—450. Van Nostrand, Princeton, New Jersey, 1963
6. NEUMAYER, J. J.: Anal. Chim. Acta, **20**, 519 (1959)
7. KNAUER, H.: Wissenschaftlicher Gerätebau 1. Berlin, 33
8. GLASSTONE, S.: Textbook of Physical Chemistry, 2nd Ed., (a) p. 711, (b) p. 713. Macmillan, London, 1960
9. WEAST, R. C., SELBY, S. M., HODGMAN, C. D.: Handbook of Chemistry and Physics, 46. Ed., D—3, The Chemical Rubber Co., 1965—1966
10. HILL, A. U.: Proc. Series A, **127**, 9 (1930)
11. MÜLLER, R. H., STOLTEN, H. J.: Anal. Chem. **25**, 1103 (1953)
12. FINAR, I. L.: Organic Chemistry, Volume 1, 5th Ed., p. 672. Longmans, 1967

Alfy Badie SAKLA
A. H. BADRAN
N. A. SAYED
Cairo University, Giza, Egypt.

Acta Chimica Academiae Scientiarum Hungaricae, Tomus 74 (1), pp. 59–70 (1972)

THEORETICAL INVESTIGATION OF THE ELECTRONIC SPECTRA OF MONOSUBSTITUTED BENZENE DERIVATIVES

Á. I. KISS and J. SZŐKE

(Department of Physical Chemistry, Technical University, Budapest and Central Research Institute for Physics, Budapest)

Received June 1, 1971

The electronic structures and spectra of monosubstituted benzenes containing fluoro-, chloro-, hydroxy-, amino-, and carbonyl-groups as well as their combinations were calculated by the Pariser—Parr—Pople method. The calculations reproduced the experimental singlet energies, polarization directions and lowest energy band intensities fairly well. The starting parameters giving the best energies are equally well applicable to simple and complex substituents, and the correlation between the electronic structure of the molecules and the mesomeric effect of the substituents is in accord with the expectations. Deviations found for halogen derivatives may be caused by failure of the calculations to account for some important additional effects.

1. Introduction

Many authors have dealt with the calculation of the π-electronic structure and spectra of monosubstitutedbenz enes by the Pariser–Parr–Pople (PPP) method, taking very different starting values. PPP-type calculations have been published for benzene derivatives *e.g.* in the following papers: hydroxyl [1—4], amino [2—11], fluoro [12, 13], chloro [12, 14, 15], and carbonyl derivatives [16, 17]. It is believed that no calculations have been performed as yet on derivatives containing complex substituents.

The aim of our work is to determine the best characteristic starting values (I, A, β) for the PPP calculation of π-electron systems, which could be applied to a great number of analogous compounds. In this paper we propose starting values suitable for the calculation of both simple (C_6H_5X) and complex (C_6H_5COX) derivatives (X = F, Cl, OH, NH_2).

2. Calculation method

The PPP method is used in its original form [18, 19]. The details of the method will not be given here, as they can be found in Refs [20, 21]. Starting from Hückel MO's, the computer program used calculates the Pople SCF MO's followed by a configuration interaction treatment between all singly excited states. The computation produces the charge density–bond order matrix, the singlet and triplet transition energies, the magnitude and direction of transi-

tion moments, the total π-electron energy, and the π-electron contribution to the dipole moment.

The computation requires as starting values the resonance integrals $\beta_{\mu\nu}$, the molecular geometry, the ionization potentials, electron affinities, and the virtual charges of π-electrons. The two-center repulsion integrals, $\gamma_{\mu\nu}$, are calculated by the MATAGA—NISHIMOTO approximation [22].

The calculations were carried out on the ICT 1905 computer of the Central Research Institute for Physics, Budapest.

3. Determination of the starting parameters

The electronic spectra recorded in saturated hydrocarbon solvents were used as reference data for the compounds investigated, because the vapour spectra of the more complex derivatives are not available. The electronic transitions are characterized by λ_{max} and ε_{max} values. As the determination of the 0,0 band position is uncertain, the calculated energies have been fitted to the experimental band maxima.

The molecular geometries were considered as sets of fixed values taken from experimental data [23]. The C—C bond length in the benzene ring was taken as equal to 1.397 Å, the C—O distance in phenol 1.36 Å, the C—N distance in aniline 1.38 Å, the C—F distance in fluorobenzene 1.30 Å, the C—Cl distance in chlorobenzene 1.69 Å, and all bond angles as equal to 120°. The $C_{aromatic}$—$C_{aldehyde}$ distance in benzaldehyde is 1.50 Å, the C=O distance 1.215 Å, and the angles are 120°, as in acetaldehyde. As bond distances and angles of the substituted carbonyl groups, the data for the corresponding methyl derivatives were used [23].

The atomic ionization potential, I_μ, and the one-center repulsion integrals, $\gamma_{\mu\mu}$, were considered as fixed. The I_μ and $\gamma_{\mu\mu}$ values for atoms contributing one electron to the π system were taken from the table of HINZE and JAFFÉ [24], as in Ref. [3]. For evaluation of the I_μ values of atoms contributing two electrons, KWIATKOWSKI's approximation [8] was used:

$$I_\mu = I_{CH_3X} + \gamma_{\mu\mu}$$

For the I_{CH_3X} values the following experimental ionization potentials were taken: CH_3F 12.61 eV [25], CH_3Cl 11.34 eV [26], CH_3OH 10.83 eV [27], CH_3NH_2 8.97 eV [28]. The $\gamma_{\mu\mu}$ values for N and O were the same as in BAILEY's work [3], those for F and Cl the same as in FORD's paper [12]. The values used are listed in Table I.

The $\beta_{\mu\nu}$ values were varied in a comparatively wide range. The aromatic β_{C-C} value of —2.39 eV [18] was chosen so as to obtain best agreement for

Table I

Atomic parameters used in the calculations

	Ċ	Ṅ	N̈	Ȯ	Ö	F̈	C̈l
I_μ	11.16	14.12	25.73	17.70	30.07	34.00	24.37
$\gamma_{\mu\mu}$	11.13	12.34	16.76	15.23	19.24	21.39	13.03
A_μ	0.03	1.78	8.97	2.47	10.83	12.61	11.34

the lowest energy electronic transition of benzene. The deviation from the experimental value is 0.53%. Fig. 1 shows the dependence of the first three transition energies on β_{C-C}. This best aromatic β_{C-C} value was used for all further benzene derivatives.

In the substituted benzenes the $\beta_{\mu\nu}$ values of the bond between the substituent and the ring carbon atom, as well as those of the bonds within the

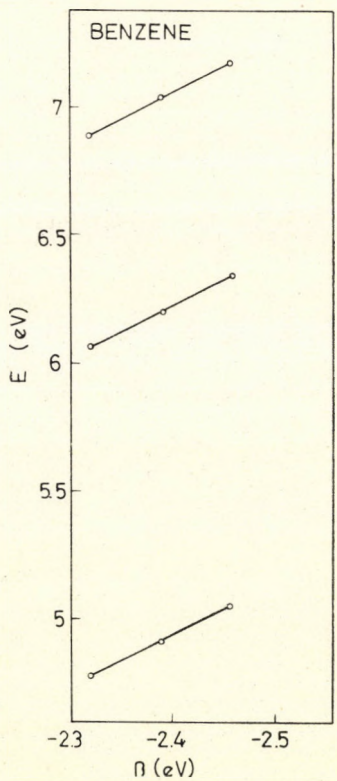

Fig. 1. The calculated singlet energies of benzene as a function of β_{C-C}

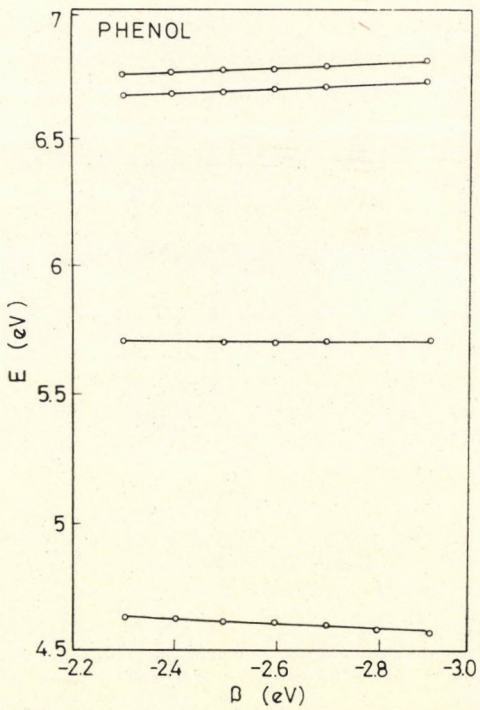

Fig. 2. The calculated singlet energies of phenol as a function of β_{C-O}

substituent were varied. As an example, we show the transition energies for phenol as a function of β_{C-X} (Fig. 2).

With benzaldehyde the β values between the aromatic and the aldehyde carbon atom, and those between the aldehyde carbon and the oxygen atom

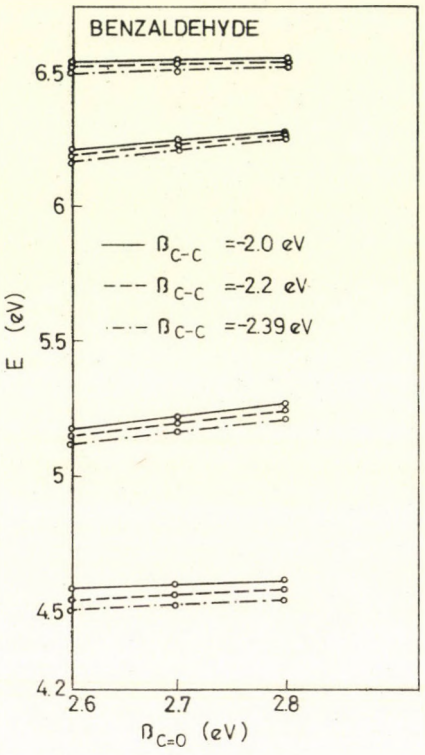

Fig. 3. The calculated singlet energies of benzaldehyde as a function of $\beta_{C=O}$

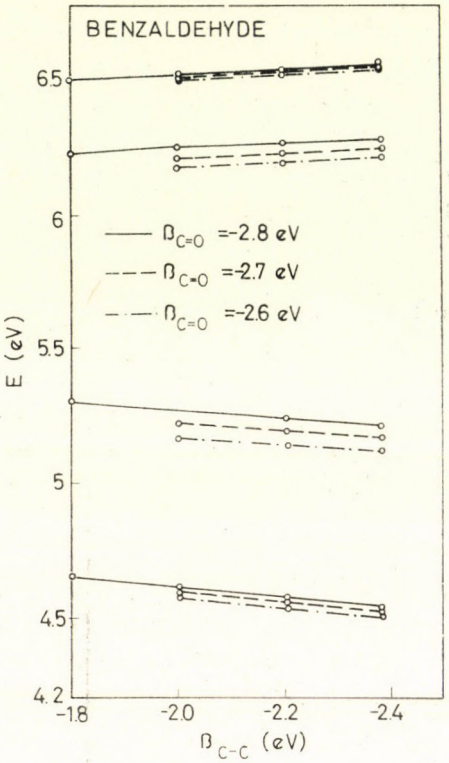

Fig. 4. The calculated singlet energies of benzaldehyde as a function of β_{C-C}

were varied simultaneously. The dependences of the calculated energies on $\beta_{C=O}$ and β_{C-C} are shown in Figs 3 and 4, respectively. The best agreement for the two experimental band energies was obtained with $\beta_{C-C} = -2.39$ and $\beta_{C=O} = -2.7$ eV.

For studying the substituted carbonyl groups, —2.39 eV was chosen for the β_{C-C} value between the aromatic and the aldehyde carbon atom. The values of $\beta_{C=O}$ and β_{C-X} (X = F, Cl, OH, NH_2) were varied.

The calculated best energies and the corresponding $\beta_{\mu\nu}$ values, together with the experimental energies, are collected in Table II. The $\beta_{\mu\nu}$ values that give singlet transition energies in best agreement with the experimental values

Table II

Calculated and experimental spectral data

Compound Best $\beta_{\mu\nu}$ (eV)	Calculated			Experimental			Ref.
	E (eV)	f	α^0	E (eV)	λ_{max} (nm)	log ε	
1	2	3	4	5	6	7	8
1. Benzene							
$\beta_{C-C} = -2.39$	4.9073	0		4.8811	254	2.40	29
	6.2047	0		6.0774	204	3.94	
	7.0303	1.2008	90	6.7380	184	4.83	
	7.0303	1.2008	0	6.7380	184	4.83	
2. Fluorobenzene							
$\beta_{C-F} = -2.20$	4.7576	0.0172	90	4.7502	261	3.08	29
	5.9294	0.1109	0	6.1073	203	3.88	
	6.8357	1.0284	270				
	6.8366	1.1632	0				
3. Chlorobenzene							
$\beta_{C-Cl} = -2.20$	4.7165	0.0222	90	4.6784	265	2.43	29
	5.7920	0.2323	0	5.7400	216	3.92	
	6.7419	1.0711	0	6.5253	190	4.74	
	6.7487	0.9071	270	6.5253	190	4.74	
4. Phenol							
$\beta_{C-O} = -2.50$	4.6134	0.0411	90	4.5749	271	3.28	
	5.7030	0.2518	0	5.8759	211	3.72	
	6.6747	0.8078	270				
	6.7580	1.0664	0				
5. Aniline							
$\beta_{C-N} = -2.30$	4.3785	0.0600	90	4.3049	288	3.27	
	5.3143	0.4175	0	5.2982	234	3.95	
	6.3236	0.3917	270				
	6.6464	0.8098	0				
6. Benzaldehyde							
$\beta_{C-C} = -2.39$	4.5264	0.0260	111	4.4598	278	2.97	
$\beta_{C=O} = -2.70$	5.1664	0.5749	191.6	5.1550	240.5	4.03	
	6.2440	0.3975	279.7				
	6.5471	0.6481	195.1				
7. Benzoyl fluoride							
$\beta_{C=O} = -2.70$	4.6232	0.0178	115.2	4.4838	276.5	3.04	
$\beta_{C-F} = -2.20$	5.3627	0.4975	10.5	5.3904	230	3.99	
	6.3866	0.3759	112.3				
	6.5904	0.7978	207.0				
8. Benzoyl chloride							
$\beta_{C=O} = -2.60$	4.5962	0.0197	115.0	4.3886	282.5	3.10	
$\beta_{C-Cl} = -1.80$	5.2819	0.5344	8.9	5.1443	241	4.18	
	6.1306	0.0111	266.7				
	6.4119	0.6858	103.6				
	6.5687	0.7235	199.9				
9. Benzoic acid							
$\beta_{C=O} = -2.60$	4.6430	0.0155	119.2	4.5248	274	3.02	
$\beta_{C-OH} = -2.50$	5.3798	0.5091	11.8	5.3670	231	4.20	
	6.1591	0.0100	44.3				
	6.4892	0.7199	95.4				
	6.6027	0.7571	190.4				
10. Benzamide							
$\beta_{C=O} = -2.80$	4.6817	0.0127	121.9	4.5919	270	2.90	
$\beta_{C-N} = -2.30$	5.5000	0.4089	15.1	5.5973	221.5	4.00	
	5.5446	0.1410	314.0				
	6.3753	0.1153	116.8				
	6.6010	0.6313	138.3				
	6.6199	0.8088	41.8				

also correlate reasonably well with the bond distances $r_{\mu\nu}$ (Table III). With shorter bond length the interaction generally becomes greater, *i.e.* the $\beta_{\mu\nu}$ value decreases.

Table III

Bond parameters used in the calculation

	r_{C-X}	β_{C-X}
—C—F	1.30	—2.20
—C—Cl	1.69	—2.20
—C—OH	1.36	—2.50
—C—NH_2	1.38	—2.30

	r_{C-C}	$r_{C=O}$	r_{C-X}	$\beta_{C=O}$	β_{C-X}
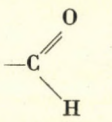	1.50	1.215	—	—2.70	—
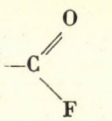	1.50	1.16	1.37	—2.70	—2.20
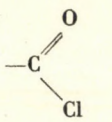	1.50	1.17	1.82	—2.60	—1.80
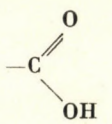	1.50	1.245	1.31	—2.60	—2.50
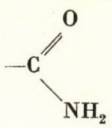	1.53	1.21	1.36	—2.80	—2.30

4. Results and discussion

The correlations between the calculated results and the various structural characteristics of the molecules considered are discussed in the following sections.

4.1. *Singlet energies*

The experimental and calculated energies and oscillator strengths are collected in Table II, from which it may be seen that the calculated best energies are in good agreement with the experimental ones. The experimental energies for the simple C_6H_5X derivatives decrease in the order $-H > -F > -Cl > -OH > -NH_2$. The agreement for the first band is satisfactory but for the second band there is some deviation with the halogens, so that the order of these bands does not agree with the experimental order.

Our results are in good agreement with the data given in the literature.

With the C_6H_5COX derivatives, the energies of the first and second $\pi \rightarrow \pi^*$ bands increase in the following order:

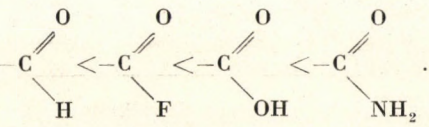

For both bands this order corresponds to the experimental one, and is in keeping with the increase in the +M effect of the X group (X = F, OH, NH_2), which determines the —M effect of the —COX group [30]. The results of the calculations are in full accordance with the experimental interpretation of the spectra, except that the energies calculated for benzoyl chloride are between those for benzaldehyde and benzoyl fluoride, whereas the experimental energies are, in fact, smaller than those for benzaldehyde. The weak acceptor effect of the chlorine atom assumed for benzoyl chloride [30] is clearly not taken into account, the chlorine atom being treated as a weak donor.

Among the compounds investigated, the worst correspondence was obtained with benzoyl chloride, for which the largest deviation of the calculated values from the experimental ones is 4.8%.

The calculated first and second band energies are shown as functions of the experimental values in Figs 5 and 6.

4.2. *Ground state charge densities*

The charge density values corresponding to the best energies given above are in accordance with the electronic structure of the molecules investigated. The charge density on the X atom in the C_6H_5X derivatives decreases in the order $-F > -Cl > -OH > -NH_2$, as would be expected from the theoretical values of the +M effect in the ground state. The other charge densities and bond orders vary in the expected manner, too. Table IV contains the charge densities of the molecules investigated.

The charge densities of the C_6H_5COX derivatives for the $\beta_{\mu\nu}$ values giving the best energies are presented in Table IV. The charge density on

atom X decreases in the order —Cl > —F > —OH > —NH_2, and increases on the carbonyl carbon and oxygen atoms, as well as on the *o*- and *p*-carbon atoms, in the order —H < —Cl < —F < —OH < —NH_2, in conformity

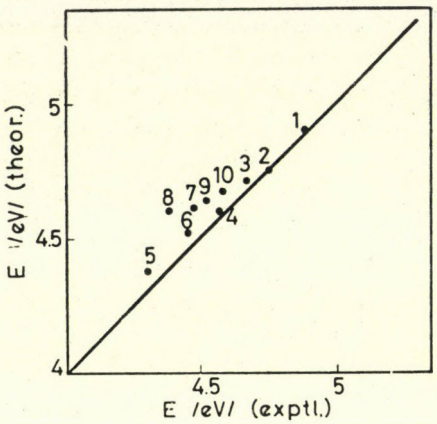

Fig. 5. Correlation between the calculated and experimental α band energies

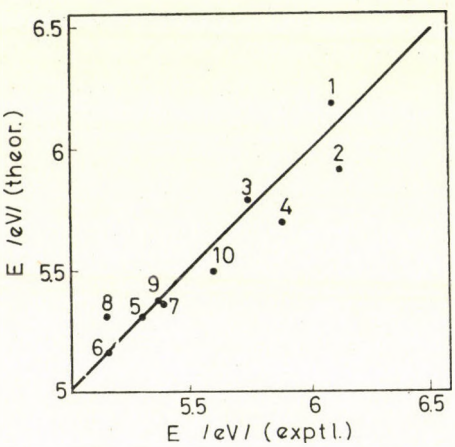

Fig. 6. Correlation between the calculated and experimental *p* band energies

with an increase of the +M effect (*i.e.* decrease of the —M effect of the —COX group in the ground state).

It is evident that the charge density on the X atom decreases more in the C_6H_5COX derivatives than in the C_6H_5X compounds. It should be noted that the chlorine atom loses less charge with respect to the fluorine atom in benzoyl chloride than in chlorobenzene, which indicates that the former is a weaker donor, in accordance with the experimental spectra. The difference resulting from the calculation is not as large as would be expected from the

Table IV

Calculated charge densities

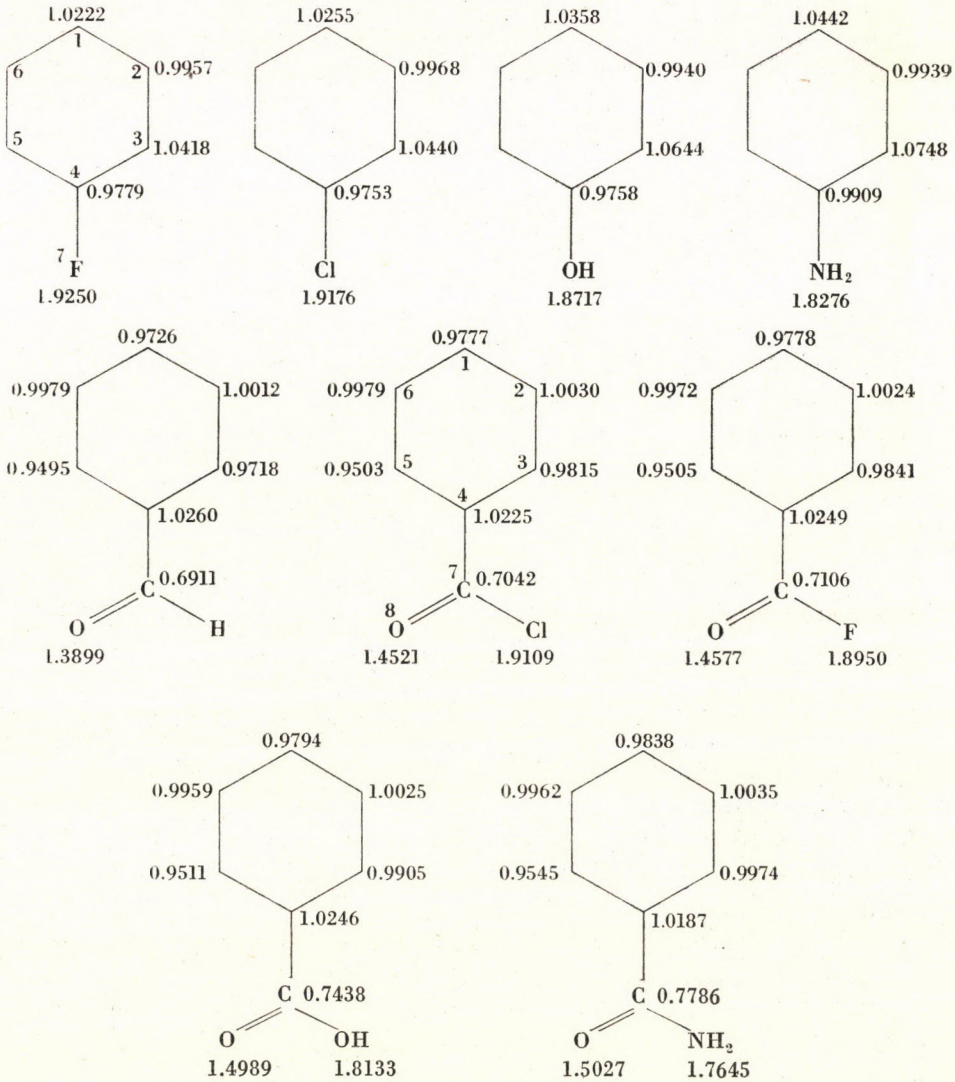

experimental data, perhaps because there is an additional effect dominating in the excited states. The charge density of the carbonyl oxygen atom varies in parallel to the oxygen basicity. WOJTKOWIAK *et al.* [31] recently reported a basicity order obtained from a consideration of the thermodynamic properties of the $C_6H_5COX.I_2$ complexes, which is in general agreement with the results of the present calculations. The deviation observed with the halogen derivatives presumably arises from the fact that the PPP calculation does

not take into account the inductive effect, which, according to WOJTKOWIAK *et al.* [32], is important for benzoyl halides.

It should be mentioned that charge densities in excellent agreement with the observed quantities are obtained for the $\beta_{C=O}$ and β_{C-X} values giving the best energies; with other β values the correlation was worse.

4.3. *Oscillator strengths*

The band intensities belonging to the best energies give good agreement for the first band (Table II). The order of the calculated and experimental intensities of the C_6H_5X derivatives is the same, with the exception of the fluorine derivative, which has a very high experimental value. Among the experimental intensities of the C_6H_5COX derivatives, benzoyl chloride has the highest value for the first band; among the calculated values, however, that of benzaldehyde is the highest. Otherwise, the following order holds for both the calculated and the experimental intensities:

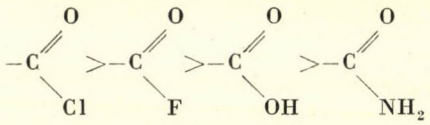

The second band intensity failed to give good agreement with the experimental data.

4.4. *Polarization directions*

The polarization of the calculated bands is given in Table II. The α values measure the angle from the positive y axis in clockwise direction, with the ring-substituent axis lying in the —y direction. The first band of the C_6H_5X compounds is polarized perpendicularly to ($A_1 \rightarrow B_1$), and the second band in parallel to ($A_1 \rightarrow A_1$), the ring-substituent axis. This result is in full accordance with the experimental polarization values for *p*-dimethoxybenzene [33] and the aromatic amines [34]. The third and fourth bands show perpendicular and parallel polarization, respectively.

The allowed bands of the C_6H_5COX derivatives have the same polarization as the C_6H_5X compounds. The polarization directions are somewhat altered because of the conformation of the carbonyl bond. The results obtained are in agreement with the experimental polarization values for benzaldehyde [35]. The first $\pi \rightarrow \pi^*$ band of benzaldehyde is polarized perpendicularly to the carbonyl-bond-benzene axis ($A_1 \rightarrow B_1$).

4.5. *Triplet energies*

As the energies and relative intensities of the singlet–triplet transitions of all three bands are known only for benzene [36], only this compound will

be considered here. The agreement between the calculated and the experimental values is poor (Table V) using $\beta_{C-C} = -2.39$ eV, the best value for singlet–singlet transitions. The triplet energies vary with β_{C-C} in the same way as the singlet energies, thus an acceptable result may be expected only for much lower β_{C-C} values. The second band is doubly degenerate, in accordance with DOERING's band assignment [36].

Table V

Energy of the calculated and experimental singlet–triplet transitions, in eV

Calculated energy	Experimental energy	Relative intensity	Excited state symmetry
2.4905	3.95	medium	$^3B_{2\mu}$
4.0037			
	4.75	strong	$^3E_{1\mu}$
4.0037			
4.9073	5.60	weak	?

(The accuracy of the experimental energies is $\pm$ 0.05 eV)

5. Conclusions

The singlet transition energies of the C_6H_5X and C_6H_5COX compounds calculated here are in good agreement with the experimental data. The charge density-bond orders belonging to the $\beta_{\mu\nu}$ values producing the best energies correspond to the theoretical predictions. The oscillator strengths vary in the same order as the experimental intensities with the first $\pi \rightarrow \pi^*$ bands only; for the singlet–triplet transition energies the agreement is poor.

Except for the chloro derivatives, the same β_{C-X} values produce the best energies and charge densities with both the C_6H_5X and C_6H_5COX compounds and, therefore, seem to be transferable. The reason for the deviations with the halogen derivatives may be that, apart from the +M effect, other effects (*e.g.* inductive effect, d-orbitals) not considered in the PPP calculations play an important role. The neglect of such additional effects may also be the reason for the fact that smaller differences are obtained between the calculated energies than are observed between the experimental values.

We conclude that in its original form the PPP method yields suitable results for the singlet–singlet energies, as well as for the charge densities and bond orders. In order to obtain a better approximation for the oscillator

strengths and the singlet–triplet transition energies, a more accurate method is needed. Investigations in this direction are in progress.

*

The authors are greatly indebted to Mrs. Borbála HETZER for her very valuable assistance.

REFERENCES

1. FORSÉN, S., ALM, T.: Acta Chem. Scand., **19**, 2027 (1965)
2. BILLINGSLEY, F. P., BLOOR, J. E.: Theor. Chim. Acta, **11**, 325 (1968)
3. BAILEY, M. L.: Theor. Chim. Acta, **13**, 56 (1969)
4. TICHY, M., ZAHRADNIK, R.: J. Phys. Chem., **73**, 534 (1969)
5. FISCHER-HJALMARS, I.: Arkiv Fysik, **21**, 123 (1962)
6. LABHART, H., WAGNIERE, G.: Helv. Chim. Acta, **46**, 1314 (1963)
7. KLESSINGER, M.: Theor. Chim. Acta, **5**, 236 (1966)
8. KWIATKOWSKI, J. S.: Acta Phys. Polon., **29**, 477(1966); **30**, 529 (1966)
9. LIPTAY, W., EBERLEIN, W., WEIDENBURG,H., ELFLEIN, O.: Ber. Bunsenges. physik. Chem., **71**, 548 (1967)
10. FISCHER-HJALMARS, I., SUNDBOM, M.: Acta Chem. Scand., **22**, 607 (1968)
11. NISHIMOTO, K., FORSTER, L. S.: Bull. Chem. Soc. Japan, **41**, 2254 (1968)
12. FORD, B.: Theor. Chim. Acta, **10**, 342 (1968)
13. CHALVET, O., LEIBOVICI, C.: Theor. Chim. Acta, **13**, 297 (1969)
14. GRABE, B.: Acta Chem. Scand., **22**, 2237 (1968)
15. CHALVET, O., LEIBOVICI, C.: Theor. Chim. Acta, **14**, 65 (1969)
16. JENSEN, H., SKANCKE, P. N.: Acta Chem. Scand., **22**, 2899 (1968)
17. EDWARDS, T. G., GRINTER, R.: Mol. Phys., **15**, 357 (1968)
18. PARISER, R., PARR, R. G.: J. Chem. Phys., **21**, 466, 767 (1953)
19. POPLE, J. A.: Trans. Faraday Soc., **49**, 1375 (1953)
20. PARISER, R.: J. Chem. Phys., **24**, 250 (1956)
21. PARR, R. G.: Quantum Theory of Molecular Electronic Structure. Benjamin, New York 1963
22. MATAGA, N., NISHIMOTO, K.: Z. physik. Chem. N. F., **13**, 140 (1957)
23. SUTTON, L. E., Ed.: Tables of Interatomic Distances and Configuration in Molecules and Ions. Spec. Publ. No. 11, Chem. Soc., London 1958; Supplement, Spec. Publ. No. 18, Chem. Soc., London 1965
24. HINZE, J., JAFFÉ, H. H.: J. Am. Chem. Soc., **84**, 540 (1962)
25. DIBELER, V. H., REESE, R. M.: J. Res. Nat. Bur. Stand., **54**, 127 (1955)
26. DIBELER, V. H., REESE, R. M.: Anal. Chem., **30**, 604 (1958)
27. MORRISON, J .D., NICHOLSON, A. J. C.: J. Chem. Phys., **20**, 1021 (1952)
28. WATANABE, K.: J. Chem. Phys., **26**, 542 (1957)
29. DMS Uv Atlas of Organic Compounds, Vol. I—IV Butterworths, Verlag Chemie 1968
30. KISS, Á. I., HORVÁTH, G.: Acta Chim. Acad. Sci. Hung., **66**, 431 (1970)
31. GUIHENEUF, G., LAURENCE, C., WOJTKOWIAK, B.: Compt. rend. C, **271**, 389 (1970)
32. GUIHENEUF, G., LAURENCE, C., WOJTKOWIAK, B.: Bull. soc. chim. France, 1970, 571
33. ALBRECHT, A. C., SIMPSON, W. T.: J. Chem. Phys., **23**, 1480 (1955)
34. KALANTAR, A. H., ALBRECHT, A. C.: Ber. Bunsenges. physik. Chem., **68**, 361, 377 (1964)
35. SHIMADA, R., GOODMAN, L.: J. Chem. Phys., **43**, 2027 (1965)
36. DOERING, J. P.: J. Chem. Phys., **51**, 2866 (1969)

Árpád István KISS; Budapest XI., Budafoki út 8.
József SZŐKE; Budapest XII., Konkoly Thege M. út.

Acta Chimica Academiae Scientiarum Hungaricae, Tomus 74 (1), pp. 71–77 (1972)

DISTRIBUTIONS IN TIME AND SPACE, RESPECTIVELY, IN FIXED BED MULTISTAGE EXCHANGE PROCESSES OF LINEAR KINETICS

(SHORT COMMUNICATION)

Á. PETHŐ

(Central Research Institute for Chemistry of the Hungarian Academy of Sciences, Budapest)

Received October 1, 1971

1. Statement of the problem

Let us consider a cascade of similar cells (numbered by $m = 0, 1, 2, \ldots$) containing two phases from which let the one be fixed and the other flow from one cell into the other in the direction of increasing cell numbers. Let the volumes of the phases in the single cells be independent of the cell number. Consider now a solute which is capable of being sorbed in the fixed phase, supposing perfect mixing in both phases. Under such conditions the process, namely *convection* (in the mobile phase) as well as *sorption* (in the stationary phase) of the solute can be described by two independent variables: by the *cell number m* and by the *time t*. (*Cf.* the case when both space and time are discontinuous [1, 2] and continuous [3, 4], respectively.)

Let us now define $W_m^{(t)}$ as the *flux*, *i.e.* the amount of the solute transferred by convection in the mobile phase in unit time, related to the mth cell, further $T_m^{(t)}$ as the *amount of the solute* both in the mobile and the stationary phase, related to the mth cell. With these quantities the *Fokker—Planck-equation* of the process reads

$$W_m^{(t)} - W_{m-1}^{(t)} + \frac{dT_m^{(t)}}{dt} = 0\,, \tag{1.1}$$

where $W_{-1}^{(t)}$ (the value of $W_{m-1}^{(t)}$ if putting $m = 0$) denotes the *boundary condition;* if the input of the solute takes place momentaneously, we have

$$W_{-1}^{(t)} = \delta^{(t)}\,, \tag{1.2}$$

where by $\delta^{(t)}$ the Dirac delta function is denoted. On the other hand, the *initial condition* for Eq. (1.1) should be

$$T_m^{(0)} = 0\,, \tag{1.3}$$

i.e. at the beginning of the process no solute has yet been present in the system.

Let us now define the amount of the solute in the mobile phase: $Y_m^{(t)}$, related to the mth cell, further the *characteristic time* τ as

$$\tau = \frac{\text{volume of the mobile phase in a cell}}{\text{flow rate of the mobile phase}} .$$

Thus the relation between $W_m^{(t)}$ and $Y_m^{(t)}$ is the following:

$$W_m^{(t)} = \frac{1}{\tau} Y_m^{(t)} . \tag{1.4}$$

In order to define the *sorption kinetics* for the process, the amount of the solute in the fixed phase, related to the mth cell, should first be introduced:

$$X_m^{(t)} = T_m^{(t)} - Y_m^{(t)} . \tag{1.5}$$

Now we will stipulate the following relation between $X_m^{(t)}$ and $Y_m^{(t)}$:

$$X_m^{(t)} = Kf^{(t)} * Y_m^{(t)}, \tag{1.6}$$

denoting by * the *convolution* of two functions. In this equation the function $f^{(t)}$ should be such for which

$$\int_0^\infty f^{(t)} dt = 1 , \tag{1.7}$$

and $K \geq 0$ is called the *equilibrium constant* of the sorption (see also the Appendix). Introducing the new constants

$$p = \frac{K}{1+K} , \qquad q = \frac{1}{1+K} , \tag{1.8}$$

in view of Eqs (1.5)—(1.6) we have

$$T_m^{(t)} = \frac{1}{q} [pf^{(t)} + q\delta^{(t)}] * Y_m^{(t)} . \tag{1.9}$$

(Note that, if no sorption takes place, $p = 0$ and $q = 1$.) The system of Eqs (1.1)—(1.2)—(1.3)—(1.4)—(1.9) constitutes the basis of what follows.

2. The distribution of the residence times

Let us consider a particle of the solute and the time ϑ_m when this particle has left the mth cell. This time will be called the *residence time* of the particle at the place m. The quantity ϑ_m may be considered as a random variable, its

probability density function will obviously be

$$\frac{d}{dt}\mathfrak{P}(\vartheta_m \leqq t) = W_m^{(t)}, \tag{2.1}$$

where $\mathfrak{P}(\vartheta_m \leqq t)$ is the probability of ϑ_m being not greater than t.

Taking the *Laplace transform* of Eqs (1.1)—(1.4)—(1.9), after eliminating $T_m^{(t)}$ and $Y_m^{(t)}$, we obtain

$$\mathfrak{L}W_m^{(t)} \equiv W_m(s) = \left\{1 + \frac{\tau s}{q}[pf(s) + q]\right\} W_{m+1}(s), \tag{2.2}$$

which is a difference equation; the boundary condition will be the transform of Eq. (1.2):

$$W_{-1}(s) = 1. \tag{2.3}$$

Let us now determine the *generating function* of $W_m(s)$: multiplying Eq. (2.2) by z^{m+1} and summing up from $m = 0$ to ∞, taking Eq. (2.3) into consideration as well, we have

$$\sum_{m=0}^{\infty} W_m(s) z^m \equiv W(z, s) = \frac{1}{\left\{1 + \frac{\tau s}{q}[pf(s) + q]\right\} - z}. \tag{2.4}$$

(Note that

$$W(z, 0) = \frac{1}{1 - z}, \quad i.e. \quad W_m(0) = \int_0^{\infty} W_m^{(t)}\, dt = 1,$$

which is a physical triviality.)

By means of the Laplace transform of $W_m^{(t)}$ one has for the *mean* (expected value) and *variance* (dispersion) of the residence times [5]

$$\mathfrak{E}(\vartheta_m) = -\left.\frac{dW_m(s)}{ds}\right|_{s=0}, \tag{2.5}$$

$$\mathfrak{D}^2(\vartheta_m) + \mathfrak{E}^2(\vartheta_m) = \left.\frac{d^2 W_m(s)}{ds^2}\right|_{s=0}. \tag{2.6}$$

Taking the generating functions of Eqs (2.5)—(2.6) we may write

$$\sum_{m=0}^{\infty} \mathfrak{E}(\vartheta_m) z^m = -\left.\frac{\partial W(z, s)}{\partial s}\right|_{s=0}, \tag{2.7}$$

$$\sum_{m=0}^{\infty} \left[\mathfrak{D}^2(\vartheta_m) + \mathfrak{E}^2(\vartheta_m)\right] z^m = \left.\frac{\partial^2 W(z, s)}{\partial s^2}\right|_{s=0}. \tag{2.8}$$

From these equations, in view of Eq. (2.4), one finally obtains

$$\mathcal{E}(\vartheta_m) = \frac{\tau}{q}(m+1)\,, \tag{2.9}$$

$$\mathcal{D}^2(\vartheta_m) = \left(\frac{\tau}{q}\right)^2 (m+1)\left[1 - \frac{2pq}{\tau} f'(0)\right], \tag{2.10}$$

where $f'(0)$ stands for $[df/ds]_{s=0}$.

3. The distribution of the displacements

Let us now turn our attention to the displacement (or position) η_t of a particle of the solute at time t. The quantity η_t may be considered as a random variable, its *probability distribution* obviously becomes

$$\mathcal{P}(\eta_t \leq m) = T_m^{(t)}\,. \tag{3.1}$$

Taking the Laplace transform of Eqs (1.4)—(1.9) we have

$$\mathcal{L}T_m^{(t)} \equiv T_m(s) = \frac{\tau}{q}\left[pf(s) + q\right] W_m(s)\,; \tag{3.2}$$

thus the generating function of $T_m(s)$ will be, taking Eq. (2.4) also into consideration, as follows:

$$\sum_{m=0}^{\infty} T_m(s) z^m \equiv T(z,s) = \frac{\frac{\tau}{q}\left[pf(s)+q\right]}{\left\{1 + \frac{\tau s}{q}\left[pf(s)+q\right]\right\} - z}\,. \tag{3.3}$$

(Note that

$$T(1,s) = \frac{1}{s}\,, \quad \text{i.e.} \quad \sum_{m=0}^{\infty} T_m^{(t)} = 1\,,$$

which is a physical triviality.)

By means of the generating function of $T_m^{(t)}$ one has for the *mean* and *variance* of the displacements [5]

$$\mathcal{E}(\eta_t) = \left.\frac{dT^{(t)}(z)}{dz}\right|_{z=1}, \tag{3.4}$$

$$\mathcal{D}^2(\eta_t) - \mathcal{E}(\eta_t) + \mathcal{E}^2(\eta_t) = \left.\frac{d^2T^{(t)}(z)}{dz^2}\right|_{z=1}. \tag{3.5}$$

Writing the Laplace transform of Eqs (3.4)—(3.5) we have

$$\mathfrak{L}\mathcal{E}(\eta_t) = \left.\frac{\partial T(z,s)}{\partial z}\right|_{z=1}, \tag{3.6}$$

$$\mathfrak{L}[\mathcal{D}^2(\eta_t) - \mathcal{E}(\eta_t) + \mathcal{E}^2(\eta_t)] = \left.\frac{\partial^2 T(z,s)}{\partial z^2}\right|_{z=1}. \tag{3.7}$$

Regarding Eqs (3.6) and (3.7), in view of Eq. (3.3), one obtains

$$\mathfrak{L}\mathcal{E}(\eta_t) = \frac{\frac{q}{\tau}}{[pf(s)+q]s^2}, \tag{3.8}$$

$$\mathfrak{L}[\mathcal{D}^2(\eta_t) - \mathcal{E}(\eta_t) + \mathcal{E}^2(\eta_t)] = \frac{2\left(\frac{q}{\tau}\right)^2}{[pf(s)+q]^2 s^3}. \tag{3.9}$$

Now, instead of giving the inverse transforms of these equations, we rather determine *asymptotic* relations for large values of t. This may be done by expansion into power series of the right-hand sides of Eqs (3.8)—(3.9):

$$\frac{1}{pf(s)+q} = 1 - \left.\frac{pf'(s)}{[pf(s)+q]^2}\right|_{s=0} s + \ldots = 1 - pf'(0)s + \ldots,$$

$$\frac{1}{[pf](s)+q^2} = 1 - 2pf'(0)s + \ldots.$$

That is,

$$\mathfrak{L}\mathcal{E}(\eta_t) = \frac{q}{\tau}\left[\frac{1}{s^2} - \frac{pf'(0)}{s} + \ldots\right]$$

and

$$\mathfrak{L}[\mathcal{D}^2(\eta_t) - \mathcal{E}(\eta_t) + \mathcal{E}^2(\eta_t)] = 2\left(\frac{q}{\tau}\right)^2\left[\frac{1}{s^3} - \frac{2pf'(0)}{s^2} + \ldots\right].$$

Taking the inverse transforms, we obtain the asymptotic relations:

$$\mathcal{E}(\eta_t) \approx \frac{q}{\tau}[t - pf'(0)] \approx \frac{q}{\tau}t \tag{3.10}$$

and

$$\mathcal{D}^2(\eta_t) - \mathcal{E}(\eta_t) + \mathcal{E}^2(\eta_t) \approx \left(\frac{q}{\tau}\right)^2[t^2 - 4pf'(0)t],$$

i.e.

$$\mathcal{D}^2(\eta_t) \approx \frac{q}{\tau}\,t\left[1 - \frac{2pqf'(0)}{\tau}\right]. \tag{3.11}$$

(Concerning the mathematical justification of the above procedure see [6].)

4. Application of a central limit theorem of probability theory

By Eq. (2.4) the generating function of $W_m(s)$ was given; hence, $W_m(s)$ can be obtained as

$$W_m(s) = \left\{1 + \frac{\tau s}{q}\left[pf(s) + q\right]\right\}^{-(m+1)}.$$

One can now apply the central limit theorem of *Lindeberg—Lévy* [5] obtaining the result that ϑ_m, if *standardised*, is asymptotically normally distributed: *i.e.* for $m \to \infty$ we have

$$W_m^{(t)} \approx \frac{1}{\sqrt{2\pi}\sigma} e^{-\frac{(t-\mu)^2}{2\sigma^2}}$$

where

$$\sigma^2 \equiv \mathfrak{D}^2(\vartheta_m) \quad \text{and} \quad \mu \equiv \mathfrak{E}(\vartheta_m),$$

see Eqs (2.9)—(2.10).

A similar statement is true for $T_m^{(t)}$ as well, due to the fact that the distributions of ϑ_m and η_t are interconnected according to the Fokker—Planck-equation [see Eq. (1.1)]:

$$\int_0^t W_m^{(t')} dt' + \sum_{k=0}^{m} T_k^{(t)} = 1.$$

Therefore, for $t \to \infty$ we have

$$T_m^{(t)} \approx \frac{1}{\sqrt{2\pi}\sigma} e^{-\frac{(m-\mu)^2}{2\sigma^2}}$$

where

$$\sigma^2 \equiv \mathfrak{D}^2(\eta_t) \quad \text{and} \quad \mu \equiv \mathfrak{E}(\eta_t),$$

see Eqs (3.10)—(3.11).

Appendix

By Eq. (1.6) the *sorption kinetics* has been defined. In the special case of the so-called *linear* sorption kinetics:

$$\frac{\partial X_m^{(t)}}{\partial t} = k\left[KY_m^{(t)} - X_m^{(t)}\right], \tag{1}$$

where $k > 0$ is the *sorption rate constant*, for $f(s)$ we have

$$\mathfrak{L}f^{(t)} \equiv f(s) = \frac{k}{k+s},$$

that is

$$f'(0) = -\frac{1}{k}. \tag{2}$$

In the limiting case $k \to \infty$ in Eq. (1) we will say that *sorption equilibrium* has been established. Now we have

$$f(s) = 1\,,$$

that is

$$f'(0) = 0\,. \tag{3}$$

REFERENCES

1. PETHŐ, Á.: Chem. Eng. Sci. **22**, 1793 (1967)
2. PETHŐ, Á.: Remarks on a paper of MEDGYESSY, P., RÉNYI, A., TETTAMANTI, K., VINCZE, I.: Studia Sci. Math. Hung. In press.
3. PETHŐ, Á., SCHAY, G.: Chromatographia **2**, 158 (1969), Acta Chim. Acad. Sci. Hung. **62**, 395 (1969)
4. PETHŐ, Á.: Chem. Eng. Sci. **25**, 769 (1970)
5. FELLER, W.: An Introduction to Probability Theory and its Applications I.—II. Wiley, 1966
6. SAUER, R., SZABÓ, I.: Mathematische Hilfsmittel des Ingenieurs I. Springer, 1967

Árpád PETHŐ; Budapest II., Pusztaszeri út 57—69.

Acta Chimica Academiae Scientiarum Hungaricae, Tomus 74 (1), pp. 79–85 (1972)

ACIDE INHALTSSTOFFE DER TORFFULVOSÄUREFRAKTION

W. WILDENHAIN und G. HENSEKE

(Sektion Chemie der Bergakademie Freiberg/Sachs.)

Eingegangen am 14. Juni 1971

Durch Heißwasserextraktion gewonnene Torffulvosäuren werden an aktiviertem Wofatit E adsorbiert und mit verschiedenen Lösungsmitteln fraktioniert. Im NaOH-Eluat sind die Ligninspaltstücke *p*-Hydroxybenzoe-, Vanillin-, Protocatechu-, *p*-Hydroxyzimt- und Ferulasäure nachweisbar. Daneben gelang die Identifizierung anderer Pflanzeninhaltsstoffe oder -abbauprodukte wie Kaffee-, Glyoxyl-, Brenztrauben-, Hydroxybrenztrauben-, Oxalessig-, α-Ketoglutar-, Lävulin-, *p*-Hydroxyphenylbrenztrauben- und 4-Hydroxy-3-methoxyphenylbrenztraubensäure. Ihre Stellung im Humifizierungsprozeß wird diskutiert.

Für die Aufklärung des Humifizierungsprozesses ist die Kenntnis der in der Torffulvosäurefraktion vorhandenen niedermolekularen Inhaltsstoffe von Interesse. Durch Heißwasserextraktion isolierte Fulvosäuren lassen sich an Wofatit E mit Wasser, Aceton–Wasser (9 : 1), Dimethylformamid–Wasser (9 : 1) und 0,5proz. Natronlauge fraktionieren [1]. Das NaOH-Eluat wurde nach Passage des Ionenaustauschers Wofatit KPS 200 i. Vak. bei 40 °C weitgehend eingeengt und an Kieselgel im System Benzol/Dioxan/Eisessig (90 : 25 : 4) chromatographiert. Trotz erheblicher Schwanzbildung können mit verschiedenen Sprühreagenzien [2] einzelne Substanzflecke bzw. -zonen unterschieden werden (s. Tab. I).

Substanz 1 ist eine phenolische Ketosäure, deren Hydroxylgruppe aufgrund der Färbungen mit 4-Aminoantipyrin und 2,6-Dibromchinonchlorimid nicht *p*-ständig zur Carbonylfunktion angeordnet sein kann. Farbreaktionen mit Bromkresolgrün, Diphenylpikrylhydrazyl, *o*-Dinitrobenzol und Titanchlorid sowie der negative 4-Aminoantipyrin-Test in Gegenwart von Luftsauerstoff charakterisieren Substanz 2 als eine 2,3- ider 3,4-Dihydroxyzimtsäure. Die Substanzflecke 3 und 7 geben im Unterschied zur Substanz 1 Indikationen für *p*-Hydroxyphenylketosäuren. Auf eine 2,3- oder 3,4-Dihydroxybenzoesäure- bzw. -phenylalkansäure-Struktur weisen vor allem die Farbreaktionen der Verbindung 4 mit 4-Aminoantipyrin und Luftsauerstoff sowie Bromkresolgrün hin. Substanz 5 dürfte aufgrund der dunkelbraunen Färbung mit 4-Aminoantipyrin und $K_3[Fe(CN)_6]$ keine Phenolcarbonsäure darstellen. Wahrscheinlicher ist hingegen das Vorliegen einer Hydroxyzimtsäure, da das Tricyanvinylphenolat-Ion farblich mit dem der Substanz 2 fast identisch ist.

Infolge des blaugrünen Tetracyanäthylen-π-Komplexes muß das Molekül mindestens noch einen weiteren als Elektronendonator fungierenden Substituenten enthalten. Substanz 6 gibt mit Tetracyanäthylen und nachfolgender NaOH-Behandlung nahezu die gleiche Farbreaktion wie Verbindung 4, so daß eine ähnliche Konstitution zu erwarten ist. Es läßt sich allerdings keine *o*-Dihydroxy-Gruppierung nachweisen. Die am meisten bewegliche Substanz zeigt Ketosäureeigenschaften. Auffallend ist das Ausbleiben sämtlicher Phenolreaktionen. *o*-Dinitrobenzol verursacht eine Braunfärbung, die nicht erklärt werden kann.

Eine spektroskopische Charakterisierung der mit den angeführten Sprühreagenzien differenzierten Substanzflecke bzw. -zonen ist durch die gleichzeitig mitverteilten Huminstoffe unmöglich (vgl. [4]). Deshalb schien nur die Überführung der Inhaltsstoffe des NaOH-Eluats in geeignete Derivate erfolgversprechend zu sein. Die Umsetzung mit 2,4-Dinitrofluorbenzol lieferte ein gelbes Reaktionsprodukt, das an Kieselgelschichten im System Cyclohexan/Cyclohexanol (75 : 10) in 6 Komponenten zerlegt werden konnte (s. Tab. II).

Aus dem IR-Spektrum der Substanz 1a läßt sich anhand des Quotienten aus den prozentualen Maximalabsorptionen der bei 1542 cm^{-1} liegenden NO_2-Bande und der Carbonylfrequenz ein Zahlenwert von 1,43 berechnen, der einem mit zwei Hydroxylgruppen substituierten Benzolkern entspricht [5]. Die Absorption bei 993 cm^{-1} und Schulter bei 1637 cm^{-1} zeigen den olefinischen Charakter an. Analoge Eigenschaften besitzt Substanz 2. Mit der Identität des Bis-DNP-Äthers der 3,4-Dihydroxyzimtsäure (Kaffeesäure) konnte diese Korrelation bestätigt werden. Substanz 2a gibt oberhalb 2400 cm^{-1} ein breites Absorptionsgebiet, das für Carboxylgruppen typisch ist. Im Bereich der paraffinischen CH-Valenzschwingungen tritt lediglich ein schwacher Peak zwischen 2858 und 2849 cm^{-1} auf. Die Anwesenheit von Methoxylgruppen wird durch die CH_3-Deformation bei 1473 cm^{-1} und intensive Bande der sym. COC-Valenzschwingung bei 1038 cm^{-1} bewiesen. Der Benzolkern der ursprünglichen Verbindung enthält aufgrund des »Quotienten« [5] von 1,01 nur eine OH-Funktion. Absorptionen bei 1642 und 984 cm^{-1} rühren von C=C-Valenz- und CH-Waggingschwingungen olefinischer Gruppierungen her. Somit ist das Verhalten dem der Substanz 5 ähnlich. Von den verbleibenden Strukturvarianten zeigt das Spektrum des DNP-Äthers der 4-Hydroxy-3-methoxyzimtsäure (Ferulasäure) einen kongruenten Kurvenverlauf. Die Olefinbanden bei 1640 und 991 cm^{-1} und der »Quotient« von 1,06 charakterisieren Substanz 3a im Zusammenhang mit der OH-Valenzabsorption der Carboxylgruppe als Derivat einer Monohydroxyzimtsäure. Tatsächlich liefert der DNP-Äther der *p*-Hydroxyzimtsäure (*p*-Cumarsäure) ein identisches Spektrum. Die reine Verbindung besitzt fast den gleichen R_F-Wert wie Ferulasäure und ist daher im Substanzfleck 5 mitenthalten. Im Spektrum des DNP-Derivates 4a wird das Auffinden aliphatischer CH-Valenzschwingungen durch das breite OH-Absorptionsgebiet

Tabelle I

Farbreaktionen des chromatographierten NaOH-*Extraktes*

Substanzfleck (Nr.) R_F-Wert × 100	1 11	2 19	3 25	4 38	5 44	6 50	7 63	8 89
p-Nitrobenzoldiazonium-fluoroborat	orange +++	hellbraun +++	violett ++	braun +++	rotbraun ++	graubraun +++	oliv ++	
4-Aminoantipyrin + $K_3[Fe(CN)_6]$	++	++		++	dunkelbraun +	+++		
4-Aminoantipyrin + Luftsauerstoff [3] Tetracyanäthylen				+++	blaugrün ++			
Tetracyanäthylen + NaOH	braun ++	blaugrün ++		weinrot +++	blau +++	rot ++		
2,6-Dibromchinonchlorimid + 0,1 *N* NaOH	++	++		grün ++	++	++		
Diphenylpikrylhydrazyl		+++		+++				
$TiCl_3$ + Pyridin + CH_3OH		+++		++				
$TiCl_4$ + Pyridin + CH_3OH		++		+				
$TiCl_3$ + CH_3OH		rotbraun ++		braun ++				
o-Dinitrobenzol		rotviolett +++		rotviolett +++				braun +++
Bromkresolgrün	+++	+++	+++	+++	+++	+++	+++	+++
2,4-Dinitrophenylhydrazin	++		+++				+++	+++

+++ = stark positiv ++ = positiv + = schwach positiv

der Carboxylgruppe mit einzelnen Maxima erschwert. Andererseits geben die CH_3-Deformationsbande bei 1472 cm^{-1} und der intensive Peak der sym. COC-Valenzschwingung bei 1032 cm^{-1} einen sicheren Hinweis für das Vorhanden-

Tabelle II

Dünnschichtchromatographie der DNP-*Äther des* NaOH-*Eluats*

Substanz	R_F-Wert × 100
1a	20
2a	29
3a	37
4a	54
5a	61
6a	69

Tabelle III

Im Rahmen dieser Arbeit hergestellte Vergleichssubstanzen, die bisher in der Literatur nicht bekannt sind

Nr.	Verbindung	Summenformel (Mol.—Gew.)	Analyse			F. °C (Lsgm.)
			ber. C gef.	H	N	
1a	3,4-Bis-[2,4-dinitrophenoxy]-zimtsäure	$C_{21}H_{12}N_4O_{12}$ (512,4)	49,23 49,35	2,36 2,32	10,94 10,79	120—123 (Eisessig/Wasser)
2a	4-[2,4-Dinitrophenoxy]-3-methoxyzimtsäure	$C_{16}H_{12}N_2O_8$ (360,3)	53,34 53,64	3,36 3,38	7,78 7,53	266 (Zers.) (Essigester/Cyclohexan)
3a	4-[2,4-Dinitrophenoxy]-zimtsäure	$C_{15}H_{10}N_2O_7$ (330,3)	54,54 54,26	3,05 3,11	8,48 8,51	238 (Zers.) (Aceton/Wasser)
6a	3,4-Bis-[2,4-dinitrophenoxy]-benzoesäure	$C_{19}H_{10}N_4O_{12}$ (486,3)	46,09 46,49	2,07 2,02	11,52 11,53	125—127 (DMF/verd. Essigsäure)

Für die bereits von GRASSMANN und Mitarb. [18] dargestellte 4-[2,4-Dinitrophenoxy]-3-methoxybenzoesäure [F. 185° (Chloroform)] ermittelten wir einen abweichenden Schmelzpunkt [F. 220—222° (Äthanol/Wasser)].

sein von Methoxylgruppen. Aus dem Zahlenwert des »Quotienten« von 0,99 läßt sich eine mit 2,4-Dinitrofluorbenzol verätherbare Hydroxylfunktion pro Benzoleinheit ableiten. Diese Parameter entsprechen dem Verhalten der Substanz 6. Durch Spektrenvergleich konnte die Struktur der DNP-Vanillinsäure sichergestellt werden. Substanz 5a ergibt einen »Quotienten« von 1,05 sowie eine breite, von der Carboxylgruppe herrührende OH-Bande und erfüllt damit ebenfalls die Bedingungen des Substanzfleckes 6. Der DNP-Äther der *p*-Hy-

droxybenzoesäure zeigt in den spektralen Eigenschaften völlige Übereinstimmung. Das am schnellsten wandernde Derivat 6a weist keine aliphatischen CH-Absorptionen auf. Ferner korreliert der »Quotient« von 1,56 mit den Strukturindizes der Substanz 4. Somit stehen lediglich 2,3- oder 3,4-Dihydroxybenzoesäure zur Diskussion. Letztere Verbindung liefert in Form des Bis-DNP-Äthers ein kongruentes Spektrum.

Hydrogenolyse der Ketosäure-2,4-dinitrophenylhydrazone des NaOH-Eluats zu Aminosäuren

Aus dem entionisierten NaOH-Eluat lassen sich 2,4-Dinitrophenylhydrazone ausfällen, die größtenteils saure Eigenschaften besitzen. Eine Identifizierung der Ketosäurederivate gelingt durch Hydrogenolyse [6] zu den entsprechenden Aminosäuren, die chromatographisch leicht bestimmt werden können. Nach dieser Methodik erhält man ein Aminosäuregemisch, das sich an luftgetrockneten Kieselgelschichten bei zweidimensionaler Arbeitsweise in den Laufmittelsystemen $CHCl_3/CH_3OH$/17proz. NH_3 (2 : 2 : 1 v/v) und Phenol/Wasser (75 : 15 g/g) [7] in Glutaminsäure, Serin, Glykokoll, Asparaginsäure, Alanin, γ-Aminovaleriansäure, Tyrosin und 4-Hydroxy-3-methoxyphenylalanin auftrennen läßt. Die Aminosäuren resultieren aus den 2,4-Dinitrophenylhydrazonen von α-Ketoglutar-, Hydroxybrenztrauben-, Glyoxyl-, Oxalessig-, Brenztrauben-, Lävulin-, *p*-Hydroxyphenylbrenztrauben- und 4-Hydroxy-3-methoxyphenylbrenztraubensäure.

Diskussion

Aus dem NaOH-Eluat der an alkalisch aktiviertem Wofatit E selektiv adsorbierten Torffulvosäurefraktion wurden *p*-Hydroxybenzoe-, Vanillin-, *p*-Hydroxyzimt-, Ferula- und Protocatechusäure in Form von Derivaten abgeschieden. Damit gelang erstmalig der Nachweis dieser Ligninspaltstücke in einem Torfheißwasserextrakt [8]. Kürzlich identifizierten CHESHIRE und Mitarb. [9] bei der Behandlung einer Torfhuminsäure mit Wasser bzw. Salzsäure unter verschiedenen Bedingungen Vanillin-, Syringa- und Protocatechusäure. Bisher waren derartige Verbindungen nur durch alkalische Hydrolyse [10] oder oxydativen Abbau [11] von Torf erhältlich. Die Stellung der Ligninspaltprodukte im Humifizierungsprozeß ist bereits umfassend abgehandelt worden [12]. Ein analoges Reaktionsverhalten ist auch für die im NaOH-Eluat nachweisbare Kaffeesäure zu erwarten. Letztere Verbindung ist im Pflanzenreich weit verbreitet und findet sich fast immer in auffallend hohen Konzentrationen in verwesendem Pflanzenmaterial. Durch Hydrogenolyse

der sauren 2,4-Dinitrophenylhydrazone gelang die Identifizierung zahlreicher Ketosäuren. Bemerkenswert ist die in Torffulvosäuren vorkommende 4-Hydroxy-3-methoxyphenylbrenztraubensäure, die von NORD und Mitarb. [13], [14] beim mikrobiellen Fichtenligninabbau als Intermediärprodukt erkannt wurde. Unter Berücksichtigung des Lignins der Gräser und Moose dürfte *p*-Hydroxyphenylbrenztraubensäure eine analoge Stellung einnehmen. Daneben ist ihre Bildung durch oxydative Desaminierung von Tyrosin denkbar. An Protocatechusäure wird in Gegenwart von Bakterien wie Pseudomonas fluorescenz, die beim Torfbildungsvorgang bedeutungsvoll sind, enzymatisch Sauerstoff addiert, wobei die entstehende Carboxymuconsäure unter formaler Wasseranlagerung und Abspaltung von CO_2 in β-Ketoadipinsäure übergeht [15]. Da aber β-Ketosäuren unbeständig sind und leicht decarboxylieren, wäre die Folgereaktion zu Lävulinsäure, die sich im NaOH-Eluat nachweisen läßt, verständlich. Bei der durch Sauerstofftransferasen verursachten Spaltung des Benzolringes erhielten FUKUZUMI und Mitarb. [16] u. a. α-Ketoglutarsäure, die ebenfalls von uns in der Torffulvosäurefraktion aufgefunden wurde. Als weitere Bildungsmöglichkeit kommt die oxydative Desaminierung von Glutaminsäure in Frage. Derselbe Syntheseweg ist auch für Glyoxyl-, Brenztrauben-, Hydroxybrenztrauben- und Oxalessigsäure diskutabel. Diese Verbindungen können den Mikroorganismen als Kohlenstoffquelle dienen. Andererseits stellten MORTENSEN und MARCUSIU [17] in 6*N* HCl-Hydrolysaten bodenorganischer Substanz α-Ketosäuren fest, so daß deren Beteiligung am Aufbau der Humusstoffe nicht auszuschließen ist.

Experimentelle Methodik

Die Isolierung und Fraktionierung der Fulvosäuren, die chromatographischen Trennoperationen einschließlich Transfer DC → IR sowie die Abscheidung der 2,4-Dinitrophenylhydrazone erfolgten nach der bereits publizierten Vorschrift [1].

Darstellung der DNP-Äther

1g Extrakt des entionisierten NaOH-Eluats löst man zusammen mit 390 mg 2,4-Dinitrofluorbenzol in 30 ml DMF, fügt 10 ml Wasser zu und stellt mit festem $NaHCO_3$ einen pH-Wert von 7—7,5 ein. Nach Stehen der Mischung über Nacht werden 20 ml Äthanol und 140 ml Wasser mit einmal zugegeben, wobei sich der ursprüngliche Niederschlag auflöst. Die klare Lösung fällt man mit 2*N* CH_3COOH vorsichtig bei stetem Rühren und fügt am Ende 2*N* HCl bis pH 3 zu. Sofern die Fällung langsam erfolgt, erhält man ein gut filtrierbares Produkt, das abgesaugt, mit wenig 50 proz. Methanol und viel Wasser ausgewaschen und im Vakuumexsikkator über P_2O_5 getrocknet wird. Zur Dünnschichtchromatographie verwendet man acetonische Lösungen.

LITERATUR

1. WILDENHAIN, W., HENSEKE, G.: J. Prakt. Chem. **312**, 690 (1970)
2. WILDENHAIN, W., HENSEKE, G.: Z. Anal. Chem. **229**, 271 (1967)
3. LA RUE, T. A., BLAKLEY, E. R.: Anal. Chim. Acta **31**, 400 (1964)
4. MAEDER, H.: Dissertation, Univ. Gießen 1960

5. WILDENHAIN, W., HENSEKE, G.: Z. Chem. **7**, 425 (1967)
6. ALFTHAN, M., VIRTANEN, A. I.: Acta Chem. Scand. **9**, 186 (1955)
7. RANDERATH, K.: Dünnschicht-Chromatographie. Verlag Chemie, Weinheim/Bergstr., 1962
8. WILDENHAIN, W., HENSEKE, G.: Z. Chem. **5**, 457 (1965)
9. CHESHIRE, M. V., CRANWELL, P. A., FALSHAW, C. P., FLOYD, A. J., HAWORTH, R. D.: Tetrahedron **23**, 1669 (1967)
10. MORITA, H.: Can. J. Biochem. Physiol. **43**, 1277 (1965)
11. MORITA, H.: J. Org. Chem. **27**, 1079 (1962)
12. WILDENHAIN, W.: Freiberger Forschungsh. A447 (1969)
13. ISHIKAWA, H., SCHUBERT, W. J., NORD, F. F.: Arch. Biochem. Biophys. **100**, 131 (1963)
14. NORD, F. F.: Tappi **47**, 624 (1964); Geochim. Cosmochim. Acta **28**, 1507 (1964)
15. STANIER, R. Y., INGRAHAM, J. L.: J. Biol. Chem. **210**, 799 (1954)
16. FUKUZUMI, T., MINAMI, K., SCHIBAMOTO, S.: J. Japan Wood Res. Soc. [Nippon Mokuzai Gakkaishi] **5**, 96 (1959)
17. MORTENSEN, J. L., MARCUSIU, E. C.: Soil Sci. Soc. Am. Proc. **27**, 653 (1963)
18. GRASSMANN, W., ENDRES, H., BROCKHAUS, R., MERKLE, K.: Chem. Ber. **90**, 2416 (1957)

Wolfgang WILDENHAIN
Günter HENSEKE
92 Freiberg (Sachs.), Leipziger Straße. DDR.

Acta Chimica Academiae Scientiarum Hungaricae, Tomus 74 (1), pp. 87–97 (1972)

AROMATIC SULFENYL CHLORIDES, V

REACTION OF SULFENYL CHLORIDE WITH N²-ARYLDITHIOCARBAZATES, O-ALKYL-THIOCARBAZATES AND O-ARYL SUBSTITUTED PHENYLTHIOCARBAMATES

F. KLIVÉNYI, G. STÁJER, E. A. SZABÓ, J. PINTYE and E. VINKLER

(Institute of Pharmaceutical Chemistry, Medical University, Szeged)

Received June 17, 1971

The reactions of *p*-toluenesulfenyl chloride with ammonium N²-aryldithiocarbazates, O-ethyl-thiocarbazate esters and O-aryl arylthiocarbamate esters were examined. IR spectroscopic analysis of the products revealed that the arylsulfenyl cation attacked at the sulfur atom in all cases. The reaction of thiocarbazate esters was accompanied by elimination of alkyl halide to give S-aryl substituted dithiopercarbazate esters. The sulfenylation reaction did actually proceed with O-aryl arylthiocarbamate esters in the above depicted manner only if the O- or the N-aryl ring contained substituent(s) in the *ortho* position allowing the formation of the thiol tautomer and a stable disulfide.

As a continuation of investigations on the sulfenylation reaction by means of *p*-toluenesulfenyl chloride **(I)** of compounds containing sulfur and nitrogen, the present communication deals with the reactions of dithiocarbazate salts, O-alkyl-thiocarbazates and O-arylthiocarbamates. The site of attack of the arylsulfenyl cation has been decided by infrared spectrometry.

Reaction of p-toluenesulfenyl chloride with N²-aryldithiocarbazates

Ammonium N²-aryldithiocarbazates **(II)** reacted smoothly with *p*-toluenesulfenyl chloride to give the corresponding S-*p*-tolyl-aryltrithiopercarbazates **(III)** in satisfactory yields (Eq. 1).

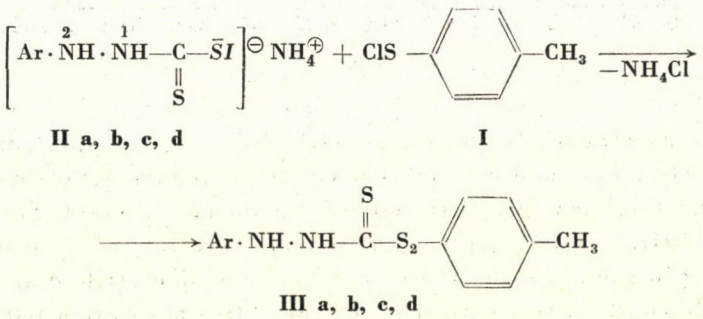

II a, b, c, d **I**

III a, b, c, d (1)

$Ar(a) = C_6H_5$; $Ar(b) = C_6H_4 \cdot Cl\,p$; $Ar(c) = C_6H_4Br\,p$; $Ar(d) = C_6H_4 \cdot NO_2\,p$

The spectra of the 'carbazates' **(II)** (*cf.*, *e.g.*, the spectrum of **IIa**; Fig. 1) possess the νNH_4^+, δNH_4^+, (νNH), βNH, $\nu C{=}S$, as well as the $\gamma C_{Ar}H$ and

$\gamma C_{Ar}C_{Ar}$ bands, characteristic of mono- (in the case of **IIa**) and *p*-disubstitution **(IIb, c, d)**, respectively. Presumably, the νNH_4^+, νNH, as well as the δNH_4^+ and $\nu C{=}S$ bands overlap and appear as such (*cf.* Table I).

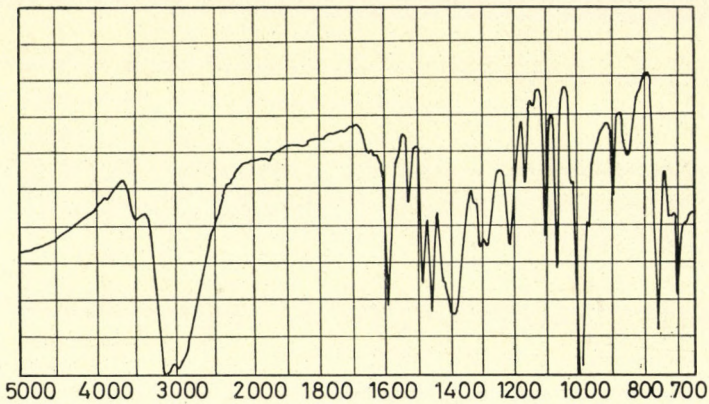

Fig. 1

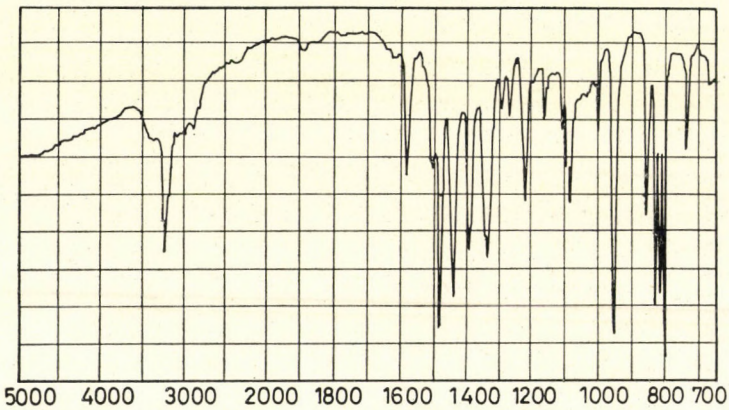

Fig. 2

In the spectra of 'trithio esters' **(III)** (*cf.*, *e.g.*, the spectrum of **IIIb**; Fig. 2), the stretching and deformation vibration frequencies of the NH_4^+ ion are missing, while the νNH, βNH and $\nu C{=}S$ bands are present. The spectrum of compound **IIIa** has a $\gamma C_{Ar}H$ band, proving the presence of a *p*-disubstituted benzene ring in the molecule. In the case of compounds **IIIb, c** and **d**, where the molecule contains two such benzene rings, two absorption bands appear in the region characteristic of *p*-disubstitution (*cf.*, *e.g.*, Fig. 2). Accordingly, sulfenylation has been accomplished and since similar spectra show that compounds **II** are transformed to analogous derivatives, the substitution could take place on the sulfur atom only (*cf.* Table I).

Table I

Some more important absorption bands in the infrared spectra of compounds **II**—**V** *recorded in KBr pellets*

Frequency, cm^{-1}	**IIa** Fig. 1	**IIIa**	**IIIb** Fig. 2	**IIIc**	**IIId**	**IV** Fig. 3	**V** Fig. 4
νNH_4^+	3350 2100	—	—	—	—	—	—
νNH	overlap with the νNH_4^+ band	3500 2700	3250	3450	3400 3200	3300 3200	3300 3200
βNH	1590	1490	1480	1480	1590	1480	1490
$\nu C=S$	overlap with the δNH_4^+ band	1340	1330	1330	overlap with the $\nu_s NO_2$ band	1340?	—
$\gamma C_{Ar}H$	760	750	—	—	—	750	740
$\gamma C_{Ar}C_{Ar}$ mono	700	690	—	—	—	700	690
$\gamma C_{Ar}H$ *p*-di	—	820	830 810 800	820 810 800	830 810	—	800
$\nu_s C—O—C$	—	—	—	—	—	1240 1200	—
$\nu_{as} C—O—C$						1050	
$\nu_{as} NO_2$	—	—	—	—	1510 1360	—	—
$\nu_s NO_2$					1300		
ν amide I	—	—	—	—	—	—	1680 1650

The strong absorption band appearing at 995—945 cm^{-1} in the spectrum of compounds **IIIa, b, c, d** can most probably be assigned to the (NH)—NH—C—(S)—S— group. The corresponding band appears in the spectrum of compound **II** at 1000 cm^{-1}.

Reaction of p-toluenesulfenyl chloride with O-ethyl-thiocarbazate

According to HARRIS [1] the reaction of N-substituted ethyl-thiocarbamates and sulfenyl chloride gives rise to substitution at the sulfur atom with simultaneous elimination of ethyl chloride to give compounds of the 'carbamoyl disulfide' type. In his opinion the temporarily formed hydrogen chloride is responsible for the above reaction, as the ester group is not split off in the presence of pyridine.

According to our experiments, ethyl N^2-phenyl-thiocarbazate **(IV)** reacts similarly with *p*-toluenesulfenyl chloride in respect of the overall change, but

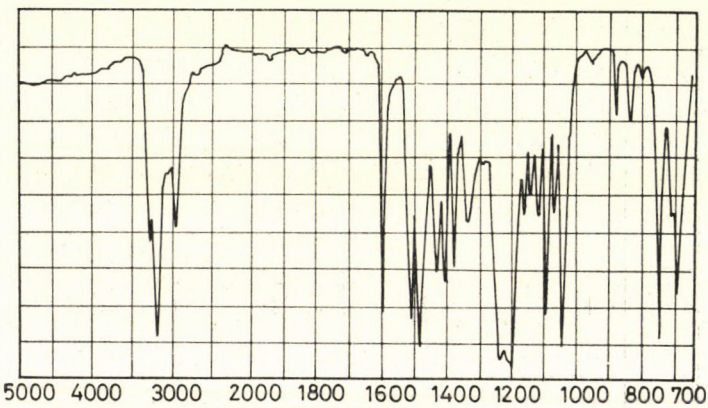

Fig. 3

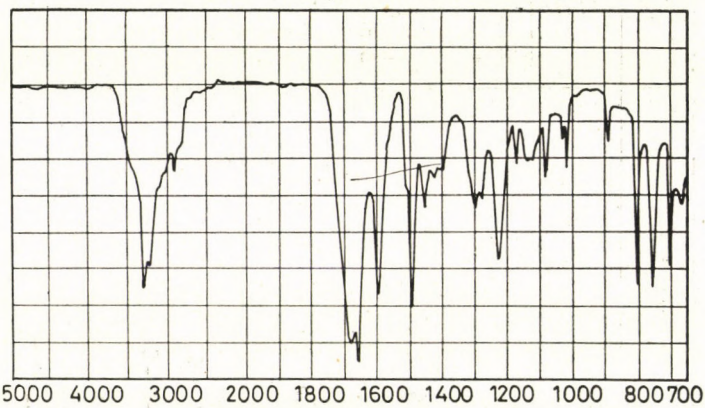

Fig. 4

the elimination of ethyl chloride occurs in the presence of pyridine, too (Eq. 2). Hence the reaction proceeds proably by a different route and even the assumption of the intermediary formation of sulfenate ester (—C(S)—O—S—Ar) seems reasonable.

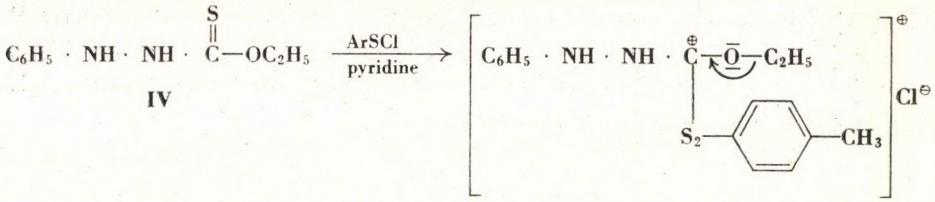

(2)

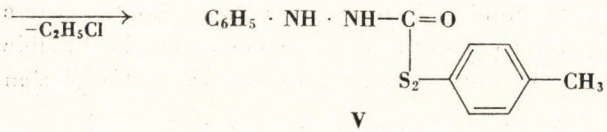

In the spectrum of compound **IV** (*cf.* Fig. 3) there appear the νNH, βNH, νC—O—C, νC=S, and the $\gamma C_{Ar}H$ and $\gamma C_{Ar}C_{Ar}$ bands characteristic of monosubstitution. The elementary composition of the sulfenylated product **(V)** does not depend on whether the reaction is accomplished in the presence or

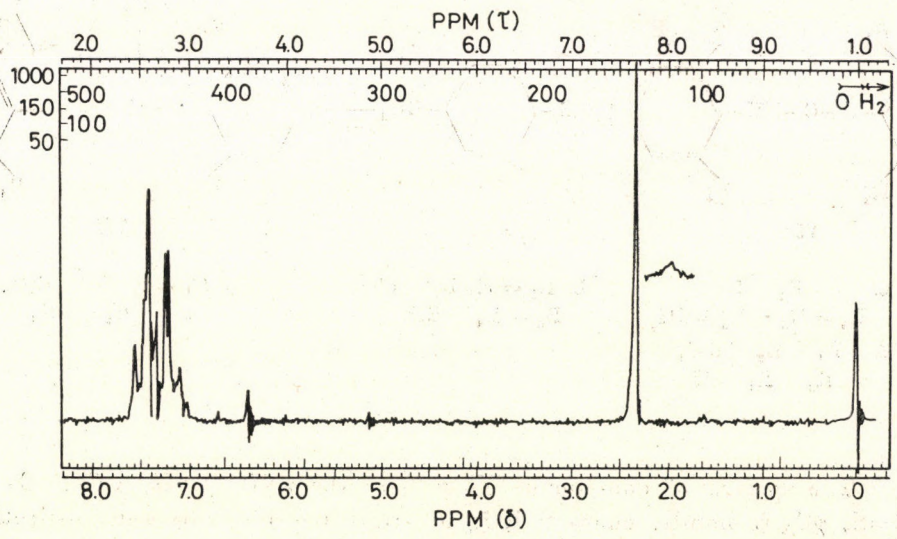

Fig. 5

in the absence of pyridine. As a proof of the presumed structure of compound **V**, the bands associated with the vibrations of the ethoxyl and the thiocarbonyl groups, present in the spectrum of the starting material, are missing from the spectrum of the product, while the amide-I band and the $\gamma C_{Ar}H$ band indicating the incorporation of a *p*-disubstituted benzene ring are present (*cf.* Fig. 4). The absence of the ethoxyl group is also proved by the NMR spectrum (Fig. 5), which is devoid of the characteristic triplet (methyl) and quartet (methylene) signals of the ethyl group (δCH_3 singlet 2.34 ppm, ArH multiplet 420—460 H_2(9H), δNH $\sim$ 10.3 ppm).

Reaction of p-toluenesulfenyl chloride with O-aryl substituted phenylthiocarbamates

It appeared to be of interest to examine the sulfenylation reaction of the various substituted and sterically hindered O-aryl arylthiocarbamate esters **(VI)** prepared by WALTER and BODE [2] and to decide whether the aryl halide elimination reaction observed by HARRIS [1] occurs during the sulfenylation reaction.

It has been observed that the reaction of O-aryl-N-arylthiocarbamate esters **(VI)** with *p*-toluenesulfenyl chloride gives rise to the formation of the corresponding O-(phenyl)-N-aryl-S-(*p*-toluenesulfenyl)-isothiocarbamates **(VII)** (Eq. 3).

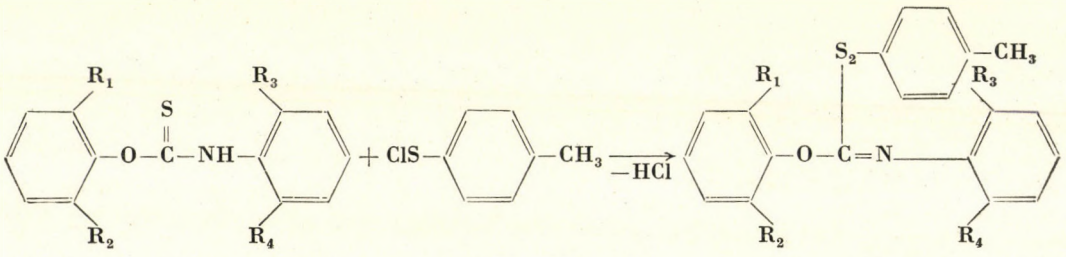

VI **I** **VII** (3)

a. $R_1 = H$, $R_4 = R_2 = R_3 = CH_3$

b. $R_1 = H$, $R_2 = Cl$, $R_3 = R_4 = CH_3$

c. $R_1 = H$, $R_2 = C_6H_5$, $R_3 = R_4 = CH_3$

d. $R_1 = R_2 = CH_3$, $R_3 = R_4 = H$

The spectra of compounds **VI** possess the νNH, βNH, $\nu_s C_{Ar}$—O—C, νC=S, $\gamma C_{Ar}H$ bands, characteristic of trisubstitution and *o*-disubstitution (*cf.*, *e.g.*, the spectrum of **VIa**, Fig. 6, and Table II).

The thioamide group frequencies are missing in the spectrum of compounds **VII** (*cf.*, *e g.*, the spectrum of compound **VIIa**, Fig. 7). On the other hand, the stretching vibration of a conjugated C=N double bond, as well as the $\gamma C_{Ar}H$ band characteristic of *p*-disubstitution appear.

On basis of these infrared spectroscopic data the conclusion may be drawn that also in this case sulfenylation process is at the sulfur atom, but the elimination of aryl halide does not accompany the reaction.

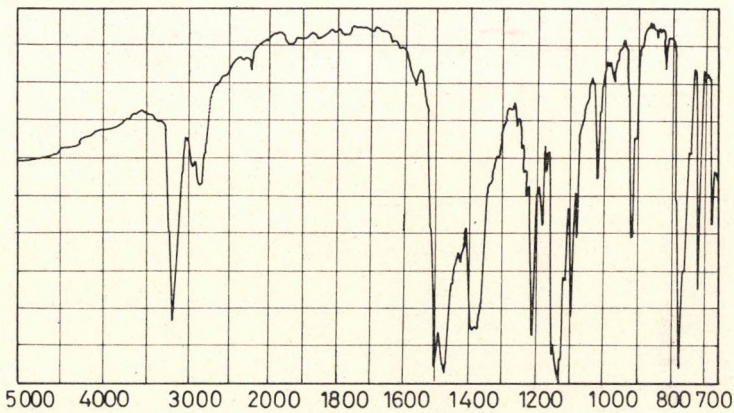

Fig. 6

The sharp absorption band appearing at 930—920 cm^{-1} in the spectrum of compounds **VI** is presumably associated with the thiourethane group.

The absorption band at 910—890 cm^{-1} in the spectrum of compounds **VII** is also associated with the vibration of the —S—C(O—)=N group the displacement towards lower vibration being the consequence of sulfenylation.

It was observed in further experiments that O-phenyl N-arylthiocarbamates which possess both of the unsubstituted phenyl group (**VI**; $R_1=R_2=R_3=R_4=H$) give rise on sulfenylation to rather unstable products. In the reaction mixture phenol, phenylisothiocyanate and *p*-tolyl-disulfide, beside unchanged starting material were identified by thin-layer chromatography.

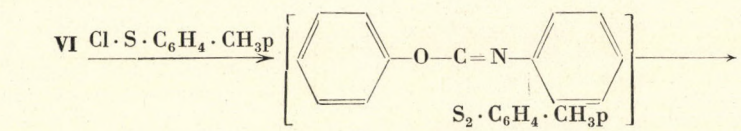

(4)

$$\longrightarrow C_6H_5OH + C_6H_5{-}N{=}C{=}S + (CH_3 \cdot C_6H_4 \cdot S)_2 + C_6H_5 \cdot O \cdot \underset{\displaystyle NH \atop \displaystyle |\ \ \ \

Table II

Some more important absorption bands in the infrared spectra of compounds **VI—VII** *recorded in KBr pellets*

Frequency, cm^{-1}	**VIa** Fig. 6	**VIb**	**VIc**	**VId**	**VIIa** Fig. 7	**VIIb**	**VIIc**	**VIId**
νNH	3180	3200	3250	3100	—	—	—	—
βNH	1470	1470	1470	1540	—	—	—	—
$\nu_s C_{Ar}$—O—C	1160—1120	1130	1170—1120	1160—1140	1140—1120	1140—1100	1140—1100	1200—1120
νC = S	1210?	1390?	1250, 1220?	1360	—	—	—	—
νC = N	—	—	—	—	1640	1630	1650	1640
$\gamma C_{Ar}H$ tri-	770	760	770	770	780 770	770 760	780 770	770 760
$\gamma C_{Ar}H$ *o*-di-	overlap	730	740	—	740	730	740	—
$\gamma C_{Ar}H$ *p*-di-	—	—	—	—	800	800	810	810
$\gamma C_{Ar}H$	—	—	—	740	—	—	—	—
$\gamma C_{Ar}C_{Ar}$ mono-	—	—	—	690	—	—	—	700

These results support the assumption that substitution in the *ortho* position of both the O-phenyl and N-phenyl rings renders possible or facilitates the formation of stable disulfides.

Experimental

All melting points are uncorrected. The IR spectra were recorded with a Spectromom 2000 instrument in potassium bromide pellets.

S-*p*-Tolyl N²-phenyltrithiopercarbazate (IIIa)

A solution of 3.2 g (0.02 mole) *p*-toluenesulfenyl chloride in 30 ml ether was added dropwise with stirring to a suspension of 4.0 g (0.02 mole) ammonium N²-phenyldithiocarbazate [3] in 50 ml dry ether at room temperature, the mixture was stirred until the red colour of the solution vanished and then filtered. The filtrate was evaporated to give 2.8 g (46%) residue, which was crystallized from benzene to obtain brownish-white lustrous needles, m.p. 90—95 °C (unsharp).

$C_{14}H_{14}N_2S_3$ (306.47). Calcd. C 54.87; H 4.60; N 9.14. Found C 54.88; H 4.62; N 8.94%.

S-*p*-Tolyl N²-(p-chlorophenyl)-trithiopercarbazate (IIIb)

4.7 g (0.02 mole) ammonium N²-(*p*-chlorophenyl)-dithiocarbazate was treated with 3.2 g (0.02 mole) *p*-toluenesulfenyl chloride as described in the first experiment to give 3.1 g (46%) of the crude product, which was crystallized from a 2 : 10 : 1 mixture of benzene–petroleum ether–abs. ethanol to obtain yellowish-white slack needles, m.p. 111—113 °C.

$C_{14}H_{13}ClN_2S_3$ (340.9). Calcd. C 49.33; H 3.84; N 8.22. Found C 49.17; H 3.81; N 8.25%.

S-*p*-Tolyl N²-(p-bromophenyl)-trithiopercarbazate (IIIc)

5.6 g (0.02 mole) ammonium N²-(*p*-bromophenyl)-dithiocarbazate was treated with 3.2 g (0.02 mole) *p*-toluenesulfenyl chloride as described in the first experiment and the reaction mixture worked up similarly to give 3.5 g (45%) crude product. Recrystallization from a 2 : 10 : 1 mixture of benzene–petroleum ether–abs. ethanol gave pale yellow lustrous needles, m.p. 113—114 °C (d).

$C_{14}H_{13}BrN_2S_3$ (385.35). Calcd. C 43.64; H 3.40; N 7.27. Found C 43.56; H 3.53; N 7.38%.

S-*p*-Tolyl N²-(*p*-nitrophenyl)-trithiopercarbazate (IIId)

2.4 g (0.01 mole) ammonium N²-(*p*-nitrophenyl)-dithiocarbazate was treated with 1.6 g (0.01 mole) *p*-toluenesulfenyl chloride in abs. ether as described in the first experiment to give, after working up of the reaction mixture, 1.4 g (39%) crude product. Recrystallization from a 3 : 5 : 1 mixture of benzene–petroleum ether–ethanol gave a red powder, m.p. 132—134 °C (d).

$C_{14}H_{13}N_3O_2S_3$ (351.46). Calcd. C 47.84; H 3.73; N 11.96. Found C 47.95; H 4.08; N 11.53%.

S-*p*-Tolyl N²-phenyldithiopercarbazate (V)

3.9 g (0.02 mole) O-ethyl N²-phenylthiocarbazate [4] was dissolved in 50 ml abs. ether and the solution treated dropwise with a solution of 3.2 g (0.02 mole) *p*-toluenesulfenyl chloride in ether. (In a parallel experiment the ethereal ester solution was mixed with 2 g pyridine before addition of the sulfenyl chloride.) After vanishing of the red colour, the solutions were washed successively with 1 *N* HCl and water until neutral, dried and evaporated. The residue was 3.5 g (60%) in both cases. Crystallization from benzene–petroleum ether (1 : 3) gave colourless needles, m.p. 140—142 °C (decomposition with gas evolution).

$C_{14}H_{14}N_2OS_2$ (290.4). Calcd. C 57.90; H 4.80; N 9.65. Found C 58.17; H 5.00; N 9.49%.

O-(2'-Phenylphenyl) S-(*p*-toluenesulfenyl)-2,6-dimethylphenylisothiocarbamate (VIIc)

6.67 g (0.02 mole) O-(2'-phenylphenyl) 2,6-dimethylphenylthiocarbamate [2b] was treated with 3.2 g (0.02 mole) *p*-toluenesulfenyl chloride as described in the first experiment

and the reaction mixture was worked up similarly with the only modification that the ethereal solution was washed with water until free of acid and dried. Evaporation of the solvent gave 6.1 g (67%) crude product. Crystallization from benzene–petroleum ether (1 : 2) yielded colourless lustrous prisms, m.p. 74—75 °C.

$C_{28}H_{25}NOS_2$ (455.64) Calcd. C 73.81; H 5.54; N 3.07; S 14.07. Found C 74.14; H 5.73; N 2.87; S 13.72%.

O-(2'-Methylphenyl) S-(*p*-toluenesulfenyl)-2,6-dimethylphenylisothiocarbamate (VIIa)

5.4 g (0.02 mole) O-(2'-methylphenyl) 2,6-dimethylphenylthiocarbamate [5] was allowed to react with 3.2 g (0.02 mole) *p*-toluenesulfenyl chloride as described in the preparation of **V** and worked up similarly. Evaporation of the solvent left a viscous oil, which was chromatographed on a silica gel column with a 1 : 1 mixture of benzene and petroleum ether. The medium fraction solidified on standing overnight. The crude product weighed 4.4 g (56%). Recrystallization from petroleum ether gave colourless needles, m.p. 68—69°C.

$C_{23}H_{23}NOS_2$ (393.57). Calcd. C 70.20; H 5.89; N 3.56. Found C 70.12; H 6.10; N 3.47%.

O-(2'-Chlorophenyl) 2,6-dimethylphenylthiocarbamate (VIb)

24.2 g (0.2 mole) 2,6-dimethylaniline was allowed to react with 20.7 g (0.1 mole) O-(2'-chlorophenyl) chlorothiocarbonate [2a] as described by WALTER and BODE [5] to give 15 g (51%) crude product. Recrystallization from benzene–alcohol–petroleum ether (1 : 1 : 2) yielded colourless lustrous needles, m.p. 130—140 °C (unsharp).

$C_{15}H_{14}ClNOS$ (291.8). Calcd. C 61.74; H 4.84; N 4.80. Found C 61.94; H 4.95; N 5.01%.

O-(2'-Chlorophenyl) S-(*p*-toluenesulfenyl)-2,6-dimethylphenylisothiocarbamate (VIIb)

5.8 g (0.02 mole) O-(2'-Chlorophenyl) 2,6-dimethylphenylthiocarbamate **(VIb)** was reacted with 3.2 g (0.02 mole) *p*-toluenesulfenyl chloride as described in the preparation of **V** and the reaction mixture worked up similarly to give 3.9 g (47%) crude product. Recrystallization from benzene–petroleum ether (1 : 2) resulted in colourless needles, m.p. 98—100 °C.

$C_{22}H_{20}ClNOS_2$ (413.99). Calcd. C 63.83; H 4.87; N 3.38. Found C 64.17; H 5.03; N 3.53%.

O-(2,6-Dimethylphenyl) S-(*p*-toluenesulfenyl)-phenylisothiocarbamate (VIId)

5.14 g (0.02 mole) O-(2,6-dimethylphenyl) N-phenylthiocarbamate [2a] was treated with 3.2 g (0.02 mole) *p*-toluenesulfenyl chloride as described in the preparation of **V** and the reaction mixture worked up similarly to give 4.1 g (54%) crude product. Recrystallization from petroleum ether gave colourless lustrous needles, m.p. 85—86 °C.

$C_{22}H_{21}NOS_2$ (379.52). Calcd. C 69.62; H 5.58; N 3.69. Found C 69.92; H 5.65; N 3.50%.

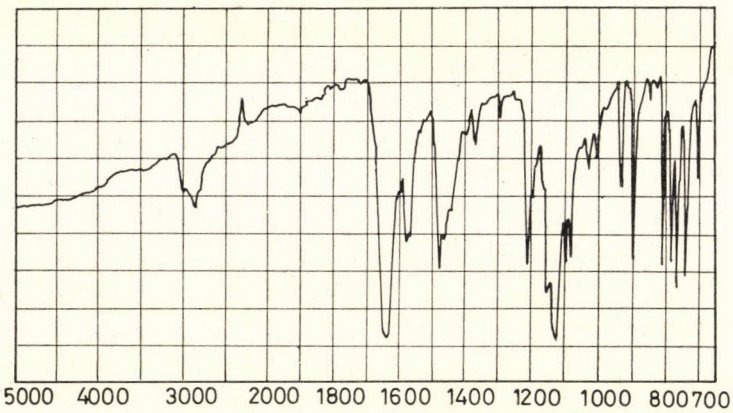

Fig. 7

Reaction of *p*-toluenesulfenyl chloride with O-aryl-N-aryl-thiocarbamates (VI)

2.3 g (0.01 mole) O-(aryl)-N-aryl-thiocarbamates **(VI)**, 0.8 g pyridine and 1.6 g (0.01 mole) *p*-toluenesulfenyl chloride were reacted and worked up similarly as described in the preparation of **V** to give a redbrown oil. A sample of it parallel with authentic substances, was

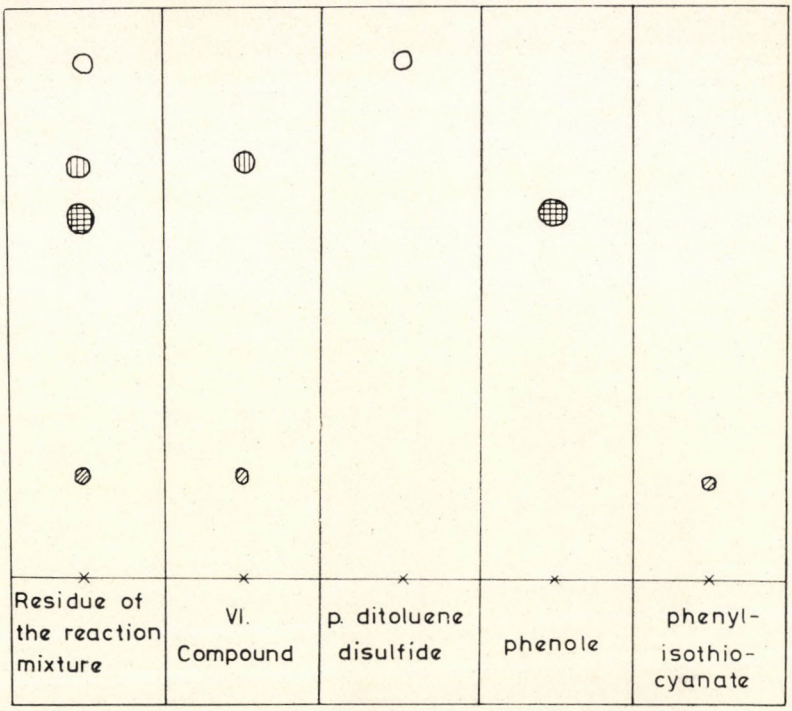

Fig. 8

tested by thin-layer chromatography. Absorbent: Kieselgel GF_{254} Merck; solvent: petroleum ether–ethylacetate (5 : 1).

Developing: the plate was placed in chlor-gas, and sprayed with *o*-toluidine (added KI) in water–acetic acid (cf. Fig. 8).

*

The authors are indebted to Dr. P. Sohár, C. Sc., for his valuable comments on the IR and NMR spectra as well as for his precious suggestion concerning the structure of compound **V**.

REFERENCES

1. Harris, J. F.: J. Am. Chem. Soc. **82,** 155 (1960)
2. Walter, W., Bode, K. D.: *(a)* Ann. **681,** 71 (1965); *(b)* **692,** 111 (1966)
3. Heller, G., Bauer, W.: J. pract. Chem. **65,** 382 (1902)
4. Wheeler, H. L., Barnes, B.: Am. Chem. Journal **24,** 65 (1900); ref. C. II 583 (1900)
5. Walter, W., Bode, K. D.: Ann. **698,** 122—130 (1966)

Ferenc Klivényi
Géza Stájer
Enikő A. Szabó
János Pintye
Elemér Vinkler
Szeged, P. O. Box 121, Hungary

Acta Chimica Academiae Scientiarum Hungaricae, Tomus 74 (1), pp. 99—113 (1972)

CONVERSIONS OF TOSYL AND MESYL DERIVATIVES OF THE MORPHINE GROUP, X*

14-HYDROXYMORPHINE DERIVATIVES, I. AZIDO AND AMINO COMPOUNDS

S. MAKLEIT, L. RADICS,** R. BOGNÁR, T. MILE and É. OLÁH

*(Institute of Organic Chemistry, L. Kossuth University, Debrecen and **Central Research Institute of Chemistry, Hungarian Academy of Sciences, Budapest)*

Received June 21, 1971

The azidolysis of the 6-O-tosylates and 6-O-mesylates of 14-hydroxycodeine was studied.

Several new saturated and unsaturated amino compounds were prepared from the new azido derivatives by various methods of reduction selected according to the structure of the starting material and the nature of the desired reduced product.

The azidolysis of 6-O-tosyl-14-hydroxycodeine carried out under various conditions can give both 6-deoxy-6-azido-14-hydroxyisocodeine and 8-deoxy-8-azido-14-hydroxypseudocodeine. The isolated 6-deoxy-6-azido compound can be isomerized to the 8-deoxy-8-azido derivative. The rate of isomerization is not affected by the addition of azide anion.

The experimental data support a new interpretation of the nucleophilic substitution reactions of the 6-O-tosyl and 6-O-mesyl derivatives of the morphine group according to which the C_8-pseudo derivatives, as thermodynamical isomers, are formed through the C_6-iso compounds, as kinetic products, quite independently of the possibility of isolation of the C_6-iso compounds. Thus, the conversions accompanied by allylic rearrangement take place in two steps, by an S_N2 and an S_Ni' reaction.

We published recently [1] a systematic study of the nucleophilic substitution reactions of 6-O-tosyl and 6-O-mesyl morphine derivatives carrying no substituent in position 14 (morphine, codeine, dihydromorphine and dihydrocodeine).

On the basis of the theoretical and practical pharmacological results of these experiments, it appeared desirable to study the similar reactions of morphine derivatives carrying a 14-positioned hydroxyl group.

In the present work the azidolysis of the 6-O-tosyl **(IIIa, IVa)** and 6-O-mesyl **(IIIb, IVb)** derivatives of 14-hydroxycodeine **(I)** and of 14-hydroxydihydrocodeine **(II)** is described. The preparation of 6-O-tosyl-14-hydroxycodeine **(IIIa)** and 6-O-tosyl-14-hydroxydihydrocodeine **(IVa)** and their nucleophilic substitution reactions with some anions ($Cl^{\ominus}$, $Br^{\ominus}$, $I^{\ominus}$, $H^{\ominus}$, $CH_3COO^{\ominus}$) have been reported by CURRIE *et al.* [2] and by SEKI [3].

However, the nucleophilic substitution reactions of a number of important anions such as the anion N_3 investigated by us, have not been studied; for this reason, the theoretical evaluation of the investigations carried out so far [2, 3] is, in our opinion, still incomplete.

* Part IX: R. BOGNÁR, S. MAKLEIT, T. MILE, L. RADICS: Monatsh. f. Chem. **103**, 143 (1972) and Magy. Kém. Foly. **78**, 163 (1972)

The course of our present investigations was as follows. Thebaine **(V)** was converted with hydrogen peroxide in acetic acid [4] or, more expediently in formic acid [3], into 14-hydroxycodeinone **(VI)**. This can be reduced with sodium borohydride in aqueous dioxan [2] in a stereospecific way to obtain 14-hydroxycodeine **(I)** which has its C-6 hydroxyl group in a *quasi-equatorial* position, *i.e.* in a position below the plane of the ring C of flat boat conformation [5]. When compound **(I)** is treated with *p*-toluenesulfonylchloride at 0°C

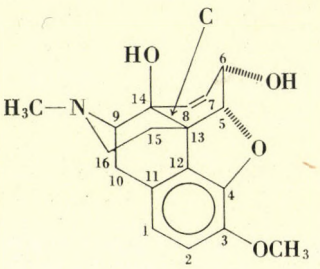

I

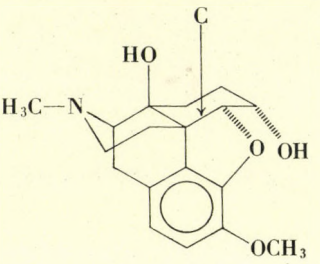

II

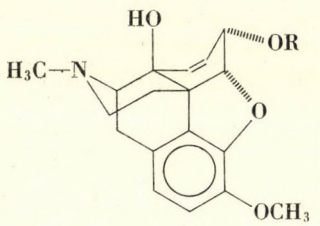

R = Ts: **IIIa**
R = Ms: **IIIb**

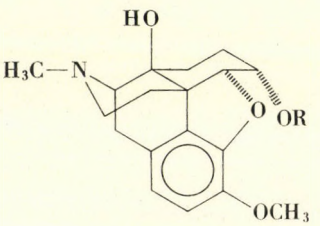

R = Ts: **IVa**
R = Ms: **IVb**

Fig. 1

in the presence of pyridine [2], 6-O-tosyl-14-hydroxycodeine **(IIIa)**, and similarly, with methanesulfonylchloride, the hitherto unknown 6-O-mesyl-14-hydroxycodeine **(IIIb)** is obtained.

When these compounds which are very suitable for nucleophilic substitution reactions [6] are treated with sodium azide in the dipolar aprotic solvent dimethylformamide, two products are formed depending upon the conditions of reaction: 6-deoxy-6-azido-14-hydroxyisocodeine **(VII)** is obtained at 100 °C in 4 hrs, whereas 8-deoxy-8-azido-14-hydroxypseudocodeine **(VIII)** is the product when the reaction is carried out at the same temperature but for 8 hrs.

This is the first case in the series of morphine alkaloids when both the $\alpha(\text{-}C_6)$ and $\beta(\text{-}C_8)$ isomers could be prepared from the same initial substance simply by altering the conditions of reaction.

By heating the isolated 6-deoxy-6-azido-14-hydroxyisocodeine **(VII)** for 6 hrs in dimethylformamide, it can be isomerized to 8-deoxy-8-azido-14-hydroxypseudocodeine **(VIII)**.

In our opinion, these experimental results are of prominent importance from the aspect of elucidating the mechanism of the nucleophilic substitution reactions of the 6-O-tosyl and 6-O-mesyl derivatives.

The reduction of the azido derivatives to amino derivatives was attempted in our experiments by several methods [7].

6-Deoxy-6-azido-14-hydroxyisocodeine **(VII)** was successfully reduced to 6-deoxy-6-amino-14-hydroxyisocodeine **(IX)** by the method developed for steroids by DREFAHL *et al.* [8], using hydrazine hydrate and Raney nickel. The similar reduction of the 8-azido derivatives **(VIII)** did not afford a homogeneous product; therefore reduction with lithium aluminium hydride was applied which gave 8-deoxy-8-amino-14-hydroxypseudocodeine **(XVII)**.

Concerning the above discussed reactions, it seems necessary to mention the following:

The conversion of 6-O-tosyl-14-hydroxycodeine **(IIIa)** and of 6-O-mesyl-14-hydroxycodeine **(IIIb)**, into 6-deoxy-6-azido-14-hydroxyisocodeine **(VII)** occurs according to an S_N2 mechanism. This is supported by the evidence listed below.

(*a*) The dipolar aprotic solvent dimethylformamide does not facilitate the cleavage of the tosyloxy group as an anion, which would result in the formation of the carbonium ion required for an S_N1 reaction, as this solvent, owing to its structure, does not solvate anions [9].

The carbonium ion which may occasionally form has the character of an allyl cation, the stability of which is, however, decreased by the inductive effect of the oxygen atom present in the dihydrofuran ring [10].

For the sodium azide used as a reagent, the applied solvent is favourable, because it solvates only the Na^+ cations and provides in this way the existence of "free" N_3 anions of a concentration required for the nucleophilic attack.

(*b*) In considering the steric position of the azido group, one must take into account, in the knowledge of the stereochemical properties of the molecule, that there is no steric hindrance to a substitution from the so-called 'iso-side'.

(*c*) Besides these rather general remarks, the chemical and stereochemical properties of 6-deoxy-6-azido-14-hydroxyisocodeine **(VII)** and thus also the mechanism of the reaction are unequivocally proved by the fact that the catalytic hydrogenation of **(VII)** affords 6-deoxy-6-amino-14-hydroxydihydroisocodeine **(X)** the structure of which has been proved.

(*d*) Lastly, the experience that compound **(VII)** can be isomerized to **(VIII)**, also confirms the suggested structure.

As regards the formation of 8-deoxy-8-azido-14-hydroxypseudocodeine **(VIII)**, this takes place by an S_N2 reaction followed by allylic rearrangement.

In this case the allylic rearrangement is presumed to occur by an S_Ni' reaction. In this interpretation it is necessary to emphasize that as far as the final result is concerned this reaction is identical with an S_N2' reaction, but it occurs

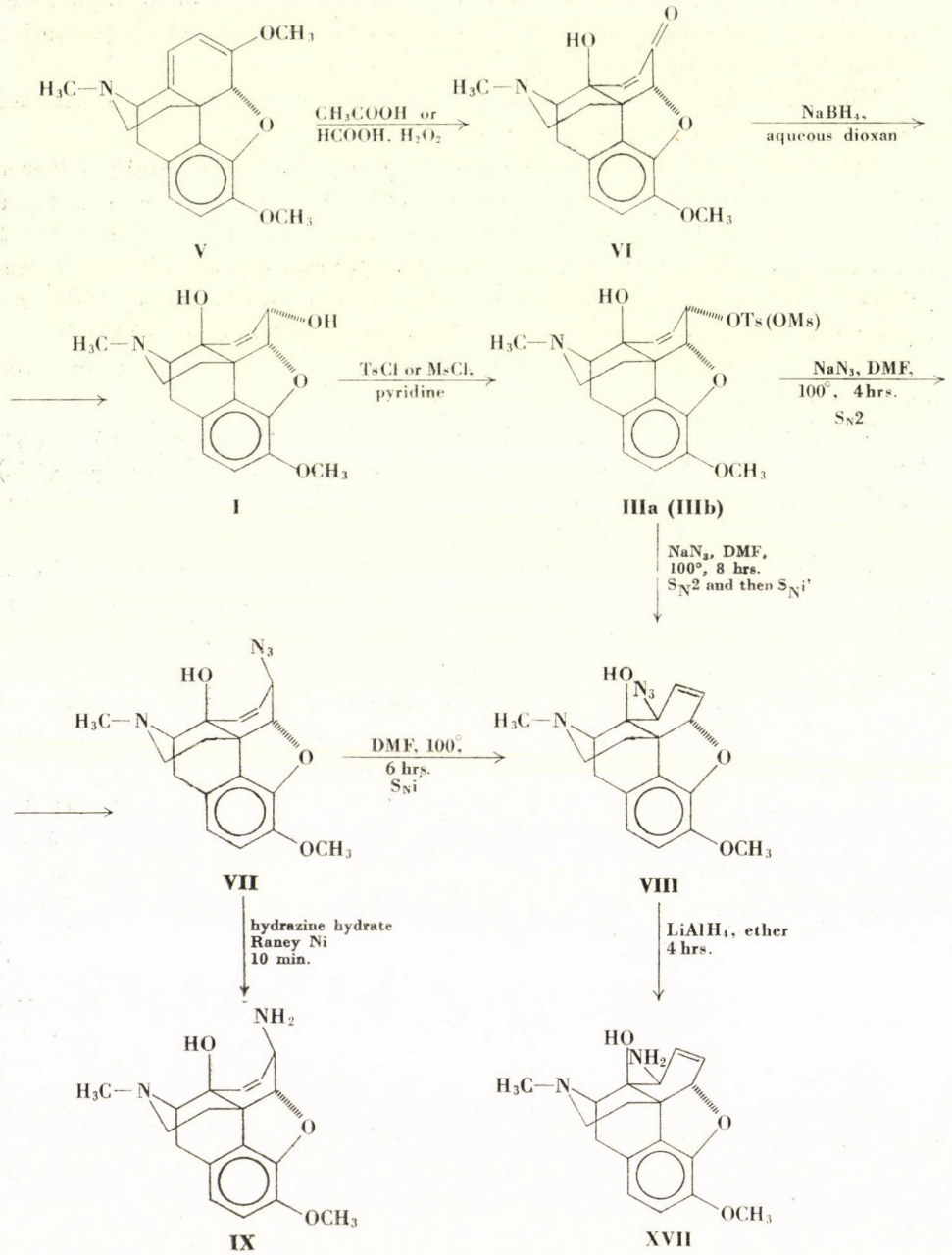

Fig. 2

by a different course. 'Pure' S_N2' reactions take place only under defined stereochemical conditions: the *cis* relationship of the entering and leaving groups is indispensable [11].

In 6-O-tosyl-14-hydroxycodeine **(IIIa)**, the leaving tosyloxy group is located below the plane of the ring C in a *quasi-equatorial* position, whereas

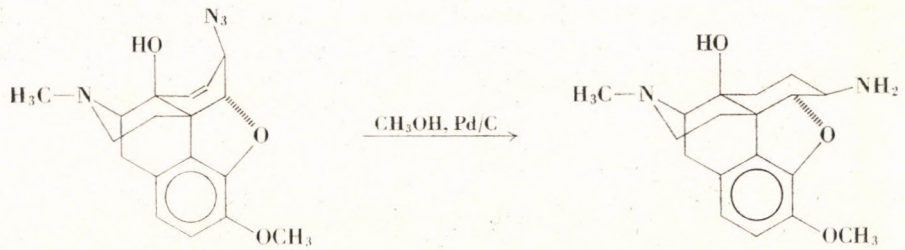

VII X

Fig. 3

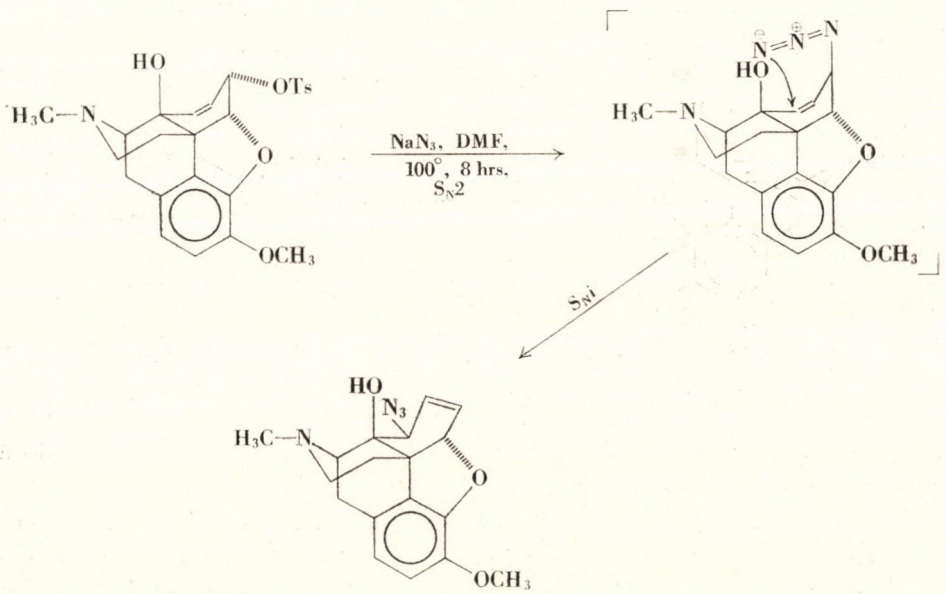

Fig. 4

the newly formed, introduced azide anion of 8-deoxy-8-azido-14-hydroxypseudocodeine **(VIII)**, in spite of being located *quasi-equatorially* above the plane of the C ring, is in *trans* orientation; therefore the '*cis*' rule does not hold for the reaction.

Consequently, the formation of 8-deoxy-8-azido-14-hydroxypseudocodeine **(VIII)**, even if this is the main trend of the reaction, takes place

through 6-deoxy-6-azido-14-hydroxyisocodeine **(VII)**, which is then rearranged to the C_8 compound. The C_6 product is probably kinetically controlled while the C_8 product is the thermodynamical isomer.

This assumption was also confirmed by our experimental results obtained when 6-O-tosylcodeine **(XI)** [12] and 6-O-tosylisocodeine **(XII)**, carrying only a hydrogen atom in position 14, were subjected to reaction with lithium chloride [10] under identical conditions. The reaction of 6-O-tosylcodeine with lithium chloride yielded α-chlorocodide (6-deoxy-6-chloroisocodeine) **(XIII)**,

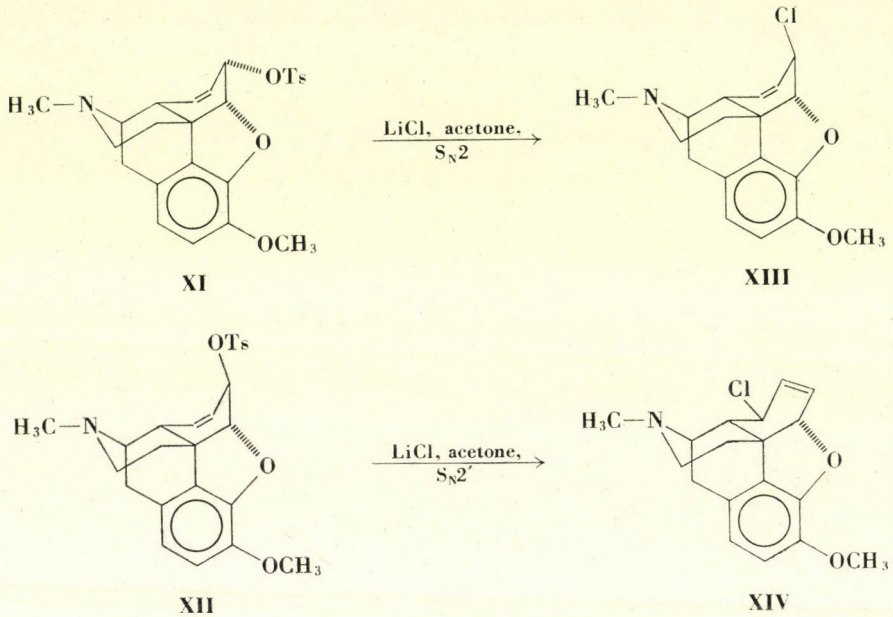

XI **XIII**

XII **XIV**

Fig. 5

whereas a similar treatment of 6-O-tosylisocodeine gave β-chlorocodide (8-deoxy-8-chloropseudocodeine) **(XIV)**.

In the latter conversion the entering and leaving groups are in the *cis* orientation, and thus an S_N2' reaction may take place. The conversions discussed above prove unequivocally the role of the stereochemical properties of the initial compounds in the mechanism of the reactions.

Starting with 14-hydroxydihydrocodeine, the following reactions were carried out:

14-Hydroxydihydrocodeine **(II)** [2] obtained by the catalytic reduction of 14-hydroxycodeine **(I)** was converted, as described above, into the 6-O-tosyl derivative [2] **(IVa)**, and into the hitherto unknown 6-O-mesyl derivative **(IVb)**. Compound **(IVb)** has also been prepared by the catalytic reduction of 6-O-mesyl-14-hydroxycodeine **(IIIb)**.

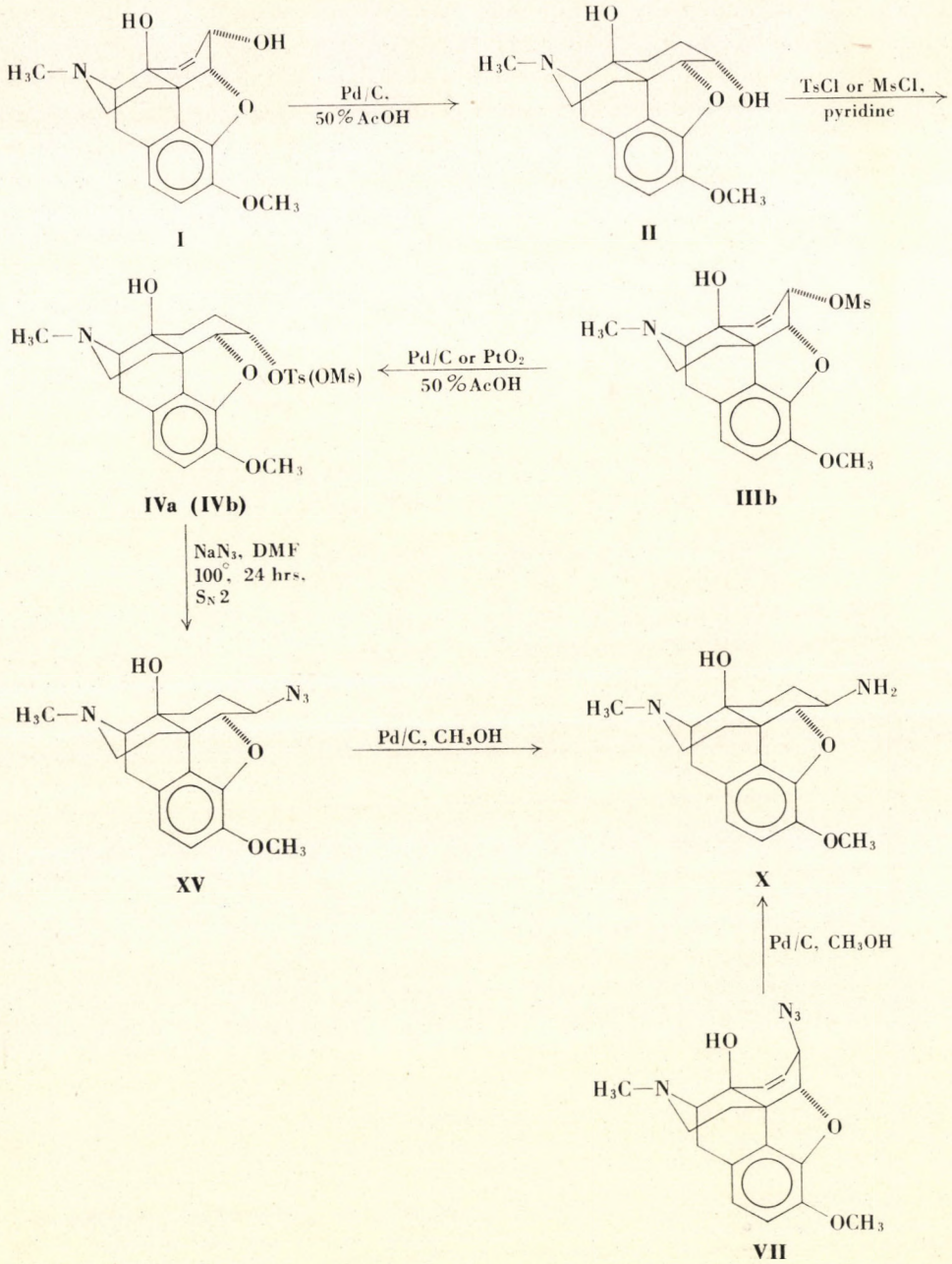
HO
OH
H3C—N
O
OCH3
I
Pd/C,
50% AcOH
HO
H3C—N
O OH
OCH3
II
TsCl or MsCl,
pyridine
HO
H3C—N
O OTs(OMs)
OCH3
IVa (IVb)
Pd/C or PtO2
50% AcOH
HO
OMs
H3C—N
O
OCH3
IIIb
NaN3, DMF
100°, 24 hrs,
SN2
HO
N3
H3C—N
O
OCH3
XV
Pd/C, CH3OH
HO
NH2
H3C—N
O
OCH3
X
Pd/C, CH3OH
N3
HO
H3C—N
O
OCH3
VII

Fig. 6

The azidolysis of **IVa** afforded 6-deoxy-6-azido-14-hydroxydihydroisocodeine **(XV)**. The catalytic reduction of the product resulted in 6-deoxy-6-amino-14-hydroxydihydroisocodeine **(X)**. The conversion tosyloxy → azide occurs, as proved by our conclusions derived from the azidolysis of the unsaturated compound, according to an S_N2 mechanism. Consequently, the structure of the product is given by the above formula correctly.

The structure and steric structure of **VII** is unequivocally confirmed by the fact that this compound can be hydrogenated to **X**, whereas the hydrogenation of **VIII** affords a compound other than **X**, namely 8-deoxy-8-amino-14-hydroxydihydropseudocodeine **(XVI)**.

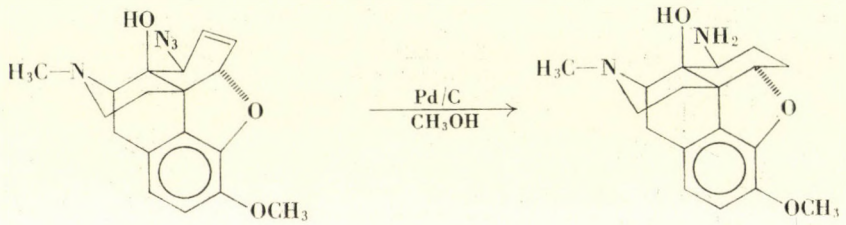

VIII **XVI**

Fig. 7

The data of nuclear magnetic resonance and of X-ray analysis proving the structures and steric structures of the new morphine derivatives prepared by us will be described in detail in another paper.

Experimental

Only the preparation of new compounds are described in detail; for known compounds reference is made to the literature.

The homogeneity of the compounds was checked in each case by thin-layer chromatography, using silica gel (Kieselgel) G, Merck adsorbent, a 8 : 2 mixture of benzene-methanol as the developing solvent, and Dragendorff's reagent for detection.

Melting points were measured in open capillaries. Infrared spectra were obtained with a UNICAM SP 200 G spectrophotometer in KBr pellets or in carbon tetrachloride solution with a Zeiss UR 10 instrument. The values given in the text refer to carbon tetrachloride solutions unless stated otherwise.

14-Hydroxycodeine (I)

It was prepared from thebaine [2], through 14-hydroxycodeinone [3, 4].

14-Hydroxydihydrocodeine (II)

It was prepared from 14-hydroxycodeine as described by CURRIE *et al.* [2].

6-O-Tosyl-14-hydroxycodeine (IIIa)

This compound can be prepared by the method described by CURRIE *et al.* [2].

6-O-Mesyl-14-hydroxycodeine (IIIb)

It was prepared on the analogy of **IIIa**. 5.0 g of 14-hydroxycodeine gave 4.16 g (67%) of **IIIb**, m.p. 146°C (from methanol); $[\alpha]_D$—192° (chloroform, 0.5).

$C_{19}H_{23}O_6NS$ (393.448). Calc. S 8.14; N 3.56. Found S 8.18, 8.13; N 3.51, 3.53%. IR: ν_{OH} 3310 cm^{-1}.

6-O-Tosyl-14-hydroxydihydrocodeine (IVa)

It can be prepared as described by CURRIE *et al.* [2].

6-O-Mesyl-14-hydroxydihydrocodeine (IVb)

(*a*) Compound **II** was treated in the same way as given for **IIIa**. 2.0 g of 14-hydroxydihydrocodeine gave 0.5 g (20%) of **IVb**, m.p. 98—99°C (from cyclohexane): $[\alpha]_D$ —137.6° (chloroform, 0.436).

$C_{19}H_{25}O_6NS$ (395.464). Calc. S 8.11; N 3.54. Found S 7.43, 7.44; N 3.73, 3.74%.

(*b*) **IIIb** was reduced in 50% acetic acid in the presence of 10% Pd/C catalyst. 1.0 g of 6-O-mesyl-14-hydroxycodeine gave 0.22 g (22%) of **IVb**, m.p. 95°C (from cyclohexane): $[\alpha]_D$ —131.9° (chloroform: 0.432). Found S 7.53, 7.57; N 3.45, 3.48%.

(*c*) **IIIb** was hydrogenated in 50% acetic acid in the presence of platinum dioxide catalyst. 1.0 g of 6-O-mesyl-14-hydroxycodeine yielded 0.2 g (20%) of **IVb**, m.p. 97—98°C (from cyclohexane); $[\alpha]_D$ —143.5° (chloroform: 0.39). Found S 7.51, 7.60; N 3.55; 3.66%.

6-Deoxy-6-azido-14-hydroxyisocodeine (VII)

To a solution of 3.0 g of 6-O-tosyl-14-hydroxycodeine **(IIIa)** in 90.5 ml of dimethylformamide, a solution of 0.52 g of sodium azide (0.25 mole excess) in 6.8 ml of water was added, and the mixture was kept for 4 hrs at 100°C. The reaction mixture was poured into 460 ml of ice-water, extracted with 3×110 ml of ether and the ethereal phase was washed with 2×40 ml of water saturated with sodium chloride. After drying the ethereal phase over magnesium sulfate, the solvent was evaporated and the dry residue dissolved in anhydrous ether, then recrystallized from anhydrous ether to yield 0.93 g (38%), of 6-deoxy-6-azido-14-hydroxyisocodeine, m.p. 124—125°C; $[\alpha]_D$ —337.5° (chloroform; 0.474).

$C_{18}H_{20}O_3N_4$ (340.372). Calcd. N 16.46. Found N 16.60, 16.63%. IR: ν_{N_3} 2105; ν_{OH} 3415 cm^{-1}.

8-Deoxy-8-azido-14-hydroxypseudocodeine (VIII)

It was prepared from 6-O-tosyl-14-hydroxycodeine (IIIa) in the same way as described for VII, with the difference that the reaction mixture was kept at 100 °C for 8 hrs.

The reaction mixture consisted of 5.0 g of IIIa in 150 ml of dimethylformamide, and 0.83 g of sodium azide (0.25 mole excess) in 10.0 ml of water. The reaction mixture was poured into 800 ml of ice-water extracted with 3×200 ml of ether, the ethereal phase washed with 2×70 ml of water saturated with sodium chloride, dried over magnesium sulfate, and evaporated to dryness.

The residue was crystallized from ether and a mixture of ether and petroleum ether, or from aqueous acetone to obtain 1.72 g (46.5%) of VIII, m.p. 110°C; $[\alpha]_D$ —78.4° (chloroform; 0.446).

$C_{18}H_{20}O_3N_4$ (340.372). Calcd. N 16.46. Found N 16.62, 16.74% IR: ν_{N_3} 2105; ν_{OH} 3415 cm^{-1}.

Isomerization of 6-deoxy-6-azido-14-hydroxyisocodeine to 8-deoxy-8-azido-14-hydroxypseudocodeine

0.3 g of 6-deoxy-6-azido-14-hydroxyisocodeine **(VII)** was dissolved in 9 ml of dimethylformamide, and kept 6 hrs at 100°C. Processing of the reaction mixture gave 0.25 g (83.3%) of a product which was identical in all respects with 8-deoxy-8-azido-14-hydroxypseudocodeine.

6-Deoxy-6-amino-14-hydroxyisocodeine (IX)

To a solution of 0.83 g of 6-deoxy-6-azido-14-hydroxyisocodeine **(VII)** in 106.4 ml of anhydrous ethanol, 0.85 ml of 85% hydrazine hydrate and about three pinches of Raney nickel catalyst were added, and the mixture was boiled for 10 min. on a water-bath. The catalyst was removed by filtration, the solution was evaporated to dryness, and the residue crystallized from a mixture of ether and petroleum ether to yield 0.55 g (72.5%) of **IX**, m.p. 116—117°C; $[\alpha]_D$ —154.6° (chloroform; 0.582).

$C_{18}H_{22}O_3N_2$ (314.372). Calcd. N 8.9.Found N 9.12, 9.31%. IR: ν_{NH} 3280; ν_{OH} 3410 cm^{-1}.

6-Deoxy-6-amino-14-hydroxydihydroisocodeine (X)

It was prepared by the conversion: **XV** → **X**. The product proved to be completely identical with the compound formed in the way to be described later.

6-O-Tosylcodeine (XI)

It was prepared from codeine, according to KARRER and WIDMARK [12].

6-O-Tosylisocodeine (XII)

This compound was prepared analogously to isoneopine-O-tosylate, as described by TAKEDA, INOUE and KUGITA [13].

α-Cholorocodide (XIII)

It was prepared from 6-O-tosylcodeine, according to STORK and CLARKE [10].

β-Chlorocodide (XIV)

170 mg of 6-O-tosylisocodeine **(XII)** was allowed to react with lithium chloride in an acetone according to STORK and WHITE [11], and the product was isolated by preparative thin-layer chromatography. The identity of the product (40 mg) with β-chlorocodide was proved by thin-layer chromatography. The infrared spectrum obtained in chloroform solution also confirmed that the compound was identical with β-chlorocodide: the characteristic maximum of the spectrum appeared at 902 cm^{-1}.

6-Deoxy-6-azido-14-hydroxydihydroisocodeine (XV)

A solution of 5.9 g of sodium azide (a tenfold molar excess) in 21.5 ml of water was added to a solution of 4.3 g of 6-O-tosyl-14-hydroxydihydrocodeine **(IVa)** in 128 ml of dimethylformamide, and the mixture was kept at 100°C for 24 hrs. It was then poured into 500 ml of water, extracted with 3×100 ml of ether, the ethereal phase washed with 2×50 ml of water saturated with sodium chloride, dried, and evaporated to dryness.

Recrystallization from a mixture of acetone and water gave 2.08 g (31%) of **XV**, m.p. 137—138°C; $[\alpha]_D$ —207.8° (chloroform; 0.38).

$C_{18}H_{22}O_3N_4$ (342.388). Calcd. N 16.36. Found N 16.12, 15.95%. IR: ν_{N_3} 2106; ν_{OH} 3415 cm^{-1}.

6-Deoxy-6-amino-14-hydroxydihydroisocodeine (X)

(*a*) A solution of 0.5 g of 6-deoxy-6-azido-14-hydroxydihydroisocodeine **(XV)** in 30 ml of methanol was reduced in the presence of 10% palladium-on-carbon to obtain 0.43 g (93%) of **X**, m.p. 147—148° C (from ether); $[\alpha]_D$ —137.3° (chloroform; 0.415).

$C_{18}H_{24}O_3N_2$ (316.388). Calcd. N 8.86. Found N 9.23, 9.37%. IR: ν_{OH} 3415; ν_{NH} 3390 cm^{-1}.

(*b*) The same product was obtained from 6-deoxy-6-azido-14-hydroxyisocodeine **(VII)** in the way described under (*a*). The product had m.p. 140° C; mixed m.p. with the product of (*a*): 138—142 °C; [α]d —141.3° (chloroform; 0.382). IR: ν_{NH} 3390; ν_{OH} 3415 cm^{-1}.

8-Deoxy-8-amino-14-hydroxydihydropseudocodeine (XVI)

XVI was prepared from 8-deoxy-8-azido-14-hydroxypseudocodeine **(VIII)**, on the analogy of the preceding reaction, in methanolic solution, in the presence of 10% palladium-on-carbon. Yield: 75%; m.p. 175—178° C (from ether), $[\alpha]_D$ —79.3° (chloroform, 0.353). IR_{KBr}: ν_{NH} 3350 cm^{-1}.

8-Deoxy-8-amino-14-hydroxypseudocodeine (XVII)

A solution of 1.2 g of 8-deoxy-8-azido-14-hydroxypseudocodeine **(VIII)** in 100 ml of anhydrous ether was added by drops with stirring, to a boiling suspension of 0.54 g of lithium aluminium hydride in 75 ml of anhydrous ether. The reaction mixture was refluxed for 3 hrs, then it was processed in the usual way; the product was recrystallized from anhydrous ether to obtain 280 mg (25%) of **XVII**, m.p. 160° C; $[\alpha]_D$ —141.6° (chloroform; 0.48 g).

$C_{18}H_{22}O_3N_2$ 314.372. Calcd. N 8.9. Found N 8.83; 8.96%. IR_{KCl}: ν_{NH} 3310 cm^{-1}.

*

The authors' thanks are expressed to Department I for Natural Sciences of the Hungarian Academy of Sciences, and to the Tiszavasvári Alkaloida Chemical Works for a financial support of the present studies, as well as to the Analytical Laboratory of this Institute for the microanalyses and for recording and evaluating the infrared spectra. Thanks are due to Mr. G. KISS for his industrious and expert assistance in the experimental work.

REFERENCES

1. MAKLEIT, S.: Bulletin of Narcotics (in press)
2. CURRIE, A. C., GILLON, J., NEWBOLD, G. T., SPRING, F. S.: J. Chem. Soc. **1960,** 773
3. SEKI, I.: Ann. Sankyo Res. Lab. **17,** 1 (1965)
4. LUTZ, R. E., SMALL, L.: J. Org. Chem. **4,** 220 (1939)
5. RÜLL, T.: Bull. soc. chim. France **1963,** 586
6. GOULD, E. S.: Mechanismus und Structur in der organischen Chemie, 2. Aufl. Verlag Chemie GmbH, 1964
7. BOYER, J. H., CANTER, F. C.: Chem. Rev. **54,** 1 (1954)
   BOSE, A. K., KISTNER, J. F., FARBER, L.: J. Org. Chem. **27,** 2925 (1962)
   JARREAU, F. X., KHUONG-HUU, Q., GOUTAREL, R.: Bull. soc. chim. France **1963,** 1861
   OHRUI, H., EMOTO, S.: Carbohyd. Res. **10,** 221 (1969)
   ALI, Y., RICHARDSON, A. C.: Carbohyd. Res. **5,** 441 (1967)
   BOYER, J. H., ELLZEY, S. E.: J. Org. Chem. **23,** 127 (1958)
8. DREFAHL, G., PONSOLD, K., SCHUBERT, G.: J. prakt. Chem. **311,** 919 (1969)
9. BERTHO, A.: Ann. **714,** 155 (1968)
   CAVÉ, A., JARREAU, F.X., KHOUNG-HUU, O., LEBOEF, M. M., SERBEN, N., GOUTAREL, R.: Bull. soc. chim. France **1967,** 701
10. STORK, G., CLARKE, F. H.: J. Am. Chem. Soc. **78,** 4619 (1956)
11. STORK, G., WHITE, W. N.: J. Am. Chem. Soc. **78,** 4609 (1956)
12. KARRER, P., WIDMARK, G.: Helv. Chim. Acta **34,** 34 (1951)
13. TAKEDA, M., INOUE, H., KUGITA, H.: Tetrahedron **25,** 1839 (1969)

Sándor MAKLEIT
Rezső BOGNÁR
Teréz MILE
Éva OLÁH
Debrecen 10. Szerves Kémiai Intézet, Hungary
Lajos RADICS; Budapest II., Pusztaszeri út 57—69.

Acta Chimica Academiae Scientiarum Hungaricae, Tomus 74 (1), pp. 111–113 (1972)

CONVERSIONS OF TOSYL AND MESYL DERIVATIVES OF THE MORPHINE GROUP, XI*

14-HYDROXYMORPHINE DERIVATIVES, II HALOGEN COMPOUNDS

S. MAKLEIT, L. RADICS,** R. BOGNÁR and T. MILE

*(Institute of Organic Chemistry, L. Kossuth University, Debrecen and **Central Research Institute of Chemistry, Hungarian Academy of Sciences, Budapest)*

Received June 21, 1971

The known compounds 6-deoxy-6-chloro-14-hydroxyisocodeine, 8-deoxy-8-bromo-14-hydroxypseudocodeine and 8-deoxy-8-bromo-14-hydroxypseudocodeine have been prepared by nucleophilic substitution of the tosyloxy group in 6-(*p*-toluenesulfonyloxy)-14-hydroxycodeine with halogen anions; the physical constants of these compounds are given.

The hitherto unknown isomerization reaction of 6-deoxy-6-chloro-14-hydroxyisocodeine to 8-deoxy-8-chloro-14-hydroxypseudocodeine has been achieved.

6-Deoxy-6-fluoro-14-hydroxyisocodeine, not yet described in the literature, has also been prepared. The constitutions and steric structures of the compounds were examined by IR and NMR analysis.

Nucleophilic substitution reactions with halogen anions of 6-(*p*-toluenesulfonyloxy)-14-hydroxycodeine were first reported by SEKI [1].

In the course of a systematic investigation of these reactions in our laboratory, it appeared necessary to complete SEKI's results with some theoretical aspects and practical data, and to describe in detail the experimental conditions of preparing the halogen derivatives, as well as the characteristic properties of these compounds. SEKI's paper [1] does not include experimental details.

The following compounds were synthesized according to SEKI: 6-deoxy-6-chloro-14-hydroxyisocodeine **(I)**, 8-deoxy-8-bromo-14-hydroxypseudocodeine **(II)** and 8-deoxy-8-iodo-14-hydroxypseudocodeine **(III)**.

The isomerization of 6-deoxy-6-chloro-14-hydroxyisocodeine to 8-deoxy-8-chloro-14-hydroxypseudocodeine **(IV)** was not examined by SEKI. According to our experience, this isomerization can also be accomplished. However, while in the case of 6-deoxy-6-chloroisocodeine containing a hydrogen atom in position 14 it is sufficient to reflux a solution of the starting material in bromobenzene for one hour only [2] to accomplish the isomerization process, *i.e.* transformation into 8-deoxy-8-chloropseudocodeine, in the case of **IV** the presence of the 14-hydroxyl group makes necessary to reflux its solution in bromo-benzene for 50 hours in order to achieve the isomerization leading to 8-deoxy-8-chloro-14-hydroxypseudocodeine.

* Part X: S. MAKLEIT, L. RADICS, R. BOGNÁR, T. MILE, É. OLÁH: Magy. Kém. Foly. **78**, 223 (1972) and Acta Chim. Acad. Sci. Hung. **74**, 99 (1972)

For pharmacological tests it was desirable to prepare 6-deoxy-6-fluoro-14-hydroxyisocodeine **(V)**.

Based on our earlier experience [3] in the preparation of halogen derivatives of codeine containing hydrogen atom in position 14, the fluoro derivative was prepared by the reaction of 6-(*p*-toluenesulfonyloxy)-14-hydroxycodeine and tetrabutyl-ammonium fluoride in acetonitrile.

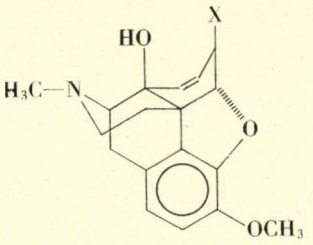

I: X=Cl
V: X=F

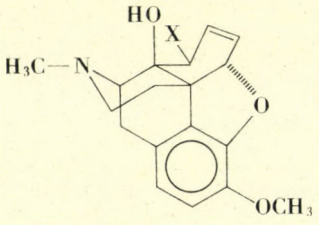

II: X=Br
III: X=I
IV: X=Cl

With this synthesis all the halogen derivatives obtainable from 6-(*p*-toluenesulfonyloxy)-14-hydroxy-codeine became known. The constitutions and steric structures of the compounds are supported by IR and NMR spectroscopic analysis.

It has been found that the characteristic IR spectroscopic features of the halogen derivatives containing hydrogen atom in position 14 [4] also apply to the corresponding 14-hydroxy halogen derivatives and hence the IR spectroscopic data are equally useful in the determination of structural problems (position of the substituent) of these codeine derivatives (C_6 halogen: absorption at 10.7 μ, C_8 halogen: absorption at 11.1 μ).

Detailed NMR spectroscopic data proving the constitutions and the steric structures of the new morphine derivatives prepared in our laboratory will be published elsewhere.

Experimental

6-Deoxy-6-fluoro-14-hydroxyisocodeine (V)

A mixture of 9.0 g (0.019 mole) of 6-(*p*-toluene-sulfonyloxy)-14-hydroxycodeine ($C_{25}H_{27}O_6NS$, 471.790) and 8.03 g (0.03 mole) of tetrabutylammonium fluoride in 54.6 ml abs. acetonitrile was refluxed for 4 hrs, cooled and poured into 54 ml of water. The mixture was extracted with three 120 ml portions of chloroform; the combined chloroform extracts were washed twice with 40 ml of water, dried over anhydrous magnesium sulfate and evaporated. The residue was extracted with 3×120 ml warm ether and the ethereal extract was evaporated. The residue was crystallized from methanol to give 2.5 g (41%) of 6-deoxy-6-fluoro-14-hydroxy-isocodeine, m.p. 181—182 °C; $[\alpha]_D$ —98° (*c* 0.5, chloroform).

$C_{18}H_{20}FNO_3$ (323.348). Calcd. F 5.88%. Found F 5.71%.

6-Deoxy-6-chloro-14-hydroxyisocodein (I)

A solution of 10.1 g (0.021 mole) of 6-(*p*-toluene-sulfonyloxy)-14-hydroxycodeine and 3.5 g (0.083 mole) of lithium chloride in 387 ml abs. acetone was refluxed for 24 hrs, cooled, and poured into 1680 ml of water. The solution was extracted with three 100 ml portions of benzene, the combined organic phase was washed with 3×150 ml water, dried over anhydrous magnesium sulfate and evaporated. The residue was crystallized from ethanol (25 ml) to give 3.76 g (53%) of 6-deoxy-6-chloro-14-hydroxyisocodeine **(I)**, m.p. 166° C; $[\alpha]_D$ —298° (*c* 0.5, chloroform) ($C_{18}H_{20}ClNO_3$, 339.805).

8-Deoxy-8-chloro-14-hydroxypseudocodeine (IV)

A solution of 2.0 g of 6-deoxy-6-chloro-14-hydroxyisocodeine in 40 ml of bromobenzene was refluxed for 50 hrs. The solution was cooled and extracted with 2×40 ml of 10% hydrochloric acid; the combined aqueous phase was treated with 10% ammonium hydroxide solution until alkaline, and then extracted with three 50 ml portions of chloroform. The chloroform extracts were washed with 2×30 ml of water, dried over anhydrous magnesium sulfate and evaporated. The residue was crystallized from ethanol to give 0.4 g (20%) of 8-deoxy-8-chloro-14-hydroxypseudocodeine **(IV)**, m.p. 174—175° C; $[\alpha]_D$ —92° (*c* 0.5, chloroform).

8-Deoxy-8-bromo-14-hydroxypseudocodeine (II)

A solution of 3.0 g (0.0063 mole) of 6-(*p*-toluenesulfonyloxy)-14-hydroxycodeine and 2.4 g of anhydrous lithium bromide (0.027 mole) in 115 ml of abs. acetone was refluxed for 6 hrs, poured into 500 ml of water, and the mixture was extracted with three 100 ml portions of benzene. The combined benzene extract was washed with 2×50 ml of water, dried over anhydrous magnesium sulfate and evaporated. The residue was twice recrystallized from methanol (5 and 7 ml, respectively) to give 0.2 g (8.3%) of 8-deoxy-8-bromo-14-hydroxypseudocodeine **(II)**, m.p. 155—156 °C; $[\alpha]_D$ —26° (*c* 0.5, chloroform) ($C_{18}H_{20}BrNO_3$, 384.264).

8-Deoxy-8-iodo-14-hydroxypseudocodeine (III)

A solution of 3.0 g (0.0063 mole) of 6-(*p*-toluene-sulfonyloxy)-14-hydroxycodeine and 4.1 g of (0.034 mole) sodium iodide in 115 ml of abs. acetone was refluxed for 3 hrs, cooled and poured into 500 ml of water. The solution was extracted with three 100 ml portions of benzene, the combined organic phase was washed with 2×50 ml of water, dried over anhydrous magnesium sulfate and evaporated. Crystallization of the residue from 25 ml of methanol gave 0.95 g (35%) of 8-deoxy-8-iodo-14-hydroxypseudocodeine **(III)**, m.p. 146—147° C (d.), $[\alpha]_D$ +34° (*c* 0.5, chloroform) ($C_{18}H_{20}INO_3$, 431.268).

*

The authors express their thanks to Department I of Natural Sciences of the Hungarian Academy of Sciences and to Tiszavasvári Alkaloida Chemical Works for financial support of this work. We also thank the Analytical Laboratory of this Institute for the microanalyses, as well as for the recording and evaluation of the infrared spectra. We thank Mr. G. Kiss for his valuable technical assistance.

REFERENCES

1. Seki, I.: Ann. Sankyo Res. Lab. **17**, 1 (1965)
2. Small, L. F., Faris, B. F., Mallonee, J. L.: J. Org. Chem. **5**, 334 (1940)
Speyer, E., Rosenfeld, A.: Ber. **58**, 1113 (1925)
3. Bognár, R., Makleit, S., Radics, L.: Magy. Kém. Foly. **76**, 461 (1970)
Bognár, R., Makleit, S., Radics, L.: Acta Chim. Acad. Sci. Hung. **67**, 63 (1971)
4. Stork, G., Clarke, F. H.: J. Am. Chem. Soc. **78**, 4619 (1956)

Sándor Makleit
Rezső Bognár
Teréz Mile
Debrecen 10. Szerves Kémiai Intézet, Hungary.
Lajos Radics; Budapest II., Pusztaszeri út 57—69.

RECENSIONES

Topics in Current Chemistry. 13/2. Photochemistry

pp. 227—450, Springer Verlag, 1969

It seems to be almost commonplace to say of one or another branch of chemical research that it has undergone fundamental transformation during the last decades, and its rapid advancement is due to the development of new aspects, new experimental techniques and a more profound theoretical foundation. This process is, however, perhaps nowhere else so emphasized as in the field of organic photochemistry. Organic photochemical reactions have been known since the beginning of organic chemical research and the work in this field, at least to a certain extent, has been continuous. The results of modern physics greatly promoted the elucidation of the theoretical fundamentals, but really rapid advancement occurred parallel to the development of quantum chemistry, since this latter led to a deeper understanding of the electron structure of molecules and electron excitation processes. Investigation of the excited states and their transformations, the concept of energy transfer, as well as modern separation techniques and structure investigation methods had a decisive influence on the development of modern photochemistry.

The purpose of the book "Photochemistry" was not, of course, to deal with the general problems of modern photochemistry. The five comprehensive reviews discuss the photochemistry of one, well-defined smaller group of compounds, assuming general photochemical knowledge of the reader. In spite of this, the book can be useful not only for those working in the restricted fields discussed, but also for researchers engaged in other fields of photochemistry and those intending to get acquainted with photochemistry more thoroughly. The five reviews are independent of one another in respect of the compounds treated and the primary aspects of research were also different; still, these individual, very specialized topics give the reader an almost general picture of photochemistry as a whole. In discussing the photochemistry of *o*-quinones and α-diketones or compounds with cycloheptatriene skeleton, the mechanisms from the organic chemical point of view are in the foreground, while in the paper dealing with the photochemistry of metal carbonyls, metallocenes and olefin complexes, the spectroscopic characteristics and primary photochemical processes are emphasized. In the radiation chemistry of alcohols kinetic considerations prevail and finally the review on the photochemical reactions of polymers pays special attention mainly to practical aspects.

The paper "Photochemistry of *o*-quinones and α-diketones" (M. B. RUBIN, Dept. of Chemistry, Technion, Haifa, Israel) deals with a group of compounds (benzil, diacetyl, phenantrenequinone) which have been the model compounds of photochemical research for a long time and studied in great detail. After reviewing the spectroscopic characteristics, individual examples of homolytic splitting and cycloaddition reactions are discussed, followed by a very thorough treatment of the most important photochemical reaction of this type of compounds, *i.e.*, the hydrogen abstraction process. The radical products of the primary process (one of them being the semidion radical directly detectable by the ESR method) can react further in various ways, depending on the chemical properties of the dione and the hydrogen donating agent. The paper also mentions shortly the photochemical reaction which these compounds undergo in the presence of oxygen.

The paper "Photochemical reactions of cycloheptatriene and related compounds" (L. B. JONES and V. K. JONES, Dept. of Chemistry, Univ. of Arizona, Tucson, Arizona, USA) seems to relate to a narrower field; it deals with the photochemical reactions of some other conjugated trienes and even of benzene, in addition to those mentioned in the title. The various cyclization and migration reactions are characterized, in general, by high selectivity. The review mentions some interesting examples of the validity of the Woodward—Hoffman rule.

In respect of the literature reviewed, the paper "Photochemistry of metal carbonyls, metallocenes and olefin complexes" (E. KOERNER von GUSTORF and F. W. GREVELS, Max-Planck

Institut für Kohlenforschung, Abt. Strahlenchemie, Mülheim/Ruhr, GFR), rises above the other works published in the book. Its main purpose is — according to the authors — to inform researchers of organometallic compounds on the possibilities offered by photochemistry in preparative work and studies of the mechanism; this aim is realized by this review on a high level. The discussion of substitution, addition and elimination reactions of metal carbonyls calls attention to very interesting possibilities, and the summary of the cycloaddition and polymerization reactions of olefin complexes and of the photochemistry of ferrocene deserve interest.

In the paper "Radiation chemistry of alcohols" (C. V. SONNTAG, Institut für Strahlenchemie, Kernforschungszentrum, Karlsruhe, GFR) the discussion of actual photochemical reactions is a small part only, in accordance with the limited number of results obtained in this field. The effect of ionizing radiations is, however, treated in great detail. Particular interest is attached to the chapter on the role of solvated electrons, and to the evaluation of the homogeneous kinetic treatment and the description of the linear energy transfer (LET) effects.

J. L. R. WILLIAMS (Eastman Kodak Co., Rochester, N. Y., USA) reviews in his paper "Photopolymerization and photochemical cross-linking of polymers" a field narrower than that expected on the basis of the title, and actually surveys the practical processes directly applicable in picture fixing procedures. The problem of photopolymerization, in accordance with its theoretical importance, would deserve a more detailed kinetic discussion and the characteristic photochemical polymerization reactions discovered in the last years could have been included. However, the paper gives a very good survey of the selected field.

In conclusion, it can be stated that the volume "Photochemistry" contains very valuable material for the specialists of the field as well as for those taking interest in its general problems, thus it can be a useful help in further research of photochemistry. Chemists engaged in this branch of science would surely welcome the publishing of similar books in the future.

B. TURCSÁNYI

R. C. HADDON, V. R. HADDON and L. M. JACKMAN: *NMR Spectroscopy of Annulenes*

pp. 116, Springer Verlag, Berlin, Heidelberg, New York 1971

The book is actually the second part of the 16th volume of the series "Fortschritte der Chemischen Forschung, Topics in Current Chemistry", therefore it begins with page 103.

In the modern literature, the concepts of "aromatic character" and "aromaticity" are differentiated. The appearance of the latter property can be examined most expediently by means of NMR spectroscopy, and one of its most characteristic definitions is in connection with the phenomenon of ring current.

Thus, the introductory part deals with the definition given by HÜCKEL, stating that systems comprising $4n + 2$ electrons are expected to show aromatic properties, and its up-to-date, extended variations are also discussed. This is followed by a short review of the bond relations in annulenes (Bond Alteration in Annulenes) (3 pages), the conditions of aromaticity (Criteria of Aromaticity) (3 pages), then the theories dealing with magnetic properties of annulenes are surveyed in detail (Theory of the Magnetic Properties of Annulenes) (14 pages). It is praiseworthy that this latter part avoids detailed calculations and gives a short and lucid treatment of the most important approximations.

In the next chapter (28 pages) the NMR spectra of annulenes are summarized in a well-constructed table and a very interesting, thorough discussion. Special interest is attached to an analysis of the NMR spectra obtainable on "freezing out" one of the conformers from among the several existing forms of annulenes.

In Section F, the NMR spectra of quasi-annulenes are described on equally high level and in a rather large extent (50 pages) as compared with the size of the book. Therefore, in contrast with the title of the book, preponderance is slightly shifted from annulenes to quasi-annulenes. A short Addendum and reference list are the final parts of the book.

The three authors discuss the subject expertly; instead of a collection of data, the book presents enjoyable reading containing valuable discussions.

Cs. SZÁNTAY

Kelso B. MORRIS: *Fundamental Chemical Equilibria. Nonionoc-Ionic*

pp. 110, Gordon and Breach Science Publishers, New York, London, Paris, 1971

The purpose of this book consisting of 110 pages and published in 1971 by Gordon and Breach Science Publishers, New York, London, Paris, is to facilitate the chemical studies of university students. In this small monograph the author relied on his educational experience in selecting some fields of chemical equilibria considered by him to be of the greatest importance for students, and limited the mathematical apparatus of the treatment to the minimum necessary for the explanation of the problems discussed.

The book consists of four chapters. The first chapter (22 pages) introduces the thermodynamic principles of chemical equilibria. This chapter also presents the necessary mathematical fundamentals required for the use of the five thermodynamic functions of state *(U, H, S, A, G)* and for the deduction of various simple correlations. The last section of the chapter deals shortly with gaseous equilibria. In the second and third chapter homogeneous and heterogeneous equilibria are discussed (in 30 and 20 pages, respectively). In the discussion the Brønsted acid-base theory is applied. The fourth chapter (22 pages) is concerned with reduction–oxidation equilibria and galvanic cells. Special attention is paid to the elucidation of electrochemical conventions. The treatment also involves actual examples, as well as calculation exercises together with the method of solving. The four chapters are followed by unsolved calculation problems (only numerical results are given) and tables.

On the basis of the treatment of the material the book can be regarded as a university study-aid. It seems to be necessary at places where general chemistry of introductory character is omitted from the university course and physical chemistry is treated on purely mathematical basis. This conclusion can be drawn from the structure of the book. Namely, the first chapter is recapitulation-like, *i.e.* it is designed for students who have learned thermodynamics, while the treatment applied in the other three chapters is on the level of general chemistry. (In the thermodynamical part an inconsistency should be noted: Principle I is given as $dU = \delta Q - \delta W$, but $-\delta W$ is interpreted as the work carried out *by* the system.) If the program of the university course teaches physical chemistry on the basis of former studies in general and fundamental analytical chemistry, the book can be utilized in teaching the latter subjects. The electrochemical examples are very wide-ranging and the exercises comprised in the book can also be helpful in teaching.

Gy. VARSÁNYI

M. B. NEIMAN and D. GÁL: *The Kinetic Isotope Method and Its Application*

pp. XII + 309, Akadémiai Kiadó, Budapest and Elsevier Publishing Co., Amsterdam, 1971

The significance of the kinetic isotope method manifests itself in studies of the kinetics and mechanism of complex reactions, where the reactants are converted to products via a number of consecutive, competitive, reversible and irreversible steps. By permitting direct experimental observation of the rate of formation and consumption of certain intermediates and the identification of the precursors, the kinetic isotope method provides us with information necessary for the justification of a supposed mechanism, which is not attainable by other methods. Many highly important results were obtained by the intuitive application of the kinetic isotope methods in the field of oxidation and cracking reactions, heterogeneous catalysis, hydrogenation, polymerization, isomerization, etc. Recently the method was successfully applied in the study of various biologically important phenomena connected with *e.g.*, metabolism and transport processes.

Thus this monograph is a considerable contribution to the literature of chemical kinetics; stimulates and encourages the application of stable and radioactive isotopes in the studies of chemical mechanism.

The monograph consists of 10 chapters. The first describes the kinetics and sequence of intermediate formation in complex reactions, the second deals with the theoretical background of the kinetic isotope method, the third with methods to determine reaction order. Chapter 4 deals with the investigation of complex reactions in which perfect mixing occurs.

These chapters allow a comparison with classical methods, indicating the advantages of the tracer technique in producing information on complex reactions which cannot be obtained by other methods.

The following topics are discussed: thermal decomposition reactions (Chapter 5), gas phase oxidation of hydrocarbons (Chapter 6), competitive radical reactions (Chapter 7), liquid phase oxidation reactions (Chapter 8), heterogeneous catalysis (Chapter 9) and biochemical applications (Chapter 10).

In this last chapter the authors attempt to give comprehensive and unambiguous definitions of concepts, such as "turnover time", "turnover rate", "open" and "closed" systems, used in different senses.

The monograph provides a wide survey in presenting the applications of method, and it is of special value that the authors have made a very careful, critical selection of the papers published in this field. They follow, as far as possible, a uniform treatment of the problems and present the results in great detail. The readers can check directly the reliability of the conclusions drawn from the experimental results. This makes the monograph a most valuable practical book too.

E. KŐRÖS

A. LÁSZLÓ und M. BAKOS: *A vegyészmérnöki tudomány klasszikusai. Válogatott tanulmányok. (Klassiker des Chemie-Ingenieurwesens. Ausgewählte Studien.)*

403 Seiten, Verlag Tankönyvkiadó, Budapest 1971

Dieses — für Studenten und beginnende Chemie-Ingenieure bestimmte — Hilfsbuch enthält dreizehn Studien von zwölf verschiedenen Verfassern in der Originalsprache und in wortgetreuer ungarischer Übersetzung. Die ausgewählten Studien repräsentieren je einen wichtigen Meilenstein der etwa 50 jährigen Geschichte des Chemie-Ingenieurwesens (chemical engineering) und ihre Verfasser zählen heute bereits zweifellos zu den Klassikern dieser neuen technischen Wissenschaft.

Die Herausgabe des Buches dient in erster Linie didaktischen Zielen und scheint eine in ihrer Art sehr nützliche, neue Wege suchende, interessante Initiative zu sein. Das Buch ermöglicht es den Studenten, die kennzeichnenden Züge der Denkart der Chemie-Ingenieure, den Vorgang der Entwicklung dieser Denkart sowie die wichtigsten Gebiete und Probleme des Chemie-Ingenieurwesens aus den primären Quellen kennen zu lernen; diese Quellen wären für Studenten sonst nur schwer zugänglich. Zugleich gibt das Buch eine Anregung zum Lernen von Fremdsprachen und führt den Leser in das Studium der ausländischen Fachliteratur ein. In dieser Hinsicht ist es als glücklich zu bezeichnen, daß unter den Originalmitteilungen Texte in englischer, russischer, deutscher und französischer Sprache zu finden sind.

Auch die kurzen, in ungarischer Sprache geschriebenen Einleitungen zu den einzelnen Studien verfolgen didaktische Ziele; sie lenken die Aufmerksamkeit des Lesers auf die wichtigsten Zusammenhänge, informieren ihn über neuere Ergebnisse in dem Problemenkreis der Studie und helfen ihm, diese in den Lehrstoff des Universitätsstudiums einzufügen.

Der einleitende Aufsatz ist die in der ersten Nummer der Zeitschrift Chemical Engineering Science in 1951 erschienene Arbeit von J. CATHALA, worin der Verfasser das Wesen und die Konzeption dieser neuen Disziplin auf exakte Art formuliert und die Ursachen und wesentlichen Phasen ihrer Entwicklung zusammenfaßt.

Der Verfasser des nächsten Aufsatzes ist W. NUSSELT (1916). Diese Studie, worin der Verbrennungsprozeß der Steinkohle am Rost behandelt wird, ist ein gutes Beispiel der Gestaltung der Denkweise des Chemie-Ingenieurs.

Eines der wichtigsten Gebiete des chemical engineering sind die Grundoperationen (unit operations). Die nächsten vier Studien sind klassische Beispiele für die Theorie der Absorption sowie für die Entwicklung der Kenntnisse, die zur Projektierung von Destillations- und Absorptionskolonnen nötig sind. Ihre Verfasser sind W. K. LEWIS und W. G. WHITMAN (1924), R. HIGBIE (1935), W. L. MCCABE und E. W. THIELE (1925) und T. H. CHILTON und A. P. COLBURN (1935).

Wie bei den technischen Wissenschaften im allgemeinen, ist auch im Chemie-Ingenieurwesen die Untersuchung der Analogien von großer Bedeutung. Dies wird durch die grundlegende Arbeit von Th. KÁRMÁN (1939) über die Analogie zwischen der Flüssigkeitsreibung und der Wärmeübertragung vorgeführt.

Das nächste umfassende Gebiet ist die Untersuchung der Kinetik der chemischen Vorgänge und die daraus entwickelte Reaktortechnik. Die Anfänge dieser Forschungen können

auf die Studie von Langmuir im Jahre 1908 zurückgeführt werden, worin die Reaktionsgeschwindigkeit in strömenden Systemen erstmalig behandelt wurde. In der wissenschaftlichen Fundierung der Reaktortechnik wird heute die Tätigkeit von DAMKÖHLER als grundlegend betrachtet. Eine seiner Mitteilungen (1936) ist im Buch enthalten. Auch eine Studie von C. WAGNER (1945) über die thermische Stabilität der Reaktoren sowie zwei Abschnitte aus dem Buch von D. A. FRANK-KAMENETSKY »Diffusion und Wärmeübertragung in der chemischen Kinetik« über weitere Grundprobleme der kontaktkatalytischen Reaktoren bzw. über periodische Vorgänge sind in der Auswahl enthalten. Die Sammlung der Beispiele wird durch einen Aufsatz von E. W. THIELE (1939) über einzelne Probleme der Kontaktkatalyse abgeschlossen.

Einige Worte über die Übersetzung: meiner Meinung nach ist die Methode der wortgetreuen Übersetzung, die bei dem vorliegenden Buch aus didaktischen Günden gewählt wurde, nur eine der bestehenden Möglichkeiten. Ohne Zweifel bedeutet eine derartige Übersetzung denen, die sich im Übersetzen von fremdsprachigen Fachtexten üben wollen, viel Hilfe. Allerdings ergibt sich daraus an vielen Stellen des Buches ein etwas fremdartiges Ungarisch.

B. ZSADON

W. SCHULZE: *Radiochemie*

Band 4005 der Sammlung Göschen, 157 Seiten, Walter de Gruyter Verlag, Berlin—New York, 1971

Der Chemiker von heute muß die Radiochemie kennen, da sie weitverbreitet auf zahlreichen Gebieten der Forschung angewendet wird. Außer ihrer praktischen Verwendung führte die Entdeckung der künstlichen Radioisotopen z. B. in der analytischen Chemie zu verschiedenen, in der »inaktiven Chemie« unbekannten Methoden.

Das vorliegende Buch von Werner SCHULZE leistet dem Chemiker wertvolle Hilfe, die Grundbegriffe, Meßmethoden, Fehlerrechnung und besonderen Arbeitsverfahren dieses Wissenszweiges kennen zu lernen und zu verstehen. Der logische Aufbau des Stoffes weist auf eine gründliche Kenntnis des Gegenstandes hin. Obwohl die Behandlung knapp gefaßt ist, bleibt sie stets klar und verständlich.

Einleitend werden die Arten der Kernstrahlung und die Wechselwirkungen zwischen Materie und Strahlung kurz behandelt. Anschließend folgt das Messen der Strahlung, angefangen von den Ionisationskammern bis zu den modernen Halbleiter- und Szintillationsdetektoren. Ein besonderes Kapitel ist den verschiedenen Methoden der Fehlerrechnung gewidmet. Bevor der Leser in die radiochemischen Arbeitsverfahren eingeweiht wird, gibt der Verfasser einen kurzen Überblick über die Vorschriften und Gefahren beim Arbeiten mit strahlenden Stoffen, ohne jedoch die Fragen des Strahlenschutzes eingehend zu behandeln, da der Umfang des dünnen Buches dies nicht ermöglicht.

Die radiochemischen Verfahren weichen von den bekannten chemischen Verfahren ab, da die Kernreaktionen in der Mehrzahl der Fälle nur Mikromengen an Produkten liefern und bei diesen Mengen andere Gesetzmäßigkeiten herrschen, als in der Makrochemie. In dem Kapitel über diese Verfahren werden die komplizierten Probleme der Trennung, die Technik der Trägerbereitung sowie der Isotopenaustausch behandelt. Dabei befaßt sich das Kapitel mit analytischen Methoden, mit der Verdünnungsanalyse und den verschiedenen Arten der Aktivierungsanalyse. Auch die Koinzidenzmethode und die Autoradiographie werden hier erwähnt.

Das letzte Kapitel behandelt die präparative Herstellung der Radionuklide, d. h. die Kernreaktionen, die chemische und radiochemische Reinheit der Präparate, die Forderungen gegenüber den Targetstoffen, die in Kernspaltungsreaktionen entstandenen Nuklide. Endlich wird die Herstellung von markierten anorganischen und organischen Molekülen, die in den heutigen Forschungen eine wichtige Rolle spielen, kurz berührt. Die durch WILZBACH entwickelte Technik wird hervorgehoben, mit deren Hilfe solche organische Verbindungen mit Tritium markiert werden können, die auf synthetischem Wege bisher nicht zugänglich waren.

Das Verständnis des Stoffes wird durch einige gut überblickbare Tabellen und durch 33, in ihrer Einfachheit recht anschauliche Abbildungen erleichtert. Alle, die die Grundbegriffe und Methoden der Radiochemie in kurzer Zeit kennen zu lernen wünschen, werden das Büchlein mit Freude begrüßen. Dabei kann auch der Spezialist der Radiochemie das Buch als nützliches Hilfsmittel verwenden.

Frau I. INZELT

HOLLÓ—KURUCZ—BORÓDY: *The Applications of Molecular Distillation*

pp. 210, 36 Figs., 34 Tables, Akadémiai Kiadó
(Publishing House of the Hungarian Academy of Sciences), Budapest, 1971

Among the monographs spreading nowadays on the bookshelves of libraries one over and over has the impression that, in spite of the fact that the epoch of polyhystors had passed, the publication of works dealing with particular topics seems to be in vain, since there is no practicable way to comprehend the branching results of the developments in science.

If there are exceptions proving the rule, this book certainly is; it establishes the use of specialized experts in the endeavour of imparting their skill to chemists and chemical engineers working to solve their everyday problems.

The monograph consists of five main chapters, the first dealing with the theory, the second and third with the different apparatuses and auxiliary equipments of molecular distillation while the fourth and fifth ones as well as the supplementary tables review the laboratory and industrial applications of this unique method of separation.

The theoretical considerations in the parallel treatment of regular distillation and the differences thereof in the interpretation of the phenomena in high vacuum are excellent. The reader becomes imperceptibly acquainted with proper definitions such as elimination curve, distillability, initial temperature of molecular distillation and straight off gets a lot of examples how to perform indulgent distillation of thermolabile substances.

The authors emphasize the importance of technical details, first of all the equipments ensuring and the devices measuring high vacuum.

The appropriately successive treatment makes a digression to the laboratory applications and summarizes a great deal of work from the preparative and separation points of view, relying also on the wide-spread experiences of the authors of their own. A rich compilation surveys the fractionation of fat components, glycerides, waxes, etc.

The review of industrial applications stresses the importance of the refining of edible oils, mono- and triglycerides, the separation of non-fatty constituents of fats and the distillation of tall oils, mineral oils, plasticizers, etc.

Perhaps the only topic missing is a comprehensive hint revealing those fields where — up to now — molecular distillation has not been used though potentionally it might be.

As a final recapitulation the reader is fully convinced of the features provided by molecular distillation as a separation method and on the side holds possession of a new tool with the aid of which a couple of different problems can successfully be settled. The Publishing House of the Hungarian Academy of Sciences rendered the specialists working both in industry and research a reliable service by issuing this monograph.

T. LENGYEL

INDEX

BRUCKNER, V.: László (Ladislaus) VARGHA† 1

PHYSICAL CHEMISTRY – PHYSIKALISCHE CHEMIE – ФИЗИЧЕСКАЯ ХИМИЯ

MÓGER, D., MINK, GY. and NAGY, F.: Study of the Catalytic Hydrogenation (Deuteration) of Cyclohexene on a Platinum Catalyst. Aging of the Catalyst During the Reaction 27

SOLYMOSI, F. and BÁNSÁGI, T.: Stabilities of Ammonium Halates in the Solid Phase. Study of the Effects of Aging and Various Additives on the Thermal Decomposition of Ammonium Chlorate 35

SAKLA, A. B., BADRAN, A. H. and SAYED, N. A.: Thermoelectric Microdetermination of Molecular Weights of Organic Compounds in Homogeneous Binary Solvent Systems Using Thermistors 51

KISS, Á. I. and SZŐKE, J.: Theoretical Investigation of the Electronic Spectra of Monosubstituted Benzene Derivatives 59

PETHŐ, Á.: Distributions in Time and Space, Respectively, in Fixed Bed Multistage Exchange Processes of Linear Kinetics (Short Communication) 71

ORGANIC CHEMISTRY – ORGANISCHE CHEMIE – ОРГАНИЧЕСКАЯ ХИМИЯ

WILDENHAIN, W. und HENSEKE, G.: Acide Inhaltsstoffe der Torffulvosäurefraktion (Acidic Substances of Turffulvonic Acid Fraction) 79

KLIVÉNYI, F., STÁJER, G., SZABÓ, E. A., PINTYE, J. and VINKLER, E.: Aromatic Sulfenyl Chlorides, V. Reaction of Sulfenyl Chloride with N^2-Aryldithiocarbazates, O-Alkyl-Thiocarbazates and O-Aryl Substituted Phenylthiocarbamates 87

MAKLEIT, S., RADICS, L., BOGNÁR, R., MILE, T. and OLÁH, É.: Conversions of Tosyl and Mesyl Derivatives of the Morphine Group, X. 14-Hydroxymorphine Derivatives, I. Azido and Amino Compounds 99

MAKLEIT, S., RADICS, L., BOGNÁR, R. and MILE, T.: Conversions of Tosyl and Mesyl Derivatives of the Morphine Group, XI. 14-Hydroxymorphine Derivatives, II. Halogen Compounds 111

RECENSIONES 115

Printed in Hungary

A kiadásért felel az Akadémiai Kiadó igazgatója — Műszaki szerkesztő: Zacsik Annamária

A kézirat nyomdába érkezett: 1972. IV. 7. Terjedelem: 10 ív 12 old. A/5 ív, 57 ábra

72.74206 Akadémiai Nyomda, Budapest — Felelős vezető: Bernát György

ACTA CHIMICA

ТОМ 74 — ВЫП. 1

РЕЗЮМЕ

Изучение каталитического гидрирования (дейтерирования) циклогексена на платиновом катализаторе

Старение катализатора в ходе реакции

Д. МОГЕР, ДЬ. МИНҚ и Ф. НАДЬ

Гетерогенное каталитическое гидрирование циклогексена изучалось в реакторе, в котором при помощи постоянного шлифования платины в ходе реакции был обеспечен всегда свежий катализатор. Было установлено, что наряду с гидрированием одновременно протекает крекинг циклогексена. В результате разложения на поверхности катализатора образуются отложения хемосорбированного угля и CH-(метин-) радикалы. Полагалось, что старение катализатора вызвано в первую очередь накоплением вышеупомянутых продуктов разложения, т. е. уменьшением числа свободных активных центров. Скорость крекинга уменьшается с уменьшением активности катализатора значительнее, чем скорость гидрирования; поэтому эти два процесса протекают с соизмеримыми скоростями лишь в случае свежих катализаторов.

Эффект старения и различных добавок на термическую стабильность хлората аммония

Ф. ШОЙМОШИ и Т. БАНШАГИ

Изучалось влияние различных параметров, таких, как старение, газы разложения, инородные вещества и др. на разложение и взрыв хлоратов аммония. Наиболее поразительный эффект наблюдался в присутствии NH_3; последний значительно увеличивает стабильность соединения. Среди различных добавок кислоты вызывают ускорение разложения. Со старением стабильность уменьшается, что приводит к взрывам при пониженных температурах. Подробные исследования были также проведены с твердым остатком разложения.

Микроаналитическое определение молекулярных весов органических соединений в гомогенных бинарных смесях растворителей термоэлектрическим методом, используя термисторы

А. Б. САҚЛА, А. Х. БАДРАН и Н. А. САЙЕД

Термометрическое определение молекулярных весов органических соединений в гомогенной бинарной системе растворителей, используя термисторы, имеет относительную погрешность определения меньше, чем 2%. Метод может быть использован в качестве простой и надежной процедуры определения поведения гомогенной бинарной системы с точки зрения закона Рауля.

Теоретическое изучение электронных спектров монозамещенных производных бензола

А. ҚИШ и Й. СЁҚЕ

С помощью метода Паризер—Парр—Попла были рассчитаны электронные спектры монозамещенных бензолов, содержащих фтор-, хлор-, гидрокси-, амино- и карбонилгруппы, а также их комбинации. Расчеты с хорошим приближением дают эксперименталь-

ные величины энергии, направления поляризации и интенсивности первой полосы. Исходные параметры, дающие оптимальные величины энергии, с успехом применяются как к простым, так и к комбинированным замещенным. Была найдена корреляция, соответствующая ожидаемой, между электронным строением молекул и мезомерным влиянием заместителей. Отклонения, наблюдаемые для галогенов, могут быть вызваны, помимо мезомерного влияния, другими возможно важными влияниями.

Кислые компоненты фракции Фульвоновой кислоты торфа

В. ВИЛЬДЕНГАЙН и Г. ГЕНСЕКЕ

Фульвоновые кислоты, полученные путем экстракции торфа горячей водой, были адсорбированы на Wofatit E, а затем фракционированы различными растворителями. В щелочном (NaOH) элюате были обнаружены следующие продукты расщепления лигнина: п-гидроксибензолная, ванилиновая, протокатеховая и п-гидроксикоричная кислоты, а также 3-метиловый эфир кофейной кислоты. Помимо этого удалось идентифицировать другие растительные соединения или продукты их расщепления, а именно: кофейная, глиоксиловая, пировиноградная, гидроксипировиноградная, оксалуксусная, кетоглутаровая, левулиновая, п-гидроксифенилпировиноградная и 4-гидрокси-3-метоксифенилпировиноградная кислоты. Обсуждается их роль в процессе гумификации.

Исследования в области ароматических сульфенилхлоридов, V

Реакция сульфенилхлорида с N^2-арилдитиокарбазатом, О-эфиром тиокарбазиновой кислоты и О-ариловым эфиром фенилтиокарбаминовой кислоты

Ф. КЛИВЕНИ, Г. ШТАЙЕР, А. Э. САБО, Й. ПИНТЕ и Э. ВИНКЛЕР

Была изучена реакция арилсульфенилхлорида с аммонийной солью N^2-арилдитиокарбазиновой кислоты, О-этиловым эфиром тиокарбазиновой кислоты, а также с О-ариловыми эфирами арилтиокарбаминовых кислот. На основе ИК исследований было найдено, что замещение арилсульфенилового катиона происходит на атоме серы во всех трех случаях. В ходе реакции эфира тиокарбазиновой кислоты, с отщеплением алкилгалоида, происходит образование S-арилового эфира замещенной дитиоперкарбазиновой кислоты. Реакция сульфенилирования О-ариловых эфиров арилтиокарбаминовой кислоты протекает указанным способом лишь в том случае, если в О- или N-ариловом кольце имеется орто-заместитель, что позволяет образование таутомерного тиола и стабильного дисульфида.

Изучение реакций тозиловых и мезиловых производных в ряду морфина, X

14-Гидроксиморфиновые производные, I. Азидовые и аминовые соединения

Ш. МАКЛЕЙТ, Л. РАДИЧ, Р. БОГНАР, Т. МИЛЕ и Э. ОЛАХ

Был исследован азидолиз 14-гидроксикодеина, а также 6-О-тозиловых и 6-О-мезиловых эфиров 14-гидроксидигидрокодеина.

Из полученных новых азидо-производных — соответственно строению и природе желаемых восстановленных продуктов — восстановлением, осуществляемым различными методами, были получены новые насыщенные и ненасыщенные амино-производные.

На основе азидолиза 6-О-тозил-14-гидроксикодеина, проводимого в различных условиях реакции, были приготовлены как 6-дезокси-6-азидо-14-гидроксиизокодеин, так и 8-дезокси-8-азидо-14-гидроксипсевдокодеин. Полученное 6-дезокси-6-азидо-соединение было изомеризовано в 8-дезокси-8-азидо-производное. Скорость изомеризации не зависит от прибавления азидного аниона.

Эти экспериментальные данные подтверждают те новые представления относительно реакций нуклеофильного замещения, осуществленных авторами на примере 6-О-тозиловых и 6-О-мезиловых производных морфиновых алкалоидов, согласно которым, независимо от возможности изолирования C_6-изосоединения, C_8-псевдопроизводные как термодинамические изомеры образуются через C_6-изосоединения как кинетические продукты. Т. о., реакции, протекающие через аллильную миграцию, протекают в две ступени — согласно S_N2 и S_Ni' механизмам.

Исследование реакций тозиловых и мезиловых производных в ряду морфина, XI

14-Гидрокси-морфиновые производные, II. Галогеновые соединения

Ш. МАКЛЕЙТ, Л. РАДИЧ Р. БОГНАР и Т. МИЛЕ

Из 6-О-тозил-14-гидроксикодеина на основе нуклеофильного замещения галоидными ионами были получены уже известные 6-дезокси-6-хлор-14-гидроксиизокодеин, 8-дезокси-8-хлор-14-гидроксипсевдокодеин и 8-дезокси-8-бром-14-гидроксипсевдокодеин, а также сообщаются их до сих пор не приводимые данные.

Была осуществлена неизвестная до сих пор изомеризация 6-дезокси-6-хлор-14-гидроксиизокодеина в 8-дезокси-8-хлор-14-гидроксипсевдокодеин.

Был синтезирован ранее неизвестный 6-дезокси-6-фтор-14-гидроксиизокодеин. Строение и пространственная структура этих соединений были исследованы с помощью ИК и ЯМР спектроскопии.

COORDINATION CHEMISTRY: EXPERIMENTAL METHODS

by *K. Burger*

The experimental methods used for the investigation of the structure of coordination compounds are described; such as electron excitation and infrared spectrometry, the method based on the application of the Mössbauer effect, magnetic susceptibility measurement, nuclear magnetic resonance and electronspin resonance spectroscopy, X-ray structure analysis, thermal analysis (TG, DTG, DTA), investigation of optical rotatory dispersion and circular dichroism.

Apart from the brief description of the fundamental principles and ways of investigations of the various experimental methods, the author made efforts to present the possibilities of application thereof in coordination chemistry in the broadest possible range.

In English · Approx. 290 pages · 114 figures · Cloth

THE BUTTERWORTH GROUP — London

AKADÉMIAI KIADÓ — Budapest

A co-edition — distributed in the socialist countries by Kultura, in all other countries by The Butterworth Group, London.

QUANTENCHEMIE

von J. Ladik

Dieses Traktat wünscht Physikern und Chemikern eine Einführung in die quantenchemische Analyse der Elektronenstruktur von Molekülen, also in die Quantenchemie zu geben. Die interessantesten Abschnitte des Werkes sind: Abschnitt II über die quantenchemischen Annäherungsmethoden zur Behandlung des Mehrkörper-Problems, die neuesten »ab initio« Berechnungen, ferner die Beschreibung der neuen Methode zur Bestimmung von quantenchemischen Integralen mit mehreren Zentren.

In deutscher Sprache · Etwa 350 Seiten · Ganzleinen

Herausgegeben von

FERDINAND ENKE VERLAG
Stuttgart

AKADÉMIAI KIADÓ
Budapest

Vertrieben in den sozialistischen Ländern von KULTURA, Budapest, in allen anderen Ländern von FERDINAND ENKE VERLAG, Stuttgart.

The Acta Chimica publish papers on chemistry in English, German, French and Russian.

The Acta Chimica appear in volumes consisting of four parts of varying size, 4 volumes being published a year.

Manuscripts should be addressed to

Acta Chimica
Budapest 112/91 Műegyetem

Correspondence with the editors should be sent to the same address.

The rate of subscription is $ 16.00 a volume.

Orders may be placed with "*Kultúra*" Foreign Trade Company for Books and Newspapers (Budapest I., Fő utca 32. Account No. 43-790-057-181) or with representatives abroad.

Les Acta Chimica paraissent en français, allemand, anglais et russe et publient des mémoires du domaine des sciences chimiques.

Les Acta Chimica sont publiés sous forme de fascicules. Quatre fascicules seront réunis en un volume (4 volumes par an)

On est prié d'envoyer les manuscrits destinés à la rédaction à l'adresse suivante:

Acta Chimica
Budapest 112/91 Műegyetem

Toute correspondance doit être envoyée à cette même adresse.

Le prix de l'abonnement est de $ 16.00 par volume.

On peut s'abonner à l'Entreprise pour le Commerce Extérieur de Livres et Journaux «*Kultúra*» (Budapest I., Fő utca 32. Compte-courant No. 43-790-057-181) ou à l'étranger chez tous les représentants ou dépositaires.

«*Acta Chimica*» издают трактаты из области химической науки на русском, французском, английском и немецком языках.

«*Acta Chimica*» выходят отдельными выпусками разного объема. 4 выпуска составляют один том. 4 тома публикуются в год.

Предназначенные для публикации рукописи следует направлять по адресу:

Acta Chimica
Budapest 112/91 Műegyetem

По этому же адресу направлять всякую корреспонденцию для редакции.

Подписная цена — $ 16.00 за том.

Заказы принимает предприятие по внешней торговле книг и газет «*Kultúra*» (Budapest I., Fő utca 32. Текущий счет № 43-790-057-181) или его заграничные представительства и уполномоченные.

Reviews of the Hungarian Academy of Sciences are obtainable at the following addresses:

ALBANIA

Drejtorija Qändrone e Pärhapjes
dhe Propagandimit tä Librit
Kruga Konferenca e Päzes
Tirana

AUSTRALIA

A. Keesing
Box 4886, GPO
Sydney

AUSTRIA

GLOBUS
Höchstädtplatz 3
A-1200 Wien XX

BELGIUM

Office International de Librairie
30, Avenue Marnix
Bruxelles 5
Du Monde Entier
5, Place St. Jean
Bruxelles

BULGARIA

HEMUS
11 pl Slaveikov
Sofia

CANADA

Pannonia Books
2, Spadina Road
Toronto 4, Ont.

CHINA

Waiwen Shudian
Peking
P. O. B. 88

CZECHOSLOVAKIA

Artia
Ve Smečkách 30
Praha 2
Poštovní Novinová Služba
Dovoz tisku
Vinohradská 46
Praha 2
Mad'arská Kultura
Václavské nám. 2
Praha 1
SLOVART A. G.
Gorkého
Bratislava

DENMARK

Ejnar Munksgaard
Nörregade 6
Copenhagen

FINLAND

Akateeminen Kirjakauppa
Keskuskatu 2
Helsinki

FRANCE

Office Internationa de Documentation
et Librairie
48, rue Gay-Lussac
Paris 5

GERMAN DEMOCRATIC REPUBLIC

Deutscher Buch-Export und Import
Leninstraße 16
Leipzig 701
Zeitungsvertriebsamt
Fruchtstraße 3—4
1004 Berlin

GERMAN FEDERAL REPUBLIC

Kunst und Wissen
Erich Bieber
Postfach 46
7 Stuttgart S.

GREAT BRITAIN

Blackwell's Periodicals
Oxenford House
Magdalen Street
Oxford
Collet's Subscription Import
Department
Dennington Estate
Wellingsborough. Northants.
Robert Maxwell and Co. Ltd.
4—5 Fitzroy Square
London W. 1

HOLLAND

Swetz and Zeitlinger
Keizersgracht 471—487
Amsterdam C.
Martinus Nijhof
Lange Voorhout 9
The Hague

INDIA

Hind Book House
66 Babar Road
New Delhi 1

ITALY

Santo Vanasia
Via M. Macchi 71
Milano
Libreria Commissionaria Sansoni
Via La Marmora 45
Firenze
Techna
Via Cesi 16
40135 Bologna

JAPAN

Kinokuniya Book-Store Co. Ltd.
826 Tsunohazu 1-chome
Shinjuku-ku
Tokyo
Maruzen and Co. Ltd.
P. O. Box 605
Tokyo-Central

KOREA

Chulpanmul
Phenjan

NORWAY

Tanum-Cammermeyer
Karl Johansgt 41—43
Oslo 1

POLAND

RUCH
ul. Wronia 23
Warszawa

ROUMANIA

Cartimex
Str. Aristide Briand 14—18
Bucureşti

SOVIET UNION

Mezhdunarodnaya Kniga
Moscow G—200

SWEDEN

Almquist and Wiksell
Gamla Brogatan 26
S—101 20 Stockholm

USA

F. W. Faxon Co. Inc.
15 Southwest Park
Westwood Mass. 02090
Stechert Hafner Inc.
31. East 10th Street
New York, N. Y. 10003

VIETNAM

Xunhasaba
19, Tran Quoc Toan
Hanoi

YUGOSLAVIA

Forum
Vojvode Mišića broj 1
Novi Sad
Jugoslovenska Knjiga
Terazije 27
Beograd

ACTA CHIMICA

ACADEMIAE SCIENTIARUM HUNGARICAE

ADIUVANTIBUS

V. BRUCKNER, GY. DEÁK, K. POLINSZKY,
E. PUNGOR, G. SCHAY, Z. G. SZABÓ

REDIGIT

B. LENGYEL

TOMUS 74 FASCICULUS 2

AKADÉMIAI KIADÓ, BUDAPEST

1972

ACTA CHIM. (BUDAPEST) ACASA 74 (2) 121—266 (1972)

ACTA CHIMICA

A MAGYAR TUDOMÁNYOS AKADÉMIA KÉMIAI TUDOMÁNYOK OSZTÁLYÁNAK IDEGEN NYELVŰ KÖZLEMÉNYEI

SZERKESZTI

LENGYEL BÉLA

TECHNIKAI SZERKESZTŐK

DEÁK GYULA és HARASZTHY-PAPP MELINDA

Az Acta Chimica német, angol, francia és orosz nyelven közöl értekezéseket a kémiai tudományok köréből.

Az Acta Chimica változó terjedelmű füzetekben jelenik meg, egy-egy kötet négy füzetből áll. Évente átlag négy kötet jelenik meg.

A közlésre szánt kéziratok a szerkesztőség címére (Budapest 112/91 Műegyetem) küldendők.

Ugyanerre a címre küldendő minden szerkesztőségi levelezés. A szerkesztőség kéziratokat nem ad vissza.

Megrendelhető a belföld számára az „Akadémiai Kiadó"-nál (Budapest V., Alkotmány utca 21. Bankszámla 05-915-111-46), a külföld számára pedig a „Kultúra" Könyv- és Hírlap Külkereskedelmi Vállalatnál (Budapest I., Fő utca 32. Bankszámla: 43-790-057-181) vagy annak külföldi képviseleteinél és bizományosainál.

Die Acta Chimica veröffentlichen Abhandlungen aus dem Bereiche der chemischen Wissenschaften in deutscher, englischer, französischer und russischer Sprache.

Die Acta Chimica erscheinen in Heften wechselnden Umfanges. Vier Hefte bilden einen Band. Jährlich erscheinen 4 Bände.

Die zur Veröffentlichung bestimmten Manuskripte sind an folgende Adresse zu senden:

Acta Chimica
Budapest 112/91 Műegyetem

An die gleiche Anschrift ist auch jede für die Redaktion bestimmte Korrespondenz zu richten. Abonnementspreis pro Band: $ 16.00.

Bestellbar bei dem Buch- und Zeitungs-Außenhandels-Unternehmen »*Kultúra*« (Budapest I., Fő utca 32. Bankkonto No. 43-790-057-181) oder bei seinen Auslandsvertretungen und Kommissionären.

THIS ISSUE IS DEDICATED TO

PROFESSOR TIBOR ERDEY-GRÚZ

AN OUTSTANDING SCIENTIST OF PHYSICAL CHEMISTRY,
PRESIDENT OF THE HUNGARIAN ACADEMY OF SCIENCES,

IN COMMEMORATION OF HIS

70TH BIRTHDAY

BY HIS PUPILS AND COLLEAGUES

Acta Chimica Academiae Scientiarum Hungaricae, Tomus 74 (2), pp. 123—133 (1972)

UNTERSUCHUNG DER IONISATION VON METALLEN UND DER NEUTRALISATION VON METALLIONEN MIT DER ROTIERENDEN RING-SCHEIBENELEKTRODE, IX

L. KISS, J. FARKAS und Á. FÓTHI*

(Lehrstuhl für physikalische Chemie und Radiologie, L. Eötvös Universität, Budapest)

Eingegangen am 1. Juli 1971

Aufgrund der in unseren früheren Mitteilungen festgestellten Zusammenhänge hinsichtlich der in zwei Einelektronenschritten verlaufenden Ionisation von Metallen und Reduktion von Metallionen wurden die an der rotierenden Scheibenelektrode meßbaren Polarisationskurven und die an der Ringelektrode meßbaren Oxydationsgrenzströme für einige Fälle berechnet.

In unseren vorangegangenen Mitteilungen [1, 2] wurden Zusammenhänge bei den an rotierenden Ring-Scheibenelektroden verlaufenden Vorgängen festgestellt, für den Fall, daß an der Scheibenelektrode folgende Reaktionen vor sich gehen:

$$\mathrm{Me} \underset{k_{k_1}}{\overset{k_{a_1}}{\rightleftharpoons}} \mathrm{Me}^{+} + e \qquad \text{(I)}$$

$$\mathrm{Me}^{+} \underset{k_{k_2}}{\overset{k_{a_2}}{\rightleftharpoons}} \mathrm{Me}^{++} + e \qquad \text{(II)}$$

Es wurde die Gleichung der an der rotierenden Scheibe gemessenen Polarisationskurve für jenen Fall berechnet, in welchem im Vorgang Diffusions- und Übertrittspolarisation gleichzeitig auftreten. Demgemäß ist

$$j = k_{a_1} \frac{X_1 + \dfrac{2k_{a_2}}{1 + \dfrac{k_{k_2}}{X_2}}}{X_1 + k_{k_1} + \dfrac{k_{a_2}}{1 + \dfrac{k_{k_2}}{X_2}}} - k_{k_1} - \frac{\dfrac{k_{a_2}}{1 + \dfrac{k_{k_2}}{X_2}}}{X_1 + k_{k_1} + \dfrac{k_{a_2}}{1 + \dfrac{k_{k_2}}{X_2}}} - X_1 c_{1\infty} - \frac{c_{2\infty}}{\dfrac{1}{X_2} + \dfrac{1}{k_{k_2}}} \frac{X_1 + 2k_{k_1}}{X_1 + k_{k_1} + \dfrac{k_{a_2}}{1 + \dfrac{k_{k_2}}{X_2}}} \qquad (1)$$

* Lehrstuhl für numerische und Computer-Mathematik, L. Eötvös Universität, Budapest.

j = die Scheibe durchfließende Stromdichte, $c_{1\infty}$ und $c_{2\infty}$ = Konzentration der Me^{+} bzw. Me^{2+}-Ionen im Inneren der Lösung,

$$X_i = 0{,}62 F D_i^{2/3} \nu^{-1/6} \omega^{1/2} \tag{2}$$

$i = 1, 2$; F = Faradaysche Konstante, D_i = Diffusionskoeffizient der Me^{+} bzw. Me^{2+}-Ionen, ω = Winkelgeschwindigkeit der rotierenden Elektrode, ν = kinematische Viskosität der Lösung,

$$k_{a_1} = k'_{a_1} \exp\left\{\frac{\alpha_1 F\varphi}{RT}\right\} \tag{3}$$

$$k_{k_1} = k'_{k_1} \exp\left\{-\frac{(1-\alpha_1)F\varphi}{RT}\right\} \tag{4}$$

$$k_{a_2} = k'_{a_2} \exp\left\{\frac{\alpha_2 F\varphi}{RT}\right\} \tag{5}$$

$$k_{k_2} = k'_{k_2} \exp\left\{-\frac{(1-\alpha_2)F\varphi}{RT}\right\} \tag{6}$$

k'_{a_1}, k'_{k_1}, k'_{a_2}, k'_{k_2} sind vom Elektrodenpotential unabhängige Konstanten, α_1 und α_2 sind Übertrittsfaktoren, φ = Potential der Scheibenelektrode.

Es wurde der Ausdruck für den an der Ringelektrode gemessenen Grenzstrom I_h des Me^{+}-Ions angegeben [1, 3]:

$$I_h = r_1^2 \pi \left[N \frac{j + X_1 c_{1\infty} + 2c_{2\infty} \dfrac{X_2 k_{k_2}}{X_2 + k_{k_2}}}{1 + \dfrac{2k_{a_2}}{X_1 + \dfrac{X_1}{X_2} k_{k_2}}} + (S - N) X_1 c_{1\infty} \right] \tag{7}$$

N und S sind hier von den geometrischen Abmessungen der Elektrode abhängige Konstanten [3, 4, 5] und r_1 ist der Radius der Scheibenelektrode.

Wie bereits im vorangegangenen [1, 2] gezeigt wurde, ändert sich bei Veränderung des Elektrodenpotentials (der Stromdichte) der Neigungswinkel der Polarisationskurve $\varphi - \log j$ wegen dem Übergang aus dem einen diskutierten Grenzfall in den anderen. Der Mechanismus des eigentlichen Elektrodenvorganges (Ladungsübertritt) bleibt also unverändert, dennoch ändert sich jener Parameter, aus dem oft Schlüsse auf den Mechanismus des Vorganges gezogen

werden. Um die Verhältnisse besser und vollständiger überblicken zu können, wurden deshalb aufgrund der Gleichungen (1) und (7) für verschiedene Werte von k'_{a_i} und k'_{k_i} in zwei aufeinanderfolgenden Einelektronen-Übertrittsreaktionen mit Hilfe eines Computers folgende Berechnungen durchgeführt: es wurden die Polarisationskurven der an der rotierenden Scheibenelektrode verlaufenden Vorgänge und die an der die Scheibenelektrode umgebenden Ringelektrode meßbaren, durch das Intermediärprodukt bestimmten Oxydationsgrenzströme in Abhängigkeit von der die Scheibenelektrode durchfließenden Stromdichte (bzw. vom Potential) bei verschiedenen Umdrehungszahlen der rotierenden Elektrode berechnet.

Dabei war die Einheit von k_{a_1} $A \cdot \text{cm}^{-2}$, die Einheit von k_{a_2}, k_{k_1}, k_{k_2} und X_i $A \cdot \text{cm} \cdot \text{Mol}^{-1}$. Im weiteren wurde für F, α_i, D_i und ν mit folgenden Werten gerechnet: $F = 10^5$ C $\cdot$ Mol^{-1}, $\alpha_i = 0{,}5$, $D_i = 10^{-5}$ cm^2 s^{-1} und $\nu = 10^{-2}$ cm^2 s^{-1}. Mit diesen Werten gerechnet ist $X_i = X'_i f^{1/2}$ mit $X'_i = 20$ $A \cdot \text{cm} \cdot \text{Mol}^{-1}\,\text{min}^{1/2}$ und $f =$ Umdrehungszahl der Elektrode in min^{-1}. Als Temperaturwert wurde $T = 298$ °K gewählt. Der Wert von f wurde in den Berechnungen zwischen 10^1 und 10^5 min^{-1} verändert. Die Umdrehungszahl von 10/min entspricht der in der Lösung auftretenden natürlichen Konvektion [6]. Demgemäß ergaben sich für die Berechnungen folgende Werte: $X^{(1)} \simeq \simeq 62$ $A \cdot \text{cm} \cdot \text{Mol}^{-1}$, $X^{(5)} \simeq 6{,}2 \cdot 10^3$ $A \cdot \text{cm} \cdot \text{Mol}^{-1}$. Die Umdrehungszahl von 10^5/min wäre experimentell mit der Annahme der laminaren Strömung [1, 3] kaum zu vereinbaren, jedoch war unser Ziel bei der Berechnung der Kurven, die Wirkung der Umdrehungszahl zu untersuchen, und diese Wirkung ist bei der extrem hohen Umdrehungszahl viel auffallender. Es wurde in allen Fällen mit einer Oberfläche der rotierenden Scheibenelektrode von 1 cm^2 und einem Wert von 0,1 für die Konstante N gerechnet.

Bei der Berechnung der im weiteren vorzuführenden Kurven wurde angenommen, daß $c_{1\infty} \simeq 0$ und (mit Ausnahme von Abb. 7) $c_{2\infty} \simeq 0$ ist, d. h. daß die Konzentrationen des Intermediärions und des Endprodukt-Ions im Inneren der Lösung praktisch gleich Null sind. Dies bedeutet zugleich, daß unter solchen Bedingungen nicht von einem Austauschstrom der einzelnen Vorgänge gesprochen werden kann, und daß diese Vorgänge keine kathodischen Polarisationskurven besitzen. Demzufolge vereinfacht sich Gl. (1), da es sich um einen in zwei Einelektronenschritten verlaufenden Vorgang handelt, folgenderart:

$$j = k_{a_1} \frac{X_1 + \dfrac{2k_{a_2}}{1 + \dfrac{k_{k_2}}{X_2}}}{X_1 + k_{k_1} + \dfrac{k_{a_2}}{1 + \dfrac{k_{k_2}}{X_2}}} \tag{8}$$

Aus Gl. (8) ist ersichtlich, daß der jeweilige Ausgangswert von k'_{a_1} die Form der Polarisationskurve nicht beeinträchtigt, sondern nur ihre Lage verschiebt.

In den Abbildungen 1—7 werden einige aufgrund von Gl. (1) und Gl. (7) berechnete Polarisationskurven φ — lg j sowie die an der Ringelektrode meßbaren Grenzströme in Abhängigkeit von der die Scheibenelektrode durchfließenden Stromdichte (lg I_h — lg j) dargestellt. Die Werte der beim Rechnen

Tabelle I

Bei der Berechnung der Polarisationskurven und der an der Ringelektrode meßbaren Grenzströme angewendete Parameter

Nr. der Abbildung	k'_{a_1} $A \cdot cm^2$	k'_{k_1} $A \cdot cm \cdot Mol^{-1}$	k'_{a_2} $A \cdot cm \cdot Mol^{-1}$	k'_{k_2} $A \cdot cm \cdot Mol^{-1}$	$c_{2,\infty}$ $Mol \cdot cm^{-3}$
1	10^{-6}	10^{10}	10^{5}	10^{4}	0
2	10^{-6}	10^{10}	10^{2}	$\simeq 0$	0
3	10^{-1}	10^{8}	1	10	0
4	10^{-6}	10^{8}	10^{6}	10^{6}	0
5	10^{-5}	$\simeq 0$	10^{6}	10^{8}	0
6	10^{-6}	10^{8}	10^{3}	10^{8}	0
7	10^{-6}	10^{8}	10^{3}	10^{2}	10^{-9} / 10^{-3}

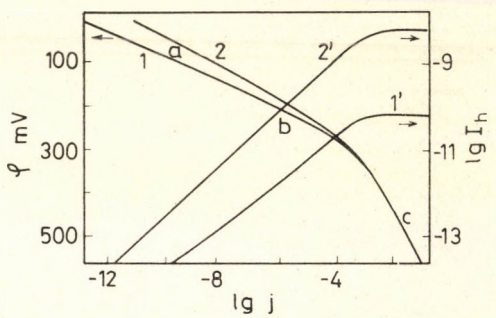

Abb. 1. Polarisationskurven (Kurve 1 und 2) und Oxydationsgrenzstrom (Kurve 1′ und 2′) bei natürlicher Konvektion (Kurve 1 und 1′) und bei einer Umdrehungszahl der Elektrode von 10^5/Minute (Kurve 2 und 2′); $k'_{a_1} = 10^{-6}$ $A \cdot cm^{-2}$, $k'_{k_1} = 10^{10}$ $A \cdot cm \cdot Mol^{-1}$, $k'_{a_2} = 10^{5}$ $A \cdot cm \cdot Mol^{-1}$, $k'_{k_2} = 10^{4}$ $A \cdot cm \cdot Mol^{-1}$

verwendeten (im vorangegangenen noch nicht angegebenen) Parameter sind in Tab. I zusammengestellt.

Aus den für $\varphi = 0$ angenommenen Geschwindigkeitskonstanten zur Berechnung der Kurven in Abb. 1 (s. Tab. I) ist ersichtlich, daß bei geringen

anodischen Stromdichten und natürlicher Konvektion

$$k_{k_1} \gg X_2 \frac{k_{a_2}}{k_{k_2}} \gg X_1 \quad \text{und} \quad k_{k_2} \gg X_2$$

ist. Unter diesen Bedingungen erhält man aus Gl. (8) den folgenden einfacheren Zusammenhang [1]:

$$j = 2X_2 \frac{k'_{a_1} k'_{a_2}}{k'_{k_1} k'_{k_2}} \exp\left\{\frac{2F\varphi}{RT}\right\} \tag{9}$$

woraus sich ein Neigungswinkel der Polarisationskurve von $\simeq$29 mV ergibt (s. Strecke *a* der Kurve 1). Bei hoher Umdrehungszahl der Elektrode wird k_{k_2} auf der Strecke *a* kommensurabel mit X_2, folglich steigt der Neigungswinkel der Polarisationskurve durch die Rührwirkung an und das System nähert sich jenem Zustand, worin die Polarisationskurve durch folgende Gleichung beschrieben wird [1]:

$$j = 2 \frac{k'_{a_1} k'_{a_2}}{k'_{k_1}} \exp\left\{\frac{(1+\alpha_2)F\varphi}{RT}\right\} \tag{10}$$

Dieser Fall wird bei der anodischen Auflösung von Kupfer in sauren Sulfatlösungen realisiert [7].

Auf der Strecke *b* beginnt die Kommensurabilität von k_{k_2} und X_2 bereits bei natürlicher Konvektion, da der Wert von k_{k_2} wegen dem Positiverwerden des Potentials abnimmt und folglich der Neigungswinkel der Polarisationskurve zunimmt. Bei hoher Umdrehungszahl der Elektrode ist dagegen der Neigungswinkel der Polarisationskurve $\simeq$40 mV, da die Bedingungen erfüllt sind, bei denen die Polarisationskurve durch Gl. (10) beschrieben wird [1].

Bei weiterer Zunahme der anodischen Polarisation gelangt man zur Bedingung $k_{k_1} \ll k_{a_2}$ und die Kurve wird durch folgende Gleichung beschrieben [1]:

$$j = 2k'_{a_1} \exp\left\{\frac{\alpha_1 F\varphi}{RT}\right\} \tag{11}$$

Hier ist der Neigungswinkel 118 mV und die Umdrehungszahl der Elektrode übt keine Wirkung aus.

Wie aus Abb. 1 ersichtlich ist, steigt der Oxydationsgrenzstrom I_h des Intermediärproduktes mit der Stromdichte monoton an. Sobald die Bedingung $k_{k_1} \ll k_{a_2}$ erfüllt ist, wird I_h (wie aus Gl. 7 hervorgeht) vom Potential der Scheibenelektrode bzw. von der Stromdichte unabhängig; die Grenzstromkurve in Abb. 1 wird zu einer Geraden, die parallel zur Abszisse verläuft. Aus Gl.

(7) folgt, daß die Grenzstromkurve unter den gegebenen Bedingungen in sämtlichen Stromdichtebereichen von der Umdrehungszahl der Elektrode abhängig ist. Auf der Strecke *c*, wo der Verlauf der Polarisationskurve von der Rührwirkung unabhängig ist, beträgt das Verhältnis der am Ring meßbaren Grenzströme gemäß Gl. (7):

$$\frac{I_h^{(5)}}{I_h^{(1)}} = 10^2,$$

$I_h^{(5)}$ = Grenzstrom bei der Umdrehungszahl von 10^5/min,
$I_h^{(1)}$ = Grenzstrom bei der Umdrehungszahl von 10/min.

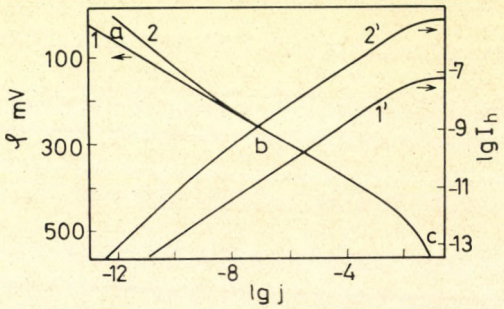

Abb. 2. Polarisationskurven und Oxydationsgrenzstrom. Bezeichnung der Kurven wie in Abb. 1. $k'_{a_1} = 10^{-6}\ A \cdot \mathrm{cm}^{-2}$, $k'_{k_1} = 10^{10}\ A \cdot \mathrm{cm} \cdot \mathrm{Mol}^{-1}$, $k'_{a_2} = 10^2\ A \cdot \mathrm{cm} \cdot \mathrm{Mol}^{-1}$, $k'_{k_2} \simeq 0$

Bei den Kurven in Abb. 2 wurde die Bedingung $k'_{k_2} \simeq 0$ gewählt (s. Tab. I) und k'_{a_2} ist mit $X_1^{(1)}$ kommensurabel (s. Zähler in Gl. 8). Demzufolge ergibt sich bei geringer anodischer Polarisation (Strecke *a*) ein höherer Neigungswinkel als 40 mV für Kurve 1. Mit zunehmender Umdrehungszahl, da dann die Bedingung $X_1^{(5)} \gg k_{a_2}$ erfüllt wird, ergibt sich folgende Annäherungsgleichung für die Polarisationskurve:

$$j = X_1 \frac{k'_{a_1}}{k'_{k_1}} \exp\left\{\frac{F\varphi}{RT}\right\} \tag{12}$$

und demgemäß beträgt der Neigungswinkel $\simeq$60 mV.

Bei zunehmender anodischer Stromdichte wird X_1 bei natürlicher Konvektion früher k_{a_2} vernachlässigbar als bei hoher Umdrehungszahl der Elektrode. Demzufolge wird die Polarisationskurve in diesem Fall bereits von verhältnismäßig geringen anodischen Stromstärken an durch Gl. (10) beschrieben (Strecke *a*). Auf der Strecke *b* nimmt k_{a_2} einen ziemlich hohen Wert an und die Kurve wird — unabhängig von der Rührwirkung — durch Gl. (10) beschrieben.

Auf der Strecke *c* beträgt der Neigungswinkel der Kurve — gemäß Gl. (11) — 118 mV.

Die Grenzstromkurven $\lg I_h$—$\lg j$ verlaufen in diesem Fall ähnlich wie in Abb. 1.

Bei den in Abb. 3 vorgeführten Kurven wurden die Ausgangswerte der Geschwindigkeitskonstanten (s. Tab. I) so gewählt, daß

$$k'_{k_1} \gg X_2 \frac{k'_{a_2}}{k'_{k_2}}$$

sein soll, demgemäß wird die Polarisationskurve bei geringer anodischer Polarisation (Strecke *a*) durch Gl. (12) beschrieben und die Rührwirkung verändert

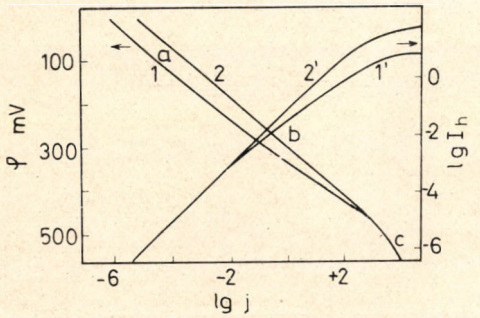

Abb. 3. Polarisationskurven und Oxydationsgrenzstrom. Bezeichnung der Kurven wie in Abb. 1. $k'_{a_1} = 10^{-1}\ A \cdot \mathrm{cm}^{-2}$, $k'_{k_1} = 10^8\ A \cdot \mathrm{cm} \cdot \mathrm{Mol}^{-1}$, $k'_{a_2} = 1\ A \cdot \mathrm{cm} \cdot \mathrm{Mol}^{-1}$, $k'_{k_2} = 10\ A \cdot \mathrm{cm} \cdot \mathrm{Mol}^{-1}$

den Neigungswinkel von ≃60 mV nicht, sondern verschiebt nur die Kurve in Richtung negativeren Potentials. In diesem Fall wird die Geschwindigkeit des Vorganges durch die Diffusion des Intermediärproduktes bestimmt. Dieser Fall wird bei der anodischen Auflösung von Kupfer in sauren chloridhaltigen Lösungen realisiert [8].

Bei stärker anodischer Polarisation (Strecke *b*) und natürlicher Konvektion wird die Bedingung $X_2 \ll k_{a_2}$ erfüllt; da hier noch $k_{k_1} \gg k_{a_1}$ ist, wird die Polarisationskurve durch Gl. (10) beschrieben, d. h. es handelt sich um reine Übertrittspolarisation. Bei hoher Umdrehungszahl der Elektrode ist jedoch der geschwindigkeitsbestimmende Schritt wiederum die Diffusion des Intermediärproduktes (Kurve 2, Strecke *b*). Es handelt sich also hier um den ungewöhnlichen Fall, daß die Übertrittspolarisation durch die Rührwirkung in Diffusionspolarisation übergeht. Die Ursache hierfür, worauf bereits im vorangegangenen hingewiesen wurde, ist, daß die Diffusion des Intermediärproduktes von der Oberfläche weg und die weitere Reaktion des Intermediärproduktes parallele Vorgänge sind.

Bei hoher anodischer Polarisation (Strecke *c*) beträgt der Neigungswinkel gemäß Gl. (11) $\simeq$118 mV und ist von der Umdrehungszahl unabhängig.

Die Grenzstromkurve $\lg I_h - \lg j$ ist auf der Strecke *a* von der Umdrehungszahl der Elektrode unabhängig, solange $X_1 \gg k_{a_2}$ ist (s. Gl. 7). Bei höheren anodischen Stromdichten ist der Verlauf der Kurven ähnlich wie in Abb. 1 und 2.

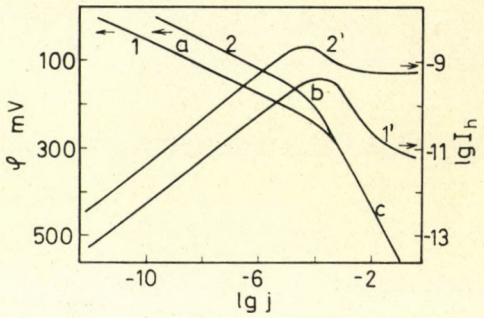

Abb. 4. Polarisationskurven und Oxydationsgrenzstrom. Bezeichnung der Kurven wie in Abb. 1. $k'_{a_1} = 10^6\ A \cdot \mathrm{cm}^{-2}$, $k'_{k_1} = 10^8\ A \cdot \mathrm{cm} \cdot \mathrm{Mol}^{-1}$, $k'_{a_2} = 10^6\ A \cdot \mathrm{cm} \cdot \mathrm{Mol}^{-1}$, $k'_{k_2} = 10\ A \cdot \mathrm{cm} \cdot \mathrm{Mol}^{-1}$

In Abb. 4 beträgt der Neigungswinkel der Polarisationskurve auf Strecke *a* gemäß Gl. (9) $\simeq$29 mV. Am Anfang der Strecke *b* ist

$$k_{k_1} \ll X_2 \frac{k_{a_2}}{k_{k_2}} \quad \text{und} \quad X_1 \ll X_2 \frac{k_{a_2}}{k_{k_2}},$$

demgemäß wird die Polarisationskurve von hier an durch Gl. (11) beschrieben. Die Grenzstromkurve nimmt auf der Strecke *a* monoton zu; dagegen nimmt $\lg I_h$ auf der Strecke *b* mit $\lg j$ ab, weil — wie aus Gl. (7) ersichtlich ist — eine Änderung von $\simeq$120 mV dazu nötig ist, um im Ausdruck für I_h den Zähler (j) um eine Größenordnung zu erhöhen, während der Nenner bereits bei einer Änderung von $\simeq$60 mV um eine Größenordnung zunimmt. Wird dann bei der weiteren Steigerung der anodischen Polarisation $k_{k_2} \ll X_2$, so ändert sich I_h nicht mehr mit j (Strecke *c*).

In Abb. 5 wird ein ziemlich extremer Fall vorgeführt. Auf der Strecke *a* der Polarisationskurve besitzt der Neigungswinkel einen Wert zwischen 60 und 118 mV, da im Zähler und Nenner des Bruches in Gl. (8) Glieder von kommensurabiler Größenordnung enthalten sind. Aus der Gleichung geht auch hervor, daß die Änderung der hydrodynamischen Verhältnisse keine Wirkung auf die Polarisationskurve ausübt. Der Neigungswinkel ändert sich zu 118 mV,

sobald die Bedingung

$$X_1 \ll \frac{k_{a_2}}{1 + \frac{k_{k_2}}{X_2}}$$

erfüllt wird; im weiteren wird die Polarisationskurve durch Gl. (11) beschrieben.

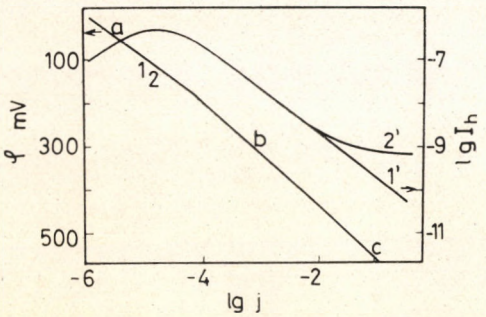

Abb. 5. Polarisationskurven und Oxydationsgrenzstrom. Bezeichnung der Kurven wie in Abb. 1. $k_{a_1} = 10^5\ A \cdot cm^{-2}$, $k_{k_1} \simeq 0$, $k_{a_2} = 10^6\ A \cdot cm \cdot Mol^{-1}$, $k_{k_2} = 10^8\ A \cdot cm \cdot Mol^{-1}$

$\lg I_h$ nimmt — wie aus Gl. (7) ersichtlich — solange mit $\lg j$ zu, bis X_1 viel kleiner wird als

$$\frac{k_{a_2}}{1 + \frac{k_{k_2}}{X_2}}$$

Danach nimmt $\lg I_h$ mit $\lg j$ ab, weil — wie in Abb. 4 — der Zähler von I_h bei einer Änderung von 120 mV, der Nenner dagegen bei einer Änderung von 60 mV um eine Größenordnung zunimmt. Aus Gl. (7) folgt, daß der Wert von I_h nur dann anfängt von der Umdrehungszahl der Elektrode abzuhängen, wenn k_{k_2} mit X_2 kommensurabel ist und dann von j unabhängig wird, wenn $k_{k_2} \ll X_2$ ist.

Ein interessanter Fall ist in Abb. 6 dargestellt. Auf der Strecke *a* wird die Bedingung erfüllt, die der Strecke *a* in Abb. 3 entspricht, während bei positiveren Potentialen die Bedingungen für die Strecken *a* und *b* in Abb. 4 erfüllt werden (Strecke *b* und *c* in Abb. 6).

In Abb. 7 wird ein Fall gezeigt, in welchem die Konzentration des Me^{2+}-Ions, d. h. des stabilen Endproduktes im Inneren der Lösung, höher als Null ist. Im gewählten Fall werden die Zusammenhänge φ — $\lg j$ und $\lg I_h$ — $\lg j$ nur bei natürlicher Konvektion untersucht. Die anodische Polarisationskurve wird bei geringen Stromdichten durch Gl. (10), bei hohen Stromdichten durch Gl. (11) beschrieben (Kurve 1). Der kathodischen Polarisationskurve entspricht

bei $c_{2,\infty} = 10^{-9}$ Mol · cm^{-3} die Kurve 2, bei $c_{2,\infty} = 10^{-3}$ Mol · cm^{-3} die Kurve 3. Da bei katodischer Polarisation $k_{k_1} \gg k_{a_2}$ ist, ergibt sich — wie aus Gl. (1) unmittelbar erkennbar ist [2]

$$j = -2k_{k_2}c_{2,\infty}, \tag{13}$$

und demgemäß beträgt der Neigungswinkel $\simeq$118 mV. Infolge des Kathodenvorganges biegt sich die anodische Polarisationskurve in der Nähe des sich einstellenden Gleichgewichtspotentials von ihrem ursprünglichen Verlauf ab.

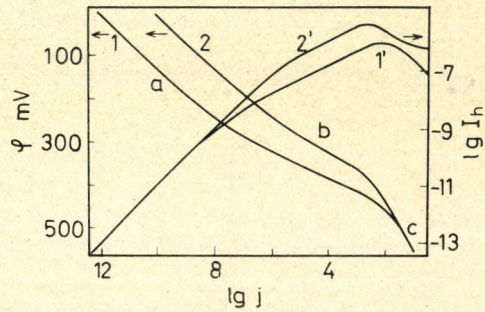

Abb. 6. Polarisationskurven und Oxydationsgrenzstrom. Bezeichnung der Kurven wie in Abb. 1. $k_{a_1} = 10^{-6}$ A · cm^{-2}, $k_{k_1} = 10^{8}$ A · cm · Mol^{-1}, $k_{a_2} = 10^{3}$ A · cm · Mol^{-1}, $k_{k_2} = 10^{8}$ A · cm · Mol^{-1}

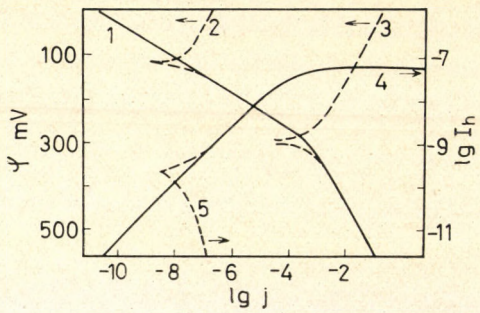

Abb. 7. Polarisationskurven (Kurven 1, 2 und 3) und Oxydationsgrenzstrom (Kurven 4 und 5) bei natürlicher Konvektion, in Gegenwart von Me^{2+}-Ionen in der Lösung. Kurve 1 — anodische Polarisationskurve. Kurven 2 und 3 — kathodische Polarisationskurven. $c_{2,\infty}$ bei Kurven 2 und 5 $= 10^{-9}$ Mol · cm^{-3}, $c_{2,\infty}$ bei Kurve 3 $= 10^{-3}$ Mol · cm^{-3}. $k_{a_1} = 10^{-6}$ A · cm^{-2}, $k_{k_1} = 10^{8}$ A · cm · Mol^{-1}, $k_{a_2} = 10^{3}$ A · cm · Mol^{-1}, $k_{k_2} = 10^{2}$ A · cm · Mol^{-1}

Ohne Metallionen ist der Charakter der Kurve lg I_h — lg j (Kurve 4) ähnlich wie in Abb. 1 und 2. Bei kathodischer Polarisation und $c_{2,\infty} = 10^{-9}$ Mol · cm^{-3} verläuft die Änderung des Grenzstromes mit der kathodischen Stromdichte nach Kurve 5. Bei hoher Metallionenkonzentration (10^{-3} Mol · · cm^{-3}) ändert sich der Grenzstrom — wie auch aus Gl. (7) hervorgeht — nur

wenig mit der Stromdichte j. Im untersuchten Fall entspricht dieser Änderung annähernd die horizontale Strecke der Kurve 4.

Aus den vorgeführten Beispielen geht hervor, daß bei der in Einelektronenschritten verlaufenden anodischen Auflösung von Metallen die Tafelsche Konstante b der anodischen Polarisationskurve einen Wert zwischen 29 mV und 118 mV besitzen kann. Demgemäß ist es kaum möglich, allein aus dem Neigungswinkel der Polarisationskurven verläßliche Folgerungen hinsichtlich des Reaktionsmechanismus zu ziehen, besonders dann, wenn die Rührwirkung nicht untersucht wird und wenn es nicht möglich ist, Messungen in einem weiten Stromdichtebereich durchzuführen.

Die angeführten Beispiele zeigen andererseits daß der Grenzstrom an der Ringelektrode und seine Änderung mit der Stromdichte der Scheibenelektrode einen ausreichend verläßlichen Stützpunkt zur Feststellung des Stufenmechanismus bieten. Wie aus den Abbildungen ersichtlich ist, kann der Zusammenhang zwischen I_h und j in den einzelnen Stromdichtebereichen durch folgenden Ausdruck angegeben werden:

$$I_h \approx j^n, \tag{14}$$

wo der Wert von n zwischen $+1$ und -1 liegen kann. Aus Abb. 3 und 6 ist ersichtlich, daß n gleich 1 ist, wenn die Steilheit der Polarisationskurve 59 mV beträgt, d. h. wenn die Kinetik des Vorganges durch die Diffusion der Me^{2+}-Ionen von der Elektrodenoberfläche weg bestimmt wird. In den Abbildungen 4, 5 und 6 ist n in bestimmten Bereichen negativ und in Abb. 5 besitzt n über eine mehrere Größenordnungen umfassende Änderung der Stromdichte den Wert von -1.

LITERATUR

1. Kiss, L., Farkas, J.: Magy. Kém. Foly. **76,** 113 (1970); Acta Chim. Acad. Sci. Hung. **64,** 241 (1970)
2. Kiss, L., Farkas, J.: Magy. Kém. Foly **76,** 120 (1970); Acta Chim. Acad. Sci. Hung. **65,** 7 (1970)
3. Kiss, L., Farkas, J.: Magy. Kém. Foly. **77,** 121 (1971); Acta Chim. Acad. Sci. Hung. **69,** 167 (1971)
4. Iwanow, Ju. B., Lewitsch, B. G.: Dokl. AN SSSR **126,** 1029 (1959)
5. Albery, W. J., Bruckenstein, S.: Trans. Farad. Soc. **62,** 1920 (1966)
6. Marchiano, S. L., Arvia, A. J.: Electrochim. Acta **15,** 325 (1970)
7. Kiss, L., Farkas, J.: Magy. Kém. Foly. **76,** 389 (1970); Acta Chim. Acad. Sci. Hung. **66,** 395 (1970)
8. Kiss, L., Farkas, J., Kőrösi, A.: Magy. Kém. Foly. **76,** 569 (1970); Acta Chim. Acad. Sci. Hung. **67,** 179 (1971)
9. Kiss, L., Farkas, J.: Magy. Kém. Foly. **77,** 35 (1971); Acta Chim. Acad. Sci. Hung. **68,** 359 (1971)

László Kiss
József Farkas
Ákos Fóthi
Budapest VIII., Puskin u. 11—13.

Acta Chimica Academiae Scientiarum Hungaricae, Tomus 74 (2), pp. 135–142 (1972)

ANODIC BEHAVIOUR OF IRON IN FORMAMIDE SOLUTIONS

L. KISS, M. LAKATOS-VARSÁNYI and DO NGOC LIEN

(Department of Physical Chemistry and Radiology, L. Eötvös University, Budapest)

Received March 13, 1972

The anodic dissolution and passivation of iron have been studied by galvanostatic and potentiostatic methods in anhydrous formamide containing KCl, $KClO_4$, CH_3COOH and CH_3COONa, as well as added water. It has been established that in the active state iron is uniformly dissolved in solutions containing acetic acid and sodium acetate. In solutions containing only potassium chloride or potassium perchlorate, pitting is observed. In solutions of acetic acid and sodium acetate the passivation of iron requires the presence of water.

The anode processes occurring on metals, thus the ionization of metals, have been studied almost exclusively in aqueous solutions. Investigations on the dependence of anodic metal dissolution on the composition of non-aqueous solutions may provide new information concerning the nature of these processes. For this purpose we studied [1, 2] the anodic behaviour of iron in acetic acid, a solvent of low dielectric constant. We have established that the rate of active anodic dissolution is influenced by the acetate ion concentration in a manner analogous to the effect of hydroxide ions in aqueous solutions. Passivation independent of the convection in the solution is observed only in the presence of sodium acetate solutions containing water.

In the present paper we report on studies performed in formamide, a solvent with properties different from those of acetic acid. Similarly to acetic acid, formamide is also capable of self-dissociation [3] but its dielectric constant is as high as 111.3 at 25 °C [4], therefore, it readily dissolves a variety of salts. It does not undergo either oxidation or reduction in a wide range of potentials [5, 6], thus is a suitable solvent for electrochemical studies. The anodic behaviour of various metals was recently investigated in formamide containing sulfamic acid [7]; the electropolishing of many metals was found to be feasible in this solvent.

Similarly to studies in acetic acid solutions, we have investigated the anodic dissolution of active iron by a galvanostatic method, and the development of passivation by a potentiostatic technique.

Experimental

The experimental methods, the quality and preparation of iron and the other chemicals were the same as described earlier [1, 2].

Commercial formamide usually contains water and decomposition products (formic acid and ammonia) as impurities. A check with Bromothymol Blue indicated the absence of formic acid in the product used by us. The amount of water found by the K. Fischer titration was 0.5—1.0 g/l. For drying and purification, the solvent was left standing over sodium sulfate or a molecular sieve for 2—3 days. After decanting, the solvent was subjected to 2—3-fold distillation under reduced pressure at 95—110 °C. The acid and water content of the distillate were re-checked. The water content of solutions prepared with the formamide purified in the above way was generally less than 0.08%. The solutions referred to in this paper as anhydrous contained the above amount of water as a maximum. All the potentials given are against an aqueous, saturated calomel reference electrode.

Results and discussion

Study of active dissolution

The anodic dissolution of iron has been studied by galvanostatic techniques in anhydrous formamide solutions containing KCl, $KClO_4$, CH_3COOH and CH_3COONa, as well as in formamide containing water.

In order to check whether or not the anodic dissolution of iron is the only process occurring under the present conditions we determined the efficiency of anodic dissolution by measuring the weight loss of the anode and the amount of charge that had passed through the electrode. The charge of dissolved iron was found to be 2 for active dissolution. This permits the conclusion that no process other than the ionization of iron does take place on the electrode at detectable rates. When studying the efficiency of dissolution (in solutions containing CH_3COONa and water) at potentials corresponding to the transpassive section of the potentiostatic curve, a value of —12% was found, indicating that besides dissolution some components of the solution undergo oxidation at the electrode.

The anodic polarization curve of iron is shown in Fig. 1 (φ is the electrode potential, j the current density) for solutions containing acetic acid, acetic acid and potassium chloride or potassium perchlorate. The experimental points obtained in the various solutions lie practically on the same straight line whose slope $b \approx 60$ mV. The effect of added water on the polarization curve in acetic acid is shown in Fig. 2. The rate of the process is found to increase if water is added to this medium.

The φ *vs.* $\lg j$ curve determined in formamide containing 0.5 mol/dm^3 sodium acetate is shown in Fig. 3. As compared with the polarization curves in acetic acid, the one obtained in CH_3COONa solution is shifted towards negative potentials (*cf.* Fig. 1), *i.e.* the rate of the process has increased. From Fig. 3 it is also apparent that the addition of water significantly increases the rate of anodic dissolution of iron in this case, too. According to Figs 2 and 3, the slope of the φ *vs.* $\lg j$ straight lines $b \approx 60$ mV.

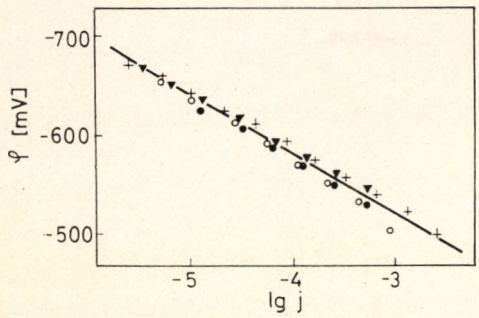

Fig. 1. Galvanostatic φ *vs.* lg j curves. Composition of the solutions: + 0.5 mol/dm³ CH_3COOH; ● 0.5 mol/dm³ CH_3COOH + 0.5 mol/dm³ $KClO_4$; ▼ 0.1 mol/dm³ CH_3COOH + 0.25 mol/dm³ KCl; ○ 1.0 mol/dm³ CH_3COOH + 0.5 mol/dm³ $KClO_4$

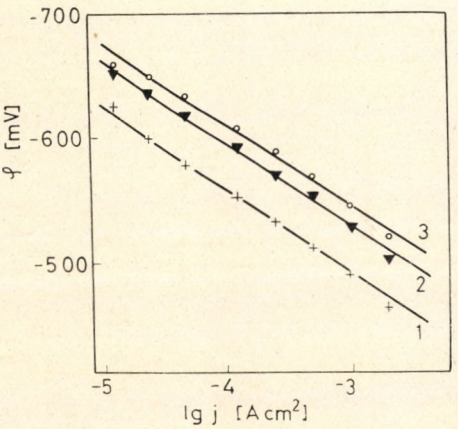

Fig. 2. Effect of water on the galvanostatic φ *vs.* lg j curve in formamide containing 0.5 mol/dm³ acetic acid. Water content: *1.* 0.06; *2.* 5.0; *3.* 10%

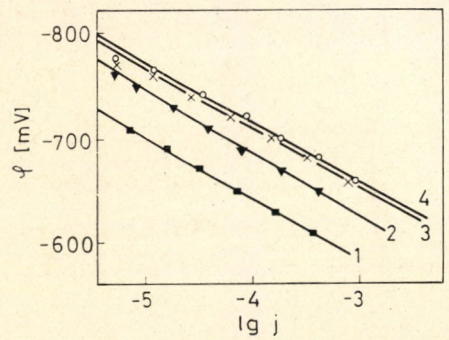

Fig. 3. Effect of water on the galvanostatic φ *vs.* lg j curve in formamide containing 0.5 mol/dm³ CH_3COONa. Water content: *1.* 0.03; *2.* 1.5; *3.* 5.0; *4.* 8%

We have attempted the determination of the φ *vs.* lg j relationship also in 0.5 mol/dm³ KCl and $KClO_4$ in formamide. As can be seen in Fig. 4, upon changing the anodic current in these solutions, the electrode potential remains practically unchanged. The variation of the electrode potential with time after switching on the current is exemplified by Fig. 5, in which the curve for a KCl solution reveals a maximum. Similar curves have been obtained for $KClO_4$ solutions, too.

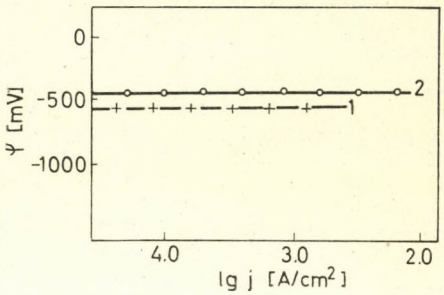

Fig. 4. φ *vs.* lg j curves *1.* in 0.5 mol/dm³ KCl, and *2.* 0.5 mol/dm³ $KClO_4$ solution

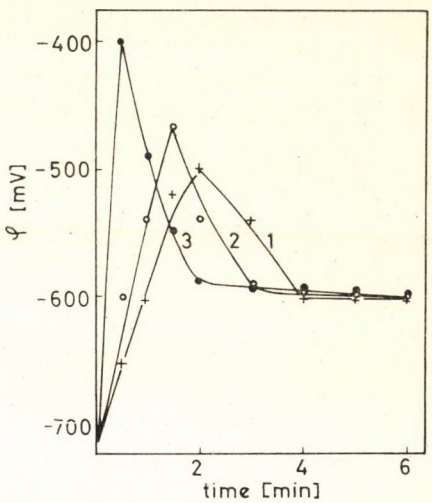

Fig. 5. Potential *vs.* time relationship in 0.5 mol/dm³ KCl at various currents. *1.* 50; *2.* 100; *3.* 200 μA

The shape of the polarization curve and of the galvanostatic potential *vs.* time curves (*cf.* Figs 1, 4, 5) indicates pitting of the metal [8]. In fact, the formation of pits on the electrode surface is visible within a short time ($\simeq$1 mA/cm², 60 min.). The charge of dissolved iron remains 2 even at very positive potentials (*e.g.* at 1.2 V, for 0.5 mol/dm³ KCl).

It follows from the results presented that the adsorption of acetic acid or acetate ions on the iron surface promotes the uniform anodic dissolution of active iron.

Similarly as in anhydrous acetic acid, the increasing concentration of acetate ions increases the rate of the anode process also in formamide media. As shown by Figs 2 and 3, added water in acetic acid increases the rate of the anode process to a lesser extent than in the presence of sodium acetate. This is probably due to the stronger adsorption of acetic acid and acetate relative to water in the former case, which implies a weaker effect of water on the anode process. In the second case, sodium acetate undergoes hydrolysis, resulting in the formation of acetic acid and hydroxide ions. The latter is known to increase the rate of dissolution of iron and thus to promote its passivation. The results described permit the conclusion that the mechanism of anodic dissolution of iron in the present case is similar to that assumed in acetic acid. At present this conclusion is supported only by the value of $b \approx 60$ mV and by the increase of the rate of dissolution with increasing acetate ion concentration. Thus similar dissolution mechanisms may be assumed in solvents of significantly different nature. This is probably due to the decisive role of adsorbed species (acetate ions and acetic acid molecules in the present case) in the mechanism of dissolution.

Study of the passivation

The passivation of the iron electrode in formamide solutions was studied by the steady-state potentiostatic method described previously. The measurements were carried out in solutions containing sodium acetate and acetic acid, in the presence of various amounts of water.

Characteristic potentiostatic curves obtained in sodium acetate solutions are shown in Fig. 6. Accordingly, the passivation of iron does not take place in anhydrous formamide. It can be observed that in the presence of 10% water the rate of the passive dissolution is lower than at higher water contents. Similar phenomena were observed by SCHWABE and SCHMIDT [9, 10] for the dissolution of nickel in dimethylformamide—water mixtures containing 2 N H_2SO_4. The explanation lies probably in the different solubility of the surface layers of iron in the given solvent mixtures.

According to Fig. 6, in an anhydrous sodium acetate solution, at potentials above 100 mV, a plateau is observed, *i.e.* the rate of anodic dissolution of iron does not change with the potential. This indicates that a salt has been deposited on the iron surface and the rate of the process is controlled by the diffusion of this salt into the bulk of the solution. The results shown in Fig. 7 lend support to this assumption. In the case of a rotating-disc electrode, the

current density corresponding to the plateau increases with increasing speed of rotation. In this context it is necessary to call attention to the fact that the initial step of passivation often consists in salt deposition on the surface [11, 12]. However, no true passivation occurs if the reactivation is very fast owing to the composition of the solution. There is no passivation either if, as in the present case, the molecules required for passivation are present in the solution in insufficient amounts only.

The potentiostatic polarization curves of the iron electrode obtained in anhydrous formamide and in formamide—water mixtures in the presence of

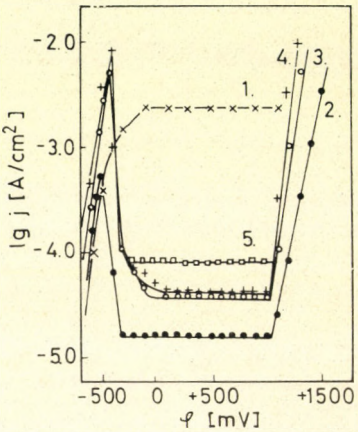

Fig. 6. Potentiostatic lg j *vs.* φ curves in 0.5 mol/dm³ CH_3COONa. Solvent composition: *1.* anhydrous formamide; *2.* 90% formamide—10% water; *3.* 80% formamide—20% water; *4.* 50% formamide—50% water; *5.* 100% water

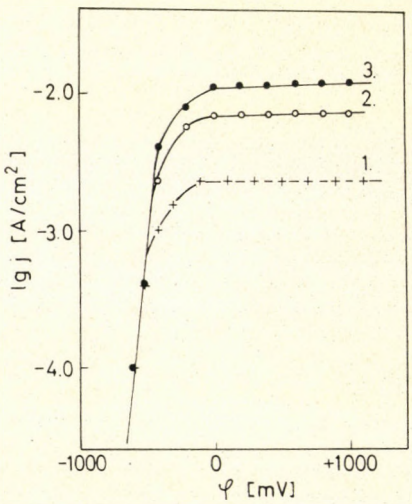

Fig. 7. Effect of the speed of rotation of the iron disc electrode on the lg j *vs.* φ relationship in anhydrous formamide containing 0.5 mol/dm³ CH_3COONa. *1.* 0; *2.* 2120; *3.* 3820 r.p.m.

acetic acid and sodium acetate are shown in Figs 8 and 9. According to these, no passivation occurs if the acetic acid contains 5% water (Fig. 8), but the iron undergoes passivation upon the addition of sodium acetate to the solution. 10% of water already causes passivation in acetic acid too (Fig. 9). In the presence of sodium acetate, however, passivation begins at more negative potentials and the rate of dissolution in the passive state is lower. In agree-

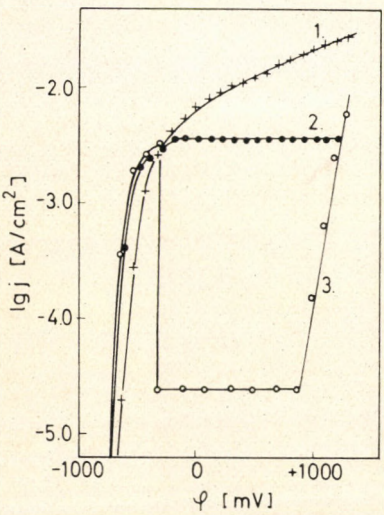

Fig. 8. Potentiostatic lg j *vs.* φ curves. Composition of the solutions: *1.* 0.5 mol/dm³ CH_3COOH in anhydrous formamide; *2.* 0.5 mol/dm³ CH_3COOH in 95% formamide + 5% water; *3.* 0.5 mol/dm³ CH_3COOH + 0.5 mol/dm³ CH_3COONa in 95% formamide +5% water

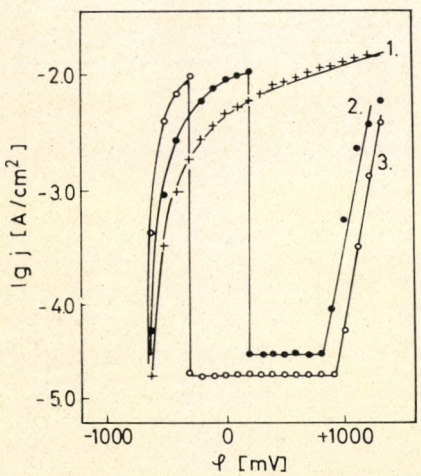

Fig. 9. Potentiostatic lg j *vs.* φ curves. Composition of the solutions: *1.* 0.5 mol/dm³ CH_3COOH in anhydrous formamide; *2.* 0.5 mol/dm³ CH_3COOH in 90% formamide + 10% water; *3.* 0.5 mol/dm³ CH_3COOH + 0.5 mol/dm³ CH_3COONa in 90% formamide +10% water

ment with the interpretation of the results concerning the anodic dissolution of iron in the active state, this phenomenon may be explained by enhanced passivation due to the adsorption of hydroxide ions formed upon the hydrolysis of sodium acetate.

As shown by the present results and those reported earlier [1, 2], passivation is promoted by the components of the solution which accelerate dissolution of the active state (H_2O, CH_3COONa). Analogous phenomena are observed in aqueous solutions with other constituents (*e.g.* the effect of OH ions) [13].

If there is dissolved KCl or $KClO_4$ in the formamide, iron does not undergo passivation even in the presence of water but salt deposition on the iron surface occurs instead. This is probably due to the very high rate of active dissolution as compared with the rate of formation of the passivating oxide layer on the surface [12].

REFERENCES

1. Kiss, L., Do Ngoc Lien, Varsányi, L. M.: Annales Univ. Sci. Budapest, Sectio Chim., **12,** 145 (1971)
2. Kiss, L., Do Ngoc Lien, Varsányi, L. M.: Acta Chim. Acad. Sci Hung., **70,** 313 (1971)
3. Jander, J., Lafrencz, Ch.: Wasserähnliche Lösungsmittel, p. 180. Verlag Chemie, 1968
4. Jander, G., Spandau, H., Addison, C. C.: Chemie in niederen Fettsäuren und ihren Derivaten, p. 259. Akademie-Verlag, Berlin
5. Charlot, G., Bandoz-Lambling, J., Tremillon, B.: Electrochemical Reactions, p. 354. Elsevier, Amsterdam—New York, 1962
6. Bard, A. J.: Electroanalytical Chemistry, Vol. 3, p. 84. M. Dekker Inc., New York, 1969
7. Menzies, J. A., Marshall, G. W., Griffin, C. B.: Corr. Sci., **9,** 287 (1969)
8. Kaeshe, H.: Corrosion, **17,** 389 (1969)
9. Shmidt, V.: Zashchita Metallov, **5,** 608 (1969)
10. Schwabe, K., Schmidt, W.: Corr. Sci., **10,** 143 (1970)
11. Gerischer, H.: Angew. Chem., **70,** 285 (1958)
12. Schwabe, K.: Werkstoffe und Korr., **18,** 961 (1967)
13. Kolotyrkin, Ya. M.: Zashchita Metallov, **3,** 131 (1967)

László Kiss
Magda Lakatos-Varsányi
Do Ngoc Lien
Budapest VIII., Puskin u. 11—13.

Acta Chimica Academiae Scientiarum Hungaricae, Tomus 74 (2), pp. 143—150 (1972)

NEW METHOD FOR THE DETERMINATION OF STABILITY CONSTANTS OF MOLECULAR COMPLEXES FROM SELF-DIFFUSION DATA

STUDY OF THE FORMATION EQUILIBRIUM OF THE PYRIDINE–IODINE MOLECULAR COMPLEX IN CARBON TETRACHLORIDE

B. LÉVAY

(Department of Physical Chemistry and Radiology, L. Eötvös University, Budapest)

Received December 14, 1971

The self-diffusion coefficient of iodine dissolved in pyridine-containing carbon tetrachloride was measured as a function of the pyridine concentration at 25 °C and 35 °C.

A new method was developed for the determination of the equilibrium constant for the formation of a 1 : 1 molecular complex. The equilibrium constants for the formation of the pyridine–iodine complex at 25 °C and 35 °C were calculated from the self-diffusion data to be 108 dm^3/mol and 70 dm^3/mol, respectively. The enthalpy for the formation of the complex was found to be —7.9 kcal/mol.

The self-diffusion coefficients of the complex at 25 °C and 35 °C are 1.01×10^{-5} cm^2/s and 1.20×10^{-5} cm^2/s, respectively.

The ratio of the self-diffusion coefficients of the complex and the free iodine molecule is 0.685; this value supports the view that the iodine atoms in the complex molecule lie in the plane of the pyridine ring and in a common straight line with the nitrogen atom.

In our earlier publications [1, 2] an attempt was made to use self-diffusion measurements in binary liquid mixtures to obtain information on the structures of the liquids. In the systems studied the interactions between the individual molecules may be quite complicated, and thus the variation of the self-diffusion coefficient gave information only on the changes arising as the resultant of these interactions (*e.g.* on the stabilization of the structure of water in the case of aqueous mixtures of low alcohol content).

With a view to the further elucidation of the nature of solutions it was considered desirable to clarify the connection between the intermolecular interactions and the self-diffusion coefficient in systems for which the interaction between the molecules has already been demonstrated and studied in a quantitative way by other methods.

For this purpose it seemed suitable from several points of view to select as model the reversible formation of a charge-transfer complex [3] from iodine and some appropriate donor molecule such as pyridine, and to follow this process by measuring the self-diffusion coefficient of iodine. For complex formation in a non-coordinating solvent it is necessary to consider only the interaction of iodine with the donor, and interaction with the solvent molecules can be neglected to a first approximation.

Experimental

The self-diffusion coefficient of iodine was measured by the open-ended capillary method, in essentially the same way as previously reported [1], but with the following minor modifications.

In order to further decrease the convection of the solution upon immersion of the capillaries into the diffusion vessel, instead of immersing the capillaries into the solution, the solution was slowly admitted to the diffusion vessel beside the capillaries. Further, since the γ-radiation of the ^{131}I used as tracer permits the measurement of the activity in the capillaries without the removal of the material from the capillaries, it was necessary to prevent the evaporation of the material during the measurement. For this purpose one drop of a rapidly drying lacquer was applied to the opening of the capillary. This sealed the capillary adequately for several hours (this was checked by the frequent repetition of the activity measurement), but could readily be removed after the measurement.

The γ-radiation of ^{131}I was measured with a scintillation detector. For each sample the time necessary for the receipt of 10^5 impulses was measured.

The material used in the experiments were Reanal products of p.a. quality; they were further purified and dried.

The iodine was powdered with 1% KI and 1% CaO and freshly sublimed.

The pyridine was refluxed with solid KOH for 2 hours, left to stand until cool, poured off from the KOH and fractionally distilled. In this way the water content of the main fraction was less than 0.01 wt.%. The water content was determined by Karl Fischer's titration.

The carbon tetrachloride was purified similarly to the pyridine, then dried with anhydrous magnesium perchlorate and again distilled.

The solutions were mixed by weight. The diffusion experiments were carried out in a thermostat with an accuracy of ± 0.01 °C at 25 and 35 °C.

The self-diffusion measurement was performed twice for each solution of different composition, with 6 capillaries at a time in a glass capillary holder. The relative error of the determination of the self-diffusion coefficient, as characterized by the scatter of the measurements, was $\leqslant 1\%$.

It was possible to compare our measured self-diffusion coefficients with the literature data only in the case of iodine dissolved in carbon tetrachloride. As shown by the data for 25 °C in Table I, the agreement is satisfactory.

Table I

Self-diffusion coefficient of iodine dissolved in carbon tetrachloride at 25 °C

$D \cdot 10^5$ cm^2/s	Method	Reference
1.50	diaphragm cell	[4]
1.447	capillary cell	[5]
1.474	capillary cell	[6]
1.47	capillary cell	our data

The concentration of iodine taken in the experiments was in all cases 1×10^{-3} mol/dm^3. In our experience a precipitate resulted after a certain time when pyridine was added to higher concentrations of iodine, whereas this was not observed with the above concentration.

The pyridine concentration was varied in the range 2×10^{-3}—8×10^{-2} mol/dm^3.

Experimental results

At both temperatures the self-diffusion coefficient of iodine decreased with increasing concentration of pyridine added to the solution (Fig. 1, Table II). The data refer to the average rates of self-diffusion of iodine in the various

states. This decrease is practically completely the result of the interaction between pyridine and iodine, for our measurements indicated that in the concentration range studied there was no discernible change in the viscosity of the solution.

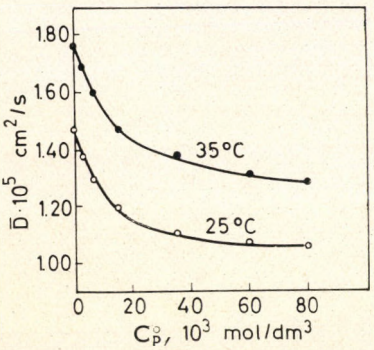

Fig. 1. Variation of the self-diffusion coefficient of iodine with the pyridine concentration in carbon tetrachloride solution ($c^\circ_{I_2} = 1 \times 10^{-3}$ mol/dm^3)

Table II

Self-diffusion coefficient of iodine in carbon tetrachloride as a function of the pyridine concentration ($c^\circ_{I_2} = 1 \times 10^{-3}$ mol/dm^3)

$c^\circ_{py} \cdot 10^3$ mol/dm^3	$\bar{D} \cdot 10^5$ (measured) cm^2/s		$\bar{D} \cdot 10^5$ (calculated) cm^2/s	
	25 °C	35 °C	25 °C ($K_c = 108$ dm^3/mol)	35 °C ($K_c = 70$ dm^3/mol)
0	1.47	1.76	1.466	1.759
2	1.38	1.69	1.390	1.694
6	1.30	1.60	1.294	1.600
15	1.19	1.47	1.188	1.479
35	1.10	1.38	1.107	1.366
60	1.07	1.31	1.071	1.310
80	1.06	1.28	1.057	1.287
—	—	—	1.009	1.202

Discussion

In the explanation of the experimental results the starting point was the well-substantiated fact that pyridine and iodine react to give a 1 : 1 charge-transfer complex, in accordance with the following equilibrium process:

$$C_5H_5N + I_2 \rightleftharpoons C_5H_5N \cdot I_2 \qquad (1)$$

In a solution containing pyridine, therefore, iodine is in two states, and the self-diffusion coefficients in the two states are different. Under otherwise identical conditions, the complex formed by the linking of the two molecules will clearly diffuse more slowly than the free iodine, and this is the cause of the decrease of the average self-diffusion coefficient as a result of the increase of the pyridine concentration.

Under the simplest conditions the average self-diffusion coefficient of a molecule consists of the sum of the self-diffusion coefficients $\bar{D}_i$ corresponding to the different states i:

$$\bar{D} = \sum_i X_i D_i \tag{2}$$

where X_i is the fraction of the molecule under consideration in state i. Under the above conditions Eq. (2) is also valid if the different states i can transform into each other, assuming that the rate of this transformation is fairly large compared with the rate of self-diffusion. The time spent by the relevant molecule in any individual state is proportional to the frequency of that state. This latter condition holds in the case of the formation of the pyridine–iodine complex, and thus Eq. (2) can be applied to process (1):

$$\bar{D} = (1 - X_K)\, D_{I_2} + X_K D_K = D_{I_2} - (D_{I_2} - D_K) X_K \tag{3}$$

where D_{I_2} and D_K are the self-diffusion coefficients of the free I_2 molecule and the pyridine–iodine complex, respectively, and X_K is the fraction of the total iodine in the molecular complex.

Hence, with the increase of the proportion of the molecular complex, the self-diffusion coefficient decreases linearly from the value corresponding to the self-diffusion coefficient of the free I_2 molecule to the limiting value corresponding to the complex molecule.

For given pyridine and iodine concentrations, the proportion of I_2 in the complex is determined by the equilibrium constant of reaction (1); this can be expressed in terms of the concentrations in mol/dm^3:

$$K_c = \frac{c_K}{(c^\circ_{I_2} - c_K)(c^\circ_{py} - c_K)} \tag{4}$$

where $c^\circ_{I_2}$ and c°_{py} are the concentrations of I_2 and pyridine initially taken, and c_K is the equilibrium concentration of the complex. The relation between K_c and X_K is obtained from the relation:

$$X_K = \frac{c_K}{c^\circ_{I_2}} \tag{5}$$

by substituting for c_K in Eq. (4):

$$K_c = \frac{X_K}{(1 - X_K)(c^\circ_{py} - X_K c^\circ_{I_2})} \tag{6}$$

The relation between K_c and the measured self-diffusion coefficients is obtained from Eqs (3) and (6):

$$\frac{1}{K_c} = \frac{\bar{D} - D_K}{D_{I_2} - \bar{D}} c^\circ_{py} - \frac{\bar{D} - D_K}{D_{I_2} - D_K} c^\circ_{I_2} \tag{7}$$

As a result of the complexity of Eq. (7) it is not suitable for the evaluation of a series of experimental data and hence for the calculation of the equilibrium constant K_c and the self-diffusion coefficient D_K of the complex molecule.

With certain approximations Eq. (7) can be written in several forms which give linear plots permitting the calculation of K_c and D_K from the graphically determined slope and intercept. A relation is thus obtained which is analogous to relations (*e g.* the BENESI—HILDEBRAND equation [3]) widely used for the determination of equilibrium constants by spectroscopic and NMR methods. These approximations, however, generally require a special choice of the concentration conditions, and even then there is a fair degree of uncertainty in the evaluation.

In place of this evaluation of the data, the following method was selected. Different K_c values were assumed, the X_K values corresponding to the individual K_c values were calculated from Eq. (6), and these were then used to calculate, by the method of least squares, the parameters of the straight line best corresponding to Eq. (3). An examination was next made of the quality of the fit of the straight lines calculated with the different K_c values. The scatter of the experimental points compared to the points of the calculated straight line was regarded as a measure of this; it is described by the following

$$s = \sqrt{\frac{\Sigma \Delta_i^2}{n - k}} \tag{8}$$

where Δ_i is the difference between the i-th experimental point and that calculated, n is the number of measurements, and k is the number of constants in the formula used in the calculations (in our case the equation of the straight line, thus $k = 2$).

s showed a minimum as a function of K_c, and the value of K_c corresponding to this minimum was accepted.

As a result of the above calculations, values of 108 $\pm$ 10 dm^3/mol and 70 $\pm$ 7 dm^3/mol were obtained for the equilibrium constant at 25 °C and

35 °C, respectively, while the corresponding values for the self-diffusion coefficient of the pyridine–iodine complex were 1.01×10^{-5} cm^2 · s^{-1} and $1.20 \times \times 10^{-5}$ cm^2 · s^{-1}, respectively.

Figure 2 gives the experimental data plotted in accordance with Eq. (3) from the above K_c values. The calculated values of the self-diffusion coefficients are listed in the last two columns of Table II. In both cases the agreement between the calculated and measured data is satisfactory.

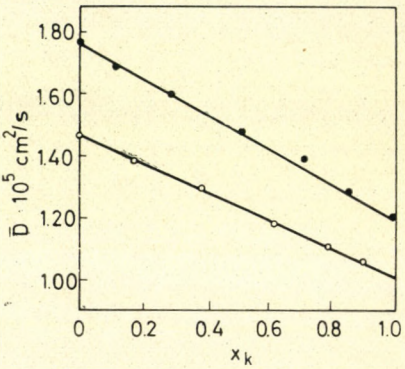

Fig. 2. Self-diffusion coefficient of iodine plotted as a function of its proportion in the pyridine–iodine complex (calculated with equilibrium constants $K_c = 108$ dm^3/mol at 25 °C, and $K_c = 70$ dm^3/mol at 35 °C)

An approximate value of the enthalpy of formation of the complex can be determined from the equilibrium constants measured at the two temperatures; this was found to be $\Delta H = -7.9$ kcal/mol, while the value of the entropy change at 25 °C $\Delta S = -17.2$ cal · mol^{-1} · K^{-1}.

The quotient of the self-diffusion coefficients of the pyridine–iodine complex and the free iodine molecule was, to a very good approximation, the same at the two temperatures, with an average value of $D_K/D_{I_2} = 0.685$.

According to the above, the interaction leading to the formation of a complex between pyridine and iodine can be followed by the measurements of the self-diffusion coefficient of one of the components, and conversely, assuming a complex-formation equilibrium, the variation of the self-diffusion data with the composition can be quantitatively interpreted.

In this way a new method has been derived for the determination of the equilibrium constant for the formation of the molecular complex.

Table III lists the equilibrium constants for the pyridine–iodine system in carbon tetrachloride at 25 °C measured by various authors. As can be seen, our value is in satisfactory agreement with the results measured by spectroscopic methods.

Table III

Equilibrium constant for the formation of the pyridine–iodine complex at 25 °C in carbon tetrachloride

K_c (dm³/mol)	Reference
101	[7]
107	[8]
105	[9]
111	[10]
109	[11]
108	our data

Our values calculated for the enthalpy and entropy of complex formation, —7.9 kcal/mol and 17.2 cal · mol^{-1} · K^{-1}, respectively, are in agreement with the literature values observed in carbon tetrachloride, —7.47 kcal/mol and 15.8 cal · mol^{-1} · K^{-1} [9], and with the value of the heat of formation, 7.95 kcal/mol, calculated from the heats of dissolution [12].

From the self-diffusion coefficient of the molecular complex, conclusions may be drawn about the form and size of the complex in solution. This may help in the choice between different assumptions as to the structure of the complex.

Some information regarding the dimensions of the complex and the spatial configuration of the molecules comprising it may be given by the quotient of the self-diffusion coefficients of the complex and of the free iodine molecule.

It has so far not proved possible to prepare the pyridine–iodine complex in crystalline form. With regard to its structure it is probable that, similarly to the complexes pyridine–iodine monochloride and 4-picoline–iodine, the two iodine atoms lie in the plane of the ring and in a straight line with the nitrogen atom [13, 14]. In the view of REID and MULLIKEN, however, only one of the iodine atoms lies in the plane of the ring [15].

In the former case the dimensions of the iodine molecule and the pyridine ring [16, 17] indicate that the form of the complex approximates a strongly stretched ellipsoid of rotation. The volume of this is about 2.5 times that of the free iodine molecule, and the ratio of the major and minor semi-axes is at least $\varrho = 3$. In the second case, however, the molecule is much less stretched, and the ratio of the axes does not exceed $\varrho = 2$. The iodine molecule can be regarded as an ellipsoid of rotation for which $\varrho \sim 1.75$.

If the calculations of PERRIN [18] referring to the diffusion coefficients of ellipsoids of rotation are applied to the above models, the ratio of the self-diffusion coefficients of the complex and the free iodine molecule emerges as

$\sim$0.67 in the first case, and $\sim$0.76 in the second. The experimentally found value of 0.685 therefore corresponds to the structure assuming the two iodine atoms to lie in the plane of the pyridine ring and in a common straight line with the nitrogen atom.

*

The author wishes to express his thanks to Professor Tibor ERDEY-GRÚZ, and to Dr. Miklós ORBÁN for useful consultations and their valuable advice, and to Mrs. B. JANKÓ for her assistance in the experimental work.

REFERENCES

1. ERDEY-GRÚZ, T., CSÁNYI-FODOR, P., LÉVAY, B., GYŐRI-SZILÁGYI, E.: Magy. Kém. Foly. **77,** 145 (1971)
2. ERDEY-GRÚZ, T., LÉVAY, B.: Magy. Kém. Foly. **77,** 149 (1971)
3. FOSTER, R.: Organic Charge-Transfer Complexes. Academic Press, London, New York 1969
4. STOKES, R. H., DUNLOP, P. J., HALL, J. R.: Trans. Faraday Soc., **49,** 886 (1953)
5. HAYCOCK, E. W., ALDER, B. J., HILDEBRAND, J. H.: J. Chem. Phys., **21,** 1601 (1953)
6. NAKANISHI, K., OZASA, T.: J. Phys. Chem., **74,** 2956 (1970)
7. POPOV, A. I., RYGG, R. H.: J. Amer. Chem. Soc., **79,** 4622 (1957)
8. MAKI, A. G., PLYLER, E. K.: J. Phys. Chem., **66,** 766 (1962)
9. MCKINNEY, W. J., POPOV, A. I.: J. Amer. Chem. Soc., **91,** 5215 (1969)
10. BHASKAR, K. L., SINGH, S.: Spectrochim. Acta, **23A,** 1155 (1967)
11. MCKINNEY, W. J., WONG, M. K., POPOV, A. I.: Inorg. Chem., **7,** 1001 (1968)
12. HARTLEY, K., SKINNER, H. A.: Trans. Faraday Soc., **26,** 621 (1950)
13. HASSEL, O., ROMMING, C.: Acta Chem. Scand., **10,** 696 (1956)
14. HASSEL, O., ROMMING, C., TUFTE, T.: Acta Chem. Scand., **15,** 967 (1961)
15. REID, C., MULLIKEN, R. S.: J. Amer. Chem. Soc., **76,** 3869 (1954)
16. MULLIKEN, R. S.: J. Amer. Chem. Soc., **72,** 600 (1950)
17. ALMENNINGEN, A., BASTIANSEN, O., HANSEN, L.: Acta Chem. Scand., **9,** 1306 (1955)
18. PERRIN, F.: J. Phys. Radium, **7,** 1 (1936)

Béla LÉVAY; Budapest VIII., Puskin u. 11—13.

Acta Chimica Academiae Scientiarum Hungaricae, Tomus 74 (2), pp. 151—158 (1972)

INVESTIGATION OF THE ANTIMONY CONTENT OF CALCIUM HALOPHOSPHATE LUMINESCENT POWDERS BY MÖSSBAUER SPECTROSCOPY

A. VÉRTES,* V. FRAKNÓY-KŐRÖS,** B. LÉVAY,* P. A. GELENCSÉR** and M. RANOGAJEC-KOMOR*

*(*Department of Physical Chemistry and Radiology, L. Eötvös University, Budapest **Tungsram Research Institute, Budapest)*

Received December 20, 1971

In a Mössbauer investigation of calcium halophosphate luminescent powders containing antimony, a semi-empirical method has been developed for the determination of the optimum layer thickness of the absorber, and of the minimum measuring time necessary to attain the required accuracy. The Mössbauer spectra of a few luminescent powders, prepared in different ways, have been recorded. On the basis of the isomer shift values, the electron configuration of antimony in the luminescent powders is similar to that of antimony in Sb_2O_3, but it may have a stronger ionic character, depending on the conditions of preparation. Values of line broadening are indicative of antimony present in the same oxidation state, but located at sites of slightly different environment.

The β-decay of the radioactive isotope ^{121m}Sn leads to the formation of ^{121m}Sb with a half-life of 76.3 years. The average life-time of ^{121m}Sb is 5.07×10^{-9} s. It is de-excited into its ground state by emitting 37.2 keV γ-radiation. This energy transition of antimony can be utilized in Mössbauer spectroscopy [1].

The use of the above antimony isotope in Mössbauer spectroscopy is impeded by several circumstances. As well-known, the magnitude of the Mössbauer effect (f) can be given by the following expression:

$$f = \exp\left(-\frac{3E^2}{4Mc^2k\Theta}\right) \tag{1}$$

where E is the energy of γ-radiation,
M is the mass of the Mössbauer atom,
c is the velocity of light,
k is the Boltzmann constant, and
Θ is the Debye temperature.

According to Eq. (1), f decreases exponentially with E^2. On the other hand, 37.2 keV can be considered already as a high energy (*e.g.* in the case of ^{57}Fe, $E = 14.4$ keV), and this reduces the magnitude of the effect.

The spin of the ^{121m}Sb nucleus is $I = 7/2+$ in the excited state, and $I = 5/2+$ in the ground state. This means that in the case of the criterion

$\Delta m_I \leqslant 1$, the Mössbauer spectrum of antimony is split into 8 lines as a result of the Stark effect, which lie rather close to each other, so that they are exhibited in the Mössbauer spectrum only as line broadening, and not as separate lines. This is the reason why the half-width of the Mössbauer lines of antimony is $\Gamma \approx 3$ mm/s, a rather large value, which makes the evaluation of the spectra difficult.

In the majority 37.2 keV gamma photons of ^{121m}Sb produce a photoeffect in the K shell of antimony or the tin parent element in the form of internal conversion or self-absorption, which gives rise to characteristic K_α X-rays with an energy of $\sim$24 keV. The intensity of this radiation is by several orders of magnitude higher than that of the 37.2 keV γ-radiation of the source. Using a NaI(Tl) scintillation crystal the 37.2 keV photons can be detected more efficiently as the escape peak of the iodine ($\sim$9 keV).

Among luminescent powders used in fluorescent lamps, halophosphates are employed most widely. The first data relevant to luminescent powders of this type were published in 1949 [2, 3]. The chemical composition of calcium halophosphate luminescent powders activated by antimony and manganese can be described by the formula $3\ Ca_3(PO_4)_2 \cdot CaX_2$ (X = Cl, F or Cl + F). The crystal structure is that of synthetic apatite, in which Sb and Mn are incorporated as activators. Antimony plays the role of primary activator, *i.e.* it takes up the ultraviolet energy and transmits it to the manganese centers. The spectrum of the emitted light exhibits the emission maxima characteristic of both antimony and manganese, the ratio of the two bands depending on the manganese content. It is assumed that the activators can be incorporated at two Ca sites of different symmetry of the crystal lattice. There are several concepts concerning the distribution of antimony and manganese between the two different sites [4]. As concerns the antimony centers, we thought that the Mössbauer spectra of these luminescent powders will provide a new aspect for elucidating the problem: we might obtain useful data on the energy state of the nuclides of the incorporated Sb-centers and on their interaction with neighbouring atoms of the crystal lattice.

With increasing concentration of the activators, the luminescence efficiency decreases considerably on account of the so-called concentration quenching (secondary effects). Optimum efficiency is attained when antimony is incorporated in an amount of about 0.5—1.0% w/w. It follows from this, as well as from the circumstances listed above, that Mössbauer spectroscopy will yield information on the oxidation state, electron configuration and the incorporation into the crystal lattice of antimony present in luminescent powders only if the conditions of measurement are optimized to a maximum. This justifies the purpose of the present work, which deals with the semi-empirical determination of the optimum layer thickness of the absorber and of the measuring time needed.

In the case of a low source activity and a low concentration of the Mössbauer nuclei, thus, also in the case of luminescent powders, conditions prevail, owing to which the per cent extent of nuclear resonance absorption will exceed the magnitude of statistical error only if an appropriately long measuring time is chosen. Therefore, in the case of a measuring apparatus of stable operation, the statistical error may be reduced below the required limit by increasing adequately the measuring time. However, the measuring time needed for this may be so long that it cannot be realized in practice without extensive optimization of the relevant parameters. Under given conditions (source activity, concentration, etc.), the thickness of the absorber layer is the most important parameter, the proper selection of which will ensure optimal measuring conditions. On the other hand, it is desirable in such cases to estimate under optimum conditions the necessary measuring time.

With a sample of given composition, the increasing layer thickness increases, on the one hand, the number of Mössbauer nuclei in the radiation path, and thereby the extent of nuclear resonance absorption, while, on the other hand, the general absorption by the matrix elements also increases simultaneously. This latter may result under otherwise identical conditions in a higher statistical error. The increase in layer thickness gives rise, therefore, to two effects acting in opposite directions, so that an optimum value is to be expected.

Let us first investigate the dependence of the per cent extent of nuclear resonance absorption on the layer thickness. Let us designate by I_0 the intensity measurable per channel of the spectrum in the absence of the test sample. Upon introducing a sample of surface density d, this intensity will be decreased according to the following relationship:

$$I = I_0 \exp(-\mu d) \tag{2}$$

in the whole velocity interval of the spectrum due to general mass absorption (photoeffect, Compton scattering), where μ is the general mass absorption coefficient of the sample. The intensity reduced by general absorption is further decreased by nuclear resonance absorption. The reduced intensity, observable at the position of the corresponding Mössbauer line is thus:

$$I_M = I \cdot \exp(-\mu_M x_M d) = I_0 \exp - [(\mu + \mu_M \cdot x_M)d] \tag{3}$$

where μ_M is the mass absorption coefficient for the resonance absorption of the Mössbauer nucleus, and x_M is the weight fraction of the Mössbauer nucleus in the sample.

From Eqs (2) and (3), the per cent extent of resonance absorption (S_M) will be:

$$S_M = \frac{I - I_M}{I} \cdot 100 = 100\left[1 - \exp(-\mu_m \cdot x_M \cdot d)\right] \tag{4}$$

In view of the fact that the exponent is sufficiently small at small concentrations, the terms with powers higher than 1 can be neglected in the expansion. The following simplified expression is obtained for the extent of resonance absorption:

$$S_M = 100\mu_M \cdot x_M \cdot d \tag{4a}$$

Thus, matrix elements do not influence the relative extent of resonance absorption, which increases in the case of samples of the given low concentration linearly with the thickness of the layer. Let us now investigate the effect of the layer thickness on the statistical error. If we continue measurement at the intensity I defined above for time t, the relative statistical error (S_H) of the pulses $I \cdot t$ collected per channel is

$$S_H = 100\frac{\sqrt{It}}{It} = \frac{100}{It}\ \% \tag{5}$$

On the basis of Eqs (2) and (5) the measuring time needed to attain the given statistical error is:

$$t = \frac{10^4}{S_H^2 I} = \frac{10^4}{S_H^2 I_0}\exp(\mu d) \tag{6}$$

The measurement time belonging to the given statistical error increases exponentially with the thickness of the layer, while the extent of resonance absorption only linearly. Let the requirements towards the measurement be such that the per cent extent of resonance absorption shall be k times the statistical error. In this case, from Eqs (5) and (4a) the measuring time required to fulfil the condition $S_M = k \cdot S_H$ is:

$$t = \frac{1}{I_0}\left(\frac{k}{\mu_M \cdot x_M}\right)^2 \cdot \frac{1}{d^2}\exp(\mu d) \tag{7}$$

With all other parameters constant, t exhibits a minimum as a function of d. For the optimum layer thickness belonging to the minimum value of t, $d_{\text{opt}} = \frac{2}{\mu}$ is obtained. Substitution of this value into Eq. (7) gives the minimum

measuring time belonging to the optimum layer thickness:

$$t_{\min} = \frac{1}{I_0}\left(\frac{ke}{2x_M}\,\frac{\mu}{\mu_M}\right)^2 \tag{8}$$

Without simplifications, *i.e.* using Eq. (4) instead of (4a), the expression

$$d_{\text{opt}} = \frac{\ln(1+B)}{\mu_M x_M} \tag{9}$$

is obtained for the optimum layer thickness, and

$$t_{\min} = \frac{1}{I_0}\left(\frac{k}{B}\right)^2 (1+B)^{(2/B+2)} \tag{10}$$

for the minimum measuring time. In these equations

$$B = \frac{2\mu_M x_M}{\mu}\,.$$

Thus, for the determination of the optimum layer thickness only the mass absorption coefficient of the sample with respect to the given radiation must be known. If the composition of the sample is known, this value can be evaluated on the basis of data published in the literature. However, in the case of multicomponent mixtures, as *e.g.* calcium halophosphate luminescent powders, the experimental determination is simpler and also more suitable for practical purposes. For the evaluation of the minimal measuring time required, the mass absorption coefficient μ_M pertinent to the resonance absorption of the Mössbauer nucleus must also be known. This can be determined experimentally with the aid of Eqs (4) and (4a) on the basis of the per cent absorption measured for a sample of known composition.

Experimental

After suitable modification, the experimental set-up described earlier [7] became suitable for use in the velocity range of about ± 20 mm/s required for the measurement of antimony. ^{121m}Sn with an activity of 0.1 mCi was used as source in the form of $CaSnO_3$(Sb). Antimony oxides used in the experiments were of analytical purity. In our present work, calcium halophosphate samples prepared in different ways have been compared by Mössbauer spectroscopy [2, 3]. In the measurement the absorbers were kept at the temperature of liquid nitrogen. Isomer shift and line width values are subject to errors of ± 0.2 mm/s. Isomer shift values are referred to the $CaSnO_3$(Sb) source, and data taken from the literature have also been recalculated to this source with the aid of known isomer shift values pertinent to sources of different composition.

Results and discussion

The general mass absorption coefficients needed for the evaluation of the optimal layer thickness were determined empirically, and were found to be 2.1 cm^2/g in the case of luminescent powders. On the basis of the Mössbauer spectrum of Sb_2O_3 (Fig. 1) a value of 5.4 cm^2/g was obtained for μ_M. (Surface density of the sample was 20 mg/cm^2, S_M is 5%.) From this, the optimum

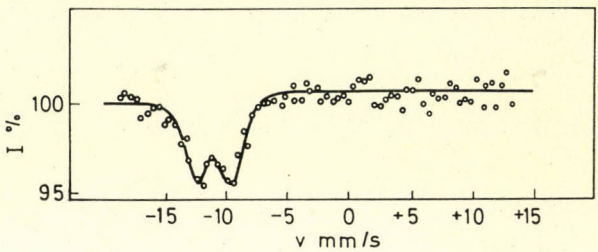

Fig. 1. Mössbauer spectrum of Sb_2O_3

layer thickness of the absorber $d_{opt} = 0.91$ g/cm^2. On the basis of this, the measuring time necessary in the case of a sample containing 1% of Sb, under observation of the requirement that the per cent intensity of the Mössbauer lines should be twice the value of the standard deviation (*i.e.* $k = 2$), is $t_{min} \sim 7$ days at the temperature of liquid nitrogen. ($I_0 = 4.8 \cdot 10^3$ count day^{-1} $channel^{-1}$.)

Table I contains the Mössbauer parameters of the antimony oxide samples investigated by us, as well as those of a few antimony compounds published in the literature. The parameters of the Mössbauer spectra of halo-

Table I

Absorber	Isomer shift mm/s	Reference
SbF_3	—14.7	[8]
$SbCl_3$	—13.8	[8], [10]
Sb_2O_3	—10.5	[9]
Sb_2O_3	—11.0	*
SbF_5	+ 2.3	[8]
Sb_2O_5	0.0	[9]
Sb_2O_5	+ 0.5	*
$SbCl_5$	— 3.2	[8]

* present work

phosphate luminescent powders, recorded under optimum measuring conditions, are given in Table II. Samples 1—4 were prepared under different conditions. Sample 4 was after-treated, the pertinent data are included in Table II under No. 5.

Table II

Sample No.	Isomer shift* mm/s	Line width* mm/s
1	—11.0	3.0
2	—11.1	2.8
3	—15.0	3.0
4	—12.5	4.5
5	—12.5	3.7

* Error: ± 0.2 mm/s.

The value of the isomer shift depends on the density of *s* electrons at the nucleus. However, as has been shown for iron by WALKER *et al.* [5], this value is influenced also by the shielding effect of the *p*, *d* and *f* electrons. On the other hand in addition to the oxidation number, the electron density depends among others also on the covalency of the bond, so that the isomer shift gives information also on this. The WALKER—WERTHEIM—JACCARINO diagram [5] gives for iron the theoretical isomer shift values, belonging to various electron configurations, and agrees well with the experimental data. On the principle of the WWJ diagram, RUBY [6] has performed similar calculations for antimony. The expected isomer shifts for antimony atoms in different oxidation states and electron configurations referred to a $CaSnO_3$ source are listed in Table III.

Table III

Absorber	Sb^{3+}	Sb	Sb^{5+}
Electron configuration	$5s^2\ 5p^0$	$5s^2\ 5p^3$	$5s^0\ 5p^0$
Isomer shift, mm/s	—24	—8	+5

The theoretically expected limiting values of —24 and +5 mm/s cannot be measured in practice, because there is no completely ionic antimony either in the +3 or in the +5 oxidation state.

On the basis of this, the following can be established for the luminescent powder samples investigated. As concerns the isomer shift values, the electron configuration of antimony in samples 1 and 2 is, within experimental error, the same as that of antimony in Sb_2O_3. Antimony in the other samples has

a more ionic character (the 5 *p* orbital is less occupied). This behaviour is most pronounced in sample 3. Samples 4 and 5 occupy an intermediate position. On the basis of literature data mentioned earlier it can be assumed that the decreased occupation of the 5 *p* orbital is caused by antimony–halogen bonds (neighbourhood).

The line broadening (*e.g.* in the case of sample 4) is probably due to the fact that the sample contains more than one kind of antimony in the same oxidation state but of a slightly different electron configuration. Each of these gives a separate line but, owing to the small difference between the isomer shifts, superposition is manifested only as line broadening, no separate lines being observed. The decrease of line width on after-treatment of the sample might be indicative of the removal of one of the components.

The difference in electron configuration may be caused *e.g.* by the fact that antimony is located in the crystal at lattice sites of different environment, at one of the cation sites of different symmetry, or in interstitial positions. In the spectra of the luminescent powders, the line intensity of Sb(V) does not attain the limit required by unequivocal evaluation, which means that less than 10% of the total amount of antimony is present as Sb(V).

On the basis of these measurements, orientative at present, it can be established that the circumstances of preparation of calcium halophosphate luminescent powders affect the Mössbauer parameters indicative of the chemical environment of antimony in the luminescent powder. For further conclusions, extensive experimental work has still to be performed.

*

The authors wish to thank Mrs. L. SUBA for her valuable assistance in the measurements.

REFERENCES

1. SNYDER, R. E., BEARD, G. B.: Phys. Letters, **15,** 264 (1965)
2. MCKEAG, A. H., RANBY, P. W.: Alkaline earth halophosphate phosphors. U. S. Patent No. 2,488,733
3. JENKINS, H. G., MCKEAG, A. H., RANBY, P. W.: J. Electrochem. Soc., **96,** 1 (1949)
4. JOHNSON, P. D.: Luminescence of Organic and Inorganic Materials, Ed. H. P. Kallmann and G. M. Spruch. J. Wiley, New York 1962
5. WALKER, L. R., WERTHEIM, G. K., JACCARINO, V.: Phys. Rev. Lett., **6,** 98 (1961)
6. RUBY, S. L., KALVIUS, G. M., BEARD, G. B., SNYDER, R. E.: Phys. Rev., **159,** 239 (1967
7. SÓOS, J., VÉRTES, A.: Magy. Kém. Lapja, **12,** 690 (1968)
8. BOWEN, L. H., STEVENS, J. G., LONG, G. G.: J. Chem. Phys., **51,** 2010 (1969)
9. LONG, G. G., STEVENS, J. G., BOWEN, L. H.: Inorg. Nucl. Chem. Lett., **5,** 779 (1969)
10. RUBY, S. L., SHENOY, G. K.: Phys. Rev., **186,** 326 (1969).

Attila VÉRTES
Béla LÉVAY
Mária RANOGAJEC-KOMOR
Budapest VIII., Puskin u. 11—13.

Vera FRAKNÓY-KŐRÖS
Péter GELENCSÉR
Budapest IV., Váci út 77.

Acta Chimica Academiae Scientiarum Hungaricae, Tomus 74 (2), pp. 159—161 (1972)

INVESTIGATION OF THE HYDROLYSIS OF ANTIMONY CHLORIDE BY MÖSSBAUER SPECTROSCOPY

A. VÉRTES, M. RANOGAJEC-KOMOR and M. SUBA

(Department of Physical Chemistry and Radiology, L. Eötvös University, Budapest)

Received December 20, 1971

The hydrolysis of $SbCl_3$ has been investigated by Mössbauer spectroscopy. It has been found that hydrolysis proceeds stepwise, and the donicity of hydroxide in the solution is greater than that of chloride.

In the present work, the hydrolysis of $SbCl_5$ and $SbCl_3$ has been studied by means of the Mössbauer effect.

The spectra were recorded with a Ca $^{121}Sn/^{121}Sb/O_3$ source. Both the source and absorbent were kept at liquid nitrogen temperature. The concentration of the solutions was 1 mol Sb/1000 g solvent. Absorbers were prepared by quick freezing. The surface density of Sb in the absorbers was 30 mg/cm^2.

The other conditions of the investigation of antimony by Mössbauer spectroscopy are reported in a separate paper [1].

Results and discussion

The results of investigation of antimony chloride hydrolysis by Mössbauer spectroscopy are summarized in Table I and Fig. 1. Measurements pertinent to Sb(III) were carried out by us, while the data on Sb(V) were measured by BRYUCHANOV and co-workers [2], and the Mössbauer spectrum of $SbCl_3$ was recorded by BOWEN *et al.* [3].

In the works cited, the source was $^{121}Sn/^{121}Sb/O_2$. Differences in the experimental conditions (chemical composition and cooling of the source) may cause deviations of the same magnitude as the experimental error ($\Delta\delta = \pm 0.2$ mm/s), so that they could be disregarded in evaluation of the results. [The differences due to the conditions do not cause difficulties in the evaluation, because they remain constant within a single series of experiments with Sb(III) or Sb(V), respectively and, on the other hand, isomer shifts serving as basis of our conclusions exceed by more than an order of magnitude the inaccuracies mentioned above.]

Table I

Composition of the solution	δ (mm/s)
$SbCl_3 \cdot xH_2O$	—13.8±0.2
Sb(III) in 8 *M* HCl	—17.4±0.2
Sb(III) in 5 *M* HCl	—15.0±0.2
Sb(III) in 1 *M* HCl	—15.2±0.2
$NaSb(OH)_4$	— 8.9±0.2
$SbCl_5$	— 3.5±0.3
$HSbCl_6 \cdot H_2O$	— 3.0±0.2
Sb(V) in 11 *M* HCl	— 2.7±0.2
Sb(V) in 9 *M* HCl	— 2.0±0.2
Sb(V) in 6 *M* HCl	— 0.8±0.2
$NaSb(OH)_6$	+ 0.5±0.2

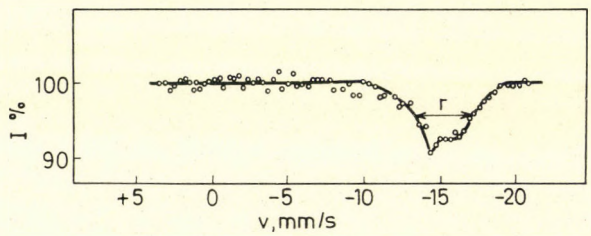

Fig. 1. Mössbauer spectrum of $SbCl_3$ in 1 *M* HCl solution

On the basis of the data measured the following can be established: The ratio of the measured and natural line broadenings is:

$$\Gamma_{\text{measured}} \approx 2\Gamma_{\text{natural}} \quad (\Gamma_{\text{measured}} \sim 3 \text{ mm/s}).$$

This result shows that the Mössbauer spectra do not contain large quadrupole splitting, so that the asymmetry of the charge distribution in the neighbourhood of the Mössbauer nuclei is not considerable. It follows from this that the coordination number of antimony is six in solution (octahedral symmetry).

The hydrolysis of both Sb(III) and Sb(V) occurs in a stepwise manner: δ changes gradually with the acid concentration.

In the case of Sb(III), in 5 *M* and 1 *M* HCl solutions the isomer shift is the same within the experimental error, and this value is closer to that measured in a concentrated acid solution than to the isomer shift of $NaSb(OH)_4$. This result suggests that in these Sb(III) solutions the concentration of the monohydroxide is substantially higher than that of the dihydroxide. At the two acid

concentrations mentioned above, more than 90% of the antimony is present as the monohydroxide:

$$SbCl_i^{(i-3)-} + H_2O \rightleftharpoons [Sb(OH)Cl_k]^{(k-2)-} + H^+ \ldots {}^*K_1 > 10$$

$$[Sb(OH)Cl_k]^{(k-2)-} + H_2O \rightleftharpoons [Sb(OH)_2Cl_l]^{(l-1)-} + H^+ \ldots {}^*K_2 < 10^{-1}$$

The Mössbauer results are in good qualitative agreement with the spectrophotometric data of BONNER and GOISKI [4], who found that the spectrophotometric curves of Sb(III) do not change in the concentration interval between 6 and 12 *M* HCl, so that hydrolysis begins only at lower acid concentrations.

As concerns the electronic structure of Sb(III) and Sb(V) in solution, it can be established that in the case of both Sb(III) and Sb(V), the density of *s* electrons at the nucleus, $|\psi_s(0)|^2$, increases with increasing extent of Cl coordination. (In the case of ^{121}Sb, the radius of the excited nucleus is smaller than that of the ground state and, therefore, the value of the isomer shift decreases with increasing *s* electron density $|\psi_s(0)|^2$ at the absorber nucleus.) This effect means that in the case of Sb, the bond with OH increases the occupation of the 5 *p* and 5 *d* orbitals more strongly than the bond with Cl.

These results indicate that the Sb–OH bonds are more covalent than the Sb–Cl linkage.

On comparing the δ value of $SbCl_3$ with δ values measured in Sb(III) solutions in concentrated hydrochloric acid, the conclusion can be drawn that chloride coordination in such solutions is more extensive ($SbCl_4^-$) than in solid antimony chloride.

WILLIS *et al.* have studied the rate of hydrolysis of the $SbCl_6^-$ ion by spectrophotometry [5]. They found that the first step of hydrolysis [$SbCl_6^- \xrightarrow{k} Sb(OH)Cl_5^-$] is slow ($k \sim 3 \cdot 10^{-5}\ s^{-1}$), while further hydrolysis is rapid. In this way, the attainment of equilibrium in antimony chloride solutions of various hydrogen ion concentrations is a slow process which may require several weeks. (This circumstance must be taken into consideration in the measurements.)

REFERENCES

1. VÉRTES, A., FRAKNÓY-KŐRÖS, V., LÉVAY, B., GELENCSÉR, P. A., RANOGAJEC-KOMOR, M.: Acta Chim. Acad. Sci. Hung. **74**, 151 (1972)
2. BRYUCHANOV, V. A., YOFA, B. Z., SEMENOV, S. I.: Radiokhimiya, **11**, 362 (1969)
3. BOWEN, L. H., STEVENS, J. G., LONG, G. G.: J. Chem. Phys., **51**, 2010 (1969)
4. BONNER, N. A., GOISKI, W.: J. Am. Chem. Soc., **83**, 85 (1962)
5. WILLIS, S. B., NEUMANN, H. M.: J. Am. Chem. Soc., **91**, 2924 (1969)

Attila VÉRTES
Mária RANOGAJEC-KOMOR
Magdolna SUBA

Budapest VIII., Puskin u. 11—13.

Acta Chimica Academiae Scientiarum Hungaricae, Tomus 74 (2), pp. 163—168 (1972)

MAGNETIC PROPERTIES OF THE BINUCLEAR ION $[Fe_2(OH)_2(H_2O)_8]^{4+}$

K. LÁZÁR,* M. HORVÁTH-PARDAVI** and A. VÉRTES*

(*Department of Physical Chemistry and Radiology, Eötvös Loránd University, Budapest, and **Central Physical Research Institute of the Hungarian Academy of Sciences, Budapest)

Received December 20, 1971

It was found from a study of the magnetic susceptibilities and Mössbauer effects of the polymerization products formed on the hydrolysis of iron(III) perchlorate solutions that the number of spin-free 3d electrons per iron atom in these is about three.

Introduction

In the majority of the many publications dealing with the hydrolysis of iron(III) salts mention is made of the polynuclear hydrolysis products, including the binuclear 'dimer' [1—17]. Two types of structure can be conceived for the 'dimer':

$$[(H_2O)_5Fe-O-Fe(H_2O)_5]^{4+} \quad \text{and} \quad \left[(H_2O)_4Fe\begin{matrix}H\\O\\O\\H\end{matrix}Fe(H_2O)_4\right]^{4+}$$

In general the latter is considered probable [1—5], but in the opinion of ROPARS *et al.* [6] both structures occur.

The magnetic properties of the dimer are dealt with in a number of publications [1—3, 6—8]. MULAY and SELWOOD [1] assumed it to be diamagnetic, but other authors now regard it as paramagnetic [2, 3, 6]. The data of MULAY and SELWOOD were used by MÁTHÉ and BAKK-MÁTHÉ [2] to calculate the magnetic moment of the dimeric molecule. The calculation is complicated by the fact that various hydrolysis products can be found in the solution the susceptibility of which is measured [1, 2, 4, 6, 7, 9—13]. Susceptibility values measured at different pH values were used in their calculations by MÁTHÉ and BAKK-MÁTHÉ.

In the present paper the magnetic moment of the dimer ion is calculated from measurements at different temperatures.

If it is assumed that:

(i) the Curie law is valid in the temperature range studied in this system (the straight line of Figure 1 passes through the origin, $\Theta = 0°$);

(ii) the susceptibilities of the individual components are additive (Wiedemann rule);

(iii) the mononuclear hydrolysis products have susceptibilities corresponding to the theoretical 5.92 BM [2, 6, 7];

(iv) the magnetic moments are not significantly affected by freezing; then a relation can be obtained for the susceptibility of the dimer.

The measured susceptibilities are comprised of the susceptibilities of the monomeric hydrolysis products and of the dimer:

$$\varkappa_T = m\frac{C_m}{T} + \frac{c-m}{2}\frac{C_d}{T} \tag{1}$$

where $\varkappa_T$ is the susceptibility of a solution whose iron molarity is c and whose monomer molarity is m, measured at temperature T, and C_m and C_d are the values of the Curie constants for the monomer and dimer. The value of C_m is known: 4.345 K. (In taking the molarity of the dimer as $\frac{c-m}{2}$, the hydrolysis products containing more than two iron atoms have been neglected.)

Experimental conditions

Iron(III) perchlorate solutions, with concentrations of 0.6 and 0.9 mole/dm^3, were prepared by the dissolution of metallic iron in perchloric acid, oxidation with hydrogen peroxide, and then the removal of the excess hydrogen peroxide and perchloric acid. The pH was adjusted to 1.4 $\pm$ 0.1 by the addition of sodium hydrogen carbonate. The susceptibility was determined in a Foner vibration magnetometer to an accuracy of $\pm 3 \times 10^{-8}$ in a magnetic field of 10 kOe ($\approx$ 0.8 MAm^{-1}). The quantity of solution measured was about

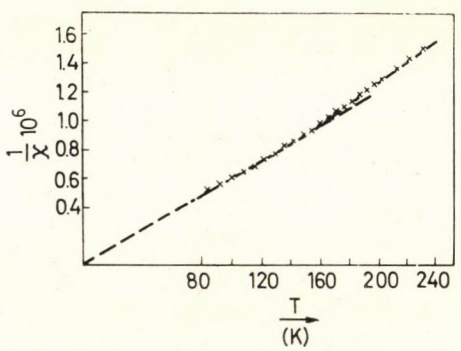

Fig. 1. Reciprocal of the susceptibility of a sample containing 4.765×10^{-5} mole iron as a function of temperature. (The individual points have already been corrected for the diamagnetic contributions of the solvent and the other ions.) The break at 170 °K is probably connected with the fact that an eutectic or crystal hydrate segregations begin to form in the solution at this temperature

0.1 g. The measurements were made in the range 80—260 °K. The results are shown in Figure 1.

In an exactly similar way, a 1.0 mole/dm^3 solution was prepared with a pH of 1.6. This was left to stand for several days, and the Mössbauer spectrum of the precipitate formed was taken at liquid nitrogen temperature (Fig. 2).

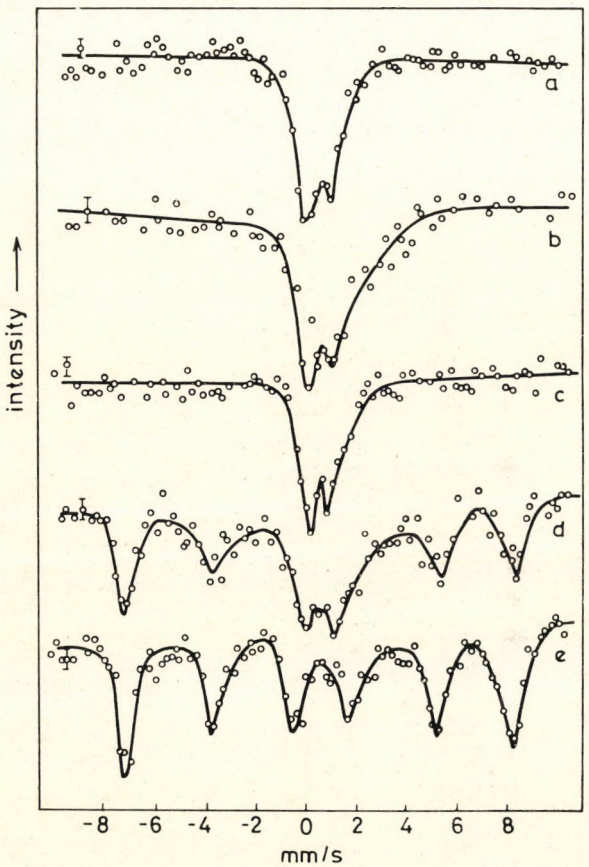

Fig. 2. Mössbauer spectra of a 1.0 mole/dm^3 iron(III) perchlorate solution of pH 1.6. a — pure solution, b — the clear part of the solution on precipitation, c — the precipitate in a 22-day-old solution, d — the precipitate in a 110-day-old solution, e — the precipitate in a 380-day-old solution

Results and discussion

After the insertion of the experimental results, equation (1) can be written in the form

$$\frac{C_d}{C_m} = 2\,\frac{3.772 - m}{4.765 - m} \tag{2}$$

The curve corresponding to equation (2) is given in Figure 3.

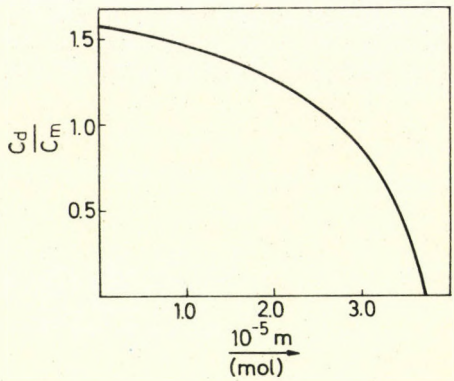

Fig. 3. The C_d/C_m—m value pairs of equation (2)

For the determination of the magnetic moment it is also necessary to know the amount of monomer in the solution. This can be found from a knowledge of the hydrolysis constant of the dimer

$$K_{22} = \frac{[[Fe_2(OH)_2]^{4+}[H^+]^2}{[Fe^{3+}]^2} \tag{3}$$

The following values have been calculated by various authors for K_{22} at 25 °C:

Table I

Method	$K_{22} \times 10^3$	Ref.
Proton magnetic resonance	1.00	[6] (at 22 °C)
Potentiometry	1.22±0.1	[9]
Spectrophotometry	1.9 ±0.6	[14]
Potentiometry	4.4	[15]
Magnetic susceptibility	7.3 ±0.8	[1]
Proton magnetic resonance	10	[7] (at 20 °C)
Mössbauer spectroscopy	13.5 ±5	[16] (at 20 °C)
Magnetic susceptibility	32	[2]
Spectrophotometry Magnetic susceptibility	75 ±10	[8]

Using the value $K_{22} = 13.5 \pm 5 \times 10^{-3}$, calculated from the paper of KOMOR *et al.* [16], the value of C_d/C_m is found to be 1.42.* This corresponds

* The calculations here were performed with the result of the Mössbauer measurement because this method measures the amount of dimer directly.

to $C_d = 6.17$. Then, from the relation $\mu_{\text{eff}} = 2.84\ C_d^{0.5}$, the magnetic moment of the dimer is 7.03 ± 0.1 BM. This corresponds to 3.05 unpaired electrons per iron atom. It must be noted, however, that the antiferromagnetic coupling between the iron atoms may distort this result a little, and this may mean a further uncertainty corresponding to $\sim \pm 0.5$ unpaired electrons.

If the calculation is carried out with the lowest and the highest K_{22} values from Table I (*i.e.* 1.00×10^{-3} and 85×10^{-3}), the values found for the magnetic moment are 5.0 and 7.3 BM.

It should be noted that in spite of the fact that the measurements were carried out in frozen solution between 80 and 260 °K, the K_{22} value determined at 25 °C can be used for the calculation of the final result; the dimer molecule decomposes very slowly [17], and thus the concentration relations of the solution did not change significantly during the short time of the freezing.

Our result differs from the value, $\mu_{\text{eff}} = 6.2$ BM, found by MÁTHÉ and BAKK-MÁTHÉ.

The Mössbauer measurements lead to a value of 480 kOe ($\approx$38 MAm^{-1}) for the internal magnetic field in the precipitate formed on the long standing of the solution. In the case of the iron(III) ion the Fermi contact interaction is decidingly responsible for the magnetic splitting:

$$H_c = K \sum_{ns} \left(\varrho_{s\uparrow}(0) - \varrho_{s\downarrow}(0) \right) \tag{4}$$

(The size of the magnetic field is proportional to the difference in the densities of the *s* electrons of opposite spins.) The polarizing effect of the *d* electrons is the reason that the spins of the *s* electrons of the individual shells do not compensate each other completely. If there are several unpaired *d* electrons in the system (the value of the spin is high), then the value of the magnetic field H_c is also high, while with fewer unpaired *d* electrons the value of H_c is smaller too. If the increase of the magnetic field caused by each electron (approximately 125 kOe) $\approx$ 10 MAm^{-1} [18] is compared with the measured value of 480 kOe ($\approx$38 MAm^{-1}), and if it is considered that about 10% of this originates from the orbital momentum, then it can be said that the number of unpaired *d* electrons per iron atom calculated from the Mössbauer measurements is close to the value calculated from the susceptibility.

It must be noted that the precipitate formed after long standing is not a dimer, but a polymer. Thus, the fact that the results obtained with the above two methods are almost identical indicates that the electronic structures of the iron atoms in the dimer and in the polymer are also very similar.

REFERENCES

1. MULAY, L. N., SELWOOD, P. W.: J. Am. Chem. Soc. **77,** 2693 (1955)
2. MÁTHÉ, J., BAKK-MÁTHÉ, E.: Rev. Roum. Chim. **11,** 225 (1966)
3. SCHUGAR, H., WALLING, C., JONES, R. B., GRAY, H. B.: J. Am. Chem. Soc. **89,** 3712 (1967)
4. WENDT, H.: Inorg. Chem. **8,** 1527 (1969)
5. PO, H. N., SUTIN, N.: Inorg. Chem. **10,** 428 (1971)
6. ROPARS, C., ROUGÉE, M., MOMENTEAU, M., LEXA, D.: J. Chim. Phys. Physico-chim. Biol. **65,** 816 (1968)
7. BROERSMA, S.: J. Chem. Phys. **26,** 1405 (1957)
8. MULAY, L. N., NAYLOR, M. C.: Advances in the Chemistry of the Coordination Compounds — Proc. 6th ICCC, New York, 1961, p. 520.
9. HEDSTRÖM, B. O. A.: Arkiv Kemi **6,** 1 (1954)
10. MILBURN, R. M., VOSBURGH, W. C.: J. Am. Chem. Soc. **77,** 1352 (1955)
11. STUMM, W., MORGAN, J. J.: J. Am. Water Works Assoc. **54,** 971 (1962)
12. SCHINDLER, P., MICHAELIS, W., FEITKNECHT, W.: Helv. Chim. Acta **46,** 444 (1963)
13. BEHAR, B., STEIN, G.: Isr. J. Chem. **7,** 827 (1969)
14. MILBURN, R. M.: J. Am. Chem. Soc. **79,** 537 (1957)
15. ZVJAGINTSEV, O. E., LJAKHMANOV, S. B.: Zh. Neorg. Khim. **13,** 1230 (1968)
16. KOMOR, M., VÉRTES, A., DÉZSI, I., RUFF, I.: Acta Chim. Acad. Sci. Hung. **66,** 285 (1970)
17. VÉRTES, A., KOMOR, M., DÉZSI, I., BURGER, K., SUBA, M., GELENCSÉR, P.: Proc. 3rd Symp. Coord. Chem. (Debrecen, 1970), Akadémiai Kiadó, Budapest, 1970, p. 477
18. WATSON, R. E., FREEMAN, A. J.: Phys. Rev. **123,** 2027 (1961)

Károly LÁZÁR
Márta PARDAVI-HORVÁTH
Attila VÉRTES

Budapest VIII., Puskin u. 11—13.

Acta Chimica Academiae Scientiarum Hungaricae, Tomus 74 (2), pp. 169—178 (1972)

A STUDY OF THE POSITIVE ION EMISSION OF MOLYBDENUM BY MEANS OF A TIME-OF-FLIGHT MASS-SPECTROMETER

R. KARÁCSONYI, O. KAPOSI, M. RIEDEL, I. HOBINKA and I. PODMANICZKY

(Department of Physical Chemistry and Radiology, L. Eötvös University, Budapest)

Received January 24, 1972

Molybdenum filaments produced by powder metallurgy were heated at predetermined rates per determined final temperatures, and the positive ions emitted by the filaments during heating were studied. It has been found that besides K^+, and Na^+, emitted during the entire time of heating, at higher temperatures also Rb^+ ions were emitted.

The curves representing ion intensities in function of time showed two maxima and an exponentially descending branch in every case both for potassium and sodium. We ascribed the first maxima to the desorption at increasing temperature of impurities earlier accumulated on the surface. We suggest the second are due to several superimposed phenomena, *viz.* diffusion, evaporation of the matrix metal, oxidation of the metal, and evaporation of the oxides.

Contribution of potassium ions to the total ion current emitted increases if the rate of heating is increased.

Ratios of ions emitted at second heating by filaments allowed to stand showed that sodium approximates, or reaches, initial concentrations on the surface earlier than does potassium. This can be explained by the ratio of their ionic radii, since this ratio affects rates of diffusion; thus it seems to be likely that measurements of ion emissions will be suitable for the determination of diffusion coefficients.

In earlier communications [1, 2, 3] we have reported on a study, by means of time-of-flight mass-spectrometry, of the emission of positive ions of tungsten. A more thorough knowledge of the process of the emission and of the several part processes requires the study of the thermal positive ion emission of incandescent metals of high melting point. The importance of molybdenum in industrial practice, *e.g.* in electronics, justifies our endeavour to find out what kind of ions are emitted from molybdenum heated to high temperatures, the dependence of the emission on temperature and other parameters.

We started our studies with relatively few previous results at hand.

WAHLIN [4] reported that investigating the emission of molybdenum alkali ions could be detected emitted for a short time.

SMITH [5] carried out more detailed studies on the thermal emission of tungsten, and of molybdenum. He found that the two metals emitted potassium, sodium and aluminium ions. Above 2300 °K also molybdenum ions could be detected.

LICHTMANN [6] studied the emission of molybdenum coated with a thin layer of aluminium. Potassium, sodium and aluminium ions were detected. He also investigated the effect of temperature upon the emission [7].

DOBRECOV [8], EVANS [9], MEYER [10], and WILSON [11] determined the ion emission efficiency of various alkali ions on molybdenum surfaces.

BAKULINA *et al.* [12] detected WO_3^+ and MoO_3^+ ions in the emission of tungsten, and molybdenum, respectively.

Experimental apparatus

A time-of-flight mass-spectrometer was used in this study of the spontaneous thermal positive ion emission of molybdenum. The advantage of this instrument, compared to those used in former studies, resides in the possibility to follow the process of emission in time. The instrument was designed by MATUS [13]. A research team in the Central Research Institute for Physics, and the staff of the Department of Physical Chemistry at the L. Eötvös University were the first to use a time-of-flight mass-spectrometer as an analyser in ion emission studies [1, 2, 3]. The resolution of the instrument was comparatively low, about 100, however, our interest in ions emitted having been confined to low mass number species this did not cause any disadvantage.

A detailed description of the instrument, and the technique of its application, have been published earlier [1, 2, 3, 14, 15].

The reproducible heating of the metal filaments was carried out by an electronic regulating circuit [2].

In our experiments molybdenum filaments (0.1 mm in diameter) produced by powder metallurgy were used.

The spectra in the screen of the oscilloscope were filmed with a Pentaflex 16 mm camera; for the evaluation of the films a photo-projector was used.

Experimental results

1. *The character of the ions emitted*

All the filaments studied emit potassium and sodium ions of high intensity. At higher temperatures, besides the attenuated peaks due to K^+ and Na^+, a peak caused by Rb^+ emerged with gradually increasing amplitude. In the moments just preceding the burning of the filament the height of the Rb^+ peak substantially surpassed the initial K^+ and Na^+ amplitudes. We have not been able to detect the emission of aluminium ions, claimed by SMITH [5].

2. *Character of the heating curves*

For recording ion-intensity versus time, we varied the heating rate $\frac{\Delta T}{\Delta t}$ of the filaments on the one hand [this is an average derivate of the function $T = f(t)$; in our experiments the values were chosen between 25 °K · s^{-1} and 10 500° K · s^{-1}] and the speed of filming, from 5 frames per second to 64 frames per second, on the other hand. Variation in the heating rate has been regarded necessary in order to separate the overlapping part processes of emission, *i.e.* from the characteristic sections of $I = f(t)$ curves some conclusions could be drawn concerning the part processes. The increase of the frequency of the exposures at filming promised to reveal something about the possible fine structure of the $I(t)$ curves.

With each filament studied we found that the K^+ ions produce $I(t)$ curves with two maxima and a closely exponential decay (*cf.* Fig. 1).

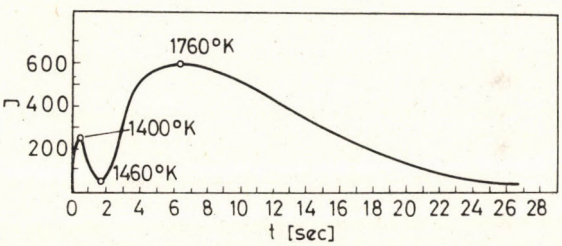

Fig. 1. K^+ ion emission of molybdenum filament as a function of time. The final temperature was 1760 °K. The intensity of ion current is given in arbitrary units

On these curves the 'location' by time of the maxima is quite straightforwardly defined.

The 'location' by temperature of the first maximum shows values rather divergent from one filament to the other.

The 'location' by temperature of the second maximum in the case of rapid heatings, *i.e.* from 1000° to 10 500° per second, was found unequivocally defined by the final temperature. In ranges of lower heating rates, the location of the second maximum varied within wide limits both by time and by temperature. These findings partly support LICHTMANN's results [7] in connexion with the ion emission of molybdenum. However, LICHTMANN's data and our findings diverge in the location, according to temperature, of the intensity maxima. If the final temperature of the filaments was raised without a change in the rate of heating the following could be observed:

a) The significant intensity difference between the first and the second maxima became less in such a way that the first maximum increased and the second one decreased.

b) Also the minimum that separated the two maxima became less, in other words, at its minimum section the curve became filled up (*cf.* Fig. 2).

An increase in the frequency of exposure in filming did not reveal any significant change in the structure of the curves, only some low-amplitude peaks superimposed on the smooth course of the curves became visible, *i.e.* the pulsation mentioned by LICHTMANN.

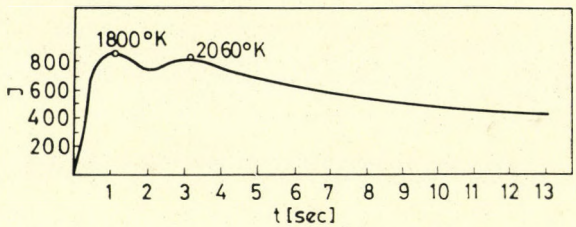

Fig 2. Variation of K^+ ion emission from molybdenum filament as a function of time. The final temperature was 2060 °K

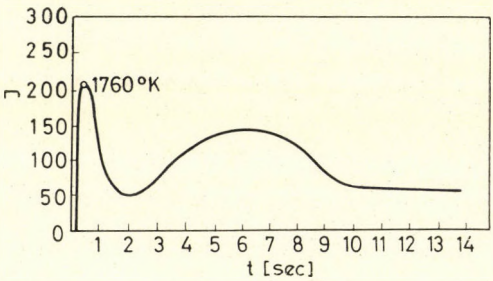

Fig. 3. Variation of Na^+ ion emission from molybdenum filament as a function of time. Final temperature 1800 °K

On the $I = f(t)$ curve for sodium ion at rather low frequencies of exposure (5 to 20 frames per second), *i.e.* at low resolution, two well-separated maxima appeared (*cf.* Fig. 3).

The location of these maxima, even by time, was less distinct than in the case of potassium. The ratio of the intensities of the first and the second maxima, also the ratio of the intensities of the same maximum but of different filaments showed much greater deviations than found with potassium.

With lower heating rate the amplitude of the maxima was generally higher than that shown by filaments exposed to higher heating rates, while the final temperature was the same.

3. *Total ion current*

The area circumscribed by our $I = f(t)$ curves and the co-ordinate axes is proportional to the total quantity of ion emitted. The relevant integrals were calculated. Considering that at the 20th to 25th second of heating every

curve reached its exponentially decreasing section mentioned before, the calculation of the integrals was carried out in two steps. Using SIMPSON's formula [16], first, approximate integrals for the first 25 seconds were computed, then the descending branch of a curve was approximated by the least squares method to an $I = A \cdot 10^{-Bt}$ exponential function. As the concrete exponential function was known, we could integrate from the 25th second to infinity. The sum of the two integrals $\int_0^{25} + \int_{25}^{\infty}$ was considered to be proportional to the total ion quantity emitted.

The integral values for the whole domain $0 \rightarrow \infty$ were found to be constant, and independent of the rate of heating. The integrals for the first 25 secondschanged with heating rates; the relevant data are collected in Table I.

Table I

$\frac{\Delta T}{\Delta t}$	$\int_0^{25} I(dt)$, K^+	$\int_0^{25} I(dt)$, Na^+
1000....10 500	1500....11 000	270....4 300
70.... 200	5700.... 8 200	1200....1 800
40.... 100	8200....33 000	900....7 300
25.... 35	4700....12 000	650....1 100

The highest integral values were found at low heating rates, *i.e.* for $40 < \frac{\Delta T}{\Delta t}\left[\frac{°K}{s}\right] < 100$. If similar integrals for filaments of other cross sections are compared with data in Table I, we find that the integrals change in the sense suggested by the change of surface area of the filament and nearly in the same proportion.

In most cases the amount of potassium ions emitted from a filament was greater than that of sodium. Using filaments of various cross sections we found that increase of this cross section favoured the emission of potassium. When, in the case of filaments of 0.1 mm in diameter, the heating rate decreases, the ratio $\int K^+$ to $\int Na^+$ increases, *i.e.* the slower the heating the higher the proportion of K^+ emitted in reference to Na^+. This ratio was found to vary between 4.0 and 8.5.

4. *Repeated heatings*

a) *Filaments purified by short heat treatment flashing*

In this series of experiments we heated the filaments for a short time ($\sim$1 second) to about 2000 °K. With filaments thus pre-treated heating tests described above were then carried out. The aim of this pre-treatment was the

removal, by flashing, of the impurities accumulated on the surface and thus to start the heating with a purified surface of the filaments.

Compared to the results of previous experiments, a decrease in the number of emitted ions could be observed as a difference, and the descending branch of the curve turned less steep (Fig. 4). The character of the $I(t)$ curves did not change by short purification of the surface.

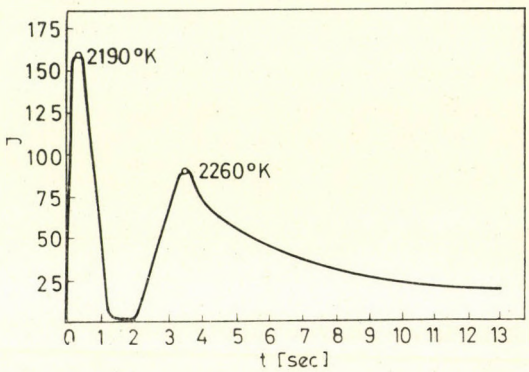

Fig. 4. Change in K^+ ion emission from annealed Mo filament upon repeated heating-up. Final temperature 2260 °K

b) *Repeated heating of filaments allowed to stand after the first heating*

In this series of experiments, immediately after the first heating or after standing for a certain period of time at some chosen temperature, the filaments were heated again. From a comparison of $I(t)$ curves from the first heating with $I(t)$ curves from the second one we expected to obtain some information about the time needed for the heated filaments to have their surface covered again with alkali ions as they had been before heat treatment. Our findings we can summarize as follows:

First heating of filaments	$I_{K+} = 2064$
not annealed	$I_{Na+} = 1107$
Same filament, at second	$I_{K+} = 593$
heating immediately after the first	$I_{Na+} = 575$

The integrated emission values for filaments heated a second time after standing subsequently to their first heating are gathered in Table II. The integrated values are expressed in arbitrary units.

Table II

Time allowed for standing	Temperature maintained during standing					
	−180 °C		25 °C		100 °C	
	$\int I_{K^+}\, dt$	$\int I_{Na^+}\, dt$	$\int I_{K^+}\, dt$	$\int I_{Na^+}\, dt$	$\int I_{K^+}\, dt$	$\int I_{Na^+}\, dt$
600 hours	526	764	950	1081	—	—
1200 hours	636	966	1652	1584	2156	1480

Discussion

1. *Character of heating curves*

We assume that the first maximum on the $I = f(t)$ curves is due to the desorption of impurities accumulated on the surface. Since desorption is a rapid process it follows that the location in time of this maximum might be quite invariable by changes in heating rates. Already during desorption those part processes begin which will cause further increase of emission (second maximum). These are

a) *Recrystallization*

From studies that have dealt with recrystallization processes occurring during the heat treatment of molybdenum [17] we know that molybdenum prepared in powder metallurgy turns into a macrocrystalline phase between 1670 and 1700 °K. The disappearance of boundaries between crystallites and the structural changes that bring forth new boundary surfaces impart substantial mobility to contaminants within the body of the metal substrate: this facilitates the migration of the contaminants towards the surface. Thus this part process enhances the emission.

b) *Vapour pressure of molybdenum increased by temperature*

The vapour pressure of molybdenum is substantially increased by increasing the temperature [18]. Molybdenum which evaporates uncovers its layers under the surface, and forestalling the diffusion brings the impurities on the filament surface. Thus a higher vapour pressure leads to an increased emission. At 2000 °K the amount of impurities arriving at the surface because of the evaporation of the metal is commensurable with the amount brought to the surface by diffusion [18].

c) *Oxidation of molybdenum, and evaporation of the oxide from the surface*

BERKOWITZ-MATTUCK and BÜCHLER [19] have carried out detailed studies on the oxidation of molybdenum and on the desorption of the oxides. These authors have found that the intensity of MoO_2^+ has a maximum at 1900 °K and that of MoO_3^+ at 1600 °K.

Experiments with tungsten have shown that oxygen enhances ion emission [15]. Due to coverage with oxygen the work function becomes greater and thus ionic desorption gains preference. We assume that in the case of molybdenum also another effect of oxygen in favour of ion emission might be considered, this being just the intensive formation of oxides and their evaporation from the surface. This process facilitates ion emission in a way as does the evaporation of the metal.

d) *Changes in the efficiency of ionisation by temperature*

Many factors affect $\alpha = \frac{N^+}{N^0}$ (the degree of ionisation), *e.g.* coverage of surface, value of external electrical field, temperature, etc. [20], therefore it is rather difficult to follow the changes of α during the heating experiments. For pure molybdenum surfaces we present our data in Table III, calculated according to the Saha formula, presupposing an $\alpha = f(T)$ function with a single variable. The work function for polycrystalline molybdenum is 4.12 eV [18].

Table III

	1000 °K	1500 °K	2000 °K	2300 °K
K^+	$9.84 \cdot 10^{-2}$	$9.18 \cdot 10^{-2}$	$9.09 \cdot 10^{-2}$	$9.00 \cdot 10^{-2}$
Na^+	$8.89 \cdot 10^{-6}$	$1.86 \cdot 10^{-4}$	$8.99 \cdot 10^{-4}$	$1.44 \cdot 10^{-3}$

In the case of potassium the rather slow decrease of α with temperature favours a more rapid decay of the curves; in the case of sodium, however, α is greatly increased by temperature and therefore, if no other effects influence the ion emission, increase of α will lead to increased ion emission.

e) *Increase of diffusion with temperature*

Data found in the literature on the diffusion of alkali metals in molybdenum [21, 22] reveal quite substantial differences in the values of diffusion coefficients. Irrespective of the numerical value of the diffusion coefficient,

increase of temperature helps to increase the amount of impurities being carried to the surface and consequently increases the ion intensity found in our experiments.

2. *Comparison of amounts of ions emitted during annealing*

Table I shows the greatest amount of ions emitted at heating rates between 40 and 100 °K · s^{-1}. If we suppose that impurities carried by dislocations play an important role in our measurements of emission then this is supported by the fact that at high heating rates the contaminant alkalies lag behind the rapidly advancing dislocations and their arrival on the surface is an effect brought about by some slower processes.

3. *The ratio of emitted K^+ to Na^+ is increased when the heating rate is reduced*

This phenomenon supports our remarks made in connexion with Par. 2. The ratio of atomic radii $R_K : R_{Na}$ is 1.273. It is more difficult for potassium ions to proceed to the surface by diffusion through the metal lattice than for sodium ions. This is shown also by KARPMAN's result [23] that the activation energies of diffusion for potassium, and sodium, in molybdenum are as shown in Table IV.

Table IV

Polycrystalline molybdenum		Molybdenum single crystal	
K	13 700 cal · $mole^{-1}$	K	25 043 cal · $mole^{-1}$
Na	13 250 cal · $mole^{-1}$	Na	21 250 cal · $mole^{-1}$

Thus, if we suppose that in our measurements an important role must be attributed to impurities carried by dislocations then we might expect that at low heating rates the ratio $\frac{K^+}{Na^+}$ is greater than at high heating rates where, as mentioned, contaminant alkali ions are apt to lag behind the dislocations which proceed at higher speed, and shall have to be carried to the surface *e.g.* by diffusion through the lattice of the matrix metal.

4. *Repeated heating*

Ion emission from filaments at a second heating after standing suggests that accumulation of sodium on the surface proceeds more quickly than accumulation of potassium. This is explained by the ratio of their atomic radii ($R_K : R_{Na} = 1.273$). Diffusion, as one of the processes that govern the concentration of surface contaminants, favours that of the smaller species.

Further research project

Since, in ultimate analysis, emission should be considered as the result of several part processes, these latter should be studied in detail. Due to their point occurrence the individual part processes cannot be studied separately, therefore we regard it as important to perform the mathematical analysis of the intensity *vs.* time curves of emissions.

REFERENCES

1. KAPOSI, O., MATUS, L., SÜLI, M.: Magy. Kém. Foly. **73,** 245 (1967)
2. KAPOSI, O., RIEDEL, M., MATUS, L.: Magy. Kém. Foly. **74,** 429 (1968)
3. KAPOSI, O., RIEDEL, M., STANISLAV, D.: Magy. Kém. Foly. **75,** 324 (1969)
4. WAHLIN, H. B.: Phys. Rev. **34,** 164 (1929)
5. SMITH, P.: Phys. Rev., **35,** 381 (1930)
6. LICHTMANN, D.: J. Vacuum Sci. **2,** 2 (1965)
7. LICHTMANN, D.: J. Appl. Phys. **36,** 2323 (1965)
8. DOBRECOV, L. N.: J. Exp. Theor. Phys. USSR **6,** 552 (1965)
9. EVANS, R. C.: Proc. Cambridge Philos. Soc. **29,** 552 (1933)
10. MEYER, E.: Ann. Phys. **4,** 357 (1930)
11. WILSON, R. G.: J. Appl. Phys. **37,** 4125 (1966)
12. BAKULINA, J. N., ZANDBERG, E. J., IONOVA, N. I.: Zh. Tekhn. Fiz. **35** 562 (1965)
13. MATUS, L.: KFKI Közl. **13,** 4 (1965)
14. RIEDEL, M.: Thesis, Budapest, 1968
15. KAPOSI, O.: Thesis, Budapest, 1970
16. BJEZIKOVICS, Sz.: Közelítő Számítások (Approximation Calculus). Tankönyvkiadó, Budapest, 1952
17. DAVIS, G. L.: Metal Treatment, p. 495, 1958
18. NORTHCOST, L., FINNISTON, H. M.: Molybdenum. 1956, Butterworths, London
19. BERKOWITZ-MATTUCK, J. B., BÜCHLER, A.: J. Chem. Phys. **39,** 2722 (1963)
20. MOESTA, H.: Chemisorption und Ionisation in Metall-Metall Systemen. 1968, Springer, Berlin
21. BENEDIKTOVA, G. P., DUBININ, G. N.: Met. i Term. Obrab. Met. **5,** 55 (1966)
22. CORNIDES, I.: Naturwissenschaften **45,** 6 (1958)
23. KARPMAN, M. G., DUBIBIN, G. N.: Met. i Term. Obrab. Met. **3,** 46 (1967)

Rezső KARÁCSONYI
Olivér KAPOSI
Miklós RIEDEL
Ildikó HOBINKA
István PODMANICZKY

Budapest VIII., Puskin u. 11—13.

Acta Chimica Academiae Scientiarum Hungaricae, Tomus 74 (2), pp. 179–183 (1972)

AN INTERPRETATION OF THE BEHAVIOUR OF SCINTILLATION SYSTEMS BY THE SPECTRAL PROPERTIES OF THE COMPONENTS

P. FODOR-CSÁNYI

(Department of Physical Chemistry and Radiology, L. Eötvös University, Budapest)

Received February 21, 1972

Three independent groups of phenomeny — phosphorescence, chemiluminescence and light output of the system — are interpreted by the spectral properties of the components of scintillation systems, and on the basis of energy transfer via radiation.

Though liquid scintillators have been used extensively during the last 20 years, a large number of questions still await for answer in connection with the mechanism of energy transfer in liquid scintillation systems. In course of our recent studies three major groups of phenomena have been observed, offering a more detailed interpretation of energy transfer mechanism. Apparently these three groups are not connected with each other, though all the phenomena can be interpreted by the spectral properties of the components of scintillation systems. On this basis, we have concluded that energy transfer via radiation may have a greater role in scintillation mechanism than supposed earlier. In the present paper the experimental observations and the considerations leading to the above conclusion are described.

The phenomena mentioned above can be divided in three groups: those connected 1. with phosphorescence, 2. with chemiluminescence, and 3. with the light output of the scintillation systems.

1. The problem of phosphorescence

It has been stated that the measured phosphorescence (in a single-photomultiplier scintillation counter) of the whole system cannot be obtained as a sum of the individual phosphorescence intensities originating from the sample container, solvent, additive materials, etc. [1, 2]. This was concluded by reexamining the method of LLOYD *et al.* [3] by using an optical filter to eliminate phosphorescence. They claim that the optical filter decreases the sensitivity of the photocathode to the emission range of the scintillator molecule, thus decreasing the intensity of phosphorescence.

This is valid only if the phosphorescence of the individual components is examined separately. In the presence of scintillator molecules, however, the

phosphorescence of the sample container, the solvent and the additive materials increases. This phenomenon, called by us "the introduction of phosphorescence" can be explained by the emission of a part of phosphorescence (not detectable in the absence of scintillator molecules) at the emission wavelength of the scintillator. If the absorption band of the scintillator molecule is in the transmission range of the optical filter, and its emission band has a longer wavelength, the intensity of phosphorescence decreases significantly.

Thus it can be taken experimentally as proved that phosphorescence is absorbed by the scintillator to a great extent.

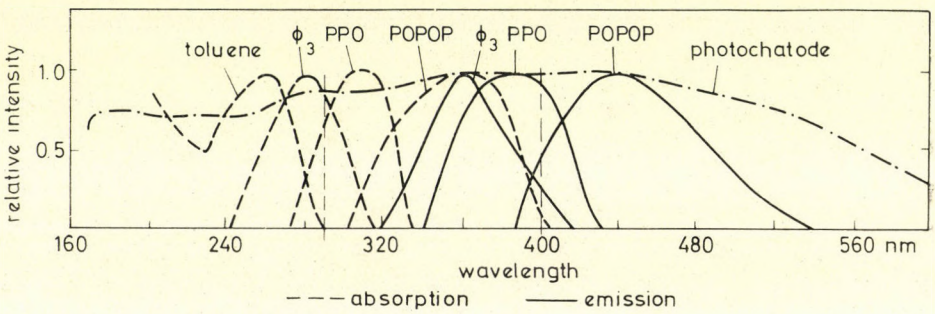

Fig. 1

An increase and decrease in phosphorescence can be illustrated by the following examples:

a) System:

Toluene (absorption band: 230—276 nm), *p*-terphenyl (absorption band: 240—320 nm, emission band: 320—420 nm), Chance OX7 optical filter (transmission range: 230—400 nm), EMI 9514 S photomultiplier (160—600 nm). The limit of UV transmission of pyrex sample container is 290 nm, therefore the system is sensitive between 290 and 400 nm (Fig. 1).

In the system phosphorescence between 200 and 300 nm (which is undetectable when measuring the individual components) is absorbed by toluene or *p*-terphenyl, and is limited on the emission wavelength of *p*-terphenyl and so the intensity of phosphorescence increases.

b) System:

Toluene, POPOP (absorption band: 270—400 nm, emission band: 390—530 nm), Chance OX7 optical filter, EMI 9514 S photomultiplier. The system is sensitive between 290 and 400 nm (Fig. 1).

Phosphorescence between 290 and 400 nm is absorbed by the scintillator and therefore its intensity decreases the emission band of the scintillator not being detectable.

2. The problem of chemiluminescence

The intensity of phosphorescence can be reduced to a suitable level by means of a coincidence circuit. The intensity of chemiluminescence is much greater than that of phosphorescence, therefore its intensity is very high after the coincidence circuit, too, but the mechanism — discussed above — the absorption and remission of light has a great importance in this case, too.

There are two types of the chemiluminescence reactions: The wavelength of chemiluminescence might be either in the insensitive or in the sensitive range of the system (photocathode + sample container), being either less than 290 nm or between 290 and 600 nm. These two types of chemiluminescence [4] can be illustrated by the following examples using a dual-photomultiplier scintillation counter.

c) System:

Dioxane; Hyamine hydroxide (HyOH); EMI 9635 QA photomultiplier tube (160—600 nm); pyrex sample container. The sensitivity range is between 290 and 600 nm.

d) System:

System *c);* PPO (absorption band: 280—330 nm; emission band; 340—430 nm); POPOP; naphthalene (absorption band: 180—330 nm). The sensitivity range is between 290 and 600 nm.

In system *c)* chemiluminescence between dioxane and HyOH is unmeasurable;* in system *d)* PPO + POPOP + naphthalene can absorb the chemiluminescence and remit it in the sensitive range of the system with the mechanism discussed with system *a)* in connection with "the introduction of phosphorescence".

e) System:

Dioxane; blood + dimethyl sulfoxide + H_2O_2 + HyOH; EMI 9635 QA photomultiplier; pyrex sample container.

f) System:

System *e);* PPO; POPOP; naphthalene.

The sensitivity range of the systems *e)* and *f)* lies between 290 and 600 nm.

g) System:

System *f);* Chance OX7 optical filter. The sensitivity range is between 290 and 400 nm.

In system *e)* chemiluminescence is measurable without any scintillator. The result is the same with system *f).* But in system *g)* chemiluminescence between 290 and 400 nm is absorbed by the scintillator, shifter and naphtha-

* In another way it has been concluded that the source of chemiluminescence is the reaction between dioxane and HyOH. The scintillator, shifter and naphthalene do not play any role.

lene, and therefore the intensity of chemiluminescence decreases strongly, the emission band of POPOP is undetectable. The mechanism is the same as with system *b)*.

3. The problem of light output

In agreement with the considerations described above, it is possible to identify the relations between the behaviour of scintillation system and the absorption and emission spectra of components. These are the following [5]:

a) In the case of good solvent + scintillator pairs, the absorption bands of the scintillators are overlapped by those of the solvents; *e.g.* PBD, 2-(4-methoxyphenyl)-5-phenyloxazole, PPO, *p*-terphenyl, 2-(4-fluorophenyl)-5-phenyloxazole in toluene (Fig. 1).

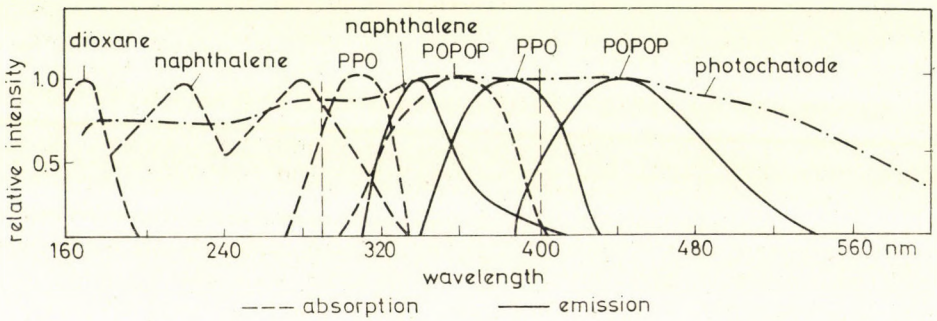

Fig. 2

On the other hand, bad solvent + scintillator pairs are those in which the absorption band of the scintillator lies far from that of the solvent; *e.g.* 2-(4-iodophenyl)-5-phenyloxazole in toluene or *p*-terphenyl in 1,4-dioxane (Fig. 2).

b) The absorption bands of good shifters overlap the emission bands of the scintillators; *e.g.* PPO + POPOP, PPO + α-NPO, *p*-terphenyl + POPOP (Fig. 1).

c) The absorption bands of diluters (decreasing the light output of the systems only slightly) are usually at wavelengths shorter than that of the absorption band of the solvent; *e.g.* ethanol and methanol, with absorption bands between 70 and 200 and up to 200 nm, respectively.

d) The absorption bands of quenchers (decreasing considerably the light output of the system) are either in the range of the absorption bands of solvents or in that of scintillators; *e.g.* chlorobenzene, cyclohexanone, thiophene, triethylamine, water with absorption bands between 235 and 270, up to 300, up to 250, up to 250 and up to 180 nm, respectively.

e) The wide absorption band of the additive material (increasing the light output) overlaps the absorption band of solvent and scintillator and that of water, too; *e.g.* naphthalene (Fig. 3).

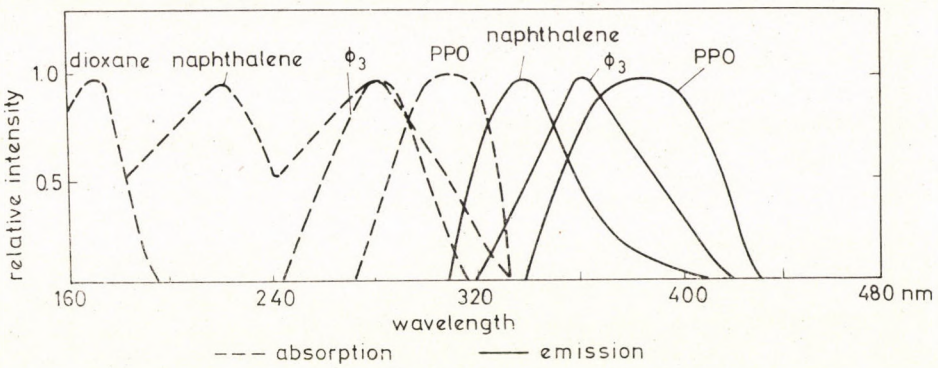

Fig. 3

Conclusion

From the experimental results it is obvious that the behaviour of liquid scintillation systems is determined by the spectral properties of their components. This must be taken into account for all models of scintillation mechanism. In our opinion, the considerable influence of the spectral properties of the components on the behaviour of the scintillation system points to the significant role of energy transfer via radiation in this mechanism.

REFERENCES

1. Fodor-Csányi, P., Lévay, B.: Acta Chim. Acad. Sci. Hung., **47**, 343 (1966)
2. Fodor-Csányi, P., Lévay, B.: Int. J. Appl. Rad. Isotopes **20**, 223 (1969)
3. Lloyd, R. A., Ellis, S. C., Hallowes, K. H.: Symposium on the Detection and Use of Tritium in Physical and Biological Sciences, Vienna, 3—10 May, 1961
4. Nicoll, D. R., Ewer, M. J. C., Fodor-Csányi, P.: Int. J. Appl. Rad. Isotopes, in press
5. Fodor-Csányi, P., Inzelt, Gy.: Int. J. Appl. Rad. Isotopes, **22**, 159 (1971)

Piroska Fodor-Csányi; Budapest VIII., Puskin u. 11—13.

Acta Chimica Academiae Scientiarum Hungaricae, Tomus 74 (2), pp. 185–191 (1972)

EFFECT OF MERCURY IMPURITIES ON THE HYDROGEN OVERVOLTAGE ON GALLIUM ELECTRODES

K. SZABÓ, L. MIHÁLYI and J. MIKA

(Department of Physical Chemistry and Radiology, L. Eötvös University, Budapest)

Received March 13, 1972

The effect of ppm impurities of Hg on the hydrogen overvoltage on solid and liquid gallium electrodes has been investigated. On both solid and liquid gallium, the overvoltage was found to increase with increasing mercury content.

At identical impurity levels, the increase of η is greater on the solid than on the liquid electrode. The overvoltage on contaminated solid electrodes is, in all cases studied, higher than on the liquid electrodes ($\eta_s > \eta_l$).

On the solid electrodes the capacity decreases with increasing Hg contamination, *i.e.* with increasing η. The C *vs.* φ curves are shifted in the positive direction upon increasing the impurity level of liquid electrodes.

The experimental results can be interpreted in terms of the adsorption of Hg on the gallium surface. The mechanism of action of the Hg impurity seems to be different on solid and on liquid electrodes.

In a previous paper [1] we have reported that the overvoltage of hydrogen on a high-purity (99.9999%) liquid or solid gallium electrode increases in the presence of a small amount of copper impurity.

Since the surface tension of copper [2] ($\sigma \approx 1066$ dyn $\cdot$ cm^{-1}) is greater than that of gallium [3] ($\sigma \approx 648$ dyn $\cdot$ cm^{-1}), the adsorption of copper on the gallium surface is unlikely. Evidence against adsorption is also provided by the increase of η in the presence of copper impurities: the overvoltage of hydrogen is lower on copper than on gallium, therefore, one would expect the decrease of η as a result of adsorption.

Our experimental results [1] can thus be interpreted by assuming that copper causes migration to the surface of those impurities which are originally present in gallium and have a tendency to adsorption. Such phenomenon has been observed in the Hg–Cd–K system, too, where the addition of Cd increases the surface concentration of K of the amalgam [4].

It is also conceivable that the Cu impurity brings about a change in the structure of metallic gallium which, in turn, results in an increased capacity of the electrode/electrolyte interface.

It was found expedient to study the effect of impurities that are adsorbed on the surface of the gallium electrode, *e.g.* mercury. The surface tension of mercury (465 dyn $\cdot$ cm^{-1}) [2] is lower than that of gallium.

The effect of mercury impurities on the overvoltage of hydrogen on gallium has been studied [5, 6]. BUTLER [5] investigated this effect on a dropping

gallium electrode and observed the increase of η with increasing amount of mercury.

In a recent study FRUMKIN *et al.* [6] compared the effect of Hg on η observed on a gallium electrode with electrocapillary measurements. From the latter results they calculated the surface concentration of Hg(Γ) for the gallium electrode and thus correlated the variation of η with Γ. At low Hg concentrations [6] η was found to increase linearly with Γ; at higher amounts of the impurity the increase is steeper than linear.

The η *vs.* Γ curve tends to the overvoltage measured on pure mercury as a limiting value. To interpret the effect of Hg impurities, the authors assume that the given current density is due to the sum of hydrogen evolution on the free gallium surface (i_1) and on the surface of adsorbed mercury (i_2).

The above authors [5, 6] studied the effect of Hg impurities only in liquid gallium. It was of interest to investigate the influence of mercury on the overvoltage of hydrogen on solid gallium electrodes. We have, therefore, studied this effect on solid and liquid gallium electrodes, completing the kinetic measurements with capacity determinations.

Experimental

The measurements have been performed by means of the apparatus and procedure described earlier [7, 8]. The hydrogen overvoltage and the differential capacity of the electrode/electrolyte boundary layer have been measured in 1 *M* HCl, on solid and liquid electrodes prepared from gallium samples with 7×10^{-4}—2.5×10^{-2} atom % mercury. The experiments with the solid electrodes were carried out at 28 °C, those with the liquid electrodes at 32 °C. The samples were prepared by adding a $Hg(NO_3)_2$ solution to high-purity liquid gallium in dilute nitric acid. Metallic mercury has deposited on the gallium surface. After about 60—80 sec, the $Hg(NO_3)_2$ solution was decanted from the gallium, which was then washed several times to remove traces of $Hg(NO_3)_2$. The gallium contaminated with mercury in the above manner was kept for a prolonged time at 60—80 °C to promote uniform distribution of the mercury. The remaining samples were prepared by dilution with gallium from the one containing the largest amount of mercury. The Hg content of the individual samples was determined analytically.* $Hg(NO_3)_2$ was prepared by dissolving doubly distilled mercury in reagent grade nitric acid. The basis metal used in the experiments contains the following impurities (in ppm): Cu 0.5, Al 0.2, Si 0.2, Mg 0.1. The mercury contents of the individual samples are listed in Table I.

The η *vs.* lg i curves for the solid gallium electrodes contaminated to various extents are shown in Fig. 1a, those for the liquid electrodes with the same impurity concentrations in Fig. 1b. As can be seen from the Figures, η increases with increasing mercury concentration on both the solid and the liquid electrodes. The change of η is much greater on the solid than on the liquid electrode at the same concentration of mercury. In Fig. 2 is shown the variation of the overvoltage with the Hg concentration at constant current density i. The difference between the two kinds of electrode is even more apparent from Fig. 2.

On solid gallium, a small amount of Hg brings about a sharp increase of η, the rate of increase being smaller at higher Hg concentrations. As shown by Figs 1 and 2, for the contaminated samples studied in the present work the hydrogen overvoltage on the solid electrode

* The mercury analyses have been performed in the Research Institute for Non-ferrous Metals, by polarography after enrichment with dithizone.

Table I

No. of sample	(Hg) atom %	Solid			Liquid		
		b_1/mV	$-\lg i$ point of break	b_2/mV	b_1/mV	$-\lg i$ point of break	b_2/mV
1	0	83.7	3.60	42	110	—	—
2	7×10^{-4}	129	2.76	109.5	118.7	2.66	86.3
3	2.4×10^{-3}	132.5	2.69	105.7	119.3	2.56	92.7
4	1.04×10^{-2}	126	2.50	112.5	118.5	2.64	92.2
5	2.54×10^{-2}	142	2.57	119.5	136.1	2.50	101

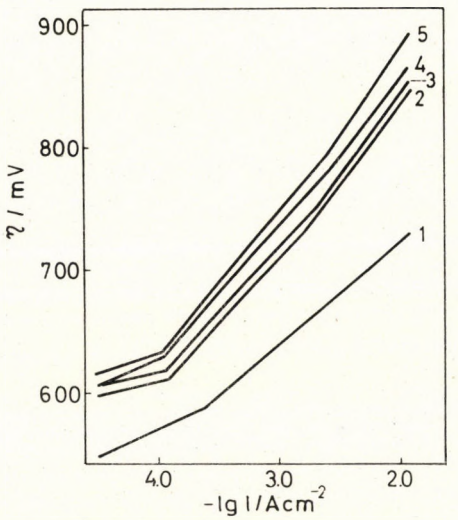

Fig. 1a. η *vs.* lg i curves for solid gallium electrodes containing various amounts of Hg impurity, in 1 *M* HCl; 1–0, 2–7×10^{-4}, 3–2.4×10^{-3}, 4–1×10^{-2}, 5–2.5×10^{-2} atom % Hg

(η_s) is greater than that on the liquid electrode (η_l), contrary to the case of pure gallium electrodes where $\eta_s < \eta_l$.

For a sample containing 2.5×10^{-2} atom % of Hg, the value of η at $i = 10^{-3}$ A · cm^{-2} exceeds that for the pure gallium electrode by ~150 mV (solid) and ~25 mV (liquid).

The shape and slope of the η *vs.* lg i curves are different for the pure and the contaminated gallium electrodes (Fig. 1a).

Two sections can be distinguished on the polarization curve for pure gallium: an upper, steep section with $b \approx 84$ mV and a lower, less steep region with $b \approx 42$ mV. The two sections intersect at $i \approx 2.5\times10^{-4}$ A · cm^{-2}. The polarization curves on the solid, contaminated gallium electrode reveal 3 sections, the 2 steeper ones intersecting at $i \approx 2.5\times10^{-3}$ A · cm^{-2}. The value of b on the contaminated samples is higher than in the case of pure gallium.

The variation of the slope and other parameters of the polarization curve with the extent of contamination with Hg is shown in Table I. The first section ($i < 10^{-4}$ A · cm^{-2}) of the η *vs.* lg i curves for the contaminated sample probably corresponds to the spontaneous dissolution of gallium.

The slope of the η *vs.* lg i curves for the liquid electrodes contaminated with mercury is greater than that measured on pure gallium electrodes (*cf.* Table I).

In this case too a break can be observed on the polarization curves of contaminated electrodes at $i \approx 2.5 \times 10^{-3}$ A · cm^{-2}. No such break is found on the polarization curves of pure, liquid gallium electrodes.

The differential capacity of the electrode/electrolyte boundary layer has been measured by the a.c. bridge method [8] with simultaneous recording of the polarization curves.

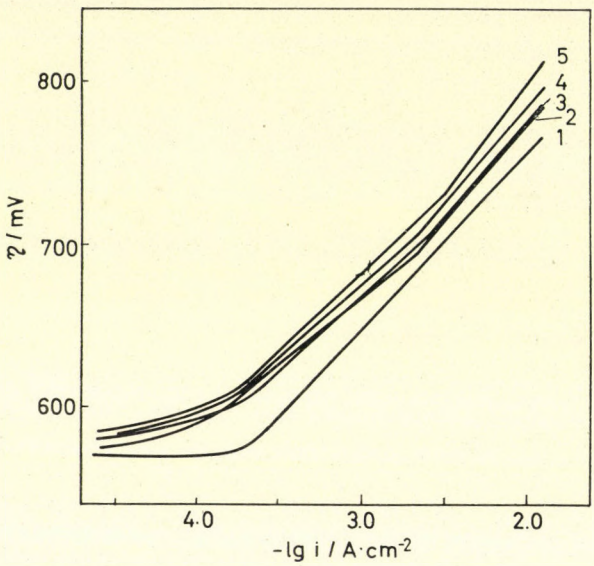

Fig. 1b. η *vs.* lg i curves for liquid gallium electrodes containing various amounts of Hg impurity, in 1 M HCl: 1–0, 2–7×10^{-4}, 3–2.4×10^{-3}, 4–1×10^{-2}, 5–2.5×10^{-2} atom % Hg

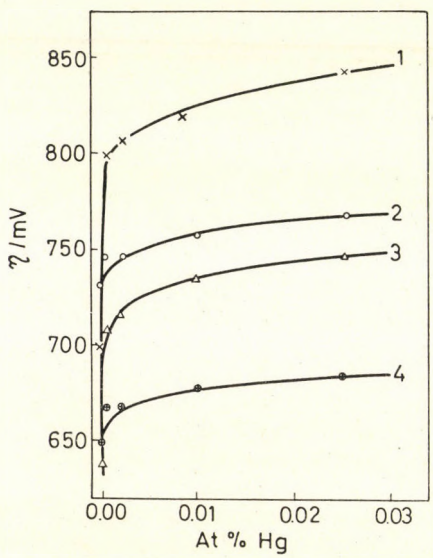

Fig. 2. η *vs.* atom % Hg curves for solid (1, 3) and liquid (2, 4) gallium electrodes (1, 2 – i = $= 5.6 \times 10^{-3}$ A · cm^{-2}; 3, 4 – $i = 10^{-3}$ A · cm^{-2})

The C *vs.* φ curves for the liquid and solid gallium electrodes are shown in Fig. 3. The capacity measured for the solid gallium electrode strongly decreases relative to the pure metal value already at the lowest Hg concentration.

Upon further increase of the Hg concentration, the capacity drops but slightly. At $\varphi = -0.62$ V the capacity of the sample containing 2.5×10^{-2} atom % Hg is by $\sim$230 μF lower than that of a pure gallium electrode.

The C *vs.* φ curves for the liquid gallium electrode are shifted in the positive direction with increasing amount of the Hg impurity. The electrode potential at $C = 100\,\mu$F of the sample containing 2.5×10^{-2} atom % Hg is by about 60 mV more positive than in the case of pure gallium. The C *vs.* φ curves recorded on the liquid, contaminated samples reveal a slight maximum in the vicinity of 0.65—0.71 V.

We have investigated the variation of the overvoltage at constant current density upon freezing the liquid, contaminated gallium.

In Fig. 4 is shown the variation of the potential upon freezing of a liquid electrode containing 2.5×10^{-2} atom % Hg, as a function of time. As can be seen from the Figure, η changes suddenly upon the liquid $\rightarrow$ solid transformation and within a short time reaches the value measured on the solid electrode at the same extent of contamination.

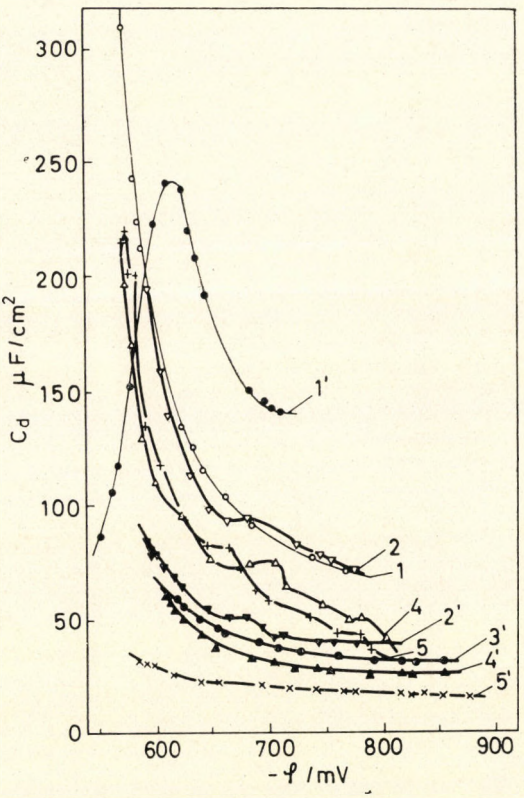

Fig. 3. C *vs.* φ* curves for liquid and solid gallium electrodes containing various amounts of Hg impurity (liquid samples: $1-0$, $2-7\times10^{-4}$, $4-1\times10^{-2}$, $5-2.5\times10^{-2}$ atom % Hg; solid samples: $1'-0$, $2'-7\times10^{-4}$, $3'-2.4\times10^{-3}$, $4'-1\times10^{-2}$, $5'-2.5\times10^{-2}$ atom % Hg)

* The φ values are against the normal hydrogen electrode.

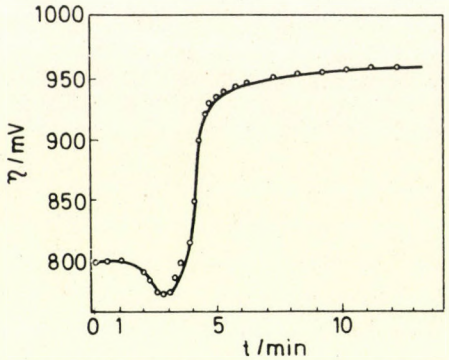

Fig. 4. Variation of η with time for the gallium electrode containing 2.5×10^{-2} atom % Hg at $t = 28$ °C and $i = 2.5 \times 10^{-2}$ A · cm^{-2}

Interpretation of the results

The experimental data show that the overvoltage of hydrogen increases with increasing concentration of the Hg impurity on both the solid and liquid electrodes. The experimental fact that at a given Hg concentration the change of the overvoltage is much greater on the solid than on the liquid electrode indicates that the impurity exerts its influence in different ways in the two states.

In the interval of impurity concentrations studied by us the overvoltage on the solid electrode is greater than that on the liquid electrode ($\eta_s > \eta_l$), in contrast to pure gallium where $\eta_s < \eta_l$.

The effect of Hg impurities on liquid gallium electrodes can be interpreted in the manner described by FRUMKIN [6]. According to this, the overall rate of the process is determined by the evolution of hydrogen on the free gallium surface and on the surface covered with mercury. Thus at constant current density (i) the variation of the overvoltage with the Hg concentration can be given by the following expression:

$$\Delta\eta \simeq \frac{RT}{F} \ln (1 - \Theta) \tag{1}$$

where Θ is the coverage of the electrode surface by mercury.

Accordingly, the overvoltage increases with the increasing amount of Hg impurity adsorbed on the electrode surface, Θ, in turn, is proportional to the concentration of the Hg impurity, in agreement with the behaviour observed for liquid gallium electrodes.

The positive shift of the capacity curves for contaminated samples can be interpreted in a similar manner.

The capacity of the gallium electrode contaminated with Hg can be regarded as two capacitances connected in parallel, viz. the capacity of the

pure gallium surface (C'_{Ga}) and that of the surface fraction covered with mercury (C'_{Hg}):

$$C = C'_{Ga} + C'_{Hg} \tag{2}$$

where

$$C'_{Ga} = C_{Ga}(1 - \Theta)$$

and

$$C'_{Hg} = C_{Hg}\Theta$$

Upon rearrangement, Eq. (3) gives

$$C = C_{Ga} - (C_{Ga} - C_{Hg})\Theta \tag{3}$$

where C_{Ga} and C_{Hg} denote the capacity measured on pure gallium and mercury, respectively.

Eq. (3) shows that the capacity decreases with increasing coverage by mercury, which is in line with the experimental results provided that Θ is proportional to the Hg concentration. The data of the C *vs.* φ curves in combination with Eq. (3) give $\Theta \approx 0.35$ at $\varphi = -0.62$ V for the liquid gallium electrode containing 2.5×10^{-2} atom% Hg (in the calculation $C_{Hg} = 20$ $\mu F \cdot cm^{-2}$ was used).

Substitution of the Θ value thus obtained into Eq. (1) yields $\Delta\eta \approx 20$—25 mV for the sample of given contamination (the experimental value is $\Delta\eta \approx$ ≈ 30—35 mV). The deviation between the measured and calculated values is due to experimental errors and the approximate nature of expression (1) [6]. The approximate agreement of the measured and calculated $\Delta\eta$ values lends support to the assumed mechanism of action of the Hg impurity. Our results on liquid gallium are in good agreement with the data of FRUMKIN *et al.* [6]. On solid gallium low concentrations of Hg already cause a great increase in η, with a simultaneous, strong decrease of the capacity (Figs 1, 1a, 2 and 3). In the case of the solid electrode variation of the experimental η values cannot be interpreted in the same way as with the liquid electrode. We assume that in this case the adsorption of the Hg impurity on the electrode surface reduces the bond energy of the adsorbed H atoms (W), which results in an increase of the overvoltage. In agreement with this, the electrode capacity decreases with increasing η, which can be attributed to the decreased concentration of adsorbed H atoms on the surface.

With the solid gallium electrode, the effect of Hg impurity is similar to that of surface oxides [7], inasmuch as these also increase the value of η and reduce the capacity.

The rapid increase of the overvoltage upon freezing of liquid gallium (Fig. 4) also indicates that the Hg impurity acts by different mechanisms on solid and liquid electrodes.

Further work is needed to elucidate the effect of Hg impurities on the electrochemical properties of gallium.

REFERENCES

1. SZABÓ, K., MIKA, J., MIHÁLYI, L.: Magy. Kém. Foly. **76,** 563 (1970)
2. DEMCHENKO, V. V.: Zhurn. Fiz. Khim., **36,** 2524 (1962)
3. POLYANOVSKAYA, N. S., FRUMKIN, A. N.: Elektrokhimia **3,** 1129 (1967)
4. LAZAREV, V. B.: Elektrokhimia **3,** 300 (1967)
5. BUTLER, I. N., MEEHAN, M. L.: Trans. Faraday Soc. **62,** 3524 (1966)
6. FRUMKIN, A., POLYANOVSKAYA, N., BAGOTSKAYA, I., GRIGOREV, N.: J. Electroanal. Chem. **33,** 319 (1971)
7. SZABÓ, K.: Magy. Kém. Foly. **73,** 174 (1967)
8. SZABÓ, K., EGRESSY, Cs.: Magy. Kém. Foly. **74,** 200 (1968)

Kálmán SZABÓ
László MIHÁLYI
József MIKA

Budapest VIII., Puskin u. 11—13.

Acta Chimica Academiae Scientiarum Hungaricae, Tomus 74 (2), pp. 193—197 (1972)

STUDY OF THE A. C. CORROSION OF NICKEL BY LINEAR POLARIZATION

J. Dévay, B. Lengyel, Jr., Sayed Sabet Abd El Rehim* and J. Bakos

(Department of Physical Chemistry, University of Chemical Engineering, Veszprém and Research Group of Electrochemistry, Hungarian Academy of Sciences, Veszprém)

Received March 2, 1972

The corrosion of nickel under a.c. conditions was investigated in 5% NaCl solution by the linear polarization method. This technique consists of the superposition of a.c. on the cell controlled by a potentiostat in respect to the d.c. The effect of a.c. on the polarization resistance, *i.e.* the corrosion current density was measured. The corrosion of nickel, *i.e.* the magnitude of the corrosion current density, was increased by a.c. to an extent depending on the current density and frequency of the latter.

It is well known that, due to the asymmetric polarizability of the electrodes [1], the polarization of the latter, *i.e.* the rate of the electrode reaction is affected by a.c. to an extent depending on its frequency and current density. Consequently, the a.c. modifies the corrosion of a homogeneous metal surface [2—5] and produces points having different potentials because of an uneven current distribution, *i.e.* local elements [2, 6, 7] are produced. The corrosion by stray direct currents [8, 9, 10] is affected too and the d.c. intensity due to the local elements is altered [2, 11, 12]. These a.c. effects are superimposed on each other.

The method of linear polarization has been widely employed for the determination of the rate of corrosion [13].

The theory of mixed potentials defines the potential of a metal in contact with a solution not containing the respective metal ions as the steady state developed between anodic metal dissolution and the cathode process. The current densities of the anode and cathode processes are equal at this potential; the corresponding current is referred to as corrosion current density (i_{corr}). The corrosion current density can be evaluated from the slope of the approximately linear section of the polarization curve in the neighbourhood (a few mV's) of the corrosion potential according to the following formula:

$$i_{corr} = \left(\frac{di}{dE}\right)_{i=0} \cdot \frac{b_1 \cdot b_2}{(b_1 + b_2) \cdot 2.3} \qquad (1)$$

* On leave from Ain-Shamps University, Cairo, Egypt.

where $\left(\frac{dE}{di}\right)_{i=0} = R_P$ is the polarization resistance, E is the electrode potential, i is the current density and b_1 and b_2 are the Tafel slopes of the corresponding anode and cathode processes, respectively, *i.e.*:

$$b = \frac{d\eta}{d \lg i} \tag{2}$$

where η is the overvoltage.

If the cathode process is assumed to be the reduction of hydrogen ions, $b_1 = 0.12$ V, while $b_2 = 0.06$ V in the case of the anodic oxidation of a divalent metal. Thus Eq. (1) can be rewritten in a simpler form

$$i_{corr} = 0.017 \cdot \left(\frac{di}{dE}\right)_{i=0} \tag{3}$$

where the current density is given in A/cm^2 and the electrode potential in V.

The following technique was employed in the study of the effect of a.c. Alternating current was superimposed on the cell controlled by a potentiostat with respect to the d.c. and the effect of a.c. on the corrosion current density was measured by the method of linear polarization. Thus the change in the corrosion current density of the system can be followed in a relatively rapid and simple manner.

The measuring equipment is shown in Fig. 1. Nickel electrode M_1 having a surface area of 1 cm^2, normal calomel electrode K_1 and platinum electrodes E_1 and E_2 were immersed in the glass cell containing the electrolyte. The electrodes were connected to potentiostat P, type IP-410-B of Bulgarian make. A filter circuit composed of R_2 (1 MOhm) and condenser C (10 μF) was inserted between calomel K_1 and the potentiostat while self-inductance H_1 (21 H) and variable resistance R_1 were inserted in the circuit of electrodes E_1 and E_2. The reference voltage of the potentiostat was controlled by a type EMG 1117/1 sawtooth generator (MG_2) and thus the working electrode was polarized at a uniform rate from cathodic to anodic potentials. Potentiometer R_P served to adjust a constant d.c. voltage. The latter was the starting potential of the polarization to which the voltage of MG_2 varying linearly in time was impressed at a constant rate of 30 mV/min. The d.c. current flowing through the cell generated a voltage drop on standard resistance R_m (5 KOhm) connected to the symmetrical input of the Y axis of a type EFKI X—Y recorder. The reference voltage of the potentiostat controlled by MG_2 was connected to the X-axis of the X—Y recorder. Vacuum tube voltmeter V_1 of a high input impedance served for the measurement of the potential difference between working electrode M_1 and reference electrode K_1.

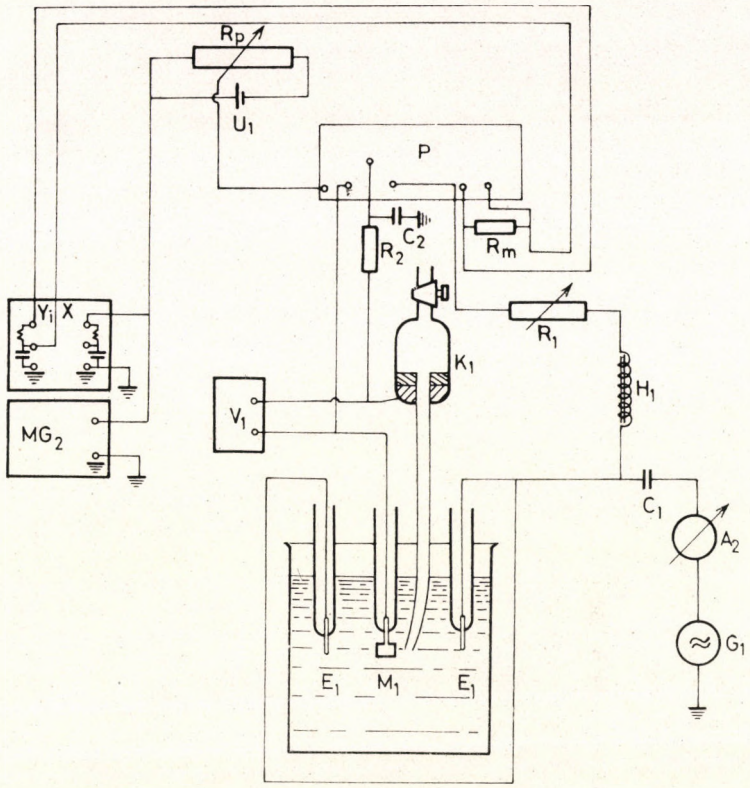

Fig. 1. Measuring equipment for the determination of polarization resistance

The a.c. was supplied by a type HGH HZ—GZ a.c. generator (G_1) connected to platinum electrodes E_1, E_2 and nickel electrode M_1 through ammeter A_1 and condenser C_1 (10 μF).

Condenser C_1 and self-inductance H_1 served to separate the d.c. and a.c. circuits. The time constant of the control system was increased by resistance R_1 in series with self-inductance H_1 to prevent oscillation. The filter circuit R_2, C_2 prevented the flow of a.c. to the potentiostat.

The experiments were performed in 5% NaCl solution. The solution was deaerated by introduction of nitrogen gas. The nickel electrodes contained 0.1 to 0.9% manganese, 0.1 to 0.9% magnesium, 0.1 to 0.9% silicon, 0.01 to 0.09% aluminium, 0.01 to 0.09% cobalt, 0.001 to 0.009% copper, 0.005 to 0.05% iron, and 0.001 to 0.05% antimony. Prior to the measurement the nickel electrodes were cleaned with emery paper, degreased by a suitable solvent and etched in 20% hydrochloric acid at room temperature until a constant weight was attained.

Figs 2 and 3 represent the effect of a.c. of various intensity on the corrosion current density at 100 and 500 Hz frequency, respectively. The corrosion current density increases with increasing a.c. density. Inspection of Figs 2 and 3 reveals a decrease in the corrosion current density with increasing a.c. frequencies at identical current densities.

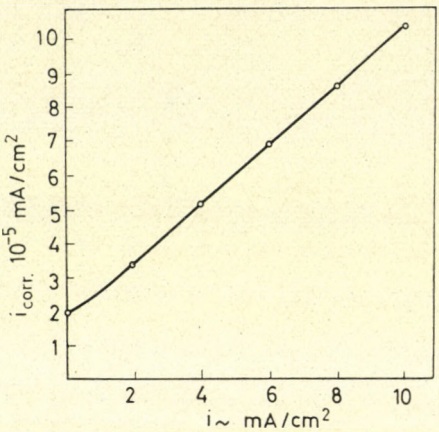

Fig. 2. Effect of a.c. density on the corrosion current density ($f = 100$ Hz)

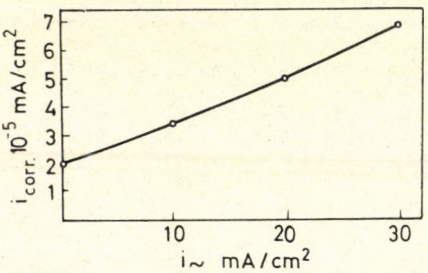

Fig. 3. Effect of a.c. density on the corrosion current density ($f = 500$ Hz)

Fig. 4 shows the effect on the current density of the a.c. frequency at a current density of the latter equal to 10 mA/cm^2. It is apparent that the intensity of the corrosion current, *i.e.* the corrosion of nickel electrodes decreases with increasing frequency.

This phenomenon can be explained in terms of changing polarization and potential of the electrodes, which exhibit a non-linear polarization curve, under a.c. conditions. The effect is due to the distortion of the periodic, sinusoidal potential variations generated by the a.c. in the case of a non-linear polarization curve, which shifts the time average of the electrode potential [1, 6, 7].

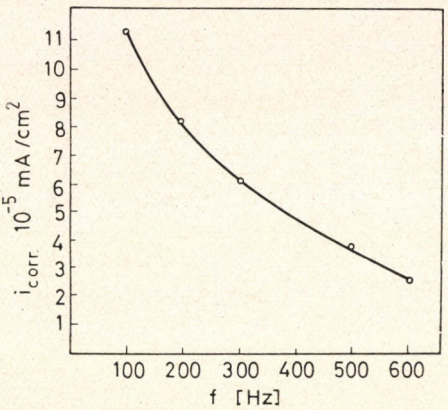

Fig. 4. Effect of the a.c. frequency on the corrosion current density ($i_{\sim} = 10$ mA)

Thus the corrosion of nickel is increased by a.c. to an extent depending on the frequency and current density of the latter. The influence of a.c. on corrosion can be investigated by the method of linear polarization, though the accuracy of this technique is not always satisfactory. The method is rapid and gives a good basis for the measurement of the corrosion current density under a.c. conditions, especially in the case of comparative studies.

REFERENCES

1. Dévay, J.: Veszprémi Vegyipari Egyetem Közleményei, **10,** 129 (1966)
2. Erdey-Grúz, T., Dévay, J., Szegedi, R., Gáldi, A.: Acta Chim. Acad. Sci. Hung., **38,** 325 (1963)
3. Erdey-Grúz, T., Dévay, J., Vajasdy, I.: Acta Chim. Acad. Sci. Hung., **40,** 289 (1964)
4. Dévay, J., Sayed Sabet Abd El Rehim, Takács, V.: Acta Chim. Acad. Sci. Hung., **52,** 201 (1967)
5. Dévay, J., Sayed Sabet Abd El Rehim, Takács, V.: Acta Chim. Acad. Sci. Hung., **52,** 63 (1967)
6. Dévay, J., Szegedi, R., Lábody, I.: Acta Chim. Acad. Sci. Hung., **42,** 191 (1965)
7. Erdey-Grúz, T., Dévay, J., Szegedi, R.: Acta Chim. Acad. Sci. Hung., **35,** 29 (1963)
8. Dévay, J.: Acta Chim. Acad. Sci. Hung., **44,** 385 (1965)
9. Dévay, J.: Acta Chim. Acad. Sci. Hung., **42,** 255 (1965)
10. Dévay, J., Lengyel, B., Jr., Kraxner, M.: Acta Chim. Acad. Sci. Hung., **58,** 129 (1968)
11. Erdey-Grúz, T., Dévay, J., Szegedi, R., Vajasdy, I.: Acta Chim. Acad. Sci. Hung., **34,** 301 (1962)
12. Dévay, J., Lengyel, B. Jr.: Acta Chim. Acad. Sci. Hung., **46,** 325 (1965)
13. Fontana, M. G., Green, N. D.: Corrosion Engineering. New York 1967

József Dévay
Béla Lengyel Jr. } Veszprém, Schönherz Z. u. 10, Hungary.
Sayed Sabet Abd El Rehim; Ain-Shamps University, Cairo, Egypt.
József Bakos; Veszprém, Schönherz Z. u. 10. Hungary.

Acta Chimica Academiae Scientiarum Hungaricae, Tomus 74 (2), pp. 199—203 (1972)

ELECTROCHEMICAL METHOD FOR THE INVESTIGATION OF THE CORROSION RESISTANCE OF PAINT COATINGS

J. DÉVAY, F. JANÁSZIK, L. MÉSZÁROS and F. HORKAY*

*(Department of Physical Chemistry, University of Chemical Engineering, Veszprém, Research Group of Electrochemistry, Hungarian Academy of Sciences, Veszprém and *BUDALAKK Paint and Synthetic Resin Factory, Budapest)*

Received March 2, 1972

An electrochemical experimental method has been elaborated for the examination of corrosion processes occurring on paint-coated steel surfaces in a highly polluted atmosphere.

The method is based on measuring the polarization resistance of the electrode immersed in corrosive media. The results of the experiments are in good agreement with practical experience.

The measurements were carried out on samples pretreated by different methods and exposed to corrosion effects of various nature, intensity and duration. After pretreatment the samples were coated with paint.

Paint systems which exhibit anticorrosive effects both simultaneously with the formation of the coating and during various corrosion influences become increasingly important in preventing the corrosion of metal surfaces. Several active components are generally contained in the first layer of such coatings, which is in immediate contact with the metal surface. One of these components is usually an acid or ester suitable for the formation of a passive layer by facile reaction with the metal surface under the effect of humidity. The other is generally a compound of low solubility — though not insoluble in water — *viz.* a pigment which gradually dissolves from the coating. This pigment ensures the continuous flow to the metal surface of such ions which react with the anodically dissolved metal ions during wear and form a passive layer preventing the corrosion of the metal surface.

The quality and concentration of the active compound in the case of a given binder depend on the nature of the metal, the potential and purity of the surface as well as on the chemical composition and structure of the corrosion protective surface layer either formed spontaneously or by a chemical or electrochemical method.

The problem is involved and a number of methods can be employed to examine the various surface layers. In the present communication we report on the study of the effect of the surface layer on the rate of metal corrosion disregarding the composition of these layers. An experimental technique was developed which is suitable for investigating the passivation by chemical

processes occurring on the metal surface during application of the coating as well as for the study of changes in the passivation during corrosion.

The method consists essentially in the electrochemical measurement of the rate of corrosion. The organic coating was dissolved from the metal surface by a suitable solvent mixture prior to the electrochemical investigation as its high electric resistance would have impeded the measurements, and the structure of the surface layer would have been strongly altered by the reactions of the active component of the coating during the electrochemical test. However, the protective layer and the corrosion products firmly adhering to the metal surface were not removed by the solvent mixture composed of chlorinated hydrocarbons of low molecular weight as well as an ester and ketone.

The technique known as "linear polarization method" in the literature was employed to determine the corrosion current density characteristic of the corrosion rate of metal plates prepared according to the above procedure. The measurement consisted in the determination of the polarization resistance of the electrode immersed in the corrosive medium. The polarization resistance is

$$R_p = \left(\frac{dE}{di}\right)_{i=0} \tag{1}$$

$\left(\frac{dE}{di}\right)_{i=0}$ is the slope of the polarization curve of the electrode at the potential where $i = 0$. This slope can be evaluated by graphical differentiation of the nearly linear polarization curve in the vicinity (within a few mV's) of the corrosion potential where $i = 0$. The corrosion current density is given by the following formula [1]:

$$i_c = \frac{0.026}{R_p} \tag{2}$$

The polarization measurements have been carried out in 0.1 n $NaNO_3$ as an electrolyte because this does not react with the surface layer and has but a weak corrosion effect. The polarization measurements were performed with a potentiostat while the polarization curves were automatically recorded on an X—Y recorder.

Experiments on model metals and paints proved the reliability of the method.

In the following the results of a series of experiments pertaining to a given problem will be discussed in detail.

We modelled the conditions encountered in the application of paint to steel surfaces exhibited to an atmosphere severely polluted by industrial gases. The variation of the rate of corrosion was measured on steel surfaces

Table I

Pre-treatment	Treatment before coating	Metal without coating	Corrosion current density, $\mu A/cm^2$					
			Plates after removal of coating		Plates exposed to salt mist chamber		Plates exposed to sulphur dioxide chamber	
			after 300 hrs					
			Promet	Pellikor	Promet	Pellikor	Promet	Pellikor
	I	35.0	4.0	0.9	83	0.9	5.9	0.9
	II	22.0	4.7	2.0	46	3.2	6.1	0.4
	III	16.0	4.3	1.6	34	8.3	1.4	0.6
A	IV	26.0	2.6	1.3	31	4.3	18.0	0.3
	V	6.4	4.0	1.2	45	3.5	13.0	0.3
	VI	14.0	4.3	1.6	23	3.2	4.4	0.3
	VII	17.0	7.3	1.7	33	2.7	2.1	1.0
	I	5.1	2.7	2.0	1010	0.4	2.4	0.4
	II	5.3	5.2	3.2	1230	0.4	2.5	0.7
	III	7.9	5.3	2.3	1450	0.4	2.6	1.5
B	IV	2.5	3.3	1.3	1620	0.2	1.9	0.4
	V	1.2	1.9	1.0	1230	0.1	1.8	0.5
	VI	7.3	2.4	2.4	1010	0.4	2.7	0.3
	VII	17.0	6.9	2.6	1140	0.9	2.9	0.5
	I	59.0	3.9	7.6	6.5	0.8	3.2	6.6
	II	18.0	4.1	14.0	19.0	0.4	8.4	10.0
C	III	38.0	6.4	25.0	13.0	2.2	14.4	15.0
	IV	7.8	4.8	16.0	4.8	0.8	5.1	3.0
	V	6.7	3.0	22.0	5.6	0.5	4.8	0.8
	VI	9.8	5.6	23.0	7.5	1.7	4.6	6.3
	VII	20.0	8.8	22.0	6.5	1.9	5.4	7.7
	I	25.0	10.0	14.0	7.9	5.6	4.2	0.4
	II	50.0	32.0	36.0	27.0	9.6	3.5	3.5
D	III	53.0	60.0	80.0	18.0	12.2	2.1	5.8
	IV	44.0	4.7	1.8	9.8	1.7	1.9	1.0
	V	11.0	3.5	8.4	12.4	0.3	4.7	0.8
	VI	37.0	31.0	17.8	14.9	1.9	5.3	1.9
	VII	42.0	29.0	10.3	24.0	1.9	3.9	5.4

A — sand blasted surface,
B — hand polished surface,
C — surface treated with Ferrofixol,
D — surface treated with Mavebit,
I — without exposure,
II — exposure to mixed industrial atmosphere for 168 hrs,
III — exposure to mixed industrial atmosphere for 236 hrs,
IV — exposure to ammonia for 72 hrs,
V — exposure to ammonia for 168 hrs,
VI — exposure to saturated water vapour for 24 hrs,
VII — exposure to saturated water vapour for 72 hrs.

which were cleaned by a mechanical method or pretreated by a chemical procedure, and the metal was exposed to various corrosion effects for different periods of time between the cleaning procedure and the paint application. We intended to determine whether or not the quality and extent of contamination reached a critical value by which the formation of a passive layer was overcompensated by anodic metal dissolution. The iron oxide layer was removed from the metal surface used in the experiments either by *(A)* sand blasting, or *(B)* manual polishing, or else the iron oxide was chemically converted to an iron oxide–iron phosphate layer by treatment with *(C)* Ferrofixol (an aqueous solution containing condensed amines and other organic compounds). After pretreatment the plates were exposed to an atmosphere containing either 3% ammonia or a mixture of corrosive gases, both saturated with water at 40 °C, for various lengths of time. Both adsorption and chemisorption could occur at the temperature of the gas chamber. After this treatment the plates were coated either with Promet (a paint of vinyl resin base containing a reactive component) or Pellikor (a synthetic alkyde resin paint containing a chromate pigment having an inhibitor effect). The coated surfaces were exposed to a mist containing 0.05 mol/l NaCl solution and to a water vapor atmosphere containing 0.05 mol/l SO_2 gas. The changes on the metal–paint boundary layer were examined by the above procedure after 300 hrs.

The results are summarized in Table I. The corrosion current density values measured on iron plates which were not painted and not exposed to corrosion effects are also listed in order to facilitate comparison of the data. It is apparent from the results that the metal surface was passivated simultaneously with the application of the coating in the case of the primers used in this investigation. The corrosion protective effects of the various pretreatments are clearly different. It is noteworthy that manual polishing considerably increases the metal surface as the latter is engraved by the hard granules of the polishing material. Thus the amount of active compounds present in the solution was not sufficient for passivating the surface of increased area. This fact accounts for the intense corrosion observed especially under the effect of highly aggressive chloride ions. The presence of contaminations affected the values of the corrosion current density to an identical extent regardless of the pretreatment. A very small corrosion current density was observed on surfaces contaminated by ammonia. The results of these experiments lead to the conclusion that the above method permits evaluation of the corrosion protection due to the chemical change occurring at the boundary layer of the metal and the paint coating without the determination of the structure and the composition of the boundary layer.

REFERENCE

1. FONTANA, M. G., GREEN, N. D.: Corrosion Engineering. New York, 1967

József DÉVAY
Ferenc JANÁSZIK
Lajos MÉSZÁROS
Ferenc HORKAY

Veszprém, Schönherz Z. u. 10, Hungary.

Acta Chimica Academiae Scientiarum Hungaricae, Tomus 74 (2), pp. 205—211 (1972)

THIRD HARMONIC COMPONENT OF THE ELECTRODE CURRENT DUE TO A SINUSOIDAL A.C. VOLTAGE IN CASE OF DIFFUSION AND TRANSFER POLARIZATION

DÉVAY, J., MÉSZÁROS, L. and GARAI, T.

(Department of Physical Chemistry, University of Chemical Engineering, Veszprém and Research Group of Electrochemistry, Hungarian Academy of Sciences, Veszprém)

Received March 2, 1972

Formulas are derived relating to the third harmonic component of the a.c. passing through an electrode under the effect of a small amplitude a.c. voltage superimposed on the d.c. polarizing potential. The expressions relating to reversible polarographic reactions are derived as a limiting case.

In a previous communication [1] we presented a mathematical analysis of the harmonic components of the current flowing through an electrode polarized by a small amplitude sinusoidal a.c. voltage superimposed on the d.c. potential in the case of diffusion and transfer polarization. Expressions were derived for the dependence of the fundamental and second harmonic a.c. components on the potential, the amplitude and frequency of the a.c. voltage, the concentration of the electroactive species as well as on the kinetic parameters of the electrode reaction (heterogeneous rate constant and transfer coefficient).

Very little interest has been directed to the third or higher harmonic a.c. components under the above conditions. PAYNTER and REINMUTH [2] were the first to report on measurements of the third and fourth harmonic components of the polarographic a.c. MCCORD, BROWN and SMITH [3] derived the formula of the third harmonic a.c. as a function of the potential for reversible polarographic reactions starting from the relations of TACHI and KAMBARA [4]. The applicability of the measurement of the third harmonic a.c. component in a.c. polarographic analysis was investigated recently [5, 6].

In the present paper we extend to the third harmonic a.c. component the harmonic analysis of the current flowing through the electrode polarized by a small amplitude sinusoidal a.c. voltage superimposed on the d.c. potential. The amplitude of the third harmonic a.c. component is derived in an explicit form for the potential range of the total polarographic wave in the case of a combined diffusion and transfer process assuming linear diffusion. The formulas relating to reversible polarographic reactions are obtained from the above relations as a limiting case when the rate of the charge transfer reaction is very large as compared to the rate of diffusion.

The mathematical treatment is the same as that given in the previous communication [1], thus the detailed discussion will be omitted. The additional calculations related to the third harmonic a.c. component of the current are presented after a short summary of the derivation of the formulas.

The relation between the overpotential and the current density in the case of diffusion polarization combined with a transfer reaction is represented by the following expression [7]:

$$i_t = i_0 \left\{ \frac{C_1(0,t)}{C_{10}} e^{\frac{\alpha z F}{RT}\eta} - \frac{C_2(0,t)}{C_{20}} e^{-\frac{(1-\alpha)zF}{RT}\eta} \right\}, \tag{1}$$

where i_t is the current density corresponding to the transfer reaction, i_0 is the exchange current density, α is the transfer coefficient, $C_1(0, t)$ and $C_2(0, t)$ are the instantaneous concentrations of the reduced and oxidized species, respectively, at the electrode surface (*i.e.* at $x = 0$ and time t), while C_{10} and C_{20} are the bulk concentrations in the solution, which are independent of time and the distance from the electrode surface.

In our case the instantaneous value of the overpotential (η) imposed on the electrode by a potentiostat at a given time t is expressed by the following periodic equation

$$\eta = \eta_{=} + \eta_{\sim} \sin \omega t\,, \tag{2}$$

where $\eta_{=}$ is the d.c. component of the overpotential and $\eta_{\sim}$ is the peak value of the alternating voltage superimposed on the d.c. potential.

The ions reduced or oxidized in the electrode reaction are supplied by diffusion to the electrode surface, thus the concentrations $C_1(0, t)$ and $C_2(0, t)$ can be determined using the familiar differential equation of diffusion; as linear diffusion is assumed, this will be:

$$\frac{\partial^2 C_k(x,t)}{\partial x^2} = \frac{1}{D_k} \frac{\partial C_k(x,t)}{\partial t}\,, \quad (k = 1, 2) \tag{3}$$

where $C_1(x, t)$ and $C_2(x, t)$ are the concentrations of the reduced and oxidized forms, respectively, of the potential-determining ions as a function of time and the distance from the surface of the electrode, and D_1 and D_2 denote the corresponding diffusion coefficients.

The initial and the boundary conditions needed to solve differential equation (3) are given by

$$D_1 \left.\frac{\partial C_1}{\partial x}\right|_{x=0} = -D_2 \left.\frac{\partial C_2}{\partial x}\right|_{x=0} \tag{4}$$

an equation expressing the continuity of mass transport, and by the following equations implying that both components had been present in a homogeneous distribution before the reaction took place and their concentrations did not vary in time; furthermore, that concentration changes during the electrode process take place only in the Nernst-type diffusion layer, δ_1 and δ_2 being the thicknesses of diffusion layers corresponding to the reduced and oxidized species, respectively.

$$C_1(x,t)|_{t\leq 0} = C_{10}\,, \qquad C_2(x,t)|_{t\leq 0} = C_{20} \tag{5}$$

and

$$C_1(x,t)|_{x\geq \delta_1} = C_{10}\,, \qquad C_2(x,t)|_{x\geq \delta_2} = C_{20} \tag{6}$$

The diffusion current density expressed by the concentration of the oxidized form of the reaction component is

$$i_d = -zFD_2 \left.\frac{\partial C_2}{\partial x}\right|_{x=0} \tag{7}$$

The boundary condition representing the relation between concentrations and overpotential is obtained by combining Eqs (7) and (1), (the latter relates to the transfer current density):

$$-zFD_2 \left.\frac{\partial C_2}{\partial x}\right|_{x=0} = i_0 \left\{ \frac{C_1(0,t)}{C_{10}} e^{\frac{\alpha zF}{RT}\eta} - \frac{C_2(0,t)}{C_{20}} e^{-\frac{(1-\alpha)zF}{RT}\eta} \right\} \tag{8}$$

(It is evident that the current density given by Eq. (1) is equal to the diffusion current [Eq. (7)] as diffusion precedes the transfer reaction and only the electroactive species which have reached the electrode surface by diffusion can take part in the charge transfer process.)

The total current $i(t)$ passing through unit area of the electrode surface is given by the sum of the transfer current and the current flowing through the capacitance of the double layer

$$i(t) = i_0 \left\{ \frac{C_1(0,t)}{C_{10}} e^{\frac{\alpha zF}{RT}\eta} - \frac{C_2(0,t)}{C_{20}} e^{-\frac{(1-\alpha)zF}{RT}\eta} \right\} + C\frac{d\eta}{dt}\,, \tag{9}$$

where C is the capacitance of the double layer per unit area of the electrode, a value approximately independent of the potential (linear element from an electric point of view) [8].

Taking into consideration Eq. (2), it is obvious that the second term at the right-hand side of Eq. (9) contains only the periodic signal of angular frequency ω. Thus the presence of higher harmonics, *i.e.* the deviation of the

current from the sinusoidal form, is caused only by the nonlinearity of the electrode process, in the present case by that of the diffusion and transfer polarizations.

The solution of differential equation (3) will be given using the above boundary and initial conditions after the steady state has been attained (*i.e.* after the decay of the transient phenomena following the switching on of the d.c. potential and a.c. voltage). Eqs (1) and (8), used as boundary conditions immediately yield the transfer current density, while the total current density will be given by Eq. (9).

The variation of the concentrations at the electrode surface will be given by a periodic function as the potential of the electrode is also a periodic function of time.

Thus the solution of differential equation (3) after the decay of transient phenomena [9] is

$$C_1(x, t) = (A_1 + \Delta A_1)x + B_1 + \Delta B_1 +$$

$$+ \sum_{n=1}^{\infty} e^{-\sqrt{\frac{n\omega}{2D_1}}x} \left\{ a_{n_1} \cos\left(n\omega t - \sqrt{\frac{n\omega}{2D_1}}x \right) + b_{n_1} \sin\left(n\omega t - \sqrt{\frac{n\omega}{2D_1}}x \right) \right\};$$

$$C_2(x, t) = (A_2 + \Delta A_2)\, x + B_2 + \Delta B_2 +$$

$$+ \sum_{n=1}^{\infty} e^{-\sqrt{\frac{n\omega}{2D_2}}x} \left\{ a_{n_2} \cos\left(n\omega t - \sqrt{\frac{n\omega}{2D_2}}x \right) + b_{n_2} \sin\left(n\omega t - \sqrt{\frac{n\omega}{2D_2}}x \right) \right\}, \qquad (10)$$

where $A_1x + B_1$ and $A_2x + B_2$ are the changes in the concentrations of the reduced and the oxidized species, respectively, as functions of the distance from the electrode surface in the case of direct potential polarization (according to Nernst's assumption of the diffusion layer), while ΔA_1, ΔB_1 and ΔA_2, ΔB_2 are the changes in the coefficients of the above expressions caused by the a.c. voltage as a consequence of the nonlinearity of the electrode process.

The determination of the unknown coefficients of Eq. (10) is performed, as in the previous study [1], by substituting Eq. (10) into the initial and boundary conditions [Eqs (4), (5), (6) and (8)] except that the expression in the right-hand side of Eq. (8) is approximated by its third order Taylor polynomial instead of the second order one and Eq. (10) representing the periodical changes in the concentrations is replaced by its third order Fourier polynomial. Thus a comparison of the coefficients gives the change in the d.c. current under the effect of an a.c. voltage corresponding to the Faradaic rectification, the amplitude of the first and second harmonic a.c. components, as in the previous communication [1], and the amplitude of the third harmonic

component of the a.c.

$$|i_3| = \sqrt{2}\,|\psi_3| \sqrt{\frac{A^2 + B^2}{(\varphi_1 + \psi_3)^2 + \psi_3^2}}, \tag{11}$$

where

$$A = \frac{\lambda_4 \eta_\sim^2}{8} a_{12} + \frac{\lambda_2 \eta_\sim}{2} b_{22};$$

$$B = \frac{\lambda_4 \eta_\sim^2}{8} b_{12} - \frac{\lambda_2 \eta_\sim}{2} a_{22} + \frac{\lambda_3 \eta_\sim^2}{24};$$

$$a_{12} = \frac{\psi_1 \Phi \eta_\sim}{(\varphi_1 + \psi_1)^2 + \psi_1^2};$$

$$b_{12} = -\frac{(\varphi_1 + \psi_1)\Phi \eta_\sim}{(\varphi_1 + \psi_1)^2 + \psi_1^2};$$

$$a_{22} = \frac{(\psi_2 + \varphi_1)(1/4\lambda_1 \eta_\sim^2 + 1/2\lambda_2 b_{12} \eta_\sim) + 1/2\psi_2 \lambda_2 a_{12} \eta_\sim}{(\varphi_1 + \psi_2)^2 + \psi_1^2};$$

$$b_{22} = \frac{-(\psi_2 + \varphi_1)\,1/2\lambda_2 a_{12} \eta_\sim + \psi_2(1/4\lambda_1 \eta_\sim^2 + 1/2\lambda_2 b_{12} \eta_\sim)}{(\varphi_1 + \psi_2)^2 + \psi_2^2};$$

$$\varphi_1 = -i_0 \left\{ \sqrt{\frac{D_2}{D_1}} \frac{e^{\frac{\alpha z F}{RT}\eta_=}}{C_{10}} + \frac{e^{-\frac{(1-\alpha)zF}{RT}\eta_=}}{C_{20}} \right\};$$

$$\Phi = i_0 \frac{zF}{RT} \left\{ \frac{\bar{C}_1(0)}{C_{10}} \alpha e^{\frac{\alpha z F}{RT}\eta_=} + \frac{\bar{C}_2(0)}{C_{10}} (1 - \alpha)\, e^{-\frac{(1-\alpha)zF}{RT}\eta_=} \right\};$$

$$\lambda_1 = i_0 \left(\frac{zF}{RT}\right)^2 \left\{ \frac{\bar{C}_1(0)}{C_{10}} \alpha^2 e^{\frac{\alpha z F}{RT}\eta_=} - \frac{\bar{C}_2(0)}{C_{20}} (1 - \alpha)^2 e^{-\frac{(1-\alpha)zF}{RT}\eta_=} \right\};$$

$$\lambda_2 = -i_0 \frac{zF}{RT} \left\{ \sqrt{\frac{D_2}{D_1}} \alpha \frac{e^{\frac{\alpha z F}{RT}\eta_=}}{C_{10}} - (1 - \alpha) \frac{e^{-\frac{(1-\alpha)zF}{RT}\eta_=}}{C_{20}} \right\};$$

$$\lambda_3 = i_0 \left(\frac{zF}{RT}\right)^3 \left\{ \frac{\bar{C}_1(0)}{C_{10}} \alpha^3 e^{\frac{\alpha z F}{RT}\eta_=} + (1 - \alpha)^3 \frac{\bar{C}_2(0)}{C_{20}} e^{-\frac{(1-\alpha)zF}{RT}\eta_=} \right\};$$

$$\lambda_4 = -i_0 \left(\frac{zF}{RT}\right)^2 \left\{ \sqrt{\frac{D_2}{D_1}} \frac{\alpha^2}{C_{10}} e^{\frac{\alpha z F}{RT}\eta_=} + \frac{(1 - \alpha)^2}{C_{20}} e^{-\frac{(1-\alpha)zF}{RT}\eta_=} \right\};$$

$$\psi_n = -zFD_2 \sqrt{\frac{n\omega}{2D_2}}, \qquad (n = 1, 2, 3);$$

further

$$\bar{C}_1(0) = C_{10}\left(1 - \frac{i^*_=}{i_{da}}\right),$$

$$\bar{C}_2(0) = C_{20}\left(1 - \frac{i^*_=}{i_{dk}}\right)$$

where i_{da} and i_{dk} are the limiting current densities of the anode and cathode processes, respectively, and $\bar{C}_1(0)$ and $\bar{C}_2(0)$ are the concentrations of the potential-determining ions in the oxidized and reduced form, respectively, on the surface of the electrode in the case of $\eta_\sim = 0$; and

$$i^*_= = \frac{i_0\left\{e^{\frac{\alpha zF}{RT}\eta_=} - e^{-\frac{(1-\alpha)zF}{RT}\eta_=}\right\}}{1 + i_0\left\{\frac{e^{\frac{\alpha zF}{RT}\eta_=}}{i_{da}} - \frac{e^{-\frac{(1-\alpha)zF}{RT}\eta_=}}{i_{dk}}\right\}}$$

is the equation of the d.c. polarization curve. It is apparent that the expression of the third harmonic a.c. component (Eq. (11)) is a complicated function of the kinetic parameters of the electrode reaction and it can be evaluated by computer techniques only. The results of the latter calculations will be reported later.

The expressions relating to reversible polarographic reactions can be derived from Eq. (11). Polarographic reactions are termed reversible if the rate of the transfer reaction is high compared to the rate of diffusion (thus the rate of the electrode reaction is controlled by diffusion). Accordingly, i_0, the exchange current density, proportional to the rate of the charge transfer reaction is large, *i.e.* $i_0 \to \infty$ in a limiting case.

A derivation similar to the one presented in the Appendix of the previous communication [1] yields

$$i_{3\,\mathrm{rev}} = \lim_{i_0 \to \infty} i_3 =$$

$$= \frac{(zF)^4}{(RT)^3}\frac{\sqrt{3\omega}}{192}\left(C_{10}\sqrt{D_1} + C_{20}\sqrt{D_2}\right)\frac{\left|3 - 2ch^2\frac{zF}{2RT}\eta_=\right|}{ch^2\frac{zF}{2RT}\eta_=} \cdot \eta^3_\sim. \qquad (12)$$

The result agrees with that derived by McCord *et al.* [3] employing a different method.

REFERENCES

1. DÉVAY, J., MÉSZÁROS, L., GARAI, T.: Acta Chim. Acad. Sci. Hung., **58,** 141 (1968)
2. PAYNTER, J., REINMUTH, W. H.: Anal. Chem., **34,** 1355 (1962)
3. MCCORD, T. G., BROWN, E. R., SMITH, D. E.: Anal. Chem., **38,** 1615 (1966)
4. TACHI, I., KAMBARA, T.: Bull. Chem., Soc. Japan, **28,** 35 (1955)
5. NEEB, R.: Z. Anal. Chem., **180,** 401 (1962)
6. DÉVAY J., GARAI T., MÉSZÁROS L., PALÁGYI-FÉNYES, F.: Magy. Kém. Foly., **75,** 460 (1969)
7. KORTÜM, G.: Treatise on Electrochemistry, p. 478. Elsevier, Amsterdam 1965
8. Cf. Ref. [7], p. 63.
9. SOMMERFELD, A.: Partielle Differentialgleichungen der Physik, p. 63. Akad. Verlag, Leipzig 1962

József DÉVAY
Lajos MÉSZÁROS
Tibor GARAI

Veszprém, Schönherz Z. u. 10, Hungary.

Acta Chimica Academiae Scientiarum Hungaricae, Tomus 74 (2), pp. 213—224 (1972)

COMPARATIVE STUDY OF THE VARIATIONS IN THE PROPERTIES OF BINARY SOLUTIONS ON TEMPERATURE CHANGE OR ON ADDITION OF A THIRD COMPONENT, AND ITS APPLICATION TO THE VISCOSITY OF METAL CHLORIDE—HCl—H_2O SYSTEMS

E. Berecz and I. Báder

(Department of General and Physical Chemistry, Technical University of Heavy Industry, Miskolc)

Received March 6, 1972

A study was made on the relations between the property changes resulting in binary solution systems from the temperature change or from the addition of a third component. The possibilities of the general description of these phenomena were considered. It was shown how the connection between the two effects can be plotted on the ternary and binary diagrams, while the method was applied to the comparative study of systems of the type metal chloride–HCl–H_2O. The deduced relations were applied to the viscosity conditions in the $MgCl_2$–HCl–H_2O and CsCl–HCl–H_2O systems, and conclusions were drawn as to the isothermal concentration dependence of the structures of the two binary aqueous salt solutions, to the dissociation relations for the HCl added to the binary systems, and its dependence on the corresponding salt concentrations.

In our research work in connection with the investigation of the structure of solutions of strong electrolytes we have been studying some properties measured experimentally (viscosity, conductivity, vapour pressure, density, solubility) or calculated from the experimental data (molar volume, activation thermodynamic functions, etc.) in the total concentration range of AX–BX–H_2O solutions. These are used to gain a deeper insight into the structure of concentrated and moderately concentrated solutions, regarding which there are relatively insufficient reliable informations so far. The study of such ternary solutions is considered as a means of obtaining information on the structure of the constituent binary systems AX–H_2O and BX–H_2O. Thus, we have studied how a third component added to a binary solution affects the properties of the initial binary system as a function of concentration of the latter, and compared the relations between the property changes ΔZ, resulting from the variation of the temperature in the binary system, or the addition of a third component.

A qualitative discussion of the latter effect has been given in an earlier paper [1]. In the present paper an attempt is made to give a general and exact description of the effect; further, the possibility of plotting of connec-

tion of both effects is demonstrated on the ternary diagram, an its applicability is illustrated by the comparative study of metal chloride–HCl–H_2O systems.

The property change ΔZ, resulting from the temperature change Δt, in the binary system AX–H_2O (or BX–H_2O) can be compared with the property change ΔZ, following the addition of the component BX (or AX) to the binary solution AX–H_2O (or BX–H_2O) of a given initial concentration, in two ways:

a) investigating as a function of the concentration m_{AX} (or m_{BX}) those amounts BX (or AX) added to the binary aqueous solution AX–H_2O (or BX–H_2O) of a given concentration m_{AX} (or m_{BX}), which produce the same property change ΔZ as a given constant temperature change Δt applied to the binary solution AX–H_2O of the same concentration m_{AX};

b) keeping the property change ΔZ produced by either of the two methods (temperature variation or the addition of a third component) at a constant value, to study the variation of the mutual ratio of the Δt and Δm_{BX} (or Δm_{AX}) required to produce the constant ΔZ as a function of the concentration m_{AX} (or m_{BX}) of the corresponding binary aqueous solution.

For the case of the addition of BX to the binary aqueous solution of AX, method *a)* can be carried out in accordance with the following principles (the treatment below is also valid for the addition of AX to the binary BX solution, of course, the relevant indices simply being interchanged):

Let $\left(\frac{\Delta Z}{\Delta t}\right)^{\text{binary}}_{m'_{AX}}$ be the temperature coefficient of the property Z of the binary aqueous solution of AX at various binary aqueous solution concentrations m'_{AX}, for the case of a temperature change Δt beginning from the temperature t_2;* and let $\left(\frac{\Delta Z}{\Delta m_{BX}}\right)^{\text{ternary}}_{t,\, m''_{AX}}$ be the BX-concentration coefficient of the property Z of the binary aqueous solution of AX for the addition of BX to binary aqueous solutions of AX of various concentrations m''_{AX} at constant temperature t, *i.e. under isothermal conditions*. The ternary upper index indicates that a ternary system was produced by the addition of BX to the binary AX solution.

Let the initial compositions of the binary aqueous solutions, the temperature of which is varied and to which the third component is added, be the same:

$$m'_{AX} = m''_{AX} = m_{AX} \tag{1}$$

Moreover, let the temperature change Δt producing the property change ΔZ within the same experimental series (in accordance with the conditions of

* It is also important to take the initial temperature t_2 into consideration, for although Δt is the same if the temperature is reduced from *e.g.* 50 to 30 °C, or from 30 to 10 °C, the ΔZ values in the two cases are not identical.

method *a)* be constant in the whole AX–H_2O concentration range:

$$\Delta t = t_2 \pm t_1 = \text{constant} \neq f(m_{AX}); \tag{2}$$

and let also the addition of the amount of BX necessary to produce the property change ΔZ in the case of the validity of condition (1) take place in the whole binary AX–H_2O concentration range under isothermal conditions:

$$t_2 = \text{constant} \tag{3}$$

The two effects changing Z (the variation of the temperature and the addition of the third component) can now most simply be compared by taking the ratio of the above coefficients of the change Z produced in the two ways. When conditions (1), (2) and (3) all hold, the ratio of the two coefficients can be written as follows:

$$\frac{\left(\frac{\Delta Z}{\Delta t}\right)^{\text{binary}}_{m_{AX}, t_2}}{\left(\frac{\Delta Z}{\Delta m_{BX}}\right)^{\text{ternary}}_{m_{AX}, t_2}} = M' \tag{4}$$

where

$$M' = f(m_{AX}, \Delta t = t_2 \pm t_1, t_2) \tag{5}$$

From (4) we have

$$\left(\frac{\Delta Z}{\Delta t}\right)_{m_{AX}, t_2} = M' \left(\frac{\Delta Z}{\Delta m_{BX}}\right)_{m_{AX}, t_2} \tag{6}$$

The comparison of the changes of Z due to the two effects is made still easier if, in the case when conditions (1), (2) and (3) hold simultaneously, the changes ΔZ produced by the two means are also taken as identical at the various binary concentration m_{AX}:

$$\Delta Z^{(\Delta t)}_{m_{AX}, \Delta t, t_2} \equiv \Delta Z^{(\Delta m_{BX})}_{m_{AX}, t_2} \tag{7}$$

That is, in this case m_{BX} in (4) and (6) means just the amount of BX which produces an identical change in Z as the changing in t.

Accordingly, since $t = t_2 \pm t_1$ and t_2 is constant in the whole binary AX–H_2O concentration range, (4) and (6) assume the following forms:

$$\frac{(\Delta m_{BX})_{m_{AX}, t_2}}{(\Delta t)_{m_{AX}, t_2}} = M \tag{8}$$

and

$$(\Delta m_{BX})_{m_{AX}, t_2} = (\Delta t)_{m_{AX}, t_2} M = K_{\Delta t, t_2} \cdot M \tag{9}$$

where

$$K_{\Delta t, t_2} = \text{constant.}$$

Eq. (9) is the equation of those curves on the isotherm ternary diagram (Figure 1) which connect the ternary concentrations for which the addition of the appropriate amount of BX at a given temperature to the binary AX–H_2O

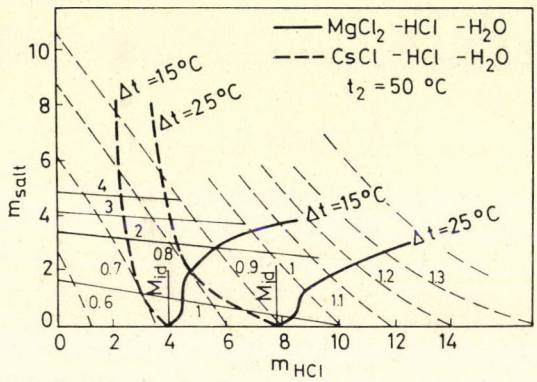

Fig. 1

solution of given concentration m_{AX} causes the same change ΔZ, as that resulting from the change in the temperature t_2 of the binary AX–H_2O solution of given concentration m_{AX} by the constant Δt in the whole AX–H_2O concentration range. Consequently, M means physically a concentration change Δm_{BX} which, under isothermal (t_2 = constant) conditions, produces the same property change in the binary aqueous AX system as a 1 °C changing in the temperature within the temperature range $\Delta t = t_2 \pm t_1$ in a binary aqueous AX solution with identical concentration.

According to Eq. (5), M' and also the corresponding Δm_{BX} are functions of m_{AX}, $\Delta t = t_2 \pm t_1$ and t_2. If the latter two parameters are constant in the whole binary AX–H_2O concentration range (as is the case here), M' and the corresponding M, and hence Δm_{BX} too, are simply functions of the concentration of AX. If M were not to change with the linear increase of the concentration of the binary AX solution, this would mean that the ratio of Δm_{BX} and Δt producing the property change ΔZ, would remain the same, independently of the concentration in the binary aqueous AX solution; and [since according to condition (2) Δt is constant in the whole binary concentration range] nor would the value of Δm_{BX} change with the concentration of AX (the straight

lines M_{id} in Figure 1). This would indicate that (at least as regards the effect on the property Z) the addition of the third component BX would produce the same change in the structural relations in the whole binary AX–H_2O concentration range, and hence with the increase of m_{AX} there would be no change in the structure of the binary solution or at least the change too would be linear in the whole concentration range. On the other hand, if M changes non-linearly with m_{AX}, or changes linearly only in certain sections (see the other M curves in Figure 1), the cause must be sought in the structural changes occurring on the increase of the concentration in the aqueous solution of AX. As a result of this, because of the various structural arrangements and interactions which develop, the amount of BX $(\Delta m_{BX})_{\Delta t, t_2}$ — required to attain the ΔZ produced by the temperature change Δt — exerts different effects in the various AX concentration intervals.

As we have seen, M characterizes the mutual relation of the effects of the temperature change and of the addition of the third component on the property change ΔZ. Thus, if it is assumed that the increase (decrease) of the temperature leads only to the decrease (increase) of the structural ordering without a change in the number of ions in the binary aqueous solution, then the value of M and the extent and direction of its variation as a function of the concentration of AX may also be good characteristics of what type of effect is exerted by the addition of the third component on the structures of binary aqueous salt solutions of given concentration. A proof for this is provided by the fact that according to our findings the line of curve M in ternary metal chloride–HCl–H_2O systems will vary with the nature of the salt component of the binary aqueous salt solution, and will be characteristic.

Let us apply the above relations to the system $MgCl_2$–HCl–H_2O studied by us [2]. In this case let AX = $MgCl_2$, BX = HCl, $t_2 = 50$ °C, $\Delta t = t_1 - t_2 = 35—50$ °C = —15 °C, or $t_1 - t_2 = 25 - 50$ °C = — 25 °C, $\Delta Z = \Delta\eta$ the viscosity change, and for the complete $MgCl_2$–H_2O concentration range that

$$\left(\frac{\Delta\eta}{\Delta t}\right)^{\text{binary}} < 0$$

Accordingly, Eq. (9) assumes the following form:

$$(\Delta m_{HCl})_{m_{MgCl_2},\, t_2=50°C} = -(\Delta t)_{t_2,\, \Delta t} \cdot M = K_{\Delta t,\, t_2} \cdot M \qquad (10)$$

Eq. (10) gives an equation for the curves shown in Figure 1, which relate to the two different temperature decreases Δt (a temperature change of $-\Delta t$) of 15 and 25 °C starting from $t_2 = 50$ °C. The two curves connect those HCl concentrations for which the addition of the corresponding amount of HCl to the $MgCl_2$–H_2O binary solutions of given concentration produces the same

viscosity change at $t_2 = 50$ °C as the decrease of the temperature of such a binary $MgCl_2$–H_2O solution by 15 or 25 °C from $t_2 = 50$ °C and $K'_{t,t_2} = 15$ °C, $K''_{t,t_2} = 25$ °C, respectively.

It can be seen from Figure 1 that even in the case of extremely dilute initial $MgCl_2$–H_2O binary system (*i.e.* practically in water) the viscosity is increased to such a large extent by a temperature decrease of 15 °C that under isothermal conditions this could only be achieved by the addition of 4 *m* HCl. It is also clear that, with the exception of moderately concentrated $MgCl_2$ solutions, the more concentrated the initial $MgCl_2$ solution at a given temperature (here 50 °C) the more the HCl required for the viscosity increase produced to be equivalent to that due to the 15 °C temperature decrease of the 50 °C binary $MgCl_2$–H_2O with the corresponding concentration.

A different behaviour is observed for the moderately concentrated $MgCl_2$ solutions: In the initial concentration range 0.5—1.5 *m* $MgCl_2$ the amount of HCl which must be added to give just the same viscosity change in the binary solutions under isothermal conditions as the decrease of the temperature of these solutions by 15 or 25 °C is practically constant. According to our assumption, this corresponds to those conditions for which the rearrangement of the hydrate shell and the increase of the ion-ion interaction resulting from the addition of the given amount of HCl will produce the same viscosity change as a function of the $MgCl_2$ concentration in the given range, as that due to the temperature decrease in binary $MgCl_2$ solutions in this concentration range. In more dilute solutions the latter effect will be the dominant one, while in more concentrated $MgCl_2$ solutions the former effect will prevail.

The increase in viscosity due to a decrease in temperature is so large that it is not possible by the addition of HCl to concentrated binary aqueous $MgCl_2$–H_2O solutions to produce a viscosity increase equivalent to that resulting from a temperature decrease of 35 °C, for example (the HCl exerts a very strong salting-out effect on the $MgCl_2$ and the vapour pressure of HCl rapidly attains a value of 1 atm). Likewise even in the case of less concentrated aqueous salt solutions, it would be possible to produce it only by the addition of 13—14 *m* HCl.

Figure 2 gives a plot of $M = \left(\frac{\Delta m_{HCl}}{\Delta t}\right)_{\Delta t, t_2}$ as a function of the concentration of the binary $MgCl_2$–H_2O solution for $\Delta t = 25$ and 15 °C. It can be seen that the plot is not linear in either case, merely approaching linearity through the various sections. Nevertheless, the slope of the linear section varies, showing that there are concentration intervals with different, dominant structural rearrangements as the concentration changes in the binary system. It is also clear that for the whole $MgCl_2$ concentration range

$$M_{\Delta t=25°,\, t_2=50°} > M_{\Delta t=15°,\, t_2=50°} \qquad (11)$$

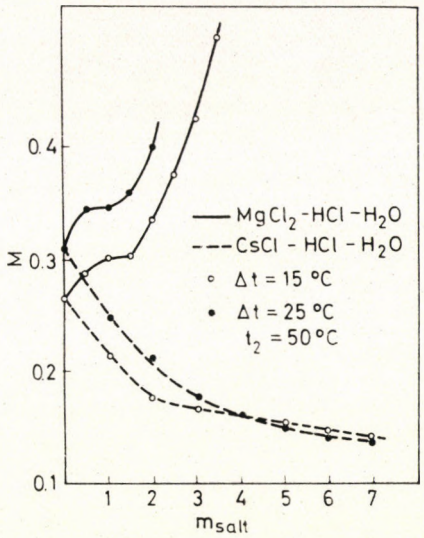

Fig. 2

that is

$$\left(\frac{dM}{d\Delta t}\right)_{t_2} > 0 \tag{12}$$

and

$$\left(\frac{dM}{dt_1}\right)_{t_2} < 0 \tag{13}$$

Thus, starting from t_2 the value of M increases with the increase of Δt (temperature decrease!), *i.e.* with the decrease of t_1.

Let us now turn to the monovalent Cs^+ ion, which is much larger (r = = 1.69 Å) than the Mg^{2+} ion (r = 0.65 Å), thus to the CsCl–HCl–H_2O system [3]. It can be seen from both Figures 1 and 2 that the M curves for the $MgCl_2$ and CsCl systems differ, indicating that the shapes of the curves and hence the structures of the binary aqueous $MeCl_x$–H_2O solutions are mainly determined by the size and charge of the cation of the salt.

Let us now use method *b)* as outlined in the introduction to compare the effects of the temperature change and the addition of a third component on the variation in the property Z. In this case it will be compared that temperature change t and that amount of the third component m_{BX} which must be added to produce a given — in the whole binary aqueous AX concentration range — constant property change Z. In the case of method *a)*, therefore, t was constant and Z and m_{BX} depended on the concentration of the binary aqueous AX

solution, whereas in the present case Z is constant and t and m_{BX} depend on the concentration of AX.

In spite of the fact that the number of dependent variables in method *b)* is apparently unchanged, nevertheless the method seems to be more applicable from a certain point of view, because in this case it is possible to compare two factors which bring about only one given, constant effect, and to study their dependence on the concentration of AX too, and, as will be seen later [Eq. (17)], this does in fact decrease the number of variable parameters to be considered by one.

Let $\left(\frac{\Delta t}{\Delta Z}\right)^{\text{binary}}_{t_2, m'_{AX}}$ be the temperature change corresponding to unit ΔZ-change, *i.e.* the temperature change producing unit ΔZ-change, starting from a temperature, t_2.

Similarly, let $\left(\frac{\Delta m_{BX}}{\Delta Z}\right)^{\text{ternary}}_{t_2, m''_{AX}}$ be the amount of the third component corresponding to unit ΔZ-change, *i.e.* the amount of the third component producing unit ΔZ-change under isothermal conditions with $t_2 = \text{constant}$.

On the analogy of Eq. (4), the ratio of the two coefficients can be written as follows:

$$\frac{\left(\frac{\Delta m_{BX}}{\Delta Z}\right)^{\text{ternary}}_{t_2, m''_{AX}}}{\left(\frac{\Delta t}{\Delta Z}\right)^{\text{binary}}_{t_2, m'_{AX}}} = N' \tag{14}$$

Similarly, if (1) and (3) hold, and

$$\Delta t = t_2 \pm t_1$$

and if

$$(\Delta Z)_{\Delta t, t_2} \equiv (\Delta Z)_{\Delta m_{BX}, t_2} = \text{constant} \neq f(m_{AX}) \tag{15}$$

then (14) assumes the following form:

$$\left(\frac{\Delta m_{BX}}{\Delta t}\right)_{t_2, m_{AX}} = N \tag{16}$$

where

$$[N = f m_{AX}]_{t_2} \tag{17}$$

According to (17), therefore, and in contrast with (5), N is no longer a function of Δt, and thus there is indeed one fewer independent variable involved in considerations with method *b)*.

Eq. (16) gives the ratio of the two independent effects in the case of identical changes ΔZ, constant in the whole binary aqueous AX solution concentration range, and produced by the two independent methods (*i.e.* temperature variation and addition of the third component). Eq. (17) shows that this ratio depends only on the concentration of the binary aqueous AX solution if the temperature t_2 is also constant.

N may therefore be considered as that amount of BX corresponding to the temperature change Δt and added to the binary aqueous salt solution under isothermal conditions (t_2 = constant), which produces a given — in the whole binary aqueous AX concentration range — constant property change ΔZ.

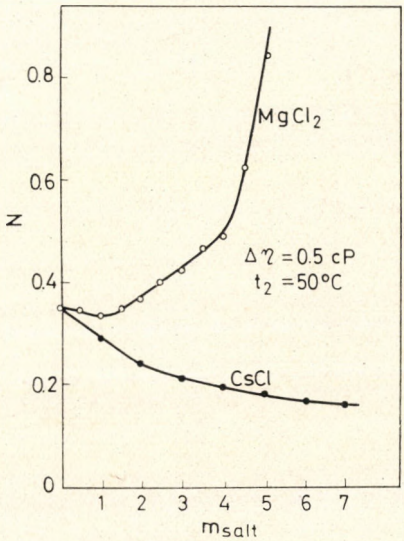

Fig. 3

Both (8) and (16) have their own advantages. The advantage of the use of (8) is that, as we have seen, it gives the equation of the thick curves in Figure 1. In spite of the fact that as a principle a corresponding curve cannot be drawn on the ternary diagram of type 1, the advantage of using (16) is that the dependence of N on the concentration of the binary aqueous AX solution under isothermal conditions (t_2 = constant) is much more expressed, as can be seen in Figure 3. Thus, it may possibly become easier to draw conclusions for the dependence on the structure of the binary aqueous solution, and hence for the structure of the binary aqueous solution too.

Let us apply method *b)* to the systems CsCl–HCl– H_2O and $MgCl_2$–HCl–H_2O, assuming the dependence of N on the concentration of the CsCl or $MgCl_2$ solution as obtained from (16) (Figure 3). The symbols used in connection with method *a)* are also used in this case.

The curves given in Figure 3 in fact exhibit a more expressed line than the M curves in Figure 2 for the several given temperature decreases Δt. In addition, the curves are very different. This shows well that for the same molalities the structures of the two solutions differ considerably (a solution of $MgCl_2$ contains 1.5 times as many ions and twice as much charge as an equimolal solution of CsCl; in the latter solution, therefore, there are much more free water molecules because of the very different sizes of the cations and a 100% difference in the cation charge). Three concentration ranges can be well distinguished in the N curve for $MgCl_2$, these three sections being to a good approximation linear. It holds for them that

$$\frac{dN}{dm_{MgCl_2}} = \alpha_{MgCl_2} \begin{cases} \alpha^{I}_{MgCl_2} = N_{\alpha^{I}_{MgCl_2}} + k^{I}_{MgCl_2} m_{MgCl_2} & (k^{I}_{MgCl_2} < 0) \\ \alpha^{II}_{MgCl_2} = N_{\alpha^{II}_{MgCl_2}} + k^{II}_{MgCl_2} m_{MgCl_2} & (k^{II}_{MgCl_2} > 0) \\ \alpha^{III}_{MgCl_2} = N_{\alpha^{III}_{MgCl_2}} + k^{III}_{MgCl_2} m_{MgCl_2} & (k^{III}_{MgCl_2} \gg 0) \end{cases} \tag{18}$$

On the other hand, the N curve for the CsCl–HCl–H_2O system exhibits only two linear sections, where

$$\frac{dN}{dm_{CsCl}} = \alpha_{CsCl} \begin{cases} \alpha^{I}_{CsCl} = N_{\alpha^{I}_{CsCl}} + k^{I}_{CsCl} m_{CsCl} & (k^{I}_{CsCl} < k^{I}_{MgCl_2} < 0) \\ \alpha^{II}_{CsCl} = N_{\alpha^{II}_{CsCl}} + k^{II}_{CsCl} m_{CsCl} & (k^{I}_{CsCl} < k^{II}_{CsCl} < 0) \end{cases} \tag{19}$$

It is remarkable that in both systems interval I extends to the limit of complete hydration [4, 5], that is while it is still possible for the added HCl to be hydrated by the free water molecules, or for the structural free water fraction* to increase or decrease as a result of the change of Δt.

This clearly shows that a structure differing from the previous ones is formed in the binary solution after the attainment of the limit of complete hydration, which can therefore be determined from the N curves. In this case

* The views of a number of authors [6, 7] can be generalized by saying that liquid water consists of at least two fractions: a statistically "quasicrystalline" water fraction, where the water molecules are bounded relatively strongly by hydrogen bonds — this is termed "structural" (ice-like, clustered, etc.) water —, and a fraction consisting of monomers, this is termed "monomeric" water. At a given temperature there is an equilibrium between the two forms. This can be described by the relation

$$\frac{[H_2O]_{structural}}{[H_2O]_{monomeric}} = K \tag{20}$$

Decrease in temperature shifts the equilibrium toward the polymeric state (the structural form), and consequently there is an increase in the viscosity of the water. This is also true for dilute salt solutions with concentrations less than the limit of complete hydration. On the other hand, the isothermal addition of the third salt component does not change the equilibrium, but only decreases the absolute amounts $[H_2O]_{structural}$ and $[H_2O]_{monomeric}$.

processes can take place such as the decrease of the extent of the hydrate shell, the number of hydrated water molecules, possibly — in the case of small ions of high charge — new, more complex ion-ion and ion-solvent associates, which can be affected by the change of temperature and by the addition of Δm_{HCl} in different manner the previous structure. Interval II gives information as to the concentration range for the formation of this new structure and to its relative strength. In this interval, for instance, N increases as a function of the $MgCl_2$ concentration, but not as a function of the CsCl concentration; in the latter case the slope is merely somewhat greater (less negative) than in the first interval.

The N curve for $MgCl_2$ begins to rise very sharply at concentrations near to saturation. This must obviously be related with the formation of a further, third solution structure, considered as a statistically quasicrystalline pre-structure approaching the solid phase with the composition of $MgCl_2 \cdot 6H_2O$ which separates from the saturated solution. The change in the temperature is able to produce only slight variation in this latter solution structure (only the solid $MgCl_2 \cdot 6H_2O$ gets precipitated both from the saturated binary and the hydrochloric acid-containing ternary $MgCl_2$ solutions in the temperature range 0—100 °C [8]), but very much HCl is required to produce the same change $\Delta\eta$ as the increase of viscosity due to the temperature increase. This shows that in such concentrated $MgCl_2$ solutions the degree of dissociation of dissolved HCl is very low. A large part of it merely undergoes physical dissolution, remaining as an undissociated, uncharged, quasi-inert molecule. It weakens the structure which has developed, and the ion-ion interactions producing an increase in viscosity are increased only by the small amount of charge carriers resulting from the very slight dissociation.

That such a statistically quasicrystalline pre-structure does in fact exist, and that the HCl added to such solutions dissociates only very slightly, has emerged from our earlier measurements [2]. It was found that there is also a sudden and great increase in the entropy of activation of viscous flow in this concentration range, while in such concentrated solutions the addition of HCl decreases the viscosity of the binary $MgCl_2$ solution, and also barely increases the specific conductivity.

Interval III does not appear with the CsCl–HCl–H_2O system, and thus the quasicrystalline pre-arrangement and the repression of the dissociation of the HCl do not occur (or to an extremely small extent only) in such systems. This is shown by the fact that anhydrous CsCl falls out from its saturated solutions over a wide temperature range [9], while our own results [3] indicate that when HCl is added to even the most concentrated aqueous CsCl solutions the viscosity and the specific conductivity continue to increase. Similarly in this concentration range there is no increase in the curve of the concentration dependence of the entropy of activation of viscous flow.

At present for the structural relations of solutions between the limit of complete hydration and the starting point of quasicrystalline pre-arrangement (or the saturation concentration in the case of CsCl) we can only say from the shapes of the N curves that such rearrangements occur and structures are formed which differ increasingly from the structure of free water with the increase of the concentration, and in the case of small cations with high charge they point at the quasicrystalline structure, while for large cations with small charge they alter linearly up to the saturation, without any particular structural changes. Still further efforts are required to study this region more extensively.

REFERENCES

1. BERECZ, E.: Z. Phys. Chem. **229,** 173 (1965)
2. BERECZ, E., BÁDER, I.: unpublished data
3. BERECZ, E., CZAKÓ-NAGY, I.: Proceedings of the 16th meeting of the C.I.T.C.E. 1965. 165—167 (1965); CZAKÓ-NAGY, I.: Thesis. L. Eötvös University, Budapest, 1965
4. BERECZ, E., ACHS-BALLA, M.: Acta Chim. Acad. Sci. Hung. accepted for publication
5. MISHCHENKO, K. P., SUKHOTYIN, A. M.: Izv. Sekt. Platin. **26,** 203 (1951)
6. ERDEY-GRÚZ, T.: Transport Processes in Aqueous Solutions. Akadémiai Kiadó, Budapest, (1971)
7. SAMOILOV, O. YA.: Struktura vodnikh rastvorov elektrolitov i gidratatsia ionov. Izd. A. N. SSSR Moscow, 1957
8. Spravochnyik po rastvorimostyi. Tom I. Goskhimizdat 1953, 622.
9. PLYUSHCHEV, V. E., KUZNYETSOVA, T. P.: Tr. Mosk. Inst. Tonkoi Khim. Teknol. **6,** 15 (1956)

Endre BERECZ
Imre BÁDER
} Miskolc, Egyetemváros, Hungary.

Acta Chimica Academiae Scientiarum Hungaricae, Tomus 74 (2), pp. 225—232 (1972)

SELECTIVE POISONING OF Pt CATALYSTS BY CO_2 CHEMISORPTION, I

REACTION OF CO_2 WITH ADSORBED HYDROGEN

F. NAGY, GY. MINK and D. MÓGER

(Central Research Institute for Chemistry, Hungarian Academy of Sciences, Budapest)

Received March 6, 1972

A tracer investigation of the chemisorption of CO_2 on a Pt surface covered by hydrogen has led to the following conclusions:

1. Chemisorption may be described by the overall reaction:

$$H_{2(a)} + CO_2 = CO_{(a)} + H_2O$$

2. Chemisorbed CO cannot be removed at room temperature either by evacuation or with hydrogen.

3. CO chemisorption proceeds at a measurable rate which can be described as the sum of three reactions, all first order with respect to the adsorbed hydrogen. There is a difference of nearly one order of magnitude between the rate constants of these reactions, therefore, the different active sites of the Pt surface can be selectively blocked by CO chemisorption.

Platinum catalysts are widely used in catalytic hydrogenation, dehydrogenation and reforming reactions, both in the gas and liquid phase. Pure Pt catalysts are, however, generally not applicable for practical purposes, especially in the case of gas-phase reactions for, in parallel with the main reaction, side-reactions with products of low hydrogen content, occasionally carbon deposits, will occur on the surface, which leads to a rapid decrease in the activity of the catalyst [1, 2].

In fact, the purpose of applying different alloys has been to reduce the activity of the Pt catalyst towards side-reactions. In case the surface of a pure Pt catalyst cannot be considered homogeneous in respect to the catalytic activity, it may be assumed that the undesirable side-reactions are 'initiated' only at certain points of the surface and the polymers of low hydrogen content, or the carbon deposits thus formed, block part of the surface, which results in the decrease of catalytic activity towards the main reaction. If this assumption holds true, the stabilization of catalytic activity towards the main reaction can be achieved by selective poisoning of the catalyst by chemisorption. The poisoning agent is required to undergo truly selective chemisorption on the active sites and, on the other hand, should not be susceptible to displacement, under the experimental conditions, by the components of the main reaction either through competitive adsorption or chemical reactions.

The catalytic activity of Pt in hydrogenation reactions is closely related to its ability to adsorb hydrogen. Early observations regarding the heterogeneous activity of the Pt surface also refer to the inhomogeneity of hydrogen adsorption. A number of studies on hydrogen adsorption both in the gas and liquid phase confirm that hydrogen is adsorbed on Pt surfaces in different forms involving different binding energies [3—10]. In view of the above, it seems reasonable to carry out selective poisoning with a reagent that is adsorbed through the displacement of hydrogen from the surface sites which it occupies, and whose product of chemisorption cannot be displaced either by hydrogen or by the substrate under the conditions of hydrogenation. According to our studies, the most suitable procedure for this purpose is to allow chemisorption of carbon dioxide at room temperature on the Pt catalyst covered by hydrogen. The chemisorption of CO_2 can be described by the following overall reaction:

$$H_{2(a)} + CO_2 = CO_{(a)} + H_2O \qquad (1)$$

where subscript (*a*) refers to the adsorbed state.

According to the above explanation, which remains to be verified by experiments, the conditions of applying CO_2 are that

1. CO_2 should undergo chemisorption on a Pt surface only as a result of reaction (1);

2. At room temperature, the adsorbed CO should not be removable either by evacuation or with hydrogen;

3. The reaction of carbon dioxide with different types of adsorbed hydrogen should occur at different rates in order to ensure selective poisoning.

Experimental

The study of CO_2 chemisorption has been carried out by a method described earlier [11], in which $^{14}CO_2$ is used as tracer. The accumulation of chemisorbed CO on the surface and its removal in desorption measurements were followed by measuring the radioactivity of the catalyst.

The fulfilment of condition (1) has been proved by removing the chemisorbed carbon monoxide with ^{18}O-labelled oxygen in the form of CO_2 and determining the ^{18}O content of the carbon dioxide by mass spectrometry.

Apparatus

A plastic scintillator (Sc) (a solid solution of PPO and dimethyl-POPOP in polystyrene) is glued to the bottom of the metal reactor (Fig. 1) and isolated from the gas phase by a thin mica sheet. Isolation is required in order to avoid contamination of the scintillator by CO_2 and other gases readily absorbed by polystyrene [12—14], resulting in a pronounced 'memory' effect. The cata-

lyst powder (Ads) is pressed into a pellet and placed on the mica sheet. The gas space (Gas) is immediately over the catalyst and constitutes part of a gas circulation system. In order to avoid poisoning of the catalyst by grease, all valves have been made of metal. The reactor is connected to a vacuum system

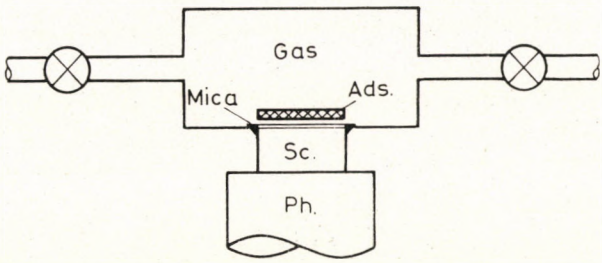

Fig. 1. Schematic diagram of the measuring section. Gas — gas space, Mica — thin mica sheet, Ads — adsorbent, Sc — scintillator, Ph — phototube

which allows evacuation to 10^{-3}—10^{-4} Torr. The scintillator is mounted directly onto the phototube (Ph). Radioactivity is measured by a type GAMMA NP—244 counter.

In the case of ^{18}O measurements, an MI 1305 type mass spectrometer was used for the determination of the isotope content of carbon dioxide.

Principle of tracer chemisorption measurements

When ^{14}C-labelled gases are used, radiation from the free gas phase will not reach the scintillator if the catalyst layer is thicker than 25 mg · cm^{-2}. The measured count rate (ΣI) can be expressed in this case as the sum of the following three terms:

$$\Sigma I = I_a + I_p + I_b \qquad (2)$$

where I_a denotes the radiation from the adsorption phase, I_p is the radiation wom the free gas held in the pores, and I_b stands for the background radiation.

The value of I_b can be directly measured. For a given catalyst, porosity ard specific activity of carbon dioxide, I_p is proportional to the gas pressure, *ie.*

$$I_p = ap \qquad (3$$

where p is the pressure of labelled gas and a the proportionality factor.

Determining the chemisorption of carbon dioxide by a volumetric method, we have found that chemisorption reaches the saturation level already at a low CO_2 pressure [11]. If, after having reached chemisorption equilibrium (*i.e.*

ΣI remains unchanged in time), the pressure of labelled carbon dioxide is altered, we may calculate proportionality factor a on the basis of relationship (3). The knowledge of this, in turn, allows determination of the I_p value in the course of chemisorption, at any gas pressure. If I_b and I_p are known, one may calculate I_a and its time dependence from the ΣI values determined in the course of sorption, using Eq. (2). Under given experimental conditions (catalyst, porosity and specific activity), I_a is proportional to the specific adsorption of the labelled component, *i.e.*

$$I_a = \Sigma I - I_p - I_b = b\Gamma \tag{4}$$

where b is a proportionality factor and Γ denotes the specific adsorption.

Materials and procedure

The Pt powder was prepared by the reduction of hexachloroplatinic acid. The catalyst was purified in perchloric acid by repeated anodic and cathodic polarization. Purification was carried out in an electrolyzer with a platinum plate constituting the bottom. After being washed in distilled water and dried in air, the catalyst powder was pressed into a pellet (thickness 0.2—0.3 mm; diameter 2 cm) and placed into the reactor.

Hydrogen was purified by diffusion through a Pd thimble. Oxygen was obtained from a cylinder and passed through a trap cooled by liquid nitrogen. ^{14}C-labelled carbon dioxide was prepared from labelled $BaCO_3$ (specific activity: 3.2 mCi/mmol) with sulfuric acid.

The catalyst covered with hydrogen was obtained by allowing 300 Torr of hydrogen to circulate in the reactor at room temperature for about 2 hrs. The water formed was collected in a trap cooled by liquid nitrogen. After treatment with hydrogen at room temperature, the reactor was evacuated to 10^{-3} Torr.

In the case of chemisorption measurements, labelled carbon dioxide was allowed to circulate at constant pressure and the count rate (ΣI) was determined as a function of time.

The adsorbed CO was removed by alternative treatment of the catalyst with oxygen and hydrogen until the radioactivity dropped to the background value.

In order to confirm the unambiguity of reaction (1), the following measurements were performed in the presence of a relatively large amount of catalyst in a volumetric adsorption system. The catalyst was first treated with hydrogen, the vessel was evacuated to 10^{-3} Torr, and inactive carbon dioxide (50—60 Torr) was allowed into the system. After complete chemisorption (about 1 day), the apparatus was evacuated to 10^{-3} Torr and ^{18}O-enriched oxygen was allowed into the adsorption vessel. The ^{18}O content of oxygen was about 20.1%. Measurements with radioactive carbon dioxide have shown that oxygen removes the chemisorbed carbon monoxide within a few minutes. Accordingly, after about 10—15 min, the adsorption vessel was evacuated through a trap cooled with liquid N_2 and the ^{18}O content of the carbon dioxide collected in the trap was determined by mass spectrometry.

Results and discussion

In order to verify that the chemisorption of carbon dioxide on the surface of the Pt catalyst treated with hydrogen (condition 1) occurs exclusively by overall reaction (1), carbon monoxide was removed with oxygen containing 20.1% of ^{18}O. The ^{18}O content of the carbon dioxide formed was found to be $10.5 \pm 0.6\%$, consequently 0.5 mol of oxygen was required to convert the

chemisorbed product into 1 mol of carbon dioxide. This means that the chemisorbed product on the surface was of the composition CO, which proves that the chemisorption of carbon dioxide on the hydrogen-covered Pt surface takes place according to overall reaction (1).

To confirm the validity of condition (2), after the chemisorption of radioactive CO_2 had reached equilibrium, we examined the variation of I_a upon evacuation and treatment with hydrogen. According to these measurements, no decrease in the I_a values can be observed, which means that CO is so strongly chemisorbed that it cannot be removed from the surface either by evacuation or by treatment with hydrogen.

The chemisorption of carbon dioxide on the Pt catalyst treated with hydrogen occurs at a finite rate, which can be followed by measuring I_a as a function of time (t) (*cf.* Table I). A number of kinetic equations have been studied in view of their applicability for the mathematical description of the experimental data given in Table I. The following expression was found to be the most suitable:

$$(I_a)_c = A_1(1 - e^{-k_1 t}) + A_2(1 - e^{-k_2 t}) + A_3(1 - e^{-k_3 t}) \tag{5}$$

where A_1, A_2, A_3 as well as k_1, k_2 and k_3 are constants.

According to investigations by CVETANOVIĆ *et al.* [10], four different kinds of adsorbed hydrogen (α, β, γ and δ) can be identified on the Pt surface. Of these, α and β are hydrogen molecules adsorbed on one or two sites, respectively, while γ and δ are regarded as hydrogen atoms adsorbed at one or two sites, respectively. Type α was found to be stable only at low temperatures, therefore, only types β, γ and δ should be taken into account here. Empirical equation (5) can be interpreted by the following mechanism:

$$H_{2(a)} + CO_2 \xrightarrow{r_\beta} CO_{(a)} + H_2O, \quad \text{(slow)} \tag{6}$$

$$H_{(a)} + CO_2 \xrightarrow{r_\gamma r_\delta} COOH_{(a)}, \quad \text{(slow)} \tag{7}$$

$$H_{(a)} + COOH_{(a)} \longrightarrow CO_{(a)} + H_2O, \quad \text{(fast)}$$

According to relations (6) and (7), the system of kinetic equations for chemisorption is:

$$r_\beta = -\frac{d\theta^\beta_{H_2}}{dt} = \frac{d\theta^\beta_{CO}}{dt} = k'_\beta \theta^\beta_{H_2} f(p_{CO_2}) \tag{8}$$

$$r_\gamma = -\frac{1}{2}\frac{d\theta^\gamma_{H}}{dt} = \frac{d\theta^\gamma_{CO}}{dt} = k'_\gamma \theta^\gamma_{H} f(p_{CO_2})$$

$$r_\delta = -\frac{1}{2}\frac{d\theta^\delta_{H}}{dt} = \frac{d\theta^\delta_{CO}}{dt} = k'_\delta \theta^\delta_{H} f(p_{CO_2}) \tag{9}$$

where r is the rate of chemisorption, θ denotes the coverage of the surface, k' stands for the rate constant of chemisorption, and p_{CO_2} designates the pressure of carbon dioxide. Upper indices β, γ and δ refer to different 'adsorption sites' or forms of adsorption.

Taking into account relationships (6) and (7), the solution of the system of equations is:

$$\theta^{\beta}_{CO} = (\theta^{\beta}_{H_2})_0(1 - e^{-k_\beta t})$$

$$\theta^{\gamma}_{CO} = \frac{1}{2}(\theta^{\gamma}_{H})_0(1 - e^{-k_\gamma t}) \tag{10}$$

$$\theta^{\delta}_{CO} = \frac{1}{2}(\theta^{\delta}_{H})_0(1 - e^{-k_\delta t})$$

where 0 refers to time $t = 0$ and

$$k_\beta \equiv k'_\beta f(p_{CO_2})$$

$$k_\gamma \equiv k'_\gamma f(p_{CO_2}) \tag{11}$$

$$k_\delta \equiv k'_\delta f(p_{CO_2})$$

According to relationship (4), I_a is proportional to the amount of adsorbed CO, which is, on the other hand, proportional to the coverage (θ). This means that

$$I_a \sim \theta_{CO} = \theta^{\beta}_{CO} + \theta^{\gamma}_{CO} + \theta^{\delta}_{CO} \tag{12}$$

On the basis of the relationships (10) and (12),

$$I_a \sim (\theta^{\beta}_{H_2})_0(1 - e^{-k_\beta t}) + \frac{1}{2}(\theta^{\gamma}_{H})_0(1 - e^{-k_\gamma t}) + \\ + \frac{1}{2}(\theta^{\delta}_{H})_0(1 - e^{-k_\delta t}) \tag{13}$$

Comparison of the expression found suitable for describing the experimental results with Eq. (13) obtained from the above mechanism shows the two relationships to be analogous. At present, it is not possible to define the correlation between the constants of Eqs (5) and (13) as this would require further comparison with other experimental data, *e.g.* temperature-programmed desorption (TPD) measurements. The time dependence of I_a, determined experimentally for different Pt samples at 35 and 58 Torr of CO_2 and the $(I_a)_c$ values calculated on the basis of Eq. (5) are listed in Table I. The

Table I

Variation of the measured (I_a) *and calculated* $[(I_a)_c]$ *count rates during the chemisorption of* $^{14}CO_2$ *on Pt powders covered with hydrogen;* $\delta = \dfrac{(I_a)_c - I_a}{(I_a)_c}$

$p(^*CO_2) = 35$ Torr				$p(^*CO_2) = 58$ Torr			
t (s)	$I_a \times 10^{-3}$ $\left(\frac{\text{counts}}{20\ \text{s}}\right)$	$(I_a)_c \times 10^{-3}$ $\left(\frac{\text{counts}}{20\ \text{s}}\right)$	δ (%)	t (s)	$I_a \times 10^{-3}$ $\left(\frac{\text{counts}}{20\ \text{s}}\right)$	$(I_a)_c \times 10^{-3}$ $\left(\frac{\text{counts}}{20\ \text{s}}\right)$	δ (%)
0	0	0	0	0	0	0	0
10	8.0	7.7	—3.9	5	17.0	15.4	—10.4
35	15.7	15.0	—4.7	20	34.6	34.6	0.0
60	19.8	20.3	+2.5	35	45.0	44.8	—0.4
85	24.0	24.0	0.0	50	54.6	52.6	—3.8
110	27.3	27.0	—1.1	65	61.0	59.8	—2.0
135	29.3	29.5	+0.7	80	67.0	65.4	—2.4
160	31.8	31.7	—0.3	95	71.0	71.2	+0.3
185	33.5	33.6	—0.3	110	75.4	75.2	—0.3
210	35.0	35.3	+0.9	125	79.4	79.0	—0.5
235	36.5	36.8	+0.8	140	82.4	82.6	+0.2
260	38.0	37.7	+0.5	155	85.2	85.8	+0.7
285	39.2	39.4	—0.5	170	87.6	88.6	+1.1
310	40.7	40.5	—0.5	185	91.0	91.2	+0.2
360	42.5	42.5	0.0	200	91.0	93.6	+2.8
410	44.2	44.1	—0.2	215	95.0	95.6	+0.6
460	45.8	45.7	—0.2	230	96.6	97.8	+1.2
510	46.8	46.9	+0.2	245	98.6	99.4	+0.8
560	48.6	48.2	—0.8	260	101.0	101.4	+0.4
610	49.5	49.3	—0.4	290	104.0	104.4	+0.4
660	50.8	50.5	—0.6	320	107.0	107.4	+0.4
710	51.6	51.4	—0.4	350	110.6	110.0	—0.5
810	53.2	53.3	+0.2	380	112.6	112.6	0.0
910	55.2	54.9	—0.5	410	115.0	114.6	—0.3
1010	57.0	56.5	—0.9	440	117.0	116.8	—0.2
1110	58.0	57.8	—0.3	500	120.6	120.4	—0.2
1210	58.5	59.0	+0.8	560	123.0	123.6	+0.5
1310	60.3	60.1	—0.3	620	127.0	126.4	—0.5
1410	60.5	61.3	+1.3	680	128.6	128.8	+0.2
1510	62.0	62.1	+0.2	740	131.0	131.0	0.0
1710	63.0	63.7	+1.1	800	133.6	132.8	—0.6
1910	65.2	65.0	—0.3				
2110	66.0	66.2	+0.3				
2310	67.2	67.1	—0.1				
2510	68.0	67.9	—0.1				

last column shows the relative difference between the measured and calculated count rates. As can be seen from Table I, the measured and calculated values are in good agreement.

The constants of Eq. (5) are given in Table II. As shown by the table, the A constants of Eq. (5), which are proportional to the initial coverage of

Table II

Constants of kinetic equation (5) applied in the calculations

p_{CO_2} Torr	k_j; 10^{-2} s^{-1}			A_j; $10^3 \frac{\text{counts}}{20\ s}$			A_j/A_3		
	1	2	3	1	2	3	1	2	3
35	5.32	0.99	0.0944	9.5	22.9	39.1	0.24	0.58	1
58	18.35	1.42	0.0966	19.6	49.2	77.2	0.25	0.64	1

the different kinds of adsorbed hydrogen, are comparable. [The proportionality is strictly valid only if reaction (7) consists of sequences $H_\gamma + H_\gamma$ and $H_\delta + H_\delta$, *i.e.* $H_\gamma + H_\delta$ or $H_\delta + H_\gamma$ type processes do not occur.] On the other hand, the rate constants (k) in Eq. (5) differ by orders of magnitude. Consequently, by a proper choice of the chemisorption time one may achieve blocking of adsorption sites 1 or 1 + 2 with the chemisorbed carbon monoxide. Accordingly, the method allows poisoning of the platinum catalyst with a fair degree of selectivity.

REFERENCES

1. Móger, D., Mink, Gy., Nagy, F.: Magy. Kém. Foly., **76,** 408 (1970)
2. Mink, Gy., Móger, D., Nagy, F.: Magy. Kém. Foly., **76,** 411 (1970)
3. Telcs, I., Jáky, M.: Acta Chim. Acad. Sci. Hung. **58,** 275 (1968)
4. Pliskin, W. A., Eischens, R. P.: Z. phys. Chem., **24,** 11 (1960)
5. Mignolet, J. C. P.: J. Chim. Phys., **54,** 19 (1957)
6. Suhrmann, R., Wedler, G., Gentsch, H.: Z. phys. Chem., **17,** 350 (1958)
7. Sachtler, W. M. H., Dorgelo, G. J. H.: Z. phys. Chem., **25,** 69 (1960)
8. Kubokawa, Y., Takashima, S., Toyama, O. J.: J. Phys. Chem., **68,** 1244 (1964)
9. Giordano, N., Moretti, E.: J. Catalysis, **17,** 190 (1970)
10. Tsuchiya, S., Amenomiya, J., Cvetanović, R. J.: J. Catalysis, **19,** 245 (1970); **20,** 1 (1971)
11. Nagy, F., Mink, Gy., Móger, D., Király, J.: International Symposium on Heterogeneous Catalysis, Varna, 1971
12. Weller, S., Steiner, W.: Chem. Engng. Prog., **46,** 585 (1950)
13. Brown, W. E., Sauber, W. J.: Mod. Plast., **36/12,** 107 (1959)
14. Bockman, D. D., Brandt, D. C., Babb, A. L.: Int. J. Appl. Rad. Isotopes **18,** 728 (1967)

Ferenc Nagy
György Mink
Dezső Móger

Budapest II., Pusztaszeri út 57—69.

Acta Chimica Academiae Scientiarum Hungaricae, Tomus 74 (2), pp. 233–238 (1972)

EFFECT OF THE STRUCTURE OF LIQUID MIXTURES ON THE EQUILIBRIA OF POLYMER GEL-ALIPHATIC ALCOHOL-WATER SYSTEMS

M. NAGY,* E. WOLFRAM,* GY. INZELT** and GY. BEKE**

*(*Department of Colloid Chemistry and Technology, L. Eötvös University, Budapest and ** Department of Physical Chemistry and Radiology, L. Eötvös University, Budapest)*

Received April 1, 1972

The selective sorption isotherms of methanol, ethanol and *n*-propanol have been determined in aqueous solutions at 25 °C in the range of 0—25 mol% of alcohol.

In this concentration interval the sorption coefficient may assume several extrema and in some cases even changes sign. The alcohol concentration corresponding to maximum alcohol sorption is comparable with the concentration of maximum stabilization.

The complicated shape of the isotherms is due to the simultaneous effect of several factors. These effects may be interpreted in terms of structural stabilization of the mixtures, as well as specific interactions between the components of the mixture and the sorbents.

Studies on the equilibria between chemically cross-linked macromolecular gels and solvent mixtures may provide a wide variety of information not only about the interaction of the components with the macromolecules but also about changes in the structure of the liquid mixture. The latter effects are the more important, the less the deviation between the interaction energies of the components with each other and with the macromolecules. In addition to their theoretical and practical importance, the application of alcohol–water mixtures in the present work is motivated by the fact that their properties are extensively covered in the literature and numerous structural models are available [1].

In the studies we have used poly(vinylalcohol) (PVA) gels cross-linked with succinic dialdehyde and gelatin cross-linked with chromium alum, in combination with mixtures of water with methanol, ethanol and *n*-propanol. All experiments have been performed at 25 °C.

Experimental

The experimental method and the preparation of gels have been described elsewhere [2, 11]. The characteristic data for the gels are listed in Table I.

The selective sorption coefficient (γ_M) was calculated from the equation

$$\gamma_M = \frac{(x_0 - x_e)n_0}{n_p}$$

where x_0 and x_e are the mole fraction of alcohol in the initial and equilibrium mixture, respectively, n_0 is the amount (in mol) of the solvent components in the system, and n_p is the number of monomer units (mol) in the polymer. In this case γ_M denotes the amount of excess alcohol (mol) bound by 1 mol of monomer units, a quantity analogous to the Gibbs adsorption.

Table I

Characteristic data for the gels used

	$\nu \times 10^{-18}$ (cm^{-3})	w_p (w/w%)	V/V_0
PVA	1.08	4.92	27.5
Gelatin			
I	5.55	6.99	24.0
II	6.24	8.34	21.5

ν — number of cross-links in 1 cm^3 of the swollen gel;
w_p — polymer concentration in the gel;
V/V_0 — degree of swelling in distilled water

Results and discussion

The sorption isotherms of methanol, ethanol and *n*-propanol on the two gels are shown in Figs 1—5. These curves of rather complicated form reveal, in fact, maxima and minima, their shape being modified by individual effects (*e.g.* PVA–methanol–water). It is remarkable that the equilibrium alcohol concentrations corresponding to the extrema of the selective sorption coefficient γ_M are approximately equal for the two, chemically strongly different gels. Naturally, the numerical values of γ_M are different.

The interpretation of the results involves consideration of the interactions between the macromolecules and the components of the solvent mixture, as well as the factors influencing the structure of the mixtures. There are two main types of interaction between the polymers and alcohols studied: the alcohol molecules can be attached to the macromolecules either by hydrogen bonds or, especially in the case of higher alcohols, by hydrophobic bonding.

In considering the structure of alcohol–water mixtures, the theory of SAMOYLOV [3] may serve as a guideline: the structure of ice persists in small regions of liquid water. The lattice defects of this ice-like structure are occupied by the molecules of the non-electrolyte. To fill all of the cavities, 17 mol% of non-electrolyte would be required. This is approximately correct for methanol, whereas the actual amount is lower in the case of ethanol and *n*-propanol. This is obviously due to the fact that the latter molecules may occupy more than one defect site (cavity) at a time. The structure of water is stabilized

until there are available cavities for the alcohol molecules. In this range the derivative of the partial molar volume with respect to the concentration is negative. At higher concentrations this derivative changes sign [4], indicating that the structure-loosening and -modifying effect of the alcohol becomes predominant. These two effects are more pronounced at lower temperatures [5, 6].

The presence of macromolecules, however, requires that specific effects be also taken into account. In our opinion, the macromolecular chains inside the gel may also modify the structure of water, presumably by a mechanism different from that operative in the case of small molecules: owing to the closely spaced, identical groups (*e.g.* the hydroxyls of PVA), this effect may be cooperative in nature.

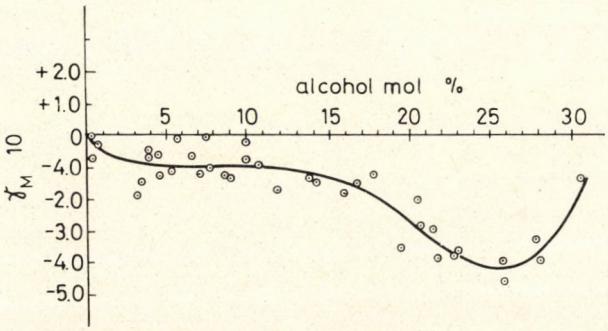

Fig. 1. Sorption isotherm of methanol–water mixtures on PVA gel

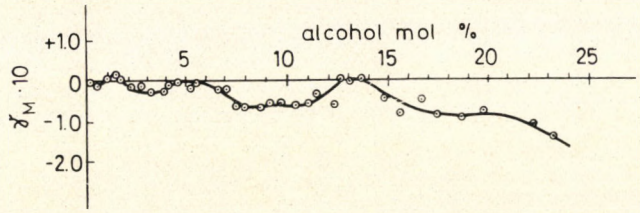

Fig. 2. Sorption isotherm of ethanol–water mixtures on PVA gel

The sorption isotherm of the methanol–water mixture (Fig. 1) has a minimum at 25 mol%, and the value of γ_M is negative in the concentration range studied. An explanation for this may be that the hydration of PVA in methanol–water mixtures is energetically more favourable than its solvation by methanol molecules. The minimum is probably due to changes in the solvent structure.

The isotherms of the ethanol–water mixtures (Figs 2 and 3) are more complicated in shape, which is probably associated with the predominance of

hydrophobic interactions. This receives support from the fact that in the case of gelatin, possessing a greater number of larger hydrophobic side chains, the effect is even more pronounced (Fig. 3). After the initial negative alcohol sorption, γ_M even changes sign.

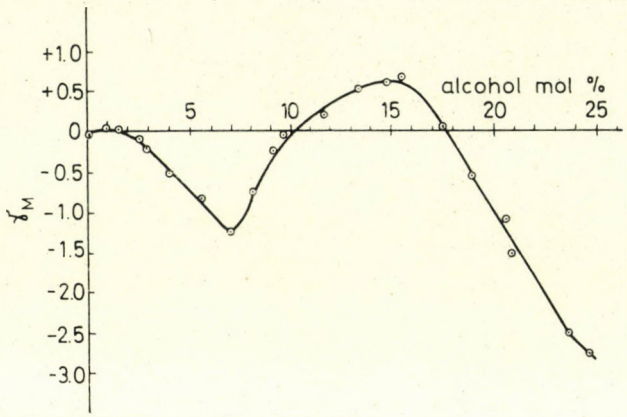

Fig. 3. Sorption isotherm of ethanol–water mixtures on gelatin I

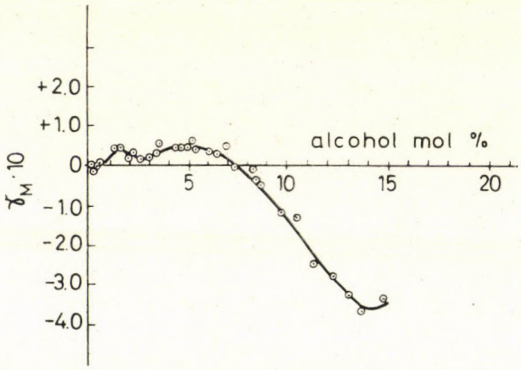

Fig. 4. Sorption isotherm of *n*-propanol–water mixtures on PVA gel

Table II

Alcohol concentrations characteristic of

Alcohol	Minimum of partial molar volume	Minimum of self-diffusion coefficient for		Maximum of viscosity
		water	alcohol	
Methanol	17—19 [4]	15—20 [5]	17—24 [7]	20—25 [6]
Ethanol	8 [4]	—	—	20—25 [8]
n-Propanol	4— 5 [4]	—	—	20—25 [9]

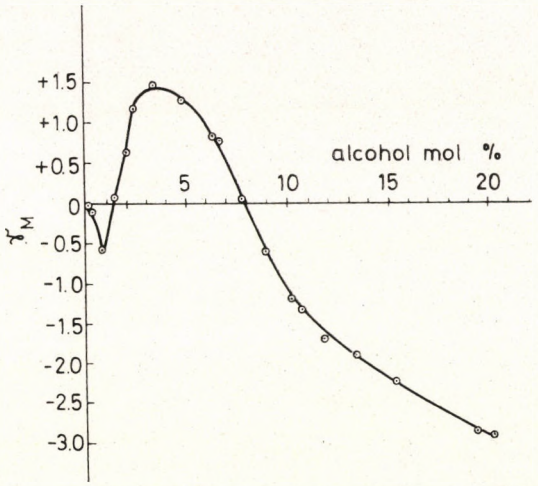

Fig. 5. Sorption isotherm of *n*-propanol–water mixtures on gelatin II

In the case of *n*-propanol, the isotherms are similar to the above. An initial positive region is observed owing to the pronounced hydrophobic interaction (Figs 4 and 5). The minimum at very low alcohol concentrations with gelatin is probably due to the start of the hydration process.

The concentrations or concentration intervals characteristic of changes in the structure of the alcohol–water mixtures, determined by various methods, are summarized in Table II, together with the equilibrium alcohol concentrations corresponding to the extrema of the sorption isotherms.

Although it cannot be unambiguously established at present whether the changes in the structure detected by other methods correspond to the minimum, maximum or the azeotropic point ($\gamma_M = 0$) of the sorption isotherm, the results clearly indicate that the concentration intervals of structural changes are in the vicinity of the extrema of the sorption isotherms.

structural changes in alcohol–water mixtures

Walden product KCl and KF	Minimum of the heat of mixing	Minimum of the relaxation time	Gel sorption			
			PVA		Gelatin	
			min.	max.	min.	max.
8—10 [6]	22—25 [1]		25	—	—	—
8—10 [8]	15 [1]	2—4 [10]	8	13	7	15
8—10 [9]	10 [1]		3	4.5	1	4.5

REFERENCES

1. ERDEY-GRÚZ, T.: Transport Processes in Aqueous Solutions (in Hungarian). Akadémiai Kiadó, Budapest, 1971; FRANKS, F., IVES, D. J. G.: Quart. Rev., **20,** 1 (1966)
2. NAGY, M., WOLFRAM, E., HORVÁTH, M.: Annales Univ. Sci. Budapestinensis, Sec. Chim., **11,** 57 (1969)
3. BUSLAYEVA, M. N., SAMOYLOV, S. YA.: Zhurn. Strukt. Khim., **4,** 502 (1963)
4. NAKANISHI, K.: Bull. Chem. Soc. Japan, **33,** 793 (1960)
5. ERDEY-GRÚZ, T., FODOR-CSÁNYI, P., LÉVAY, B., SZILÁNYI-GYŐRI, E.: Magy. Kém. Foly., **77,** 145 (1971)
6. ERDEY-GRÚZ, T., KUGLER, E., REICH, A.: Acta Chim. Acad. Sci. Hung., **13,** 429 (1958)
7. INZELT, GY.: Thesis, Budapest 1970
8. ERDEY-GRÚZ, T., KUGLER, E., HIDVÉGI, J.: Acta Chim. Acad. Sci. Hung., **19,** 89 (1959)
9. ERDEY-GRÚZ, T., KUGLER, E., MAJTHÉNYI, L.: Electrochim. Acta, **13,** 947 (1968)
10. MATIASH, I. V., YASHKITCHEV, V. I.: Zhurn. Strukt. Khim., **5,** 13 (1964)
11. INZELT, GY.: Ph. D. Thesis, Budapest 1972

Miklós NAGY
Ervin WOLFRAM
György INZELT
Gyula BEKE

Budapest VIII., Puskin u. 11—13.

Acta Chimica Academiae Scientiarum Hungaricae, Tomus 74 (2), pp. 239–251 (1972)

STUDY OF THE OXIDATION OF *n*-HEPTANE

Z. G. SZABÓ, I. GALIBA and D. GÁL

(Department of Inorganic and Analytical Chemistry, L. Eötvös University, Budapest)

Received February 21, 1972

The effect of the wall on the oxidation of *n*-heptane was studied in a specially designed apparatus. It was found that, depending on its position in the reactor, the wall and its various coatings exert a strong effect on the composition of the product. A reaction scheme was proposed for the oxidation of *n*-heptane, and on the basis of this an interpretation was given of the much-debated mechanism of formation of acetone. The scheme was brought into conformity with the experimental results. It is assumed that the wall affects primarily the isomerization.

In spite of the large number of papers published in this field in recent years, the mechanism of the oxidation of hydrocarbons is still far from having been completely elucidated. The application of gas chromatographic analysis of the products meant a great step forward in the study of these reactions, while an advance in the research into the mechanism was provided by the assumption of isomerization steps [1, 2]. The latter raises certain energetic problems, including the questions of the formation of transition complexes, the ring-member number, etc. In addition, the role of the wall of the reaction vessel in the gas-phase oxidation of hydrocarbons is still largely unclarified. At the Seventh Symposium on Combustion, SZABÓ [3] expressed the view that the role of the wall of the reaction vessel in the oxidation of hydrocarbons appears primarily not in the initiation, but in the breaking down of the chains already formed.

Earlier investigations have indicated that the nature of the wall of the reaction vessel is of importance with respect to the nature and life-time of the radicals formed [4—8]. It may be presumed, therefore, that the wall plays an important role in the isomerization [2]. In order to throw further light on these phenomena, an experiment was begun to study the nature of the wall effect. A moving-wall apparatus was constructed [9] for the investigation of the selective wall effect, and the oxidation of *n*-heptane was chosen as model reaction.

Experimental

The *n*-heptane was oxidized in a flow system. The reactor was a Pyrex tube, 480 mm long and 14 mm in diameter, into which extended a sintered-glass wall pretreated in various ways [9]. The treatments comprised the washing of the wall surface with a 10% NaOH solution, conc. HNO_3, or a saturated Na_2HPO_4 solution, respectively. The PbO layer was prepared

by transferring a saturated solution of $Pb(NO_3)_2$ in 90% ethanol to the sintered-glass surface, where it was first dried, and then kept at 450 °C for several hours. The yellow modification develops. Attempts had previously been made by the sublimation of solid PbO according to HOARE and WALSH [10], but these experiments did not result in a uniform coating of the wall.

The reaction vessel was heated by an electric furnace lined with copper. An indicating electrical multipoint controller was used to stabilize the temperature; this ensured the desired temperature of 229 °C to an accuracy of ± 1 °C in that length of the reaction space where the experiments were carried out.

The reaction zone was divided into six different sections by changing the depth of protrusion of the wall, and the reactions were carried out for these various 'wall positions'. The space after the wall was cooled to quench any further reaction. A double-walled glass tube fixing the wall in the reactor was used for this purpose, previously cooled by compressed air being circulated through it. Preliminary investigation showed that the temperature in this section was decreased to such an extent (by about 100 °C) that no oxidation could occur.

The composition of the reaction mixture was the following: oxygen flow rate 120 ml/min; the amount of heptane flowing into the reactor could be calculated from its pressure, and corresponded to the saturated vapour pressure of heptane at 32 °C.

Analysis of the products

The total peroxide content was determined by the iodometric analysis of the mixture condensed during one hour continuous reaction [11]. The aldehydes and ketones formed in the reaction were determined gas chromatographically. According to SCHRÖDER *et al.* [12], the boiling-point range of the mixture formed in the oxidation comprises about 300 °C. It contains some 75 compounds of the homologous series. Naturally the polarities are very different, and this makes the separation more difficult. A further problem is that at low conversions the residual *n*-heptane is present in extremely high amounts compared to the products.

A study was not made of the concentrations of all the products formed in the low-temperature oxidation of *n*-heptane; measurements were made for only a few of the products which can be readily determined gas chromatographically, such as acetaldehyde, propionaldehyde, butyraldehyde, acetone and methyl ethyl ketone.

A β-ray ionization detector was used in the measurements, the column consisted of a 10% squalane, 5% ethyleneglycol-bis-(propionitrile ether) and 5% silicone grease D.C. mixture liquid phase on a silanized porolite carrier about 2.5 m long. Calibration curves were prepared for the evaluation of the experimental chromatograms. These showed that in the concentration range employed the relations between the amounts and the peak-heights were linear. The results of the chromatographic measurements were given as a function of the reciprocal of the space velocity.

Results

It was found from the iodometric measurements that there was no significant build-up of peroxide, and the accumulation which did occur was independent of the wall position.

For purposes of comparison oxidation reactions were also carried out without the use of the wall, by cooling the reaction volume beyond the corresponding wall position; in effect, this means different reaction times, and gives the mixtures of oxidation products formed during these reaction periods. The reaction is not completely quenched even after the cooling, and with the increase of the reaction volume the concentrations of all the products formed in the reaction increase. The analytical results were obtained from the calibration curves in units of mmole/l (Table I).

Table I

Amounts of oxidation products in the case of uninfluenced experiments

Wall position	Acetaldehyde	Propional-dehyde	Acetone	Butyral-dehyde	Methyl ethyl ketone
	mmole/l				
0	2.785	1.474	4.200	0.737	4.571
I	2.942	1.765	4.856	0.828	5.782
II	3.185	1.880	5.342	1.000	6.834
III	3.494	2.057	6.885	1.377	9.271
IV	6.473	4.014	8.321	2.571	14.571
V	11.320	6.485	15.571	4.034	23.313

The values obtained are given in Fig. 1 as a function of the reciprocal of the space velocity. It can be well seen from the Figure that the amounts of the products measured by gas chromatographic analysis increase monotonously with the increase of the reciprocal of the space velocity. Methyl ethyl ketone is formed in the greatest amount, followed in turn by acetone, acetaldehyde, propionaldehyde, and least of all butyraldehyde. Thus, the ketones are formed in greater amounts than any of the aldehydes (in mmole/l).

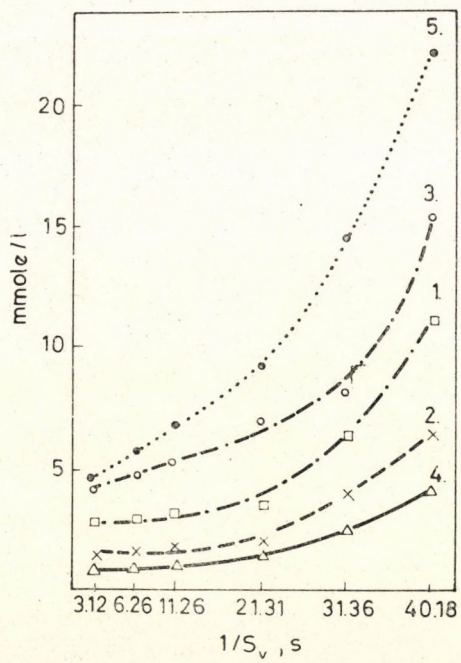

Fig. 1. Concentrations of reaction products without wall. 1. acetaldehyde; 2. propionaldehyde; 3. acetone; 4. butyraldehyde; 5. methyl ethyl ketone

Table II

Amounts of oxidation products in the case of sodium hydroxide coating

Wall position	Acetaldehyde	Propional-dehyde	Acetone	Butyraldehyde	Methyl ethyl ketone
	mmole/l				
0	1.694	0.628	2.056	0.788	5.220
I	5.967	2.572	4.524	2.204	10.260
II	3.30	1.964	4.00	1.028	5.620
III	14.76	9.976	19.312	4.640	23.428
IV	15.40	10.740	15.120	5.804	29.028
V	8.327	5.740	10.192	3.768	20.068

NaOH wall-coating. The amounts of the individual products obtained at different wall positions in this case are given in Table II. Since it is difficult to compare the numerical data, for the sake of clarity the experimental results were also compared with the wall-free values; in this way a series of reduced curves was obtained which provided direct information on whether the reac-

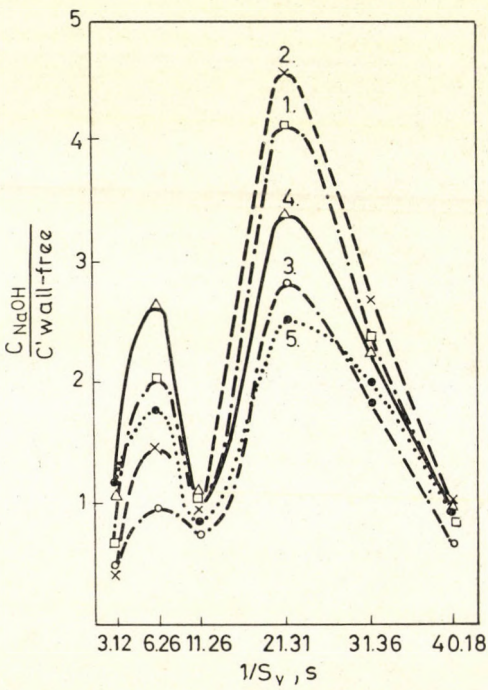

Fig. 2. Relative concentrations of reaction products in the case of sodium hydroxide-coated wall. 1. acetaldehyde; 2. propionaldehyde; 3. acetone; 4. butyraldehyde; 5. methyl ethyl ketone

tion was catalyzed or inhibited (Fig. 2). The following conclusions can be made from these curves: as compared with the monotonously increasing curves for the wall-free reaction, two sharp maxima appear, the first at wall position I, the second and larger one at wall position III. Whereas the aldehydes were formed to comparatively low extents in the 'wall-free' reaction, their amounts are higher with the sodium hydroxide coating. For example, in wall position I the amount of butyraldehyde is increased by a factor of 2.7 compared to the wall-free reaction; at the same time the methyl ethyl ketone is increased only about 1.7 times, while the acetone is practically unchanged and exhibits no maximum. In wall position III, however, the curve of acetone too increases, but nevertheless the maxima for acetone and methyl ethyl ketone are the lowest. Since these are relative maxima, this does not mean that the absolute values for these ketones are lower than those for the aldehydes in the case of the NaOH-coated wall. The amount of butyraldehyde is only a few mmole/l even in the catalyzed case, but the two maxima on the above curve definitely show that there is a significant change in the amount of product accumulated, and this clearly points to the effect of the sodium hydroxide treatment. In the second maximum the amount of propionaldehyde is 4.8 times higher than in the wall-free reaction. In wall positions 0, II and V the values lie about unity, which means that there is no wall effect; the fluctuations can be explained by the uncertainty in the temperature and the poorer reproducibility of the measurements. The amount of acetaldehyde is significantly increased at both maxima. The increase here is also considerable in absolute value, because this is the aldehyde formed in highest amount.

Lead oxide wall-coating. In this case the individual reaction products are formed in relatively low amounts (Table III). The diagram showing the com-

Table III

Amounts of oxidation products in the case of lead oxide coating

Wall position	Acetaldehyde	Propional-dehyde	Acetone	Butyral-dehyde	Methyl ethyl ketone
	mmole/l				
I	2.575	2.294	1.575	0.957	1.60
II	3.423	2.794	2.160	1.574	2.45
III	7.647	5.072	3.280	1.723	3.61
IV	5.735	3.814	4.162	2.039	6.26

parative values (Figure 3) illustrates that there is a marked difference between the ketones and the aldehydes. While acetone and methyl ethyl ketone give weakly rising straight lines, but nevertheless are within the 'inhibition' zone,

the aldehydes give curves which lie above unity and which exhibit *one* maximum. The various maxima are found in the regions of wall positions II and III.

If the wall is treated with *nitric acid* before the reaction, the reduced curves exhibit two maxima and one minimum (Figure 4). The maxima are at positions II and IV, and the minimum at position III. Acetone forms an

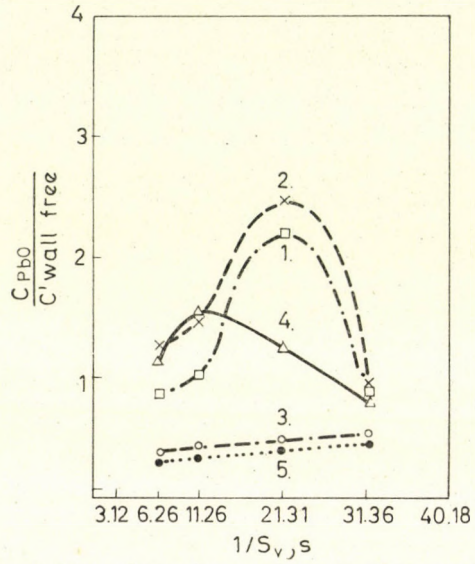

Fig. 3. Relative concentrations of reaction products in the case of lead oxide-coated wall. 1. acetaldehyde; 2. propionaldehyde; 3. acetone; 4. butyraldehyde; 5. methyl ethyl ketone

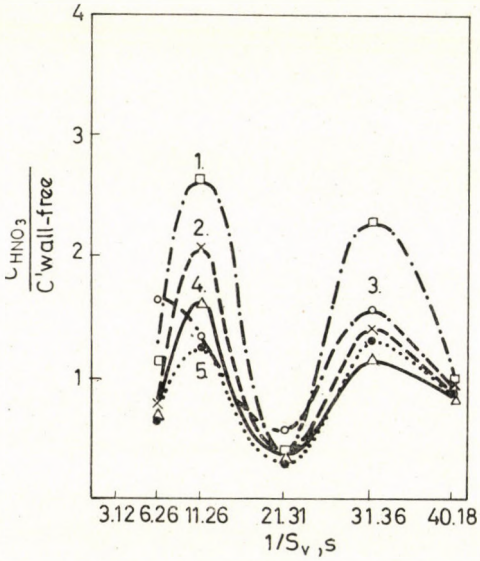

Fig. 4. Relative concentrations of reaction products in the case of nitric acid-treated wall. 1. acetaldehyde; 2. propionaldehyde; 3. acetone; 4. butyraldehyde; 5. methyl ethyl ketone

exception: the first maximum appears at wall position I, that is somewhat before those for the other substances. The second maximum is relatively significant in the case of acetone. The nitric acid exerts the greatest effect on acetaldehyde. Both maxima are very large, while there is a very strong inhibition effect in wall position III. In general, it can be said that the nitric acid treatment promotes the accumulation of the aldehydes to the greatest extent.

In the case of the *Na_2HPO_4 treatment*, there are maxima in the build-up of the products at wall position 0 (Figure 5). After this the amounts of all the products gradually decrease to wall position II; here there is a slight inhibition

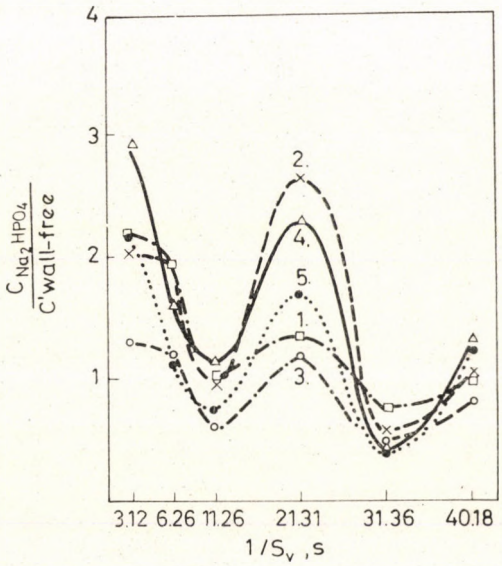

Fig. 5. Relative concentrations of reaction products in the case of disodium hydrogen phosphate-coated wall. 1. acetaldehyde; 2. propionaldehyde; 3. acetone; 4. butyraldehyde; 5. methyl ethyl ketone

for acetone and methyl ethyl ketone, while the relative values for the aldehydes are not affected. At wall position III strong maxima appear, being greatest for propionaldehyde and butyraldehyde. Although acetaldehyde and acetone exhibit the same tendency, the curves barely exceed the unity line indicating the non-catalyzed reaction. The curve for acetaldehyde is less structured than those for the other aldehydes. The maximum on the relative curve for methyl ethyl ketone is considerable, but the effect is very much smaller for acetone.

Discussion

A detailed account was given above of the changes observed when a wall with a large surface pretreated in various ways was placed into the reaction space of a flow reactor, at different points of the reaction zone. *The different*

wall positions therefore corresponded to different conversions. To a rough, first approximation, it can be assumed that at the beginning of the reactor the wall affects primarily the initial steps, while in a later section it has an effect on the chain carriers which propagated the chain further on, the intermediates and the end-products. This effect may vary depending on the conversion. Studies of a similar nature have so far not been reported in the literature.

In general two stages can be distinguished with respect to the various wall coatings. For instance, on treatment with HNO_3 or NaOH two maxima can be seen, whereas after Na_2HPO_4 treatment two minima are found. The PbO coating is an exception, its effect depends on the compounds formed. With this coating the relative curves exhibit at most only one maximum.

The experimental results were evaluated in the following way. All the possible reaction steps were collected, and the most probable of these were selected in accordance with the following considerations:

(a) the validity of the principle of the conservation of spin;

(b) the internal isomerization takes place primarily via complexes of 4 or 6 centres;

(c) consideration of the bond strengths for the calculation of the activation energies;

(d) it is always the C–C bond adjacent to the O–O group which breaks.

In this way it was possible to produce a mechanism scheme by means of which the pathways of the formation of the oxidation products could be followed. Each product may be formed in several ways, in spatial or in surface reactions. The composition of the product varies according to which route predominates.

The overall reaction scheme is enclosed on the following page.

The primary step of the oxidation is today generally accepted to be the splitting off of a hydrogen atom to give a hydrocarbon radical: [1] → [2]. The hydrogen may be split off as a result of attack by O_2, ·OH, HO_2· or RO_2·. In the case of oxygen as reaction partner the activation energy of the process is the greatest; LISCHKE *et al.* [13] report 36 kcal/mole, and TIPPER [5] 43 kcal/mole in the cold-flame region. The splitting off due to ·OH is not selective, and its activation energy is 1—2 kcal/mole [14]. If the attacking radical is HO_2· or RO_2·, then according to FISH [1], in support of SZABÓ [15], OTOZAI [16], BENSON [17] and KNOX [2], the activation energy of the splitting off of hydrogen is 6—15 kcal/mole. It cannot be given more accurately than this.

The step following the primary one is the formation of the peroxy radical [3]. The activation energy of this reaction is practically zero. At temperatures above 300 °C the process is displaced towards hydrogen extraction, with the formation of HO_2· and an olefin.

Four different peroxy radicals can presumably be formed in the oxidation of *n*-heptane; these may be generated only in primary steps but in later

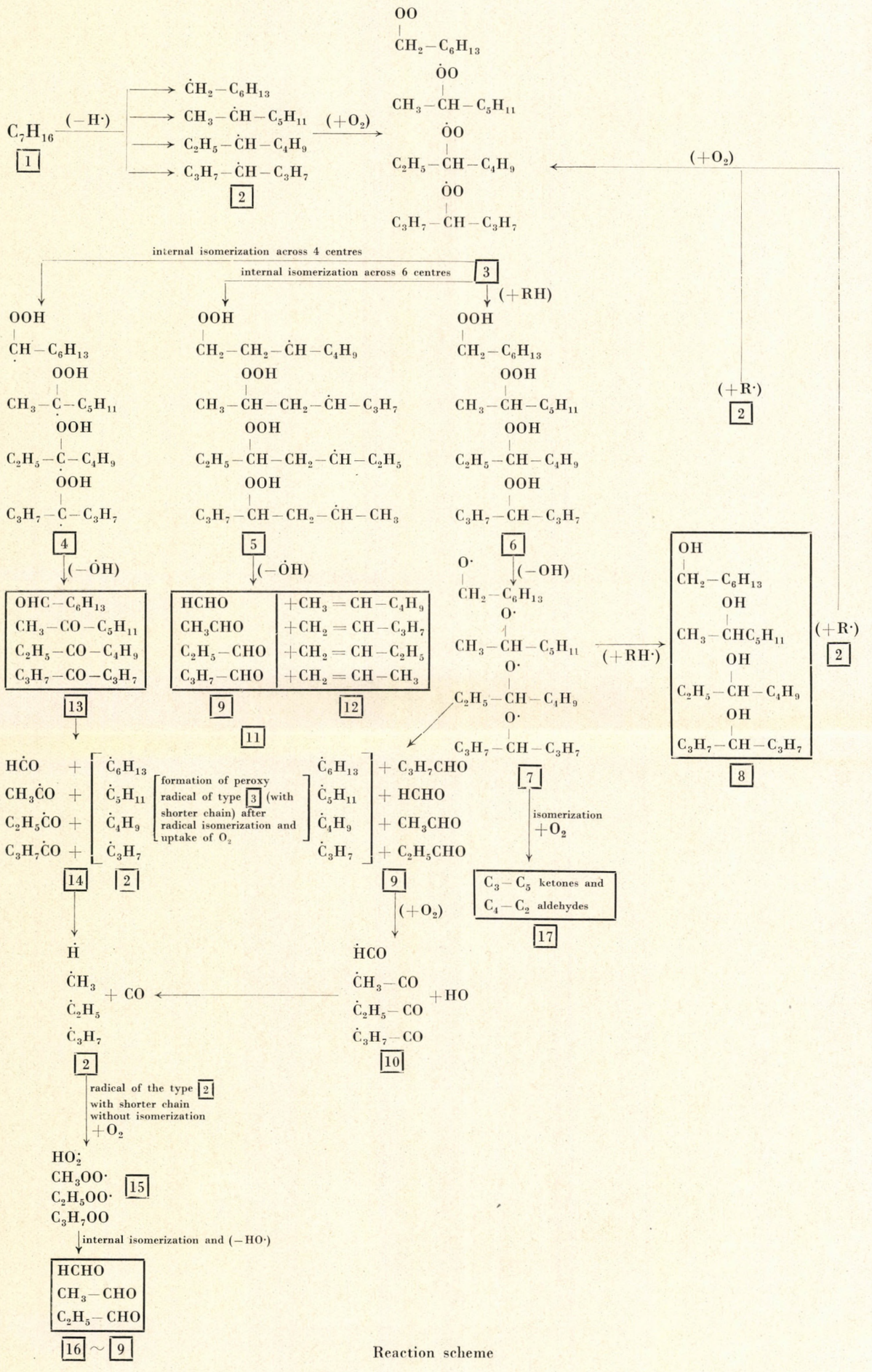

Reaction scheme

cycles too, but they enter the chain process here (3 → 6, 7 → 8). The peroxy radicals thus formed can react further in *three* ways, which are the precursors of the four main end-product cycles (alcohol, aldehyde, ketone, olefin) in the oxidation of heptane.

One of these routes is internal isomerization through a transition state of four centres. This leads to ketones *via* 3 → 4 → 13.

Long-chain ketones are formed only in this way. Shorter-chain ketones are, however, also found as reaction products; their formation can be conceived by the same cycle, with the difference that the above processes are repeated by *shorter* alkyl radicals formed in the steps 13 → 2 and 14 → 2. Their formation will be discussed later on. Acetone forms an exception, and must be dealt with separately.

The energy requirements of the isomerization 3 → 4 have not been completely elucidated. According to KNOX [2], the activation energy of such a process is 22—27 kcal/mole in the case of the rearrangement of a secondary hydrogen in the β-position, and this will naturally be connected with a lower activation energy. FISH [1] assumes rearrangement *via* a cyclic transition state, the activation energy of which is 17 kcal/mole for 5 or 7-membered rings, and 11.1 kcal/mole for 6-membered rings, in the case of the shorter-chain hydrocarbons. BENSON [18] also considers the four-centre rearrangement to be likely, and estimates its activation energy as about 20 kcal/mole. The route 3 → 4, therefore, is probably not very fast, whereas analogies indicate that the step 4 → 13 can take place fairly easily [2]. It is not necessary to consider an extensive decomposition of the ketones formed, because the value of the activation energy calculated from the bond dissociation energies by Szabó's formula, $E = \Sigma D_i - \alpha \Sigma D_j$, amounts to 65 kcal/mole.

The second route for the further reaction of the peroxy radicals is the internal isomerization *via* six centres 3 → 5. Splitting off the ·OH from the hydroperoxy radicals thus formed gives olefins 12 and aldehydes 9. Our experiments were carried out at low temperature, the conversion was very small, and the measurements are characterized by the fact that we are at the beginning of the reaction. Since unsaturated hydrocarbons were not found among our products, the route 3 → 4 is taken to be preferred to 3 → 5. If olefin does form, then it is transformed to the hydroperoxy radical by reaction with $HO_2\cdot$ according to equation (8) of FISH [1].

The *third* cycle propagates the interaction with the hydrocarbon molecule itself which produces the hydroperoxide molecule 6 and regenerates the radical 2. This is energetically similar to the step 1 → 2, since there also $RO_2\cdot$ was assumed as the hydrogen-abstracting radical.

There is no extensive accumulation of the hydroperoxide molecule, because it is converted to the alkoxy radical 7 by the elimination of ·OH. The alkoxy radicals can react further in two ways, and one of these is represent-

ing the fourth product cycle. If there is a repeated hydrogen abstraction from an original hydrocarbon molecule, then with the simultaneous regeneration of the radical [2] a new molecule, the alcohol [8], is obtained. These compounds were not found among the products, and were probably quickly further oxidized. (The course of this, however, is unexplored.) The decomposition of the alkoxy radicals leads to the development of the aldehyde cycle [9]. The other product of the splitting is an alkyl radical, which by means of isomerization and O_2-uptake provides peroxy radicals of type [3], but with shorter chains; these can similarly react further by the above cycles [11]. Similar shorter-chain alkyl radicals may also be formed by the decomposition of the ketones [13] → → [14]; as a result of the higher activation energy, however, this is much less probable than the decomposition of the alkoxy radicals. There are also acyl radicals among their decomposition products, but these readily eliminate CO with the formation of new, already still shorter alkyl radicals via the reaction path [14] → [2].

It is much more likely, however, that the aldehydes formed in step [9] are oxidized and the acyl radicals so formed undergo a decomposition similar to the route [14] → [2]. If the radicals formed are oxidized without isomerization, this provides the peroxy radicals [15], which undergo internal isomerization and split off ·OH to give aldehyde end-products similar to [9].

The aldehydes may therefore appear among the products *via* a number of pathways. On examination of the analytical results obtained in this work it is striking that the aldehydes are found in relatively low amounts. Their oxidation is assumed in the reaction scheme, but attention must also be drawn to the fact that although the thermal decomposition of the aldehydes begins only at 400—500 °C, in the presence of oxygen sensitized decomposition and oxidation occur at much lower temperatures [20—22]. The decomposition of ketones (acetone) can be induced only in the region of 450 °C.

It was mentioned earlier that the formation of acetone must be dealt with separately. Although there are three places in the reaction scheme where propyl radicals are formed, as precursors for acetone formation, it is still necessary for them to isomerize. This can take place on the wall:

$$\dot{C}H_2-CH_2-CH_3 \xrightarrow{\text{wall}} CH_3-\dot{C}H-CH_3 \xrightarrow{O_2}$$

$$\xrightarrow{O_2} CH_3-\underset{\displaystyle OO\cdot}{\underset{|}{CH}}-CH_3 \longrightarrow CH_3-\overset{\displaystyle O}{\overset{\|}{C}}-CH_3 + \cdot OH$$

Considering a remark by BENSON [23], another route for the formation of acetone can be derived from the oxidation scheme in the following way: The alkoxy radicals [7] can react further not only by the two pathways already

discussed (C–C bond splitting, or abstracting hydrogen from another heptane molecule), but can also undergo internal isomerization to form an alcohol radical:

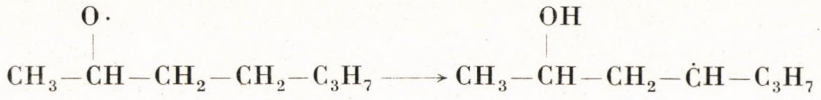

The latter takes up another oxygen molecule:

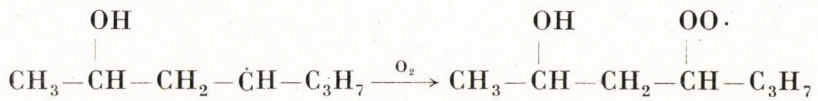

nd then isomerizes:

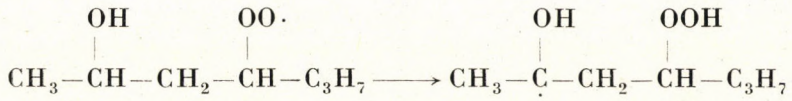

ollowed by decomposition in an exothermic process:

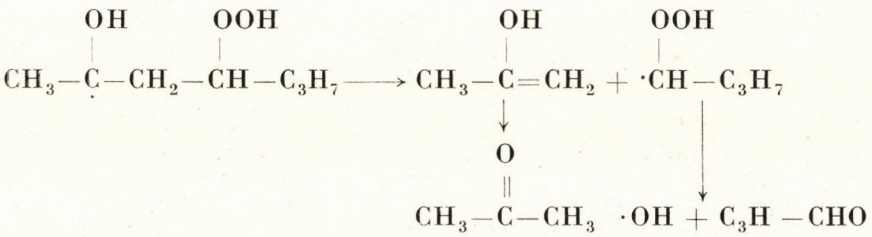

Thus, the formation of acetone can be explained by this series of elementary steps with no difficulty, *via* the enol-keto transformation.

Table IV shows the reaction steps of the above scheme grouped according to the individual products. It can be seen from the Table that acetaldehyde, for instance, may be formed in the system *via* five different routes. (Steps playing a part in the formation of a given product are given within a square frame.) Similarly, there are five different routes for the formation of propionaldehyde, three for butyraldehyde, and so on. The various formation pathways, however, can contain the same steps, too.

If the oxidation scheme is compared with the product distribution, the following conclusions can be made.

The data of the wall-free experiments are in agreement with the proposed mechanism as follows. It is probable that the routes [3] → [4] and [3] → [5], that is the formation of aldehydes and ketones by internal rearrangement, are

Table IV

Pathways of the formation of the products

Acetaldehyde	[1]	[2]	[3]	4	5	[6]	[7]	8	[9]	10	11	12	13	14	15	16	17
	[1]	[2]	[3]	[4]	5	6	7	8	9	10	11	12	[13]	[14]	[15]	[16]	17
	[1]	[2]	[3]	4	5	[6]	[7]	8	[9]	[10]	11	12	13	14	[15]	[16]	17
	[1]	[2]	[3]	4	[5]	6	7	8	[9]	10	11	12	13	14	15	16	17
	[1]	[2]	[3]	4	5	[6]	[7]	8	9	10	11	12	13	14	15	16	[17]
Propionaldehyde	[1]	[2]	[3]	4	5	[6]	[7]	8	[9]	10	11	12	13	14	15	16	17
	[1]	[2]	[3]	[4]	5	6	7	8	9	10	11	12	[13]	[14]	[15]	[16]	17
	[1]	[2]	[3]	4	5	[6]	[7]	8	[9]	[10]	11	12	13	14	[15]	[16]	17
	[1]	[2]	[3]	4	[5]	6	7	8	[9]	10	11	12	13	14	15	16	17
	[1]	[2]	[3]	4	5	[6]	[7]	8	9	10	11	12	13	14	15	16	[17]
Butyraldehyde	[1]	[2]	[3]	4	5	[6]	[7]	8	[9]	10	11	12	13	14	15	16	17
	[1]	[2]	[3]	4	[5]	6	7	8	[9]	10	11	12	13	14	15	16	17
	[1]	[2]	[3]	4	5	[6]	[7]	8	9	10	11	12	13	14	15	16	[17]
Acetone	[1]	[2]	[3]	4	5	[6]	[7]	8	9	10	11	12	13	14	15	16	[17]
Methyl ethyl ketone	[1]	[2]	[3]	4	5	[6]	[7]	8	9	10	11	12	13	14	15	16	[17]
	[1]	[2]	[3]	[4]	5	6	7	8	9	10	11	12	[13]	14	15	16	17

preferred to the route [3] → [6]. For this reason alcohols were not detected, and the peroxides did not accumulate. The fact that ketones were formed in greatest amounts has already been explained by the induced decomposition and oxidation of the aldehydes which has been observed at this temperature.

In the case of the NaOH coating the amounts of aldehydes are larger (by a factor of five for a certain wall position) than for the wall-free reaction. At the same time, however, the amounts of ketones are also greater than in the wall-free state. If the mechanism and the experimental data are compared, the step [3] → [4] is the starting point of a process which leads to both ketones and aldehydes, and therefore it appears obvious that the wall exerts an effect on the isomerization step [3] → [4]. It is, however, difficult to explain the appearance of the maximum in the vicinity of wall position III.

With the lead oxide coating the amounts of ketones decrease considerably, and the product curve rises in proportion to the residence time, but to

a small extent only. Here too there is a maximum in the case of the aldehydes, and in contrast with the ketones their amounts increase. This shows that the lead oxide inhibits the internal isomerization taking place through four centres, and thus either the reaction path [3] → [5] or [3] → [6] must prevail. Since the abstraction of hydrogen from the starting hydrocarbon occurs with higher probability from a secondary carbon atom, it is understandable that acetaldehyde and propionaldehyde will be formed primarily, because these result from the step [5] → [9] and the step [15] → [9], while butyraldehyde is formed only *via* a primary radical.

In the case of the wall treated with Na_2HPO_4, the relative accumulations of propionaldehyde and butyraldehyde are the most significant; these are formed in the lowest amounts in the wall-free reaction. This suggests that here the isomerization [3] → [4] predominates.

With the HNO_3-treated wall, the acetaldehyde exhibits significant maxima at positions II and IV. Here, too, the relative increase of the amounts of ketones is less considerable.

REFERENCES

1. Fish, A.: Adv. in Chem. **76,** 69 (1968)
2. Knox, J. H.: Adv. in Chem. **76,** 1 (1968)
3. Szabó, Z. G.: Seventh Symposium on Combustion, Butterworths, London, 1958, p. 118
4. Egerton, A. C., Minkoff, C. J., Salooja, K. C.: Combustion and Flame **1,** 257 (1957)
5. Bonner, B. M., Tipper, C. F. H.: Combustion and Flame **9,** 387 (1965)
6. Cartlidge, J., Tipper, C. F. H.: Proc. Roy. Soc. **261,** 388 (1961)
7. Salooja, K. C.: Combustion and Flame **9,** 219 (1965)
8. Knox, J. H.: Combustion and Flame **9,** 297 (1965)
9. Szabó, Z. G., Galiba, I., Gál, D.: Acta Chim. Acad. Sci. Hung. **42,** 339 (1964)
10. Hoare, D. E., Walsh, A. D.: Proc. Roy. Soc. **A215,** 454 (1952)
11. Kokatnur, B. R., Jellin, M.: J. Am. Chem. Soc. **63,** 1432 (1941)
12. Schröder, E., Öhlmann, G., Leibnitz, E.: Z. Physik. Chem. **225,** 168 (1964)
13. Lischke, G., Öhlmann, G., Schirmer, W.: Z. Physik. Chem. **230,** 73 (1965)
14. Bérces, T., Trotman-Dickensom, A. P.: J. Chem. Soc. (London) **1961,** 4281
15. Szabó, Z. G.: Chem. Soc. London, Spec. Publ. **16,** 113 (1962); Szabó, Z. G., Bérces, T.: Z. Physik. Chem. N. F. **57,** 113 (1968)
16. Otozai, K.: Bull. Soc. Chem. Japan **24,** 218 (1951)
17. Benson, S. W.: J. Am. Chem. Soc. **87,** 972 (1965)
18. Benson, S. W.: Personal communication, Edinburgh, 1970
19. Szabó, Z. G., Bérces, T.: Z. Physik. Chem. N. F. **57,** 3 (1968)
20. Gál, D., Galiba, I., Szabó, Z. G.: MTA Oszt. Közl. **8,** 3 (1957)
21. Nicolause, M., Letort, M.: Compt. rend. **226,** 77 (1948)
22. McDowell, C. A., Farmer, J. B.: Fifth Symposium on Combustion, New York, 1955, p. 453
23. Benson, S. W.: Personal communication, Symposium on Gas-kinetics, Szeged, 1969

Zoltán Gábor Szabó; Budapest VIII., Múzeum krt. 4/b.
Ilona Galiba; Szeged, Dóm tér 7, Hungary.
Dezső Gál; Budapest II., Pusztaszeri út 57/69.

Acta Chimica Academiae Scientiarum Hungaricae, Tomus 74 (2), pp. 253—266 (1972)

STUDY OF DEGRADATION IN DIMETHYLSILOXANE CONTAINING POLYMERS BY DYNAMIC THERMOGRAVIMETRY AND PYROLYSIS GAS CHROMATOGRAPHY

B. LENGYEL, T. SZÉKELY and G. GARZÓ

(Research Group for Inorganic Chemistry, Hungarian Academy of Sciences, Budapest)

Received February 28, 1972

The thermal degradation of poly(dimethylsiloxanes) (PDMS) with various terminal groups, and with titanium and potassium as heteroatoms has been studied. The thermogravimetric evaluation of the kinetics was performed by the DDTG method proposed by the authors. As a further development of this method a novel calculation procedure was elaborated permitting the separation and accurate kinetic description of several consecutive degradation processes reflected by the changes in weight. All derivatives of PDMS were found to exhibit a degradation step which is characterized by an activation energy of 43—46 kcal/mol.

It was shown by pyrolysis gas chromatography that this decomposition step is characterized by product ratios practically independent of the pyrolysis temperature between 400 and 600 °C, the molecular weight of the sample and the nature of the terminal group. Thus the possibility of an end group initiation must be excluded. In the presence of a heteroatom (a terminal K atom, or a Ti atom in the chain), however, initiation by the terminal atom and catalytic depolymerization take place.

The experimental results and the calculated data support the mechanism proposed by THOMAS and KENDRICK for the degradation of PDMS.

Introduction

Poly(dimethylsiloxane) (PDMS) serves as the basis of a number of silicone products widespread in industrial manufacture. Besides, the derivatives of PDMS play a significant role in inorganic polymer chemistry. Accordingly, it is quite obvious that the thermal stability of PDMS and of its derivatives have been attracting the interest of scientists since more than two decades. Despite the great number of results published in this field there is no agreement as regards the interpretation of thermal degradation and the determination of the factors limiting thermal stability. This is particularly true for the assumptions concerning the mechanism and mainly the initiation of these reactions.

It has been shown already by the very first studies [1] that the thermal degradation of PDMS affords exclusively cyclic oligomers, *i.e.* depolymerization occurs instead of pyrolysis. It is also known [2, 3] that depolymerization is catalyzed by alkali metal oxides and hydroxides, in the presence of which it takes place significantly faster or at temperatures lower by 150—200 °C.

KUCERA [4] and LEWIS [5] have pointed out that the thermal stability can be greatly improved by removing these catalytic traces. In view of this it

is rather difficult to distinguish catalytic and non-catalytic depolymerization experimentally. Thus the problem of the actual, intrinsic thermal stability of PDMS remains unsolved.

The role of the catalyst seems to be another unsolved problem. The depolymerizing effect of metals is regarded by a number of authors, *e.g.* by NOLL [6], as an inverse process of the known polymerization reaction catalyzed by acids and bases.

According to RODE *et al.* [7], the terminal hydroxyl group plays a decisive role in the degradation of simple siloxanes. Calculations have been carried out by these authors on the secondary bond energies expected upon the formation of the activated complex corresponding to the so-called 'back biting' mechanism. It follows from these calculations that the hydroxyl group retains its terminal position, seemingly by intramolecular transfer, while the cyclic oligomer is split off. ALEXANDROVA *et al.* [8] have shown by gas chromatography that methane is formed during degradation: this observation has been used to interpret the formation of rings and the degradation of the polymer. According to THOMAS and KENDRICK [9] the activated complex of the decomposition process is a ring formed from neighbouring segments of the intramolecular helix owing to the interaction of —Si—O— groups. The decomposition of this complex leads to a single small molecule and a new macromolecule of lower molecular weight. In terms of the kinetics of polymer degradation this process resembles initiation by random chain scission without any depropagation, followed by a single intramolecular transfer and then by recombination, since after the cleavage of the ring a chain completely similar to the initial one but of a slightly lower molecular weight is formed.

The purpose of the present work is to continue our earlier studies [10], on the kinetics of depolymerization in PDMS systems significantly differing from one another. We also intended to examine the effect of the end-group of the chain and of the heteroatoms on the mechanism of degradation. In order to solve the kinetic problem, thermogravimetric investigations (TG) have been performed. To elucidate the second group of problems experiments by pyrolysis gas chromatography (PGC) have been carried out.

Kinetic analysis of two independent reactions

The thermobalance often produces degradation curves which, already at first glance, appear to indicate two or more independent steps. The degradation of simple inorganic or organic compounds may take place in a way that the solid (or non-volatile) degradation product of the initial substance undergoes further transformation at a higher temperature with additional loss of weight. One of the best known processes of this type is the decomposition of calcium

oxalate:

$$Ca(COO)_2 = CaCO_3 + CO \tag{1}$$

$$CaCO_3 = CaO + CO_2$$

Processes of this type, with the characteristic temperature intervals of decomposition completely separated from each other, are rather rare. No difficulties are met in the kinetic analysis because the two parts of the thermogravimetric curve can be regarded independent of each other.

In the case of polymer degradation and the decomposition of some other organic substances the relation between the two chemical processes is quite different from that in the above example. Generally, the starting materials of independent reactions are present already at the beginning of decomposition but their degradation starts and proceeds at different temperatures. It is also conceivable that the two substances of different thermal stability are not present as a physical mixture but as various parts of the same molecule (*e.g.* main chain *vs.* side group, defect points *vs.* basic structure, etc.). In the case of such processes the temperature intervals of the two reactions are very rarely as far from each other as in the case of inorganic substances. Therefore, the individual TG steps overlap strongly and often cannot be distinguished by inspection of the TG curve; their existence can be detected only by a trained expert. The two reactions appear more clearly on the DTG curve. The complex character of the degradation process, however, becomes particularly conspicuous if the experimental results are treated in the way described by us earlier [10, 11, 12]. The method utilizing besides the first derivative also the second derivative (DDTG) leads to the equation

$$I \equiv \frac{(d^2w/dt^2)T^2}{(dw/dt)} = \frac{(dw/dt)T^2}{w}\, n + \frac{E(dT/dt)}{R} \equiv Kn + \frac{EB}{R} \tag{2}$$

If the process can be described in a simple 3-parameter form, and the remaining weight fraction (w) is used as the reaction coordinate then

$$-\frac{dw}{dt} = Ae^{-E/RT}\, w^n \tag{3}$$

and a linear correlation is obtained between I and K.

In the kinetic analysis of polymer degradation one rarely finds substances that can be treated in this simple way. At the beginning of thermal treatment the degradation mechanism mostly differs from that in a later phase of the process. The calculation methods described in the literature generally provide

average values for the overall process and thus lead to erroneous kinetic parameters. The initial reaction leads to particularly great distortions if the evaluation is carried out by the common method of determining the initial rates. On the basis of this method, THOMAS and KENDRICK calculated activation energies [13] for the degradation of siloxanes from the initial change amounting to only about 20% of the sample weight, and drew conclusions from the results obtained in this way.

In our opinion it is worthwhile to attempt the separation of the two reactions in all similar instances and also in the case of reactions which take place conspicuously in two steps. DOYLE [14] suggested that the point of division between the two consecutive degradation processes on the TG curve should be determined visually or by a graphical method. However, this procedure may be the source of serious error even if we neglect the cases mentioned above in which this method fails, because the two steps on the TG curve cannot be observed visually. Our kinetic treatment is based on the remaining weight fraction defined by

$$w = \frac{g_t - g_\infty}{g_0 - g_\infty} \tag{4}$$

where g_0, g_t and g_∞ are the sample weight at time zero, at an arbitrary moment t, and after the decomposition, respectively. The error according to the procedure of DOYLE is due to the more or less arbitrary choice of the initial weight The method suggested by us offers a simple means for the accurate determination of the true initial weight (g_{0_2}) of the second reaction by extrapolation. Taking into account the definition of w by Eq. (4), one can rearrange Eq. (2) using the experimental value of g_t and of its derivatives:

$$I = \frac{(d^2g_t/dt^2)T^2}{(dg_t/dt)} = \frac{(dg_t/dt)T^2}{g_t - g_\infty} n + \frac{E(dT/dt)}{R} = Kn + \frac{EB}{R} \tag{2a}$$

Equation (2a) does not contain the initial weight, whereas the final weight is identical with the last weight data measured (g_∞). The latter is zero for substances without degradation residues.

Consequently, Eq. (2a) may be used to calculate the activation energy and the apparent reaction order in that stage of the reaction where the first degradation step already does not play any role. Thus, by calculating the values of I and K from the experimental data and plotting I against K, we shall by all means find a linear section on the second part of the diagram which will be acceptable for the second reaction. On applying Eq. (2a) to this section we obtain both kinetic parameters (E_2 and n_2) for the second reaction.

The integration of Eq. (3) and substitution of Eq. (4) lead to Eq. (5), which is suitable for the calculation of the required values in all cases if $n \neq 1$:

$$\int_0^w \frac{dw}{w^n} = \frac{1-(g_t/g_0)^{1-n}}{1-n} = \frac{AE}{BR}\left(\frac{e^{-x}}{x} - \int_x^\infty \frac{e^{-u}}{u}\,du\right) \equiv \frac{AE}{BR}\,p(x) \qquad (5)$$

$$x = \frac{E}{RT} \qquad g_\infty = 0$$

On applying Eq. (5) to the second reaction and rearranging:

$$g_t^{1-n_2} = g_{t_2}^{1-n_2} = \frac{A_2E_2(n_2-1)g_{0_2}^{1-n_2}}{BR}\,p(x_2) + g_{0_2}^{1-n_2} \qquad (6)$$

From Eq. (6) now the values of g_{0_2} and A_2 can be calculated, using the weights (g_t) for the section, selected as described above, the temperature and the two kinetic parameters determined earlier.

This procedure yields all the kinetic parameters for the second reaction, moreover the extrapolated value of the initial weight which would have been the true initial weight of the sample had the first reaction not occurred and had the decomposing substance volatilizing in this reaction not been present. However, the weight g_{0_2} is also the final weight in the first reaction ($g_{\infty_1} = g_{0_2}$), whereas the initial weight of the first reaction is obtained by subtracting g_{0_2} from the initial weight of the sample (g_0). Thus, on substituting these quantities into Eq. (4) and calculating the values of g_2, g_2' and g_2'' on the basis of the known parameters A_2, E_2 and n_2 up to the temperature corresponding to the beginning of weight loss, we obtain the quantities g_{t_1}, g_1' and g_1'' by subtracting the values of g_2, g_2' and g_2'' from the experimental data (g_t) for the overall process, and from the values of g' and g'' numerically calculated from the latter. The knowledge of these data now permits to determine the *I vs. K* function for the first reaction, and to calculate the values of E_1, n_1 and A_1.

As a test of the entire technique let us now apply Eq. (5) simultaneously to both reactions in order to obtain numerically the TG curve which is characteristic for the overall process. The algorithm of this calculation is simple, and can be performed by means of a Hewlett—Packard 9100A Calculator, using an attached 9101A Extended Memory Unit, and may be plotted by means of a HP 9125 Plotter (see Figs 2 and 3).

It must be noted that actually any number of steps may be analyzed by repeating the above method. The example of two-step curves has been discussed only for the sake of simplicity.

Experimental and results

The substances investigated are listed in Table I. The applied methods were thermogravimetry and pyrolysis gas chromatography. However, both methods could not be applied in the case of all the substances. Namely, certain substances (*e.g.* that denoted by *F*), owing to their easy decomposition, did

Table I

Substances studied

Symbol	Chemical characteristics of the material
A	PDMS, volatile components removed, molecular weight 10^6;
B	PDMS, volatile components not removed;
C	PDMS, narrow fraction with Si—OH terminal groups, molecular weight 11300;
D	PDMS, narrow fraction with Si—OC_2H_5 terminal groups, molecular weight 2250;
E	PDMS, narrow fraction with Si—CH_3 terminal groups, molecular weight 8600;
F	PDMS, polydisperse, with Si—OK terminal groups;
G	Ti $\{[Si(CH_3)_2O]_{75}Si(CH_3)_2OH\}_4$ (metallosiloxane polymer with titanium as heteroatom)

not give a well-defined initial weight under the working conditions of the thermobalance. The volatile components leaving sample *A* before pyrolysis and the degradation products evolving from sample *B* during pyrolysis are identical. Consequently no distinction between *A* and *B* can be made by means of pyrolysis gas chromatography.

Thermogravimetry

From substances *A*, *B* and *C* samples not exceeding 8 mg were weighed into flat platinum pans. The measurement was carried out in high vacuum (10^{-5}) by means of the Mettler thermobalance 'Thermoanalyzer'.

The TG curves obtained are shown in Figs 1 to 3. The derivatives have been obtained from the TG curves by the mathematical method described earlier [11]. The corresponding *I vs. K* diagrams are shown in Figs 4 to 6. The extrapolation performed according to Eq. (6) is illustrated in Figs 7 and 8.

The kinetic parameters are listed in Table II.

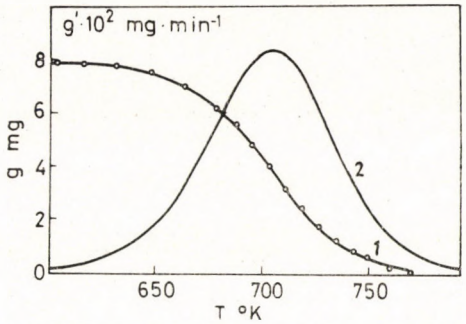

Fig. 1. Substance *A*. 1: TG curve (○ denotes the measured values); 2: DTG curve

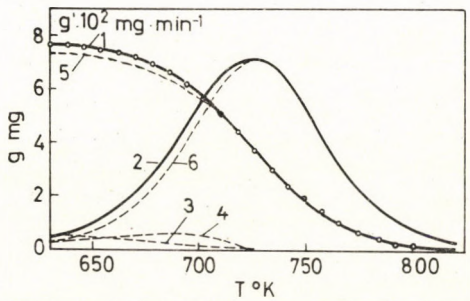

Fig. 2. Substance *B*. 1: TG curve (○ denotes the measured values); 2: DTG curve; 3: TG curve of the first reaction; 4: DTG curve of the first reaction; 5: TG curve of the second reaction; 6: DTG curve of the second reaction

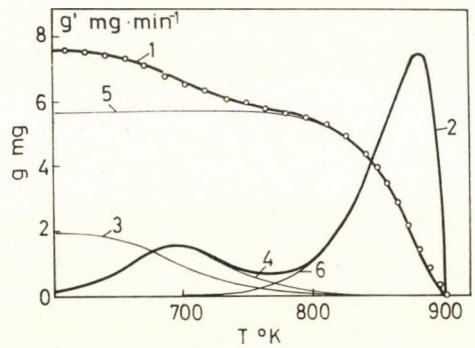

Fig. 3. Substance *G*. 1: TG curve (○ denotes the measured values); 2: DTG curve; 3: TG curve of the first reaction; 4: DTG curve of the first reaction; 5: TG curve of the second reaction; 6: DTG curve of the second reaction

It is clear from Figs 7 and 8 that the linearity required by this method is strictly met. The TG curves simulated by the computer on the basis of the calculated kinetic parameters are in excellent agreement with the measured curves. This proves the correctness of our method applied for resolving the complex process into components.

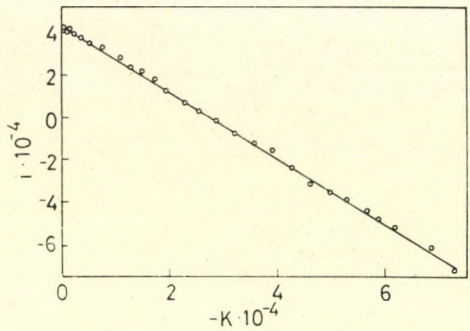

Fig. 4. Substance *A*. Plot of *I vs. K*. The points refer to values calculated from the measured data; the straight line was obtained from these data by linear regression analysis

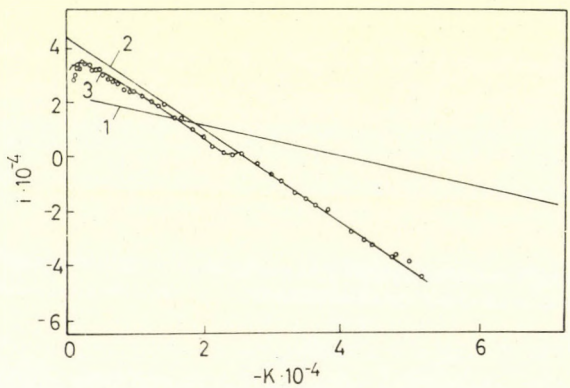

Fig. 5. Substance *B*. Plot of *I vs. K*, for 1: the first reaction in the actual temperature range of degradation; 2: the second reaction in the actual temperature range of degradation; 3: calculated curve for the overall reaction; the points denote the calculated amounts corresponding to the measured values

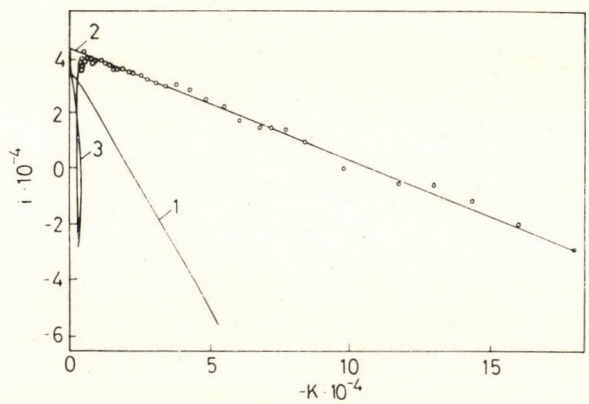

Fig. 6. Substance *G*. Plot of *I vs. K*, for 1: the first reaction in the actual temperature range of degradation; 2: the second reaction in the actual temperature range of degradation; 3: calculated curve for the overall reaction; the points denote the calculated amounts corresponding to the measured values

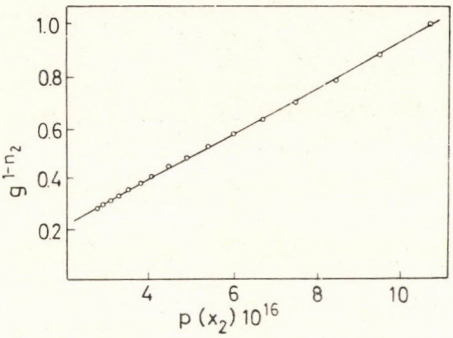

Fig. 7. Substance *B*. Determination of g_{02} on the basis of Eq. (6); the points denote the amounts calculated from the measured values

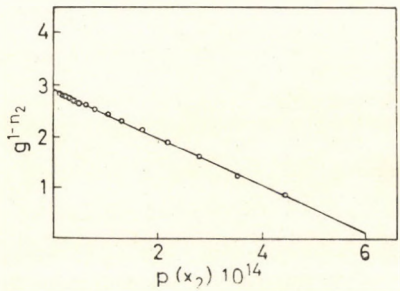

Fig. 8. Substance *G*. Determination of g_{02} on the basis of Eq. (6); the points denote the amounts calculated from the measured values

Table II

Kinetic parameters

Symbol of substance	Activation energy E, kcal/mol^{-1}	Preexponential factor A, min^{-1}	Order of reaction, n
A	42	9.8×10^{11}	1.6
B first reaction	23	1.1×10^{6}	0.6
second reaction	44	1.4×10^{12}	0.7
G first reaction	35	6.7×10^{9}	0.7
second reaction	43	2.5×10^{9}	0.4

Pyrolysis gas chromatography

By using the special micropyrolysis device (microreactor) designed earlier [15], attached directly to the gas chromatographic column, it is possible to carry out the reproducible degradation of polymers at a known temperature. The pyrolysis-chromatograms were recorded at programmed temperatures in a 50 m steel capillary column coated with APL. The quantitative evaluation was carried out by means of an electronic integrator.

We wished first to investigate the extent to which the depolymerization of PDMS depends on the terminal group, *i.e.* whether the initiation process is due to the end group of the chain or to random chain scission. For this purpose various PDMS samples were kept for the same periods (30 and 10 sec), at 450 and 600 °C, in the microreactor, and the volatile products were led directly into the column of the gas chromatograph. As regards the terminal group (trimethylsilyl), sample *E* can be considered as a completely inactive compound and presumably sample *D* is but weakly reactive. However, as already mentioned in the introduction, the opinions differ concerning the silanol group (sample *A*).

Our experiments, the results of which are summarized in Table III (1—4), have confirmed that neither the differences in the terminal groups nor the significant deviations in the molecular weights cause appreciable alterations in the distribution of the concentration of the degradation products.

Table III

Composition (in %) of pyrolysis products at 450 and 600 °C, for PDMS with various molecular weights and various terminal groups

The data are mean values calculated from several measurements
$D_n = (—Si(CH_3)_2O—)_n$ ring

Symbol of substance	No. of pyrolysis run	D_3		D_4		D_5		D_6		D_7	
		450	600	450	600	450	600	450	600	450	600
A	1	70	68	23	25	3	4	1	2	1	1
C	2	71	69	22	20	5	4	3.5	1.5	1.5	0.5
D	3	71	73	14	16	4	4	2	2	1	3
E	4	69	73	21	21	3.5	4.5	2	2	1.5	0.5
Mean value for all pyrolysis runs carried out at 450 °C		70		20		4		2		1	
Mean value for all pyrolysis runs carried out at 600 °C		70.5		20.5		4		2		1	

Moreover it is clear from Table III that the relative amounts measured at two different temperatures are identical within the experimental error. The results obtained on treating the four samples et 450 °C and 600 °C have been summarized in the two lowest rows of Table III. It can be seen that these values may be considered as identical within the experimental error.

In the products of pyrolysis carried out at 420 °C, a markedly lower amount, only 43.7%, of D_3 was found by THOMAS and KENDRICK [9]. In our opinion this may be due to certain losses during their experiment performed in vacuum, which influenced mainly the D_3 content, that of the most volatile component. As in our experiments the products were transferred directly to the gas chromatograph, any losses were excluded. Since both the above error and any possible contaminations of the sample under investigation may manifest themselves only in the decrease of the amount of D_3, in our opinion, our results are more realistic than those given by THOMAS and KENDRICK [9].

The experimental results with PDMS samples (*F* and *G*) containing potassium or titanium as heteroatoms are listed in Table IV. The univalent potassium may be located obviously only in terminal positions, whereas the tetravalent titanium at branching points of the chain. It has been known for long that the Si–OK end-groups of the siloxane chains are capable of exerting a catalytic depolymerizing effect. This is certainly reflected by pyrolysis runs 7—11. It can be seen that a significant amount of degradation products is liberated already at 150 °C as indicated by the sum of the peak areas given

Table IV

Effect of potassium and titanium on the thermal degradation of PDMS

Symbol of substance	No. of pyrolysis run	Temperature of pyrolysis (°C)	Time of pyrolysis (hr)	Total peak area on the pyrogram	Composition of pyrolysis products, %						
					D_3	D_4	D_5	D_6	D_7	D_8	D_9
C	5	150	1	400	—	—	—	—	—	—	—
	6	250	1	1 423	73	18	5	3	—	—	—
F	7	150	1	10 854	5	39	31	23	3	—	—
	8	250	1	34 330	26	29	15	21	7.5	1.5	0.5
	9	250	2	20 620	34	28	13	13	8	3	1
	10	250	4	8 568	36	13	8	21.5	15	5.5	1
	11	450	30 sec	25 403	66	25	6	2	1	—	—
G	12	250	1	21 183	41	40	13	4	—	—	—
	13	250	2	19 585	53	28	13.5	4.5	—	—	—
	14	250	6	15 083	55	17	11	11	4	—	—
	15	600	10 sec	238 483	68.5	21	4.5	2	1	—	—

as a reference number in column 5 of Table IV. For comparison also the data characterizing the behaviour of substance *C* at low temperatures are listed in Table IV. Apparently this sample does not decompose below 150 °C (5), and gives only an ill-developed chromatogram even at 250 °C (6). It is worth noting that the relative amounts found at this latter temperature closely approach the values given in Table III, though the ratio is actually shifted slightly towards D_3.

On comparing experiments 6 and 8 it is conspicuous that, as a result of initiation at the chain-end, the composition of the volatiles undergoes a shift in favour of D_4, and in general the composition becomes more uniform. This is particularly true for experiment 7 where D_3 almost disappears. It may be assumed that under the conditions of depolymerization with low activation energy, initiated by the chain-ends, *i.e.* in the case of depolymerization occurring at low temperatures, D_3 is already thermodynamically unstable owing to the strain existing in the ring, and thus 'back biting' may be commenced not nearer than at the fourth siloxane unit from the chain-end.

The results of continued pyrolysis of the same sample are given by the data of experiments 8, 9 and 10. It is of interest that with the progress of depolymerization the composition of products has a trend towards the increase, instead of decrease, in the quantity of D_3. This is rather surprising since the concentration of the catalyst increases with the decrease of the remaining amount of the sample. Since there are no reasons to assume that above a certain concentration the catalyst would turn into an inhibitor, we may draw the conclusion that in the course of the reaction the catalyst becomes deactivated.

Experiment 11 refers to the pyrolysis of sample *F* carried out for 30 sec at 450 °C. The conditions of this experiment were the same as those for samples *A* to *E* at 450 °C. On comparing these experimental results with the data in Table III, surprisingly small differences (of 4—5%) are observed. From this we may conclude that, at 450 °C, catalytic degradation due to the terminal OK groups is insignificant compared to the intrinsic degradation of PDMS. Obviously, slow heating of the sample to 450 °C would lead to complete catalytic decomposition before attaining that temperature.

At 250 °C and at the beginning of pyrolysis sample *G* shows a $D_3 : D_4$ ratio of about 1 : 1, which is characteristic of catalytic depolymerization [12], although the total amount of D_3 and D_4 is relatively higher than in the case of substance *F* with OK groups at the chain ends. Experiments 12 to 14, illustrating the course of stepwise thermal degradation of a given sample, again indicate a shift towards the product distribution characteristic of the uncatalyzed decomposition, as already seen in the case of sample *F*. Pyrolysis at 600 °C for 10 sec led to a $D_3 : D_4$ ratio of 7 : 2, thus revealing an 'intrinsic' PDMS character. Therefore at this temperature the role of initiation by chain-ends becomes already negligible.

In accordance with pyrograms 12 to 14, the thermogram of sample *G* can be interpreted by assuming that, owing to the presence of titanium, part of the substance is first decomposed catalytically at lower temperatures. The process afterwards stops due to deactivation of the 'catalyst' and it starts again as soon as the intrinsic degradation of PDMS becomes possible.

Conclusions

Both the thermogravimetric and gas chromatographic investigations carried out by us lead to the unambiguous conclusion that the depolymerization of the polydimethylsiloxane chain takes place with an activation energy of 43 to 46 kcal/mol, regardless of the nature of the heteroatom or group of atoms located in the chain or at the chain end. A characteristic product composition rather constant within a broad temperature range corresponds to this intrinsic feature. This degradation pattern is, however, distorted by catalytic degradation, evaporation or other side reactions occurring simultaneously. If, however, we succeed in taking these accompanying phenomena separately into account by means of the calculation method suggested above, we shall obtain about the same characteristic data for PDMS samples of any kind.

Consequently, we are of the opinion that the hypothesis of THOMAS and KENDRICK [9] concerning the degradation of dimethylsiloxanes seems to be confirmed. According to these authors, the initiation process in the degradation of pure PDMS (free of catalysts) is analogous to random chain scission. In concordance with others, they presume that the chain of the molecule is strongly spiralized. Between Si–O bonds of the vicinal spirals, a tetranuclear activated complex is formed, whose rearrangement is responsible for the formation of cyclic oligomers D_n. The energy requirement of this process is considerably lower than the Si–O bond energy. According to our experience, the characteristic activation energy for the degradation of dimethylsiloxane is nearly the same in the various polymers. Together with the fact that the relative amounts of the homologous degradation products are independent of the temperature within a broad range (from 450 to 600 °C), this supports the view that this depolymerization process and its products are related to a secondary molecular structure of preformed geometry and a very significant conformational energy. It also follows from the experimental results that the relative amounts of volatile products in the case of both the catalytic and noncatalytic process are primarily controlled thermodynamically and not kinetically.

REFERENCES

1. LEWIS, C. W.: J. Polym. Sci., **33,** 153 (1958)
2. DBP 875046 (1942)
3. AP 2455999 (1944)
4. KUCERA, M., LANIKOVA, J.: J. Polym. Sci., **59,** 79 (1962)
5. LEWIS, C. W.: J. Polym. Sci., **37,** 425 (1959)
6. NOLL W.: Chemie und Technologie der Silicone. Verl. Chemie, 1968.
7. RODE, V. V., VERHOTIN, M. A., RAFIKOV, S. R.: Vys. Soed., **A, 11,** 1529 (1969)
8. ALEXANDROVA, YU. A., NIKITINA, T. S.: Vys. Soed., **A, 10,** 1078 (1968)
9. THOMAS, T. H., KENDRICK, T. C.: J. Polym. Sci., A-2, **7,** 537 (1969)
10. LENGYEL, B.: Kém. Közl. **30,** 271 (1968)
11. SZÉKELY, T.: Chim. Ind. Gen. Chim., **104,** 905 (1971)
12. LENGYEL, B., SZÉKELY, T.: Monatshefte Chem. **24,** (1972).
13. THOMAS, T. H., KENDRICK, T. C.: J. Polym. Sci., A-2, **8,** 1823 (1970)
14. DOYLE, C. D.: J. Appl. Polym. Sci., **5,** 285 (1961)
15. GARZÓ, G., TAMÁS, J., SZÉKELY, T., ÚJSZÁSZI, K.: Acta Chim. Acad. Sci. Hung., **69,** 273 (1971)

Béla LENGYEL
Tamás SZÉKELY
Gabriella GARZÓ
Budapest VIII., Múzeum krt. 6—8.

INDEX

KISS, L., FARKAS, J. and FÓTHI, Á.: Untersuchung der Ionisation von Metallen und der Neutralisation von Metallionen mit der Rotierenden Ring-Scheibenelektrode, IX. (Investigation of the Ionisation of Metals and of the Neutralisation of Metal Ions on the Rotary Ring-and-Disc Electrode, IX) 123

KISS, L., LAKATOS-VARSÁNYI, M. and DO NGOC LIEN: Anodic Behaviour of Iron in Formamide Solutions 135

LÉVAY, B.: New Method for the Determination of Stability Constants of Molecular Complexes from Self-Diffusion Data 143

VÉRTES, A., FRAKNÓY-KŐRÖS, V., LÉVAY, B., GELENCSÉR, P. A. and RANOGAJEC-KOMOR M.: Investigation of the Antimony Content of Calcium Halophosphate Luminescent Powders by Mössbauer Spectroscopy 151

VÉRTES, A., RANOGAJEC-KOMOR, M. and SUBA, M.: Investigation of the Hydrolysis of Antimony Chloride by Mössbauer Spectroscopy 159

LÁZÁR, K., HORVÁTH-PARDAVI, M. and VÉRTES, A.: Magnetic Properties of the Binuclear Ion $[Fe_2(OH)_2(H_2O)_8]^{4+}$ 163

KARÁCSONYI, R., KAPOSI, O., RIEDEL, M., HOBINKA, I. and PODMANICZKY, I.: A Study of the Positive Ion Emission of Molybdenum by Means of a Time-of-Flight Mass-Spectrometer 169

FODOR-CSÁNYI, P.: An Interpretation of the Behaviour of Scintillation Systems by the Spectral Properties of the Components 179

SZABÓ, K., MIHÁLYI, L. and MIKA, J.: Effect of Mercury Impurities on the Hydrogen Overvoltage on Gallium Electrodes 185

DÉVAY, J., LENGYEL, B. JR., SAYED SABET ABD EL REHIM and BAKOS, J.: Study of the A. C. Corrosion of Nickel by Linear Polarization 193

DÉVAY, J., JANÁSZIK, F., MÉSZÁROS, L. and HORKAY, F.: Electrochemical Method for the Investigation of the Corrosion Resistance of Paint Coatings 199

DÉVAY, J., MÉSZÁROS, L. and GARAI, T.: Third Harmonic Component of the Electrode Current Due to a Sinusoidal A. C. Voltage in the Case of Diffusion and Transfer Polarization 205

BERECZ, E. and BÁDER, I.: Comparative Study of the Variations in the Properties of Binary Solutions on Temperature Change or on Addition of a Third Component, and its Application to the Viscosity of Metal Chloride–HCl–H_2O Systems 213

NAGY, F., MINK, GY. and MÓGER, D.: Selective Poisoning of Pt Catalysts by CO_2 Chemisorption, I. Reaction of CO_2 with Adsorbed Hydrogen 225

NAGY, M., WOLFRAM, E., INZELT, GY. and BEKE, GY.: Effect of the Structure of Liquid Mixtures on the Equilibria of Polymer Gel–Aliphatic Alcohol–Water Systems 233

SZABÓ, Z. G., GALIBA, I. and GÁL, D.: Study of the Oxidation of *n*-Heptane 239

LENGYEL, B., SZÉKELY, T. and GARZÓ, G.: Study of Degradation in Dimethylsiloxane Containing Polymers by Dynamic Thermogravimetry and Pyrolysis Gas Chromatography 253

Printed in Hungary

A kiadásért felel az Akadémiai Kiadó igazgatója — Műszaki szerkesztő: Botyánszky Pál

A kézirat nyomdába érkezett: 1972. VI. 14. — Terjedelem: 13 (A/5) ív, 61 ábra, 1 melléklet.

72.73749 Akadémiai Nyomda, Budapest — Felelős vezető: Bernát György

ACTA CHIMICA

ТОМ 74 — ВЫП. 2

РЕЗЮМЕ

Изучение ионизации металлов и восстановления ионов металлов с помощью вращающегося дискового электрода с кольцом, IX

Л. КИШ, Й. ФАРКАШ и А. ФОТИ

На основании уравнений, выведенных в предыдущих сообщениях [1—3], с помощью электронновычислительной машины были рассчитаны поляризационные кривые двухстадийного двухэлектронного процесса, происходящего на вращающемся дисковом электроде и предельные токи, возникающие при этом на кольцевом электроде.

Изучение анодного поведения железа в формамидных растворах

Л. КИШ, Л. М. ВАРШАНИ и ДО НГОК ЛИЕН

Было изучено гальваностатическим и потенциостатическим методами анодное растворение и пассивация железа в безводных и водных формамидных растворах KCl, $KClO_4$, CH_3COOH и CH_3COONa.

Определено, что равномерное анодное растворение активного железа происходит только в растворах, содержащих уксусную кислоту или ацетат натрия. В растворах, содержащих только хлористый калий или перхлорат калия возникает питтинг.

В формамидных растворах уксусной кислоты и ацетата натрия пассивация имеет место только в присутствии воды.

Новый метод определения констант стабильности молекулярных комплексов, исходя из данных самодиффузии, I

Исследование равновесия молекулярного комплекса пиридин-йод в четыреххлористом углероде

Б. ЛЕВАИ

Коэффициент самодиффузии йода измерялся в четыреххлористом углероде, содержащем пиридин, в зависимости от концентрации пиридина при 25 и 35°C.

Был разработан новый метод измерения константы равновесия молекулярного комплекса с составом 1 : 1. Константа стабильности для молекулярного комплекса пиридин-йод, рассчитанная из данных самодиффузии, равна 108 dm^3/моль при 25°C и 70 dm^3/моль при 35°C. Энтальпия комплексообразования равна —7,9 ккал/моль.

Коэффициент самодиффузии комплекса при 25 и 35°C равен $1{,}01 \cdot 10^{-5}$ и $1{,}20 \cdot 10^{-5}$ $см^2$/сек, соответственно.

Коэффициент самодиффузии комплекса равен 0,685 от коэффициента самодиффузии свободной молекулы йода. Это подтверждает те представления, что атомы йода в комплексе расположены в плоскости придинового кольца и на одной прямой с атомом азота.

Исследование содержания сурьмы в металлических порошках галофосфата кальция с помощью спектроскопического метода Мёссбауэра

А. ВЕРТЕШ, В. ФРКНОЙ-КЁРЁШ, Б. ЛЕВАИ, П. А. ГЕЛЕНЧЕР и М. РАНОГАЕЦ-КОМОР

В связи с исследованиями металлических порошков галофосфата кальция, содержащего сруьму, спектроскопическим методом Мёссбауэра был разработан полуэмпирический метод определения оптимальной толщины слоя абсорбента, а также минимальное время измерения, необходимое для достижения заданной точности. Были сняты спектры Мёссбауэра образцов металлического порошка, приготовленного различными способами. Согласно величине изомерного сдвига электронное строение сурьмы в металлических порошках подобно строению в SO_2O_3, но может изменяться и приобретать более ионный характер в зависимости от условий приготовления. Величина уширения полос свидетельствует о присутствии атомов сурьмы с одинаковым состоянием окисления, но с различающимся слегка окружением.

Исследование гидролиза хлористой сурьмы с помощью спектроскопического метода Мёссбауэра

А. ВЕРТЕШ, М. РАНОГАЕЦ-КОМОР и М. ШУБА

Гидролиз хлористой сурьмы был исследован с помощью спектроскопического метода Мёссбауэра. Было утсановлено, что гидролиз протекает ступенчато, и донорность гидроксида в растворе больше, чем хлорида.

О магнитных свойствах двуядерного иона $Fe_2(OH)_2(H_2O)_8^{+4}$

К. ЛАЗАР, М. ХОРВАТ-ПАРДАВИ и А. ВЕРТЕШ

При изучении магнитной восприимчивости и эффекта Мёссбауэра полимерных продуктов, образующихся при гидролизе растворов перхлората железа(III), было найдено, что на один атом железа приходится около трех 3d электронов с неспаренными спинами.

Исследование эмиссии положительных ионов молибдена на основе времен полёта в масс-спектрометре

Р. КАРАЧОНИ, О. КАПОШИ, М. РИДЕЛЬ, И. ХОБИНКА и И. ПОДМАНИЦКИ

Молибден, полученный с помощью технологии порошковой металлургии, нагревался с определенной скоростью и до заданной температуры. Исследовались ионы, эмитируемые молибденом при нагревании последнего. Было установлено, что за всё время нагрева наряду с ионами K^+ и Na^+, при более высоких температурах, наблюдается эмиссия ионов Rb^+.

Рассматриваются кривые интенсивности ионной эмиссии во времени. В каждом случае, как для калия, так и для натрия, были получены кривые с двумя максимумами, почти экспоненциально затухающие. Первый максимум приписывается десорбции примесей на поверхности, протекающей с увеличением температуры. В образовании второго максимума кривой могут принимать участие многие суперпонирующие процессы, а именно диффузия, испарение основного составляющего металла, его окисление и испарение продуктов окисления.

Было установлено, что доля калия в токе всех эмитированных ионов возрастает при уменьшении скорости нагрева.

На основе исследования отношения содержания ионов для волокон, прокаленных один раз и подвергнутых повторному нагреву, было доказано, что натрий быстрее достигает своей начальной концентрации на поверхности, чем калий. Это может быть объяснимо величинами радиусов ионов, оказывающих влияние на скорость диффузии. Таким образом, измерения ионной эмиссии могут быть также использованы для измерения коэффициентов диффузии.

Интерпретация поведения сцинтиляционных систем на основе спектральных свойств их компонентов

П. ФОДОР-ЧАНИ

Три различных типа явлений: фосфоресценция, хемилюминесценция и светоиспускание систем интерпретируются на основе спектральных свойств компонентов сцинтиляционных систем и на основе передачи энергии через радиацию.

Влияние примесей ртути на перенапряжение водорода на галлиевом электроде

К. САБО, Л. МИХАИ и Й. МИКА

Было исследовано влияние небольших количеств примесей ртути (м. д.) на перенапряжение водорода на твердом и жидком галлиевом электроде. Было установлено, что с увеличением содержания ртути увеличивается перенапряжение как на твердом, так и на жидком галлие.

Увеличение μ, при одинаковом содержании примесей, больше на твердом, чем на жидком электроде. Перенапряжение на твердом электроде, загрязненном ртутью, в изученном интервале содержания ртути, всегда больше, нежели на жидком ($\eta_{st} > \eta_l$).

В случае твердого электрода, с увеличением содержания примесей ртути, в то время как η увеличивается, величина емкости уменьшается. В случае жидкого электрода, с увеличением содержания ртути наблюдается смещение кривых $C-\varphi$ в положительном направлении.

Экспериментальные данные могут быть хорошо объяснены на основе адсорбции ртути на поверхности галлия.

На основе полученных результатов было сделано заключение о различиях в механизме влияния ртути на электроды галлия в двух различных фазах.

Исследования коррозии никеля за счет переменного тока с помощью метода линейной поляризации

Й. ДЕВАИ, Б. ЛЕНДЬЕЛ, МЛ., САЕД САБЕТ АБД ЭЛЬ РЕХИМ и Й. БАКОШ

Коррозия никеля за счет переменного тока была изучена в 5%-ом растворе NaCl с помощью метода линейной поляризации. Сущность данного метода заключается в том, что переменный ток, регулируемый с помощью потенциостата, подавался извне на ячейку, т. е. суперпонировался на постоянный ток, и было исследовано его влияние на поляризационное сопротивление и на коррозионный ток. Было установлено, что переменный ток, в зависимости от его плотности и частоты, увеличивает значение коррозионного тока, т. е. коррозию металлического никеля.

Определение защитной способности красочных покрытий от коррозии с помощью электрохимического метода

Й. ДЕВАИ, Ф. ЯНАСИК, Л. МЕСАРОШ и Ф. ХОРКАИ

Был разработан электрохимический метод исследования коррозионных процессов, протекающих на поверхности окрашенной стали под влиянием агрессивных сред.

Метод основан на измерении поляризационного сопротивления электрода, погруженного в корродирующую среду.

Исследования, проведенные на образцах, приготовленных различными путями и подвергнутых различной предварительной обработке и дальнейшему корродирующему влиянию различного качества, на протяжении различных времен и с различными интенсивностями, и лишь после этого окрашенных, приводят к результатам, согласующимся с наблюдаемыми на практике.

Третий гармонический компонент тока, возникающий за счет напряжения переменного тока синусоидного характера, в случае электродной диффузионной поляризации и поляризации переноса

Й. ДЕВАИ, Л. МЕСАРОШ и Т. ГАРАИ

Обсуждаются зависимости, касающиеся третьего гармонического компонента тока, возникающего за счет напряжения переменного тока синусоидного характера с небольшой амплитудой, суперпонируемого на напряжение постоянного тока, для случая поляризации переноса, комбинированной с диффузионной поляризацией. Полученные зависимости в предельном случае дают формулы, относящиеся к обратимым полярографическим процессам.

Исследование изменений свойств бинарных растворов, вызванных под влиянием изменения температуры и добавления к ним третьего компонента; применения на вязкость систем типа хлорит металла — $HCl—H_2O$

Э. БЕРЕЦ и И. БАДЕР

Авторами было исследовано отношение изменений свойств в бинарных системах, вызванных изменением температуры и добавлением к раствору третьего компонента. Были разработаны возможности общего описания явления и показаны возможность изображения связи двух эффектов на бинарной и тройной диаграмме а также пригодность метода для сравнительного исследования систем типа хлорид металла — $HCl — H_2O$.

Выведенные соотношения были применены на вязкость систем $MgCl_2 — HCl — H_2O$ и $CsCl — HCl — H_2O$ и были сделаны выводы относительно зависимости от концентрации структуры соответствующих бинарных растворов при изотермических условиях, а также для диссоциации HCl добавленного к бинарному раствору, и для её зависимости от концентрации соответствующих солей.

Селективное отравление платинового катализатора хемисорбцией CO_2, I

Ф. НАДЬ, ДЬ. МИНК и Д. МОГЕР

При исследовании хемисорбции двуокиси углерода на поверхности платины, покрытой водородом, с помощью радиоактивной техники было установлено, что

1. хемисорбция может быть описана следующим уравнением $H_{2(a)} + CO_2 = CO_{(a)} + + H_2O$,

2. при комнатной температуре хемисорбированную окись углерода нельзя удалить ни эвакуированием, ни с помощью водорода,

3. хемисорбция CO, протекающая с измеряемой скоростью, является суммой трех реакций, каждая из которых носит первый порядок по адсорбированному водороду. Константы скоростей этих реакций отличаются друг от друга на целый порядок, и поэтому различные активные центры платиновой поверхности могут быть селективно блокированы за счет хемисорбции CO.

Влияние строения жидких смесей на равновесие систем полимерный гель — алифатический спирт — вода

М. НАДЬ, Э. ВОЛЬФРАМ, ДЬ. ИНЗЕЛЬТ и ДЬ. БЕКЕ

Была исследована изотерма селективной сорбции метанола, этанола и н-пропанола в водных растворах при 25°C, в интервале концентраций спирта 0—25 мол.%-ов.

Коэффициент сорбции, в изученном интервале концентраций, принимает несколько граничных значений и изменяет знак. Концентрация спирта, соответствующая его максимальной сорбции, сравнима с концентрацией спирта, соответствующей максимальной стабилизации.

Сложный ход изотермы вызван одновременным проявлением многих влияний. Эти влияния могут быть объяснимы стабилизацией структур водноспиртовых смесей, а также специфическим взаимодействием компонентов смеси с сорбентом.

Окислене н-гептана

З. Г. САБО, И. ГАЛИБА и Д. ГАЛ

Исследования эффекта стенок при окислении н-гентана производились в аппаратуре, конструированной авторами. Было обнаружено, что стенки и их покрытие оказывают сильный эффект на состав продуктов, в зависимости от местонахождения покрытия, т. е. в зависимости от времени пребывания. Была составлена схема окисления гептана, а также приводится возможная интерпретация широко дискутируемого механизма образования ацетона. Демонстрируется согласованность предложенной схемы с экспериментальными данными. Полагается, что стенки оказывают эффект, в первую очередь, на изомеризацию.

Исследование деградации полимеров, содержащих диетилсилоксан с помощью динамической термогравиметрии, и пиролитической газовой хроматографии

Б. ЛЕНДЬЕЛ, Т. СЕКЕИ и Г. ГАРЗО

Была исследована термическая деградация POMS, содержащего различные конечные группы, а также титан и калий в качестве гетероатома. Термогравиметрическая оценка кинетики производилась с помощью метода DDTG. С целью дальнейшего совершенствования метода, был разработан новый способ расчета для разделения последовательных процессов разложения (изменения веса) и для кинетического описания таких сложных процессов. Было найдено, что деградация всех производных POMS протекает через ступень с энергией активации 43—46 ккал.

С помощью пиролитической газовой хроматографии было показано, что эта характерная степень разложения соответствует определенному соотношению продуктов разложения, которое в интервале 400—600°C практически не зависит от температуры пиролиза, молекулярного веса образца и конечных групп. Вследствие этого инициирование концов цепей может быть исключено. При наличии же гетероатома (в цепи Ti, а в конце цепи K) протекает инициирование концов цепи или каталитическая деполимеризация.

Экспериментальные и расчетные данные подтверждают механизм Томаса и Кендрика для разложения POMS.

The Acta Chimica publish papers on chemistry in English, German, French and Russian.

The Acta Chimica appear in volumes consisting of four parts of varying size, 4 volumes being published a year.

Manuscripts should be addressed to

Acta Chimica
Budapest 112/91 Műegyetem

Correspondence with the editors should be sent to the same address.

The rate of subscription is $ 16.00 a volume.

Orders may be placed with "*Kultúra*" Foreign Trade Company for Books and Newspapers (Budapest I., Fő utca 32. Account No. 43-790-057-181) or with representatives abroad.

Les Acta Chimica paraissent en grançais, allemand, anglais et russe et publient des mémoires du domaine des sciences chimiques.

Les Acta Chimica sont publiés sous forme de fascicules. Quatre fascicules seront réunis en un volume (4 volumes par an)

On est prié d'envoyer les manuscrits destinés à la rédaction à l'adresse suivante:

Acta Chimica
Budapest 112/91 Műegyetem

Toute correspondance doit être envoyée à cette même adresse.

Le prix de l'abonnement est de $ 16.00 par volume.

On peut s'abonner à l'Entreprise pour le Commerce Extérieur de Livres et Journaux «*Kultúra*» (Budapest I., Fő utca 32. Compte-courant No. 43-790-057-181) ou à l'étranger chez tous les représentants ou dépositaires.

«*Acta Chimica*» издают трактаты из области химической науки на русском, французском, английском и немецком языках.

«*Acta Chimica*» выходят отдельными выпусками разного объема. 4 выпуска составляют один том. 4 тома публикуются в год.

Предназначенные для публикации рукописи следует направлять по адресу:

Acta Chimica
Budapest 112/91 Műegyetem

По этому же адресу направлять всякую корреспондению для редакции.

Подписная цена — $ 16.00 за том.

Заказы принимает предприятие по внешней торговле книг и газет «*Kultúra*» (Budapest I., Fő utca 32. Текущий счет № 43-790-057-181) или его заграничные представительства и уполномоченные.

Reviews of the Hungarian Academy of Sciences are obtainable at the following addresses:

ALBANIA

Drejtorija Qändrone e Pärhapjes dhe Propagandimit tä Librit
Kruga Konferenca e Päzes
Tjrana

AUSTRALIA

A. Keesing
Box 4886, GPO
Sydney

AUSTRIA

GLOBUS
Höchstädtplatz 3
A-1200 Wien XX

BELGIUM

Office International de Librairie
30, Avenue Marnix
Bruxelles 5
Du Monde Entier
5, Place St. Jean
Bruxelles

BULGARIA

HEMUS
11 pl Slaveikov
Sofia

CANADA

Pannonia Books
2, Spadina Road
Toronto 4, Ont.

CHINA

Waiwen Shudian
Peking
P. O. B. 88

CZECHOSLOVAKIA

Artia
Ve Směčkách 30
Praha 2
Poštovní Novinová Služba
Dovoz tisku
Vinohradská 46
Praha 2
Mad'arská Kultura
Václavské nám. 2
Praha 1
SLOVART A. G.
Gorkého
Bratislava

DENMARK

Ejnar Munksgaard
Nörregade 6
Copenhagen

FINLAND

Akateeminen Kirjakauppa
Keskuskatu 2
Helsinki

FRANCE

Office International de Documentation et Librairie
48, rue Gay-Lussac
Paris 5

GERMAN DEMOCRATIC REPUBLIC

Deutscher Buch-Export und Import
Leninstraße 16
Leipzig 701
Zeitungsvertriebsamt
Fruchtstraße 3—4
1004 Berlin

GERMAN FEDERAL REPUBLIC

Kunst und Wissen
Erich Bieber
Postfach 46
7 Stuttgart S.

GREAT BRITAIN

Blackwell's Periodicals
Oxenford House
Magdalen Street
Oxford
Collet's Subscription Import Department
Dennington Estate
Wellingsborough. Northants.
Robert Maxwell and Co. Ltd.
4—5 Fitzroy Square
London W. 1

HOLLAND

Swetz and Zeitlinger
Keizersgracht 471—487
Amsterdam C.
Martinus Nijhof
Lange Voorhout 9
The Hague

INDIA

Hind Book House
66 Babar Road
New Delhi 1

ITALY

Santo Vanasia
Via M. Macchi 71
Milano
Libreria Commissionaria Sansoni
Via La Marmora 45
Firenze
Techna
Via Cesi 16.
40135 Bologna

JAPAN

Kinokuniya Book-Store Co. Ltd.
826 Tsunohazu 1-chome
Shinjuku-ku
Tokyo
Maruzen and Co. Ltd.
P.O. Box 605
Tokyo-Central

KOREA

Chulpanmul
Phenjan

NORWAY

Tanum-Cammermeyer
Karl Johansgt 41—43
Oslo 1

POLAND

RUCH
ul. Wronia 23
Warszawa

ROUMANIA

Cartimex
Str. Aristide Briand 14—18
Bucureşti

SOVIET UNION

Mezhdunarodnaya Kniga
Moscow G—200

SWEDEN

Almquist and Wiksell
Gamla Brogatan 26
S—101 20 Stockholm

USA

F. W. Faxon Co. Inc.
15 Southwest Park
Westwood Mass. 02090
Stechert Hafner Inc.
31. East 10th Street
New York, N. Y. 10003

VIETNAM

Xunhasaba
19, Tran Quoc Toan
Hanoi

YUGOSLAVIA

Forum
Vojvode Mišića broj 1
Novi Sad
Jugoslovenska Knjiga
Terazije 27
Beograd

27. X. 1972

Index: 26.007

ACTA CHIMICA

ACADEMIAE SCIENTIARUM HUNGARICAE

ADIUVANTIBUS

V. BRUCKNER, GY. DEÁK, K. POLINSZKY,
E. PUNGOR, G. SCHAY, Z. G. SZABÓ

REDIGIT

B. LENGYEL

TOMUS 74 FASCICULUS 3

AKADÉMIAI KIADÓ, BUDAPEST

1972

ACTA CHIM. (BUDAPEST) ACASA 2 74 (3) 267–385 (1972)

ACTA CHIMICA

A MAGYAR TUDOMÁNYOS AKADÉMIA KÉMIAI TUDOMÁNYOK OSZTÁLYÁNAK IDEGEN NYELVŰ KÖZLEMÉNYEI

SZERKESZTI

LENGYEL BÉLA

TECHNIKAI SZERKESZTŐK

DEÁK GYULA és HARASZTHY-PAPP MELINDA

Az Acta Chimica német, angol, francia és orosz nyelven közöl értekezéseket a kémiai tudományok köréből.

Az Acta Chimica változó terjedelmű füzetekben jelenik meg, egy-egy kötet négy füzetből áll. Évente átlag négy kötet jelenik meg.

A közlésre szánt kéziratok a szerkesztőség címére (Budapest 112/91 Műegyetem) küldendők.

Ugyanerre a címre küldendő minden szerkesztőségi levelezés. A szerkesztőség kéziratokat nem ad vissza.

Megrendelhető a belföld számára az „Akadémiai Kiadó"-nál (Budapest V., Alkotmány utca 21. Bankszámla 05-915-111-46), a külföld számára pedig a „Kultúra" Könyv- és Hírlap Külkereskedelmi Vállalatnál (Budapest I., Fő utca 32. Bankszámla: 43-790-057-181) vagy annak külföldi képviseleteinél és bizományosainál.

Die Acta Chimica veröffentlichen Abhandlungen aus dem Bereiche der chemischen Wissenschaften in deutscher, englischer, französischer und russischer Sprache.

Die Acta Chimica erscheinen in Heften wechselnden Umfanges. Vier Hefte bilden einen Band. Jährlich erscheinen 4 Bände.

Die zur Veröffentlichung bestimmten Manuskripte sind an folgende Adresse zu senden:

Acta Chimica
Budapest 112/91 Műegyetem

An die gleiche Anschrift ist auch jede für die Redaktion bestimmte Korrespondenz zu richten. Abonnementspreis pro Band: $ 16.00.

Bestellbar bei dem Buch- und Zeitungs-Außenhandels-Unternehmen »*Kultúra*« (Budapest I., Fő utca 32. Bankkonto No. 43-790-057-181) oder bei seinen Auslandsvertretungen und Kommissionären.

Acta Chimica Academiae Scientiarum Hungaricae, Tomus 74 (3), pp. 267—72 (1972)

CONTRIBUTIONS TO THE ANALYSIS OF OSMIUM COMPOUNDS

P. ORSÓS and J. NYILASI

(Department of General and Inorganic Chemistry of the L. Eötvös University, Budapest)

Received August 25, 1971

A method was developed for the quantitative determination of potassium nitrido-osmate in the presence of osmium tetroxide and potassium osmate. The method is based on the property of OsO_4 that it can be expelled quantitatively from sulfuric acid solution by boiling, and determined by photometrically in form of its thiourea complex. Certain oxidizing agents (H_2O_2, $K_2Cr_2O_7$) oxidize potassium osmate to osmium tetroxide, whereas not potassium nitrido-osmate. When the distillation is carried out in the presence of these oxidizing agents, only osmium present in form of OsO_4 or K_2OsO_4 can be removed and measured quantitatively. If, the oxidation is carried out in the presence of HNO_3 or $HClO_4$, or such oxidizing agents, which have a more positive standard redox potential than about +1.5 V ($KMnO_4$, $K_2S_2O_8$), the osmium content of $KOsO_3N$ can also be converted into OsO_4, *i.e.* the total osmium content can be measured. The difference of the two determinations yields the quantity of osmium present in form of potassium nitrido-osmate.

The studying of the reactions of osmium compounds with amines [1], necessitated the quantitative determination of the osmium content of various osmium compounds in the presence of each other. The literature contains volumetric [2], gravimetric [3] and spectrophotometric [4] methods which have been developed for the determination of osmium, only in ores and alloys. An essential step in these processes is the distillation of the volatile osmium tetroxide. Our main concern was to elaborate a method for the quantitative determination of osmium, present in various osmium compound, in different oxidation states.

In the present paper we report on the quantitative determination of potassium nitrido-osmate ($KOsO_3N$) in the presence of osmium tetroxide (OsO_4) and potassium osmate (K_2OsO_4), respectively. OsO_4 used was a Merck p.a. preparation. Potassium nitrido-osmate and potassium osmate were prepared by us from OsO_4 [5].

Since potassium nitrido-osmate is non volatile and stabile against certain oxidizing agents from the other two osmium compounds it can be separated. OsO_4 can be expelled quantitatively from sulfuric acid solution by boiling and simultaneous air purge, and can be determined photometrically through its thiourea complex. Among the oxidizing agents listed below, there are some which oxidize K_2OsO_4 to osmium tetroxide, but not $KOsO_3N$. Further there are oxidizing agents which oxidize $KOsO_3N$ also to osmium tetroxide.

Experimental

The following p.a. grade oxidizing agents applied in an about houndredfold excess, were examined: 2 *M* HNO_3, 2 *M* $HClO_4$, 5 *M* $HClO_4$, H_2O_2, $KMnO_4$, $K_2Cr_2O_7$, $K_2S_2O_8$, $KClO_4$, $KBrO_3$, KIO_3 and KO_4 in medium 1 *M* sulfuric acid. The procedure is the following:

Osmium tetroxide, or potassium nitrido-osmate or potassium osmate solution, containing about 1 mg of osmium, is transferred into flask (1) of the apparatus, shown in the figure. The volume of the solution is made up to 50 ml. 20 ml of water is introduced into flask (2), and a 1 : 1 hydrochloric acid : ethanol mixture containing 2 per cent of thiourea is filled into flasks (3), (4) and (5), and into the bubbler (6). Flasks (3), (4) and (5) are placed into an ice bath, and after the starting circulation of the cooling water a slow stream of air is passed through the system by means of a water jet pump, connected to the bubbler. Then the oxidiz-

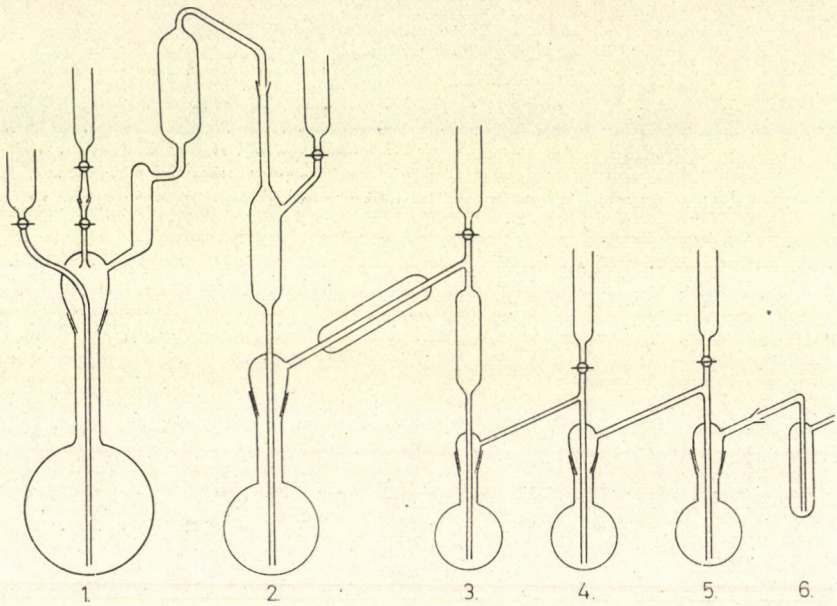

Fig. 1

ing agent is introduced into flask (1), and such quantity of water and sulfuric acid, respectively, to adjust to the required acid concentration if the final volume is 100 ml. First, the content of flask (1) is boiled for about 60 minutes, while keeping the volume of the liquid constant (by replacing the evaporated water time by time). Following this, the content of flask (2) is acidified in the same way as that of flask (1), then boiled for about 20 minutes. During distillation, the content of flask (3), and to a slighter extent that of the receiver (4) turn red, because OsO_4 forms a red complex with thiourea. After boiling, flasks 3, 4 and 5 are placed for 15 minutes into a water-bath kept at 80 °C, to allow the colour to develop completely. The content of the flasks are then poured into a 50 ml flask, and the flask is filled up with a 1 : 1 hydrochloric acid : ethanol mixture to the mark. This solution is filtered and placed into a 1 cm cell, and measured at 485 nm with a Hilger Uvispec photometer against a blank.

Results

Osmium tetroxide can be distilled quantitatively from 1 *M* sulfuric acid by boiling for 30 minutes, and can be determined by the thiourea method.

OsO_4 is not liberated from potassium nitrido-osmate when boiled in sulfuric acid. The same was found when hydrogen peroxide, potassium bichromate,

potassium perchlorate, potassium iodate or potassium periodate was present in the reaction mixture (Table I).

2 *M* nitric acid, potassium permanganate or potassium persulfate (the latter two in 1 *M* sulphuric acid) oxidize $KOsO_3N$ quantitatively osmium tetroxide. Osmium tetroxide can be distilled from the reaction mixture.

Other oxidizing agents ($KClO_3$, $KBrO_3$, 2 and 5 *M* $HClO_4$, resp.) convert nitrido-osmate only partially into osmium tetroxide. Our experiments showed that in the case of $KBrO_3$ and 5 *M* $HClO_4$ the oxidation is quantitative, when the following double distillation procedure is applied:

In the first distillation flasks (3), (4) and (5) a 3 percent H_2O_2 contain solution as osmium collector (6). After about an hour distillation, the combined contents of these flasks are poured into flask (1), which has been cleaned previously. Now 20 ml of a 30 percent H_2O_2 solution is used as oxidizing agent. From the solution made up with water and the appropriate amount of sulfuric acid to 100 ml, another distillation is carried out. Instead of water a 1 percent $KMnO_4$ solution is placed into flask (2) for the decomposition of H_2O_2 carried over. This double distillation method gives very good results, when potassium bromate or 5 *M* perchloric acid is used, but not in the case of potassium chlorate and 2 *M* perchloric acid.

It is a known fact that potassium osmate undergoes disproportionation in neutral medium:

$$2\ OsO_4^{2-} + 2\ H_2O \rightleftharpoons OsO_4 + OsO_2 + 4\ OH^-$$

Thus by acidification, the equilibrium can be shifted to the right. We expected therefore that from a sulfuric acid solution half of the osmium content of K_2OsO_4 can be removed as OsO_4. Our results showed, however, that the measured OsO_4 quantity was not in stoichiometric relation with K_2OsO_4 as expected from the disproportionation reaction.

Potassium osmate can be converted into osmium tetroxide, and after distillation measured quantitatively in form of a thiourea complex, if the oxidation is performed in 1 *M* sulfuric acid solution with potassium permanganate, potassium persulfate, potassium bichromate or 2 *M* nitric acid. The oxidation of potassium osmate into osmium tetroxide is quantitative also in the case, when halogenates, perhalogenates ($KClO_3$, $KClO_4$, $KBrO_3$, KIO_3, KIO_4) or 2 *M* perchloric acid are used, and the double distillation method described above is applied.

The determination of $KOsO_3N$ in the presence of OsO_4 or K_2OsO_4 can be carried out as follows:

In a 1 *M* sulfuric acid solution osmium, present in form of OsO_4 and K_2OsO_4, respectively, is determined by an oxidation with hydrogen peroxide or potassium bichromate. The total osmium content is determined from a

Table I

Oxidizing agent	$KOsO_3N$	K_2OsO_4
	mg weighed: 1.75 mg found:	mg weighed: 2.28 mg found:
HNO_3 (2 *M*)	1.74	2.26
	1.71	2.26
	1.71	2.25
$HClO_4$ (2 *M*)	0.11	2.29
	0.17	2.25
	0.09	2.24
$HClO_4$ (5 *M*)	1.73	2.27
	1.76	2.30
	1.75	2.26
H_2O_2	—	2.25
	—	2.27
	—	2.28
$KMnO_4$	1.77	2.30
	1.74	2.22
	1.71	2.25
$K_2Cr_2O_7$	—	2.32
	—	2.25
	—	2.26
$K_2S_2O_8$	1.73	2.28
	1.75	2.22
	1.75	2.22
$KClO_3$	0.14	2.23
	0.20	2.25
	0.19	2.24
$KClO_4$	—	2.22
	—	2.27
	—	2.25
$KBrO_3$	1.72	2.26
	1.70	2.30
	1.70	2.31
KIO_3	—	2.23
	—	2.20
	—	2.25
KIO_4	—	2.24
	—	2.29
	—	2.28

second sample after oxidation with 2 *M* nitric acid, or with potassium permanganate or potassium persulfate in 1 *M* sulfuric acid solution. The quantity of osmium present in the form of potassium nitrido-osmate is obtained from the difference of the two measurements (Table II).

Table II

Weighed Os:		
In form of OsO_4	0.65 mg	1.31 mg
In form of K_2OsO_4	0.65 mg	1.31 mg
In form of $KOsO_3N$	1.14 mg	1.14 mg
Total	2.44 mg	3.76 mg
Quantity of Os determined after oxidation with hydrogen peroxide	1.27 mg	2.57 mg
Quantity of Os determined after oxidation with nitric acid	2.38 mg	3.70 mg
Quantity of Os found in form of $KOsO_3N$	1.11 mg	1.13 mg

REFERENCES

1. NYILASI, J., ORSÓS, P., POMOGÁTS, E.: Magy. Kém. Foly. **76,** 380 (1970); Acta Chim. Acad. Sci. Hung. **66,** 251 (1970)
2. CROWELL, W. R., KIRSCHMAN, H. D.: Am. Chem. Soc. **51,** 175 (1929)
   SAITO, S.: Bull. Inst. Phys. Chem. Res. Tokyo **8,** 164 (1929)
   RYABCHIKOV, D. I.: Neorg. Khim. Akad. Nauk. USSR **22,** 35 (1948); J. Applied Prikl. Khim USSR **17,** 326 (1944)
   CROWELL, W. R.: J. Am. Chem. Soc. **54,** 1324 (1932)
   CROWELL, W. R., BAUMBACH, H. I.: J. Am. Chem. Soc. **57,** 2607 (1935)
   CROWELL, W. R., KIRSCHMAN, H. D.: J. Am. Chem. Soc. **51,** 1965 (1929)
   RYABCHIKOV, D. I.: Zhur. Analit. Khim. **1,** 47 (1946)
   SYROKOMSKIJ, V. S.: Dokl. Acad. Nauk USSR **46,** 280 (1945)
   BEAMISH, F. E.: The analytical chemistry of the noble metals. Pergamon Press, I. edition (1966)
   SAXENA, O C.: J. Chem. UAR **11,** 339 (1968); Mikrochem. J. **12,** 609 (1967)
3. GILCHRIST, R., WICHERS, E.: J. Am. Chem. Soc. **57,** 2565 (1935)
   OGBURN, S. G., MILLER, L. F.: J. Am. Chem. Soc. **52,** 42 (1930)
   HOFFMAN, I., SCHWEITZER, D. E., RYAN, D. E., BEAMISH, F. E.: Analyt. Chem. **25,** 1091 (1935)
   WILSON, R. F., BAYE, L. J.: Talanta **1,** 351 (1958); J. Am. Chem. Soc. **80,** 2652 (1958)
   SPACU, P., GHEORGHIU, C.: Z. analyt. Chem. **174,** 340 (1960)
   MUSH, A., PIETSCH, R.: Z. analyt. Chem. **137,** 321 (1952)
4. SHIOKAWA, T.: Sci. Rep. Research Inst. Tohoku Univ. Ser. A. **2,** 287, 293 (1950); J. Chem. Soc. Japan **70,** 314, 353, 355 (1949)
   BOGNÁR, J., SÁROSI, S.: Magy. Kém. Foly. **67,** 193 (1961)
   SAUERBRUNN, R. B., SANDELL, E. B.: Mikrochim. Acta 22 (1953)
   STEELE, E. L., YOE, J. H.: Anal. Chim. Acta **20,** 205 (1959), Analyt. Chem. **29,** 1622 (1957)
   MAJUMDAR, A. K., SEN GUPTA, J. G.: Anal. Chim. Acta **20,** 532 (1959)
   TSCHUGAJEFF, L.: C. **167,** 235 (1918)
   SAUERBRUNN, R. B., SANDELL, E. B.: J. Am. Chem. Soc. **75,** 3554 (1953)

DWYER, F. P., GIBSON, N. A.: Analyst. **76,** 104 (1951)
AYRES, G. H., WELLS, W. N.: Anal. Chem. **22,** 317 (1950)
BARDODEJ, Z.: Chem. Listy **48,** 1870 (1954)
YOE, J. H., OVERHOLSER, L. G.: Ind. Eng. Chem. Anal. Ed. **14,** 435 (1942)
GOLDSTEIN, G.: U. S. At. Energy Comm. ORNL-2862, 71 (1960)
GOLDSTEIN, H., MANNING, D. L., MENIS, O., DEAN, J. A.: Talanta **7,** 296, 301, 307 (1961)
BAIULESCU, G. H., LAZAR, C., CRISTESCU, C.: Anal. Chim. Acta. **24,** 463 (1961)
WINGFIELD, H. C., YOE, J. H.: Anal. Chim. Acta **14,** 446 (1956)
MAJUMDAR, A. K., SEN GUPTA, J. G.: Anal. Chim. Acta **21,** 260 (1959); **22,** 306 (1960); Z. analyt. Chem. **179,** 13 (1961)
MAJUMDAR, A. K., SAVARIAR, C. P.: Anal. Chim. Acta **21,** 146 (1959)
5. GMELINS Handbuch der Anorg. Chemie **66,** 66, 69 (1939) Inorg. Synt. **6,** 204 (1960)
6. WESTLAND, A. D., BEAMISH, F. E.: Anal. Chem. **26,** 739 (1954); Mikrochim. Acta **5,** 625 (1957)

Piroska ORSÓS
János NYILASI } Budapest VIII., Múzeum krt. 6—8.

Acta Chimica Academiae Scientiarum Hungaricae, Tomus 74 (3), pp. 273—79 (1972)

THERMODYNAMIC DATA OF TRANSITION METAL COMPLEXES WITH D-GLUCOSAMINIC ACID

A. GERGELY and I. SÓVÁGÓ

(Institute of Inorganic and Analytical Chemistry, L. Kossuth University, Debrecen)

Received September 2, 1971

The stability constants of the cobalt(II), nickel(II), copper(II) and zinc(II) complexes of D-glucosaminic acid (GAA) were determined pH-metrically at 25 °C at an ionic strength of 0.05 *M*. The enthalpy and entropy data for these complexes were obtained calorimetrically.

The stability constants of the GAA complexes are almost the same as those of the alanine and norleucine complexes. At the same time the corresponding ΔH values are larger and the ΔS values smaller than those of the alanine and norleucine complexes. It was concluded from the thermodynamic data that the hydroxyl groups of the GAA participate in complex formation in the undissociated form.

Introduction

The study of the equilibria and thermodynamics of complexes with amino acids containing alcoholic hydroxyl groups has recently received increasing attention. The stability constants and thermodynamic parameters of certain transition metal complexes of serine and threonine have been determined by a number of authors [1—9]. On the basis of the stability data and, in part, of thermodynamic data, these authors make conclusions on the bonding conditions in these complexes. Thus, SHARMA [5], FREEMAN and MARTIN [6] and LETTER and BAUMAN [7] in general exclude the possibility that the alcoholic hydroxyl groups are involved in the complex bonding. In contrast, STACK and SKINNER [8] conclude from calorimetric thermodynamic data that the alcoholic hydroxyl groups do participate in the bonding in the inner coordination sphere. On the other hand, RAJU and MATHUR [9] conclude from thermodynamic data obtained with the temperature coefficient method that the alcoholic hydroxyl groups occupy positions in the outer sphere.

Structural studies on the above complexes led to somewhat more unambigous conclusions. Thus, according to the circular dichroism study by KATZIN and GULYAS [10], the alcoholic hydroxyl group takes part in complex formation in the nickel(II)-serine system. According to nuclear magnetic resonance studies by MCCORMICK *et al.* [11] and BOWLES *et al.* [12], the alcoholic hydroxyl groups are involved in the bonding in the manganese(II)-serine, manganese(II)-threonine and the iron(II)-serine, iron(II)-threonine systems, but not in the corresponding copper(II) complexes [11]. From calorimetric studies [13] we

have concluded that the alcoholic hydroxyl groups participate in complex formation in the serine and threonine complexes of cobalt(II), nickel(II), copper(II) and zinc(II).

It was earlier recommended [14] to use as drugs several metal complexes of D-glucosaminic acid, which in essence can be regarded as an α-amino acid. Since the ligand also contains a number of alcoholic hydroxyl groups, it can serve as a good model for the study of the participation of these groups in complex formation. On the basis of equilibrium studies on the complexes of copper(II), setting out from the fact that the stabilities do not follow the IRVING-ROSSOTTI rule [15], in our previous papers [16, 17] we have concluded that the alcoholic hydroxyl groups may possibly take part in the complex formation. MIYAZAKI *et al.* [18] have carried out equilibrium studies on manganese(II), cobalt(II), nickel(II), copper(II) and zinc(II) complexes. In the copper(II)-D-glucosaminic acid system they presumed that the hydroxyl groups are bonded in alkaline media.

The stability constants of the complexes of D-glucosaminic acid differ strikingly from those of the corresponding glycine complexes. To obtain clear-cut conclusions, however, it is necessary to carry out other investigations as well. The aim of the present work was the equilibrium and calorimetric study of some transition metal–D-glucosaminic acid system.

Experimental

The metal salt solutions used in the experiments were prepared from Reanal chemicals of p.a. quality. Their concentrations were checked gravimetrically by precipitating the oxine complexes. D-glucosaminic acid (GAA) was prepared from chitin, *via* glucosamine hydrochloride, by the method of WALTRON and CRON [19]. The ionic strength was adjusted to 0.05 *M* with p.a. potassium chloride. The alkaline titrations were carried out with sodium hydroxide stored in a nitrogen atmosphere.

The metal: ligand ratio was 1 : 2 in the case of the copper(II) complexes, while the nickel(II), cobalt(II) and zinc(II) complexes it was 1 : 3. In all cases the GAA concentration was 0.01 *M*.

The pH measurements were made with a Radiometer pHM-4 instrument, using a G 200B glass and a K 100 calomel electrode. The temperature was adjusted to 25 ± 0.1°C with an ultrathermostat. The method proposed by IRVING *et al.* [20] was used to eliminate the error arising from the difference in the diffusion potential differences. A 0.25 *M* NaOH solution was used for the pH-metric titration and in every system three parallel titrations were carried out each containing 20 experimental points. The volume of the solution to be studied was adjusted to 25 ml in the pH-metric measurements, and to 500 ml in the calorimetric measurements. The latter were carried out in the manner reported earlier [21] with the calorimeter made by ourselves.

The relative error of the stability constants was about 0.02 log *K*. The evaluation of the experimental calorimetric data and the calculation of the stability constants from the pH-metric titration data were performed as reported in our earlier papers [21, 22].

Results and discussion

In Table I are listed the data obtained by us and by MIYAZAKI *et al.* [18] for the dissociation constants of GAA. For comparison, the corresponding data for alanine and norleucine are also given. It is clear from the Table that the *pK*

values of the three and six carbon atom alanine and norleucine are almost the same. Those of GAA, however, and particularly pK_2, according to both our own data and those of MIYAZAKI *et al.* [18], are significantly different from the above and are similar to the corresponding data for serine and threonine [7, 9, 13]. Accordingly, the presence of several alcoholic hydroxyl groups in the ligand

Table I

Protonation constants of alanine, norleucine and GAA at 25 °C and $I = 0.05$ M (KCL)

Amino acid	pK_1	pK_2	Reference
alanine	2.28	9.72	[22]
norleucine	2.23	9.69	*
GAA	2.20	9.08	this work
	2.01	9.06	[18]**

* unpublished data measured pH-metrically at 25 °C and $I = 0.05$ M (KCl)
** 30 °C and $I = 0.1$ M (KNO_3)

does not affect the stabilities of the proton complexes of the carboxyl and amino groups compared with those of the former.

The stability constants of the metal complexes are contained in Table II. For comparison the data available for the alanine and norleucine complexes are also given in this Table.

The following emerge from the data in Table II:

1. The stability constants of the alanine and norleucine complexes agree approximately with each other. (We shall return to the interpretation of the small differences between them in a subsequent paper.)

2. Considering the differences in ionic strength and temperature, the stability constants obtained by MIYAZAKI *et al.* [18] and by ourselves agree quite well with each other. The small differences can be explained by the fact that the graphical procedure, used for the calculation by the authors cited, provides less accurate constants.

3. According to both our own data and those of MIYAZAKI *et al.* [18], the stability constants of the GAA complexes are almost the same as those for the alanine and norleucine complexes. In the cases of cobalt(II) and nickel(II) the MA_2-type complexes of GAA are more stable than the corresponding alanine and norleucine complexes.

4. If the $pK_2 - \log K_n$ data are taken into consideration, the increase of the stability of the GAA complexes compared with the corresponding alanine and norleucine complexes is even more striking. Thus, compared with the

Table II

Stability data for transition metal complexes of alanine, norleucine and GAA at 25 °C and $I = 0.05$ M (KCl)

Ligand	log K_1	log K_2	log β_2	log K_1/K_2	$pK_2 - \log K_1$	$pK_2 - \log K_2$	Reference
				Co(II)			
alanine	4.35	3.51	7.86	0.84	5.37	6.21	[22]
norleucine	4.33	3.56	7.89	0.77	5.36	6.13	*
GAA	4.35	3.69	8.04	0.66	4.73	5.39	this work
	4.5	3.9	8.4	0.6	4.56	5.16	[18]**
				Ni(II)			
alanine	5.46	4.47	9.93	0.99	4.26	5.25	[22]
norleucine	5.41	4.33	9.74	1.08	4.28	5.26	*
GAA	5.39	4.46	9.85	0.93	3.69	4.62	this work
	5.6	4.4	10.0	1.2	3.46	4.66	[18]**
				Cu(II)			
alanine	8.17	6.78	14.95	1.39	1.55	2.94	[22]
GAA	8.07	6.69	14.76	1.38	1.01	2.39	this work
	8.0	6.6	14.6	1.4	1.06	2.46	[18]**
				Zn(II)			
alanine	4.60	4.07	8.67	0.53	5.12	5.65	[22]
GAA	4.63	4.01	8.64	0.62	4.45	5.07	this work
	4.90	—	—	—	4.16	—	[18]**

* unpublished data measured pH-metrically at 25 °C and $I = 0.05$ M (KCl)
** 30 °C and $I = 0.1$ M (KNO_3)

amino acid complexes, the stability constants of these complexes do not follow the IRVING—ROSSOTTI rule [15].

5. In spite of the greater bulk of the ligand it is evident from the log K_1/K_2 data that steric hindrance does not play a part in the formation of the GAA complexes.

The calorimetric titration data are given in Table III.

The values of the dissociation heats of GAA are as follows:

$$\Delta H_{D1} = 0.7 \text{ kcal/mol}; \quad \Delta H_{D2} = 10.2 \text{ kcal/mol}.$$

According to our own unpublished data, the corresponding values for norleucine are 0.7 and 10.7 kcal/mol. This difference, just as the pK_2 values, reflect the

Table III

Calorimetric titration data for the Co(II)–, Ni(II)–, Cu(II)– and Zn(II)–D-glucosaminic acid systems at 15 °C and I = 0.05 M (KCl)

NaOH*	Co(II)		Ni(II)		NaOH**	Cu(II)		Zn(II)	
ml	pH	−Q cal/l	pH	−Q cal/l	ml	pH	−Q cal/l	pH	−Q cal/l
0.5	6.386		5.373		0.5	3.213		6.006	
0.9	6.760	4.67	5.790	5.49	1.0	3.390	10.83	6.514	4.96
1.3	7.047	4.88	6.113	5.59	1.5	3.601	10.48	6.869	5.36
1.7	7.319	5.09	6.420	5.69	2.0	3.859	9.85	7.203	5.13
2.1	7.563	5.09	6.732	5.79	2.5	4.168	9.45	7.550	5.25
2.5	—	—	7.071	5.79	3.0	4.517	9.39	—	—
					3.5	4.919	9.16	—	—

* NaOH concentration = 0.990 *M*
** NaOH concentration = 1.0165 *M*

electron-attracting effect of the alcoholic hydroxyl groups. (See the data for serine and threonine [13].)

Table IV contains the thermodynamical constants calculated from the data in Table III with the use of the stability constants.

For comparison, the values for the alanine and norleucine complexes are also given in Table IV.

The following conclusions can be drawn from the data in Table IV:

1. Taking into account the error of about 0.5 kcal/mol in the ΔH data, the ΔH values of the GAA complexes are larger, and the entropy changes are smaller than the corresponding values of the alanine and norleucine complexes. This difference is particularly conspicuous in a comparison with norleucine containing six carbon atoms. According to this, the higher stability of the GAA complexes, which is expressed mainly in the pK_2 — log K_n data, is determined by the increased value of the enthalpy change.

2. The presence of the alcoholic hydroxyl groups in the GAA naturally weakens the bond between the metal and the nitrogen. On this basis, just as in the dissociation heats of the GAA, a lower enthalpy change would be expected in the metal complexes too. Just like the amino acids, the GAA ligand is bonded first of all to the metals through the oxygen of the carboxyl group and nitrogen of the amino group. The higher enthalpy change, resulting in spite of the decreased strengths of these bonds, is therefore best explained in terms of bond formation by the alcoholic hydroxyl groups in the inner coordination sphere. This assumption is in agreement with the structural studies by KATZIN and GULYAS [10] and BOWLES *et al.* [12] (and in part with those of MCCORMICK

Table IV

Enthalpy and entropy changes of D-glucosaminic acid, alanine and norleucine complexes

Ligand	$-\Delta H\beta_1$, kcal/mol	$-\Delta H\beta_2$ kcal/mol	$\Delta S\beta_2$ e.u.	Reference
		Co(II)		
alanine	1.3	3.6	24	[22]
norleucine	—	5.9	16	*
GAA	3.0	7.0	13	this work
		Ni(II)		
alanine	3.6	7.4	21	[22]
norleucine	—	7.5	19	*
GAA	4.2	8.6	16	this work
		Cu(II)		
alanine	4.9	10.4	34	[22]
GAA	6.6	12.8	26	this work
		Zn(II)		
alanine	1.5	4.3	27	[22]
GAA	1.8	5.4	22	this work

* unpublished calorimetric data

et al. [11] too), according to whom, as we have already mentioned, the alcoholic hydroxyl groups of these ligands do take part in complex formation.

3. The entropy changes characteristic of the GAA complexes, which are smaller than those of the corresponding alanine and norleucine complexes, can also be interpreted in part by the formation of further bonds. In all probability, however, a role is also played in these data by the ordering effect exerted on the water by the several hydroxyl groups in the GAA molecule.

*

The authors are indebted to T. GAÁL for his participation in the experimental work.

REFERENCES

1. PELLETIER, S.: Compt. Rend. **245,** 160 (1957)
2. IZATT, R. M., CHRISTENSEN, J. J., KOTHARI, V.: Inorg. Chem. **3,** 1565 (1964)
3. SUCHEV, A. Ya.: Zhur. Neorg. Khim. **9,** 2343 (1964)
4. KRAUSE, H. W., WILCKE, F. W., MIX, H., LANGENBECK, W.: Z. Phys. Chem. **225,** 342 (1964)
5. SHARMA, V. S.: Biochem. et Biophys. Acta, **148,** 37 (1967)
6. FREEMAN, H. C., MARTIN R. P.: J. Biol. Chem. **244,** 4823 (1969)
7. LETTER, J. E., Jr., BAUMAN, J. E., Jr.; J. Amer. Chem. Soc. **92,** 437 (1970)

8. STACK, W. F., SKINNER, H. A.: Trans. Faraday Soc. **63,** 1136 (1967)
9. RAJU, E. V., MATHUR, H. B.: J. Inorg. Nucl. Chem. **30,** 2181 (1968)
10. KATZIN, L. I., GULYAS, E.: J. Amer. Chem. Soc. **91,** 6940 (1969)
11. MCCORMICK, D. B., SIGEL, H., WRIGHT, L. D.: Biochim. Biophys. Acta, **184,** 318 (1969)
12. BOWLES, A. M., SZAREK, W. A., BAIRD, M. C.: Inorg. Nucl. Chem. Letters, **7,** 25 (1971)
13. GERGELY, A., MOJZES, J., BAZSA-KASSAI, Zs.: Magy. Kém. Foly. **78,** 76 (1972); J. Inorg. Nucl. Chem., **34,** 1277 (1972)
14. STOLL, A., HOFMAN, A.: U. S. Pat., 1 888 186 (1932)
15. IRVING, H., ROSSOTTI, H.: Acta Chem. Scand. **10,** 72 (1956)
16. GERGELY, A., SZARVAS, P., MÁCZAY, L.: Magy. Kém. Foly. **70,** 235 (1964)
17. GERGELY, A., SZARVAS, P.: Acta Chim. Acad. Sci. Hung. **45,** 203 (1965)
18. MIYAZAKI, M., SENSHU, T., TAMURA, I.: Chem. Pharm. Bull. **14,** 114 (1966)
19. WALTRON, M. L., CRON, M. I.: J. Amer. Chem. Soc. **74,** 1715 (1952)
20. IRVING, H. M., MILES, M. G., PETTIT, L. D.: Anal. Chem. Acta, **38,** 475 (1967)
21. GERGELY, A., NAGYPÁL, I., SÓVÁGÓ, I.: Magy. Kém. Foly. **76,** 550 (1970); Acta Chim. Acad. Sci. Hung. **67,** 241 (1971)
22. GERGELY, A., KIRÁLY, B., NAGYPÁL, I., MOJZES, J.: Magy. Kém. Foly. **76,** 452 (1970); Acta Chim. Acad. Sci. Hung. **67,** 133 (1971).

Arthur GERGELY
Imre SÓVÁGÓ
} Debrecen 10, Hungary.

Acta Chimica Academiae Scientiarum Hungaricae, Tomus 74 (3), pp. 281—91 (1972)

QUANTUM CHEMICAL INTERPRETATION OF THE SPECTROSCOPIC DATA OF PHARMACOLOGICALLY ACTIVE HOMOPYRIMIDAZOLE DERIVATIVES

G. NÁRAY-SZABÓ,* E. DUDAR and G. HORVÁTH
(Chemical and Pharmaceutical Works Chinoin, Budapest)

Received November 30, 1970; revised September 5, 1971

The charge distribution of 26 homopyrimidazole derivatives were calculated by the Pariser—Parr—Pople and DEL RE's semi-empirical methods, and correlations were found between the charge distribution and the positions of certain IR bands and NMR signals. An approximately linear relation holds true of the bond vibrations and the corresponding bond orders. A similar relationship exists between the NMR chemical shift of the C-2 proton of the ring and the net charge of this carbon atom. An analysis of anomalies has resulted in the elucidation of certain structural characteristics. The pH-dependence of the UV spectra of some compounds was also investigated.

Introduction

MÉSZÁROS *et al.* have recently synthesized several homopyrimidazole derivatives [1] which possess very favourable pharmacological properties. The interpretation of the UV, IR and NMR spectroscopic data has greatly contributed to the elucidation of the structural problems of these compounds. Quantum chemical calculations have now been performed to systematize these results; the charge distributions of certain compounds, and in some cases also

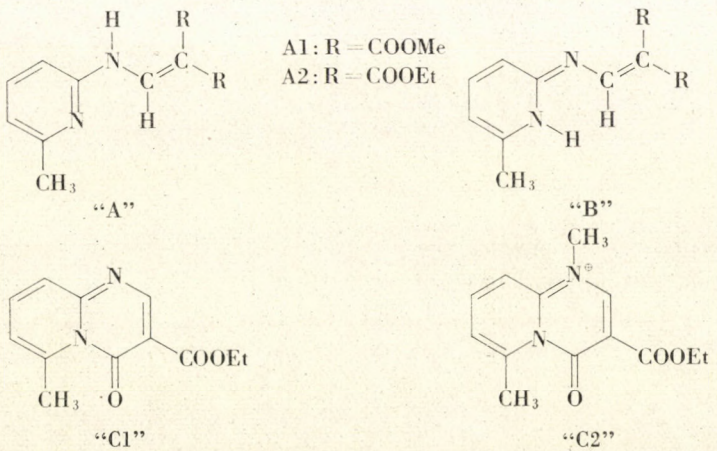

* Present address: Institute of Physics, Technical University, Budapest.

the electronic excitation energies are determined. Approximate correlations have been found between the quantum chemical parameters and spectroscopic data, and some characteristic bands of the IR and NMR spectra can be discussed on this basis. By comparing the calculated and measured UV maxima, the mechanism of an interesting acid–base equilibrium is revealed.

Calculations were performed for the following compounds:

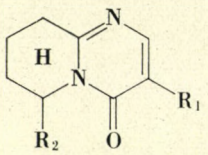

"D"

*D*1:	R_1=H	R_2=Me
*D*2:	R_1=COOH	R_2=Me
*D*3:	R_1=COOEt	R_2=H
*D*4:	R_1=COOEt	R_2=Me
*D*5:	R_1=CONH$_2$	R_2=Me

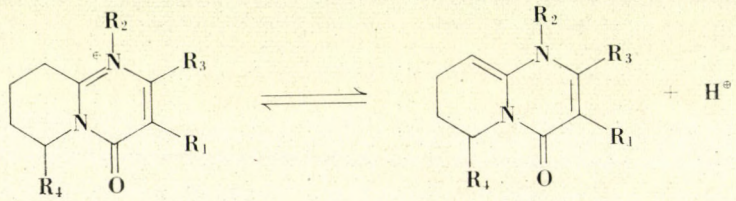

"E" "F"

*E*1:	R_1=H	R_2=H	R_3=H	R_4=Me
*E*2:	R_1=H	R_2=H	R_3=Me	R_4=Me
*E*3, *F*3:	R_1=COOEt	R_2=Me	R_3=H	R_4=H
*E*4, *F*4:	R_1=COOEt	R_2=Me	R_3=H	R_4=Me
*E*5, *F*5:	R_1=COOEt	R_2=Et	R_3=H	R_4=Me
*E*6, *F*6:	R_1=COOH	R_2=Me	R_3=H	R_4=Me
*E*7:	R_1=H	R_2=Me	R_3=H	R_4=Me
*E*8:	R_1=CONH$_2$	R_2=Me	R_3=H	R_4=Me

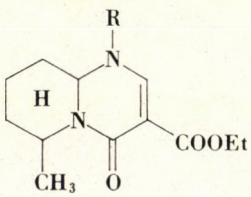

"G"

*G*1:	R=H
*G*2:	R=Me
*G*3:	R=COMe

The numbering of the rings is given in Fig. 1. For a general description and the nomenclature of the compounds discussed here, see Ref. [1].

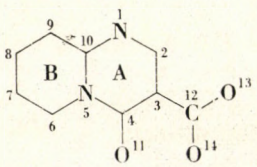

Fig. 1

Calculations

The σ and π charge distributions were individually calculated, according to the σ—π separability, applying DEL RE's [2] method to the former, and the conventional PPP-method [3, 4] to obtain the π charge distribution; these were completed by the MATAGA—NISHIMOTO approximation [5]. The parameters chosen are shown in Table I; the hybridization states of the heteroatoms attached to the carbon are given in brackets. Since no experimentally determined geometrical data were available for the compounds studied, the standard bond lengths and bond angles given in the literature [6] were used in the calculations. The bond angles were chosen within the range of 115—125° for sp^2 and between 105° and 115° for sp^3 hybridization states. The bond lengths are listed in Table II. It is well known that steric arrangement does not affect significantly the results obtainable by the PPP-method, and it has no importance at all if DEL RE's method is used, therefore the errors arising from the incertainties of the geometry can be neglected.

Table I

Parameters used for the calculations

Atom	I (eV)	E (eV)
C(sp^2)	11.42	0.58
N(sp^2)	13.83	0.45
N(sp^3)	29.16	14.49
O(sp^2)	17.28	2.70
O(sp^3)	35.76	17.70

$\beta_{CN}(sp^2) = \beta_{CC} = 1\beta$
$\beta_{CN}(sp^3) = 0.8\,\beta$
$\beta_{CO}(sp^2,\ \text{carbonyl}) = 1.6\,\beta$
$\beta_{CO}(sp^2,\ \text{carboxylic}) = 1.3\,\beta$
$\beta_{CO}(sp^3) = 0.7\,\beta$

Table II

Geometrical data

Bond	R (Å)
CC(sp^2—sp^2)	1.4—1.45
CN(sp^2—sp^2)	1.35—1.4
CN(sp^2—sp^3)	1.4
CN(amide)	1.35
CO(sp^2—sp^2)	1.2
CO(sp^2—sp^3)	1.35

The accuracy of the total-charge-density calculation was controlled by comparing the theoretical and experimentally determined* dipole moments [7, 8]. In the case of compound *D*1, which has no rotating groups, the experimental and theoretical values are 2.9*D* and 3.4*D*, respectively. The 17% difference corresponds to the usual error of calculations given in the literature [9]. In the knowledge of the error of dipole moment, the error of the charge distribution can also be estimated on the basis of statistical considerations; with compound *D*1, the value is expected to fall between 15 and 20% [10], and it is logical to presume that the errors of the calculated charge distributions for the other derivatives do not exceed the above value. On this basis, the graphically obtained correlations (Eqs (1)—(3)) can be considered significant.

In the case of quaternary ammonium bases, the conventional PPP-method fails because of the considerable polarization of the σ-core; this can, however, be corrected by means of a σ-bond polarization model [11], in which the ionization potentials (I) and electron affinities (E) of the quaternary nitrogen and the neighbouring atoms are modified. Starting with the data of Table I, the following modified values were found: $I(\mathrm{C}, sp^2) = 14.8$ eV, $I(\mathrm{N}, sp^2) = 19.0$ eV, $E(\mathrm{C}, sp^2) = 1.78$ eV, $E(\mathrm{N}, sp^2) = 4.2$ eV.

UV Spectra

The ultraviolet spectra of some compounds belonging to group E show characteristic alterations with the changes in pH, which are due to the following acid–base equilibrium, whose existence is also supported by preparative, IR and NMR evidence:

$$E^{\oplus} \rightleftharpoons F + H^{\oplus}.$$

To examine the problem more closely, the electronic excitation energies were calculated and compared with the experimental results. The data are shown in Table III. Owing to the shortcomings of the PPP-method, no difference could be observed between substituted varieties, *e.g.*, the methyl- and ethyl derivatives. The shifts of the bands due to the acid–base equilibrium can be predicted by the calculations, with the exception of the I $\pi \rightarrow \pi^*$ band of compound *E*6, although the magnitude of the experimental shifts is less than the error of the calculations. The assignments of the bands have been made, and the existence of the acid–base equilibrium can be demonstrated.

IR Spectra

In order to facilitate the systematization of the IR spectra, it was attempted to find an interrelation between certain band frequencies and the relative quantum chemical parameters. It is well known that the vibrational frequency,

* Thanks are due to Mrs. A. ILLÉNYI and to Mrs. I. GRESZ for performing the experimental work.

Table III

Singlet excitation energies

Compound		Exc. energy, eV		Compound		Exc. energy, eV	
		Exp.	Calc.			Exp.	Calc.
*E*1	I $\pi \rightarrow \pi^*$	4.44	4.00	*E*1 base	I $\pi \rightarrow \pi^*$	4.50	4.60
	II $\pi \rightarrow \pi^*$	5.45	5.95		II $\pi \rightarrow \pi^*$	5.87	6.08
*E*2	I $\pi \rightarrow \pi^*$	4.40	4.00	*E*2 base	I $\pi \rightarrow \pi^*$	—	4.60
	II $\pi \rightarrow \pi^*$	5.45	5.95		II $\pi \rightarrow \pi^*$	—	6.08
*E*3	I $\pi \rightarrow \pi^*$	4.32	3.99	*F*3	I $\pi \rightarrow \pi^*$	4.53	4.42
	II $\pi \rightarrow \pi^*$	5.34	5.53		II $\pi \rightarrow \pi^*$	5.26	5.41
*E*4	I $\pi \rightarrow \pi^*$	4.34	3.99	*F*4	I $\pi \rightarrow \pi^*$	4.68*	4.42
	II $\pi \rightarrow \pi^*$	5.30	5.53		II $\pi \rightarrow \pi^*$		5.41
	n $\rightarrow \pi^*$	3.48	—		n $\rightarrow \pi^*$	3.46	—
*E*5	I $\pi \rightarrow \pi^*$	4.76*	3.99	*F*5	I $\pi \rightarrow \pi^*$	4.68*	4.42
	II $\pi \rightarrow \pi^*$		5.53		II $\pi \rightarrow \pi^*$		5.41
	n $\rightarrow \pi^*$	3.45	—		n $\rightarrow \pi^*$	3.46	—
*E*6	I $\pi \rightarrow \pi^*$	4.43	3.99	*F*6	I $\pi \rightarrow \pi^*$	4.13	4.42
	II $\pi \rightarrow \pi^*$	5.27	5.53		II $\pi \rightarrow \pi^*$	4.84	5.41

* Bands I and II are merged

force constant and bond order are altered more or less in parallelism with one another [12]. This holds true especially of such group frequencies which are independent of the mass and combination effects [13]. The stretching frequencies originating from the vibration along the >X—Y bond, wherein X is coupled only with Y, are of this type. In these cases, a linear relationship can be found between the group frequencies and the Hammett constants [14—16], and other physical parameters [14]. Similar relations exist in some cases between the charge on atom X or the X—Y bond order and the group frequencies [17—19].

The compounds studied have two functions corresponding to the above criteria, the ester group, and the C-4 carbonyl group. The relationship of these functional groups to the corresponding quantum chemical parameters was studied, and the numerical data are given in Table IV.

The following linear relations hold true of the ester and carbonyl frequencies and the net ($\sigma + \pi$) charges of the C and O atoms:

$$\nu_{CO}\,(\text{ester}) = 1000q_C + 750q_O + 1580, \qquad (1)$$

$$\nu_{CO}\,(\text{C-4}) = -1500q_C + 500q_O + 2506. \qquad (2)$$

Table IV

IR frequency data: Charge distributions and bond orders

Compound	ν_{CO} ester	q_C	$-q_O$	d_{CO}	ν_{CO} (C-4 carbonyl)	q_C	$-q_O$	d_{CO}
*A*1 *a*	1708	0.474	0.513	0.864	—	—	—	—
*A*1 *b*	1680	0.502	0.514	0.854	—	—	—	—
*A*2 *a*	1717	0.474	0.513	0.864	—	—	—	—
*A*2 *b*	1677	0.502	0.514	0.854	—	—	—	—
*B*1 *a*	—	0.506	0.528	0.850	—	—	—	—
*B*1 *b*	—	0.513	0.531	0.846	—	—	—	—
*B*2 *a*	—	0.506	0.528	0.850	—	—	—	—
*B*2 *b*	—	0.513	0.531	0.846	—	—	—	—
*C*1	1740	0.513	0.529	0.848	1688	0.396	0.517	0.854
*C*2	1760	0.510	0.484	0.867	1705	0.390	0.458	0.887
*D*1	—	—	—	—	1662	0.401	0.500	0.863
*D*2	1722*	0.531	0.496	0.869	1615	0.411	0.494	0.872
*D*3	1757	0.517	0.499	0.869	1674	0.411	0.494	0.872
*D*4	1736	0.517	0.499	0.869	1670	0.411	0.494	0.872
*D*5	1670**	0.466	0.524	0.850	1670**	0.407	0.501	0.867
*E*1	—	—	—	—	1722	0.383	0.425	0.896
*E*2	—	—	—	—	1720	0.383	0.425	0.896
*E*3	1764	0.513	0.443	0.888	1704	0.392	0.428	0.901
*E*4	1732	0.513	0.443	0.888	1666	0.392	0.428	0.901
*E*5	1737	0.513	0.443	0.888	1670	0.392	0.428	0.901
*E*7	—	—	—	—	1712	0.383	0.425	0.896
*E*8	1660***	0.465	0.468	0.869	1720	0.390	0.430	0.900
*F*2	1732	0.519	0.518	0.857	1682	0.420	0.477	0.884
*G*1	1680	0.518	0.504	0.875	1610	0.420	0.477	0.884
*G*2	1683	0.518	0.504	0.875	1630	0.423	0.479	0.888
*G*3	1720	0.518	0.497	0.871	1670	0.422	0.472	0.886

* acid
** primary amide + C-4 carbonyl
*** primary amide

The constants in Eqs (1) and (2) were graphically determined. The calculated values are plotted versus the experimental results in Figs 2 and 4. The dependence of the band frequencies of the bond orders is illustrated in Figs 3 and 5.

Owing to the analogy in the structure, the stretching vibrations of the primary amide and the CO group of the free acid (*D*2, *D*5, *E*8) were classified together with the ester bands, though it is quite rare to discuss these bands

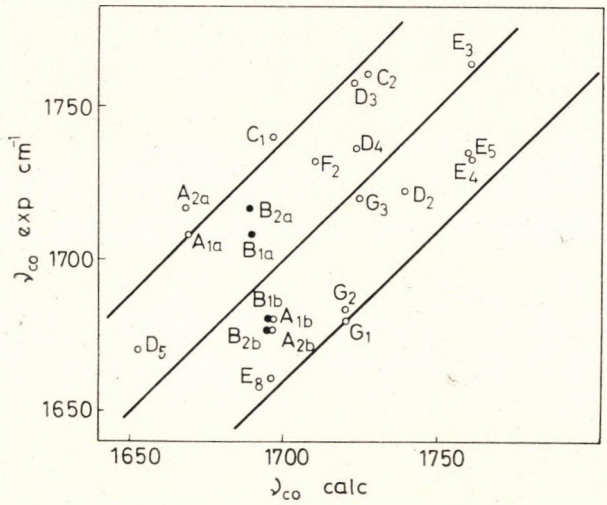

Fig. 2

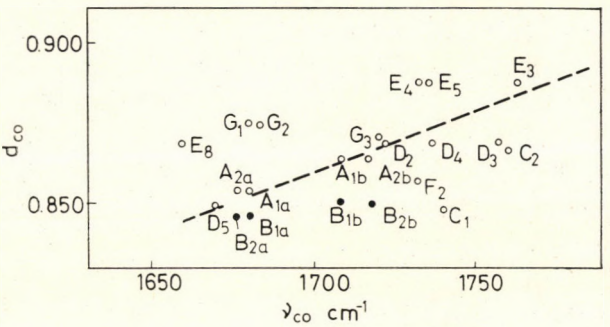

Fig. 3

together in IR spectroscopy. The reason for this is partly the fact that the different electron affinities of the OH and NH_2 groups affect the charge distribution of the CO bond to such an extent that the relative absorption band can significantly be shifted, and the relation to the ester band becomes unrecognizable. In the knowledge of the charge distribution, however, this shift can be taken into account and the approximate place of the bands are obtainable by applying Eq. (1) to the above compounds.

In the case of compound *D*5, the primary and tertiary amide bands overlap, and the frequency can be quite correctly calculated using Eq. (1) or (2). In compound *E*8 the primary amide band occurs at an extraordinarily low frequency, but here the charge distribution is also different from that of the other compounds. The band at 1720 cm^{-1} can be assigned to a tertiary amide vibration, which is shifted to rather high frequencies with the members of group *E*. The ester band of compounds *A*1 and *A*2 is split according to the

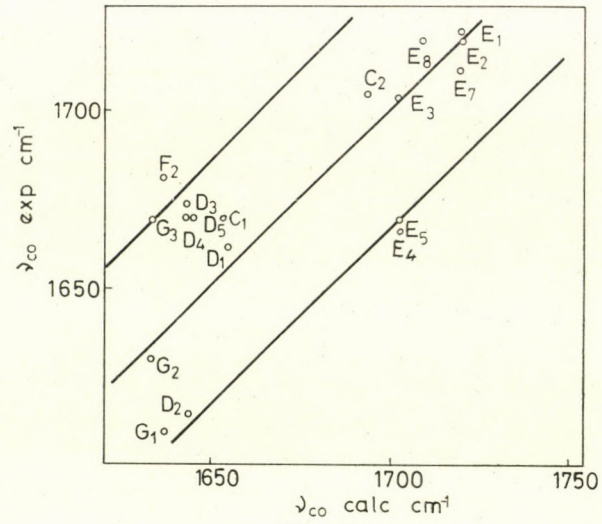

Fig. 4

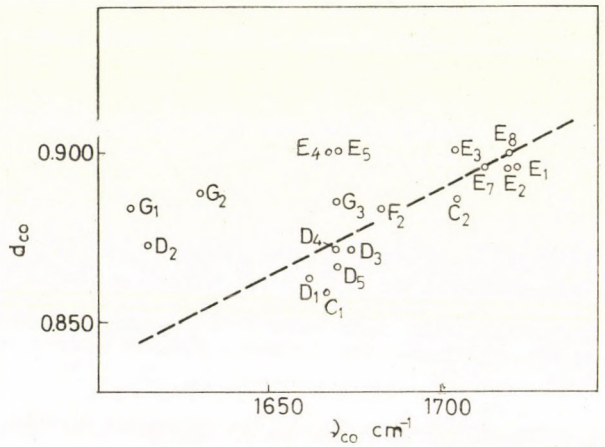

Fig. 5

different steric arrangement of the carboxyl groups. This is also reflected by the calculations, since both the charges on the carbon and oxygen atoms and the bond orders are different (see Table IV). In principle, the members of group *A* may form tautomeric couples and *B* may become stabilized under certain conditions, but no evidence was found to support this assumption. The calculations performed with two members of group *B* are indicated, for comparison, in Figs 2 and 3; the curves do not follow exactly the relationship between the frequency and bond order, but correspond rather to Eq. (1). The differences, however, are not significant, and therefore the problem cannot be decided on the basis of calculations.

NMR spectra

It is well known that the proton chemical shift is in correlation with the Hammett constant [20—22] and with the net charges of the neighbouring atoms [23—27]. DEL RE found a similar linear relationship between the charge distribution and chemical shift of amino acids [28]. Such a correlation was observed in our experiments between the chemical shift of the proton bound to C-2 of the ring and the total net ($\sigma + \pi$) charge of the same carbon atom (see Fig. 6, and Table V).

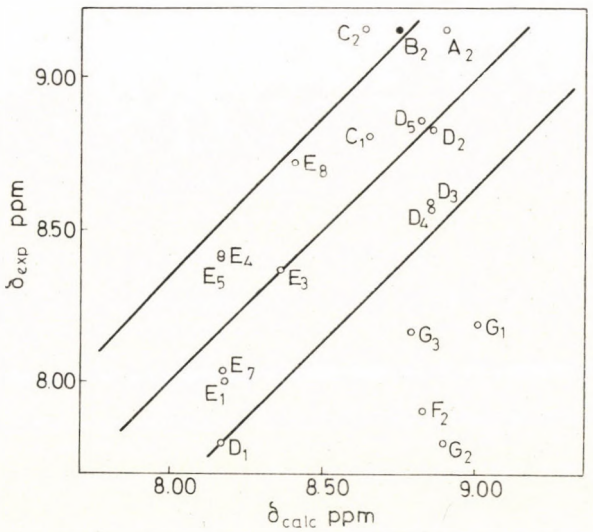

Fig. 6

The relationship can be described by the following equation:

$$\delta = 5.5q_C + 70q_H + 5.3 \tag{3}$$

The constants in Eq. (3) were determined graphically.

It can be seen that groups F and G differ substantially from the other groups; this fact can be attributed to the changes in magnetic anisotropy [29], since the conjugation in ring A involves only atoms 2—3—4—11—12—13—14, and the lone pair of nitrogen 1 is conjugated only to a very slight degree, due to the unfavourable steric position.

The point corresponding to the hypothetical compound B is also plotted in Fig. 6, but no significant difference is found with respect to group A. In case of groups D, E, F, and G, the protons attached to C-6 have chemical shifts between 4.9 and 6.2 p. p. m. $q_C = 0.016$ and $q_H = 0.042$. There is no methyl group at position 6 of compounds $D3$ and $E3$, and the chemical shift

Table V

Chemical shifts and charge distributions

Compound	Chem. shift, p. p. m.	q_C	q_H
*A*2	9.16	0.183	0.037
*B*2	—	0.154	0.037
*C*1	8.81	0.138	0.037
*C*2	9.16	0.097	0.040
*D*1	7.80	0.102	0.033
*D*2	8.83	0.174	0.037
*D*3	8.59	0.174	0.037
*D*4	8.57	0.174	0.037
*D*5	8.86	0.167	0.037
*E*1	8.00	0.015	0.040
*E*3	8.37	0.049	0.040
*E*4	8.42	0.051	0.037
*E*5	8.41	0.051	0.037
*E*7	8.03	0.015	0.040
*E*8	8.72	0.057	0.040
*F*2	7.91	0.171	0.037
*G*1	8.20	0.190	0.038
*G*2	7.80	0.183	0.037
*G*3	8.17	0.164	0.037

is accordingly 4.0 p. p. m., $q_C = -0.028$, $q_H = 0.044$. The chemical shift of the protons of the methyl group at C-6 is found between 1.09—1.45 p. p. m., $q_C = -0.113$, $q_H = 0.039$. Anomalies were found in the following cases: *A*2 ($\delta = 2.47$ p. p. m., $q_C = -0.118$, $q_H = -0.041$), *C*1 ($\delta = 3.09$ p. p. m., $q_C = 0.051$, $q_H = -0.028$), *C*2 ($\delta = 3.23$ p. p. m., $q_C = -0.051$, $q_H = -0.028$). Hyperconjugation was also taken into consideration when calculating the electron density of group *C*.

Experimental

The UV spectra were recorded on a Unicam SP 500 and SP 800, the IR spectra on a Zeiss UR 20 and Unicam SP 200, and the NMR spectra on a Perkin-Elmer R12 spectrometer. All materials used were of spectroscopical purity. The IR spectra were recorded by the KBr pellet technique, and some compounds were also examined in solution.

*

The authors are indebted to Dr. G. Biczó and Dr. J. Ladik for performing the PPP-calculations. Thanks are also due to Dr. L. Radics for recording and to Mr. P. Dvortsák for the interpretation of some NMR spectra.

REFERENCES

1. MÉSZÁROS, Z., KNOLL, J., SZENTMIKLÓSI, P.: To be published. Hungarian Pat. 156. 119 (2nd Nov., 1966); Belgian Pat. 705.934 (2nd Nov., 1966); French Pat. 78.134 (2nd Nov., 1966); UAR Pat. 8.398 (2nd Nov., 1966); GDR Pat. 64.462 (2nd Nov., 1966)
2. DEL RE, G.: J. Chem. Soc. **1958,** 4031
3. PARISER, R., PARR, R. G.: J. Chem. Phys. **21,** 466, 767 (1953)
4. POPLE, J.: TRANS. Faraday Soc. **49,** 1375 (1953)
5. MATAGA, N., NISHIMOTO, K.: Z. phys. Chem. **13,** 140 (1957)
6. SUTTON, L. E.: Tables of Interatomic Distances. The Chemical Society, Burlington House, London Wl, 1958.
7. YAMAKAWA, M., KUBOTA, T., AKAZAWA, H.: Theor. Chim. Acta **15,** 244 (1969)
8. CIGNITTI, M., PAOLONI, L.: Theor. Chim. Acta **7,** 383 (1967)
9. KÅRLSSON, G., MÅRTENSSON, O.: Theor. Chim. Acta **13,** 195 (1969)
10. MEZEY, P.: Unpublished work
11. NISHIMOTO, K., NAKATSUKASA, K., FUJISHIRO, R., KATO, S.: Theor. Chim. Acta **14,** 80 (1969)
12. SIEBERT, H.: Anwendungen der Schwingungspektroskopie in der anorganischen Chemie. Springer, Berlin—Heidelberg—New York, 1966
13. BELLAMY, L. J.: Chem. Soc. **1955,** 4221
14. FUSON, M., JOSIEN, M. L., SHELTON, E. M.: J. Am. Chem. Soc. **76,** 2526 (1954)
15. ROSETTI, G. P., SUSZ, B. P.: HELV. Chim. Acta **47,** 299 (1964)
16. STAAB, H. A.: Einführung in die theoretische organische Chemie, II. Aufl. Verlag Chemie, Weinheim, 1960
17. TANAKA J., NAGAKURA, S., KOBAYASHI, M.: J. Chem. Phys. **24,** 311 (1952)
18. BERTHIER, G., PULLMANN, B., PONTIS J.: J. Chem. Phys. **49,** 367 (1952)
19. PÁRKÁNYI, C., HORÁK V., PECKA, J., ZAHRADNIK, R.: Coll. Czechoslov. Chem. Commun. **31,** 835 (1966)
20. SPIESECKE, U., SCHNEIDER, W. G.: J. Chem. Phys. **35,** 731 (1961)
21. BOTHNER-BY, A. A., GLICK, R. E.: J. Am. Chem. Soc. **78,** 1071, (1956)
22. CARIO, P. L., DAILEY, B. P.: J. Am. Chem. Soc. **78,** 3043 (1956)
23. POPLE, J. A., SCHNEIDER, W. G., BERNSTEIN, H. J.: High-Resolution Nuclear Magnetic Resonance, pp. 257—262. McGraw Hill Book Co. Inc., New York, 1956.
24. O'REILLY, D. E., LEFTIN, H. P.: Phys. Chem. **64,** 1555 (1960)
25. SCHUG, J. L., DECK, J. C.: J. Chem. Phys. **37,** 2618 (1962)
26. SCHUG, J. L., CORPER, W. R.: Mol. Phys. **18,** 717 (1970)
27. WU, T. K., DAILEY, B. P.: J. Chem. Phys. **41,** 2796 (1964)
28. DEL RE, G.: In Electronic Aspects of Biochemistry, Ed. B. Pullmann, p. 232. Academic Press, Cambridge, 1964
29. POPLE, J. A.: J. Chem. Phys. **24,** 1111 (1956); Proc. Roy. Soc. A **239,** 541 (1957)

Gábor NÁRAY-SZABÓ
Erzsébet DUDAR
Gábor HORVÁTH
Budapest VIII., Rottenbiller u. 26.

Acta Chimica Academiae Scientiarum Hungaricae, Tomus 74 (3), pp. 293—313 (1972)

RELATIONSHIP BETWEEN THE SPIN RELAXATION AND CERTAIN CHEMICAL PROPERTIES OF PARAMAGNETIC IRON(III) SALT SOLUTIONS

A. VÉRTES* and F. PARAK**

(Department of Physical Chemistry and Radiology L. Eötvös University, Budapest, ** Physik Dep. E-15 der Technischer Universität München)*

Received June 21, 1971

Paramagnetic spin-relaxation in iron salt solutions was studied by Mössbauer spectroscopy. The chemical bonding between iron and its coordination sphere (bonding conditions) was found to influence the magnitude of the internal magnetic field pertaining to the $m_I = \pm 3/2 \rightarrow \pm 1/2$ transition of the $S_z = \pm 5/2$ Kramer doublet and by increasing the asymmetry of the $3d$ orbitals, the frequency of spin–lattic relaxation, *i.e.* the relaxation time. The method provides information on the types of solvates and complexes of iron in the solution under investigation, as well as on the relative amount of the components. The experiments have shown that the study of paramagnetic spin relaxation provides useful information on the chemical structure of the systems investigated.

Introduction

In our earlier communications [1—7] we have assumed that rapidly frozen solutions (cooled at a rate of 15 °C/sec) preserve the chemical structure they have in the liquid state. Thus the structure of complex compounds and ions formed in the course of hydrolysis, hydration and solvation remains essentially unchanged during rapid freezing.

Consequently, from the results of Mössbauer spectroscopic studies on frozen solutions, conclusions can be drawn as to the structure of the solution.

In our papers referred to above, we mentioned certain experiments which suggested (but did not prove) that rapid freezing leads to a quasi-solution structure. These experiments were of the following type.

Changes in the Mössbauer spectrum due to chemical changes brought about in the structure of the solution (*e.g.* as a result of a change in pH) can always be unequivocally interpreted [1, 5, 6].

Investigation of the Mössbauer parameters as a function of freezing rate has shown that above a threshold rate ($\sim$10 °K/sec), the Mössbauer parameters become independent of the rate of cooling [11].

It has to be mentioned here that x-ray diffraction tests [9, 10] fail to give an unequivocal answer to this problem, since the ice formed from atmospheric moisture precipitated on the sample surface under investigation has a cubic structure, which may mask the non-crystalline structure of the glass or solution under it in the course of x-ray diffraction tests. This explains why

certain authors [11] found that rapidly frozen solutions have a cubic structure while, according to others, cubic ice can be produced only by the condensation of water vapour.

Recent DTA experiments carried out by RUBY *et al.* [9] not only lend support to but provide proof for our earlier assumption that in the course of rapid freezing vitreous ice, a 'solidified solution' is formed.

When solutions rapidly frozen at liquid nitrogen temperature were heated, the DTA tests signalled an exothermic peak indicating crystallization, while when ice prepared by slow cooling was heated, this exothermic structural change could not be observed, for in the course of slow cooling, 'freezing' itself had produced crystalline structures (ice, eutectics, crystal hydrates).

In this paper we present a study of paramagnetic spin relaxation in frozen iron(III) salt solutions by means of Mössbauer spectroscopy. From the results, conclusions are drawn on the chemical properties of these solutions.

Paramagnetic spin relaxation

Mössbauer spectroscopy permits a thorough investigation of the hyperfine magnetic interactions between paramagnetic systems. Therefore, these problems have been studied by a number of authors [12—16] so that the theory of hyperfine magnetic interactions is today fairly clear and time is ripe for the utilization of these results of theoretical and partly experimental physics in some more 'practical' disciplines, *e.g.* in chemistry.

The source of the energy necessary for paramagnetic relaxation can be:

(1) energy transmission originating from the 'turning' of another spin; ($S_1 + S_2$—), the so-called spin flip-flop;

(2) liberation of a phonon from the crystal lattice surrounding the paramagnetic ion or atom.

The first case is referred to as spin–spin (*SSR*), the second as spin–lattice relaxation (*SLR*). If the average times of *SSR* and *SLR* are given the symbols τ_{SSR} and τ_{SLR}, respectively, then the time of spin relaxation (*SR*) will be

$$\tau_{SR} = \frac{1}{1/\tau_{SSR} + 1/\tau_{SLR}} \tag{1}$$

where τ_{SSR} is independent of the temperature, while τ_{SLR} is temperature dependent. For instance, in the case of rare earth metals [17]:

$$\tau_{SLR}^{-1} = (AT + Be^{-\Delta/kT} + CT^9), \ s^{-1} \tag{2}$$

where the various terms represent the possible relaxation mechanisms (so-called direct, Orbach, and indirect, Raman, mechanisms).

If the average life-time of the excited Mössbauer atom is τ_M and τ_{SR} is not less than the reciprocal frequency of the so-called Larmor precession of the magnetic momentum of the atomic nucleus

$$\tau_{SR},\ \tau_M \geq \omega_L^{-1} \tag{3}$$

then the Mössbauer nucleus 'senses' a magnetic field, hence the Mössbauer spectrum will show a Zeeman splitting.

The realization of the criterion implicit in inequality (3) may be promoted by increasing τ_{SR} or decreasing ω_L^{-1}. It follows from Eq. (1) that the increase of both τ_{SSR} and τ_{SLR} will result in the increase of τ_{SR}. The value of τ_{SSR} may be increased by increasing the distance between the paramagnetic atoms or ions (dilution), since in this way the possibility, that is the frequency, of spin–spin interaction decreases (resulting in the increase of τ_{SSR}).

The increase of τ_{SLR} can be achieved by decreasing the temperature (see *e.g.* Eq. (2)). It should be pointed out here that *SLR* — which is the interaction between lattice oscillations and the spin system — is manifest through the orbital momentum. Consequently, in the case of Fe^{3+} ions which possess a spherically symmetrical $3d^5$ external shell configuration term and ($^6S_{5/2}$ basic $L = 0$), a slow *SLR* is *ab ovo* to be expected.

In the case of the ^{57}Fe Mössbauer nucleus, depending on the effective magnetic field, the value of $10^{-8} < \omega_L^{-1} < 10^{-7}$, that is the value of ω_L^{-1} can of course be defined with the help of the external magnetic field too:

$$\omega_L = \frac{m_I}{I} g\mu_n H \tag{4}$$

where m_I is the magnetic quantum number, I the nuclear spin, g the so-called gyromagnetic factor, μ_n the nuclear magneton and H the effective magnetic field. ω_L is temperature independent.

To the description of the various interactions within the paramagnetic field the 'spin Hamiltonian' technique, frequently used in the study of electron spin resonance (*ESR*), can be applied:

$$\bar{H}_s = \bar{H}_Z + \bar{H}_{CF} + \bar{H}_{mhf} + \bar{H}_Q \tag{5}$$

where H_s is the sum of the most important interactions and the other operators (represent) the Zeeman, crystal field, magnetic hyperfine and electric hyperfine interactions in that order. The various interactions can be described in the following manner:

$$\bar{H}_Z = \beta Hgs \tag{6}$$

$$\bar{H}_{CF} = D[S_z^2 - (1/3)S(S+1)] + E(S_x^2 - S_y^2) \tag{7}$$

$$\bar{H}_{mhf} = A_z S_z I_z + A_x S_x I_x + A_y S_y I_y \tag{8}$$

$$\bar{H}_Q = P[(I_z^2 - 1/3)(I+1) + 1/3\,\eta(I_x^2 - I_y^2)] \tag{9}$$

where H is the external magnetic field, D and E are crystal field parameters, A_2, A_x and A_y are the main components of hyperfine magnetic interaction depending on the crystal field parameters of the Hamilton operator, P and η are parameters of the H operator describing electric quadrupole interaction (*e.g.* in the case of iron $P = 1/4\ e^2Q$).

The ratio $\lambda = E/D$ is used to describe the absolute magnitude of the crystal field [13], which for most systems hitherto investigated does not exceed the value of 1/3. Thus according to experience, $0 < \lambda < 1/3$.

In the vitreous systems (rapidly frozen solutions) investigated by us, $\lambda \sim 0$ and the hyperfine interactions (HFI) can be considered isotropic. Thus in the case of $H = 0$, the following Hamilton operator is obtained from Eqs (5) to (9) for the energy levels of the ^{57}Fe nucleus.

$$\bar{H} = A[I_z S_z + 1/2(S_+ I_- + S_- I_+)] + P[I_z^2 - 1/3 I(I+1)]. \tag{10}$$

It follows from Eq. (10) that, by accounting for the three Kramer doublets ($S_z = \pm 5/2, \pm 3/2, \pm 1/2$) and the nuclear spins of $I = 1/2$ and $I = 3/2$ pertaining to the ground state and to the excited state, respectively, the values obtained for the various energy levels ($\bar{H}$ eigenvalues) are:*

$$S_z = \pm 1/2 \begin{cases} I = 3/2 & 11/4\,A^* - P,\ 1/4\,A^* \left(-1 \pm \sqrt{7 - \dfrac{P}{A^*} - \dfrac{P^2}{A^{*2}}}\right) \\ & 3/4\,A^* + P,\ -13/4\,A^* - P \\ I = 1/2 & -7/4\,A,\ 1/4\,A,\ 1/4A,\ 5/4\,A \end{cases}$$

$$S_z = \pm 3/2 \begin{cases} I = 3/2 & \pm 9/4\,A^* + P,\ \pm 3/4\,A^* - P \\ I = 1/2 & \pm 3/4\,A \end{cases}$$

$$S_z = \pm 5/2 \begin{cases} I = 3/2 & \pm 15/4\,A^* + P,\ \pm 5/4\,A^* - P \\ I = 1/2 & \pm 5/4\,A \end{cases}$$

The ratio of A^* and A pertaining to the excited and ground state, respectively, is the same as the ratio of the corresponding g factors. In the case of ^{57}Fe:

$$A^*/A = -0.571 \text{ [18]}.$$

* The Kramer ground levels are due to the precession of the resultant spin vector of the electrons. According, however, to quantum mechanical concepts, the angle of this precessional movement can have only certain definite values. In the case of iron(III) for instance the eigenvalues of the precession — angle are such that the projection of the absolute spin on the precession axis is $S_z = 5/2$, $3/2$ or $1/2$.

The values obtained for the position of the Mössbauer lines from the eigenvalues pertaining to the states $I = 3/2$ and $I = 1/2$ are presented in Table I.

Table I

Position of lines

$S_z = \pm 1/2$

$7/4A - 13/4A^* - P + \delta$
$7/4A - 1/4A^*(1 + 4R)^1) + \delta$
$-1/4A - 13/4A^* - P + \delta$
$-1/4A - 1/4A^*(1 + 4R) + \delta$
$-5/4A - 1/4A^*(1 + 4R) + \delta$
$7/4A - 1/4A^*(1 - 4R) + \delta$
$-1/4A + 3/4A^* + P + \delta$
$-1/4A - 1/4A^*(1 - 4R) + \delta$
$-1/4A + 11/4A^* - P + \delta$
$-5/4A - 1/4A^*(1 - 4R) + \delta$
$-5/4A + 11/4A^* - P + \delta$

$S_z = \pm 3/2$

$\pm 3/4(A - 3A^*) + P + \delta$
$\pm 3/4(A - A^*) - P + \delta$
$\pm 3/4(A - A^*) - P + \delta$

$S_z = \pm 5/2$

$\pm 5/4(A - 3A^*) + P + \delta$
$\pm 5/4(A - A^*) - P + \delta$
$\pm 5/4(A + A^*) - P + \delta$

$R = \sqrt{7 - P/A^* - P^2/A^{*2}}$

Experimental

The solutions were prepared from metallic iron containing 90% of ^{57}Fe. (The Fe_2O_3 obtained from Oak Ridge was reduced in a H_2 atmosphere.) The pH was adjusted with $NaHCO_3$: using pH titrimeter or a precision pH paper, it was determined with an accuracy of ± 0.1 pH.

The reagents were analytical grade Mercxk preparations.

The solutions were placed in teflon sample holders provided with Hostafan windows. The path length of the gamma-rays in the solution was 1.5 mm. The sample holders with the solutions in the cryostat were immersed directly into liquid helium.

The 10 mCi, ^{57}Co Pt radiation source was kept at room temperature. The device moving the radiation source was controlled by a sinus signal. The pulses were detected by means of a 0.2 mm thick NaI scintillator and a 'Laben' type 400 channel analyzer in multi-scaler mode of operation.

For the determination and evaluation of the γ-resonance spectra an IBM 360/91 computer was used. In the course of measurements two identical spectra were recorded, so that as the first step in computer evaluation these spectra had to be united. The filling and decomposition of the individual spectral lines were performed by means of the Lorentz functions and the conventional least-squares method. Because of the complicated shape of the relaxation spectra, only the lines shown in Table II were fitted.

The number of pulses collected in each channel varied between 10^6 and 2×10^6.

Table II

1.	2.	3.	4.	5.	6.
No.	Composition of solution mol $(kg\ H_2O)^{-1}$	$H_{\delta/2}$ kOe	δ mm/sec	2 P mm/sec	Area of pair of the $\pm 5/4(A-3A^*)+P+\delta$ lines, %
1.	0.05 $FeCl_3$ + 2 HCl	549±1.4	0.22±0.05	0.10±0.05	17.5±2.4
2.	0.05 $FeCl_3$ + 2 (NaCl + HCl); pH 1	548±1.2			16.1±2.6
3.	0.05 $FeCl_3$ + 2 (NaCl + HCl); pH 2				11.4±2.1
					5.04±1.7
4.	0.2 $FeCl_3$ + 2 HCl				14.2±3.2
5.	0.2 $FeCl_3$		0.20±0.02		1.83±1.7
6.	0.5 $FeCl_3$ + 1 HCl				10.1±3.4
7.	1 $FeCl_3$ + 0.5 HCl				2.5±1.8
8.	0.025 $Fe_2(SO_4)_3$ + 1 H_2SO_4	561±1.2	0.135±0.017	0.03±0.02	19.8±3.0
9.	0.025 $Fe_2(SO_4)_3$ + 1 (Na_2SO_4 + H_2SO_4); pH 1	561±1.6	0.135±0.02	0.03±0.25	13.0±3.0
10.	0.025 $Fe_2(SO_4)_3$ + 1 (Na_2SO_4 + H_2SO_4); pH 2	558±4.9			11.4±4.0
11.	0.025 $Fe_2(SO_4)_3$ + 1 (Na_2SO_4 + H_2SO_4); pH 2.4		0.147±0.02		1.3±1.1
12.	0.3% Fe(III) + 65% HNO_3	569±1.4	0.18±0.01	0.00±0.01	27.6±1.1
13.	0.3% Fe(III) + 30% HNO_3	570±1.5	0.175±0.003	0.022±0.003	22.1±1.6
14.	0.05 $Fe(NO_3)_3$ + 2 HNO_3	568±2.1	0.155±0.02	0.03±0.02	21.3±3.00
15.	0.05 $Fe(NO_3)$ + 2 ($NaNO_3$ + HNO_3); pH 1	569±0.9	0.14±0.02	0.04±0.02	20.4±1.1
16.	0.05 $Fe(NO_3)_3$ + 2 ($NaNO_3$ + HNO_3); pH 2	567±1.3	0.145±0.04	0.05±0.04	17.7±2.5
17.	0.05 $Fe(ClO_4)_3$ + 2 $HClO_4$	582±8.0			
18.	0.05 $Fe(ClO_4)_3$ + 2 ($NaClO_4$ + $HClO_4$); pH 0.5	578±0.5	0.165±0.01	0.02±0.01	19.3±1.7
19.	0.05 $Fe(ClO_4)_3$ + 2 ($NaClO_4$ + $HClO_4$); pH 1				3.24±0.64
					19.15±1.70

20.	0.05 $Fe(ClO_4)_3$ + 2 ($NaClO_4$ + $HClO_4$); pH 2	583±96	0.155±0.016	0.05±0.02	20.5±3.0
21.	0.05 $Fe(ClO_4)_3$ + 2 ($NaClO_4$ + $HClO_4$); pH 2.3	582±1.5	0.17±0.02		18.1±2.4
22.	0.01 $Fe(ClO_4)_3$ + 2 $HClO_4$	586±4.3			9.1±3.1
23.	0.2 $Fe(ClO_4)_3$				6.0±3.8
24.	0.5 $Fe(ClO_4)_3$ + 1 $HClO_4$	583±6.0			6.5±3.0
25.	1 $Fe(ClO_4)_3$ + 0.5 $HClO_4$				3.1±1.7
26.	0.25% Fe(III) + 96% CH_3COOH		0.194±0.008	0.58±0.05	
27.	0.2% Fe(III) + 65% CH_3COOH	500±15			
28.	0.2% Fe(III) + 40% CH_3COOH	540±15			
29.	0.02 ($Fe(ClO_4)_3$ + 0.06 NTA + 1 $NaClO_4$; pH 4	546±4.0			11.2±2.2
		0	0.13±0.01	1.43±0.017	
30.	0.02 $Fe(ClO_4)_3$ + 0.06 NTA + 1 $NaClO_4$; pH 2.5	553±1.75	0.15±0.03	0.036±0.03	21.7±3.2
31.	0.02 $Fe(ClO_4)_3$ + 0.06 NTA + + 1 ($NaClO_4$ + $HClO_4$); pH 1	557±1.1			27.86±3.0
32.	0.02 $Fe(ClO_4)_3$ + 0.05 EDTA + 1 $NaClO_4$; pH 4	540±2			14.6±1.6
		463±4			11.5±2.3
33.	0.02 $Fe(ClO_4)_3$ + 0.05 EDTA + 1 $NaClO_4$; pH 3	540±1.8			21.4±2.4
34.	0.05 $Fe(ClO_4)_3$ + 1.8 $HClO_4$ + 0.17 KSCN	542±3			
35.	0.2 $K_3Fe(CN)_6$		−0.33 ±0.016	0.54±0.03	
36.	0.05 $FeSO_4$ + 1 H_2SO_4		1.025±0.004	3.30±0.007	

% = weight per cent or area-percentage

Magnetic susceptibility measurements were carried out with a Foner-type vibrational magnetometer.

The sensitivity of the measuring equipment was $\pm 10^{-9}$ cgs, while in the solutions under investigation the susceptibility corrected by a value accounting for the glass tank, varied between 0.6 and 1.5×10^{-7} cgs.

Results and discussion

The most important parameters of the Mössbauer spectra of the investigated solutions at He (4.5 °K) temperature are given in Table II. ($H_{5/2}$ is the internal magnetic field pertaining to the $S_z = 5/2$ Kramer doublet.)

The data in Table II indicate the following important correlations.

The value of $H_{5/2}$ is related to the degree of covalence of the chemical bond between iron(III) in solution and its internal ligand sphere. This may be explained by the direction of the polarization of the bonding electron pairs in the first internal ligand sphere which is opposite to the direction of the $3d^5$ electrons in high-spin iron(III), so that the bonding electron pairs can have a shielding effect on the latter. In this way the polarizing effect of the $3d^5$ electrons on the s electrons and consequently the Fermi-contact interaction too will be lower.

In agreement with the above, of the anions listed in Table II, the bonding of acetate to iron(III) involves a considerable degree of covalency. On the other hand, iron has the most markedly ionic structure in the presence of ClO_4^- ions.

The experiments have shown that the utilization of relaxation phenomena for the study of chemical bonds is an extremely sensitive method. For instance, in the case of such anions as NO_3^- and ClO_4^- it is difficult to distinguish the ligand spheres of iron by any other method (according to the literature, in the case of both anions a hexaaquo complex is formed), while the present method of investigation indicates a difference ($\Delta H_{5/2}$) one order higher than the experimental error for both anions. (This is in good agreement with some of our earlier Mössbauer spectroscopic results [6].) It should be mentioned here that the present result is not equivalent to the statement that iron(III) in NO_3^- and ClO_4^- solutions is not present as the hexaaquo complex, since the difference in $H_{5/2}$ may be due to the composition of the second ligand sphere.

In the case of some solutions listed in Table II, the Mössbauer spectrum does not show a hyperfine magnetic structure. This may have three different explanations. In the case of low-spin complexes (*e.g.* $K_3Fe(CN)_6$ solution, Table II, No. 35) the resultant spin of the $3d^5$ electrons ($S = 1/2$) is not sufficient for bringing about a polarization which would result in the Fermi-contact interaction of electrons. The other possible explanation is that the $3d$ orbital is highly symmetrical, which enhances spin-lattice interaction, that is the prob-

ability of spin-lattice relaxation ($\tau_{SLR} < 10^{-10}$ sec.). This is for instance the case with iron(II) (see Table II, No. 36).

The third reason for the lack of hyperfine magnetic structure might by the dimerization or polymerization of complex iron ions in the solution, leading to a significant increase in the probability of spin–spin relaxation. The aggregation of two molecules drastically reduces the distance between the two Fe atoms.

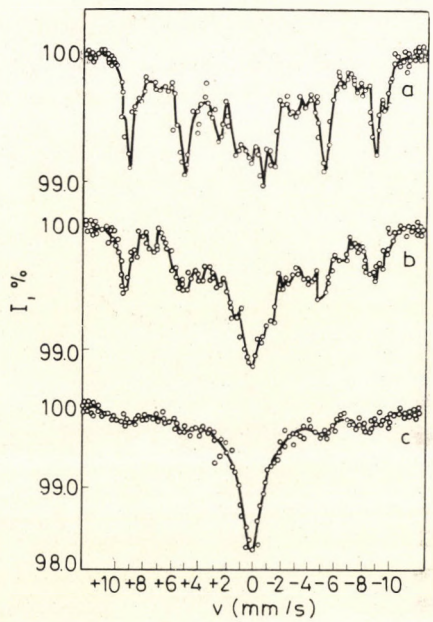

Fig. 1. Mössbauer spectra of $FeCl_3$ solutions of various concentrations. a) 0.05 mol kg^{-1} $FeCl_3$ + 2 mol kg^{-1} HCl; b) 0.2 mol kg^{-1} $FeCl_3$ + 2 mol kg^{-1} HCl; c) 0.5 mol kg^{-1} $FeCl_3$ + 1 mol kg^{-1} HCl

This is for instance the case in 96% acetic acid (Table II, No. 26). (We have shown in an earlier communication that iron polymerizes in acetic acid [3].)

From these experimental results conclusions can be drawn with respect to the correlation between the average distance of the iron(III) ions (iron(III) concentration) and τ_{SSR}. Figures 1 and 2 illustrate the Mössbauer spectra of iron(III) solutions of different concentrations in the presence of Cl^- and ClO_4^- ions. The pH of all solutions is < 0. It was found for both series of solutions that a slight hyperfine magnetic structure is apparent on the spectra even in the case of the highest concentrations (0.5 and 1 mol [kg H_2O]$^{-1}$). This hyperfine magnetic structure can be assigned to τ_{SSR} $2 \cdot 10^{-9}$. In the case of

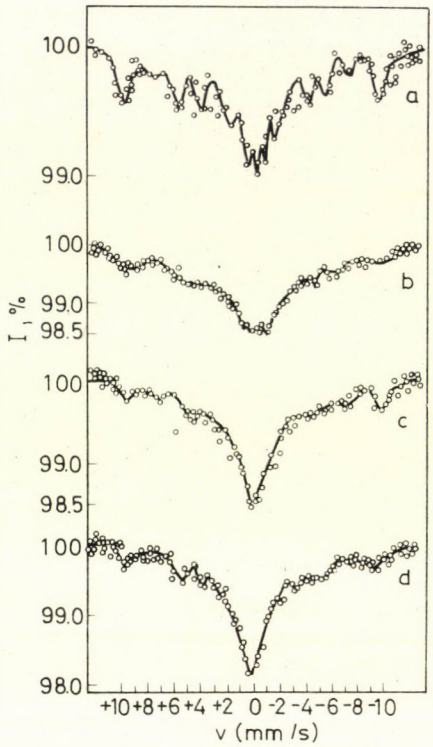

Fig. 2. Mössbauer spectra of $Fe(ClO_4)_3$ solutions of various concentrations. a) 0.01 mol kg^{-1} $Fe(ClO_4)_3$ + 2 mol kg^{-1} $HClO_4$; b) 0.05 mol kg^{-1} $Fe(ClO_4)_3$ + 2 mol kg^{-1} $HClO_4$; c) 0.5 mol kg^{-1} $Fe(ClO_4)_3$ + 1 mol kg^{-1} $HClO_4$; d) 1.0 mol kg^{-1} $Fe(ClO_4)_3$ + 0.5 mol kg^{-1} $HClO_4$

a concentration of 1 mol (kg H_2O)$^{-1}$ the average Fe–Fe distance is 11.6 Å. (If the concentration is 0.05 mol (kg H_2O^-)^1 the Fe–Fe distance is 31.7 Å.)

The decrease of the anion concentration (Fig. 3) results in an increase in the frequency of relaxation. This observation indicates that an increase in the amount of diamagnetic anions between the iron(III) ions inhibits (shields) the interactions which may raise the frequency of relaxation. The mechanism of this phenomenon is not yet clear.

Moreover, the possibility cannot be dismissed that in solutions containing nomatrix salt or acid, a slight segregation of the iron may take place during freezing, resulting in a higher probability of spin–spin relaxation.

It should be noted that a similar phenomenon has been observed when the experiments were carried out at the temperature of liquid nitrogen [19].

So far we have dealt with general properties of paramagnetic spin relaxaton in iron(III) solutions as they appear from our experimental results. We shall now investigate what further information of chemical nature can be

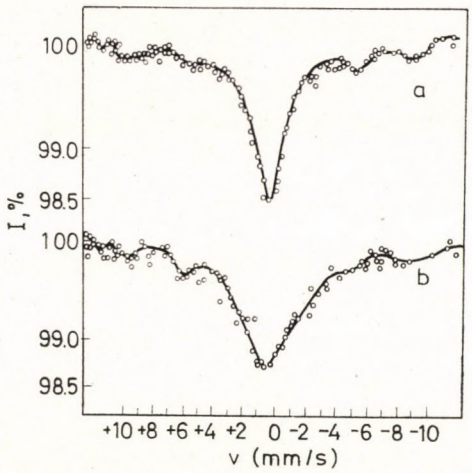

Fig. 3. Mössbauer spectra of a) 0.2 mol kg^{-1} $FeCl_3$ and b) 0.2 mol kg^{-1} $Fe(ClO_4)_3$ solutions

obtained for different solution types from paramagnetic spin relaxation as observed by means of Mössbauer spectroscopy.

Fig. 4 shows the Mössbauer spectra of *$FeCl_3$ solutions of different pH*'s. The internal part of the spectra represents the superposition of the following lines:

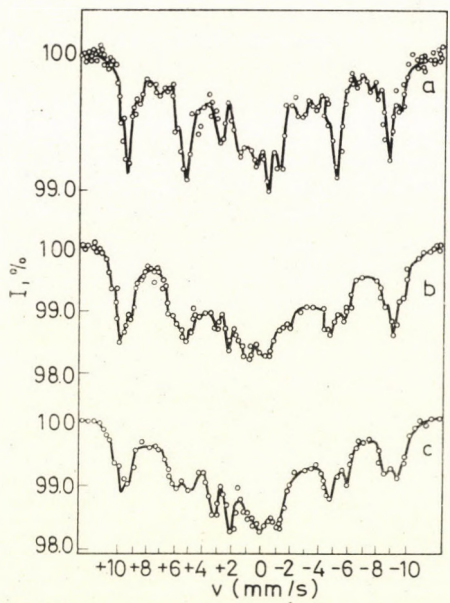

Fig. 4. Mössbauer spectra of $FeCl_3$ solutions of various pH. a) pH < 0; b) pH $= 1.0$; c) pH $= 2.0$

a) τ_{SR} pertaining to $S_z = \pm 1/2$ is significantly shorter than the relaxation times belonging to the other two Kramer doublets* [12] and, consequently, this doublet in general fails to show a hyperfine magnetic structure. In this way the resonance absorption of the iron atom in state $S_z = \pm 1/2$ raises the intensity of lines in the center of the spectrum.

b) All lines pertaining to the doublet $S_z = \pm 3/2$ (see Table I).

c) The lines resulting from the transitions $m_I = \pm 1/2 \rightarrow \pm 1/2$, pertaining to the Kramer doublet $S_z = -5/2$.

d) Lines resulting from components in the solution which, if dimerized or polymerized, lead to a $\tau_{SR} < \omega^{-1}$, hence the spectrum has no hyperfine magnetic structure.

Thus the internal part of the spectrum is the superposition of so many lines that a great uncertainty is introduced into the decomposition.

A further condition which hinders succesful decomposition of the internal lines is that a lower magnetic field is associated with the lines pertaining to the $m_I = \pm 1/2 \rightarrow \pm 1/2$ transitions of $S_z = +5/2$ and to $S_z = \pm 3/2$ and $S_z = \pm 1/2$ than to the two outer lines of the spectra ($S_z = \pm 5/2$; $m_I = +3/2 \rightarrow$ $\rightarrow 1/2$ and $m_I = -3/2 \rightarrow -1/2$). According to Eq. (4), this results, in lower ω_1 values, a fact associated with greater line width since in case of a given relaxation time, Γ is inversely proportional to ω_1 ($\Gamma \sim \omega_L^{-1}\, \tau_{SR}$). Decomposition is further hindered by the fact that the populations of the various Kramer doublets are not known.**

However, it can be ascertained even without decomposition that an increase in the pH results in an increased intensity of the spectral center, given by the following area proportions:

(for identical rate intervals)		
	pH < 0	49.2%
	pH $= 1$	55.5%
	pH $= 2$	58.6%

This increase of the area is related to the fact that the number of Fe—OH bonds increases with increasing pH and the complex ions formed, containing also "OH" and "Cl" bonds may cause dimerization. These complexes belong to category "*d*" of the above classification. We have demonstrated on the basis of electron exchange studies in an earlier paper [6] that Cl remains in the

* Transitions with $\Delta S_z > 1$ are forbidden, so that from the state $S_z = \pm 5/2$ relaxation can result only in the state $S_z = \pm 3/2$ (but *e.g.* the $S_z = +5/2 \rightarrow -5/2$ transition is not possible), that is from state $S_z = \pm 3/2$ the transitions $S_z = +3/2 \rightarrow +5/2$, $+3/2 \rightarrow +1/2$, $-3/2 \rightarrow$ $-5/2$ and $-3/2 \rightarrow -1/2$ are possible. In case of $S_z = \pm 1/2$ transition within the eigenstate, requiring less energy ($S_z = +1/2 \rightarrow -1/2$ or $-1/2 \rightarrow +1/2$) is possible, thus the probability of this last relaxation is higher than that in the first two cases.

** The populations pertaining to the various S_z values can be calculated by means of the Boltzmann statistics ($N_i = C_i e^{-Ei/KT}$), but the values of E_i are not known for the solutions under investigation.

inner coordination sphere of iron even if the pH is increased. Our present work, on the other hand, seems to indicate that this condition does not prevent dimerization through the OH or Cl bridges.

The outer lines of the spectra can only be assigned to the lines pertaining to $S_z = \pm 5/2$ ($\pm 3.391\ A + P + \delta$). The internal magnetic field, $H_{5/2} \sim$ $\sim$ 550 kOe, which can be calculated from the position of these lines seems to indicate that in the case of solutions containing 2 mol kg^{-1} of Cl^- ion, one chloride is coordinated to the majority (>60%) of iron atoms irrespective of the pH. Two pairs of lines of lower intensity corresponding to a lower, and a higher internal magnetic field are also superimposed on the pair of lines $H_{5/2} = 550$ kOe (see Fig. 4). These pairs of lines can be ascribed to the ions $[FeCl_2(H_2O)_4]^+$ and $[Fe(H_2O)_6]^{3+}$, respectively. For solutions with pH = 2 the decomposition of the two external pairs of lines will furnish the area percentages of $11.4 \pm$ $\pm 2.1\%$ and $5.0 \pm 1.7\%$. This percentage ratio is proportional to the amount of $[FeCl(H_2O)_5]^{2+}$ and $[FeCl_2(H_2O)_4]^+$ ions.*.

It follows from this that in a 2 *M* NaCl solution at pH = 2 the stability constant of the dichloride will be $\log K_2 = -0.64 \pm 0.28$.

Fig. 5 shows *the spectra of solutions containing* 1 mol kg^{-1} *of* So_4^{2-} *ion*. On spectrum pertaining to pH < 0 the appearance of all three Kramer doublets is quite clearly visible. From the value $H_{5/2} = 560$ kOe, the conclusion can be drawn that the sulfate ion is present in the inner coordination sphere of iron. As the pH increases, more and more of the iron in solution loses its hyperfine magnetic structure (HMS) which indicates the formation of hydroxo complexes with a higher degree of covalence. (We have demonstrated [4] by electron exchange studies for sulfate too that in the case of OH complex formation, and dimerization, the sulfate is still present in the inner coordination sphere of iron.) From the decomposition of spectra the following values are obtained for the amount of iron complexes with no HMS in solutions of different pH:

pH = 0	0%
pH = 1.0	$50 \pm 12\%$

* In the case of Mössbauer spectra of multicomponent samples the relationship between the areas of the various lines and the quantities of the components is described on the basis of the Lambert—Beer law by the following equation:

$$\ln\left(1 - \frac{\Sigma A_i}{I_0}\right) = -\Sigma \sigma_i n_i$$

where A_i is the area of the Mössbauer line (*s*) pertaining to the *i*-th component, σ_i is the cross-section of the resonance-absorption boundary of the *i*-th component and n_i the quantity (number of atoms) of the same component, while $(I_0 - A_i)$ is the area under the entire Mössbauer spectrum. Since in these experiments $\frac{\Sigma A_i}{I_0} < \frac{1}{100}$, the approper approximation is $\frac{\Sigma A_i}{I_0} = \Sigma \sigma_i n_i$. Assuming further that σ_i is the same for all components, the values A_i and n_i will be directly proportional to one another.

pH = 2.0	65± 8%
pH = 2.4	98.7±6%

The Mössbauer spectra of *solutions containing NO_3^- ion* are shown in Fig. 6. According to the literature, in solutions of low pH containing NO_3^-

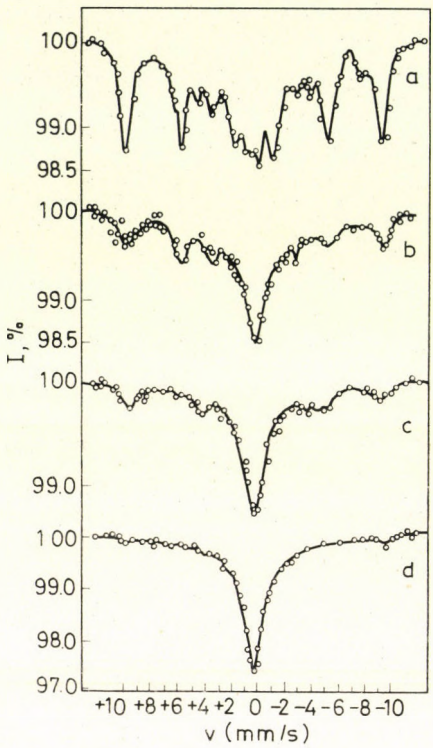

Fig. 5. Mössbauer spectra of $Fe_2(SO_4)_3$ solutions of various pH. a) pH < 0; b) pH = 1.0; c) pH = 2.0; d) pH = 2.4

and ClO_4^-, iron(III) is always present as the hexa-aquo complex. The difference between the $H_{5/2}$ values for the two anions indicates, however, as pointed out earlier, the presence of the nitrate in the outher coordination sphere of iron(III). It should be noted that the value $H_{5/2} = 570$ kOe, as measured by us in the presence of NO_3^- ions, differs from the value of 588 kOe reported by NOZIK and KAPLAN [2]. This may perhaps be attributed to the fact that the concentration of solutions investigated by us was twice as high (2 mol kg^{-1}) as that used by NOZIK and KAPLAN (1 mol/l), which causes a shift in the equilibrium of NO_3^- coordination. The difference may, however, be due also to the fairly great line width in the spectrum reported by these authors, a fact which greatly impairs

the accuracy of the determination of $H_{5/2}$ as pointed out by the authors themselves.

It appears from the measured spectra that in the case of nitrate solutions the population of the $S_z = \pm 5/2$ level is greater than that of the other two doublets.

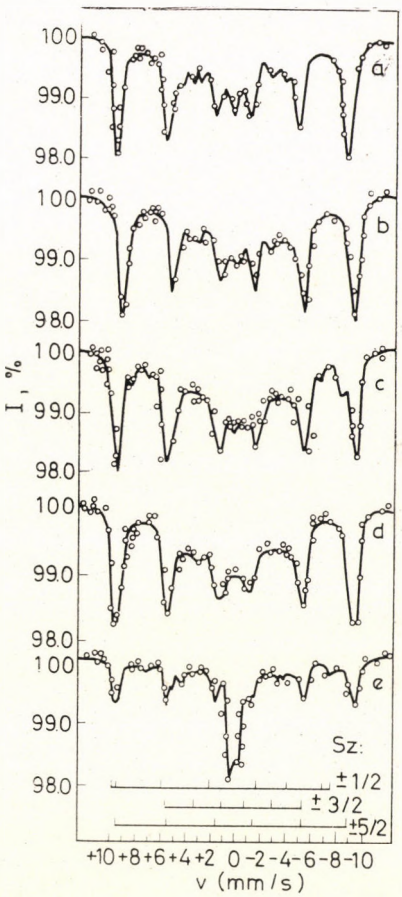

Fig. 6. Mössbauer spectra of $Fe(NO_3)_3$ solutions of various pH. a) 65% HNO_3; b) 30% HNO_3, c) 11.2 HNO_3; d) pH = 1.0; e) pH 2.0
The line intensities pertaining to the various Kramer doublets are plotted with the assumption that the population and τ_R values of the doublets are equal. This assumption is, however; not valid for practical conditions

It follows from the intensity of the lines $[\pm 5/4(A - 3A^*) + P + \delta]$ that the $S_z = \pm 5/2$ level is populated by more than 50% of the total quantity of iron. (On the basis of Boltzmann statistics it follows from this that of the three different Kramer doublets the lowest energy level belongs to $S_z = 5/2$.)

In the spectrum pertaining to pH = 2.0 the area ratio of the quadrupole pair of lines ($2P = 0.43 \pm 0.03$ mm/s), which have no hyperfine magnetic

structure is $21.8 \pm 5.6\%$. This pair of lines can in all probability be ascribed to the $[Fe_2(OH)_2(H_2O)_8]^{4+}$ complex ion.

The Mössbauer spectra of *perchlorate solutions* are shown in Fig. 7. Compared with the solutions discussed so far, a new fact arises, namely a sudden increase in the relaxation frequency, $\tau_{SR} \sim 5 \times 10^{-9}$ s, at pH < 0. (A broadening of the external lines indicates that we are dealing here not with the super-

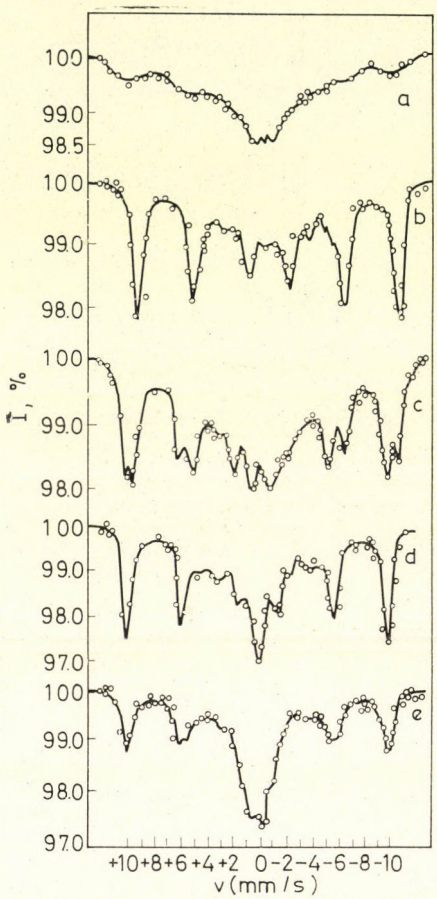

Fig. 7. Mössbauer spectra of $Fe(ClO_4)_3$ solutions of various pH. a) pH < 0; b) pH $= 0.5$; c) pH $= 1.0$; d) pH $= 2.0$; e) pH $= 2.3$

position of a new line without hyperfine magnetic structure, as is the case *e.g.* at pH 2.) The probable explanation of this phenomenon is that in frozen solutions perchlorate ions greatly loosen the structure, hence lack a stable hydration sheath and may act as phonon sources, thereby raising the probability of spin–lattice relaxation. The intensity of the line due to the dimer [20] is

60±15% at pH 2 and 67±14% at pH 2.3. (We wish to add here that the amount of the dimer can be determined more accurately from the measurement of electron exchange [23].)

Fig. 8 shows the Mössbauer spectra of some *CH_3COOH—H_2O—Fe systems*. The values of δ indicate that iron is in the oxidation state of 3^+. Nearly the whole amount (more than 90%) of the iron in 96% acetic acid furnishes a

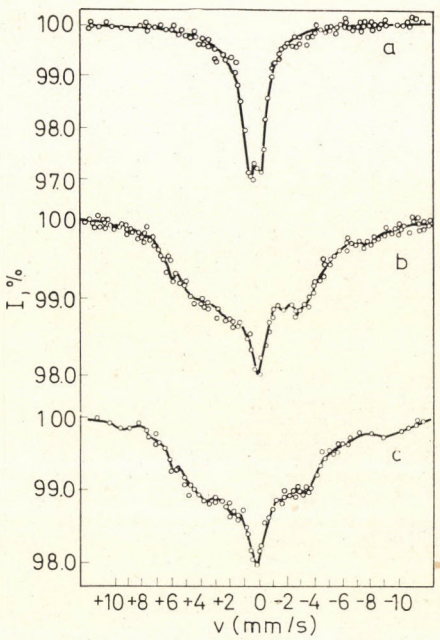

Fig. 8. Mössbauer spectra of some CH_3COOH — H_2O — Fe systems. a) 96% CH_3COOH; b) 65% CH_3COOH; c) 40% CH_3COOH

quadrupole pair of lines, thus lacks HMS. The relatively large quadrupole splitting ($2P = 0.58$ mm/s) indicates that the iron has a mixed ligand solvation shell. Since iron was dissolved in acetic acid in the presence of air, that is of oxygen, this result, namely the lack of HMS, supports our earlier supposition [3] that under such conditions polymer formation starts after dissolution.

In systems containing 35% or 60% H_2O a considerable fraction of the iron is present in a form with a hyperfine magnetic structure. This obviously indicates that in the last two cases the water molecules also participate in the formation of the inner coordination sphere of iron and hinder polymerization. The short relaxation time ($\tau_{SR} \sim 2 \times 10^{-9}$ sec), which follows from the relatively small internal magnetic field ($H_{5/2} \sim 500$ kOe) and from the shape of the spectrum, indicates that even large amounts of water do not displace the ace-

tate or OH groups, from the inner sphere owing to their stronger covalent bonding.

Iron–acetate bonds are formed in a similar manner if the solution contains ethylene-diamine-tetra-acetic acid (EDTA) or nitrilotriacetic acid (NTA).

The Mössbauer spectra of *NTA solutions of different pH* are presented in Fig. 9 (for the concentrations see Table II). At pH 4 the spectrum can be

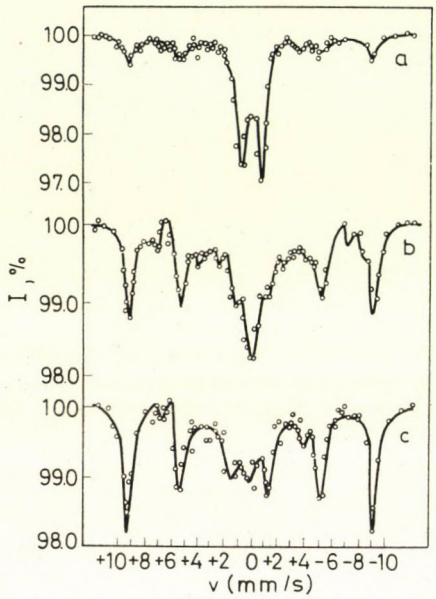

Fig. 9. Mössbauer spectra of NTA solutions of various pH. a) pH = 4.0; b) pH = 2.5; c) pH = 1.0

decomposed into a quadrupole pair of lines and a spectrum component showing Zeeman splitting.

In this solution the lack of hyperfine magnetic structure may be due either to dimerization (polymerization) or to a low-spin electron structure. To clarify this problem the magnetic susceptibility of a solution containing 0.33 mol of $FeCl_3$ and 0.68 mol of NTA per 1000 g of H_2O was measured at pH 4 the temperature interval between 95 and 295 °K. (The concentration could not be as low as that used in Mössbauer measurements, since in such a case the error of susceptibility measurements would be too high.) The experimental results follow the Curie–Weiss law with $i = 30 \pm 5°$. The 'spin-only'* value is 2.8 ± 0.2 B. M.

* The magnetic susceptibility measurements were carried out in the Central Research Institute of Physics, Hungarian Academy of Sciences, by Mrs. PARDAVI-HORVÁTH to whom the authors are indebted for her very careful work.

This value indicates low-spin structure which, however, does not unambiguously exclude the possibility of dimerization (polymerization), since similar 'spin-only' values have been found [24] in the highs-pin polynuclear iron(III) acetate complex. In the dimer (or polymer) the spin of some iron atoms may have an opposite orientation. The relatively high Weiss constant also points to an antiferromagnetic interaction and, therefore, if these experimental results are evaluated together, it appears that the quadrupole pair of lines can be ascribed to a polynuclear complex.

The value of $H_{5/2}$ gradually increases with decreasing pH (see Table II), indicating a decrease in the number of acetate bonds. The great quadrupole splitting of the complex without HMS ($2P = 1.43 \pm 0.02$ mm/s) shows that the inner coordination sphere, that is the electron structure of iron, is highly asymmetric. From the decomposition of the spectra the following values are obtained at different pH values for the component without *HMS*:

pH = 4.0	$68.9 \pm 4.5\%$
pH = 2.5	$58.5 \pm 14\%$
pH = 1.0	0%

In the case of *iron–EDTA complexes* no complete disappearance of the hyperfine magnetic structure was observed (Fig. 10). In the solution of pH 4 the lines $[\pm 5/4(A - 3A^{+}) + P + \delta]$ doubled; $(H_{5/2})_I = 540$ kOe and $(H_{5/2})_{II} = 460$ kOe. The internal magnetic field of 460 kOe indicates a strong covalence effect. Certain authors have concluded from x-ray diffraction [25] and Mössbauer measurements [26] that in the $NaFe(OH)_2$ –EDTA–$n.H_2O$ complex, iron(III) has a coordination number of seven, so that the possibility of iron's having a coordination number of seven in solution cannot be dismissed. In this case probably $(H_{5/2})_{II}$ is assigned to the complex with a coordination

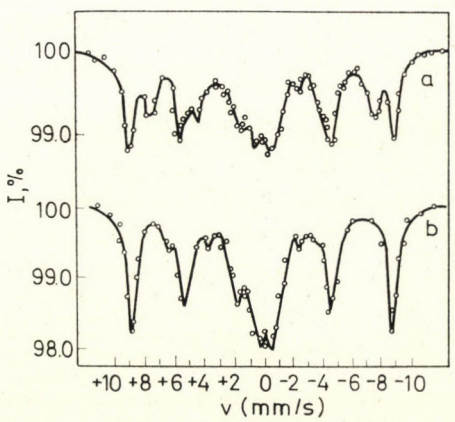

Fig. 10. Mössbauer spectra of EDTA solutions of various pH. a) pH = 4,0; b) pH = 3.0

number of seven, and $(H_{5/2})_I$ to the complex with a coordination number of six. This assumption is supported by the fact that at pH 3 only the lines of the latter complex are present, while at pH 4 the ratio of the two complexes is 14.6 : 11.5. (In the more acidic solution the number of non-coordinated acetate groups is greater.)

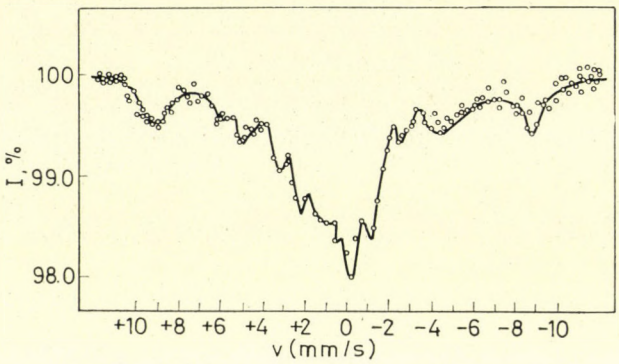

Fig. 11. Mössbauer spectra of KSCN solution

The Mössbauer spectrum of the solution containing thiocyanate is shown in Fig. 11 (for the concentrations see Table II). The spectrum is the superposition of the lines of three different complexes $(Fe(SCN)_x$, $x = 1, 2, 3)$, a fact that makes the decomposition of the spectrum extremely difficult. (The possibility of separating the three components in a spectrum recorded with higher statistics over several weeks is, however, theoretically not unlikely.) The information obtained from this spectrum is that the highest $H_{5/2} = 540$ kOe, thus the Fe–SCN bond has a higher degree of covalency than the Fe–Cl bond.

*

The authors wish to thank Prof. R. L. MÖSSBAUER for the opportunity he has given them in his Institute to perform this work which he followed with great attention and supported in many ways. They are also indebted to Professors V. A. TRUKHTANOV and K. BURGER who were always willing to participate in the discussion of the experimental results.

Thanks are due to the Humboldt Committee of the BRD for offering a scholarship to one of the authors (A. VÉRTES) for the time of his stay in Garching-München, thereby contributing to the successful performance of this work.

REFERENCES

1. VÉRTES, A.: Acta Chim. Acad. Sci, Hung. **63,** 9 (1970)
2. VÉRTES, A., BURGER, K., SUBA, M.: Acta Chim. Acad. Sci. Hung. **63,** 123 (1970)
3. VÉRTES, A., KISS, L., VARSÁNYI, M.: Acta Chim. Acad. Sci. Hung. **65,** 67 (1970)
4. VÉRTES, A., SUBA, M., KOMOR, M.: Radiochem. Radioanal. Letters **3,** 365 (1970)
5. VÉRTES, A., DÉZSI, I., SUBA, M.: Acta Chim. Acad. Sci. Hung. **64,** 347 (1970)
6. VÉRTES, A., KOMOR. M., DÉZSI, J., BURGER, K., SUBA, M., GELENCSÉR, P.: Proceedings of the 3d Symposium on Coordination Chemistry, Vol. 1, pp. 477 Debrecen, Hungary 1970
7. GREENWOOD, N. N., TURNER, G. E., VÉRTES, A.: Inorg. Nucl. Chem. Letters **7,** 389 (1971)

8. RUBY, S. L., TSENG, P. K., AWA-SHENG, LI, N.C.: Chem. Phys. Letters **2**, 39 (1969)
9. BERTIE, J. E., CALVERT, L. D., WHALLEY, E.: J. Chem. Phys. **38**, 840 (1963)
10. WELTMAN, H. J.: Report, No. *Ad* 423175 (Defense Documentation Center for Scientific and Technical Information, Cameron Station, Alexandria, Va. 1963)
11. RUBY, S. L., PELAH, J.: Research Report, Argonne National Laboratory
12. WERTHEIM, G. K., REMEIKA, J. P.: Phys. Letters, **10**, 14 (1964)
13. WICHMAN, H. H., KLEIN, M. P., SHIRLEY, D. A.: Phys. Rev. **152**, 345 (1966)
14. BLUME, M.: Phys. Rev. Letters, **14**, 96 (1965)
15. AFANASEV, 1. M., KAGAN, Y.: Zh.: Eksp. Teor. Fiz. **45**, 1660 (1963)
16. BRUCHKERR, W., RITTER, G., WEGENER, H.: Z. Physik, **236**, 52 (1970)
17. ORBACH, R.: Proc. Phys. Soc. (London) A**77**, 821 (1961)
18. PRESTON, R. S., HANNA, S. S., HEBERLE, J.: Phys. Rev. **128**, 2207 (1962)
19. PLATSHINDA, A. S. R., KOMOR, M., VÉRTES, A.: J. Radioanal. Chem. (In press.)
20. MULAY, L. N., SELWOOD, P. W.: J. Am. Chem. Soc. **77**, 2693 (1955)
21. NOZIK, A. J., KAPLAN, M.: J. Chem. Phys. **49**, 4141 (1968)
22. HUNT, J. P.: Metal Ions in Aqueous Solutions. W. A. Benjamin Inc., New York 1963.
23. KOMOR, M., VÉRTES, A., DÉZSI, J., RUFF, J.: Acta Chim. Acad. Sci. Hung. **66**, 285 (1970)
24. FIGGIS, B. N., LEWIS, J.: The magnetic properties of transition metal complexes. Progress in Inorganic Chemistry, F. A. COTTON, Ed. Vol. 6. Interscience. New York 1964; and REIFF, W. M., LONG, G. J., BAKER, W. A.: J. Chem. Soc. **90**, 6347 (1968)
25. LIND, M. O., HOARD, J. L.: Inorg. Chem. **3**, 34 (1964)
26. SPIJKERMAN, I. I., HALL, L. H., LAMBERT, I. L.: J. Am. Chem. Soc. **90**, 2039 (1968)

Attila VÉRTES; Budapest VIII., Puskin u. 11—13.
Fritz PARAK; Physik Dep. E-15 der Technischer Universität München DBR.

Acta Chimica Academiae Scientiarum Hungaricae, Tomus 74 (3), pp. 315—33 (1972)

INFRARED SPECTRA OF 1,2,3,5-TETRASUBSTITUTED BENZENE DERIVATIVES, I

G. VARSÁNYI and P. SOHÁR

(Department of Physical Chemistry, Polytechnical University and Research Institute for Pharmaceutical Chemistry, Budapest)

Received September 20, 1971

The infrared spectra of fifteen 1,2,3,5-tetrasubstituted benzene derivatives are analyzed in detail. Relations are established, partly for the frequencies and the intensities of the bands, and partly for the effects of the substituents on the electronic distributions, between the coupling of vibrations of the same symmetry and the stiffening effects of the intermolecular forces. It is clearly established that gallic acid trimethyl ether forms dimers to only a small extent, while intermolecular hydrogen bonds are formed mostly between the carboxylic hydroxyl groups and the oxygen atom of the methoxy group. The $\delta_{as}CH_3$ bands of the sterically hindered methoxy groups are strong and have anomalously low frequencies.

Introduction

In the present paper the infrared spectra of those 1,2,3,5-tetrasubstituted benzene derivatives are interpreted, in which the first atom (that bound directly to the aromatic ring) of each of the four substituents is a light atom, *i.e.* its atomic weight is less than 20.

It can be seen from Table I that with the exception of the final compound the substituents in the 1 and 3 positions are identical.

The normal vibrations of the compounds can be classified into two main groups [1]. One of these groups contains the aromatic ring vibrations, including those normal vibrations in which a decisive role is played by the stretching and bending of the bond between the first atom of the substituent and the corresponding carbon atom of the ring. There are 30 of these in each compound, and they are denoted by the Wilson numbering system [2] referring to benzene. The second group contains the internal vibrations of the substituents.

Schematic diagrams of the normal vibrations belonging to the first group are shown in Fig. 1. These 30 normal vibrations can be classified as follows:

1. Tangential skeletal vibrations (8a, 8b, 14, 19a, 19b).
2. In-plane bending C—X vibrations (3, 9a, 9b, 15).
3. In-plane bending C—H vibrations (18a, 18b).
4. Radial skeletal vibrations (1, 6a, 6b, 12).
5. C—X stretching vibrations (2, 7a, 7b, 13).
6. C—H stretching vibrations (20a, 20b).

7. Out-of-plane skeletal vibrations (4, 16a, 16b).
8. Out-of-plane C—X vibrations (5, 10a, 10b, 17b).
9. Out-of-plane C—H vibrations (11, 17a).

Table I

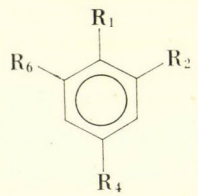

Number of compound	Substituent			
	R^2	R^1	R^3	R^5
I	OH	OMe		COOH
II	OMe	OMe		COOH
III	OEt	OMe		COOH
IV	O-*n*-propyl	OMe		COOH
V	OAc	OMe		COOH
VI	OH	OH		COOMe
VII	OH	OMe		COOMe
VIII	OMe	OMe		COOMe
IX	OMe	OMe		$CONH_2$
X	O-allyl	OMe		$CONH_2$
XI	OMe	OMe		CHO
XII	O-allyl	OMe		CN
XIII	OMe	OMe		NO_2
XIV	OH	NO_2		NO_2
XV	CO-*n*-propyl	OH	OAc	OAc

It must be noted that quite a few of the listed vibrations do not correspond to the simple classifying nomenclature: they are often mixtures of several types of vibration mode (*e.g.* the skeletal and C—X vibrations can never be separated from the C—H vibrations, or the skeletal vibrations from the vibrations of the substituents, and *vice versa*).

Experimental conditions

The compounds were studied in KBr pellets with Perkin—Elmer 457 and UR-10 spectrometers. The spectra are shown in Figs 2—16.

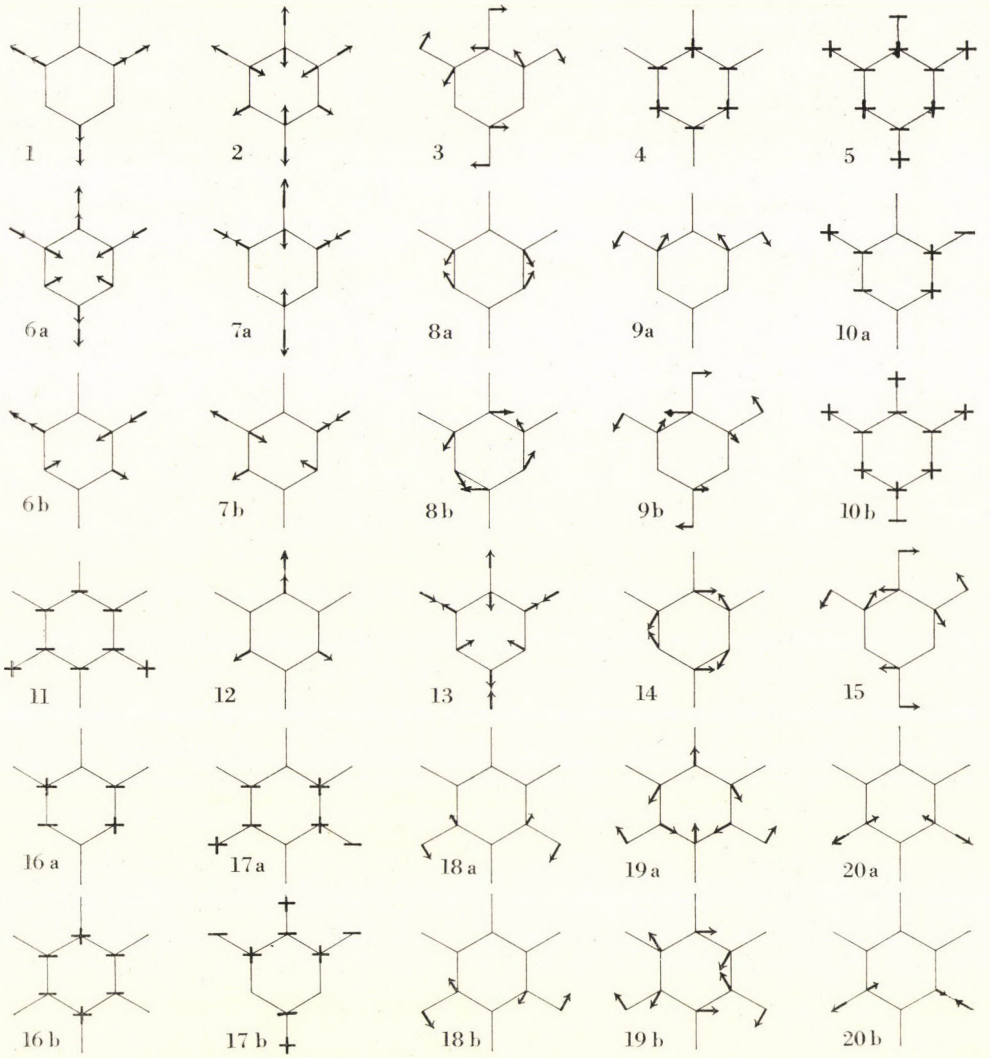

Fig. 1

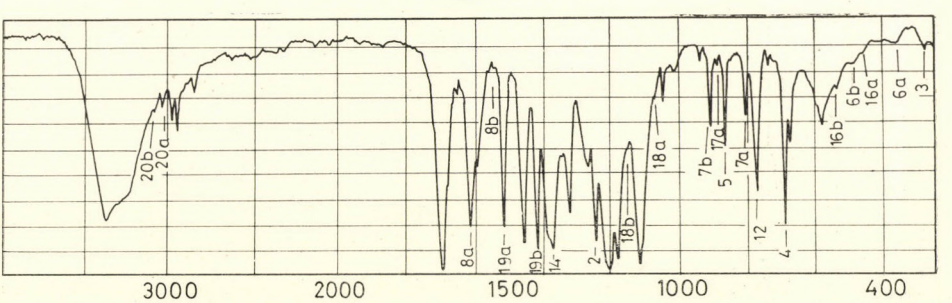

Fig. 2. 3,5-Dimethoxy-4-hydroxy benzoic acid **(I)**

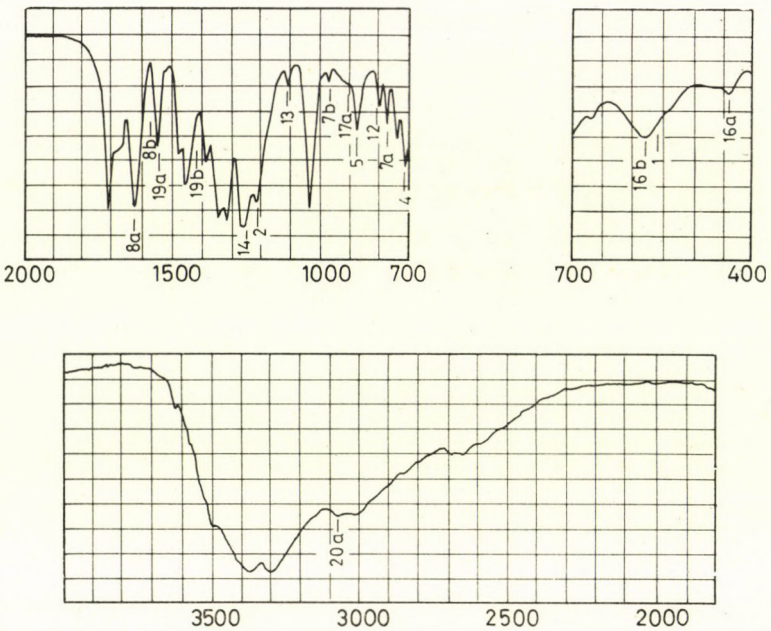

Fig. 3. 3,4,5-Trimethoxy benzoic acid **(II)**

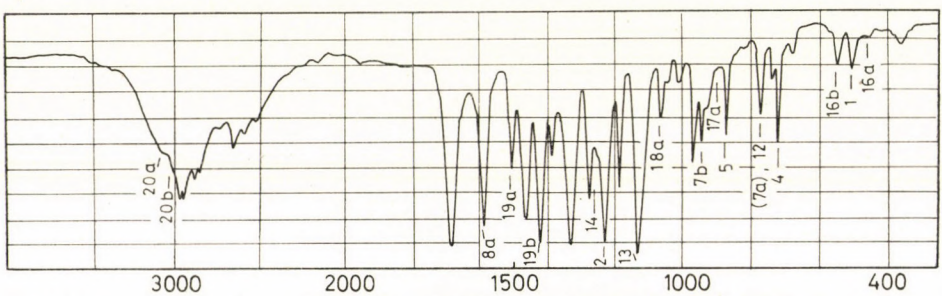

Fig. 4. 3,5-Dimethoxy-4-ethoxy benzoic acid **(III)**

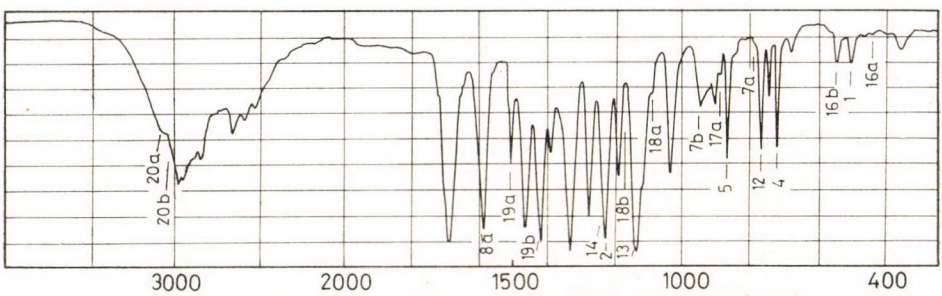

Fig. 5. 3,5-Dimethoxy-4-propoxy benzoic acid **(IV)**

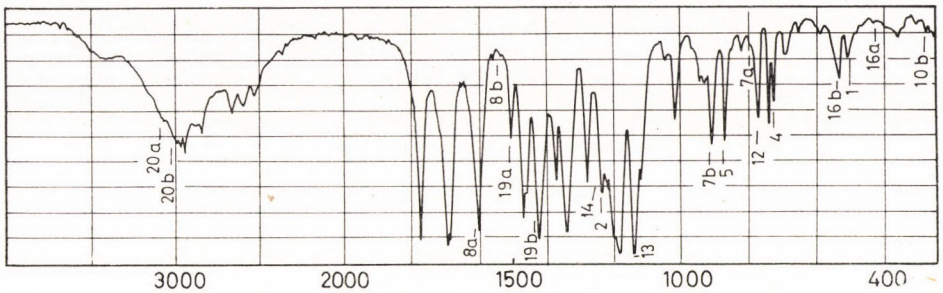

Fig. 6. 3,5-Dimethoxy-4-acetoxy benzoic acid **(V)**

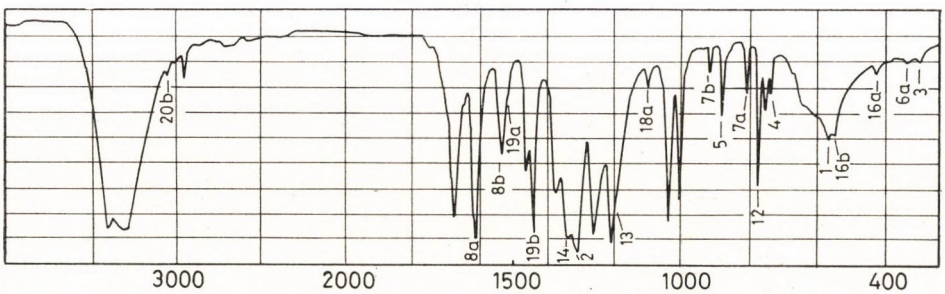

Fig. 7. Gallic acid methyl ester **(VI)**

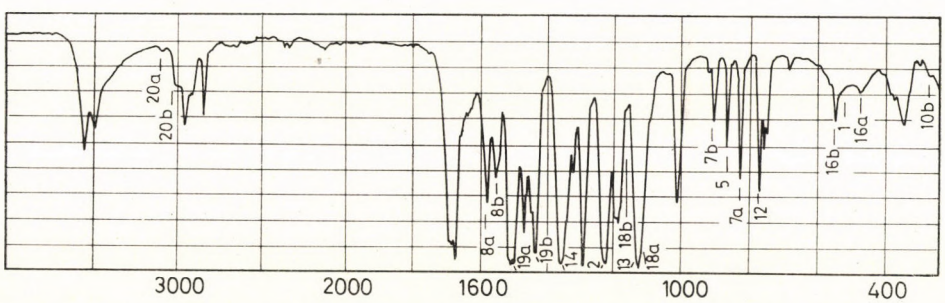

Fig. 8. 3,5-dimethoxy benzoic acid methyl ester **(VII)**

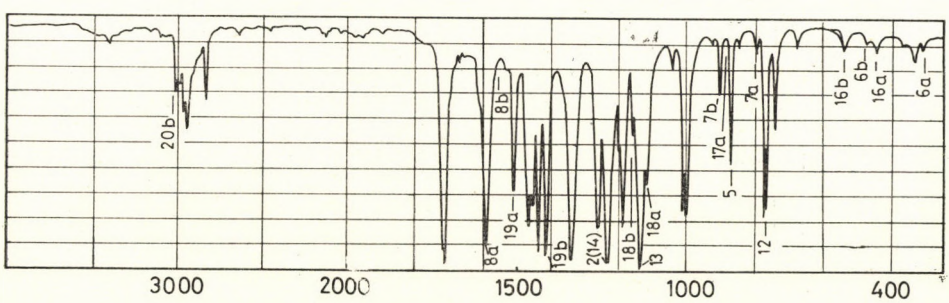

Fig. 9. 3,4,5-Trimethoxy benzoic acid methyl ester **(VIII)**

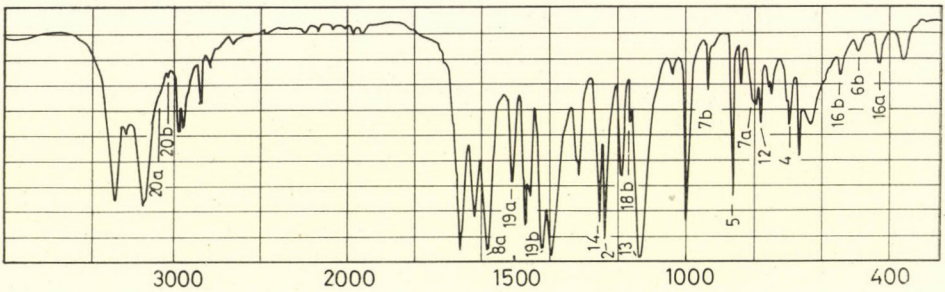

Fig. 10. 3,4,5-Trimethoxy benzoic acid amide **(IX)**

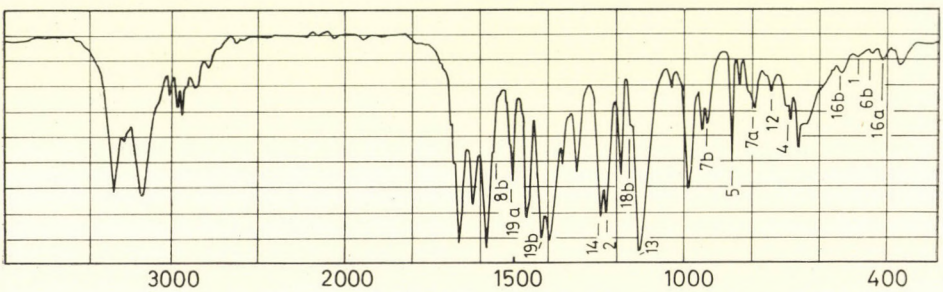

Fig. 11. 3,5-Dimethoxy-4-allyloxy benzoic acid amide **(X)**

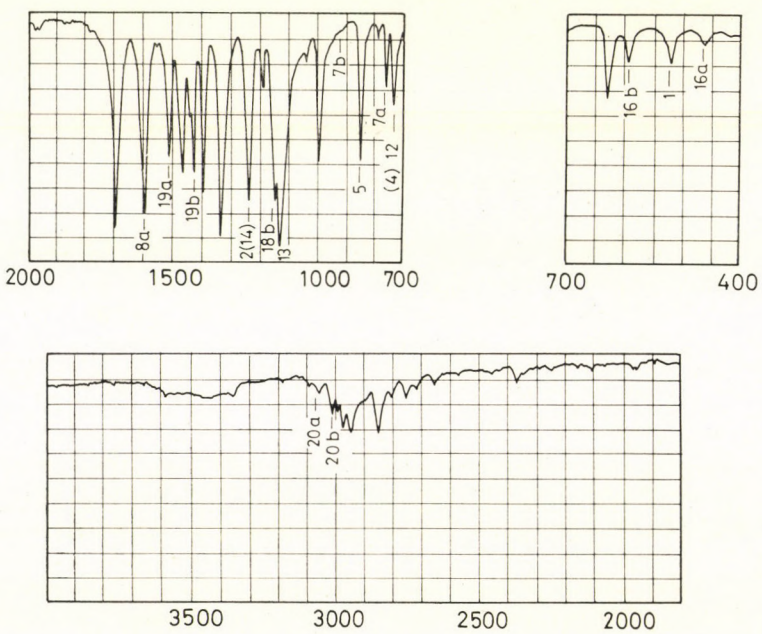

Fig. 12. 3,4,5-Trimethoxy benzaldehyde **(XI)**

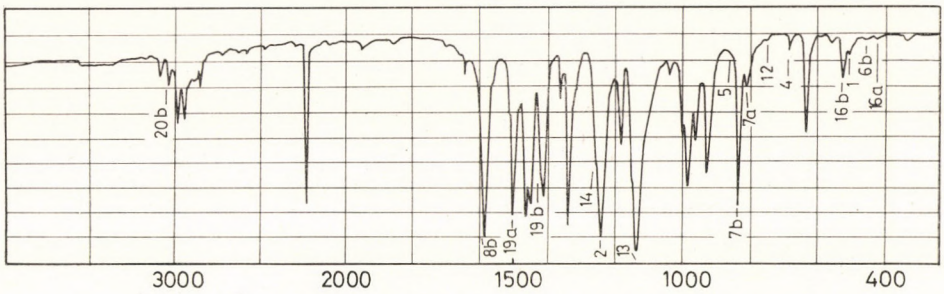

Fig. 13. 3,5-Dimethoxy-4-allyloxy benzonitrile **(XII)**

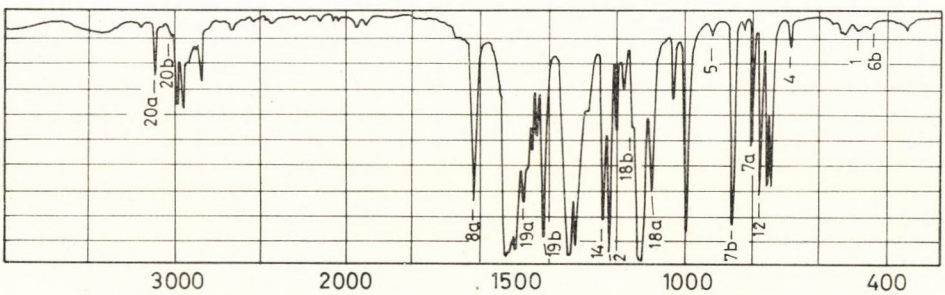

Fig. 14. 3,4,5-Trimethoxy nitrobenzene **(XIII)**

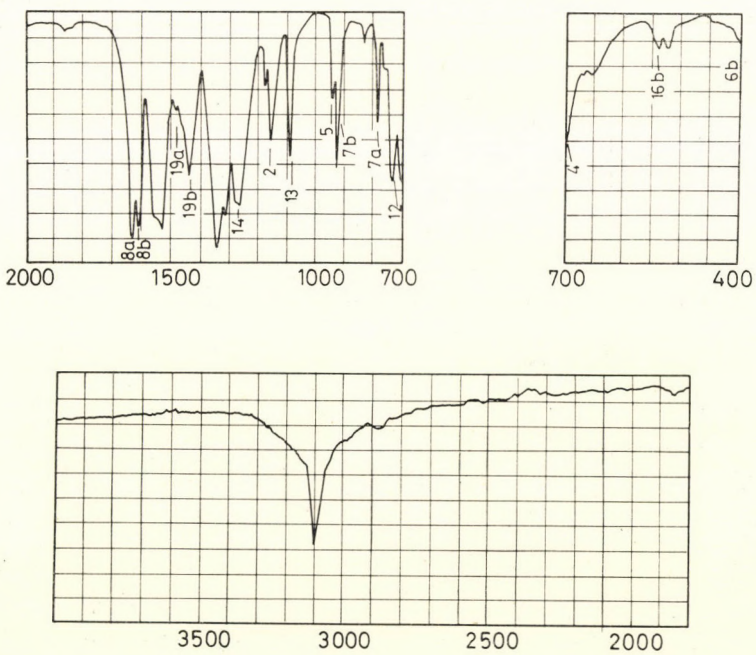

Fig. 15. Picric acid **(XIV)**

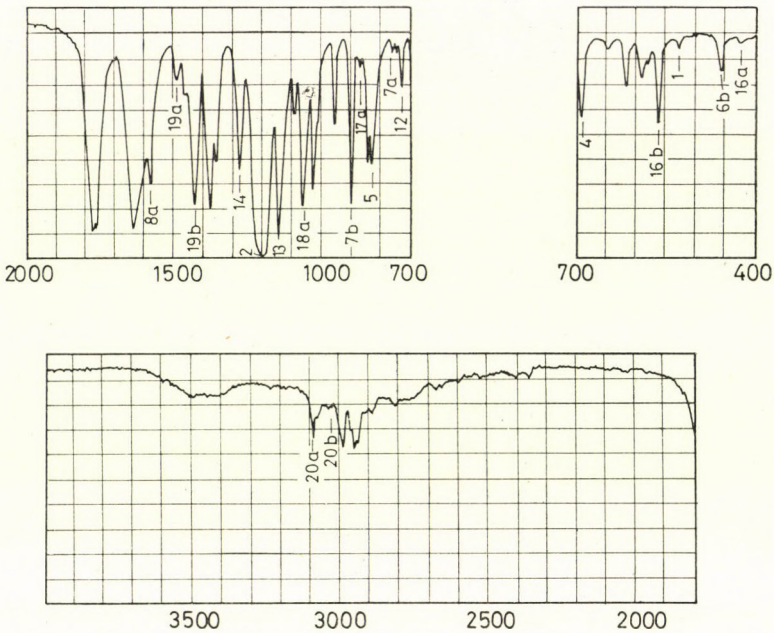

Fig. 16. 2-Hydroxy-4,6-diacetoxy propiophenone **(XV)**

Discussion

The frequency regions for the 30 normal vibrations of the aromatic ring are given in Table II.

Table II

	cm^{-1}		cm^{-1}
1	480—570	**11**	830—950
2	1150—1320	**12**	700—800
3	< 300	**13**	1090—1200
4	680—740	**14**	1230—1260*
5	< 300	**15**	< 300
6a	360	**16a**	410—480
6b	400—490	**16b**	520—600
7a	760—830	**17a**	870
7b	830—970	**17b**	< 300
8a	1570—1640	**18a**	1060—1120
8b	1530—1620	**18b**	1150—1170
9a	< 300	**19a**	1470—1550
9b	< 300	**19b**	1410—1440
10a	< 300	**20a**	3060—3120
10b	< 300	**20b**	3000—3050

* 1270 — 1380 in phenols

Tangential skeletal vibrations

The band of vibration **8a** is always strong. The frequency is strongly increased by nitro groups substituted in the 1 and 3 positions (compound **XIV**, 1637 cm^{-1}), because the vibration is coupled with the stretching vibrations of the nitro group, and as a result the frequency is shifted to higher values. The frequency ranges for the five acids, the three esters and the acid amides are 1585—1622, 1577—1613 and 1580—1583 cm^{-1}, respectively. The high frequency band of compound **VI** at 1613 cm^{-1} can be ascribed to the hydroxyl groups in the 1 and 3 positions.

The frequency of vibration **8b** is lower in every case than that of vibration **8a** (the carbon atoms substituted at positions 2 and 5 either do not vibrate at all, or do so with only a small amplitude, in vibration **8a**, see Fig. 1). The frequency of vibration **8b** is also increased by the nitro substitution. In general the band is weak; it is strong only in the spectra of the esters and of picric acid.

The band of vibration **14** is generally strong, but in a few cases an accidental degeneracy occurs with normal vibration 2. The frequency is anomalously high if there is an intermolecularly bounded hydroxyl group at position 2 in the molecule (1338—1374 cm^{-1} in compounds **I**, **VI** and **VII**), because het vibration is coupled with the βOH vibration [3]. The frequency-increasing effect of the βOH vibration in the spectrum of picric acid is partially compensated by another coupling with the components of the NO_2 vibrations of b_2 symmetry (1278 cm^{-1}).

The band of vibration **19a** is generally strong, with the exceptions of the nitro derivatives and of compound **XV** [4, 5]. The frequency and the intensity depend to a large extent on the inductive effects of the substituents (nitro and acetoxy groups). According to BROWN [6], the frequency in the nitro derivatives is a function of the Hammett σ. The frequency of vibration **19a** is anomalously high in compound **II**; this can be explained by the decreased conjugation of the groups substituted at positions 2 and 5. It can be seen from Fig. 1 that vibration **19a** is to a large extent concentrated in the stretching of the bonds adjacent to carbon atoms 2 and 5. All the fifteen compounds contain oppositely orienting substituents in the 2 and 5 positions, and therefore the quinoidal form is represented to a fairly large percentage among the mesomeric limiting structures of the ring. In this limiting structure the order of the bonds vibrating with large amplitude is smaller. The frequency is thus increased by the decreased conjugation. The decreased conjugation of compound **II** can be explained in that carboxylic acid dimers form to only a small extent in the crystal, while in contrast with this a weak hydrogen bond is formed mainly by the hydroxyl group of the carboxyl with the ether oxygen of the methoxy group at position 5. This hydrogen bond decreases the conjugation of both the

carboxyl and the methoxy group. The formation of an intermolecular hydrogen bond with such a structure can be deduced from the frequencies of other bands too (1, 2, 7a, 7b, 13, $\delta_{as}^{-}CH_3$, $\nu C{=}O$, β OH, γ OH).

The band of vibration **19b** is generally strong, but in many cases it appears only as a shoulder because of accidental degeneracy.

In-plane bending C—X vibrations

All in-plane bending C—X vibrations are of low frequency and not characteristic.

In-plane bending C—H vibrations

The band of vibration **18a** is weak in general, with the exception of compound **XV** in which the substituent to be found at position 5 (acetoxy) is exceptionally of $+M$ effect. As a consequence of this, the difference in the polarities of the 4 and 6 CH bonds is larger here. The band of vibration **18b** is always weak and not characteristic.

Radial skeletal vibrations

The band of the breathing vibration **1** is generally weak. It is of medium intensity in the spectra of the acids and of trimethoxybenzaldehyde. The vibration is sensitive to the mass of the substituents, and therefore the frequency is higher in the case of hydroxyl groups (529—565 cm^{-1}). As a result of coupling with the β_{as} NO_2 vibration, the nitro group decreases the frequency (490 cm^{-1}). The frequency is anomalously high in compound **II** (561 cm^{-1}), in which a hydrogen bond is assumed to the oxygen atom of the methoxy group at position 2. Since normal vibration **1** is radial it is perpendicular to this hydrogen bond, and this corresponds to a frequency increase.

Because of the many substituents vibration **6a** is of low frequency and cannot be identified in the spectra of the majority of the compounds. The band of vibration **6b** is also weak, with the exception of compound **XV** in which the carbon atoms have particularly variable polarities. It follows from the normal coordinate of the vibration that the variable polarity results in a large dipole moment change. In this case too the nitro group reduces the frequency (404—455 cm^{-1}).

With the exception of the allyl derivatives, the band of vibration **12** is strong. Coupling of the $\beta C{=}O$ vibration of the aldehyde and ketone groups and the $\beta_s NO_2$ vibration of the nitro groups in the 1 and 3 positions decreases the frequency (709—734 cm^{-1}). The frequency is anomalously high in compound **II** for the reason mentioned in connection with normal vibration **1.**

C—X stretching vibrations

The band of normal vibration **2** of the same phase is always strong, although in a few cases it appears as a shoulder as a result of accidental degeneracy. Its frequency depends to a large extent on the masses of the substituents in the 1 and 3 positions. In compound **VI** it is at 1313 cm^{-1}, and in the twelve 1,3-dimethoxy compounds it is between 1213 and 1248 cm^{-1}. Of these the

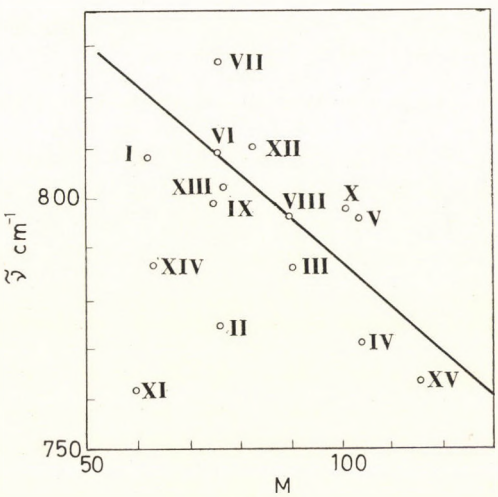

Fig. 17

frequency is the smallest in compound **II**, in which the substituents are more weakly conjugated with the aromatic ring, and thus the order of some of the C—X bonds is lower. The frequency is minimum in the spectrum of picric acid, as a result of coupling with the $\nu_s NO_2$ vibrations of the same symmetry (1159 cm^{-1}).

In normal vibration **7a** the substituents in the 2 and 5 positions vibrate with a larger amplitude than the others (see Fig. 1). The frequencies can be correlated with the masses of the substituents in the 2 and 5 positions (Fig. 17). Exceptions are compounds **XI** and **XIV**, in which the $\beta C{=}O$ frequencies of the aldehyde group and the $\beta_s NO_2$ frequencies of the nitro groups at positions 1 and 3 couple with vibration **7a** and decrease the frequency, and compound **II** which has already been mentioned several times, in which the orders of just these C—X bonds at positions 2 and 5 are lower. The frequency formula obtained for the other 12 compounds by the method of least squares is:

$$\tilde{\nu} = 873.5—0.877\ M$$

In the case of ethoxy, propoxy, acetoxy or propionyl groups at position 2 the band is weaker, but otherwise it is of medium intensity or strong.

The main factors affecting the frequency of vibration **7b** are the extent to which the molecule is stabilized by intermolecular forces, and the nature of the groups involved in this. The frequency is the greatest (968 cm^{-1}) in compound **II**, in which it is presumed that the methoxy group forms a hydrogen bond with the carboxyl group. Since the vibrational amplitude of the substituents in the 1 and 3 positions is the greatest in the vibration, the smaller order of the bonds at positions 2 and 5 does not hold good in the frequency of vibration **7b** of compound **II**. The very low intensity of the band in the spectrum of trimethoxybenzaldehyde is striking; this can be explained in that the carbonyl oxygen and the oxygens of the methoxy groups at positions 1 and 3 vibrate in opposite directions. Accordingly, there must be coupling between vibrations **7b** and $\beta C{=}O$; this is also supported by the fact that the frequency of the former vibration is relatively high (917 cm^{-1}), although there are no intermolecular hydrogen bonds. On the basis of the frequencies the compounds can be classified in the following groups:

1. Intermolecular hydrogen bond with a methoxy group (compound **II**): 968 cm^{-1}.
2. Carboxyl and acid amide dimers (compounds **III**, **IV**, **IX**, **X**): 935—944 cm^{-1}.
3. Perturbed carboxyl dimers and picric acid (compounds **I**, **V**, **XIV**): 905—915 cm^{-1}.
4. Trimethoxybenzaldehyde (compound **XI**): 917 cm^{-1}.
5. Esters and 2-hydroxy-4,6-diacetoxypropiophenone (**VI**, **VII**, **VIII**, **XV**): 899—917 cm^{-1}.
6. Other monomers (compounds **XII**, **XIII**): 832—858 cm^{-1}.

The band of vibration **13** of trigonal symmetry is strong in general. Its frequency is the lowest in the spectrum of compound **II** (1106 cm^{-1}), presumably as a result of the decreased C—X bond strengths which have already been mentioned several times, and in the spectrum of picric acid (1093 cm^{-1}), where the frequency is decreased to such an extent by the coupling with the $\nu_s NO_2$ vibrations.

C—H stretching vibrations

The bands of vibrations **20a** and **20b** in the usual frequency interval [7] are generally weak and are not characteristic.

Out-of-plane skeletal vibrations

The band of vibration **4** is strong in the spectra of the acids and acid amides. The frequency is greater than 700 cm^{-1} in the spectra of the aldehyde, the acids and the esters, and lower than this in the other spectra. Compound **I** is an exception (691 cm^{-1}).

The bands of vibrations **16a** and **16b** are weak or at most of mediu m intensity. The band of vibration **16b** in the spectrum of compound **II** is superimposed on the strong and diffuse band of the γOH vibration.

Out-of-plane C—X vibrations

All of the vibrations are of low frequency, so that they cannot be identified in the spectra in general.

Out-of-plane C—H vibrations

With the exception of the cyano and nitro derivatives vibration **11** always appears as a strong band. Its frequency can be given by the modified formula of an earlier publication [8]:

$$\tilde{\nu} = \tilde{\nu}_0 - \frac{y}{16}\left(10\,n + M + |M_m|\,\frac{m}{6}\right) \tag{1}$$

where n is the number of substituents, M is the sum of the Platt spectroscopic moments of those substituents which are in positions *ortho* or *para* to at least one hydrogen atom, M_m is the sum of the spectroscopic moments of those substituents which are in positions *meta* to at least one substituent of the same orientation, and m is the number of substituent pairs of the same orientation in positions *meta* to each other. (Thus, in compounds **XIV** and **XV** $m = 3$, and in all the other cases $m = 1$). The value of $\tilde{\nu}_0$ is defined by the following equation [8]:

$$\tilde{\nu}_0 = 932.5 - 56.9x + 4.67\ |x - 1.8|\ (x - 1.8) \tag{2}$$

x is a parameter expressing the extent of the orbital following. y characterizes the effects of the substituents on the basis of their positions and of the amplitude relations of the hydrogen atoms.* In the case of 1,2,3,5-tetrasubstitution $x = 0$ (since there are no neighbouring hydrogens), while y can have either of two values, depending on whether the two hydrogen atoms vibrate in the same ($y = 16$) or in opposite ($y = 9$) phases. Accordingly, in 1,2,3,5-tetrasubstitution $\tilde{\nu}_0 = 917\ \mathrm{cm}^{-1}$ and $n = 4$. The first term of equation (1) is therefore 877 cm^{-1}. In addition to this are the contributions from the spectroscopic moments. The modified spectroscopic moments of the substituents in positions *ortho* or *para* to hydrogens are given in Table III for the fifteen compounds.

* For the definition of x, and of y in Eq. (2), see Reference [8].

Table III

NO_2	—45	CHO	—19
COOH	—41	$OCOCH_3$	+ 8
$COOCH_3$	—38	OH	+14
$CONH_2$	—32	OCH_3	+21
CN	—20		

The nitro group behaves anomalously, in as much as the spectroscopic moments of the other substituents can not be taken into account at all in the nitro derivatives. The frequencies thus calculated and the corresponding experimental values are given in Table IV.

Table IV

Compound	Calculated cm^{-1}	Experimental cm^{-1}	Compound	Calculated cm^{-1}	Experimental cm^{-1}
I	869	869	**IX**	860	860
II	869	875	**X**	860	860
III	869	863	**XI**	847	850
IV	869	869	**XII**	848	852
V	869	871	**XIII**	912	922
VI	882	881	**XIV**	944.5	945
VII	866	864	**XV**	832	832
VIII	866	869			

Vibration **17a** is inactive in the point-group C_{2v}, and accordingly the band is very weak and can be identified in only a few cases; these are given in Table V together with the frequencies calculated from equation (1).

Table V

Compound	Calculated cm^{-1}	Experimental cm^{-1}	Compound	Calculated cm^{-1}	Experimental cm^{-1}
I	890	889	**IV**	890	886
II	890	899	**V**	869	872
III	890	883			

The characteristic vibrations of the methyl group

In the case of the methoxy group the $\nu_s CH_3$ vibration appears between 2838 and 2848 cm^{-1}, generally as a medium or strong band. In groups other than methoxy groups the band of the vibration is very weak, with a frequency

of 2905—2920 cm^{-1}. The $\nu_{as}CH_3$ is generally split into two components, in the range 2945—2990 cm^{-1}. The vibrational band of the $\delta_s CH_3$ is strong for the methoxy group, and lies between 1310 and 1345 cm^{-1}. That for other methyl groups lies between 1365 and 1390 cm^{-1}, but is much weaker. In the case of the methoxy group the bands of the $\delta^{+}_{as}CH_3$ vibrations are fairly strong; their frequency range is 1435—1475 cm^{-1}. Interesting frequency shifts can be observed for the $\delta^{-}_{as}CH_3$ vibrations. If the methoxy group is at position 2, and is thus between two other substituents, or if there is a bulky substituent (propoxy or acetoxy group) in its vicinity, then the frequency is very close to 1000 cm^{-1}. It is possible that in such a case the methyl group does not lie in the plane of the ring. The ethoxy and allyloxy groups do not cause such a decrease of the frequency. In the spectrum of compound **II**, in which methoxy–carboxyl bridges are assumed, the band of the methoxy group in the 2 position can not be identified. In the spectra of the other four trimethoxy derivatives (compounds **VIII**, **IX**, **XI** and **XIII**) the two $\delta^{-}_{as}CH_3$ bands appear regularly. The methoxy group at position 2 absorbs between 996 and 997 cm^{-1}, and those in positions 1 and 3 between 1015 and 1042 cm^{-1}, while when in the neighbourhood of propoxy and acetoxy groups they absorb at 1008—1012 cm^{-1}. The rocking bands of other methyl groups appear between 1029 and 1040 cm^{-1}.

The characteristic frequencies of the methylene group

Methylene groups are present in compounds **III**, **IV**, **X** and **XII**. The frequency ranges of the $\nu_s CH_2$ and the $\nu_{as}CH_2$ vibrations are 2880—2885 and 2935—2942 cm^{-1}, respectively. The bands of the $\beta_s CH_2$ and $\beta_{as}CH_2$ vibrations could not be identified, but in the case of the allyl group a band of medium strength appeared at 1360 cm^{-1}, which can be ascribed to the $\gamma_s CH_2$ vibration.

Other C—H vibrations in the side-chain

The νCH and βCH bands of the aldehyde group were identified at 2756 and 1398 cm^{-1}. The three νCH bands of the allyl group appear at about 3080 cm^{-1}, and in the ranges 3018—3022 and 2972—2980 cm^{-1}, respectively. The last of these three bands is the strongest. Of the in-plane bending vibrations, two can be identified satisfactorily: the one appears between 1410 and 1418 cm^{-1} as a strong band (in the acid amide this overlaps with the band of vibration **19b**), and the other is at 1315 cm^{-1} (this can be found only in the spectrum of the nitrile, **XII**, because in the spectrum of the acid amide it is masked by the $\delta_s CH_3$ band). The frequency ranges of the out-of-plane bands are 982—987, 926—930 and 630—635 cm^{-1} (in the acid amide the last of these can similarly not be separated from the amide VI band). The first of these three bands is the strongest.

$\nu C=C$ vibration

The frequency of the vibration in the allyl group is 1644—1648 cm^{-1}, while the band itself is weak.

C—(OH) vibrations of the carboxyl group

Only the strong stretching vibration band can be identified, between 1268 and 1278 cm^{-1}.

O—(CH_3) vibrations

The O—C stretching vibration of the methoxy group appears between 1179 and 1199 cm^{-1} as a relatively strong band. The stretching vibration is coupled with the $\delta_{as}^{-}CH_3$ vibration; this is generally also shown by the fact that the frequency courses of the two vibrations are opposite. Where the frequency of the $\delta_{as}^{-}CH_3$ vibration is 996—997 cm^{-1}, that of the $\nu O—(CH_3)$ is 1190—1199 cm^{-1}. In the case of methoxy groups in the 1 and 3 positions the frequency is 1179—1188 cm^{-1} if there is no steric perturbation. The splitting of the band in the spectrum of compound **III** is an interesting phenomenon; this shows that the neighbouring ethoxy group perturbs *one* of the methoxy groups. (There is also a weak shoulder on the lower wavelength side of the $\delta_{as}^{-}CH_3$ band, which may correspond to the vibration of the perturbed methoxy group.) In most cases the in-plane bending vibration too can be identified between 333 and 365 cm^{-1}.

Stretching vibrations of the C—C—C, C—O—C and O—C—C chains

The C—C—C chain occurs in the propionyl group of propiophenone (compound **XV**). The frequencies attributed to the stretching vibrations of the chain are 1094 and 957 cm^{-1}; both bands are strong. The C—O—C group can be found in the methyl esters (compounds **VI, VII** and **VIII**). The frequencies of the asymmetric stretching vibration, in which the greater role is played by the stretching of the bond between the carbonyl carbon and the ether oxygen, are 1264, 1290 and 1261 cm^{-1} in compounds **VI, VII** and **VIII**, respectively, and all three bands are very strong. The C(O)—O bond is stronger in compounds **VI** and **VII**, because the carbonyl oxygen forms a H-bond with the hydroxyl groups, this decreases the C=O bond order, and as a result the order of the C(O)—O bond increases (this is confirmed by the $\nu C=O$ frequencies). At the same time, there is coupling with the $\nu O—(CH_3)$ vibration in compounds **VII** and **VIII**, and this increases the frequency of the ester group. The frequency of compound **VII** therefore stands out, while in the case of compound **VIII** the

lower frequency corresponding to the weaker bond and the increase caused by the coupling compensate each other. The other stretching vibration of the chain similarly gives rise to a strong band, between 1004 and 1007 cm^{-1}.

The stretching frequencies of the O—C—C chain of the acetoxy group are 1182—1205 and 944—957 cm^{-1}. The 1182 and 944 cm^{-1} bands occur in the spectrum of compound **V**, in which the acetoxy group is situated between two methoxy groups. The frequency-decreasing effect of the steric hindrance does not appear in the spectrum of compound **XV**. The stretching frequencies, ascribed to the O—C—C chain of the ethoxy group are 1114 and 903 cm^{-1}, while the bands for the O—C—C—C chain of the propoxy group are 1130, 964 and 820 cm^{-1} (the 1130 cm^{-1} band is masked by the band of the 13 vibration).

νC=O vibrations

The carbonyl band can be found for compounds **I**, **III**, **IV** and **V** between 1682 and 1697 cm^{-1}. In the two strongest dimers, compounds **III** and **IV**, it is at 1684 and 1682 cm^{-1}. The frequency stands out in compound **II**, in which it is assumed that the overwhelming proportion of the carbonyl oxygen is not hydrogen-bonded. (The small amount of dimer present is indicated by a shoulder on the low-wavelength side of the band.) The stretching frequency of the carbonyl group in compound **II** is 1708 cm^{-1}. When the hydroxyl group is present in the esters the frequency is 1672—1677 cm^{-1}, and otherwise it is 1714 cm^{-1}. In compound **VII** a further carbonyl band appears at 1693 cm^{-1}, indicating two types of intermolecular coupling. The $\nu C=O$ frequency of the aldehyde, **XI**, is 1693 cm^{-1}, and that of the ketone, **XV**, is 1640 cm^{-1}. In the latter case the carbonyl forms a chelate with the hydroxyl group in the ortho position. The frequency range of the acetoxy groups (compounds **V** and **XV**) is 1763—1777 cm^{-1}. In the diacetoxy compound, **XV**, the band is split.

The amide-I vibration has in the main the nature of the $\nu C=O$ vibration. Its frequency is 1660—1662 cm^{-1}.

βC=O vibrations

The $\beta C=O$ band of the carboxyl and ester groups is weak or medium, and is found between 738 and 757 cm^{-1}. The $\beta C=O$ vibrations of the aldehyde, the acetoxy group and the ketone were identified at 788, 818 and 842 cm^{-1}, respectively. The bands at 839 and 840 cm^{-1} were ascribed to the amide-IV vibration, with mainly such a character.

γC=O vibrations

The frequencies of the bands ascribed to these vibrations are: carboxyl and ester, 668—693 cm^{-1}; aldehyde, 629 cm^{-1} (strong); acetoxy, 647—650 cm^{-1}; ketone, 587 cm^{-1}; amide-V, 655—665 cm^{-1}.

The phenolic O—H vibrations

The νOH band is generally a strong doublet between 3260 and 3560 cm^{-1}. The frequency is least in compound **I**, in which the hydroxyl group forms a bridge with the carboxyl group; here, however, the higher-frequency component belongs not to the phenolic, but to the carboxylic hydroxyl. It is greatest in compound **VII**, in which the methoxy groups adjacent to the hydroxyl group prevent the association of the ester carbonyl. (Two carbonyl bands can be found in this same spectrum !) The doublet in compound **VI** therefore arises because of two types of hydroxyl group, and that in compound **VII** as a result of two types of intermolecular bond.

The βOH frequencies are in accordance with the conclusions drawn from the stretching vibrations. Corresponding to the association, the frequencies in compounds **I**, **VI** and **XV** are 1200—1207 cm^{-1} (it is concealed by the acetoxy band in compound **XV**), and in compound **VII** is 1190 cm^{-1}. The frequency range of the γOH vibrations in the case of intermolecular bridges of different strengths is 550—590 cm^{-1}, and at the same time the bands are also very diffuse. On the other hand, in the spectrum of the chelate-forming compound **XV** the band is sharp and appears at 617 cm^{-1}.

O—H vibrations of the carboxyl group

The band of the stretching vibration is sharp in compound **I** (3405 cm^{-1}), because here the hydroxyl group does not form a bridge. In compounds **II**, **III**, **IV** and **V** can be found the characteristic band structure for bridging carboxylic hydroxyl. In the case of the dimeric structure the βOH vibration appears at 1415—1420 cm^{-1} as a strong band. In the spectrum of compound **II** (bridge formed with methoxy) it is at 1388 cm^{-1}. It cannot be identified in the spectrum of compound **I**. The γOH band is diffuse, and its frequency is 925—927 cm^{-1} in the spectra of compounds **III**, **IV** and **V**, while in the very much weaker intermolecular bond in compound **II** the band appears at a maximum of 580 cm^{-1}. The perpendicular vibration of the free hydroxyl group in compound **I** gives a band at approximately the same position as does the phenolic hydroxyl in the bridge (ca. 580 cm^{-1}).

C≡N vibrations

In the spectrum of compound **XII** the νC≡N vibration appears at 2235 cm^{-1}, and the bending at 563 cm^{-1}.

N—H vibrations

The $\nu_s NH_2$ and $\nu_{as} NH_2$ vibrations of the amino group can be found at 3185—3190 and 3355—3365 cm^{-1}, respectively, in the spectra of the two acid

amides. A band of medium strength is found alike at 747 cm^{-1} in both spectra; these are tentatively ascribed to the $\beta_{as}NH_2$ vibration of the amide group in practically a plane configuration.

Vibrations of the nitro group

The frequency range of the $\nu_{as}NO_2$ vibration is 1526—1555 cm^{-1}, and that of the ν_sNO_2 one is 1322—1348 cm^{-1}. In the spectrum of picric acid both are split by 20—25 wavenumbers, this can be explained by the chelate-formation of one of the nitro groups. The scissoring vibration appears as a weak band at 828—836 cm^{-1}, but in the spectrum of picric acid there is also a strong band at 924 cm^{-1}, which may be ascribed to the β_s NO_2 vibration of the nitro group in the chelate. The $\beta_{as}NO_2$ vibration can be found as a weak band at 524—528 cm^{-1}. The strong bands of the γ_sNO_2 vibration appear between 734 and 753 cm^{-1}, as a half-merged doublet in the spectrum of picric acid, and similarly doubled as a consequence of Fermi resonance in the spectrum of compound **XIII**.

Amide-II, amide-III and amide-IV

The amide-II band appears in both spectra at 1620 cm^{-1}, the amide-III at 1393– 1397 cm^{-1}, and the amide-VI at 630—635 cm^{-1}. The latter, in accordance with its wagging character, gives a diffuse band.

REFERENCES

1. VARSÁNYI, G.: Vibrational Spectra of Benzene Derivatives. Academic Press, New York, London, 1969
2. WILSON, E. B.: Phys. Rev. **45**, 706 (1934)
3. MECKE, R., ROSSMY, G.: Z. Elektrochem. **59**, 866 (1955)
4. KATRITZKY, A. R., JONES, R. A.: J. Chem. Soc. 3670 (1959)
5. KATRITZKY, A. R., SIMMONS, P.: J. Chem. Soc. 2051, 2058 (1959)
6. BROWN, J. F.: J. Amer. Chem. Soc. **77**, 6341 (1955)
7. HOLLY, S., SOHÁR, P.: Infrared Spectroscopy. Műszaki Kiadó, Budapest, 1968
8. VARSÁNYI, G.: Acta Chim. Acad. Sci. Hung. **57**, 51 (1968)
9. PLATT, J. R.: J. Chem. Phys. **19**, 263 (1951)

György VARSÁNYI; Budapest XI., Budafoki út 8b
Pál SOHÁR; Újpest, 1. POB 82.

Acta Chimica Academiae Scientiarum Hungaricae, Tomus 74 (3), pp. 335—43 (1972)

FERMI STATISTICAL TREATMENT OF ACID–BASE PROCESSES, II

DISTRIBUTION AND ACIDITY OF INDIVIDUAL PROTON HYDRATES IN CONCENTRATED AQUEOUS SOLUTIONS OF PERCHLORIC ACID

I. RUFF and B. LACZKÓ

(Department of Inorganic and Analytical Chemistry, L. Eötvös University, Budapest)

Received September 20, 1971

A Fermi statistical approximation has been applied to describe the resultant acidity function of concentrated aqueous perchloric acid solutions from 2 to 25 m in terms of various individual proton hydrates of different acid strength. The results indicate the presence of mono-, di-, tri-, penta-, nona-, and deca-hydrates of the hydronium ion in this concentration range.

1. Introduction

In a previous paper [1] a new definition of the pH has been given on the basis of the Fermi statistics of protons in protonic solvents. According to this definition, the pH is equal to the Fermi energy of protons, if the energy is measured in kT ln 10 units, the zero-point of the energy scale is suitably adjusted, and the concentration of the acid–base components is given in molality. The model used led to a general equation for the precise calculation of pH in any dilute acid-base system. This equation is free of any restrictions with respect to acid strength and the composition of the solution.

The mathematical advantage of the Fermi statistical treatment prompted us to extend its application to concentrated solutions. Because of the difficulties arising from the complicated nature of the interactions in such systems, the test of applicability was limited to the simplest case of aqueous perchloric acid.

2. The model

Fermi statistics gives correlation between the energy states of certain particles in a system and their distribution over these states:

$$N = \sum_{i=1}^{\infty} n_i F_i , \tag{1}$$

where N is the total number of particles whose statistics is considered, n_i is the number of possible energy levels E_i, and the function F_i is

$$F_i = 1/\{1 + \exp[(E_i - E_F)/kT]\} \tag{2}$$

E_F being the Fermi level, k the Bolzmann constant, and T the temperature in K. Thus, for the description of a system, one has to know all the energy and degeneration of all states, and the total number of particles involved. If so, the Fermi energy of the system is defined, and it represents the "average outwards behaviour" of the system.

For dilute solutions, it has been shown that the Fermi level of an acid–base system can be defined by four terms according to Eq. (1):

$$n_0 + n_a = n_0(F_h + F_p) + n_a F_a + n_b F_b\,, \tag{3}$$

where n_0, n_a, and n_b are the number of water, acid, and base molecules, respectively, while the F's correspond to the energies of protons in water (E_h), hydronium ion (E_p), acid (E_a), and base molecule (E_b). Since infinite dilution has been assumed, the number of possible levels can be simply calculated with respect to their degeneracy which is equal to the number of like molecules dissolved, there being no interaction between them, and thus no splitting occurs. (Only one proton per water molecule has been taken into account, because the dissociation of the second one can be safely neglected.) Eq. (3) is valid for univalent acids and bases. If multivalent ones are to be considered, the third and fourth terms on the right hand side of Eq. (3) must be replaced by a sum of the form $n_a(F_{a_1} + F_{a_2} + \ldots + F_{ak})$.

It has also been shown that the implicit Eq. (3) gives good results when solved with respect to E_F by numerical methods. It accurately describes the pH of the solutions of strong and weak acids and bases, hydrolyzing salts with strong–weak as well as weak–weak components, buffer solutions, etc. By certain simplifications, it can be transformed into the well-known approximate equations.

The fitting of the energy scale relative to which the levels should be measured leads to the relation [1]:

$$E_p = kT \ln n_0 \tag{4}$$

and, therefore:

$$E_h = -kT(\ln K_w + \ln n_0). \tag{5}$$

According to Eq. (4), it is very convenient to choose n_0 as having the constant value of 55.5 mol for water. This is why molality should be used, since otherwise the energy scale would be shifted with changing molarity and would depend on the density of the solution. The error caused by referring the pH to molarity becomes evident in this way, and one source of the misleading usage of 'activity coefficient' — a concept that has too many physical meanings to have any — is immediately revaeled. If Eqs (4) and (5) hold, we have:

$$\mathrm{pH} = -E_F/kT \ln 10\,. \tag{6}$$

If E_a and E_b are between the two limits of E_p and E_h, they correspond to weak acids and bases, respectively. The term strong acid means that E_a is in the energy range above level E_p, and similarly a strong base is represented by a level below E_h. Except energy, the levels are not distinguished but by their occupation in the *initial* state, while in equilibrium, every occupied state gives an acidic species and every unoccupied one corresponds to a basic species. For the four types of levels in the simplest case these conditions are shown in Table I.

Table I

No.	Symbol of the energy	Value of the levels at 298 K (kcal/mol)	Occupied state	Unoccupied state
n_0	E_p	2.38	$H_3O.^+(H_2O)_\infty$	$(H_2O)_\infty$
n_b	E_p	variable	BH^+	B
n_a	E_a	variable	HA	A^-
n_h	E_h	—21.15	$(H_2O)_\infty$	$OH^-.(H_2O)_\infty$

The energy of the (initially) acidic and basic levels should be calculated as follows:

$$E_a = -kT \ln K_a \tag{7}$$

and

$$E_b = -kT(\ln K_b - \ln K_w) \tag{8}$$

where K_a and K_b are the dissociation constants of the acid and base, respectively.

For concentrated solutions, the picture becomes much more complicated owing to several facts, *viz.*

(i) The interaction between the species is mainly of the 'charge–charge' and 'dehydration' type. This latter arises from competition between the species for water molecules which involves charge–dipole interaction, as well as hydrogen bonding. The charge–charge interaction always lowers the energy of the ions in question, while mutual dehydration increases it, affecting both ions and uncharged molecules.

In general, the result of these interactions is that the levels whose degree of degeneracy can be regarded as equal to the number of identical molecules involved in the dilute system, undergo splitting into a band. The stronger the interaction, the greater the band width.

(ii) Once a concentration has been reached above which the acid or base exhibits weak character, polymerization becomes possible, *i.e.* the protonated species form clusters like, *e.g.*, A—H . . A—H . . A^-. In other words, dehydration would compete with depolymerization. Such a behaviour can

mainly be expected for hydrogen halides, but, of course, it must exist in all cases when water tends to be the solute and base anions start to solvate their own protonated form.

Competition is reflected quantitatively in the statistical distribution. Since a very complicated problem is encountered in the usual treatment, *viz.* theoretical determination of the possible levels, and, then, description of the average behaviour of the system, we intend to apply the reverse procedure: from the knowledge of the Fermi level as a function of the concentration, let us find the energy of the states which are independent of concentration.

Let us choose the simplest possible case, the concentrated solution of an infinitely strong acid. Nmr data on perchloric acid show [2] that it behaves as a strong acid up to about 27 *m* (*m* is molality).

We can utilize, first, the simplifications following from the case chosen:

$$n_b = 0, \tag{9}$$

$$F_a = 0, \tag{10}$$

since $E_a \gg E_F$, and

$$F_h = 1, \tag{11}$$

because $E_h \ll E_F$. This latter correlation means that no H_3O^+ is formed due to the self-ionization of water which is doubtless true in concentrated acid solutions. Consider now the only remaining band, that of the hydronium ions. In constructing a model to obtain information about the structure of this band, one can introduce the following approximations.

Approximation 1: The solution is assumed to consist of a mixture of $H_3O^+ \cdot iH_2O$ species surrounded by ClO_4^- ions in such a way that (a) there are no common water molecules between two or more such proton hydrates; (b) perchlorate ions are not solvated, and the water dipoles in their vicinity (orientated in the same way whether under the influence of the negative charge of the perchlorate ion or the positive charge of the proton from the opposite direction) belong to the proton; (c) the anions, however, belong at least to two proton hydrates situated at their border line.

Approximation 2: All water molecules are involved in a hydrate, *i.e.* no water clusters are formed.

Approximation 3: Charge–charge interaction is limited to that between protons and their closest perchlorate neighbours; any other effects of this type are assumed to be shielded by this closest sphere of anions.

With these approximations the most advantageous property of the system is that the structure of the species remains unaltered with changing concentration, *i.e.* the general behaviour of the system is determined solely by their relative amount.

Thus assigning an energy E_i to the ith hydrate, one obtains

$$n_a = \sum_{i=0}^{\infty} n_i F_i \tag{12}$$

where n_i is the maximum number of the ith hydrate that can be formed. Due to the interactions to be considered, all n_i's would depend on the population of the other levels, thus, rigorously, Fermi statistics would have to be replaced by other statistics allowing this type of interactions, in which the occupation F_i would differ from that given by Eq. (2). Retaining this formula, one may introduce *approximation 4.*, *viz.* that the probability of occupation is given by the Fermi statistics even if the number of levels with identical energies is a function of the Fermi level.

The correctness of this assumption can be checked mathematically by examining whether the dependence of the Fermi energy on the concentration can be described by Eq. (12), in which the n_i's are functions of E_F but the E_i's are not.

Since it can be expected that the energy of any hydrate is lower than the energy of those containing fewer water molecules in their hydration spheres, the ith hydrate may take away water molecules from the higher ones and supply them to the lower hydrates, depending on whether the occupation of its own level or that of the levels of lower hydrates is required by the actual value of the Fermi energy. In order to formulate this, let us define the average hydration number as follows:

$$\bar{i} = \frac{n_0 - n_a}{n_a} . \tag{13}$$

Thus the plot of the total acid concentration *vs.* $\bar{i}$ gives a hyperbola:

$$n_a = \frac{n_0}{1 + \bar{i}} . \tag{14}$$

At any value of $\bar{i}$, the total concentration of the acid corresponds to the sum of individual hydrates. Consider *e.g.* the case of $\bar{i} = 1$: if no species other than $H_3O^+ \cdot H_2O$ are formed ($i = 1$), its maximum number could be $n_0/2$. However, since non-hydrated H_3O^+ may also exist at this average concentration, the value of n_1 should be corrected to $(n_0/2)\ (1 - F_0)$. (Non-hydrated H_3O^+ is the 'strongest' in taking away water molecules from the higher hydrates). Similarly, $n_2 = (n_0/3)\ [(1 - F_0)F_1]$, and following this procedure we have in general:

$$n_i = \frac{n_0}{1+i}\left[1 + \sum_{j=0}^{i-1} (-1)^{j+1} \prod_{k=i-j-1}^{i-1} F_k\right]. \tag{15}$$

Substituting this and Eq. (14) into Eq. (12), we obtain the final form:

$$\sum_{i=0}^{\infty} \frac{1}{1+i}\left[1+\sum_{j=0}^{i-1}(-1)^{j+1}\prod_{k=i-j-1}^{i-1}F_i\right]=\frac{1}{1+\bar{i}}\,. \tag{16}$$

Eq. (16) contains only the constant parameters of the energies of the levels and a single value of the Fermi energy with respect to the actual value of the average hydration number $\bar{i}$. In this way, a set of equations can be created, using the experimental data of the $E_F(\bar{i})$ function, involving as many equations of the type of Eq. (16) as there are different ones with respect of the pairs of E_F and $\bar{i}$ values taken. This set of equations permits, then, to compute the unknown, constant E_i's.

3. Results and discussion

The computer program is based on a simple iteration procedure, modifying one E_i at a concentration where its contribution to the total acidity can be expected to be significant, until the equality in Eq. (16) is satisfied to five significant digits. Iteration was started with $i = 1$, by taking small, arbitrary values for the other E_i's. If no equality could be reached owing to the wrong energy values not varied in that step, the energy, actually modified, was lowered to one half of its former value, and iteration was started again with $i = 1$. The highest possible value of the energy was allowed to be $10E_1$. If this limiting value occurred in several runs for a certain i, regardless of the starting parameters varied, we accepted it as proof of the absence of this species, *i.e.* no solution of the equation could be obtained with any value commensurable with the other energies.

The summation in Eq. (16) was made over the range of 1 to 27 for i. Since the non-existence of species with $i \geq 23$ was indicated in the above meaning, no appreciable error was caused by cutting the series at $i = 27$.

The Hammett acidity function of concentrated perchloric acid was used as the corresponding Fermi energy value. Although it is not confirmed that H_0 actually measures the activity of the protons without any correction for the indicator activities, there is no other function available in the higher concentration range. Thus *approximation 5* seems to be the choice: $E_F = -H_0 kT \ln 10$. The correctness of this assumption cannot be confirmed by any independent result, and so the further conclusions are only 'self-consistent' with respect to the model used, but it would require further proof that it reflects reality indeed.

The results of the calculation are collected in Table II. The accuracy of the energies slightly decreases with increasing i (mainly in the range of $i = 6$ to 9 and $i = 15$ to 27), as shown by repeated runs with various starting parameters.

The occupation of the individual levels is shown in Fig. 1. The deviation from the $1/(1 + \bar{i})$ curve (dotted line), which corresponds to omitting the case of $i = 22$, is quite small, though significant below 3.5 m. This can be attributed to the fact that either approximation 2 does not hold in more dilute solutions or some large hydrates are present indeed which latter interpretation is more probable in light of some new results on the mobility of protons [3].

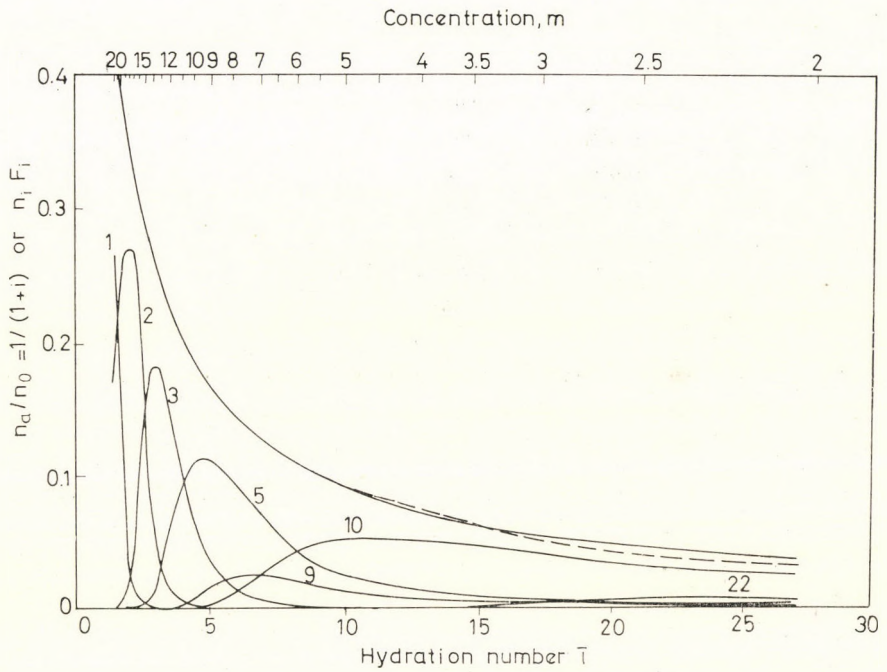

Fig. 1. Population of the individual hydronium hydrates, $n_i F_i$, *vs.* the average hydration number, $\bar{i}$ (lower scale) or concentration (in molality, upper scale). The number of additional water molecules bound to H_3O^+ are indicated by the figures next to the given curves. The hyperbola $n_a/n_0 = 1/(1 + \bar{i})$ corresponds to the amount relative to that of water

It is to be noted that — except for the case of $i = 5$ — the energy values give a reasonably series with respect to the structure of the hydrates. The symmetrical species $H_{21}O_{10}^+$ and $H_{23}O_{11}^+$ dominate in a broad range, while the asymmetrical ones ($H_{11}O_5^+$, $H_{17}O_8^+$, $H_{19}O_9^+$) do not exist practically.

The trihydrate of the hydroxonium ion, $H_9O_4^+$, has a coplanar arrangement of the four oxygen atoms [4]. Thus the nonahydrate can be considered as a trihydrate coordinating six further water molecules to its free protons. In the direction perpendicular to the plane of the trihydrate, the hydrogen bond is markedly weaker than within the plane, although it seems to compete with water molecules in the second coordination sphere. Hence, the decahy-

Table II

i	formula	E_i/kcal/mol[a]	pK_i
1	$H_5O_2^+$	10.70_0	-7.89_5
2	$H_7O_3^+$	7.89_0	-5.81_5
3	$H_9O_4^+$	5.7_9	-4.2_7
4	$H_{11}O_5^+$	none[b]	
5	$H_{13}O_6^+$	$3._9$	$-2._9$
6	$H_{15}O_7^+$	none	
7	$H_{17}O_8^+$	none	
8	$H_{19}O_9^+$	none	
9	$H_{21}O_{10}^+$	$3._8$	$-2._8$
10	$H_{23}O_{11}^+$	2.1_0	-1.5_5
11—21		none	
22	$H_{47}O_{23}^+$	uncertain ca. $1._2$	ca. —0.9
23—27		none	

[a] Energy is given relative to the zero point defined by Eq. (4), *i.e.* it is fitted to the conventional pH scale.

[b] The occurrence is negligible due to the high value of E_i.

drate has probably the same structure as the nonahydrate but stabilized by the axial water molecule in the first coordination sphere.

The predominant part of the concentration range studied is covered by the first three hydrates. The mono- and dihydrate have less symmetrical structures than the trihydrate, but they still appear in the higher concentration range simply because no hydrate-free hydronium ion can exist, it being a stronger acid than perchloric acid itself. The self-ionization of perchloric acid has not been taken into account in the equations. This is why the case of $i = 0$ could not be calculated.

The most surprising result is the relatively high population of the pentahydrate levels. This species corresponds to the tetrahydrate of $H_2O—H—OH_2^+$, and — since the same energy value was obtained even with a starting value of $E_5 = 80$ kcal/mol, *i.e.* with no pentahydrate present — one should think of some resonance between the states $(H_2O)_2—H_2O—H_3O^+—(H_2O)_2$ and $(H_2O)_2—H_3O^+—H_2O—(H_2O)_2$, resulting in stabilization. In order to prove that this result is not an artifact arising from the iteration procedure, in some runs, pentahydrate was completely omitted. In this case, the energy of the hexahydrate was lowered to 3.6 kcal/mol, but a deviation of about 10% from the $1/(1 + \bar{i})$ curve was obtained within the range of 8 to 14 m. Thus, the existence of the pentahydrate is a consequence of the model applied and not that of the actual calculation.

The results obtained indicate that Fermi statistics is mathematically suitable for describing acid–base equilibria in concentrated solutions with the given approximations, but — as already emphasized — the distribution and actual values of the energies depend on the choice of the acidity function. Thus, once an acidity function is *physically* approved, a similar calculation would yield more reliable results.

REFERENCES

1. RUFF, I.: Acta Chim. Acad. Sci. Hung. **55,** 15 (1968)
2. HOOD, G. C., REDLICH, O., REILLY, C. A.: J. Chem. Phys. **22,** 2067 (1954); HEIZINGER, K., WESTON, R. K.: J. Chem. Phys. **42,** 272 (1965)
3. J. RUFF and V. J. FRIEDRICH: J. Phys. Chem. **76.** November issue (1972)
4. GRAHN, R.: Arkiv Fysik, **21,** 1, 13 (1962)

Imre RUFF
B. LACZKÓ
} Budapest VIII., Múzeum krt. 4/b.

Acta Chimica Academiae Scientiarum Hungaricae, Tomus 74 (3), pp. 345—56 (1972)

SYNTHESIS OF SUBSTITUTED 4-HYDROXYQUINOLINE-3-CARBOXYLIC ESTERS, II

PREPARATION OF 6,7-DIISOBUTOXY-4-HYDROXYQUINOLINE-3-CARBOXYLIC ACID FROM THE NITRILE AND ITS ESTERIFICATION

J. EGRI, J. HALMOS and J. RÁKÓCZI

(EGyT Pharmacochemical Works, Budapest)

Received June 1, 1971

6,7-Diisobutoxy-4-hydroxy-3-cyanoquinoline was prepared from 3,4-diisobutoxyaniline and ethyl-ethoxymethylenecyanoacetate in one step at 255—260 °C; this compound could be hydrolyzed only under extremely vigorous conditions. The required compound, ethyl 6,7-diisobutoxy-4-hydroxyquinoline-3-carboxylate was prepared from the corresponding carboxylic acid through the acid chloride or with diazoethane, by selective esterification.

Introduction

PRICE *et al.* [1] and SNYDER and JONES [2] synthesized 7-chloro-4-hydroxy-3-cyanoquinoline by the thermal cyclization of ethyl α-cyano-β-(*m*-chloro)-anilinoacrylate; the corresponding quinoline-3-carboxylic acid was obtained by subsequent hydrolysis of the nitrile. In our present work this reaction path was utilized for the preparation of ethyl 6,7-diisobutoxy-4-hydroxyquinoline-3-carboxylate **(V)**:

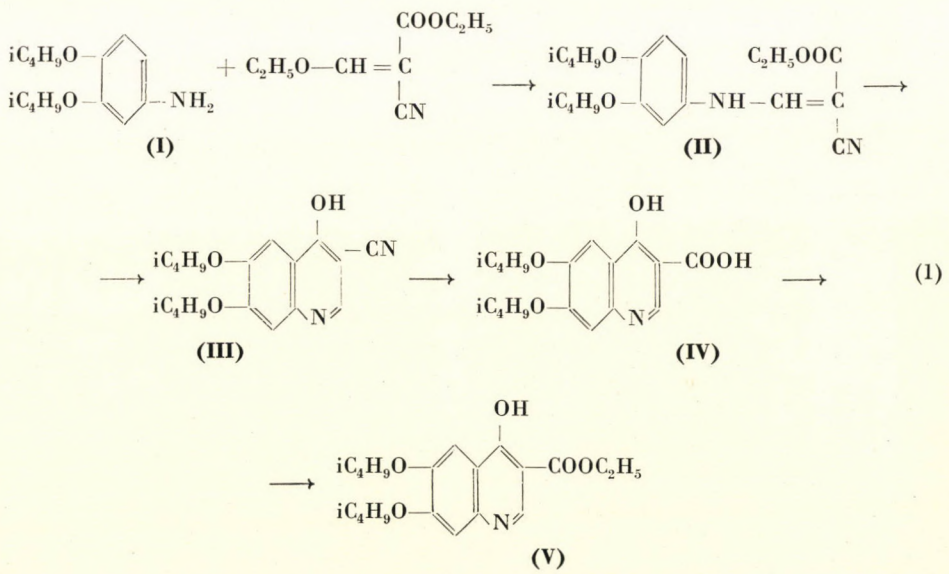

(1)

The procedures reported in the literature [1, 2] had to be modified significantly in the case of this compound; the results of our examinations are reported shortly in the following.

Results and discussion

Cyclization

Substituted 4-hydroxy-3-cyanoquinolines are prepared, in general, by the reaction of a substituted aniline, orthoformic ester and cyanoacetic ester [4], or of a substituted aniline and ethoxymethylenecyanoacetic ester [1]; the α-cyano-β-(substituted)-anilinoacrylic ester produced at 120—160 °C is isolated, purified and then cyclized into the corresponding quinoline derivative in an inert organic solvent boiling above 250 °C.

In the preparation of 6,7-diisobutoxy-4-hydroxy-3-cyanoquinoline, the reaction time of cyclization is about 6 hours at 255 °C, while the reaction of 3,4-diisobutoxyaniline and ethoxymethylenecyanoacetic ester resulting in compound **II** requires only 1—2 hours at 140 °C. Since compounds **II** and **III** are very stable and they undergo only slight decomposition even at the temperature of cyclization during 8—10 hours, it seemed reasonable to prepare compound **III** in one step, from 3,4-diisobutoxyaniline and ethoxymethylenecyanoacetic ester in the reaction medium of cyclization at 255 °C. The ring closure was effected in "Dowtherm A" (an eutectic mixture of diphenyl and diphenyl oxide). At this temperature the formation of compound **II** is a very rapid process, followed by its conversion into compound **III** obtainable in good yields (75—80%) in this way.

Hydrolysis

GILMAN and SPATZ [3] described the hydrochloric acid, sulfuric acid and sodium hydroxide hydrolyses of 3-cyanoquinoline to quinoline-3-carboxylic acid. In each case, the reaction takes place in a short time. 7-Chloro-4-hydroxy-3-cyanoquinoline can also be hydrolyzed with sulfuric acid in 1 hour [2]. On the other hand, compound **III** was found to resist hydrolysis in boiling 60% aqueous sulfuric acid at 130—140 °C for 12 hours, while at 140—150 °C a relatively violent reaction started and sulfonated nitrile was obtained.

No hydrolysis occurred on boiling for several hours in 10—15% aqueous sodium or potassium hydroxide solutions, or in boiling ethylene glycol, *i.e.* at a higher temperature.

Refluxing in 13% aqueous alcoholic (1 : 1) potassium hydroxide solutions resulted in a mixture of decreased nitrogen content; the infrared spectrum of this product showed a νC=O band at 1675 cm^{-1}, while the νCN band also appeared at 2220 cm^{-1}. (This latter band was shifted slightly as compared with the νCN peak of the pure nitrile observed at 2190 cm^{-1}. At the same time,

the $\nu C{=}O$ band was found at a higher wavenumber than that corresponding to the pure quinolinecarboxylic acid.)

Quantitative hydrolysis was achieved finally by boiling in alkaline medium for 100 hours or heating in an autoclave at 150—160 °C for 6 hours; in both cases, about 13% aqueous alcoholic (1 : 1) potassium hydroxide solution was used. The νCN peak was absent in the infrared spectrum of the product and its m. p. and infrared spectrum were identical with the data of 6,7-diisobutoxy-4-hydroxyquinoline-3-carboxylic acid prepared [5] in another way, by the alkaline hydrolysis of ethyl 6,7-diisobutoxy-4-hydroxyquinoline-3-carboxylate **(V)** obtained from the cyclization of ethyl α-carbethoxy-β-(3,4-diisobutoxyphenyl)-aminoacrylate **(VI):**

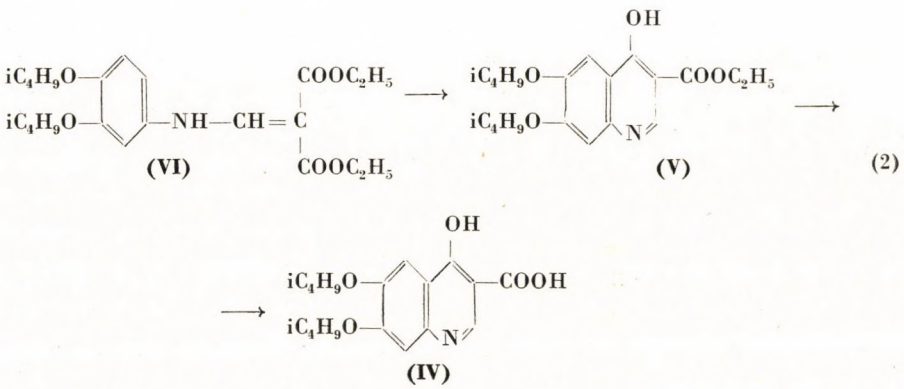

(2)

These experimental facts indicate that the hydrolysis of 6,7-diisobutoxy-4-hydroxy-3-cyanoquinoline is greatly hindered.

Esterification

The precondition of the esterification of compound **IV** was to accomplish it in a selective manner, that is, alkylation of the C—H hydroxyl group or the nitrogen atom in the ring had to be avoided.

The desired ester can be obtained from 6,7-diisobutoxy-4-hydroxyquinoline-3-carboxylic acid through its acid chloride [5]: however, this reaction is lengthy and complicated in this case, therefore, other esterification methods were also studied.

Preparation of compound **V** could not be achieved by means of diethyl sulfate, ethyl *p*-toluenesulfonate [6], ethyl iodide, ethanol in the presence of sulfuric acid [3] or in the presence of trichloroacetic anhydride [7, 8].

On the other hand, the quinolinecarboxylic ester required was obtained in quantitative yield by the reaction of compound **IV** and diazoethane. The reaction was carried out in a heterogeneous system, since the poorly soluble

compound **(IV)** could not be dissolved in the cold reaction mixture. No side reaction was observed, even when diazoethane was used in several times excess. This method permitted selective alkylation and both the C—H hydroxyl group and the ring nitrogen atom remained unchanged as indicated by the infrared spectrum of the product. The compound **V** obtained in this way was perfectly identical with ethyl 6,7-diisobutoxy-4-hydroxyquinoline-3-carboxylate prepared by Reaction (2), as shown by the mixed m. p. determination and the infrared spectra. This experience also supports the strong C=O character of the C—H hydroxyl group.

Experimental

Ethyl ethoxymethylenecyanoacetate

A mixture of 70 g cyanoacetic ester, 100 g ethyl orthoformate, 160 g acetic anhydride and 0.02 g nickel sulfate was stirred at 120—130 °C for 2.5 hrs with simultaneous removal of the ethyl acetate formed by means of distillation. After the accomplishment of the reaction, the mixture was concentrated to a head temperature of 85 °C at a pressure of 10 torr, then the unchanged cyanoacetic ester was recovered between 85 and 90 °C. The ethyl ethoxymethylenecyanoacetate distilled at 144—148 °C at 4 torr and it solidified in the receiver. The yield was 60% and 85% calculated for ethyl orthoformate and cyanoacetic ester, respectively (recovery being taken into account).

6,7-Diisobutoxy-4-hydroxy-3-cyanoquinoline (III)

23.7 g 3,4-diisobutoxyaniline, 16.9 g ethoxymethylenecyanoacetic ester and 720 ml "Dowtherm A" were mixed, the solution was heated to 255 °C in 20—30 min. and stirred at this temperature for 6 hrs, while the ethanol formed was distilled off. The solution was cooled to 20 °C, and the white crystalline substance which separated was filtered off, washed with acetone and dried. Yield: 75—80%. After recrystallization from dimethylformamide, m. p. 354—355 °C.

$C_{18}H_{22}N_2O_3$. Calcd. C 68.77; H 7.05; N 8.91. Found C 68.41; H 7.16; N 8.80%.

In the infrared spectrum the νCN band appears at 2190 cm^{-1}.

Hydrolysis of 6,7-diisobutoxy-4-hydroxy-3-cyanoquinoline

(a) 31.4 g 6,7-diisobutoxy-4-hydroxy-3-cyanoquinoline was dissolved in 420 g 50% aqueous ethanol containing 65 g potassium hydroxide, and the mixture was heated for 100 hrs under reflux. After cooling and acidifying, the product which precipitated was filtered off and washed until neutral; Yield: 98%. After recrystallization from dimethylformamide the m. p. was 268—270 °C. Mixed m. p. with 6,7-diisobutoxy-4-hydroxyquinoline-3-carboxylic acid, prepared according to Reaction (2) as reported in the literature [5], was 269—270 °C.

$C_{18}H_{23}NO_5$. Calcd. C 64.85; H 6.95; N 4.19. Found C 65.12; H 6.84; N 4.12%.

In the infrared spectrum the νCN band (2190 cm^{-1}) was missing and the νC=O band appeared at 1640 cm^{-1}.

(b) A mixture of 31.4 g 6,7-diisobutoxy-4-hydroxy-3-cyanoquinoline, 62 g potassium hydroxide and 400 g 50% aqueous ethanol was heated at 150—170 °C under pressure for 10 hrs. The mixture was cooled to 20 °C and treated as described under (a).

Esterification of 6,7-diisobutoxy-4-hydroxyquinoline-3-carboxylic acid by means of diazoethane

A solution of diazoethane prepared from 50 g nitrosoethylurea with conc. potassium hydroxide solution in 100 ml ether was added to an ethereal suspension of 33 g 6,7-diisobutoxy-4-hydroxyquinoline-3-carboxylic acid. The applied temperature was —5 °C. The suspension was agitated at —5 °C for 2 hrs and at 20 °C for 1 hr then boiled for 1 hr. The product was filtered off, washed with water and dried. Yield: 96—98%. After recrystallization from di-

methylformamide, m. p. 288—290 °C (lit. [5] m. p. 288—291 °C). Mixed m. p. with the ethyl quinoline carboxylate (m. p. 288—290 °C) prepared by the cyclization of ethyl α-carbethoxy-β-(3,4-diisobutoxyphenyl)-aminoacrylate in "Dowtherm A" at 255 °C [5] was 288—290 °C.

$C_{20}H_{27}NO_5$. Calcd. 66.46; H 7.53; N 3.87. Found C 66.83; H 7.72; N 3.74%.

In the infrared spectrum the $\nu C{=}O$ band of the corresponding quinolinecarboxylic acid was shifted from 1640 cm^{-1} to 1680 cm^{-1}.

REFERENCES

1. Price, Ch. C., Leonard, N. J., Herbrandson, H. F.: J. Am. Chem. Soc. **68,** 1951 (1946)
2. Snyder, H. R., Jones, R. E.: J. Am. Chem. Soc. **68,** 1253 (1946)
3. Gilman, H., Spatz, S. M.: J. Am. Chem. Soc. **63,** 1553 (1941)
4. Price, Ch. C., Boekelheide, V.: J. Am. Chem. Soc. **68,** 1246 (1946).
5. Watson, E. J.: Belgian Pat. 670,520; C. A. **65,** P 15350c (1966)
6. Houben-Weyl: Meth. Org. Chemie, **8,** p. 541. Georg Thieme Verlag, Stuttgart, 1952
7. Parish, R. C., Stock. L. H.: J. Org. Chem. **30,** 927 (1965)
8. Bourne, J.: J. Chem. Soc. **1949,** 2976.
9. Stanley, Ch. W.: J. Agr. Food. Chem. **14,** 321 (1966),

János Egri
József Halmos
József Rákóczi
Budapest X., Keresztúri út 30—38.

Acta Chimica Academiae Scientiarum Hungaricae, Tomus 74 (3), pp. 351—56 (1972)

SYNTHESIS OF SUBSTITUTED 4-HYDROXYQUINOLINE-3-CARBOXYLIC ESTERS, III

A ONE-STEP PROCESS STARTING FROM SUBSTITUTED PHENYLIMINO ESTERS

J. Egri, J. Halmos and J. Rákóczi

(EGyT Pharmacochemical Works, Budapest)

Received June 1, 1971

3,4-Disubstituted N-ethoxymethyleneanilines were converted into the corresponding ethyl 6,7-disubstituted-4-hydroxyquinoline-3-carboxylates in the presence of a tertiary organic base catalyst at 255—270 °C, in one step and in satisfactory yields. The procedure is suitable for continuous operation.

Introduction

In 1954, Glickman [1] patented a procedure for the preparation of N-ethoxymethylene-(*m*-chloro)-aniline and pointed out the possibility of the use of this compound in the synthesis of quinoline derivatives with antimalarial action. This can be done by allowing the imino ester to react with diethyl malonate at 140 °C for at least 24 hours, followed by the cyclization of the ethyl α-carbethoxy:β-(*m*-chloro)-anilinoacrylate formed in Reaction (1) to 7-chloro-4-hydroxy-quinoline-3-carboxylic ester in an inert organic solvent at 255—270 °C. This latter compound is an intermediate [2] in the synthesis of antimalarial drugs.

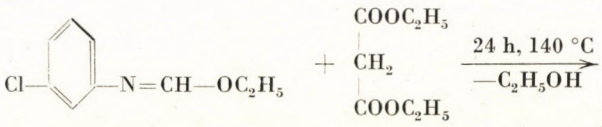

(1)

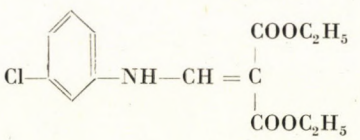

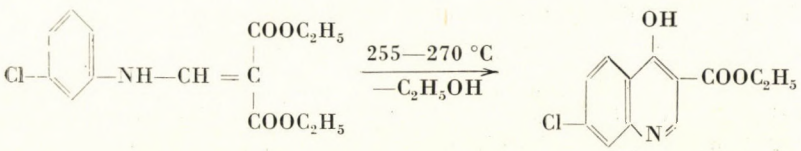

(2)

In our work we aimed at extending this method to the preparation of 6,7-dialkoxy-4-hydroxyquinoline-3-carboxylic esters having coccidiostatic action, and developing a simple, practical procedure.

Results and discussion

The starting substituted N-ethoxymethyleneanilines were synthesized according to known methods [1, 3], by the reaction of the required substituted aniline and ethyl orthoformate in the presence of a catalytic amount of *p*-toluenesulfonic acid:

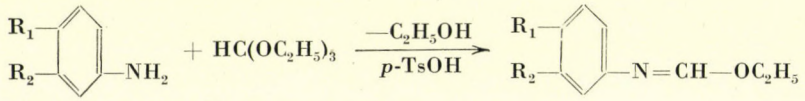

(3)

The imino esters prepared are listed in Table I, together with their m. p.'s or b. p.'s and elemental analytical data. These compounds are rather unstable and cannot be stored for a long time. In our experience, one of their decomposition products is N,N'-bis-(substituted phenyl)-formamidine:

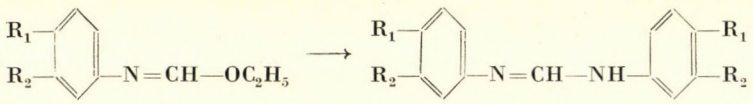

(4)

This is in agreement with the observation of PINNER [7] stating that formimino ethyl ester hydrochloride is converted into formamidine hydrochloride on heating.

In order to develop an industrially applicable quinoline synthesis, the 20—25 hr duration of Reaction (1) should be reduced; therefore, the effect on the reaction time of *(a)* increased temperature and *(b)* the use of a catalyst was studied. Reaction (1) was found to take place very rapidly in paraffin or "Dowtherm A" (a eutectic mixture of diphenyl and diphenyl oxide) solution at 255—270 °C, particularly in the presence of catalytic amounts of a high-boiling tertiary amine (*e. g.*, dimethylaniline), resulting directly in the quinoline compound required. Although the starting N-ethoxymethylene-(substituted)-anilines, as mentioned previously, are rather unstable compounds, the rate of formation of the acrylic ester at 255—270 °C is probably far higher than that of the decomposition reaction, and the acrylic ester formed *in situ* is converted immediately into the corresponding quinoline derivative. This is indicated by the rather high yields obtainable (Table II).

In this way, the synthesis of 6,7-dialkoxy-4-hydroxyquinoline-3-carboxylic esters from the corresponding imino esters can be accomplished in 30—60 min. This makes also possible carrying out the reaction continuously in a tube reactor. The paraffin solution containing the substituted aniline, malonic ester and the catalyst is circulated through the tube reactor heated to 270 °C until completion of the formation of the corresponding quinoline compound. The end product separates from the solution and can be filtered off.

Table I

New 3,4-disubstituted N-ethoxymethyleneanilines

No.	3-R_2	4-R_1	B. p. or m. p., °C	Yield %	Analysis					
					calculated %			found %		
					C	H	N	C	H	N
1	$-OCH_3$	$-OCH_3$	133—136/1.5 torr	89	63.14	7.22	6.69	63.38	7.01	6.62
2	$-OC_2H_5$	$-OC_2H_5$	150—152/4 torr	87	65.80	8.07	5.90	65.39	7.83	6.18
3	$-OiC_4H_9$	$-OiC_4H_9$	38— 42 (ethanol	91	69.59	9.27	4.77	69.42	9.47	4.71
4	$-OC_{12}H_{25}$	$-OC_{12}H_{25}$	56— 57 (ethanol)	94	76.54	11.48	2.72	76.83	11.29	2.58
5	$-OCH_3$	$-OC_{12}H_{25}$	54— 56 (ethanol)	91	72.68	10.26	3.85	72.39	10.45	3.92
6	$-OCH_2Ph$	$-OCH_2Ph$	40— 42 (methanol)	92	76.43	6.41	3.88	76.17	6.80	4.03

Acta Chim. (Budapest) 74, 1972

Table II

6,7-disubstituted 4-hydroxyquinoline-3-carboxylic ethyl esters prepared from 3,4-disubstituted N-ethoxymethyleneanilines

No.	6-R_1	7-R_2	M. p., °C	Lit m. p., °C	Mixed m. p., °C	Yield, %	Analysis					
							calculated			found %		
							C	H	N	C	H	N
1	$-OCH_3$	$-OCH_3$	285—287	280—283 [6]	—	61	60.64	5.46	5.06	60.91	5.19	5.15
2	$-OC_2H_5$	$-OC_2H_5$	280—282	275—280 [5] 285—286 [4]	—	66	62.94	6.27	4.59	63.47	6.51	4.35
3	$-OiC_4H_9$	$-OiC_4H_9$	288—290	288—291 [4]	—	79	66.46	7.53	3.87	66.22	7.68	3.99
4	$-OC_{12}H_{25}$	$-OC_{12}H_{25}$	220—222	—	221—222	76	73.80	10.15	2.39	74.02	9.98	2.47
5	$-OC_{12}H_{25}$	$-OCH_3$	249—252	—	249—251	74	69.58	8.64	3.24	69.27	8.87	3.36
6	$-OCH_2Ph$	$-OCH_2Ph$	291—293	—	291—293	59	72.71	5.40	3.26	72.38	5.23	3.39

The quinoline compounds prepared according to the above method are listed in Table II together with their m. p.'s and elemental analytical data. For the 6,7-dimethoxy-, diethoxy- and diisobutoxy derivatives the literature m. p.'s are also given in the Table; in the case of the other substances, mixed m. p.'s were measured with the corresponding 6,7-disubstituted 4-hydroxyquinoline-3-carboxylic esters prepared by independent synthesis according to literature methods [4, 5]:

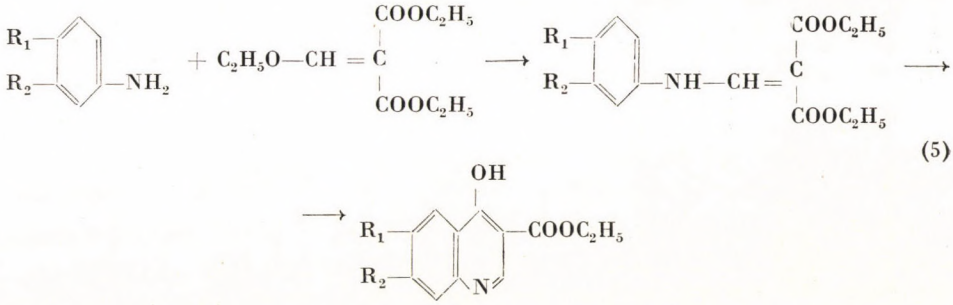

(5)

These mixed m. p.'s are also given in Table II.

Experimental

Substituted N-ethoxymethyleneanilines (General method)

A mixture of 0.1 mole of the substituted aniline, 0.15 mole ethyl orthoformate and 0.05—0.1 g *p*-toluenesulfonic acid was kept at 130—140 °C for 7—10 hrs and the ethanol formed was distilled off. The solution was evaporated and the residue distilled in vacuum (when liquid) or filtered off and recrystallized (if a crystalline substance precipitated); the yields were about 90%.

Ethyl 6,7-disubstituted-4-hydroxyquinoline-3-carboxylate (General method)

0.05 equivalent of dimethylaniline was added to an equimolar mixture of N-ethoxymethylene-(3,4-disubstituted)-aniline and diethyl malonate; the mixture was heated to 120—150 °C and added to 6—8 parts of paraffin heated to 150 °C. The solution was then heated to 270 °C and kept at this temperature for 15—30 min. After cooling to 60—70 °C, the product which separated was filtered off, washed with toluene, dried and recrystallized from dimethylformamide.

Ethyl 6,7-disubstituted-4-hydroxyquinoline-3-carboxylate (Literature procedure, general method) [4, 5]

0.1 mole of substituted aniline was allowed to react with 0.1 mole of ethoxymethylenemalonic ester at 120 °C for 2 hrs; the ethanol formed was distilled off simultaneously. After completion of the reaction, the solution was evaporated in vacuum and heated in 6—10 parts of "Dowtherm A" at 255 °C until the cyclization reaction was completed (this usually required 20—60 min.). The quinoline derivative which separated on cooling was filtered off and recrystallized from dimethylformamide. Of the compounds given in Table II, 4—6 were prepared in this way too.

REFERENCES

1. GLICKMAN, S. A.: U. S. Pat. 2,684,976; C. A. **49**, P 11005b (1955)
2. PRICE, CH. C., ROBERTS, R. M.: J. Am. Chem. Soc. **68**, 1204 (1946)
3. OLIN, J. F.: Belgian Pat. 660,485; C. A. **64**, P 2024g (1966)
4. SPENCER, C. F., ENGLE, A., YU, C. N., FINCH, R. C., WATSON, E. J., EBETINO, F. F., JOHNSON, C. A.: J. Med. Chem. **9**, 934 (1966)
5. Norwich Pharmacal Co.: Belgian Pat. 640,906; C. A. **63**, P 2962c (1965)
6. Norwich Pharmacal Co.: Brit. Pat. 942,524; C. A. **60**, P 5468f (1964)
7. PINNER, E.: BER. **16**, 358 (1883)

János EGRI
József HALMOS
József RÁKÓCZI
Budapest X., Keresztúri út 30—38.

Acta Chimica Academiae Scientiarum Hungaricae, Tomus 74 (3), pp. 357—65 (1972)

SYNTHESIS OF 2,4,6-TRIARYLPYRYLIUM FLUOROBORATES FROM AROMATIC ALDEHYDES AND ARYLMETHYL KETONES, III*

THE CLAISEN—SCHMIDT CONDENSATION

Z. CSŰRÖS, P. SALLAY and GY. DEÁK**

(Department of Organic Chemical Technology, Technical University, Budapest)

Received June 25, 1971

A quantitative method of measurement has been evolved for the investigation of the Claisen—Schmidt condensation of benzaldehyde and acetophenone in anhydrous acetic acid, in the presence of boron trifluoride catalyst, resulting in chalcone. This method was used for reaction kinetical measurements which have shown that this reaction follows second order kinetics, and it is of first order in respect of the components. In the rate equation of the reaction the exponent of the catalyst concentration is 1.5, and the activation energy is 18.3 kcal/mole.

The reaction rate and activation energy were also measured in the case of substituted benzaldehydes and acetophenones. The rate constant is altered by *para* substituents of the benzaldehyde in the order $NO_2 > CH_3 \geqslant Cl > H > CH_3O$, and by the *para* substituents of the acetophenone in the order $H > OCH_3 \approx CH_3 > Cl \gg NO_2$.

The Hammett equation holds for the substituted benzaldehydes ϱ being equal to 0.50.

The pyrylium salt synthesis [1] starting from benzaldehyde and acetophenone comprises three consecutive reactions: the Claisen—Schmidt condensation *(a)*, the Michael addition *(b)* and the final ring closure *(c)*:

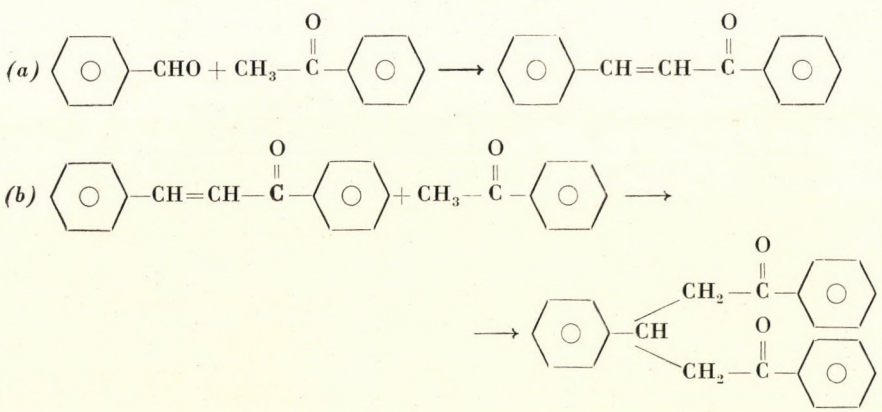

* Part II: Z. CSŰRÖS, GY. DEÁK, P. SALLAY: Acta Chim. Acad. Sci. Hung. **70**, 123 (1971.)

** Present address: Research Institute of Experimental Medicine of the Hungarian Academy of Sciences, Budapest.

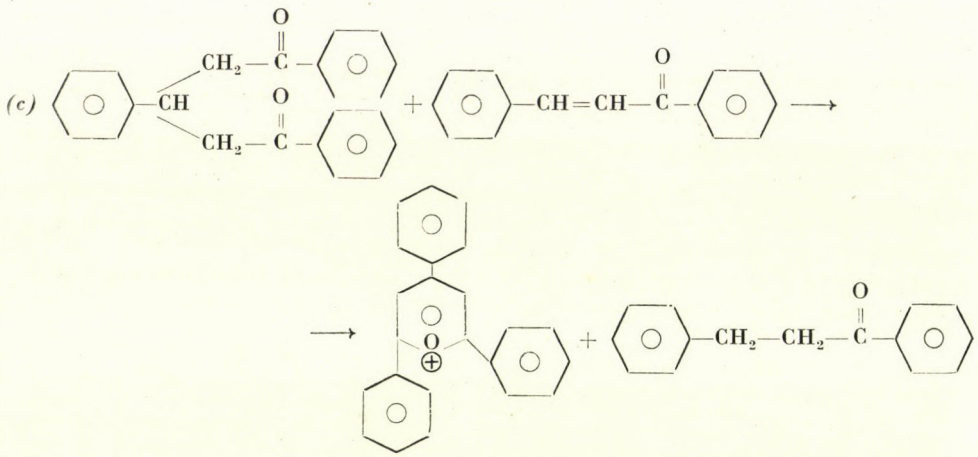

In a previous publication [2] the effect of the substituents of the benzaldehyde and acetophenone components on the yield of pyrylium salt has been investigated. It appeared interesting to examine now the effect of substitution on the reaction rate. Considering the complex nature of the overall reaction, this can be done by the reaction kinetical investigation of the single partial reactions.

The first step of the overall reaction is the condensation between benzaldehyde and acetophenone to chalcone. This reaction is catalyzed in general by bases [3], though in some cases catalysis by acids has also been reported. Thus the preparation of chalcones is catalyzed by sulfuric acid according to NOYCE and PRYOR [4], and by hydrochloric acid according to SZÉLL *et al.* [5]. Lewis acids can also be efficient: the formation of chalcones in the presence of boron trifluoride has been observed by HAUSER and BRESLOW [6], and a number of new substituted chalcones have been prepared by CSŰRÖS and DEÁK [7], using boron trifluoride in anhydrous acetic acid. In acetic acid and in the presence of sulfuric acid catalyst, the reaction is kinetically of second order [4]. According to reaction kinetical measurements, the substituents of benzaldehyde have only a weak effect on the rate constant and on the activation energy [8]. The rate constant is altered by the substituents in the following order:

$$CH_3 > Cl > H > NO_2 .$$

This order is the same as that obtained by SZÉLL *et al.* [5, 9] in their preparative experiments carried out with hydrochloric acid catalyst.

Selection of conditions suitable for following the reaction quantitative

The conditions of reaction had to be chosen in a way that only the Claisen—Schmidt condensation should take place while the other consecutive reactions remain suppressed. According to our earlier investigations [1], this

can be achieved by using a reaction mixture containing excess benzaldehyde. Therefore, a 2 : 1 molar ratio of benzaldehyde: acetophenone was applied as the initial ratio in our measurements. The actual degree of conversion was always determined by ultraviolet spectrophotometry. The ultraviolet spectra of the starting materials and of the chalcone are shown in Fig. 1. It can be seen that at 310 nm the chalcone has a very high absorption compared with the reactants, therefore the determinations were carried out at this wavelength.

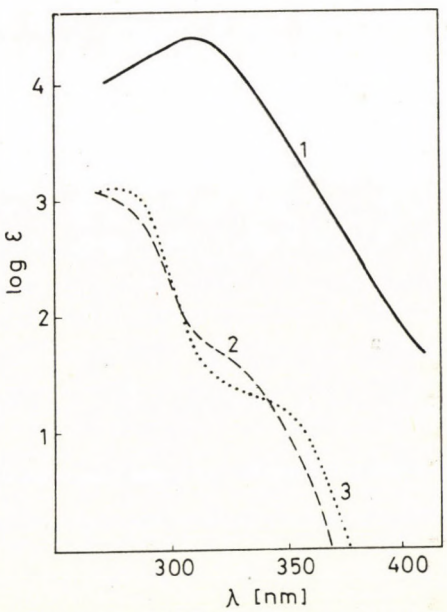

Fig. 1. Ultraviolet spectra of the components of the reaction. 1: chalcone; 2: acetophenone 3: benzaldehyde

Owing to the complexing effect of boron trifluoride, the correlation $E = \Sigma d \cdot \cdot \varepsilon_i c_i$ (where d is the optical distance, ε_i the specific extinction of the single components and c_i their concentration) valid, in general, for the extinction of multicomponent mixtures does not hold. Consequently, it was necessary to prepare a calibration diagram by the spectrophotometry of comparative mixtures corresponding to various degrees of conversion. These comparative mixtures contained aldehyde, ketone, chalcone, water and boron trifluoride in amounts corresponding to the presumed degree of conversion (Fig. 2).

Kinetical measurements

The progress in time of the reaction taking place between acetophenone and benzaldehyde at various temperatures is shown in Fig. 3. The reaction catalyzed by sulphuric acid was found to be of kinetically second order accord-

ing to NOYCE and PRYOR [4]. Presuming similar kinetics also for the reaction catalyzed by boron trifluoride, the overall order of reaction was established by plotting the linearized rate equation. It can be seen in Fig. 4 that the points of measurement lie along a straight with fair approximation, proving that the reaction follows indeed second order kinetics.

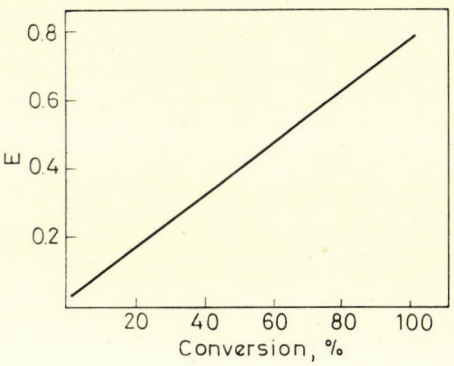

Fig. 2. Calibration diagram for following the progress of the reaction

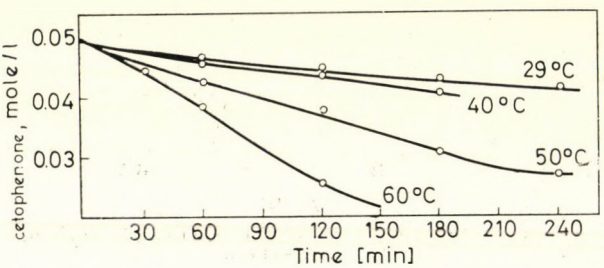

Fig. 3. Progress in time of the reaction of acetophenone and benzaldehyde at various temperatures

The partial order in respect of acetophenone was established by applying a hundredfold excess of benzaldehyde. In that case the change in the concentration of benzaldehyde during the reaction is negligible, and therefore the reaction is of first order in respect of acetophenone, as shown by Fig. 5. The rate constants measured at various temperatures are listed in Table I. From these data, the apparent activation energy can be determined by means of the Arrhenius equation. Graphic determination using the correlation $\log k$ — — $1/T$ gave the value of 18.3 kcal/mole (Fig. 6).

In further experiments, the effect of catalyst concentration on the rate of reaction was investigated. The measured rate constants are listed in Table II. No linear correlation was found between the values of k and the concentration

of boron trifluoride. The correlation can only be obtained by plotting the values of $\log k$ against $\log c_{BF_3}$ (see Fig. 7):

$$k = k'[BF_3]^n, \text{ and}$$

$$\log k = \log k' + n \log [BF_3].$$

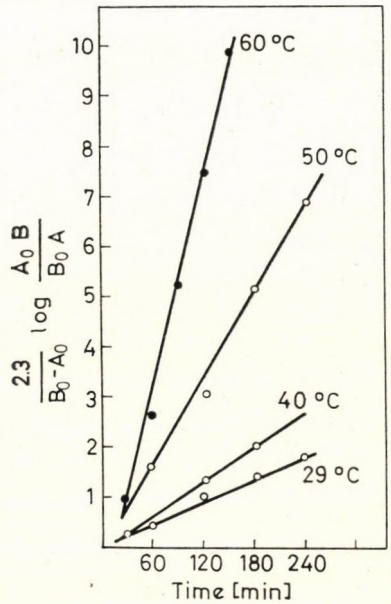

Fig. 4. Diagram of the linearized rate equation (based on Fig. 3) : A = concentration of acetophenone; B = concentration of benzaldehyde, mole/liter; A_0B_0 = initial concentrations

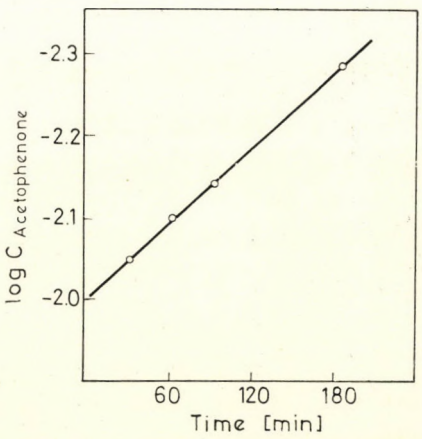

Fig. 5. Checking the partial order of the reaction

Thus, the value of n is the slope of the obtained straight and k', the rate constant independent of the catalyst.

Since in the given case the value of n is 1.5, the dependence of the rate constant on the catalyst concentration can be expressed by the formula

$$k = k' \, [BF_3]^{1.5},$$

and the rate equation of the reaction is:

$$v = k'[BF_3]^{1.5}[BzH] \, [BzMe].$$

The results obtained so far did not afford a satisfactory explanation for the value 1.5 of the exponent.

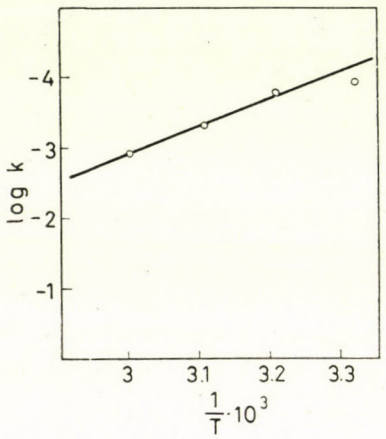

Fig. 6. Diagram of the Arrhenius equation

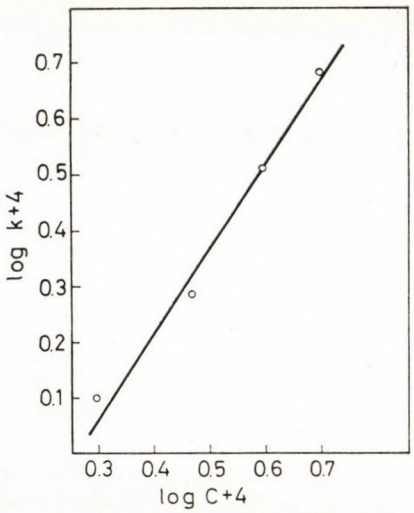

Fig. 7. Dependence of the rate constant on the catalyst concentration

Table I

Rate constants for the Claisen–Schmidt condensation of benzaldehyde and acetophenone at various temperatures

Temperature °C	$k \cdot 10^4$, $l \cdot mole^{-1} \cdot sec^{-1}$
29	1.28
40	1.95
50	4.72
60	11.95

The reaction was carried out also with initial compounds substituted in *para* position. The rate constants and the apparent activation energies calculated from the values of the rate constants are summarized in Table III.

It appears from Table III that the substituents of the benzaldehyde component have a somewhat greater influence on the reaction rate than the substituents of the acetophenone.

Table II

Dependence of the rate constants of the Claisen-Schmidt condensation on the amount of catalyst applied (at 50 °C)

Catalyst concentration, mole/liter	$k \cdot 10^4$, $l \cdot mole^{-1}$, sec^{-1}
0.2	1.25
0.3	1.94
0.4	3.20
0.5	4.72

Table III

Effect of para substituents on the rate of reaction

	$k \cdot 10^4$, $l \cdot mole^{-1} \cdot sec^{-1}$								
Temperature	Parent compound	*p*-Substituted benzaldehyde				*p*-Substituted acetophenone			
°C	H	NO_2	CH_3	Cl	OCH_3	NO_2	CH_3	Cl	OCH_3
29	1.28	1.83	1.80	1.53	0.52	0.85	0.89	0.56	0.97
40	1.95	7.50	4.44	2.92	1.30	1.28	3.47	1.35	2.28
50	4.72	9.45	6.25	4.31	3.06	2.14	4.31	1.69	3.61
60	11.95	20.30	13.60	12.10	7.36	2.92	9.87	6.11	9.72
ΔH^*, kcal/mole	18.28	15.10	14.62	14.17	16.90	8.23	15.10	15.10	15.10

The rate constants of the reaction are altered by the *para*-positioned substituents of benzaldehyde in the order

$$NO_2 > CH_3 \geqslant Cl > H > OCH_3,$$

whereas the substituents of acetophenone affect them in the order

$$H > OCH_3 \approx CH_3 > Cl \gg NO_2.$$

The Hammett equation can be applied to the reaction of substituted benzaldehydes and acetophenone. Graphic representation of the equation gives a straight line (Fig. 8) the slope of which is $\varrho = 0.50$.

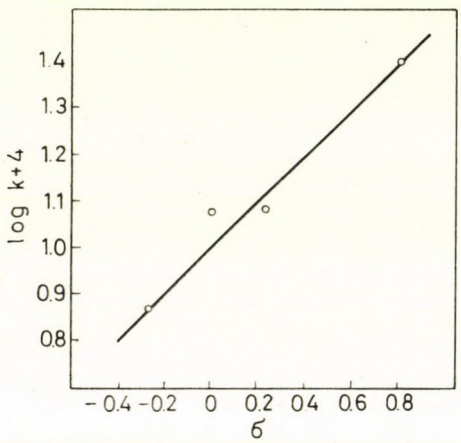

Fig. 8. Diagram of the Hammett equation

It follows that the Claisen—Schmidt condensation catalyzed by boron trifluoride is a reaction of second order where benzaldehyde is the electrophilic attacking agent.

Experimental

The benzaldehyde used was liberated from benzoic acid by treatment with sodium carbonate, distilled and stored in nitrogen atmosphere; twice-distilled acetophenone, anhydrous acetic acid, and distilled boron trifluoride acetic acid complex (BDH) were applied.

The composition and concentration of the reaction mixtures were as follows: 0.1 mole/l of benzaldehyde, 0.05 mole/l of acetophenone, and 0.5 mole/l of boron trifluoride. (One-ml portions of stock solutions of tenfold higher concentrations than those given above were measured in 10-ml volumetric flasks, and filled up to the mark with anhydrous acetic acid.) The reactions were carried out in an ultrathermostat.

Sampling method: A 0.1 ml sample was withdrawn by means of a pipette and diluted to the hundredfold volume with acetic acid: the extinction of the sample was measured with a Spektromom 201 photometer, and its composition determined by means of calibration.

REFERENCES

1. Csűrös, Z., Deák, Gy., Sallay, P.: Periodica Polytechnica **16,** 3 (1972)
2. Csűrös, Z., Deák, Gy., Sallay, P.: Acta Chim. Acad. Sci. Hung. **70,** 123 (1971)
3. Nielsen, A. T., Houlihan, W. J.: Organic Reactions, XVI. Wiley, London, 1968
4. Noyce, D. S., Pryor, W. A.: J. Am. Chem. Soc. **77,** 1937 (1955)
5. Széll, T., Eastham, A. M., Sipos, Gy.: Can, J. Chem. **42,** 2417 (1964)
6. Hauser, G. R., Breslow, D. S.: J. Am. Chem. Soc. **62,** 2385 (1940)
7. Csűrös, Z., Deák, Gy.: Magyar Tud. Akad. Kém. Tud. Oszt. Közl. **10,** 347 (1958)
8. Noyce, D. S., Pryor, W. A.: J. Am. Chem. Soc. **81,** 618 (1959)
9. Széll, T., Eastham, A. M., Sipos, Gy.: Can. J. Chem. **43,** 2134 (1965)

Zoltán Csűrös, Péter Sallay } Budapest XI., Műegyetem rkp. 3.
Gyula Deák Budapest VIII., Szigony u. 43.

Acta Chimica Academiae Scientiarum Hungaricae, Tomus 74 (3), pp. 367—70 (1972)

THE SYNTHESIS OF CALYCOSIN AND CALYCOSIN-7-β-D-GLUCOSIDE

L. FARKAS, A. WOLFNER and V. OLECHNOWICZ-STEPIEN

(Institute for Organic Chemistry, Technical University, Budapest, and Chair for Pharmacognosy of the Medical Academy, Wroclaw)

Received August 4, 1971

The synthesis of 3',7-dihydroxy-4'-methoxyisoflavone **(I)** and its 7-glucoside **(II)** is described. The identity of **I** and **II** with calycosin and its 7-glucoside, respectively, is probable, but not firmly established.

In 1967 a new isoflavone named calycosin was isolated from *Baptisia lecontei* (Leguminosae) by MABRY *et al.* [1]. Ultraviolet and nuclear magnetic resonance spectra indicated that calycosin was 3',7-dihydroxy-4'-methoxy-isoflavone **(I)**. The 7-glucoside **(II)** and 7-rhamnoglucoside of calycosin were also isolated from the same plant.

One year later an isoflavone of identical structure **(I)** was reported to be present in *Pterocarpus dalbergioides* by SESHADRI *et al.* [2]. The structure of this product, named by them 3'-hydroxyformononetin, was supported by degradation and synthesis as well [3].

Since m. p. 228—230 °C was reported for calycosin, and m. p. 245—247 °C was found for both natural and synthetic 3'-hydroxyformononetin, the identity of the two substances was questioned in SESHADRI's paper [2].*

In order to eliminate this controversy we carried out the total synthesis of 3',7-dihydroxy-4'-methoxyisoflavone-7-glucoside **(II)** and an independent synthesis of the aglycone **(I)**.

3'-Hydroxyformononetin **(I)** was first prepared [3] by acid-catalysed rearrangement of the corresponding chalcone. In our laboratory **I** was obtained by ring closure of 2,4-dihydroxyphenyl 3-hydroxy-4-methoxybenzyl ketone **(IV)** with ethyl orthoformate [4].

The ketone **IV** was prepared by Hoesch synthesis from resorcinol and (3-hydroxy-4-methoxyphenyl)acetonitrile.

WONG [5] reported difficulties when attempting the preparation of this nitrile by the azlactone method [6], so he availed himself of the less convenient

* The extremely small amounts isolated from calycosin (1.4 mg), its 7-glucoside (0.5 mg) and 7-rhamnoglucoside (0.1 mg) confined the American workers to the use of spectroscopic methods, and except for **I** no m.p.s. were given, and except for the acetate of **II** no derivatives have been prepared.

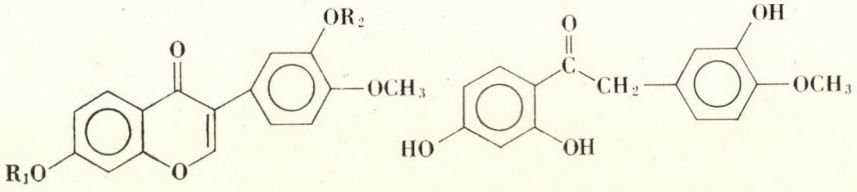

IV

I: $R^1=R^2=H$
II: $R^1=\beta$-D-glucosyl, $R^2=H$
III: $R^1=$tetraacetyl-β-D-glucosyl, $R^2=CH_3CO$

rhodanine procedure. In our hands, under selected conditions the classical azlactone approach proved to be satisfactory.

Our specimen of synthetic 3',7-dihydroxy-4'-methoxyisoflavone **(I)** as well as its acetate had m. p.'s which were in conformity with the data of the Indian authors [2, 3] and the NMR spectrum of **I** (see Experimental) was as expected. In want of a sample of natural calycosin no direct comparison was possible.

Selective coupling of 3',7-dihydroxy-4'-methoxyisoflavone with 2,3,4,6-tetra-O-acetyl-α-D-glucopyranosyl bromide in acetone in the presence of one molar equivalent of potassium hydroxide involving the more reactive 7-hydroxyl gave, after saponification, 3',7-dihydroxy-4'-methoxyisoflavone-7-β-D-glucoside (calycosin-7-glucoside?) **(II)** of m. p. 231—233 °C. The pentaacetate of **II** melted at 120—122 °C and showed the expected NMR spectrum (see Experimental). The UV spectrum of **II** is in close agreement with that reported for calycosin-7-glucoside [1].

In conclusion, the evidence produced in the present investigation seems to support the identity of calycosin and 3',7-dihydroxy-4'-methoxyisoflavone.

Experimental

7-(3-Benzyloxy-4-methoxybenzylidene)-2-phenyl-Δ^2-oxazolin-5-one

An intimate mixture of 3-benzyloxy-4-methoxybenzaldehyde [8] (23.8 g), benzoylglycine (19.7 g) and fused sodium acetate (9.8 g) was heated in acetic anhydride (60 ml) for 2 hrs on a steam bath. After cooling, the bright yellow product was filtered off, washed thoroughly with water and finally with methanol to give the crude azlactone (26.4 g; 69%), m. p. 155—156 °C. A sample recrystallized from benzene–methanol had m. p. 157—158 °C.

$C_{24}H_{19}NO_4$ (385.4). Calcd. C 74.79; H 4.97; N 3.63. Found C 74.66; H 5.00; N 3.64%.

3-Benzyloxy-4-methoxyphenylpyruvic acidoxime

The crude azlactone (23.6 g) was gently boiled for 2.5 hrs with a solution of potassium hydroxide (44 g) in water (160 ml). Hydroxylamine hydrochloride (15.2 g) was added to the chilled and filtered solution; it was allowed to stand for a few hours and then acidified, with vigorous stirring and cooling, to pH 4 with hydrochloric acid. An oily precipitate formed from which the solution was decanted and acidified to pH 1. This precipitated the oxime (13.3 g, 69%). A sample recrystallized twice from nitromethane melted at 157—158 °C (lit. m. p. [5] 155—156 °C).

3-Hydroxy-4-methoxyphenyl acetonitrile

3-Benzyloxy-4-methoxyphenyl acetonitrile (2.24 g) prepared from the above oxime as described [5] was hydrogenated in the presence of palladium-on-charcoal catalyst. The usual work-up gave a yellow oil 1.3 g which solidified on standing. A sample was several times recrystallized from chlorobenzene–ligroin to give colorless prisms, m. p. 58—59 °C.

$C_9H_9NO_2$ (163.2). Calcd. C 63.26; H 5.56; N 8.58. Found C 63.28; H 5.58; N 8.73%.

2,4-Dihidroxyphenyl 3-hydroxy-4-methoxybenzyl ketone (IV)

A solution of the above nitrile (1.2 g), dry resorcinol (1.3 g) and anhydrous zinc chloride (2 g) in dry ether (40 ml) was saturated, with stirring and cooling, with hydrogen chloride gas and then left standing overnight. The ether layer was decanted from the oil which separated, the latter was triturated with 3×20 ml of dry ether and then boiled with 40 ml of water for 90 min. On cooling the ketone crystallized. It was separated (0.8 g; 41%), m. p. 155—158 °C, and recrystallized repeatedly from aqueous ethanol. Long colorless needles, m. p. 161—162 °C.

$C_{15}H_{14}O_5$ (274.3). Calcd. C 65.69; H 5.15. Found C 65.91; H 5.09%.

3',7-Diacetoxy-4'-methoxyisoflavone

The above ketone **(IV)** (2.6 g), ethyl orthoformate (9 ml) and piperidine (1 ml) were boiled in dry pyridine (9 ml) for 3 hrs and poured into a stirred mixture of 150 ml ice-water and 15 ml conc. HCl. After a few hours the crude isoflavone was separated, dried and acetylated with acetic anhydride in pyridine on a water bath. The product which crystallized on cooling was filtered off and washed with ethanol to give the almost pure diacetate (2.5 g), m. p. 204—206 °C. Recrystallization from a large amount of ethanol raised the m. p. to 207—209 °C (lit. m. p. [2, 3] 208—209 °C).

$C_{20}H_{16}O_7$ (368.3). Calcd. C 65.21; H 4.38. Found C 65.13; H 4.34%.

3',7-Dihydroxy-4'-methoxyisoflavone (I)

Saponification of the above diacetate (0.85 g) with 1 *N* sodium methoxide (10 ml) gave **I** as colorless glistening plates (0.49 g), m. p. 248—249 °C (lit. m. p. [2, 3] 247 °C).

NMR (100 MHz, in DMSO-d^6, TMS): δ = 3.76 (s, OCH_3), (6.80—7.00 m, 5H, 6,8,2',5',6'-H), 7.95 (d, J = 8 Hz, 5-H), 8.22 (s, 2-H), 8.90 and 10.66 p. p. m. (s, 3'-OH and 7-OH).

$C_{16}H_{12}O_5$ (284.3). Calcd. C 67.60; H 4.26. Found C 67.22; H 4.24%.

3',7-Dihydroxy-4'-methoxyisoflavone-7-β-D-glucopyranoside (II)

To a suspension of **I** (0.284 g; 1 mmole) in acetone (4 ml) 9% aqueous potassium hydroxide (0.75 ml) was added and thereafter a solution of acetobromoglucose (0.50 g) in acetone (3 ml) was added dropwise with stirring. After 10 hrs more potassium hydroxide solution (0.70 ml) and acetobromglucose (0.50 g) were added. After an additional 10 hrs of stirring the solution was filtered into water (100 ml). The precipitate was separated, dried (0.3 g), and triturated with chloroform. The chloroform solution was evaporated, the residue dissolved in hot ethanol (3 ml) and 3% aqueous potassium hydroxide (2 ml). After 15 min. heating on a water bath water (1 ml) was added and the solution neutralized with 5% sulfuric acid. The glucoside (80 mg) crystallized as tiny colorless needles, m. p. 219—221 °C. Repeated recrystallizations from aqueous ethanol raised the m. p. to 231—233 °C. No m. p. was reported for the natural glucoside [1].

UV (in methanol), λ_{max} (log ε): 220 (4.37), 247 (4.25), 258 (4.27) and 2.87 (4.06) nm. (Lit. [1]: 248, 254 and 287 nm). $[\alpha]_D^{25}$ 29.1° (c = 0.99, pyridine).

$C_{22}H_{20}O_{10}.2\,H_2O$ (480.4). Calcd. C 55.02; H 5.04. Found C 55.32; H 5.39%.

3'-Acetoxy-4'-methoxy-7-hydroxyisoflavone-7-tetra-0-acetyl-β-D-glucopyranoside; calycosin pentaacetate (III)

Acetylation of **II** (50 mg) in acetic anhydride-pyridine gave after crystallization from chloroform–ethanol colorless needles (32 mg), m. p. 120—122 °C.

NMR (60 MHz, $CDCl_3$, TMS): δ = 2.08 (15H, Glucose-$(OAc)_4$) 2.32 (s, 3H, 3'-OAc);

3.86 (s, 3H, OMe), 3.18—3.35 (m, 2H, Glucose-CH_2), 5.10—5.40 (m, 4H, Glucose-CH), 6.95—7.15 (m, 3H, 2',5',6'-H), 7.35—7.55 (m, 2H, 6,8-H), 7.96 (s, 1H, 2-H), 8.22 (d, 1H, $J = 8$ Hz, 5-H).

$C_{32}H_{32}O_{15}$ (656.6). Calcd. C 58.53; H 4.91. Found C 58.07; H 4.92%.

REFERENCES

1
2. MARKHAM, K. R., MABRY, T. J., SWIFT, T. W.: Phytochemistry **7**, 803 (1968)
3. PARTHASARATHY, M. R., PURI, R. N., SESHADRI, T. R.: Indian J. Chem. **7**, 118 (1969)
4. JAIN, A. C., LAL PYARE, SESHADRI, T. R.: Indian J. Chem. **7**, 305 (1969)
. KAGAL, S. A., KARMAKAR, S. S., VENKATARAMAN, K.: Proc. Indian Acad. Sci. **44A**, 36 (1956)
5. WONG, E.: Org. Chem. **28**, 2336 (1963)
6. ADAMS, R.: Organic Reactions, Vol. III, p. 193. Wiley, New York, 1946
7. ZEMPLÉN, G., FARKAS, L.: Ber. **76**, 1110 (1943)
8. ROBINSON, R., SUGASAWA, S.:J. Chem. Soc. **1931**, 3163.

Loránd FARKAS
András WOLFNER } Budapest XI., Gellért tér 4.

Valeria OLECHNOWICZ-STEPIEN; Wroclaw, Plac Nankiera 1, Poland.

Acta Chimica Academiae Scientiarum Hungaricae, Tomus 74 (3), pp. 371—81 (1972)

THE SYNTHESES OF METHYL- AND DIMETHYL-SUBSTITUTED AMINO ACID HYDRAZIDES, AS POTENTIAL CYTOTOXIC AGENTS

M. SZEKERKE and B. SZENDE

(Institute of Organic Chemistry, L. Eötvös University, Budapest, Ist Institute of Pathology, Semmelweis Medical University, Budapest)

Received August 17, 1971

N^1-Aminoacyl-N^2,N^2-dimethylhydrazines were prepared from N-benzyloxycarbonyl amino acids by coupling the free carboxylic groups with unsym.-dimethylhydrazine in the presence of dicyclohexylcarbodiimide. In the case of dicarboxylic acids the corresponding monobenzyl esters or their dicyclohexylamine salts were used as starting materials. The blocking groups can be removed by catalytic hydrogenation in the presence of Pd-on-charcoal. Two dipeptides were also prepared, 1-(N-benzyloxycarbonyl-L-phenylalanyl-L-phenylalanyl)-2,2-dimethylhydrazine and 1-(N-*t*-butyloxycarbonyl-L-phenylalanyl-L-phenylalanyl)-2,2-dimethylhydrazine.

The synthesis of N-methylhydrazides of amino acids and dipeptides has been realised by the reductive condensation of N-protected amino acid or peptide hydrazides with formaldehyde in the presence of PtO_2 (Adams) catalyst. *p*-Toluenesulfonyl and *t*-butyloxycarbonyl N-protecting groups were employed.

The compounds were submitted to preliminary screening against different transplantable tumours. On the dose levels used only a marginal anti-tumour activity could be observed, never exceeding 50% growth inhibition.

Many papers have appeared recently concerning the toxicity and mechanism of action in the living organism of hydrazine and unsym.-dimethylhydrazine [1, 2]. Such studies have been stimulated by the use of these compounds as rocket fuels.

When testing a series of hydrazines for another purpose, 1-methyl-2-benzylhydrazine [3, 4] was found to have a pronounced tumour inhibitory effect. After the screening of several hundred analogous compounds, finally 1-methyl-2-*p*-(isopropylcarbamoyl)-benzylhydrazine hydrochloride and 1-methyl-2-*p*-allophanoyl-benzylhydrazine hydrobromide were chosen for extended biological and clinical trials.

Amino acid hydrazides substituted with alkyl, aralkyl, alicyclic, etc. radicals [5] were found to be valuable therapeutic agents. These substances are amine oxidase inhibitors; some of them show remarkable anti-depressive activity. No methyl- or dimethyl-substituted derivatives were mentioned in this series of compounds [5].

It seemed interesting therefore to synthesize some methyl- and dimethyl-substituted hydrazides of amino acids, as a new combination of two groups of biologically active compounds, and investigate their biological activity, first of all their possible tumour inhibitory potential.

The choice of the corresponding glutamic acid and aspartic acid derivatives has been based on the findings of ROBERTS *et al.* [6]; they have shown that glutamine plays a key role in the metabolism of tumour cells. This encouraged the postulation that some analogues of glutamine might function as interfering antagonists and influence the metabolic pathways of tumours. Several derivatives have been tested and some showed a considerable tumour growth inhibition, among others 1-γ-L-glutamylhydrazine [7] and 1-β-DL-aspartylhydrazine [8].

The L-asparaginase dependence of certain tumours has been demonstrated by BROOME [9], the growth of susceptible tumours being inhibited by treatment with L-asparaginase derived from either guinea pig serum or *Escherichia Coli*. Recently SCHLESINGER *et al.* [10] in a search for L-asparagine analogues found that N-benzyloxycarbonyl-L-asparagine caused a more than 50% inhibition of the growth of an L-asparaginase-sensitive murine lymphoma [11].

It is of interest to note that N-benzyloxycarbonyl-L-phenylalanine has also shown tumour inhibitory potency [12]. It has been observed that benzyloxycarbonyl derivatives of amino acids bearing an additional aromatic ring strongly inhibit a multitude of enzymes, *i.e.* rat liver asparaginase, rat liver glutaminase, rat liver glutamine synthetase, etc. The strong inhibitory activity of the derivatives containing two aromatic groups may be explained by an interaction of the aromatic rings through hydrophobic bonds with two suitable sites in the enzyme molecule. This causes inhibition either by blocking the active sites *per se*, or by exerting an allosteric effect [12].

In view of the above results we applied in most cases N-benzyloxycarbonyl protecting groups. The presence of a second aromatic ring in the molecule could be established by forming benzyl half esters in the case of glutamyl- and aspartyl derivatives. N-Benzyloxycarbonyl-phenylalanine derivatives were also synthesized.

In the case of dicarboxylic acids γ- and β-hydrazides were formed, respectively. The investigation of α-hydrazides seemed worth while too, since our previous experiences with glutamylpeptides [13] indicated that, in spite of our expectations, α-L-glutamyl-Melphalan ethyl ester was a more effective tumour inhibitor than its γ-glutamyl analogue.

A few peptide derivatives have been included in the series of our model compounds, based on indications that certain peptide derivatives of Melphalan [13, 14] and Sarcolysin [15, 16, 17] are less toxic than the parent compound, have a different spectrum of antitumour activity and may possess an improved chemotherapeutic index. The non-mustard amino acid has considerable influence on the activity; for example N-acetyl-sarcolysyl-valine ethyl ester inhibited the growth of spindle cell sarcome 45 in rats as did Sarcolysin, but damaged normal tissue, especially hemopoietic tissue to a lesser extent, suggesting a much more selective anti-tumour action [18].

N^1-Aminoacyl—N^2, N^2-dimethylhydrazines

From experiments with methylhydrazine and with unsym.-dimethylhydrazine it has been concluded [19] that the order of reactivity with respect to the formation of acylhydrazides from an ester is: $NH_2—NH_2 > CH_3NH—NH_2 > (CH_3)_2N—NH_2$. Unsym.-dimethylhydrazine did not react with simple esters larger than formates.

The synthesis of N^1-aminoacyl-N^2,N^2-dimethylhydrazines was realized therefore from N-protected amino acids by coupling the free carboxylic group in the presence of dicyclohexylcarbodiimide [20] with unsym.-dimethylhydrazine (liberated from its hydrochloride [21] with triethylamine), using acetonitril as solvent. In the case of dicarboxylic acids the corresponding monobenzyl esters, or their dicyclohexylamine salts were used as starting materials.

The N-benzyloxycarbonyl- and benzyl ester blocking groups can be removed by catalytic hydrogenation in the presence of Pd-on-charcoal. In a few cases the unprotected amino acid N,N-dimethylhydrazides were also prepared and submitted to animal tests, having a better water solubility than the protected derivatives.

The following compounds have been synthesized:

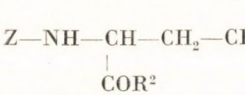

I: $R^1 = NH—N(CH_3)_2$ $R^2 = OCH_2C_6H_5$ $Z = OCOCH_2C_6H_5$

1-(α-benzyl N-benzyloxycarbonyl-γ-L-glutamyl)-2,2-dimethylhydrazine

II: $R^1 = OCH_2C_6H_5$ $R^2 = NH—N(CH_3)_2$ $Z = OCOCH_2C_6H_5$

1-(γ-benzyl N-benzyloxycarbonyl-α-L-glutamyl) 2,2-dimethylhydrazine

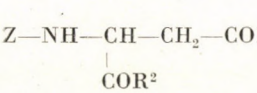

III: $R^1 = OCH_2C_6H_5$ $R^2 = NH—N(CH_3)_2$ $Z = OCOCH_2C_6H_5$

1-(β-benzyl N-benzyloxycarbonyl-α-L-aspartyl)-2,2-dimethylhydrazine

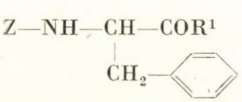

IV: $R^1 = NH—N(CH_3)_2$ $Z = OCOCH_2C_6H_5$

1-(N-benzyloxycarbonyl-L-phenylalanyl)-2,2-dimethylhydrazine

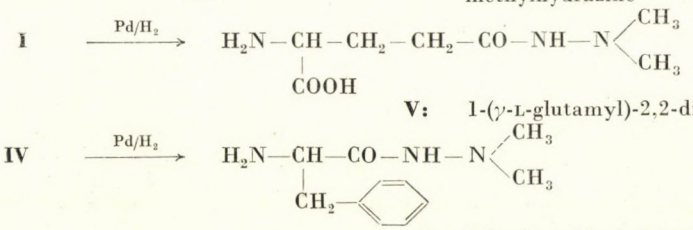

V: 1-(γ-L-glutamyl)-2,2-dimethylhydrazine

VI: 1-(L-phenylalanyl)-2,2-dimethylhydrazine

Two dipeptides, **VII** and **VIII**, were included in this series of compounds. 1-(N-Benzyloxycarbonyl-L-phenylalanyl-L-phenylalanyl)-2,2-dimethylhydrazine **(VII)** was synthesized from N-benzyloxycarbonyl-L-phenylalanine [22] and 1-(L-phenylalanyl)-2,2-dimethylhydrazine **(VI)**, using dicyclohexylcarbodiimide in tetrahydrofuran for the peptide coupling.

The second dipeptide, 1-(N-*t*-butyloxycarbonyl-L-phenylalanyl-L-phenylalanyl)-2,2-dimethylhydrazine **(VIII)** was obtained by a three-step synthesis. N-*t*-Butyloxycarbonyl-L-phenylalanine [23] and L-phenylalanine benzyl ester [24] were coupled to a dipeptide [25] by means of the mixed anhydride method. After removal of the benzyl ester group by catalytic hydrogenation in the presence of Pd/charcoal, unsym.-dimethylhydrazine was coupled to the free carboxylic group of the N-protected dipeptide [26] in the presence of dicyclohexylcarbodiimide.

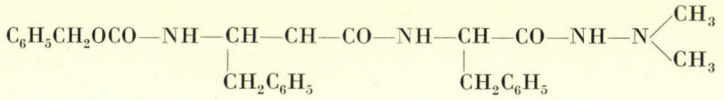

VII: 1-(N-benzyloxycarbonyl-L-phenylalanyl-L-phenylalanyl)-2,2-dimethylhydrazine

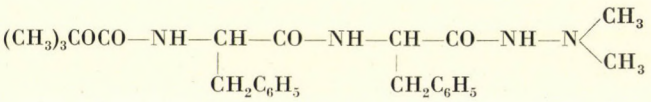

VIII: 1-(N-*t*-butyloxycarbonyl-L-phenylalanyl-L-phenylalanyl)-2,2-dimethylhydrazine

N^1-Aminoacyl-N^2-methylhydrazines

The monoacylation of methylhydrazine is complicated by the presence of two nitrogens which can undergo acylation. Considering the electron-donating character of the methyl group, acylation might be expected to occur more readily at the methyl-bearing nitrogen. Experimental evidence has shown [19] that the reaction of carboxylic acid esters with methylhydrazine yields predominantly the 1-acyl-2-methylhydrazine along with a smaller but substantial amount of the 1,1-disubstituted isomer. The reaction of an anhydride with an aqueous solution of methylhydrazine yields mainly 1-acyl-1-methylhydrazine, together with a trace of the 1-acyl-2-methyl isomer. Separation and purification of the products containing the mixture of isomers is extremely difficult and could not be effected by the usual techniques.

A suitable method for the synthesis of different N-monoalkylhydrazides of amino acids has been realized by the reductive condensation of aldehydes with the corresponding amino acid hydrazides in the presence of PtO_2 (Adams) catalyst [5, 27]. The N-methyl derivatives could be obtained by using formaldehyde as the aldehyde component. Free amino groups of amino acids would

interfere with the condensation reaction, therefore N-protecting groups were employed, such as *p*-toluenesulfonyl and *t*-butyloxycarbonyl, which are not affected by catalytic hydrogenation.

The following compounds were synthesized:

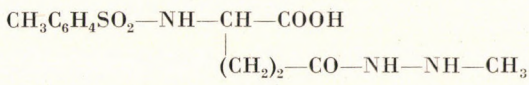

IX: 1-(N-*p*-toluenesulfonyl-γ-L-glutamyl)-2-methylhydrazine

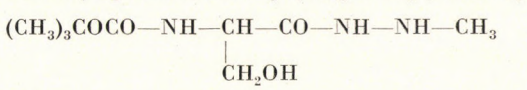

X: 1-(N-*t*-butyloxycarbonyl-L-seryl)-2-methylhydrazine

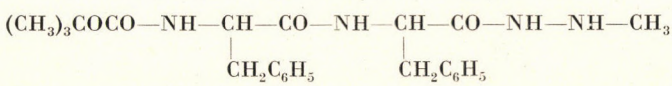

XI: 1-(N-*t*-butyloxycarbonyl-L-phenylalanyl)-
-L-phenylalanyl)-2-methylhydrazine

So far compound **XI** has been the only dipeptide derivative prepared in this series of compounds. The synthesis was achieved by coupling N-*t*-butyloxycarbonyl-L-phenylalanine [23] with L-phenylalanine methyl ester [28] using a water-soluble carbodiimide [29]. The corresponding hydrazide was obtained from the dipeptide ester with hydrazine hydrate. The last step of the synthesis was the reductive condensation of the hydrazide derivative with formaldehyde in the presence of PtO_2 catalyst.

Experimental

The compounds were checked for purity by TLC on silica gel. The most useful solvent systems were found to be: (a) MeOH—$CHCl_3$ (5 : 95); (b) Bu^nOH–AcOH–H_2O (4 : 1 : 1); (c) EtOAc–Pyr–AcOH–H_2O (60 : 20 : 6 : 11).
The spots were located with iodine vapour.

All m. p.'s are uncorrected and were taken on a Kofler apparatus

The presumed structures were confirmed by IR spectra, recorded in KBr pellets with an IR 10 spectrometer (Carl Zeiss, Jena). In a few cases the nuclear magnetic resonance spectra were also obtained in DMSO(d_6) solution using a ZKR-60 type spectrometer (Carl Zeiss, Jena).

Starting materials (prepared according to the literature)

α-Benzyl N-benzyloxycarbonyl-L-glutamate [30]
γ-Benzyl N-benzyloxycarbonyl-L-glutamate [31]
γ-Benzyl N-benzyloxycarbonyl-L-glutamic acid dicyclohexylamine salt [32]
β-Benzyl N-benzyloxycarbonyl-L-aspartate [33]
N-Benzyloxycarbonyl-L-phenylalanine [22]
unsym.-N,N-Dimethylhydrazine hydrochloride [21]
N-*t*-Butyloxycarbonyl-L-phenylalanine [23]
L-Phenylalanine benzyl ester hydrochloride [24]
N-*p*-Toluenesulfonyl-L-glutamic acid γ-hydrazide [34]
N-*t*-Butyloxycarbonyl-L-serine hydrazide [35]
L-Phenylalanine methyl ester hydrochloride [28]

N-*t*-Butyloxycarbonyl-L-phenylalanyl-L-phenylalanine methyl ester [29] Dicyclohexylcarbodiimide, N-ethyl-N'-(3-dimethylamino-propyl)-carbodiimide, isobutyl chloroformate (Fluka).

All other reagents were of analytical grade.

N^1-(N'-protected aminoacyl)-N^2,N^2-dimethylhydrazines

A mixture of the N-benzyloxycarbonylamino acid (10 mmoles) (or in the case of dicarboxylic acids the appropriate monobenzyl ester), unsym.-dimethylhydrazine hydrochloride (10 mmoles) and triethylamine (10 mmoles) was stirred in acetonitril (125 ml) for 15 min at 0 — +2 °C, followed by the addition of dicyclohexylcarbodiimide (11 mmoles). Stirring was continued in the cold for 4 hrs and then the mixture set aside for 12 hrs at room temperature. A few drops of glacial acetic acid were added, the precipitate removed, and the filtrate evaporated to dryness in vacuum. An ethyl acetate solution of the residue was washed with 5% sodium hydrogen carbonate solution and water, dried ($MgSO_4$), and the solvent removed in vacuum. The residue was purified by crystallisation from ethyl acetate–petroleum ether.

Compound	M. p., °C	Yield	Optical rotation	Analysis
I	111—2°	70%	$[\alpha]_D^{20} = -11.73°$ (c = 2.5; MeOH)	$C_{22}H_{27}O_5N_3$ (413.482) Calcd. (%) C 63.9; H 6.6; N 10.2 Found (%) C 64.1; H 7.0; N 10.0
II	141—2°	74%	$[\alpha]_D^{20} = -12.4°$ (c = 2.3; MeOH)	$C_{22}H_{27}O_5N_3$ (413.482) Calcd. (%) C 63.9; H 6.6; N 10.2 Found (%) C 64.15; H 7.05; N 10.6
III	124—5°	72%	$[\alpha]_D^{20} = -4.4°$ (c=2.7; MeOH)	$C_{21}H_{25}O_5N_3$ (399.455) Calcd. (%) C 63.15; H 6.3; N 10.5 Found (%) C 63.0; H 6.5; N 10.7
IV	142°	75%	$[\alpha]_D^{20} = +4.5°$ (c=2; EtOH)	$C_{19}H_{23}O_3N_3$ (341.417) Calcd. (%) C 66.84; H 6.79; N 12.3 Found (%) C 67.0; H 6.9; N 12.5

Catalytic hydrogenolysis of protected derivatives

The protected derivatives (10 mmoles) were dissolved in anhydrous methanol (250 ml) and hydrogenated in a stream of hydrogen at room temperature in the presence of palladium-on-charcoal (10%) until development of CO_2 was no longer detectable. The reaction mixture was filtered from the catalyst and the filtrate evaporated to dryness in vacuum.

Compound	M. p., °C	Optical rotation	Yield	Analysis
V	176—8°	$[\alpha]_D^{20} = +11.1°$ (c=2.1; water)	87.4%	$C_7H_{15}O_3N_3$ (189.221) Calcd. (%) C 44.43; H 7.99; N 22.2 Found (%) C 44.35; H 7.73; N 22.3
VI	amorphous hygroscopic solid		95.5%	$C_{11}H_{17}ON_3$ (207.281) Calcd. (%) N 20.3 Found (%) N 19.9

1-(N-Benzyloxycarbonyl-L-phenylalanyl-L-phenylalanyl)-2,2-dimethylhydrazine (VII)

N-Benzyloxycarbonyl-L-phenylalanine (10 mmoles) and 1-(L-phenylalanyl)-2,2-dimethylhydrazine (10 mmoles) **(VI)** were coupled in tetrahydrofuran (100 ml) by the dicyclohexylcarbodiimide method in the usual way.

M. p. 179—181°; $[\alpha]_D^{20} = -11°$ ($c = 2\%$; $CHCl_3$). Yield: 75%.

$C_{28}H_{32}O_4N_4$ (488.596). Calcd. C 68.83; H 6.6; N 11.47. Found C 68.82; H 6.8; N 11.27%.

1-(N-t-butyloxycarbonyl-L-phenylalanyl-L-phenylalanyl)-2,2-dimethylhydrazine (VIII)

To a cold (—5 °C) solution of N-*t*-butyloxycarbonyl-L-phenylalanine (10 mmoles) in tetrahydrofuran (50 ml) triethylamine (10 mmoles) was added followed by isobutyl chloroformate (10 mmoles). The mixture was stirred for 20 min. at —5 °C and a solution of L-phenylalanine (25 ml) was added. The solution was stirred for 3 hr at 0 °C and at room temperature overnight. The precipitate was filtered off and the solvent evaporated in vacuum. The ethyl acetate solution of the residue was washed successively with H_2O, 5% $NaHCO_3$ solution, 0.1 *N* citric acid and H_2O, dried ($MgSO_4$), and the solvent removed in vacuum. The residue was purified by crystallisation from ethyl acetate-petroleum ether. Yield 88%. The product obtained proved to be identical with the N-*t*-butyloxycarbonyl-L-phenylalanyl-L-phenylalanine benzyl ester reported in the literature [25], but prepared by a different method.

A solution of N-*t*-butyloxycarbonyl-L-phenylalanyl-L-phenylalanine benzyl ester in anhydrous methanol was subjected to catalytic reduction with palladium-charcoal according to the conventional procedure. After completion of the reaction (1/2—1 hr) and removal of the catalyst, the filtrate was concentrated under reduced pressure to a crystalline mass. Recrystallisation of the residue from ether–petroleum ether yielded a compound identical with N-*t*-butyloxycarbonyl-L-phenylalanyl-L-phenylalanine obtained previously by the saponification of the corresponding methyl ester [26].

Coupling of the N-protected dipeptide with unsym.-dimethylhydrazine in the presence of dicyclohexylcarbodiimide was achieved as described for the N-protected amino acid derivatives.

M. p. 159—160 °C; $[\alpha]_D^{20} = -6°$ ($c = 2$, MeOH). Yield: 77%.

$C_{25}H_{34}O_4N_4$ (454.579). Calcd. C 66.06; H 7.54; N 12.33. Found C 65.92; H 7.56; N 12.5%.

N-t-butyloxycarbonyl-L-phenylalanyl-L-phenylalanylhydrazide

Hydrazine hydrate (0.65 ml; 95%) was added to a solution of N-*t*-butyloxycarbonyl-L-phenylalanyl-L-phenylalanine methyl ester (10 mmoles) in dry ethanol (30 ml). The reaction mixture was kept for 5 days at room temperature. The crystals were collected and recrystallised from ethanol–ether.

M. p. 178—179 °C; $[\alpha]_D^{20} = -19.1°$ ($c = 1.98$; MeOH). Yield: 66%.

$C_{23}H_{30}N_4O_4$ (426.525). Calcd. C 64.77; H 7.1; N 13.14. Found C 64.47; H 7.5; N 13.45%.

Reaction of N-protected amino acid and peptide hydrazides with formaldehyde and simultaneous hydrogenation of the hydrazone thus formed

To a solution of the N-protected amino acid hydrazide (10 mmoles) in ethanol–water (1 : 1) (200 ml), or the N-protected peptide hydrazide (10 mmoles) in methanol–ethanol (1 : 1) (200 ml), aqueous formaldehyde solution was added (11 mmoles; 38%) and hydrogenated in the presence of PtO_2 catalyst (0.1 g). After the absorption of hydrogen had subsided (3—4 hr), the catalyst was filtered off, the filtrate concentrated in vacuum and crystallised from dry ethanol–ether.

Spectral data

NMR assignment:	δ 2.43 ppm (N—CH_3)
IR: **I:** ν_{max}:	3300, 3225 (NH); 2822, 2780 (NCH_3); 1748 (C=O, ester); 1652 (C=O, amide); 1692 (C=O, Z) cm^{-1}.
II: ν_{max}:	3300, 3225 (NH); 2780, 2795 (NCH_3); 1735 (C=O, ester); 1659 (C=O, amide); 1689 (C=O, Z) cm^{-1}.
III: ν_{max}:	3305, 3230 (NH); 2768, 2790 (NCH_3); 1735 (C=O, ester); 1660 (C=O, amide); 1686 (C=O, Z) cm^{-1}.

IV: ν_{max}: 3320, 3230 (NH); 2828, 2781 (NCH_3); 1673 (C=O, amide); 1700 (C=O, Z); 700, 740 (monosubst. aromatic ring) cm^{-1}.

V: ν_{max}: 3300—2500 (broad; NH_3^+); 1620, 1318 (CO_2^-); 2840, 2792 (NCH_3); 1679 (C=O, amide) cm^{-1}.

δ: 1558 (NH); 1595 (NH_3^+) cm^{-1}.

VII: ν_{max}: 3280, 3220 (NH, broad); 2820, 2780 (NCH_3); 1640 (C=O, amide); 1690 (C=O, Z); 700, 748 (monosubst. aromatic ring) cm^{-1}.

δ: 1548, 1532 (NH) cm^{-1}.

VIII: ν_{max}: 3325, 3292, 3241 (NH); 2822, 2780 (NH_3); 1651 (C=O, amide); 1693 (C=O, BOC); 3085, 3065, 3032 ($C_{Ar}H$); 750, 702 (monosubst. aromatic ring) cm^{-1}.

δ: 1532 (NH, amide II) cm^{-1}.

IX: ν_{max}: 3400—2000 (NH, OH); 1720 (C=O, COOH); 1655 (C=O, amide); 1335, 1165 (SO_2) cm^{-1}.

δ: 1585, (NH_2) cm^{-1}.

X: ν_{max}: 3330, 3300, 3270 (NH); 3100 (OH, broad); 1715 (C=O, BOC); 1660 (C=O, amide I) cm^{-1}.

δ: 1530 (NH, amide II).

XI: ν_{max}: 3350—3230 (NH); 1655, 164 (C=O, amide); 1689 (C=O, Z); 700, 740 monosubst. aromatic ring) cm^{-1}.

δ: 1550, 1520 (NH) cm^{-1}.

Compound	M. p., °C	Optical rotation	Yield	Analysis
IX	70—2°	$[\alpha]_D^{20} = +37.1°$ ($c = 2.1$; MeOH)	74.7%	$C_{13}H_{19}O_5N_3S$ (329.385) Calcd. (%) C 47.4; H 5.8; N 12.7; S 9.7 Found (%) C 47.1; H 6.1; N 12.5; S 9.5
X	147—8°	$[\alpha]_D^{20} = -8°$ ($c = 2$; EtOH)	78.1%	$C_9H_{19}O_4N_3$ (233.275) Calcd. (%) C 46.3; H 8.2; N 18.0 Found (%) C 46.6; H 8.4; N 18.1
XI	119—20°	$[\alpha]_D^{20} = -9.03°$ ($c = 2$; MeOH)	50%	$C_{24}H_{32}O_4N_4$ (440.552) Calcd. (%) C 65.4; H 7.3; N 12.7 Found (%) C 65.1; H 7.3; N 12.8

The degradation of deoxyribonucleic acid by methylhydrazine derivatives

The effect of 1-methyl-2-*p*-(isopropylcarbamoyl)-benzylhydrazine hydrochloride (Ro 4-6467-I) and other compounds of this type [3] on the viscosity of aqueous solutions of deoxyribonucleic acid has been examined by BOLLAG *et al.* [36].

In the presence of molecular oxygen a steady decrease of the viscosity was observed over a period of several days. From the experimental results it was concluded that this effect is due to autoxidation of the methylhydrazine derivatives leading to the formation of hydrogen peroxide. It may be assumed that slow release of hydrogen peroxide is an essential requirement for cytotoxic activity.

Experimental conditions: the solution of 0.07% w/v sodium deoxyribonucleinate (Fluka) and 10% sodium chloride to stabilize the DNA against denaturation in 1/30 molar phosphate buffer of pH = 7 was made 0.0005 molar with respect to Ro 4-6467-I. The solution was stored at 37 °C. The viscosity was measured periodically in an Ostwald type viscometer at 37 °C (sheer stress between 300 and 600 sec^{-1}).

The effect on the viscosity of aqueous DNA (REANAL) solution of two water-soluble hydrazine derivatives reported in this paper, **V** and **X**, has been investigated under similar conditions, except in a more concentrated, $2.5 \cdot 10^{-3}$ molar solution.

The results of viscosity measurements are presented in Table I and Fig. 1.

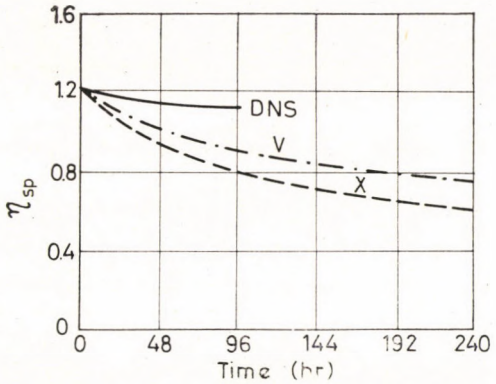

Fig. 1. **V:** 1-(γ-L-Glutamyl)-2,2-dimethylhydrazine; **X:** 1-(N-BOC-L-seryl)-2-methylhydrazine

Table I

Time, hrs	η_{isp}				
	DNA (Reanal)	DNA (Reanal) + V	DNA (Reanal) + X	DNA (Fluka)	DNA (Fluka) Ro 4-6467-I
0	1.194	1.194	1.194	0.63	0.63
24		1.194	1.114		0.38
72	1.139			0.58	
96		0.978	0.969		0.1
160					0.03
216		0.783	0.652		
Decrease	5%	35%	46%		95%

From the experimental results it can be concluded that both compounds cause a decrease in the viscosity of an aqueous DNA solution, but the process is less dramatic and also slower than in the case of Ro 4-6467-I. At the same time, it cannot be overlooked that a direct comparison between the data obtained by BOLLAG *et al.* [36] and our measurements might be incorrect, since the η_{sp} value of the control DNA solution prepared from DNA (Fluka) was about the half as much as in the case of the DNA solution used by us and prepared from a highly polymerised chicken blood DNA (REANAL, Hungary).

Biological data

Compounds **I**, **II**, **III**, **IV**, **V**, **IX** and **X** were submitted to preliminary screening and tested for anti-tumour activity on the following transplantable tumours: Yoshida subcutaneous sarcoma in rat (Wistar, random); S_{37} ascites tumour, Ehrlich ascites carcinoma and NK/Ly ascites lymphoma in mice (Swiss, random). The procedures adopted corresponded to generally accepted screening methods.

Based on toxicity estimations (LD_{50}, LD_{10}), the daily doses applied (i. p. or s. c.) for 8—10 days corresponded to the LD_{10} dose levels (**IV**, **IX**, **X**) or were somewhat higher (**I**, **II**, **III**, **V**):

I	II	III	IV	V	IX	X
50 mg/kg	50 mg/kg	50 mg/kg	1 mg/kg	50 mg/kg	5 mg/kg	10 mg/kg

Initial results of testing indicated that on the above mentioned dose levels these compounds show only borderline anti-tumour activity. Even in the case of the most active compounds **(IV, IX)** tumour growth inhibition was less than 50%. A detailed study of the tumour inhibitory properties will be published elsewhere.

*

Thanks are due to Professor V. BRUCKNER (Institute of Organic Chemistry) and Professor K. LAPIS (Institute of Pathology) for their interest in this work and for their helpful comments.

Grateful acknowledgement is due to Mrs. H. MEDZIHRADSZKY, Mrs. J. KAJTÁR and Mrs. S. KUTASSI for the microanalyses, to Drs. P. SOHÁR and P. MEZEY for NMR and F. RUFF for IR spectral measurements.

Appreciation is also expressed to A. MATTYASOVSZKY for technical assistance and to Zs. PETRES for the viscosity determinations.

This work was partly supported by the Chinoin Pharmaceutical Works, which we acknowledge gratefully.

REFERENCES

1. CORNISH, H. H., BARTH, M. L.: Toxicol. appl. Pharmacol. **6,** 568 (1964)
2. CORNISH, H. H., GEAKE, C. L., BARTH, M. L.: Biochem. Pharmacol. **14,** 1901 (1965)
3. ZELLER, P., GUTMANN, H. HEGEDÜS, B., KAISER, A., LANGEMANN, A., MÜLLER, M.: Experientia **19,** 129 (1963)
4. BOLLAG, W., GRUNBERG, E.: Experientia **19,** 130 (1963)
5. Swiss Pat. 834,391 (1960); 836,332 (1960); 843,372 (1960), F. Hofmann — La Roche Co., Basel, Switzerland.
6. ROBERTS, E., TANAKA, K. K., SIMONSEN, D. G.: Cancer Res. **16,** 970 (1956)
7. AYANGER, P., ROBERTS, E.: Growth **17,** 201 (1953)
8. MICKELSON, M. N., FLIPPIN, R. S.: Arch. Biochem. **64,** 246 (1956)
9. BROOME, J. D.: J. Exp. Med. **118,** 99 (1963)
10. SCHLESINGER, M., GROSSOWICZ, N., LICHTENSTEIN, N.: Experientia **25,** 14 (1969)
11. HARAN-GHERA M., KOTLER, M., MESHOVER, A.: J. nat. Cancer Inst. **39,** 63 (1967)
12. SPIEGELSTEIN-KLARFELD, H., LUSTIC, N.: Experientia **26,** 127 (1970)
13. SZEKERKE, M., WADE, R., BERGEL, F.: J. Chem. Soc. **1965,** 1907
14. BERGEL, F., STOCK, J. A.: J. Chem. Soc. **1960,** 3658 (and subsequent papers in this series)
15. LARIONOV, L. F., SOFINA, Z. P.: Doklady Akad. Nauk SSSR **114,** 1070 (1957)
16. LARIONOV, L. F.: Acta Un. Int. Cancr. **15,** 42 (1959)
17. LARIONOV, L. F.: in "Biological Approaches to Cancer Chemotherapy" p. 139, Academic Press, London, 1961
18. SOFINA, Z. P.: Farmakol. Toksikol. **32,** 312 (1969)
19. HINMAN, R. L., FULTON, D.: J. Am. Chem. Soc. **80,** 1895 (1958)
20. SHEEHAN, J. C., HESS, G. P.: J. Am. Chem. Soc. **77,** 1067 (1955)
21. BLATT, A. H. (editor): Org. Synth. Vol. II. p. 211, John Wiley and Sons, New York, 1943
22. GRASSMANN, W., WÜNSCH, E.: Chem. Ber. **91,** 462 (1958)
23. SCHWYZER, R., SIEBER, P., KAPPELER, H.: Helv. Chim. Acta **42,** 2622 (1959)
24. PATEL, R. P., PRICE, S.: J. Org. Chem. **30,** 3575 (1965)
25. WEYGAND, F., HUBER, P., WEISS, K.: Z. Naturforsch. **22,** 1084 (1967)
26. GERWIN, B. I., STEIN, W. H., MOORE, S.: J. Biol. Chem. **241,** 3331 (1966)
27. YALE, H. L., LOOSE, K., MARTINS, J., HOLSING, M., PERRY, F. M., BERNSTEIN, J.: J. Am. Chem. Soc. **75,** 1933 (1953)
28. BOISSONNAS, R. A., GUTTMANN, St., JAQUENOUD, P. A., WALKER, J. P.: Helv. Chim. Acta **39,** 1421 (1956)
29. NITECKI, D. E., HALPERN, B., WESTLEY, J. W.: J. Org. Chem. **33.** 864 (1968)

30. KLIEGER, E., GIBIAN, H.: Ann. **655**, 195 (1962)
31. HANBY, W. E., WALEY, S. W., WATSON, J.: J. Chem. Soc. **1950**, 3239
32. KLIEGER, E., SCHRÖDER, E., GIBIAN, H.: Ann. **640**, 157 (1961)
33. BENOITON, L.: Can. J. Chem. **40**, 570 (1962)
34. RUDINGER, J.: Coll. Czechoslow. Chem. Commun. **24**, 2013 (1959)
35. ISELIN, B., SCHWYZER, R.: Helv. Chim. Acta **44**, 169 (1961)
36. BERNEIS, K., KOFLER, M., BOLLAG, W., KAISER, A., LANGEMANN, A.: Experientia **19**, 132 (1963)

Mária SZEKERKE; Budapest VIII., Múzeum krt. 4/b.
Béla SZENDE; Budapest VIII., Üllői út 26.

RECENSIONES

B. TEŽAK and V. PRAVDIĆ, Eds.: *The Chemistry of Solid/Liquid Interfaces.*

Proceedings of the International Summer School, Dubrovnik-Cavtat, Yugoslavia. — Zagreb 1971

The collection of papers edited by B. TEŽAK and B. PRAVDIĆ and published by *Croatica Chemica Acta* under the above title, contains some of the lectures given at the Summer School held between June 23 and July 4, 1969, in Dubrovnik-Cavtat, Yugoslavia. The course has been organized by the Ruder Bošković Institute, Zagreb, under the sponsorship of the Yugoslav Federal Research Council, the corresponding Croatian federal council, and of the Nuclear Energy Council. The 18 papers included in the book were published in 1970 in Croatica Chemica Acta, together with the abstracts of other papers. As pointed out in the Introduction by Professor Težak, the initiator of this Summer School, the purpose of this collection is to arouse interest to some problems on which the Yugoslav colloid chemistry school focuses attention. To serve this objective, instead of making the book commercially available, it is sent to those interested against payment for the costs of publication.

The book is very attractively made on 10 + 300 pages. It carries numerous figures and tables, as well as subject and author indexes. The collection is not homogeneous: part of the papers can be regarded as reviews of a given field or direction of research, whereas others report on results of studies which are at present in progress. The results presented are mostly available as papers in specialist journals, some being known also as lectures of the authors in Hungary (the papers of J. LYKLEMA and M. MIRNIK at the 1st Conference on Colloid Chemistry, and of G. D. PARFITT at the Meeting of the Committee on Colloid Chemistry last year).

Although the topics discussed embrace a wide variety of fields, the papers can be roughly classed into 3 main groups. This subdivision is naturally not the only possibility since the corresponding areas often overlap.

The first group includes papers concerned with electrochemistry and the stability of sols by R. H. DOREMUS (the potential of ion-specific electrodes), L. GIERST and coworkers (effect of depolarization on the double layer), E. D. GODDARD (specific counterion effect) and J. LYKLEMA (stability of sols and the correlation between lyotropic series). The paper of M. MIRNIK on the ion-exchange theory of coagulation is very interesting and deserves attention. G. D. PARFITT treats some stability problems of non-aqueous sols. The article by W. S. STUMM and coworkers about the effect of specific interactions on the stability is also related to sol stability. A somewhat more remote aspect of the subject is represented by the papers of R. PARSONS about the transfer coefficient of electrode processes and G. H. NANCOLLAS on the thermodynamic analysis of metal complex formation in non-aqueous media. Very enlightening is B. TEŽAK's paper concerning the correlation between the so-called metoric (interphase) layers and the formation of phases.

The review by A. C. ZETTLEMOYER and F. J. MICALE on the sorption of binary liquid mixtures on solid surfaces represents a different group of subjects.

The third group includes papers on the formation of phases. A. E. NIELSEN gives a general survey of the field, A. R. DESPIC deals with the electrocrystallization of metals, R. H. DOREMUS with nucleation and crystal growth, and G. H. NANCOLLAS treats some problems of the growth of nucleation centers. The effect of intermediate phases on crystallization in the case of polymeric systems is surveyed by PETERLIN; A. G. WATSON reports on the nucleation and crystallization of common polymers and biopolymers.

The good selection of papers emphasizes that our knowledge about solid/liquid interfaces is of great importance also in the interpretation of phenomena that seem to be only remotely related to the subject of the physical chemistry of phase boundaries. Let it be sufficient to point out the electrochemical and electrokinetic phenomena at phase boundaries, or the problems of colloid stability, closely related to the latter, or of crystallization and adsorption.

The collection can be recommended primarily to scientists interested in surface chemistry, but it is not without interest for other specialists, mainly electrochemists.

I. PÁSZLI

L. EBERSON and H. SCHÄFER: *Organic electrochemistry*

Fortschritte der chemischen Forschung (Topics in Current Chemistry) 21 (182 pp). Springer Verlag, Berlin—Heidelberg—New York 1971

This issue of the well-known series (previous review, see Acta Chim. Acad. Sci. Hung. 69, 243, 1971) deals with organic electrochemistry from the preparative organic chemist's viewpoint. The amount of information and the preparative possibilities available in the field are astonishing even to the organic chemist who uses electrochemical methods fairly regularly as an analytical tool, and the review gives sufficient direct information on basic electrochemical techniques for the non-electrochemist to choose his basic instrumentation and familiarize himself with available techniques.

The organization of the book is logical and clear.

After an introduction the authors give a short classification of electroorganic reactions and a short assessment of the value of electrochemical reactions in organic systems. This introductory part is followed by a review of the methods available for gathering information on the relevant electrochemical processes in a specific system. The purpose of this part of the review is obviously to call attention to the possibilities available on the analytical side, which aid the organic preparative chemist in the choice of his final method.

The main body of the book is organized in two parts. The first contains a chapter on the experimental factors and a chapter on experimental methods and on the mechanistic considerations involved. This last chapter is especially important because the concepts and, therefore, the possibilities are in many cases different from those to which organic chemist is accustomed. The second part of the book discusses the available data on the various types of electrochemical reactions as classified in the introductory chapter. Each type of reaction is treated in a separate chapter. The titles of the chapters will suffice to give a general idea of the contents: conversion of one functional group into another functional group; electrochemical substitution; electrochemical addition; electrochemical elimination; electrochemical coupling; electrochemical cleavage; electron transfer; indirect electrochemical processes; electropolymerization and organometallics. The reviewers give a complete summary of the reactions treated and evaluate older results in the light of the greater possibilities available now. These remarks are very useful if further work is contemplated on the reactions mentioned as they show ways and means for further progress. More than 680 references covering the literature up to 1970 are included.

The reviewer thinks it appropriate to terminate this review with the conclusion quoted by the authors (Bockris 1965): "Electrochemistry nowadays has potentialities comparable with those faced by organic chemists . . . say from 1920."

M. VAJDA

R. A. HOFFMANN, S. FORSÉN and B. GESTBLOOM: *Analysis of NMR spectra*

Volume 5 of NMR Basic Principles and Progress (NMR Grundlagen und Fortschritte); Ed.: P. Diehl, E. Fluck, E. Kosfeld. Springer Verlag, Berlin—Heidelberg—New York, 1971. (165 pp)

As NMR instruments become easier to operate, organic chemists constitute an increasing percentage of users. It was realized at a very early stage that only a detailed analysis of the spectra can give the chemist *all* the information available. On the other hand, if the possibilities of gaining supplementary information by various experimental methods are fully utilized and use is made of simple calculators and tables, a greater part of moderately complex spectra can be analyzed with reasonable ease.

The ways and means for this type of analysis can be found in various standard texts but it is fairly difficult for the beginner to extract the relevant information. This is the reason why the reviewer thinks that the publication of the volume reviewed fills a real need.

The book is written with the needs of organic chemistry in mind. The first part of the book gives a brief review of the basic principles and phenomena of NMR spectroscopy, including the concepts of chemical shifts, coupling, intensities, groups of equivalent spins, time averaging phenomena, the concept of weak and strong coupling and invariance of NMR spectra. A short chapter is devoted to the possibilities of obtaining additional information on a specific compound by further spectroscopic experiments, *e.g.* double resonance techniques. The second part of the book is devoted to the analysis of spectra.

The treatment is authoritative with a clear presentation of basic concepts, stepwise procedures for the analysis of spectra. Concepts which need clarification (*e.g.* the concept of equivalence) are discussed in detail. A short chapter on the quantum mechanical treatment of NMR spectra, suggestions for further reading and some useful tables are also included.

Almost half of the book deals with the main theme: instant analysis of spectra. The authors give definite instructions for the beginner and stepwise procedures so that it is relatively easy even for the beginner to obtain a reasonable knowledge in the field. The possibilities of iterative procedures and further treatment of more complex spectra are also mentioned, although the instant analysis chapter contains data up to the ABPX and A_mB_n spin system.

The book will, no doubt, be useful for organic chemists who want to do more than first order analyses of NMR spectra.

It is regrettable that some disturbing typographical errors escaped detection.

M. VAJDA

INDEX

INORGANIC AND ANALYTICAL CHEMISTRY – ANORGANISCHE UND ANALYTISCHE CHEMIE
НЕОРГАНИЧЕСКАЯ И АНАЛИТИЧЕСКАЯ ХИМИЯ

Orsós, P. and Nyilasi, J.: Contributions to the Analysis of Osmium Compounds 267

Gergely, A. and Sóvágó, I.: Thermodynamic Data of Transition Metal Complexes with D-Glucosaminic Acid 273

PHYSICAL CHEMISTRY – PHYSIKALISCHE CHEMIE – ФИЗИЧЕСКАЯ ХИМИЯ

Náray-Szabó, G., Dudar, E. and Horváth, G.: Quantum Chemical Interpretation of the Spectroscopic Data of Pharmacologically Active Homopyrimidazole Derivatives 281

Vértes, A. and Parak, F.: Relationship Between the Spin Relaxation and Certain Chemical Properties of Paramagnetic Iron(III) Salt Solutions 293

Varsányi, Gy. and Sohár, P.: Infrared Spectra of 1,2,3,5-Tetrasubstituted Benzene Derivatives, I 315

Ruff, I. and Laczkó, B.: Fermi Statistical Treatment of Acid–Base Processes, II. Distribution and Acidity of Individual Proton Hydrates in Concentrated Aqueous Solutions of Perchloric Acid 335

ORGANIC CHEMISTRY – ORGANISCHE CHEMIE – ОРГАНИЧЕСКАЯ ХИМИЯ

Egri, J., Halmos, J. and Rákóczi, J.: Synthesis of Substituted 4-Hydroxyquinoline-3-carboxylic Esters, II. Preparation of 6,7-Diisobutoxy-4-hydroxyquinoline-3-carboxylic Acid from the Nitrile and its Esterification 345

Egri, J., Halmos, J. and Rákóczi, J.: Synthesis of Substituted 4-Hydroxyquinoline-3-carboxylic Esters, III. A One-step Process Starting from Substituted Phenylimino Esters 351

Csűrös, Z., Sallay, P. and Deák, Gy.: Synthesis of 2,4,6-Triarylpyrylium Fluoroborates from Aromatic Aldehydes and Arylmethyl Ketones, III. The Claisen—Schmidt Condensation 357

Farkas, L., Wolfner, A. and Olechnowicz-Stepien, V.: The Synthesis of Calycosin and Calycosin-7-β-D-Glucoside 367

Szekerke, M. and Szende, B.: The Syntheses of Methyl- and Dimethyl-Substituted Amino Acid Hydrazides, as Potential Cytotoxic Agents 371

RECENSIONES 383

Printed in Hungary

A kiadásért felel az Akadémiai Kiadó igazgatója — Műszaki szerkesztő: Zacsik Annamária

A kézirat nyomdába érkezett: 1972. V. 5. — Terjedelem: 10.75 (A/5) ív, 51 ábra

72.73523 Akadémiai Nyomda, Budapest — Felelős vezető: Bernát György

ACTA CHIMICA

ТОМ 74 – ВЫП. 3

РЕЗЮМЕ

Некоторые данные к аналитической химии соединений осмия

П. ОРМОШ и Й. НИЛАШИ

Был разработан метод количественного определения нитридоосмата калия в присутствии тетраокиси осмия и осмата калия. Метод основан на том, что OsO_4 может быть полностью удален из сернокислой среды с помощью кипячения и фотометрически измерен в виде тиокарбаматного комплекса. Отдельные окислители (H_2O_2, $K_2Cr_2O_7$) превращают в тетраокись осмия лишь осмат калия и не влияют на нитридоосмат калия. Т. о., проводя дестилляцию в их присутствии, может быть отделен осмий, находящийся в форме OsO_4 и K_2OsO_4, который далее количественно измеряется. Если же дестиляцию проводят в присутствии $HClO_4$, HNO_3, или в присутствии окислителей с нормальным окислительно-восстановительным потенциалом, более положительным чем + 1,5 V ($KMnO_4$, $K_2S_2O_8$), то и $KOsO_3N$ превращается в OsO_4, и, т. о., может быть измерено общее содержание осмия. Разница между двумя полученными результатами дает содержание осмия в форме нитридоосмата калия.

Термодинамические характеристики комплексов ионов переходных металлов с D-глюкозаминовой кислотой

А. ГЕРГЕЙ и И. ШОВАГО

Константы стабильности комплексов D-глюкозаминовой кислоты (ГАК) с кобальтом(II), никелем(II), медью (II) и цинком(II) были определены pH-метрически при 25° С и ионной силе 0,05 М. Энтальпии и энтропии образования этих комплексов были определены калориметрически.

Константы стабильности комплексов ГАК являются почти такими же, как и в случае аланина и норлейцина. Одновременно с этим, соответствующие величины ΔH и ΔS меньше полученных для аланина и норлейцина. Исходя из термодинамических данных, было заключено, что гидроксильные группы ГАК участвуют в образовании комплекса в недиссоциированной форме.

Квантово-химическая интерпретация спектроскопических данных фармакологически активных производных гомопиримидазоля

Г. НАРАИ-САБО, Э. ДУДАР и Г. ХОРВАТ

Распределение заряда в 26 производных гомопиримидазоля было рассчитано полуэмпирическими методами Паризер—Папп—Попла и Дель Ре. Были найдены корреляции между рассчитанными распределениями зарядов и положением некоторых ИК и ЯМР полос. Приблизительно линейное соотношение соблюдается для валентных колебаний и соответствующих порядков связей. Подобная зависимость наблюдалась между ЯМР химическим сдвигом протона на С—2 кольца и зарядом этого атома углерода. В результате анализа аномалий были объяснены некоторые структурные характеристики. Были проведены исследования зависимости УФ спектров он pH.

Зависимость между спиновой релаксацией растворов парамагнитных солей железа(III) и их некоторыми химическими свойствами

А. ВЕРТЕШ и Ф. ПАРАК

Явления парамагнитной спиновой релаксации, протекающие в растворах солей железа, изучались методом Мёссбауэра. Было установлено, что химическая связь между железом и его лигандной сферой влияет на величину внутреннего магнитного поля, относящегося к переходу $m_I = \pm 3/2 \rightarrow \pm 1/2$ дублета Крамера $S_z = \pm 5/2$, а также на частоту релаксации спин-решетка, и вследствие увеличения асимметрии электронной оболочки 3d, также на время релаксации. Метод позволяет получить информацию о числе сольватов и комплексных компонентов железа в исследуемом растворе, а также об их количественном соотношении.

Измерения свидетельствуют о том, что на основе изучения парамагнитной спиновой релаксации можно получить многостороннюю картину относительно химической структуры исследуемой системы.

ИК спектры 1,2,3,5-тетразамещенных производных бензола, I

ДЬ. ВАРШАНИ и П. ШОХАР

Подробно интерпретируются ИК спектры пятнадцати 1,2,3,5-тетразамещенных бензолов. Были установлены зависимости, с одной стороны, между частотой и интенсивностью полос, а с другой стороны, между влиянием заместителей на распределение электронной плотности, взаимодействием колебаний с одинаковой симметрией и жестким влиянием межмолекулярных сил. Однозначно было установлено, что триметиловый эфир галловой кислоты лишь в малой степени образует димеры, в большей же степени образуются водородные мостики между карбоксильной OH и кислородом метокси-группы. Полосы $\delta_{ac}CH_3$ пространственно-затрудненных метокси групп являются сильными и обладают аномально низкими частотами.

Расчеты по статистике Ферми для кислотно-основных процессов, II

Распределение и кислотность индивидуальных гидратов в концентрированных водных растворах хлорной кислоты

И. РУФФ и Б. ЛАЦКО

Приближение, основанное на статистике Ферми было использовано для описания результирующей функции кислотности концентрированных водных растворов хлорной кислоты от 2 до 25 м с различными индивидуальными протонными гидратами различной кислотности. Результаты указывают на присутствие моно-, ди-, три-, пента-, нона- и декагидратов иона гидроксониума в изученном интервале концентраций.

Синтез эфиров замещенных 4-гидрокси-3-хинолинкарбоновых кислот, II

Получение 6,7-диизобутокси-4-гидрокси-3-хинолинкарбоновой кислоты из нитрила и ее этерификация

Й. ЭГРИ, Й. ХАЛМОШ и Й. РАКОЦИ

Из 3,4-диизобутокси-анилина и цианоуксусного эфира этоксиметилена при 255—260° С в одной ступени был синтезирован 6,7-диизобутокси-4-гидрокси-3-цианхинолин, который удалось гидролизовать лишь в экстремальных условиях. Соединение, которое было целью синтеза, а именно этиловый эфир 6,7-диизобутокси-4-гидрокси-3-хинолин карбоновой кислоты, было получено из соответствующей карбоновой кислоты через хлорид кислоты, или селективной этерификацией с помощью диазоэтана.

Синтез эфиров замещенных 4-гидрокси-3-хинолинкарбоновых кислот, III

Одноступенчатый синтез из замещенных фенил-имино-эфиров

Й. ЭГРИ, Й. ХАЛМОШ и Й. РАКОЦИ

Из 3,4-дизамещенного N-этоксиметилен-анилина в присутствии четвертичного органического основания как катализатора при 255—270° С в одной ступени был получен с хорошим выходом этиловый эфир соответствующей 6,7-дизамещенной 4-гидрокси-3-хинолинкарбоновой кислоты. Данный метод пригоден и для непрерывного осуществления.

Изучение синтеза фторборатов 2,4,6-триарилпирилия из ароматических альдегидов и арилметилкетонов

З. ЧЮРЁШ, П. ШАЛЛАИ и ДЬ. ДЕАК

Был разработан количественный метод исследования реакции конденсации Кляйзена—Шмидта, приводящей к образованию халкона из бензальдегида и ацетона в среде абс. уксусной кислоты под влиянием бортрифтористого катализатора. С помощью данного метода проводились кинетические исследования реакции. Было установлено, что кинетически реакци яносит второй порядок а по компонентам — первый порядок. В уравнении скорости концентрация катализатора находится в степени 1,5. Энергия активации реакции равна 18,3 ккал/моль.

Были измерены также скорости реакции и ее энергии активации и в случае замещенных бензальдегидов и ацетофенонов. Было установлено, что заместители в бензальдегиде, находящиеся в пара-положении, изменяют скорость реакции в следующем порядке: $NO_2 > CH_3 > Cl > H > CH_3O$, а заместители в ацетофеноне, находящиеся в пара-положении — в порядке $H > OCH_3 \approx CH_3 > Cl \gg NO_2$.

В случае замещенных бензальдегидов уравнение Гамметта справедливо и $\varrho = 0{,}50$.

Синтез каликосина и каликосин-7-β-D-глюкозида

Л. ФАРКАШ, А. ВОЛЬФНЕР и В. ОЛЕХНОВИЧ-СТЕПЬЕН

Описывается синтез 3',7-дигидрокси-4'-метокси-изофлавона (I) и его 7-глюкозида (II). Идентичность I и II с каликосином и его 7-глюкозидом, соответственно, вполне вероятна, но не установлена точно.

Синтез гидразидов метил- и диметил-замещенных аминокислот, потенциально цитотоксичных агентов

М. СЕКЕРКЕ и Б. СЕНДЕ

Синтез производных N^1-аминоацил-N^2,N^2-диметилгидразина был осуществлен из N-бензилоксикарбонил-аминокислоты и асимм.-диметилгидразина с помощью дициклогексилкарбодиимида. В случае дикарбоновых кислот в качестве исходных продуктов могут быть использованы соответствующие монобензиловые эфиры или их дициклогексиламиновая соль. Защитные группы могут быть удалены с помощью каталитического гидрирования в присутствии Pd/акт. уголь. Были получены также два дипептидных производных, а именно 1-(N-бензилоксикарбонил-L-фенилаланил-L-фенилаланил)-2,2-диметилгидразин и 1-(N-*трет*-бутилоксикарбонил-L-фенилаланил-L-фенилаланил)-2,2-диметилгидразин.

Аминокислота и дипептид N-метилгидразидов могут быть получены из аминокислоты с защищенной аминогруппой или из пептид-гидразидов и формальдегида с помощью восстановительной конденсации в присутствии PtO_2 (Адамс) как катализатора; в качестве защитных групп были использованы п-толуолсульфониловая или трет-бутилоксикарбониловая группы.

С ознакомительной целью отбор соединений производился на различных экспериментальных прививочных опухолях.

Противоопухольный эффект наиболее эффективных соединений (IV, IX), на уровне изученных доз, не превышал 50%-ов.

COORDINATION CHEMISTRY: EXPERIMENTAL METHODS

by *K. Burger*

The experimental methods used for the investigation of the structure of coordination compounds are described; such as electron excitation and infrared spectrometry, the method based on the application of the Mössbauer effect, magnetic susceptibility measurement, nuclear magnetic resonance and electronspin resonance spectroscopy, X-ray structure analysis, thermal analysis (TG, DTG, DTA), investigation of optical rotatory dispersion and circular dichroism.

Apart from the brief description of the fundamental principles and ways of investigations of the various experimental methods, the author made efforts to present the possibilities of application thereof in coordination chemistry in the broadest possible range.

In English · Approx. 290 pages · 114 figures · Cloth

A joint edition with Iliffe Books LTD., London

MLV

QUANTENCHEMIE

von J. Ladik

Dieses Traktat wünscht Physikern und Chemikern eine Einführung in die quantenchemische Analyse der Elektronenstruktur von Molekülen, also in die Quantenchemie zu geben. Die interessantesten Abschnitte des Werkes sind: Abschnitt II über die quantenchemischen Annäherungsmethoden zur Behandlung des Mehrkörper-Problems, die neuesten »ab initio« Berechnungen, ferner die Beschreibung der neuen Methode zur Bestimmung von quantenchemischen Integralen mit mehreren Zentren.

In deutscher Sprache · Etwa 350 Seiten · Ganzleinen

Herausgegeben von

FERDINAND ENKE VERLAG
Stuttgart

AKADÉMIAI KIADÓ
Budapest

Vertrieben in den sozialistischen Ländern von KULTURA, Budapest, in allen anderen Ländern von FERDINAND ENKE VERLAG, Stuttgart.

The Acta Chimica publish papers on chemistry in English, German, French and Russian.

The Acta Chimica appear in volumes consisting of four parts of varying size, 4 volumes being published a year.

Manuscripts should be addressed to

Acta Chimica
Budapest 112/91 Műegyetem

Correspondence with the editors should be sent to the same address.

The rate of subscription is $ 16.00 a volume.

Orders may be placed with "*Kultúra*" Foreign Trade Company for Books and Newspapers (Budapest I., Fő utca 32. Account No. 43-790-057-181) or with representatives abroad.

Les Acta Chimica paraissent en français, allemand, anglais et russe et publient des mémoires du domaine des sciences chimiques.

Les Acta Chimica sont publiés sous forme de fascicules. Quatre fascicules seront réunis en un volume (4 volumes par an)

On est prié d'envoyer les manuscrits destinés à la rédaction à l'adresse suivante:

Acta Chimica
Budapest 112/91 Műegyetem

Toute correspondance doit être envoyée à cette même adresse.

Le prix de l'abonnement est de $ 16.00 par volume.

On peut s'abonner à l'Entreprise pour le Commerce Extérieur de Livres et Journaux «*Kultúra*» (Budapest I., Fő utca 32. Compte-courant No. 43-790-057-181) ou à l'étranger chez tous les représentants ou dépositaires.

«*Acta Chimica*» издают трактаты из области химической науки на русском, французском, английском и немецком языках.

«*Acta Chimica*» выходят отдельными выпусками разного объема. 4 выпуска составляют один том. 4 тома публикуются в год.

Предназначенные для публикации рукописи следует направлять по адресу:

Acta Chimica
Budapest 112/91 Műegyetem

По этому же адресу направлять всякую корреспонденцию для редакции.

Подписная цена — $ 16.00 за том.

Заказы принимает предприятие по внешней торговле книг и газет «*Kultúra*» (Budapest I., Fő utca 32. Текущий счет № 43-790-057-181) или его заграничные представительства и уполномоченные.

Reviews of the Hungarian Academy of Sciences are obtainable at the following addresses:

ALBANIA

Drejtorija Qändrone e Pärhapjes dhe Propagandimit tä Librit
Kruga Konferenca e Päzes
Tirana

AUSTRALIA

A. Keesing
Box 4886, GPO
Sydney

AUSTRIA

GLOBUS
Höchstädtplatz 3
A-1200 Wien XX

BELGIUM

Office International de Librairie
30, Avenue Marnix
Bruxelles 5
Du Monde Entier
5, Place St. Jean
Bruxelles

BULGARIA

HEMUS
11 pl Slaveikov
Sofia

CANADA

Pannonia Books
2, Spadina Road
Toronto 4, Ont.

CHINA

Waiwen Shudian
Peking
P. O. B. 88

CZECHOSLOVAKIA

Artia
Ve Smečkách 30
Praha 2
Poštovní Novinová Služba
Dovoz tisku
Vinohradská 46
Praha 2
Mad'arská Kultura
Václavské nám. 2
Praha 1
SLOVART A. G.
Gorkého
Bratislava

DENMARK

Ejnar Munksgaard
Nörregade 6
Copenhagen

FINLAND

Akateeminen Kirjakauppa
Keskuskatu 2
Helsinki

FRANCE

Office International de Documentation et Librairie
48, rue Gay-Lussac
Paris 5

GERMAN DEMOCRATIC REPUBLIC

Deutscher Buch-Export und Import
Leninstraße 16
Leipzig 701
Zeitungsvertriebsamt
Fruchtstraße 3—4
1004 Berlin

GERMAN FEDERAL REPUBLIC

Kunst und Wissen
Erich Bieber
Postfach 46
7 Stuttgart S.

GREAT BRITAIN

Blackwell's Periodicals
Oxenford House
Magdalen Street
Oxford
Collet's Subscription Import Department
Dennington Estate
Wellingsborough. Northants.
Robert Maxwell and Co. Ltd.
4—5 Fitzroy Square
London W. 1

HOLLAND

Swetz and Zeitlinger
Keizersgracht 471—487
Amsterdam C.
Martinus Nijhof
Lange Voorhout 9
The Hague

INDIA

Hind Book House
66 Babar Road
New Delhi 1

ITALY

Santo Vanasia
Via M. Macchi 71
Milano
Libreria Commissionaria Sansoni
Via La Marmora 45
Firenze
Techna
Via Cesi 16
40135 Bologna

JAPAN

Kinokuniya Book-Store Co. Ltd.
826 Tsunohazu 1-chome
Shinjuku-ku
Tokyo
Maruzen and Co. Ltd.
P. O. Box 605
Tokyo-Central

KOREA

Chulpanmul
Phenjan

NORWAY

Tanum-Cammermeyer
Karl Johansgt 41—43
Oslo 1

POLAND

RUCH
ul. Wronia 23
Warszawa

ROUMANIA

Cartimex
Str. Aristide Briand 14—18
Bucureşti

SOVIET UNION

Mezhdunarodnaya Kniga
Moscow G—200

SWEDEN

Almquist and Wiksell
Gamla Brogatan 26
S—101 20 Stockholm

USA

F. W. Faxon Co. Inc.
15 Southwest Park
Westwood Mass. 02090
Stechert Hafner Inc.
31. East 10th Street
New York, N. Y. 10003

VIETNAM

Xunhasaba
19, Tran Quoc Toan
Hanoi

YUGOSLAVIA

Forum
Vojvode Mišića broj 1
Novi Sad
Jugoslovenska Knjiga
Terazije 27
Beograd

ACTA CHIMICA

ACADEMIAE SCIENTIARUM HUNGARICAE

ADIUVANTIBUS

V. BRUCKNER, GY. DEÁK, K. POLINSZKY,
E. PUNGOR, G. SCHAY, Z. G. SZABÓ

REDIGIT

B. LENGYEL

TOMUS 74 FASCICULUS 4

AKADÉMIAI KIADÓ, BUDAPEST

1972

ACTA CHIM. (BUDAPEST) ACASA 2 74 (4) 387–500 (1972)

ACTA CHIMICA

A MAGYAR TUDOMÁNYOS AKADÉMIA KÉMIAI TUDOMÁNYOK OSZTÁLYÁNAK IDEGEN NYELVŰ KÖZLEMÉNYEI

SZERKESZTI

LENGYEL BÉLA

TECHNIKAI SZERKESZTŐK

DEÁK GYULA és HARASZTHY-PAPP MELINDA

Az Acta Chimica német, angol, francia és orosz nyelven közöl értekezéseket a kémiai tudományok köréből.

Az Acta Chimica változó terjedelmű füzetekben jelenik meg, egy-egy kötet négy füzetből áll. Évente átlag négy kötet jelenik meg.

A közlésre szánt kéziratok a szerkesztőség címére (Budapest 112/91 Műegyetem) küldendők.

Ugyanerre a címre küldendő minden szerkesztőségi levelezés. A szerkesztőség kéziratokat nem ad vissza.

Megrendelhető a belföld számára az „Akadémiai Kiadó"-nál (Budapest V., Alkotmány utca 21. Bankszámla 05-915-111-46), a külföld számára pedig a „Kultúra" Könyv- és Hírlap Külkereskedelmi Vállalatnál (Budapest I., Fő utca 32. Bankszámla: 43-790-057-181) vagy annak külföldi képviseleteinél és bizományosainál.

Die Acta Chimica veröffentlichen Abhandlungen aus dem Bereiche der chemischen Wissenschaften in deutscher, englischer, französischer und russischer Sprache.

Die Acta Chimica erscheinen in Heften wechselnden Umfanges. Vier Hefte bilden einen Band. Jährlich erscheinen 4 Bände.

Die zur Veröffentlichung bestimmten Manuskripte sind an folgende Adresse zu senden:

Acta Chimica
Budapest 112/91 Műegyetem

An die gleiche Anschrift ist auch jede für die Redaktion bestimmte Korrespondenz zu richten. Abonnementspreis pro Band: $ 16.00.

Bestellbar bei dem Buch- und Zeitungs-Außenhandels-Unternehmen »*Kultúra*« (Budapest I., Fő utca 32. Bankkonto No. 43-790-057-181) oder bei seinen Auslandsvertretungen und Kommissionären.

Acta Chimica Academiae Scientiarum Hungaricae, Tomus 74 (4), pp. 387–398 (1972)

IODINE EXCHANGE BETWEEN MOLECULAR IODINE AND SOME IODOMETHYLCARBONYL COMPOUNDS IN BENZENE

E. Kőrös, M. Orbán, M. Burger, K. Vörös and É. Füssy

(Department of Inorganic and Analytical Chemistry, L. Eötvös University, Budapest)

Received March 8, 1971

Iodine exchange between molecular iodine and 1-phenyl-2,3-dimethyl-4-iodoacetyl-pyrazolone (IAcpyr), monoiodoacetone (IA) and monoiodoacetic acid (IAcOH) was studied in benzene. The reactions follow the rate law, $v = k_0 \mid RCOCH_2I \mid$. The following activation parameters were obtained: for IAcpyr: $E_a = 21.2$ kcal · mole^{-1}, lg A = 11.35, $\Delta S^{\ddagger} = -9$ e.u.; for IA: $E_a = 17.8$ kcal · mole^{-1}, lg A = 6.79, $\Delta S^{\ddagger} = -28$ e.u.; for IAcOH: $E_a = 13.9$ kcal · mole^{-1}, lg A = 6.14, $\Delta S^{\ddagger} = -31$ e.u. The effect of light, oxygen and water was investigated. Based on the experimental results the authors suggested that the rate-determining steps were the formation of excited $RCOCH_2I$ species, and to a less extent the homolytic dissociation of the $RCOCH_2I$ molecules.

In preliminary communications we have reported that some iodomethylcarbonyl compounds as 1-phenyl-2,3-dimethyl-4-iodoacetyl-pyrazolone (IAcpyr) [1], monoiodoacetone (IA) [2] and monoiodoacetic acid (IAcOH) [3] exchange iodine atoms with molecular iodine. The kinetics of these exchange reactions are unlike the other iodine exchange processes, since the rates are independent on the iodine concentration.

In this publication we present our relevant studies in detail, including a thorough discussion on the mechanism of the exchange reactions.

Experimental

Reagents and their purification

^{131}IAcpyr was prepared as follows [4]: 18 g antipyrine, 20 g aluminium chloride and 1 g chloroacetyl chloride were dissolved in carbon disulphide and the mixture was kept at 50 °C for 4–5 hours. (The flask was provided with a reflux condenser.) After the evolution of hydrochloric acid had terminated the carbon disulphide was distilled off, and its last traces were removed in vacuo. The residue was treated with icy water, the separated white precipitate filtered and recrystallized twice from ethanol. 1-Phenyl-2,3-dimethyl-4-chloroacetyl-pyrazolone (ClAcpyr) separated in envelope-shaped crystals. (M.p. = 168–169 °C.)

To a saturated acetone solution of 2 g ClAcpyr a saturated acetone solution of sodium iodide (labelled with ^{131}I) was added in fivefold excess. After 3–4 hours standing the ClAcpyr was quantitatively converted to ^{131}IAcpyr. The separated sodium chloride was removed by filtration. The filtrate was kept at 30–40 °C on a water bath to expel acetone, then water was added to precipitate the ^{131}IAcpyr. The crystalline substance was washed with water to iodide-free, and dried. (Yield: 80%, m.p. = 132–133 °C.)

IA was prepared by Emmerling's method [5]. To 20 g monochloroacetone (m.p. = 118–120 °C) the saturated aqueous solution of potassium iodide was added, and then so much methanol to obtain a homogeneous liquid. After 2 days a brown oil separated, it was dried over

anhydrous sodium sulphate, and distilled in vacuo at a pressure of 2 torr and at 35 °C. Prior to distillation, iodine was removed by shaking the oil with metallic mercury.

Monoiodoacetone is both light and heat sensitive, and thus it should be stored over copper turning in a bottle wrapped in aluminium foil, at a cool place. The iodine content of IA was measured by Volhard's method, after alkaline hydrolysis.

IAcOH was recrystallized immediately before use from light petroleum. (M.p. = 82 °C.) Iodine content was measured as described above.

Labelled iodine (I—131)

Carrier-free $Na^{131}I$ solution was evaporated to dryness, then 0.5 g powdered KI, 1 g CaO and 5 g I_2 were added, and the iodine was sublimed in a tightly closed sublimation apparatus.

Benzene was purified as follows: In a separatory funnel to 500 ml benzene 25 ml concentrated sulphuric acid was added, and vigorously shaken. The sulphuric acid was separated and the procedure repeated as far as the isatin test for thiophene was negative. Benzene was washed with water and sodium carbonate solution, and again with water. Then benzene was allowed to stand over anhydrous calcium chloride for 24 hours, and over sodium metal for another 24 hours, and then fractionated. (B.p. = 80.3 °C.)

The water content of the purified benzene — determined by Karl-Fischer's method — was between 0.003 and 0.005%. Other impurities (cyclohexane, cyclohexene, toluene, ethyl benzene) were absent according to gas-chromatographic test.*

Exchange experiments

IAcpyr. It has been known from a previous study that IAcpyr exchanges with iodide ions with a considerable rate [6]. Preliminary experiments indicated that the iodine exchange between IAcpyr and molecular iodine is affected by light and dissolved oxygen. The former introduced some inaccuracy during the separation procedure, the latter during the whole exchange process.

The following procedure was adopted:

A gas (nitrogen or argon) cylinder was connected to a gas washbottle which contained benzene, and it was kept in a water-bath of approximately the same temperature as the reaction temperature. This bottle was connected to another one which was placed into an ultrathermostate. The benzene solution of IAcpyr was transferred into the second bottle and nitrogen gas (in some cases argon) of spectroscopic purity was bubbled through the solution for 30 minutes. The reaction was initiated by adding the benzene solution of iodine — which was also desaerated — to the IAcpyr solution. 5.00 ml aliquots were withdrawn at certain intervals and added to a mixture of 5.0 ml 0.01 *M* arsenic acid and 30 ml benzene in a separatory funnel. After vigorous shaking, the phases were allowed to separate, and the radioactivity of 4.00 ml of the aqueous phase was measured with a NaI(Tl) well-type scintillator. Results of this separation procedure could be reproduced within 2%. Some runs were performed after desaerating the solutions in vacuo. The iodine solution was placed into the inside vessel of the desaerating flask (Fig. 1), the IAcpyr solution into the outer part. The flask was cooled to the temperature of liquid air, evacuated with a mercury diffusion pump ($5 \cdot 10^{-4}$ torr) and then melted and agitated; the cycle freezing and evacuation was repeated five times. Then the flask was placed into a thermostate, and the reaction started by mixing the two solutions.

All the flasks used in these runs were wrapped in aluminium foil.

The three desaerating methods furnished the same results, and thus the nitrogen bubbling method was preferred.

IA. The procedure was the same as described above, except that the quenching solution was a mixture of 5.0 ml 0.1 *M* ascorbic acid and 5.0 ml benzene, and the radioactivity of 4.00 ml of the benzene phase was measured.

IAcOH. The procedure was the same as described with IAcpyr, except that the quenching solution was 3×5.00 ml 0.1 *M* perchloric acid, and the radioactivity of 4.00 ml of the aqueous phase was measured.

* The gas-chromatographic purity test of benzene was performed by Dr. T. Tóth (Eötvös University, Department of Chemical Technology), to whom the authors are indebted.

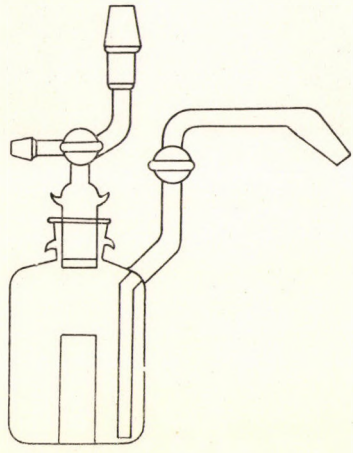

Fig. 1

Calculation of the results

The half-time of the exchange ($t_{1/2}$) was calculated graphically by plotting the logarithm of the fraction of exchange (x_t/x_∞) against time. x_∞ was obtained by multiplying the activity of 5.00 ml of the reaction mixture by the $|\,IA\,|/(|\,IA\,| + 2\,|\,I_2\,|)$. The rate of exchange ($v$) was obtained from the following relation:

$$v = \frac{|IA|2|I_2|}{|IA|+2|I_2|} \cdot \frac{0.693}{t_{1/2}} .$$

Plotting $\lg v$ against $\lg |\,I_2\,|$ and $\lg |\,IA\,|$, respectively, while the concentration of the other reactant was kept constant, the order of the reaction could be obtained.

The activation parameters (E_a, lg A and $\Delta S^{\ddagger}$) were calculated as usual.

Results

Preliminary experiments

Effect of light

IAcOH and IA decompose by the effect of natural light and the originally white crystals turn to brown. According to our spectrophotometric measurements after 140 hours, only 0.15% of the IAcOH decomposed in benzene.

We also checked the extent of the decomposition of IAcOH in benzene in the presence of iodine. The results are given in Table I.

There is practically no change in the optical density of the solutions.

Table I

$\lambda = 500$ *nm*

$\lvert IAcOH \rvert$ M	$\lvert I_2 \rvert$ M	E_1^*	E_2^{**}	Length of cell cm
$5 \cdot 10^{-4}$	$2 \cdot 10^{-3}$	0.227	0.224	0.1
$1 \cdot 10^{-3}$	$1 \cdot 10^{-3}$	0.117	0.117	0.1
$2 \cdot 10^{-3}$	$5 \cdot 10^{-4}$	0.599	0.600	1.0
—	$5 \cdot 10^{-4}$	0.597	0.595	1.0
—	$1 \cdot 10^{-3}$	0.119	0.118	0.1
—	$2 \cdot 10^{-3}$	0.217	0.214	0.1
$5 \cdot 10^{-4}$	—	0.000	0.005	1.0
$1 \cdot 10^{-3}$	—	0.003	0.000	1.0
$2 \cdot 10^{-3}$	—	0.000	0.003	1.0

* Optical density of the original solutions.
** Optical density of solutions after 6 hours, kept in dark at 60 °C.

Effect of water

Also the influence of the water content of the solvent was investigated in the case of IAcOH. The results are compiled in Table II.

Table II

$t = 45.0$ °C

$\lvert IAcOH \rvert \cdot 10^3$ M	$\lvert I_2 \rvert \cdot 10^3$ M	$k \cdot 10^6$ sec^{-1}	$\bar{k} \cdot 10^6$ sec^{-1}	Water content of benzene %
0.50	1.0	5.17		
0.70	1.0	5.08	5.40	0.02
2.0	1.0	5.78		
2.0	0.5	5.57		
0.70	1.0	4.65		
1.0	1.0	5.73	5.47	0.003
1.0	1.0	5.70		
1.0	0.5	5.47		

Effect of oxygen

Dissolved oxygen has an influence on the rate of exchange especially in the case of the IAcOH—I_2 system. Some runs were performed in benzene saturated with oxygen gas, and the results are shown in Table III.

Table III

$t = 45.0\ °C$

$\lvert IAcOH \rvert \cdot 10^3$ M	$\lvert I_2 \rvert \cdot 10^3$ M	$v_{O_2} \cdot 10^9$ $M \cdot sec^{-1}$	$v_{N_2} \cdot 10^9$ $M \cdot sec^{-1}$	v_{N_2}/v_{O_2}
0.70	3.0	3.77	4.23	1.1
1.0	0.5	3.68	6.62	1.8
1.0	1.0	3.10	5.72	1.8
1.0	3.0	2.78	6.60	2.3
3.0	1.0	8.95	19.15	2.1
5.0	3.0	3.08	31.92	10.3

v_{O_2} and v_{N_2} are the rates of the exchange measured in oxygen saturated and in nitrogen saturated benzene, respectively.

Exchange kinetics

The results of the exchange experiments with IAcpyr, IA and IAcOH are presented in Tables IV, V and VI.

The activation parameters for the three reactions are given in Table VII.

Discussion

The rate equation describing the kinetics of iodine exchange between IAcpyr, IA, IAcOH and I_2, respectively, suggests that the rate-determining step is the monomolecular transformation of $RCOCH_2I$ leading to a species which exchanges iodine rapidly with molecular iodine.

(R stands for

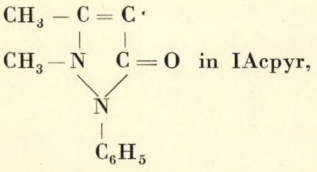

in IAcpyr,

$CH_3\cdot$ in IA, and $HO\cdot$ in IAcOH).

Table IV

t, °C	$\lvert \mathrm{IAcpyr} \rvert \cdot 10^3$ / M	$\lvert \mathrm{I_2} \rvert \cdot 10^3$ / M	$v \cdot 10^8$ / $M \cdot \mathrm{sec}^{-1}$	$k_0 \cdot 10^5$ / sec^{-1}	$\bar{k}_0$ / sec^{-1}
	2.00	1.00	1.14	0.57	
10.0	3.00	1.00	1.85	0.62	$0.60 \cdot 10^{-5}$
	4.00	1.00	2.44	0.61	$\pm 0.02 \cdot 10^{-5}$
	5.00	1.00	3.07	0.61	
	0.50	0.10	2.75	5.58	
	0.50	0.10	2.47	4.94	
	0.50	0.50	1.33	2.57	
	1.00	0.05	3.51	3.51	
	1.00	0.07	3.55	3.55	
	1.00	0.10	3.46	3.46	
	1.00	0.20	3.69	3.69	
	1.00	0.40	2.07	2.07	
	1.00	0.50	3.33	3.33	$3.24 \cdot 10^{-5}$
20.0	1.00	1.00	3.35	3.35	$\pm 0.84 \cdot 10^{-5}$
	1.00	3.00	3.21	3.21	
	1.00	5.00	3.49	3.49	
	2.00	0.10	6.56	3.28	
	2.00	0.50	5.52	2.76	
	3.00	0.10	10.30	3.43	
	3.00	0.30	7.44	2.48	
	3.00	1.00	7.22	2.42	
	3.00	5.00	6.87	2.15	
	4.00	1.00	9.06	2.27	
	5.00	0.10	18.50	3.70	
	5.00	1.00	13.80	2.78	
	5.00	5.00	16.00	3.20	
	0.50	0.10	3.76	7.53	
	1.00	0.10	8.02	8.02	
	1.00	0.50	8.55	8.55	
	1.00	1.00	7.70	7.70	
	1.00	5.00	7.20	7.20	
	1.00	10.00	8.46	8.46	$7.47 \cdot 10^{-5}$
30.0	2.00	0.50	14.80	7.40	$\pm 0.67 \cdot 10^{-5}$
	2.00	1.00	14.10	7.05	
	3.00	1.00	20.10	6.70	
	4.00	1.00	28.00	7.04	
	5.00	1.00	32.40	6.50	

Table V

t °C	$\lvert IA \rvert \cdot 10^3$ M	$\lvert I_2 \rvert \cdot 10^3$ M	$v \cdot 10^9$ $M \cdot sec^{-1}$	$k_0 \cdot 10^6$ sec^{-1}	$\bar{k}_0$ sec^{-1}
	10.0	1.0	9.72	0.97	
	10.0	7.0	8.90	0.89	
	10.0	3.0	10.20	1.00	
30.0	10.0	5.0	8.67	0.87	$1.05 \cdot 10^{-6}$
	4.0	4.0	4.75	1.19	$\pm 0.18 \cdot 10^{-6}$
	7.0	4.0	7.99	1.14	
	3.0	4.0	3.82	1.27	
	5.0	5.0	29.4	5.89	
	5.0	4.0	27.7	5.54	
	5.0	6.0	29.5	5.90	
	2.0	4.0	7.7	3.85	$4.37 \cdot 10^{-6}$
	3.0	4.0	11.7	3.89	$\pm 0.94 \cdot 10^{-6}$
	4.0	4.0	16.6	4.14	
45.0	7.0	4.0	28.8	4.11	
	1.0	1.0	3.6	3.60	
	1.0	3.0	5.5	5.50	
	10.0	1.0	39.3	3.93	
	10.0	3.0	32.8	3.28	
	10.0	5.0	35.1	3.51	
	10.0	7.0	37.9	3.79	
	10.0	1.0	124.2	12.42	
	10.0	3.0	90.2	9.02	$13.13 \cdot 10^{-6}$
	10.0	5.0	120.3	12.03	$\pm 1.03 \cdot 10^{-6}$
58.0	10.0	7.0	149.7	14.97	
	2.0	4.0	30.8	15.40	
	3.0	4.0	44.2	14.74	
	4.0	4.0	51.3	12.83	
	7.0	4.0	95.8	13.69	

Table VI

t, °C	$\lvert IAcOH \rvert$ / M $\cdot 10^4$	$\lvert I_2 \rvert$ / M $\cdot 10^4$	$v \cdot 10^9$ $M \cdot sec^{-1}$	$k_0 \cdot 10^6$ sec^{-1}	$\bar{k}_0$ sec^{-1}
	5.0	10.0	2.38	4.77	
	7.0	10.0	3.15	4.52	
	8.0	10.0	4.40	5.50	
	10.0	5.0	1.85	1.85	
	10.0	7.0	2.70	2.70	$3.16 \cdot 10^{-6}$
35.0	10.0	8.0	4.53	4.53	$\pm 1.38 \cdot 10^{-6}$
	10.0	10.0	2.20	2.20	
	10.0	10.0	2.73	2.73	
	10.0	20.0	1.97	1.97	
	10.0	30.0	2.02	2.02	
	10.0	40.0	1.97	1.97	
	5.0	10.0	2.58	5.17	
	5.0	30.0	2.88	5.97	
	7.0	10.0	3.22	4.65	
	7.0	10.0	3.57	5.08	
	8.0	10.0	4.52	5.65	
	10.0	5.0	5.47	5.47	
	10.0	5.0	7.77	7.77	
	10.0	7.0	6.87	6.87	
	10.0	8.0	7.62	7.62	$6.38 \cdot 10^{-6}$
45.0	10.0	10.0	5.73	5.73	$\pm 1.56 \cdot 10^{-6}$
	10.0	10.0	5.70	5.70	
	10.0	30.0	9.14	9.14	
	10.0	30.0	8.28	8.28	
	10.0	30.0	4.90	4.90	
	10.0	40.0	8.44	8.44	
	10.0	50.0	4.35	4.35	
	20.0	5.0	11.15	5.57	
	20.0	10.0	11.58	5.78	
	20.0	30.0	17.94	9.32	
	5.0	10.0	11.39	22.77	
	7.0	10.0	12.73	18.19	
	10.0	3.0	24.60	24.60	
	10.0	5.0	22.70	22.70	
60.0	10.0	10.0	13.47	13.47	$17.67 \cdot 10^{-6}$
	10.0	30.0	19.37	19.37	$\pm 4.96 \cdot 10^{-6}$
	10.0	50.0	12.25	12.25	
	20.0	30.0	24.35	12.17	
	20.0	40.0	27.06	13.52	

Table VII

	E_a kcal · mole^{-1}	lg A	$\Delta S^{\ddagger}$ e.u.
IAcpyr	21.2	11.35	— 9
IA	17.8	6.79	—28
IAcOH	13.9	6.14	—31

This reaction might be:

a) homolytic dissociation

$$RCOCH_2I \rightarrow RCOCH_2^{\cdot} + I^{\cdot},$$

b) heterolytic dissociation

$$RCOCH_2I \rightarrow RCOCH_2^{+} + I^{-} \text{ or } RCOCH_2^{-} + I^{+},$$

c) ion-pair formation

$$RCOCH_2I \rightarrow RCOCH_2^{+}I^{-} \text{ or } RCOCH_2^{-}I^{+},$$

d) formation of an excited molecule

$$RCOCH_2I \rightarrow RCOCH_2I_{exc.}$$

or *e)* intramolecular transformation

$$RCOCH_2I \rightarrow RC(OI)=CH_2.$$

If $I^{\cdot}$, I^{-}, I^{+}, $RCOCH_2^{-}I^{+}$, $RCOCH_2^{+}I^{-}$, $RCOCH_2I_{exc.}$ or $RC(OI)=CH^2$ exchange rapidly with iodine, the exchange reaction is described by a first order rate equation.

By inspecting the reactions one by one, the following conclusions can be drawn:

a) The homolytic dissociation might be followed by recombination reactions

$$I^{\cdot} + I^{\cdot} \rightarrow I_2$$
$$RCOCH_2^{\cdot} + {\cdot}CH_2COR \rightarrow RCOCH_2CH_2COR$$

which result in the deiodination of $RCOCH_2I$. We have experimental proof for the non-existence of such processes. Further the measured activation energies are low (between 13.9 and 21.0 kcal · mole^{-1}) to regard the homolytic dissociation as the main rate-determining step.

It is obvious from Table III that the rate of exchange decreases in the presence of oxygen. The rate-decreasing effect of oxygen is independent of the

iodine concentration and is the greater the higher is the IAcOH concentration. These findings might be compared with those of GAZITH and NOYES [7] with the benzyl iodide–iodine systems. They studied the iodine exchange by the exclusion of light between 60 and 90 °C in hexachlorobutadiene-1,3. In deaerated solvent their results could be fitted to the rate law:

$$v = k \mid \mathrm{RI} \mid \mid \mathrm{I_2} \mid^{1/2}$$

In the presence of oxygen the rate equation was different:

$$v = k' \mid \mathrm{RI} \mid^{1/2} \mid \mathrm{I_2} \mid$$

GAZITH and NOYES concluded that the oxygen inhibition depended on the $\mid \mathrm{RI} \mid / \mid \mathrm{I_2} \mid$ ratio, and was the greater, the greater was the quotient. Oxygen reacts with the benzyl radical and decreases the rate of the exchange reaction. In the rate equation describing the iodine exchange between benzyl iodide and iodine, there is iodine dependence, and thus it is obvious that the oxygen inhibition depends on the $\mid \mathrm{RI} \mid / \mid \mathrm{I_2} \mid$ ratio. In the case of the IAcOH–I_2 system the rate of iodine exchange is independent of the iodine concentration, and thus it is understandable that the v_{N_2}/v_{O_2} ratio depends only on the IAcOH concentration. This finding suggests that the homolytic dissociation of IAcOH cannot be completely excluded as a rate-determining step.

b) The heterolytic dissociation can be completely neglected, again because of the low activation energies, further of the low dielectric constant of the medium (D = 2.28), and because the rate of exchange is not affected by the water content of the solvent (see Table II).

c) The possibility of ion-pair formation depends on the nature of the group attached to the $—COCH_2I$ group. The k_0 values ($k_0 \cdot 10^5 \cdot \mathrm{sec}^{-1}$ at 30 °C) are the following:

IAcOH	IA	IAcpyr
0.215	0.107	7.50

These figures show that there is no correlation between the electron-distribution influence of the attaching group and the rate constant. (Both the OH-group and the pyrazolone-ring have electron-withdrawing character, the CH_3-group, however, is an electron-releasing one.) For this reason the ion-pair formation can be excluded as the rate determining step in the exchange.

d) The experimental results make the exchange through an excited $RCOCH_2I$ highly possible. Such mechanism has been suggested by ANBAR and REIN [8] for the iodine exchange between *o*-iodoanisole and iodine in 1-butanol. The results could be fitted to the rate law $v = k_0 \mid \mathrm{RI} \mid$. On the

basis of the values of activation parameters, effect of both the solvent and the additives, they concluded that the rate-determining step of the exchange is the formation of a low-level electronically excited molecule.

We are on the opinion that the same is valid for our systems, $RCOCH_2I$–I_2. If the interaction between $RCOCH_2I$ and the solvent is weak, the activation energy requirement of $RCOCH_2I \rightarrow RCOCH_2I_{exc.}$ is low, and the activation entropy will be a highly negative value, indicating the low probability of the above transformation. In dichloroetane — where the solvent–solute interaction is weak — the following activation parameter figures correspond to k_0:

RI	E_a kcal · mole^{-1}	$\Delta S^{\ddagger}$ e.u.
IAcpyr	9.2	—51 [9]
p-ClC_6H_4COI	7.7	—55.6 [10]
p-$NO_2C_6H_4COI$	9.9	—57.4 [10]

In a solvent (*e.g.* benzene) where the solvent–solute interaction is stronger the non-excited molecule is stabilized in relation to the excited one, followed by an increase both in its activation energy and entropy. (*E.g.* the activation parameters of the IAcpyr—I_2 exchange are the following: $E_a = 21.1$ kcal · mole^{-1}, $\Delta S^{\ddagger} = -9$ e.u.). If $RCOCH_2I$ is more strongly solvated, the activation energy of the formation of $RCOCH_2I_{exc.}$ increases further, the solvent may polarize the carbon–iodine bond, and a new mechanism (S_N2) emerges. The iodine exchange between IAcpyr and I^--ion in ethanol follows the above mentioned mechanism [6]. The same behaviour has been observed by MAY and DAUDEL [11] in the exchange reactions of iodide ion with *o*- and *p*-iodonitrobenzene, and *p*-iodophenol, respectively. In octanol the reaction follows a first-order, in acetonitrile, however, a second-order rate law.

e) The intramolecular transformation of $RCOCH_2I$ to $RC(OI)=CH_2$ as a rate-determining step is highly improbable especially in an organic solvent. We have no chemical evidence at all for the existence of the latter species.

As a conclusion it can be drawn that the non-dissociative conversion of $RCOCH_2I$ into $RCOCH_{2exc.}$ seems to be the most probable one as a rate-determining step

$$RCOCH_2I \rightarrow RCOCH_2I_{exc.}$$

which is followed by a rapid exchange reaction

$$RCOCH_2I_{exc.} + II^* \rightarrow RCOCH_2I^* + I_2$$

Since light and oxygen have some, though not significant, influence on the rate, the following route should also be taken into account to some extent:

$$RCOCH_2I \rightarrow RCOCH_2^{\cdot} + I^{\cdot} \quad \text{rate-determining step}$$

$$\left.\begin{aligned} I^{\cdot} + II^{*} &\rightarrow {\cdot}I^{*} + I_2 \\ {\cdot}I^{*} + RCOCH_2^{\cdot} &\rightarrow RCOCH_2I^{*} \end{aligned}\right\} \text{rapid}$$

Unfortunately, $RCOCH_2I_{exc.}$ could not be identified by a chemical or physical method, nevertheless this seems to be the only straightforward interpretation of the experimental findings.

REFERENCES

1. KŐRÖS, E., ORBÁN, M.: Radiochem. Radioanal. Letters, **1**, 87 (1969)
2. KŐRÖS, E., ORBÁN, M., FÜSSY, E.: Radiochem. Radioanal. Letters, **1**, 203 (1969)
3. KŐRÖS, E., ORBÁN, M., BURGER, M.: Radiochem. Radioanal. Letters, **4**, 165 (1970)
4. BENARY, E: Ber., **66**, 924 (1933)
5. EMMERLING, O.: Chem. Ber., **29**, 1558 (1896)
6. KŐRÖS, E., ORBÁN, M., BEDŐ, Zs.: Radiochem. Radioanal. Letters, **1**, 93 (1969)
7. GAZITH, M., NOYES, R. M.: J. Am. Chem. Soc., **77**, 6091 (1955)
8. ANBAR, M., REIN R.: J. Chem. Soc., **1964**, 975
9. KŐRÖS, E.. ORBÁN, M., BURGER, M., VÖRÖS, K.: Magy. Kém. Foly., **75**, 499 (1969)
0. HAMILTON, D. W., NOYES, R. M.: J. Am. Chem. Soc., **91**, 1740 (1969)
1. MAY, S., DAUDEL, R.: J. Chim. Phys., **53**, 274 (1956)

Endre KŐRÖS
Miklós ORBÁN
Mária BURGER
Klára VÖRÖS
Éva FÜSSY
Budapest VIII., Múzeum krt. 4/b.

Acta Chimica Academiae Scientiarum Hungaricae, Tomus 74 (4), pp. 399—403 (1972)

STUDY OF METAL EXCHANGE IN SOME π-BONDED COMPLEXES, II

B. R. PANCHAL and P. K. BHATTACHARYA

(Chemistry Department. M. S. University of Baroda, Baroda-2)

Received June 17, 1971
In revised form January 10, 1972

Formation constants of thioglycolic and thiolactic acid chelates of Be(II), Zn(II) and Cd(II) have been determined by the IRVING–ROSSOTTI method using least square calculations wherever possible. The values have been interpreted in terms of M–S π-interaction. The displacement of Zn(II) from the chelates by Cd(II), Hg(II) and Ag(I) has been explained by the stronger class *B* character of the latter metal ions than that of Zn(II).

Thioglycolic and thiolactic acids are known to form complexes with a number of metal ions [1–6]. Transition metal complexes of these ligands are especially interesting because of the possibility of π-interaction in the M–S bond as shown by earlier workers [7–12] and also in our previous studies [13–15]. In a recent communication from our laboratory, metal exchange in thiomalate complexes has been studied [16]. Literature data also reveal cases of the replacement of weaker acceptor metal ions by stronger ones [17–18]. In the present study, formation constants of Be^{2+}, Zn^{2+} and Cd^{2+} complexes with thioglycolic acid and thiolactic acid have been determined. Solids have been isolated by the replacement of Zn(II) by Cd(II), Hg(II) and Ag(I) in the chelates.

Experimental

The stepwise formation constants were determined by the IRVING–ROSSOTTI method [19]. The solutions containing perchloric acid, perchloric acid + ligand, perchloric acid + ligand + metal ion in a constant volume (50 ml) and at constant ionic strength (0.2 *M*) adjusted with $NaClO_4$, were titrated against standard alkali at 35 °C. The values of $\bar{n}_H$, $\bar{n}$ and *p*L were calculated from the equation given in Ref. [13]. The protonation constants were determined by the following relationship:

$$\log {}^{P}K_{n}^{H} = B + \log \bar{n}_H/(1 - \bar{n}_H)$$

where B = pH under the experimental conditions.

For the calculation of ${}^{P}K_{1}^{H}$, the points were chosen in the region where $0 < \bar{n}_H < 1$ and for ${}^{P}K_{2}^{H}$ in the region where $1 < \bar{n}_H < 2$. In the two different regions, the pH was plotted against $\log \bar{n}_H/(1 - \bar{n}_H)$ and straight lines were obtained. The average values of the protonation constants (35 °C) are

Ligand	$P_{K_1^H}$	$P_{K_2^H}$
Thioglycolic acid	9.922×10^9	2.352×10^3
Thiolactic acid	1.881×10^{10}	2.644×10^3

$\bar{n}$ and pL were calculated (at 35 °C) using known equations [13]. The formation curves obtained by the plot of $\bar{n}$ and pL are shown in Fig. 1. In cases where $\bar{n}$ exceeded 1, least squares calculations [20] were used to determine the formation constants, K_1 and K_2. In other cases, average values were obtained from the plot of pL *vs.* $\log (1 - \bar{n})/\bar{n}$ at different points. The $\log K_2$ of the thioglycolato cadmium(II) complex cannot be calculated because precipitation occurs at low pH before $\bar{n} = 0.8$.

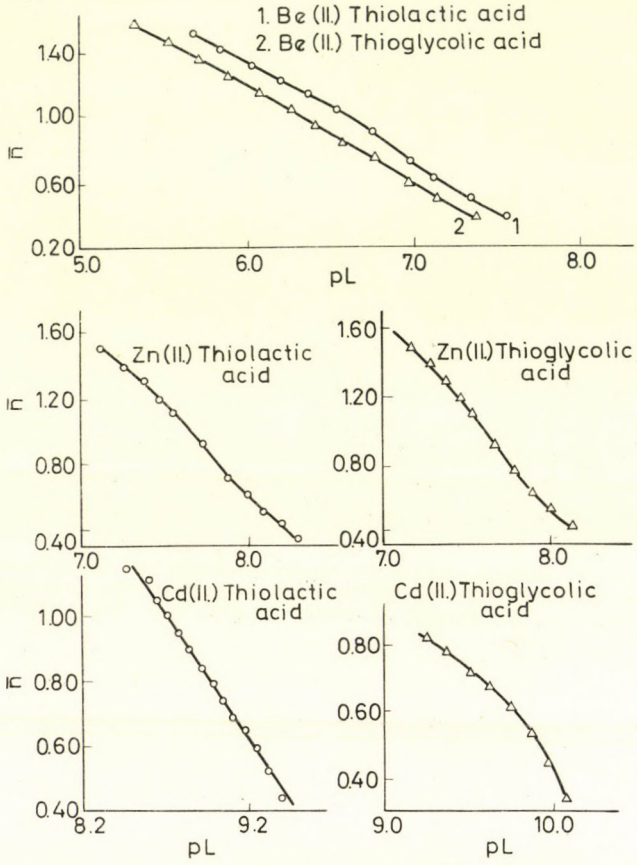

Fig. 1

Table I

Complex	$\log K_1$	$\log K_2$
Thioglycolato-beryllium(II)	7.10 ± 0.05	5.47 ± 0.05
Thiolactato beryllium(II)	7.25 ± 0.05	5.73 ± 0.05
Thioglycolato zinc(II)	7.76 ± 0.06	7.43 ± 0.06
Thiolactato zinc(II)	7.93 ± 0.06	7.32 ± 0.06
Thioglycolato cadmium(II)	9.92 ± 0.02	—
Thiolactato cadmium(II)	9.23 ± 0.02	8.08 ± 0.05

Since the Hg^{2+} and Ag^{+} complexes are formed at very low pH, their formation constants were not determined.

Preparation of thioglycolato or thiolactato complex of zinc

Zinc carbonate (1 g) was refluxed with thioglycolic or thiolactic acid (10 ml, 0.25 *M*) for about an hour. Addition of zinc carbonate was continued until an excess of it was left unreacted, indicating that the whole amount of the ligand had been consumed. The solutions were filtered. To the filtrate, alcohol (20 ml, 98%) was added to precipitate the thioglycolato or thiolactato complexes of zinc. The solids were dried in vacuum and analyzed. The analysis corresponds to a zinc to ligand ratio of 1 : 1 in both cases as shown in Table II.

Preparation of thioglycolato or thiolactato complexes of cadmium, mercury and silver from the corresponding zinc complexes

Freshly prepared thioglycolato or thiolactato complexes of zinc (1 g) were dissolved in water (30 ml). To these solutions were added the solutions of cadmium nitrate, mercuric chloride or silver nitrate (10 ml of 0.25 *M* solutions). White precipitates were obtained in the case of cadmium and mercury, and a yellow precipitate in the case of silver. They were washed with water, dried and analyzed. The results of analysis correspond to a 1 : 1 ratio of cadmium or mercury and the ligands, and to a 2 : 1 ratio of silver and the ligands, as shown in Table II.

Table II

Complex	Percentage of metal ion	
	calculated	found
Thioglycolato complexes		
$Zn[Zn(TGA)_2]\ 2H_2O$	37.66	37.16
$Cd[Cd(TGA)_2]$	55.50	54.74
$Hg[Hg(TGA)_2]$	69.00	68.52
$Ag_3[Ag(TGA)_2]$ or $Ag[Ag(TGA)]$	70.50	69.83
Thiolactato complexes		
$Zn[Zn(TLA)_2]\ 2H_2O$	34.85	34.82
$Cd[Cd(TLA)_2]$	51.90	51.57
$Hg[Hg(TLA)_2]$	65.82	65.21
$Ag_3[Ag(TLA)_2]$ or $Ag[Ag(TLA)]$	67.42	67.22

Discussion

The values of formation constants indicate that the stability order of the complexes is $Cd^{2+} > Zn^{2+} > Be^{2+}$. Since the ligands are the same, the differences in the formation constants must be attributed to the nature of the

metal ions. Beryllium, though of class *A* type [21], forms sufficiently stable complexes with the thioacids. This is because Be^{2+} has a small size and hence a stable L → M σ-bond is formed. With increasing size of the metal ion, the L → M σ-bond becomes weaker, resulting in lower values of the formation constants. However, in case of class *B* type metals [21] with filled $d\pi$ orbitals, there is an additional tendency of the metal ion to donate π-electrons to the vacant $d\pi$-orbital of sulfur. In the case of metals of the same group, other factors being similar, π-interaction is stronger with larger metal ions. It can be argued, therefore, that there is more π-interaction in the Cd—S bond than in Zn—S bond and hence cadmium complexes are more stable than zinc complexes. Mercury, with a still larger size, should have a greater tendency to donate electrons back to sulfur, resulting in a stronger M → S π-bond. Silver with its single positive charge is less electronegative and hence should also have a greater tendency to form M → L π-bonding than Cd^{2+} of almost the same size [22].

Though the concept of π-interaction explains the results satisfactorily and has now support from various accurate studies [9], the alternative explanation in terms of polarization [23] resulting in an increased strength of the M ← S σ-bond cannot be ruled out. In the case of beryllium complexes K_1/K_2 is greater and may be due to the smaller size of the metal ion, which hinders the entry of the second ligand. However, in the case of Zn^{2+} and Cd^{2+} complexes, the K_1 and K_2 values differ but slightly. The ratio K_{ML_1}/K_{ML_2} is expected to be large [24] if the π-character of the M → L bond is substantial. This points to the fact that the contribution of the M → S π-interaction is not large. Similar conclusions have been reached by PETTIT and coworkers [25].

The compounds isolated in the case of Zn(II), Cd(II) and Hg(II) correspond to the composition ML. These compounds have the composition M_2L_2 with the structure $M[ML_2]$. The composition of the silver complex, Ag_2L, corresponds to the structure $Ag[AgL]$ or $Ag_3[AgL_2]$. The experimental data are not sufficient for unequivocal determination of the structure of the compound. However, the present study confirms the fact that Cd^{2+}, Hg^{2+} or Ag^+ may displace Zn(II) from its thioacid complexes. This shows that Cd^{2+}, Hg^{2+} and Ag^+ have stronger class B character and form stronger M—S bonds than those in zinc complexes. Upon the addition of salts of the above metals to zinc complexes, therefore, the weaker Zn—S bond breaks easily, resulting in the formation of a new M—S bond.

*

The authors thank Prof. S. M. SETHNA, Head, Chemistry Dept., M.S. University of Baroda, Baroda-2 for providing the necessary laboratory facilities. We also thank the University Grants Commission, New Delhi, for providing a Junior Research Fellowship to B.R.P. Our thanks are also due to the referee for helpful suggestions.

REFERENCES

1. Bear, J. L., Choppin, G. R., Quagliano, J. V.: J. Inorg. Nucl. Chem., **25,** 513 (1963)
2. Anand, V., Deshmukh, G. S., Pandey, C. M.: Anal. Chem., **33,** 1933 (1961)
3. Perrin, D. D., Sayce, I. G.: J. Chem. Soc., 82 (1967)
4. Cefola, M., Tompa, A. S., Celiano, A. V., Gentile, P. S.: Inorg. Chem. **1,** 290 (1962)
5. Grenthe, I.: Acta Chem. Scand., **16,** 1695 (1962)
6. Buscarans, F., Casassas, E.: Anales real soc. españ. fis. y quim., **55B,** 655 (1960)
7. Harrison, S. E., Assow, J. M.: J. Chem. Phys., **40,** 465 (1964)
8. Livingstone, S. E.: Quart. Rev., **19,** 386 (1965)
9. Gerlach, D. H., Holm, R. H.: J. Amer. Chem. Soc., **91,** 3457 (1969)
10. Pettit, L. D.: Quart. Rev., **1,** 1 (1971)
11. Rickards, R., Johnson, C. E.: J. Chem. Soc., **799** (1971)
12. Bonamico, M., Dessy, G.: J. Chem. Soc., 264 (1971)
13. Reddy, M. V., Bhattacharya, P. K.: Indian J. Chem. **7,** 282 (1969)
14. Reddy, M. V., Bhattacharya, P. K.: J. Prakt. Chem., **312,** 69 (1970)
15. Reddy, M. V., Bhattacharya, P. K.: J. Inorg. Nucl. Chem. **32,** 2321 (1970)
16. Panchal, B. R., Reddy, M. V., Bhattacharya, P. K.: Indian J. Chem., **10,** 218 (1972)
17. Barnes, J. W., Dorough, G. D.: J. Amer. Chem. Soc., **72,** 4045 (1950)
18. Plumb, R. C., Martell, A. E., Barsworth, F. C.: J. Phys. and Colloid Chem., **54,** 1208 (1950)
19. Irving, H. M., Rossotti, H. S.: J. Chem. Soc., 2904 (1954)
20. Irving, H. M., Rossotti, H. S.: J. Chem. Soc., 3397 (1953)
21. Ahrland, S., Chatt, J., Davies, N. R.: Quart. Rev., **12,** 265 (1958)
22. Ahrland, S., Chatt, J., Davies, N. R., Williams, A. A.: J. Chem. Soc., 264, 1403 (1958)
23. Jørgensen, C. K.: Structure and Bonding, **3,** 106 (1967)
24. Ahrland, S., Chatt, J., Davies, N., Williams, A.: J. Chem. Soc., 276 (1958)
25. Pettit, L. D., Sherrington, C.: Progress in coordination chemistry (11th International Conference on Coordination Chemistry) Edited by C. Michael, p. 542. Elsevier Publishing Co., 1968.

B. R. Panchal
P. K. Bhattacharya
M. S. University of Baroda, Baroda–2, India.

Acta Chimica Academiae Scientiarum Hungaricae, Tomus 74 (4), pp. 405—415 (1972)

OXIDATION ON THE NICKEL HYDROXIDE ELECTRODE, VI

MECHANISM OF THE OXIDATION OF PRIMARY ALCOHOLS

G. VÉRTES and F. NAGY

(Central Research Institute for Chemistry, Hungarian Academy of Sciences, Budapest)

Received May 21, 1971

The oxidation process of primary alcohols on the nickel hydroxide electrode has been studied in order to settle the question whether the rate-determining step of the reaction is ionic or radical.

The possible processes have been selected on the basis of a method used in the study of hydrogenation. Since the reaction rate is independent of the electrode potential, it is certain that the rate-determining step of the oxidation is a radical process. The analysis of kinetic data led to the conclusion that this step should occur at the dehydrogenation of alcohol to aldehyde, more specifically at the removal of one of the hydrogen atoms.

Taking into account that identical reaction rates were observed in solutions of different hydroxide ion concentrations, as well as considering the inductive effects widely used in the discussions of organic reaction mechanisms and the analogous features between the structures of possible intermediates and those of certain stable free radicals, it seems probable that the first, rate-determining step of the oxidation reaction is the homolytic splitting of an α-C–H bond followed by the removal of a proton and an electron.

Previous communications [1] reporting our investigations on the oxidation reactions of primary alcohols on the nickel hydroxide electrode deal with the rate of the oxidation process by studying its dependence on the type and concentration of the alcohol and on the amount of charge accumulated previously on the electrode. Between these parameters, the following relation has been found:

$$w = k_0 c_a Q \tag{1}$$

where w denotes the rate of the oxidation reaction, k_0 — a rate constant varying with the type of alcohol, c_a — the concentration of the alcohol in the solution, and finally Q is the charge equivalent to the excess oxygen content relative to the amount corresponding to the $Ni(OH)_2$ composition of the electrode (active oxygen).

The mechanism of the oxidation, however, has not been discussed so far. In the investigation of the mechanism the first step is to settle whether the rate-determining step is of ionic or radical character.

Similarly to the method used in studies on the mechanism of hydrogenation reactions [2], two possible reaction routes can be assumed for the oxidation of a compound S:

(A)

$$O^* + H_2O + 2e^- \rightarrow 2OH^- \quad (a)$$

$$S \rightarrow S^{n+} + ne^- \quad (b)$$

$$S^{n+} + n\,OH^- \rightarrow Pr + n/2\,H_2O \quad (c)$$

(B)

$$S + O^* \rightarrow Pr \quad (\alpha)$$

$$(O^* + H_2O + 2e^- \rightarrow 2OH^-)$$

where O* corresponds to the active oxygen content, S^{n+} denotes the electrochemically oxidized substrate, Pr denotes the oxidized product, and n denotes the number of electrons required for the oxidation reaction. Reaction scheme (A) corresponds to the ionic, whereas scheme (B) to the atomic mechanism. It is to be noted that in the case of the radical mechanism an electrochemical reaction takes place simultaneously with the oxidation, which, on one hand, changes the amount of 'oxidizing agent' and, on the other hand, affects the electrode potential, so it cannot be neglected in this case either.

The comparison of kinetic equations derived on the basis of assuming different rate-determining steps with Eq. (1) determined experimentally appears to be helpful in the deeper understanding of the reaction mechanism.

Ionic rate-determining step

Let us first investigate the kinetic relations that should hold if the rate-determining step of the oxidation reaction is an ionic process (case A). It can be seen that the third step, (c), a reaction in solution between ions of opposite charges, cannot be rate-determining. By eliminating this possibility, only processes (a) and (b) need further discussion.

Provided that the rate-determining step is the reduction of the active oxygen of the nickel hydroxide electrode, the reaction rate should depend on the active oxygen content, the pH of the solution, and on the electrode potential. According to Eq. (1), however, the rate of the overall process is proportional to the alcohol concentration of the solution. This experimental fact, in the case of an ionic mechanism, can be accounted for only if step (b) is rate-determining. With this assumption the reaction rate can be expressed by the following equation

$$w = a\,c_a \exp(bE) \quad (2)$$

where a and b are constants and E denotes the electrode potential.

According to experimental data, the reaction rate is, indeed, proportional to the concentration of the primary alcohol. A contradiction will arise, how-

ever, if one attempts to express the potential dependence of the reaction rate by Eq. (2). In this case two problems may occur.

The first problem is that Eq. (2) gives an exact relation between the reaction rate and the electrode potential. As was shown, however, in Part IV [1] of this series, no unequivocal relation can be found between these parameters, *i.e.* the same reaction rate may correspond to different electrode potential values. This contradiction can, perhaps, be resolved by taking into account that the oxidation of alcohols takes place at the entire surface of the nickel hydroxide grains in contact with the electrolyte, whereas the electrode potential is determined by processes taking place along the surface where the grains, electrolyte and the conductor are contacted. If the degree of oxidation and the physical structure of the latter do not agree with the average of the reaction zone, the same reaction rate value may be observed in two different experiments, because the 'electrode potentials of the reaction zone' happen to be the same, although the measured electrode potentials are different.

The second problem arises from the comparison of Eq. (1) obtained experimentally with theoretical equation (2). It has been observed that the entire discharge process, from $Q = Q_0$ to $Q = 0$, obeys Eq. (1). Simultaneously with the change in Q the potential also changes monotonously: it shifts into the negative direction by about 100 mV. Accordingly, this equation is valid also while the potential is changing. This leads to the conclusion that since constant k_0 of Eq. (1) is independent of the potential (as well as, obviously, c_a), the potential dependence of Q should correspond to Eq. (2). For kinetic and thermodynamic reasons [1, 3], the electrode potential is not characteristic of the amount of nickel(III)oxide hydroxide deposited on the electrode, so the potential dependence may not, by any means, correspond to Eq. (2). Consequently, the assumption that the rate-determining step is the oxidation electrode process of the substrate, should be discarded.

Thus, it may be concluded that the rate-determining step in the oxidation of primary alcohols on the nickel hydroxide electrode cannot be an ionic process, *i.e.* a process involving charge transfer.

Radical rate-determining step

If a radical mechanism is assumed, the rate of reaction (B) should depend on the concentration of the substrate, on the active oxygen content, and on the amount of charge on the electrode. Consequently, Eq. (1), found experimentally, can be interpreted on the basis of a radical mechanism. The potential independence of the reaction rate can also be accounted for, since in the case of radical rate-controlling steps the electrode process determining the potential takes place simultaneously with the former, and so the potential has no direct role in the chemical reaction.

Accordingly, it can be concluded that the rate-determining step in the oxidation of primary alcohols on the nickel hydroxide electrode is a radical process.

The oxidation, consequently, can only take place according to a radical process given by the following equation:

$$S + n\,O^* \rightarrow Pr \qquad (\alpha)$$

As is known from our previous studies, the oxidation of primary alcohols on the nickel hydroxide electrode yields carboxylic acids according to the following equation:

$$R{-}CH_2{-}OH + 4\,NiOOH + OH^- \rightarrow R{-}COO^- + 4\,Ni(OH)_2$$

It may not be assumed that this process, requiring the transfer of four electrons, takes place in one step. Accordingly, the only conclusion from the fact that the rate-determining step is reaction (α) is that at least one step of the overall reaction should be of radical mechanism. Hence, on the basis of the available evidence the ionic or radical character of the remaining steps cannot be established.

As far as the role of nickel hydroxide is concerned, it has been assumed on the basis of published data that in 1 *N* NaOH solution, used in the experiments, the composition of the charged nickel hydroxide electrode is NiOOH, whereas that of the discharged electrode is $Ni(OH)_2$. These substances transform into each other via the following radical reaction:

$$NiOOH + H_2O \rightarrow Ni(OH)_2 + OH\cdot \qquad (\alpha_1)$$

It should be noted that chemical studies of the nickel hydroxide electrode [4] and deuterium exchange investigations [5] have led to the conclusion that the reduction of NiOOH takes place via the gain of a hydrogen ion and an electron, and not by the abstraction of oxygen. Reaction (α_1) refers to the radical version of this process. The rate of this reaction, however, is rather low, definitely lower than the rates investigated in our experiments, since otherwise this reaction would also take place in the pure background solution, which would lead to the reduction of the amount of active oxygen.

If, despite the above fact, the reduction of NiOOH is observed, namely in a radical reaction step, the hydrogen atom can only arise from the alcohol molecule according to the following reaction:

$$NiOOH + R{-}H \rightarrow Ni(OH)_2 + R\cdot \qquad (\alpha_2)$$

The consequence of reaction (α_2) is that the oxidation, or at least its rate-determining step, involves the removal of a hydrogen atom. Essentially

similar conclusions have been reached on the basis of different considerations, in a study of oxidation in non-aqueous solvents [6]. Investigations of PICKERING [7] on a series of oxide catalysts also confirm that the oxidation of alcohols takes place via dehydrogenation.

A further task is to find the steps involved in the following overall reaction:

$$R—CH_2OH + OH^- \rightarrow R—COO^- + 4H\cdot$$

The possibility of the formation of the most probable intermediate, aldehyde, had already been assumed in an earlier phase of the experiments. This possibility is also confirmed by the fact that NAKAGAWA *et al.* [8] succeeded in oxidizing primary alcohols to aldehydes by 'nickel peroxide'. (This substance is, in fact, nickel(II) hydroxide oxidized by sodium hypochlorite, and has an empirical composition of $NiO_{2.77}H_{2.85}$. As was mentioned in Part I of this series, the investigations of LABAT [9] indicate no reason to assume that nickel hydroxides would yield different substances if oxidized chemically or electrochemically; hence, by elementary algebraic calculation it is obtained that the above formula corresponds to the composition of 0.31 $Ni(OH)_2$ · 0.69 NiOOH · · 0.77 H_2O. The active oxygen content calculated from this composition is in good agreement with the experimental value of 3.5×10^{-3} g atom oxygen/g.) It was shown in our previous paper [10] that the oxidation rates of aldehydes on the nickel hydroxide electrode are higher by roughly three orders of magnitude than those of the corresponding alcohols. Provided that the reaction does proceed via an aldehyde, the rate-determining step should be searched for among the steps of the following reaction:

$$R—CH_2—OH \rightarrow R—CHO + 2H\cdot$$

Since this reaction hardly takes place in a single step (probably two steps are involved at least), equation

$$R—CH_2—OH + 2\ NiOOH \rightarrow R—CHO + 2\ Ni(OH)_2$$

is not necessarily identical with reaction (α).

Possible mechanisms of the oxidation

In relatively simple cases like the reaction discussed here the experimental fact that the reaction rate is, on the basis of Eq. (1), proportional to the alcohol concentration and to the amount of nickel(III) oxide hydroxide deposited on the electrode indicates that probably only one alcohol and one NiOOH molecule take part in the rate-determining step. As was shown above, in this step a hydrogen atom of the alcohol is removed, namely in a radical process, by the nickel hydroxide.

In the simplest case the alcohol–aldehyde reaction can take place in two ways. Either both hydrogen atoms are split off in radical processes, or one is removed in a radical and the other in an ionic process.

As far as nickel hydroxide is concerned, both ways are possible. The gain of a hydrogen atom in an ionic process is, in fact, equivalent to the electrochemical discharge of the charged nickel hydroxide electrode, *i.e.* the two processes take place in the same manner. The direct uptake of a hydrogen atom appears to be also possible, since, as mentioned earlier, NiOOH is a good hydrogen atom acceptor. This is also confirmed by several dehydrogenation experiments in non-aqueous solvents [6, 8, 11].

In the following considerations the most probable step is selected from the possible dehydrogenation steps of alcohols. In the process two hydrogens are removed from the alcohol molecule, involving the homolytic splitting of a C—H bond and that of an O—H bond. This process may take place, *e.g.* in the following order:

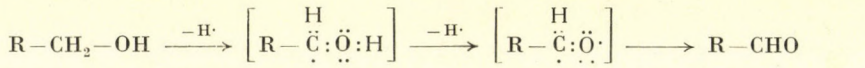

Scheme I

The radical scission of C—H bond can well be assumed; hydrogens on the α-carbon atom of alcohols can be particularly easily removed via radical mechanism. The following two examples are considered as a proof for this assumption: In the photo-oxidation process of primary alcohols in the presence of Ce(IV) ions a radical similar to the one formed in the first step of Scheme I could be detected by ESR methods [12]. In another study [13], an α deuterium substituted alcohol was reacted with methyl radicals (prepared *e.g.* from diacetyl peroxide), and CH_3D was obtained. On the other hand, no trace of such a reaction was found when reacting $(CH_3)_3C—OD$ with the same radical. This latter experiment indicates, at the same time, that the radical splitting of alcoholic O—H bonds is rather difficult. Just as the heterolytic splitting of C—H bonds appears to be hardly probable, it is more likely that, given the chance, the O—H bond of an alcoholic hydroxyl group undergoes oxidation in an ionic process; the possibility for heterolytic splitting is undoubtedly proved by the acid dissociation of alcohols. Consequently, in our opinion, the reaction route given by Scheme I is hardly probable, the homolytic splitting of the C—H bond is rather followed by the heterolytic splitting of the O—H bond by the nickel oxide hydroxide.

The ionic splitting of a bond involving hydrogen can be imagined as the removal of an electron and a proton from the molecule. Accordingly, the oxidation of alcohols to aldehydes takes place in three elementary steps: the removal of a hydrogen atom, of a proton and of an electron, respectively. By permuting these three steps, $3! = 6$ different mechanisms can be constructed,

from which the most probable one should be selected on the basis of experimental data and theoretical considerations.

a) Let us first examine the cases where the radical step comes first.

The first step given in Scheme I is still involved in these cases. The reality of this step has already been discussed. Now let us assume that the next step is the removal of an electron:

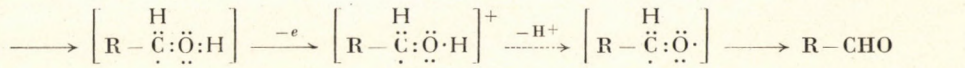

Scheme II

The radical formed *via* the abstraction of a hydrogen atom might, in principle, undergo electrochemical oxidation at the high positive potential of the nickel hydroxide electrode. The electron defect of this radical, however, exerts an electron attraction effect of some degree, and so the electron pair of the O—H bond shifts towards the oxygen atom. From this part of the molecule, due to its positive charge, a proton, having also a positive charge, can be abstracted with a higher probability.

Now let us turn to the reaction route given in Scheme III:

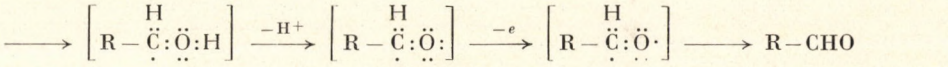

Scheme III

The reality of the second step has already been dealt with, so only the removal of the electron should be discussed here. In principle no problem occurs at the electrochemical oxidation of a negatively charged ion, even more so if the electron is removed from an oxygen atom having excess electrons.

Although it can be established at this point that the reaction can take place according to the mechanism given in Scheme III, it is worthwhile to discuss the remaining cases, too.

b) If it is assumed that the first step of the process is the removal of a proton, the reaction can no more be regarded as irreversible; first the reversible dissociation of the alcohol should be taken into account, and the abstraction of hydrogen or electron may only follow this first step.

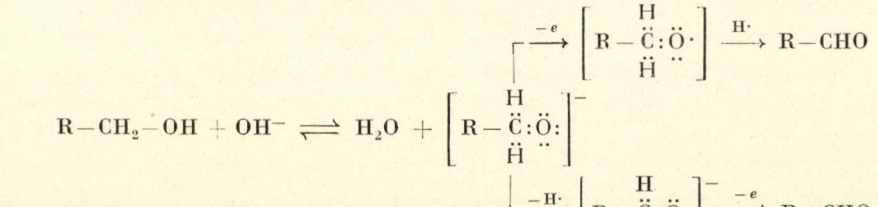

Scheme IV

Although the dissociation constant of alcohols is very low, the high hydroxide ion concentration of 1*N* NaOH solution shifts the equilibrium towards the formation of alcoholate ions. The anion formed in this equilibrium reaction may enter further reactions in the next step. Electrochemical oxidation may, presumably, take place easily since an ion of negative charge can readily lose electrons. The radical formed in the process, however, will be polarized due to the electron defect of the oxygen atom, *i.e.* the electrons of the C—O bond will be shifted towards the oxygen, whereas the electron pair of the C—H bond towards the carbon atom. Hence, the heterolytic splitting of C—H bonds becomes easier, and the homolytic splitting more difficult (relative to the unpolarized state). If, on the other hand, the alcoholate ion reacts in a way indicated by the lower arrow in Scheme IV, the above problem does not occur. The electron excess at the oxygen atom of the anion, contrary to the previous case, shifts the electron pair of the C—H bond, through the carbon atom, towards the hydrogen atom, promoting thereby the radical splitting. The radical ion formed in this process is stabilized, by the removal of an electron, at the relatively positive electrode potential of the nickel hydroxide electrode.

c) To complete the permutation of the processes, reactions starting with the removal of an electron may also be discussed. The electrochemical oxidation may, most certainly, take place at potentials exceeding the equilibrium potential by about 1000 mV. Problems occur, however, at the subsequent abstraction of hydrogen atom since, due to the electron defect, the electrons of C—H bonds are shifted towards the carbon atom, and this arrangement does not favour the homolytic decomposition.

Thus, as a first approximation, two reaction routes appear to be probable, namely those where the removal of the electron is the last step. These routes are given by Scheme III and by the lower part of Scheme IV. For deciding as to which of these possibilities is realized in the reaction, further considerations are needed.

One of the differences between the two possible mechanisms is the fact that in one of them the rate-determining step is preceded by an equilibrium process. If the first step is the radical removal of hydrogen, the next two steps, being practically irreversible, have no role, since it is only the radical step that determines the rate. In the other mechanism, however, the rate-determining process is proceeded by the dissociation of alcohol, so both processes should be taken into account. This difference may give the key to choosing between the possibilities since the shift of the dissociation equilibrium in any direction will affect the reaction rate only if the reaction takes place according to Scheme IV.

There are, in principle, two methods for shifting the dissociation equilibrium. If group R in primary alcohols of type R—CH_2—OH is varied, the

dissociability of the proton of the OH group will also change as a function of the electron attraction or repulsion properties of group R. Let us, however, consider the effect of an electron-withdrawing $\bar{R}$ group on the reaction rate. In this case the electron density on the α-carbon atom is reduced to a certain degree. As a result, the acid dissociation of the alcohol becomes easier, tending to increase the rate of a reaction according to Scheme IV with respect to the oxidation rate of the alcohol having a 'neutral' R group. An electron-withdrawing group, however, influences the reaction at other points, too. The reduction of electron density at the α-carbon atom renders the homolytic splitting of the C—H bond inevitably more difficult in the molecule, or rather in the one formed from the molecule in the dissociation process. Since the rate-determining step of the reaction represented by Scheme IV is just this process, the change of R for $\bar{R}$ would, at this point, presumably tend to decrease the reaction rate.

It could be proved by similar considerations that the situation would be no better if electron repelling groups were applied. The electron defect or excess on the α-carbon influences both the C—H and the O—H bonds, polarizing both of them in the same sense, *i.e.* shifting the electron pair of the bonds simultaneously nearer to or farther from the hydrogen. Since the homolytic splitting of a C—H bond would require a polarization opposite to that needed for the heterolytic splitting of the O—H bond, the same polarization of both bonds, obviously, promotes only one of the steps, hindering at the same time the other. To predict whether the reaction rate increases or decreases as the net result of these opposite tendencies is a task one can hardly undertake on the basis of qualitative considerations.

Another feasible method for shifting the equilibrium is the variation of hydroxide ion concentration. Should the reaction take place according to Scheme IV, the reaction rate will be proportional to the hydroxide ion concentration, since the steady-state concentration of the component taking part in the rate-determining step is, in the case of a fast pre-equilibrium, proportional to the hydroxide ion concentration. On the other hand, the rate of the reaction given by Scheme III is independent of the hydroxide ion concentration, since it is not involved in the rate-determining step, participating only in the subsequent fast, irreversible process.

The effect of hydroxide ion concentration on the oxidation rate was studied by kinetic methods and reported in Part IV of this series [1]. It has been found that on the nickel hydroxide electrode, in the concentration range of $0.01 < c_{OH^-} < 1.0$, the rate of the oxidation of ethanol is, within the experimental error, independent of the pH of the solution. This experimental fact contradicts the reaction mechanism given by Scheme IV, supporting thereby the mechanism outlined in Scheme III. Accordingly, the first step of the reaction is the homolytic splitting of the C—H bond, and this is followed

by the abstraction of a proton and finally by the removal of an electron. This mechanism can be described by the following set of equations.

$$\mathrm{R{-}CH_2{-}OH + NiOOH \xrightarrow{slow} Ni(OH)_2 + [R{-}\dot{C}H{-}OH]}$$
$$\mathrm{[R{-}\dot{C}H{-}OH] + OH^- \longrightarrow [R{-}\dot{C}H{-}O]^- + H_2O}$$
$$\mathrm{[R{-}\dot{C}H{-}O]^- \longrightarrow R{-}CHO + e^-}$$

together with the electrochemical reaction coupled with the last process:

$$\mathrm{NiOOH + H_2O + e^- \longrightarrow Ni(OH)_2 + OH^-}$$

(The radical or ionic character in the reactions does not, of course, manifest itself on a single atom; the dots in the above scheme are for illustration, assigned to the atom from which the corresponding particle has been removed.)

The mechanism outlined here is very convincingly supported also by the fact that among the possible intermediate radicals occurring in the reaction schemes the radical ion preceding the removal of electron can be regarded as the most stable one, since, based on analogous features with ketyls, a three-electron resonance state can be assumed for the C—O bond. This is of particular importance if the electrons of this three-electron bond are able to form a conjugated system with the π-electrons of an aromatic ring adjacent to the carbonyl group. This conjugation further increases the stability of the radical ion, so its formation is easier. The increasing stability of the radical ion is excellently demonstrated by the experimental fact (see Part IV [1]) that the substitution of the hydrogen or the methyl group by benzyl or 2-furyl groups increases the reaction rate by about an order of magnitude.

REFERENCES

1. Vértes, G., Horányi, G., Nagy, F.: Acta Chim. Acad. Sci. Hung., **67,** 145 (1971);
Horányi, G., Vértes, G., Nagy, F.: Acta Chim. Acad. Sci. Hung. **67,** 357 (1971);
Vértes, G., Horányi, G., Nagy, F.: Acta Chim. Acad. Sci. Hung. **68,** 217 (1971);
Vértes, G., Horányi, G., Nagy, F.: Acta Chim. Acad. Sci. Hung. **69,** 341 (1971)
2. Nagy, F., Telcs, I.: Acta Chim. Acad. Sci. Hung. **25,** 193 (1960);
Nagy, F., Telcs, I., Horányi, G.: Acta Chim. Acad. Sci. Hung. **37,** 295 (1963);
Nagy, F., Horányi, G.: Magy. Kém. Foly. **68,** 497 (1962)
3. Bourgault, P., Conway, B. E.: Can. J. Chem. **38,** 1557 (1960);
Briggs, G. W. D., Stott, G. W., Wynne-Jones, W. F. K.: Electrochim. Acta **7,** 249 (1962);
Yoshizawa, S., Takehara, Z.: CITCE Meeting, Tokyo—Kyoto 1966;
Kronenberg, M. L.: J. Electroanal. Chem. **13,** 120 (1967);
Bode, H., Dehmelt, K., Witte, J.: Z. anorg. allg. Chemie **366,** 1 (1969);
Vértes, G., Nagy, F.: Magy. Kém. Foly. **76,** 260 (1970)
4. MacArthur, D. M.: J. Electrochem. Soc. **117,** 729 (1970);
Lukovtsev, P. D., Slaidin, G. J.: Electrochim. Acta **6,** 17 (1962);
Lukovtsev, P. D., Slaidin, G. J.: Zh. Fiz. Khim. **38,** 556 (1964)

5. AIA, M. A.: J. Electrochem. Soc. **114,** 418 (1967);
AIA, M. A., KOBER, F. P.: Amer. Chem. Soc., Div. Fuels Chem. **11,** 224 (1967);
HARKEVICH, V. I., SAGOYAN, L. N.: Ukr. Khim. Zh. **31,** 1052 (1965);
ALESKEVICH, S. A., SAGOYAN, L. N.: Ukr. Khim. Zh. **31,** 1147 (1965)
6. NAKAGAWA, K., KONAKA, R., SUGITA, J.: Ann. Shionogi Res. Lab., **19,** 141 (1969);
KONAKA, R., TERABE, S., KURUMA, K.: J. Org. Chem., **34,** 1334 (1969)
7. PICKERING, W. F.: Rev. Pure and Appl. Chem., **16,** 185 (1966)
8. NAKAGAWA, K., KONAKA, R., NAKATA, T.: J. Org. Chem., **27,** 1597 (1962)
9. LABAT, J.: J. Chim. Phys., **60,** 1253 (1963)
10. VÉRTES, G., NAGY, F.: Acta Chim. Acad. Sci. Hung. **71,** 333 (1972)
11. NAKAGAWA, K., TSUJI, T.: Chem. Pharm. Bull. **11,** 296 (1963);
NAKAGAWA, K., ONOUE, H., SUGITA, J.: Chem. Pharm. Bull. **12,** 1135 (1964);
BELEW, J. S., CHWANG, T.: Chem. Comm. **1967,** 1100
12. GREATOREX, D., KEMP, T. J.: Trans. Faraday Soc. **67,** 56 (1971)
13. BARLETT, P. D., NORAKI, K.: J. Amer. Chem. Soc., **68,** 1686 (1946), *ibid.* **69,** 2299 (1947);
KHARASCH, M. S., ROWE, J. L., URRY, W. H.: J. Org. Chem. **16,** 905 (1951)

György VÉRTES
Ferenc NAGY
Budapest II., Pusztaszeri út 59—67.

Acta Chimica Academiae Scientiarum Hungaricae, Tomus 74 (4), pp. 417—437 (1972)

STUDY OF THE RATE OF SORPTION ON A SINGLE, SPHERICAL ADSORBENT PARTICLE, III

EXPERIMENTAL CONFIRMATION OF THE RATE EQUATION

K. VARGA and P. FEJES

(Radiochemistry Department of the József Attila University, Szeged)

Received July 12, 1971

The sorption rate of several hydrocarbons on porous aluminum oxide, aluminum silicate and charcoal grains was determined in an apparatus suitable for the *direct* measurement of the rate of sorption. The experimental results were evaluated by digital parameter estimation, on the basis of sorption rate equations described earlier. It turned out that the rate of sorption on the porous materials is correctly described by the rate equation(s) derived theoretically if the coverage is low, and correspondingly if the proper adsorption step following the diffusion transport processes can be described by Langmuir's linear rate equation. The values of the parameters determining the rate of sorption (the thickness of the diffusion boundary layer, the effective pore-diffusion constant, the slope of the isotherm, the coefficients of the Langmuir-type rate equation) are physically realistic. The adsorption rate constant for example agrees with the gas-kinetic collision numbers within two orders of magnitude.

1. Introduction

In the first paper of this series [1] rate relations were deduced for a system in which an adsorbate diluted with an inert gas was adsorbed on a single, porous particle. In order that the mathematical treatment be simplified as much as possible, in the *model* used to describe the system the particle was spherical, the concentration of the substrate in the gas-space was constant, and the following consecutive processes were taken into consideration:

I: transport of the substrate in the diffusion boundary layer forming around the particle;

II: diffusion process in the pores of the particle;

III: adsorption of the substrate on the surface.

Processes I and II could be formulated on the basis of Fick's First and Second Laws, respectively, and process III with the simplified Langmuir kinetic equation corresponding to a linear isotherm (in agreement with this simplification the surface coverage of the adsorbent was kept at a low value).

The radius of the particle was denoted by r_0 [cm], and the constant concentration of the gas phase by c_0 [mole $\cdot$ cm^{-3}]. The concentration function was $c(r, \tau)$ [mole $\cdot$ cm^{-3}], while the amount of substance adsorbed, referred to the apparent volume of the adsorbent, was expressed by $a(r,\tau)$ [mole $\cdot$ cm^{-3}]. In the functions the radius was denoted by r, and the time coordinate by τ. Processes I—III were taken into consideration in turn by the following relations:

$$\left.\frac{\partial c}{\partial r}\right|_{r=r_0} = K\{c_0 - c(r_0, \tau)\} \tag{1}$$

$$\frac{1}{D}\left(\frac{\partial c}{\partial \tau} + \frac{1}{\alpha}\frac{\partial a}{\partial \tau}\right) = \frac{\partial^2 c}{\partial r^2} + \frac{2}{r}\cdot\frac{\partial c}{\partial r} \tag{2}$$

$$\frac{1}{\alpha}\frac{\partial a}{\partial \tau} = k_a c - k_d a \tag{3}$$

where D [$cm^2 \cdot s^{-1}$] is the effective diffusion constant for the pore phase; $K \equiv D_g/dD$; D_g [$cm^2 \cdot s^{-1}$] is the diffusion constant of the adsorbate in nitrogen; d [cm] is the average thickness of the boundary layer around the particle; α is the free pore volume relative to the apparent volume of the adsorbent (*i.e.* the porosity); k_a [s^{-1}] and k_d [s^{-1}] are the adsorption and desorption rate constants, respectively. $k_a/k_d = \alpha q$, where q is the slope of the assumed linear adsorption isotherm. The initial condition

$$c(r, 0) = a(r, 0) = 0 \tag{4}$$

and the condition

$$c(r, \tau) < \infty \tag{5}$$

can be used for the solution of the partial differential equation system (1), (2) and (3).

The solution of problem (1)—(5) explicitly provides the amount of substrate sorbed by the particle in unit time, *i.e.* the sorption rate expressed in the dimensions [$mole \cdot s^{-1}$]:

$$\frac{dM}{d\tau} = 8\pi\alpha c_0 r_0 D \sum_{i=1}^{\infty} \frac{\left(\frac{s_i+h}{g}+1\right) e^{s_i D\tau} - e^{-hD\tau}}{\left(\frac{s_i+h}{g}+\frac{h}{s_i+h}\right)\left[\left(\frac{\omega_i}{Kr_0}\right)^2 + 1 - \frac{1}{Kr_0}\right]} \tag{6}$$

where $g \equiv k_a/D$ and $h \equiv \alpha k_d/D$. The quantities s_i and ω_i ($i = 1, 2, \ldots$) necessary for the solution of the series can be calculated from the conditions

$$s_i + [h + g + (\omega_i/r_0)^2]s_i + h(\omega_i/r_0)^2 = 0$$

and

$$\omega_i \cot \omega_i = 1 - Kr_0$$

The sorption rate equation (6) also contains rate equations valid as limiting cases for the simpler models (see models B, C and D in [1]).

In the second paper of the series we dealt with the known theoretical possibilities of digital parameter estimation; it was found that the Marquardt

modification of the Gauss–Newton method can suitably be applied as optimizing procedure for the determination of the physical parameters occurring in the sorption rate equations [2]. In addition to a few rationalizations of the calculation technique which were of minor importance, we also succeeded in developing a new principle of generating initial estimates to the minimum of the objective function by the combined application of drawing and the steepest descent method [3]. Finally, the complete optimizing algorithm was worked up for GIER and ICT 1905 computers. This made possible the evaluation of the experimental results in accordance with the four rate equations involved, that is the calculation of the values of the diffusion, equilibrium and rate constants, and also the confidence intervals of the parameter estimation.

In addition to the deduction of the theoretical rate equations and the development of the evaluation procedure, the third fundamental problem of sorption rate studies consists of the *elaboration of an experimental method* providing the most information within the framework of the given model. For this purpose some apparatus is required which is *devised in such a way that the experimental conditions be in agreement with the simplifications introduced in deducing the mathematical model. Direct measurement of the gas uptake is to be prefered* to the known indirect methods.

The object of the present paper is the confirmation of the deduced sorption rate equation(s), on the basis of the computer evaluation of the experimentally determined sorption rate curves.

2. Experimental

2.1. Experimental method

In the rate equation, forming the theoretical basis of the sorption rate studies, the value of $dM/d\tau$ is expressed as a function of time and the parameters occurring in the model. Our task is to elaborate an experimental method or apparatus which enables the quantity $dM/d\tau$ to be measured *directly* as a function of time.

In accordance with what was said in the introduction, it is favourable to measure the sorption rate on a *single*, spherical grain, under conditions such that the *concentration* of the adsorbate in the indifferent carrier gas remains almost *constant* in the course of the sorption. This condition can be fulfilled most simply by means of streaming the gas mixture. Before the measurement is begun, therefore, *a gas mixture of concentration* c_0 *must be prepared*, and then streamed through the detector with a *constant flow rate* v_0 [$cm^3 \cdot s^{-1}$]. Taking into consideration the adsorption properties of the particle, in every measurement the values of r_0, c_0 and v_0 should be selected so that the relative decrease of the amount of substance $c_0 \cdot v_0$ [$mole \cdot s^{-1}$] flowing through the detector cell in unit time (in the following: the flux) does not attain 10%. In this way the condition of constant concentration is fulfilled *practically*.

The simplified Langmuir kinetic equation was used in the models; this is presumably also valid in the range of low concentrations. It is thus desirable to carry out the measurements at a partial pressure of the adsorbate of a few Torr, *i.e.* at a concentration $c_0 \approx 10^{-8}$–10^{-7} $mole \cdot cm^{-3}$. For the measurement of such low concentrations, however, it is advisable to employ a flame ionization detector, and accordingly to use some hydrocarbon as adsorbate. The carrier gas can be nitrogen, for example.

After this there remains only one fundamental problem in the measurement: the *instantaneous* introduction of the adsorbent particle into the gas mixture. It is known from experience in gas chromatography, etc. that the problem cannot be solved by turning a tap

(and thus by 'switching over' from the inert gas with the particle present to the flow of the gas mixture). In doing this the sorption effects to be investigated become distorted, and may even be obscured, by the undefined rate of tapturning, the local pressure changes, and other unknown factors. We have succeeded in eliminating these possibilities of experimental error by *immersing the adsorbent particle in mercury* before commencing the measurement, and then at a suitable moment *introducing it momentaneously* into the flow of the gas mixture.

The apparatus is shown in Figure 1. The measurements were carried out in the following way [4].

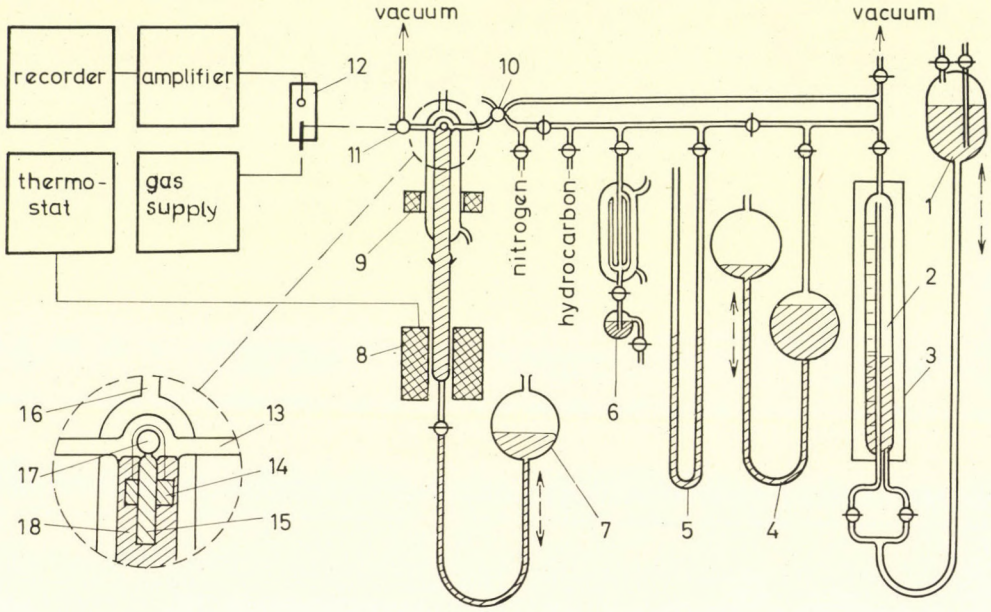

Fig. 1. Outline of the sorption rate measuring apparatus

Preparation of the particle: The adsorbent particle "17" was held on the end of the screw "15" by means of a tungsten wire net attached to the nut "14", the joint was opened, and the particle on its support was placed into the *empty* adsorbent-holder tube; this was evacuated via the three-way tap "11" and heated by the furnace "8". After the heat treatment nitrogen was admitted into the system, followed by mercury from the reservoir (adjustable height) "7". As can be seen in Fig. 1, the particle floats on the mercury, and takes up a position in line with the gas-inlet tube "13". A thermostating liquid circulates in the jacket "16" surrounding the adsorbent-holder tube. Up to the beginning of the measurement the particle was kept immersed in the mercury by means of the permanent magnet "9".

Preparation of the gas mixture: The gas burette "2" and the tap system were evacuated (10^{-2} Torr), and by means of the manometers "5" and "6" the amounts of hydrocarbon and nitrogen corresponding to the desired concentration were admitted. The *rapid and perfect mixing* of the two gases could be achieved by flushing of the contents of the gas burette into vessel "4" and back again. This mixing operation is a fundamental part of the measurement, because the accuracy of the dilution in the two-step adjustment of the very low concentrations depends on perfect mixing, and also because another condition of this is the establishment of a constant hydrocarbon flux.

Establishment of the constant flow rate: As can be seen from the Figure, the gas burette "2" and the reservoir "1" operate as a manostat. Thus, by adjustment of the height of the reservoir "1" (containing mercury!) the rate of flow of the gas from the burette can be maintained at an optional, preselected value (between the limits 0.2 and 2 ml $\cdot$ s^{-1}). Before the measurement is begun the gas mixture of concentration c_0 flows into the atmosphere with a rate v_0 through the four-way tap "10".

The taps in contact with the gas mixture (also including "11") are coated not with one of the usual "tap greases", but with a mixture of mannitol in glycerine. The hydrocarbons dissolve to a minimal extent in this polar coating.

Recording of the adsorption rate curve: Nitrogen is streamed through the cell by the suitable positioning of taps "10" and "11". In accordance with the null-signal of the detector, the recorder registers the *base line*. Tap "10" is turned, and the gas mixture is introduced. The recorder registers the detector signal y_0 [mm] proportional to the flux $c_0 \cdot v_0$. When the magnet is taken away, the particle rises up momentaneously* from the mercury and the sorption begins. The recorder now registers the $y_0 - y(\tau)$ [mm] curve. The decrease of the recorder deflection, $y(\tau)$, is proportional to the amount of substance sorbed at a given instant. The proportionality factor arises from the deflection corresponding to the total flux, and so:

$$\frac{dM}{d\tau} = \frac{c_0 v_0}{y_0} y(\tau)$$

As a result, therefore, $y(\tau)$ provides the sorption rate curve directly.

Considering that in accordance with what was said above about the fulfilment of the condition $y_0 > 10 \cdot y(\tau)$ in every experiment, it is practical to compensate electronically for 90% of the deflection after registering the flux, and then to measure the $y_0 - y(\tau)$ curve with a 10 times amplification. This enables the rate of gas uptake to be registered on the full width of the recorder paper and so the precision of the measurement can be increased.

Recording of the desorption rate curve: If it proves possible to saturate the particle with the solute (this is indicated by the deflection y_0 of the recorder), there is also the possibility of recording the desorption curve. In this case the particle is again immersed in mercury. The gas burette is filled with pure nitrogen. After the establishment of the flow rate, the base-line is plotted with appropriate sensitivity, and the particle is then introduced into the path of the 'flushing gas'.

2.2. Materials

The *choice of adsorbent* is determined by the magnitudes of many well and less well defined parameters (specific surface area, porosity, pore distribution and pore radius, activity of the surface). In the majority of the experiments aluminum oxide (Leuna catalyst carrier) and aluminum silicate (a cracking catalyst from the USSR) were used. In addition to these, a few types of charcoal were also investigated: Nuxit BO, Decolor and Akvapur (products of the Charcoal Producing Company, Budapest). The most important features of the adsorbents are given in the first part of Table I (based on [5], and in the case of the charcoal samples [6]).

The aluminum silicate catalyst was used in form of spherical particles. Grains 1–7 mm in diameter were prepared from bigger pellets by grinding. The weight of the particles was measured after drying to a constant weight in vacuo at 150 °C. The radii of the adsorbent particles were in part calculated from the weights and volumes, and in part measured directly with a caliper gauge. The two values practically agreed.

The nature of the *adsorbate* can influence the values of the physical parameters involved to a considerable extent, and so, in addition to isobutane, other hydrocarbons were also used in the experiments. The hydrocarbons studied are shown in Table II, together with the diffusion constants of the individual gases in nitrogen [7, 8], and also their molecular cross-sectional areas [9].

2.3. Experimental conditions

It is well known (see *e.g.* [10]) that the activity and the sorption capacity of porous aluminum oxides depend sensitively on the heat treatment. Accordingly, before the measurements were begun the following methods of pretreatment were applied. The air-dry aluminum

* The time required for the formation of the quasi-steady diffusion film is at most a few tenths of a second. The recording of the rapidly occurring concentration changes was impeded not only by this, but by other reasons too (*e.g.* the 1.5 s required for full-scale deflection of the recorder), and so the first part of the rate curve in the time interval 0–5 s was not used in the later evaluation (since it was really not required).

Table I

Characteristic data of the adsorbent particles applied

Adsorbent	Specific surface $F[m^2 \cdot g^{-1}]$	Porosity α	Average pore diameter [Å]	Apparent density $\varrho[g \cdot cm^{-3}]$	Particle number	Mass of particle [mg]	Radius of particle r_0 [cm]
Al_2O_3 catalyst carrier	299	0.58	55	1.390	2	14.0	0.132
					8	87.7	0.248
					11	122.5	0.275
					12	179.8	0.310
Aluminium silicate cracking catalyst	357	0.50	28	1.058	20	41.2	0.210
"Nuxit"	864	0.69	26	0.653	16	6.2	0.118
					17	15.8	0.181
"Decolor"	860	0.80	46	0.499	26	27.3	0.236
"Akvapur—FD"	379	0.62	68	0.525	23	23.1	0.219

oxide particles were *flushed* with pure nitrogen gas for 1–2 hours; alternatively, they were *evacuated* for several hours at room temperature, at a pressure of 10^{-2} Torr; as a third alternative, they were *heat-treated* for 60 min in vacuo at 150, 200 or 300 °C. A 200 °C heat-treatment was applied in all cases before the use of the aluminum silicate and charcoal particles.

For the sake of reproducibility, the measuring cell was strictly thermostated. The measurements were for the most part carried out at 20.0 °C. In the case of isobutane, however, it was expected on the basis of the known adsorption isotherm that the rate of sorption would be influenced considerably even by a relatively small *temperature change*, and hence sorption rate curves were also recorded at 40.0 and 55.0 °C.

The majority of the measurements were made at an adsorbate concentration of 0.1 vol.% (ca. 10^{-7} mole · cm^3); differences from this value by one order of magnitude (upwards or downwards) occurred only in a few cases. The applied flow rate varied between 0.1 and 2 $cm^3 \cdot s^{-1}$.

Table II

The adsorbates applied

Hydrocarbon	D_g [$cm^2 \cdot s^{-1}$] at 25 °C, in N_2	Molecular cross-sectional area, φ	
		[Å²]	[$m^2 \cdot mole^{-1}$]
Methane	0.190	17.8	$1.07 \cdot 10^5$
Ethane	0.145	23.0	$1.38 \cdot 10^5$
Propane	0.110	36.4	$2.19 \cdot 10^5$
Isobutane	0.080	50.7	$3.06 \cdot 10^5$
n-Butane	0.085	44.8	$2.70 \cdot 10^5$

2.4. Experimental results

About a hundred measurements were made. Two-thirds of the determined sorption rate curves could be evaluated. Of these, about 40 are utilized in this paper.

The effect of the *heat treatment* on the rate of sorption was studied in the aluminum oxide/isobutane system (Table III). The changes resulting from the various methods of heat treatment (primarily the increase of q) are well illustrated by Figure 2, which contains the sorption rate curves measured on particle no. 8. In order that the curves should be easy to compare, plots were made in the Figure of the ratio of the sorption rate and c_0.

The *variation of the particle radius* apparently affected the course of the sorption rate curves to a very considerable extent (see Figure 3). By increasing the particle radius (particles no. 2, 8, 11 and 12), the sorption rate curves normalized by c_0 are displaced towards higher

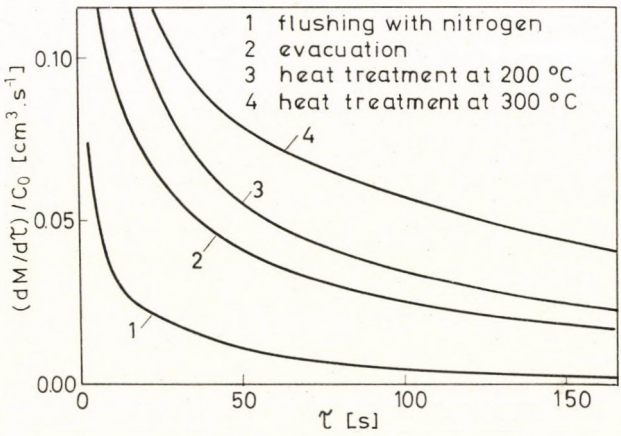

Fig. 2. Effect of the pretreatment of the adsorbent on the sorption rate (isobutane/aluminum oxide system; particle no. 8; curves 1, 2, 3 and 4 are the results of measurements 5, 4, 41 and 43, respectively)

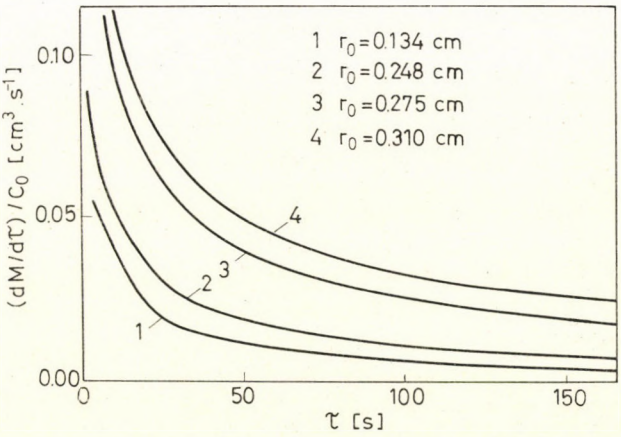

Fig. 3. Rate of sorption of isobutane on aluminum oxide particles of different sizes (curves 1, 2, 3 and 4 are the results of measurements 74, 41, 27 and 16, respectively)

Table III

Study of the rate of sorption of isobutane on aluminum oxide particles

Pretreatment		Particle no.	r_0 cm	Measurement no.	$c_0 \cdot 10^8$ mole/cm³	v_0 cm³/s	Temp. °C	q	$D \cdot 10^3$ cm²/s	$k_a \cdot 10^{-6}$ s⁻¹	k_a mole/ /(m² · s · Torr)	$k_d \cdot 10^{-6}$ s⁻¹	k'_d mole/(m² · s)	d cm
Flushing		8	0.248	5	8.00	0.489	21.0	60	5.7	59	0.0077	1.7	3.2	0.14
				6	7.59	0.495	20.0	46	5.5	13	0.0017	1.1	2.0	0.14
				7	8.09	0.501	20.5	54	6.1	42	0.0054	1.3	2.5	0.13
Evacuation (10^{-2} Torr)		2	0.132	14	5.95	0.293	25.0	147	5.0	42	0.0055	0.5	0.95	0.15
				15	5.96	0.291	25.0	170	4.5	400	0.0500	3.3	6.3	0.15
		8	0.248	1	2.05	1.38	22.6	136	6.3	67	0.0086	0.99	1.9	0.18
				9	1.54	0.451	22.0	85	5.7	280	0.036	5.7	10.5	0.13
				13	2.51	0.470	22.5	101	5.8	570	0.074	9.8	19	0.12
				2	3.96	0.506	21.0	94	5.9	230	0.030	4.2	7.9	0.26
				4	4.26	0.873	22.5	102	5.5	91	0.012	1.5	2.9	0.20
				12	7.81	0.465	22.0	92	5.7	100	0.013	1.8	3.5	0.25
		12	0.310	20	8.04	0.557	30.0	70	6.5	260	0.033	6.5	12	0.09
Heat-treatment in vacuo	150 °C	12	0.310	19	4.82	0.546	20.0	205	6.2	152	0.020	0,98	1.9	0.19
				21	7.12	0.569	40.0	103	6.6	88	0.011	1.5	2.8	0.10
				22	6.56	0.566	55.0	39	4.9	533	0.062	24	45	0.11
	200 °C	2	0.132	74	4.01	0.535	20.0	253	9.4	507	0.066	3.4	6.5	0.01
		8	0.248	41	4.01	0.553	20.0	210	10.3	930	0.12	7.6	14	0.18
		11	0.275	27	3.33	0.552	20.0	275	9.9	730	0.095	4.6	8.8	0.40
				70	46.2	1.67	20.0	230	9.7	790	0.10	5.5	10	0.04
				16	8.03	0.902	20.0	280	10.4	312	0.041	1.6	3	0.16
		12	0.310	17	7.35	0.562	20.0	313	9.3	250	0.033	1.4	2.7	0.11
				71	46.2	1.67	20.0	219	11.0	827	0.108	7.7	15	0.12
	300 °C	8	0.248	43	4.30	0.555	20.0	410	6.7	720	0.94	3.1	6.0	0.09

Table IV

Study of the rate of sorption of various hydrocarbons

Particle	Measurement no.	Adsorbate	$c_0 \cdot 10^8$ mole/cm³	v_0 cm³/s	q	$D \cdot 10^{-3}$ cm²/s	$k_a \cdot 10^{-6}$ s^{-1}	k'_a mole/ /(m² · s · Torr)	$k_d \cdot 10^{-6}$ s^{-1}	R'_d mole/(m² · s)	d cm	β
Al_2O_3	26	methane	3.85	0.555	5.4	6.4	1350	0.18	528	2860	0.23	0.021
$r_0 = 0.275$	24	ethane	4.01	0.564	15	6.0	1670	0.21	278	1170	0.43	0.035
heat-treated	25	propane	4.01	0.551	86	7.7	540	0.070	1.1	2.9	0.16	0.014
at 200 °C	27	isobutane	3.33	0.552	275	9.9	730	0.095	4.6	8.8	0.40	0.021
	28	n-butane	4.42	0.563	382	13.6	340	0.045	1.5	3.4	0.12	0.010
Aluminum	33	methane	4.42	0.561	10	4.0	1120	0.16	217	1020	0.00	0.019
silicate	32	ethane	3.59	0.560	35	3.1						
$r_0 = 0.210$	34	propane	4.82	0.564	90	6.2	170	0.024	3.8	8.6	0.19	0.005
heat-treated	31	isobutane	3.73	0.548	125	6.9	410	0.059	6.8	11	0.02	0.013
at 200 °C	36	n-butane	4.05	0.566	235	7.2	360	0.052	3.1	5.8	0.05	.012

Table V

Study of the rate of sorption of isobutane on charcoals

Adsorbent	Particle no.	r_0 cm	Measurement no.	$c_0 \cdot 10^8$ mole/cm³	v_0 cm³/s	q	$D \cdot 10^3$ cm²/s	$k_a \cdot 10^{-6}$ s^{-1}	k'_a mole/ /(m² · s · Torr)	$k_d \cdot 10^{-6}$ s^{-1}	k''_d mole/(m² · s)	d cm	β
Nuxit-BO	17	0.181	52	2.77	0.551	19 000	7.9	550	0.052	0.041	0.1	0.01	0.012
			53	45.0	1.610	1 900	8.0	240	0.023	0.18	0.41	0.11	0.005
	16	0.118	66	4.02	0.552	5 600	7.8	118	0.011	0.030	0.07	0.06	0.003
Decolor	26	0.219	82	47.8	1.68	4 800	19.0	220	0.028	0.059	0.15	0.04	0.006
Akvapur	23	0.236	86	47.8	1.68	2 900	39.0	200	0.055	0.11	0.22	0.05	0.012

ordinate values. It can be seen from Table III, however, that in spite of this the values of the various parameters determined from these curves are *independent of the particle size.*

Figure 4 shows the *temperature-dependence* of the sorption rate. In this case too it was practical to plot the curves normalized by c_0. The determined parameters can be seen in the first part of Table III. The slope of the adsorption isotherm decreases with increasing temperature, in accordance with expectations. On the other hand, the value of the effective diffusion constant exhibits a maximum at 40 °C.

The *nature of the adsorbate* affected the rate of sorption considerably. Studies were made of the sorption of methane, ethane, propane, isobutane and *n*-butane on aluminum oxide (see Fig. 5) and on aluminum silicate (see Fig. 6). In order that the effects caused by the different factors should be more easily distinguished, the curves were plotted in two different ways. The 'direct' plotting of the curves reflects primarily the effect of the slope of the iso-

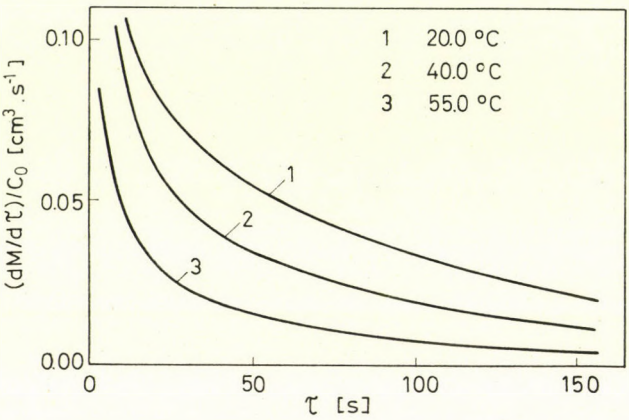

Fig. 4. Rate of sorption of isobutane at different temperatures
(aluminum oxide particle no. 12; curves 1, 2 and 3 are the results of measurements 19, 21 and 22, respectively)

therm. In the curves normalized by M_∞ (amount of material adsorbed at equilibrium [mole]), the effect of the nature of the adsorbate is reflected; it can be seen, for example, that methane is sorbed much more quickly than butane. It is clear from Table IV also that the values of the determined parameters in general follow the trends to be observed in Figs 5 and 6.

Figure 7 contains the sorption rate curves measured in the isobutane/charcoal system, and plotted in two ways (V [cm^3] is the volume of the particle). The corresponding parameter values are given in Table V. It can be seen from the normalized curves that the corresponding curves for Nuxit–BO and Decolor lie close to each other, whereas that for Akvapur lies much lower, and thus the difference in the specific surfaces of the adsorbents shows up with regard to the slopes of the individual isotherms. As a result of the very low average pore size of the Nuxit, the rate curve measured for the particle of smaller radius has a much higher slope than that for the larger particle; that is, the rate of sorption is visibly decreased by the pore-diffusion hindrance. It can also be seen from the curves measured for Nuxit and from Table V that the slope of the adsorption isotherm decreases significantly with the increase of the concentration of the adsorbate. The lower degree of curvature of the isotherm was also observed in the case of aluminum oxide (for example, see measurement no. 71 in Table III).

To complete the account of the measured adsorption rate curves, it must be mentioned that in a few cases the *desorption rate curve too* was determined. When it proved possible to attain the adsorption equilibrium reflected on the reading of the recorder then the course of the desorption rate curve measured immediately afterwards under identical conditions agreed perfectly (it was symmetrical) with that of the adsorption rate curve, while otherwise in the ratio of the amount of material adsorbed up to the interruption of the adsorption process, it turned out to be 'flatter'.

2.5. Reliability of the experimental results

The numerical results reported in the previous section were provided by a computer evaluation procedure.

At least 10, but at most 30, τ_i [s], y_i [mm] value pairs were read off the recorded plot. When supplemented by other data characteristic of the experimental conditions, these served as the input data for the optimizing procedure. In the calculation of the theoretical relation (6), accurate values were obtained in general up to 10 terms, inclusively. The optimization was carried out (in accordance with what was said in [2]) by proceeding from the most simple

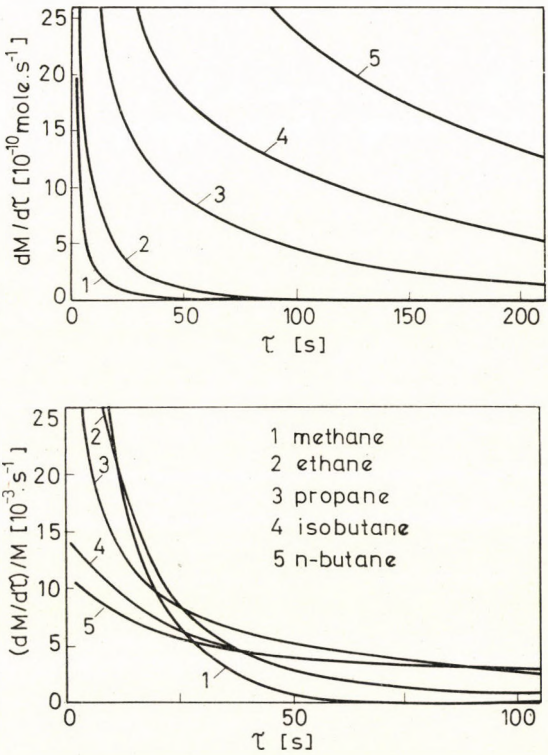

Fig. 5. Rates of sorption of different hydrocarbons on aluminum oxide
(particle no. 11; curves 1, 2 ,3, 4 and 5 are the results of measurements 26, 24, 25, 27 and 28, respectively)

model, D, to the most complex, A. In each model the computer programme provided the parameter optimum for the measurement, the measured and calculated sorption rate values relating to the chosen points of time, and also their differences, and in addition the sum of squares of the deviations. Their magnitude reveals that it was not possible to attain perfect fitting of the data with the rate equations referring to models D and B. The other two models are suitable to describe the sorption rate.

The optimizing procedure also provided the confidence intervals relating to the parameters at a 95% significance level. An enumeration of these values extending to every measurement would be very difficult to survey, and would increase the size of the above Tables unjustifiably. We consider it more practical to give one such Table, in which we show the average reliability (relating to a significance level of 95% and valid for all the models considered) of the physical parameters. In addition to this, Table VI also gives the percentage

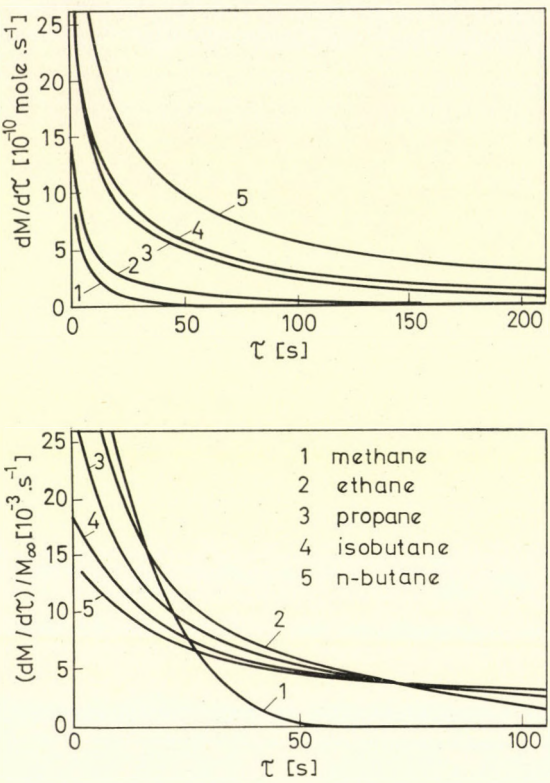

Fig. 6. Rates of sorption of different hydrocarbons on aluminum silicate (particle no. 20; curves 1, 2, 3, 4 and 5 are the results of measurements 33, 32, 34, 31 and 36, respectively)

Table VI

Error of the physical parameters

Parameter	Reliability of the estimation	Spread of the data
D	± 8%	± 7%
q	±30%	± 7%
k_a	one order of magnitude	±46%
k_d	one order of magnitude	±90%
d	±30%	±48%

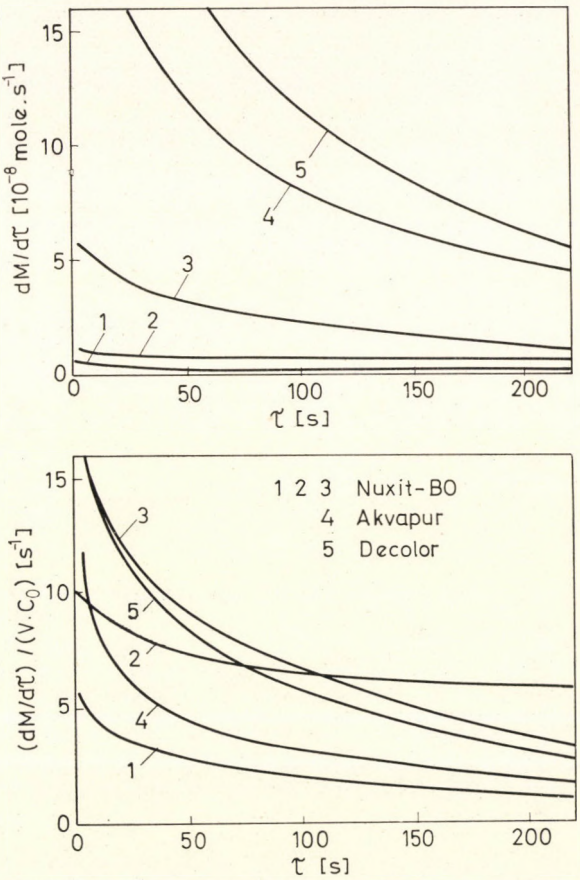

Fig. 7. Rates of sorption of isobutane on charcoals
(curves 1, 2, 3, 4 and 5 are the results of measurements 66, 52, 53, 86 and 82, respectively)

deviations of the parameters calculated from studies repeated under practically identical conditions. These latter in effect give information on the *reproducibility of the measurements*, and because of this they are not supposed to be identical with the reliability of the parameter estimation (nor because of the difference in the significance levels).

3. Conclusions

3.1. *Physical reality of the determined parameters*

Sorption equilibrium coefficient

Directly or indirectly, every model provides a value of q. The confidence interval of the parameter is the least in the case of model C (ca. $\pm 10\%$), and for this reason the q columns in Tables III—V contain the results of the evaluation in accordance with model C. It can also be seen from the Tables that

the values calculated from the ratio of k_a and k_d, in spite of their uncertainty, agree fairly well with the data in column q.

The value of q (*i.e.* the slope of the straight line joining the points of the adsorption isotherm at $c = 0$ and $c = c_0$), independently of the digital parameter estimation, can also be calculated from the amount of adsorbed material determined by numerical integration (or planimetry) of the sorption rate curves. The relation

$$M \equiv \int_0^\infty \frac{dM}{d\tau}\, d\tau \approx \alpha \cdot q \cdot V \cdot c_0$$

is valid for the amount of material sorbed, and hence

$$q \approx \frac{1}{\alpha V c_0} \int_0^\infty \frac{dM}{d\tau}\, d\tau \tag{7}$$

The value thus calculated also coincides with the above optimized values, and even agrees with the adsorption isotherms measured by other authors [5].

It can be seen from Tables III—V that the value of this parameter changes in accordance with expectations on the variation of the adsorbent and adsorbate, and of the experimental conditions. For example, on the increase of the specific surface area of the adsorbent (different adsorbents), or on the activation of the surface (heat-treatment), q increases; on the other hand, when the temperature is raised, or the adsorbate is changed for one with a lower number of carbon atoms, q decreases.

The value of q decreases appreciably with the increase of the concentration of the solute on the Nuxit–BO particles. The same was also observed to a lesser extent on aluminum oxide. According to what was said above [see Eq. (7)], this clearly indicates that in the concentration range investigated the adsorption isotherms of isobutane on charcoal adsorbents exhibit a strong downward curvature whereas this behaviour is visible to a lesser extent at the isotherms measured on aluminum oxide.

Effective diffusion coefficient. The value of D can be determined reliably by the optimizing procedure. In addition to the result of the statistics this can also be seen from the fact that when the evaluation of a given measurement was carried out by proceeding from the simplest model to the more complex ones, the otherwise small differences in the four numerical values obtained for the diffusion coefficients were not random, either. In the case of models in which no diffusion boundary layer was considered, D was always smaller than the value obtained on the basis of the more general model. This observation is in agreement with the physical picture, since a further retarding transport effect is also included in the effective diffusion coefficient determined on the basis of the simpler models, whereas the more general model proved suitable, according to the evidence, for the separation of this factor.

Although a fuller explanation is required, the value of D also follows the changes in the experimental conditions. For example, it can be seen directly from the Tables that D is smaller on aluminum silicate, with its smaller average pore diameter, than on aluminum oxide, exhibiting a greater pore diameter. The same trend can also be observed on the charcoal samples.

The effect of other factors cannot be considered so easily, since the pore diffusion characterized by D is in itself also a very complex process. To a first approximation, it is influenced by three main phenomena: the Poiseuille transport, the Knudsen diffusion and the surface migration. As will be clear from the analysis to be reported later, in the systems studied the size of the effective diffusion constant is *influenced to a considerable extent by the surface migration.*

It was interesting to observe that by increasing the temperature D reached a maximum value. This phenomenon points to surface migration; at 20 °C the amount sorbed is great, and hence the value of D is also relatively high. At 40 °C the amount adsorbed decreases appreciably, but (as characteristic for a process being activated to a small extent) the rate of surface migration increases, and because of this the value of D does not decrease. At 55 °C, however, the surface coverage is already decreased to such an extent that not even the increased temperature is able to compensate for this effect, and therefore a lower value is obtained.

The numerical value of the diffusion constant depends sharply on the nature of the adsorbate (see Table IV). On both aluminum oxide and aluminum silicate it can be observed that of the five hydrocarbons studied the effective diffusion constant of ethane is the smallest.

To decide what the role of the Knudsen diffusion is in D, the value of D_K was calculated for various adsorbates.* On the basis of the D_K values given in Table VII it can be stated that the estimated diffusion constant is approximated to by the otherwise much larger experimental value to be seen in Table IV only in the cases of methane and ethane; this is again indicative of surface migration (primarily with regard to propane and the butanes).

It can be seen from the experimental results that, in the case of the charcoals, the diffusion coefficient depends on the concentration; this is also true to a lesser extent for a few of the measurements on aluminum oxide. This too can be explained by surface migration.

The considerable symmetry in the rates of adsorption and desorption indicates that the Poiseuille transport cannot play an appreciable role. If this

* $D_K' = 2/3\ \bar{r}_p \cdot \bar{v}_a$, where $\bar{r}_p$ [cm] is the average pore radius of the adsorbent (see Table II), and $\bar{v}_a$ [cm · s^{-1}] is the average velocity of the adsorbate molecules. It holds for this latter that $\bar{v}_a = \sqrt{(8RT)/(\pi M_a)}$ where M_a is the molecular weight [g · mole^{-1}] of the adsorbate. The effective diffusion coefficient also contains the so called labyrinth factor, $\chi \approx 1/\sqrt{2}$; hence, $D_K = \chi \cdot D_K'$.

Table VII

Parameter values determined by other authors [11] or calculated theoretically

Adsorbate	$D_K \cdot 10^3$, at 20 °C [cm²/s]		k_a, at 50 °C* [s⁻¹]	k'_e, at 20 °C [mole/(m² · s · torr)]
	on aluminum oxide	on aluminum silicate		
Methane	8.1	4.0	—	8.54
Ethane	5.8	3.0	170	6.24
Propane	4.9	2.5	250	5.15
Isobutane	4.3	2.1	—	4.49
n-Butane	4.3	2.1	1500	4.49

* The adsorption rate constants were determined by SCHNEIDER and SCHMIDT [11] on silica gel, by an elution gas chromatographic method. The original units of the data given were $cm^3 \cdot s^{-1} \cdot g^{-1}$. In the absence of the apparent density relating to the adsorbent, the accurate transformation could not be made, but there is no need for this because the conversion factor as could be estimated, lies between 1 and 0.5, and thus the numerical values of the very inaccurate k_a quantities, expressed in the units used in this paper, practically do not change.

were not the case, even within the framework of the studied model (which does not take into account the curvature of the adsorption isotherm, the possibility of partially or completely irreversible adsorption, etc., which are the main causes of the asymmetry) it would have been possible to observe a slight difference between the rates of adsorption and desorption; the reason for this is simply that in the case of adsorption the adsorbate must advance in the pores of the adsorbent against a nitrogen flow of relatively low flux, while in the desorption the nitrogen causing the desorption must penetrate into the particle against a high adsorbate flux. In addition to this, the possibility of Poiseuille transport is also excluded by the very low average pore size of the adsorbents.

Rate coefficient of adsorption. Because of the otherwise understandable difficulties, this parameter can be estimated only with a high confidence interval (the order the same as the value). In the case of almost parallel measurements, however, a small fluctuation can be observed in general.

The data of Table V are by no means so clear-cut. Because of their very large fluctuations, it is only probable that on proceeding from the butanes to methane the k_a values do increase to a little extent. This increase, however, barely exceeds the error of the parameter estimation. Without reservations, therefore, it can be stated only that *the value of k_a does not increase with the increase of the carbon atom number*, whereas it may rather decrease.

On the other hand, according to the experimental result to be found in the literature, which presumably is the only one referring to this (see Table VII), the values of the adsorption rate constants in question are 5–6 orders of magnitude smaller and they change in just the opposite direction, as compared

with our data. Although attention is drawn in the publication of SCHNEIDER and SCHMIDT [11] to the inaccuracy of the given k_a values, nevertheless, no closer data relating to this are reported. In our view, their experimental method is unsuitable to determine the real value of this parameter.* As a result of the simplicity of the system studied in this work, however, it is to be expected that the description of the phenomenon is better assured by the applied model (which was the same in both cases !). In addition to this, the evaluation too was carried out on the basis of an explicit solution and using the *directly* measured sorption rate curves. The order of magnitude of the constants obtained with our method supports this expectation in all respects.

For the more direct demonstration of the physical meaning of the rate constants the k_a data given in units of s^{-1} were also calculated in units of mole $\cdot$ m^{-2} $\cdot$ s^{-1} $\cdot$ $Torr^{-1}$, and these latter k'_a values are also given in Tables III—V. The relation between the two quantities

$$k_a = RTF\,\varrho \cdot k'_a$$

can easily be proved.

The rate of physical adsorption can also be estimated theoretically on the basis of well-known relations. With the assumption of zero activation energy and a condensation coefficient value of unity ($\beta = 1$), the adsorption rate coefficient is equal to the quotient of the collision number and the pressure:

$$k'_e = 1/\sqrt{2\pi M_a RT}$$

Hence, after the substitution of the appropriate transformation constants and factors:

$$k'_e = 24.2/\sqrt{M_a T} \quad [\text{mole} \cdot \text{m}^{-2} \cdot \text{s}^{-1} \cdot \text{Torr}^{-1}]$$

The value of k'_e was calculated in every measurement. (The 'theoretical' adsorption rate constants at 20 °C for the individual hydrocarbons are given in Table VII.)

There is a difference of two orders of magnitude between the calculated k'_e and the measured k'_a values (see Tables III—V). At the same time, it is true that

$$k'_a/k'_e = \beta$$

Thus, if zero activation energy is assumed, the *condensation coefficient* can be calculated. Since this quantity is characteristic of among others the mobility of the adsorbed layer, its values are also given in Tables IV and V.

* In the relatively complex gas-chromatographic system the effects of many factors not considered by these authors can be conceived, and consequently not only the rate of the physical adsorption but also the effects of phenomena superimposed on it (or possibly concealing it) are reflected in the k_a value obtained by evaluation of the elution curves.

In the case of aluminum oxide and aluminum silicate the β values calculated by using the corresponding collision numbers fluctuate about 0.02. They are thus decidedly larger than the value of about 10^{-4} for the localized adsorption complex, and indicate mobile adsorption. This finding is in agreement with the probable surface migration.

Although for active carbons the value of the condensation coefficient ($\beta \approx 0.004$) is substantially smaller than in the former cases, the possibility of mobile adsorption is still not completely excluded.

To sum up, it can be stated that the experimentally determined k'_a values approximate the theoretically estimated k'_e values within two orders of magnitude. The relatively not very large difference can readily be explained with the value of the condensation coefficient being about 10^{-2}; this still indicates mobile physical adsorption, and at the same time also supports the physical reality of the determined k'_a values. It seems to be an interesting result that when increasing the number of carbon atoms of the solute the adsorption rate constants show a decreasing tendency, in agreement with the calculated values.

Rate coefficient of desorption. What was said in connection with the adsorption rate constants also holds as regards the reliability of the desorption rate constants. Their values too are given in two different units in the above Tables. It can be simply confirmed that the values of k_d [s^{-1}] and k'_d [mole · · $m^{-2} \cdot s^{-1}$] are related by the expression

$$k'_d = \frac{\alpha}{\varphi} k_d$$

where, assuming a mobile adsorption layer, φ is the molecular cross-sectional area of the adsorbate, expressed in units of [$m^2 \cdot mole^{-1}$] (see Table III).

From the above conclusion that the values of q and k_a are physically realistic, the same follows for k_d, too. Taking this into consideration, we should again like to draw attention to the fact that the determinations of q and k_d were performed by computer completely *independently* of each other: q and k_d acted as independent optimization parameters in the computer programme.

Thickness of the diffusion boundary layer. The inaccuracy in the determination of this parameter is relatively large. In spite of this, in all cases the thickness of the diffusion boundary layer is *very realistic*, in general being a few mm.

Although it is true that d has an acceptable order of magnitude in every measurement, its fluctuation is apparently independent of the flow rate and of the nature of the adsorbate. This could be explained simply by the inaccuracy of the estimation, but the real reason is presumably that the apparatus permitted the application of only a relatively narrow flow rate interval. In addition, the description of the transport through the boundary layer in

the *model* serving as the basis for the deduction of the rate equation is merely of an approximate nature. In reality the concentration change in the gas film is not linear, but there is an even more serious error than this: the thickness of the film varies with time (the value of d is initially 0, it then suddenly increases and after passing through a maximum approaches 0 asymptotically).

3.2. *Confirmation of the validity of the deduced sorption rate equation*

If a study is made of the conditions under which sorption rate relation (6) is suitable for the description of the rate of physical adsorption, it can easily be verified that the variation of the values of the physical constants serving to describe the processes mentioned influences the sorption rate value calculated on the basis of the equation in accordance with expectations. When this conclusion is examined for the individual parameters, the first finding is that the change of the experimental parameters which can affect the system directly is truly reflected by the measured rate curves. This is revealed by the fact that *the variation of r_0 and c_0 in the individual experiments really does not influence the values of the parameters independent of them* (q, D, etc.).

The experimental results prove that in the case of a *linear adsorption isotherm* with a constant external concentration, eq. (6) is indeed *suitable for the description of the rate of physical sorption*. At higher adsorbate concentrations, and in the case of 'active' adsorbents (*i.e.* those of high adsorption capacity, *e.g.* charcoal), the fundamental condition relating to the linearity of the isotherm is not fulfilled, and because of this the application of the equation becomes questionable. The latter finding is also supported by the difficulties of getting a good fit in such cases.

It appears from the investigations that an essential part of the mathematical model is the assumption of a *diffusion boundary layer* around the particle. Although the mathematical description of the material transport through the boundary layer was achieved in a relatively simple manner (we have already pointed out the deficiencies of the steady state approach), this nevertheless means a step forward as compared with the earlier sorption rate equations; this is shown up among others by the fact that in this way it was possible to ensure a 'perfect' fit in a large number of cases. This in itself would not be surprising, since a greater number of the parameters for describing the model leads automatically to a better fit. In this way, however, it proved possible to separate effectively the distorting effect of the material transport through the adherent film (neglected in earlier studies) from the effective diffusion constant.

As regards the description of the pore diffusion transport, the approach *must* be accepted as correct as far as the various transport processes within a particle can be described by a *single* 'constant'. Since under otherwise identical

experimental conditions, but at varying concentrations even in the case of the *same* adsorbent, the Knudsen diffusion, the surface migration and (possibly) the Poiseuille flow all vary in importance, it is not to be expected that the effective diffusion constant should remain strictly concentration-independent. In fact, it is possible on just this basis to attempt to 'break down' the effective diffusion constant for the contributions by the phenomena mentioned. (In this case the placing of D on the right-hand side of (2) in front of the differential sign is really equivalent to a new approach.) For this, however, it would have been necessary to study the change of D in a larger interval of the experimental conditions, and on several occasions in the absence of a carrier gas, which would have been beyond our present concern.

The most serious limitation is due to the use of a 'linear' kinetics (*i.e.* a kinetics in which the product of the sorbed amount and the gas concentration does not appear); at the same time this also inevitably means a linear isotherm. This simplification was inevitable in order to be able to use the Laplace transforms and to get the solution in a closed form. If non-linear kinetics had been assumed, we could have relied only on numerical methods, which are not only devoid of descriptiveness, but at the same time would have made the practical solution of the parameter estimation extremely difficult (the solution of one partial differential equation on even a high-speed computer often requires 10 minutes).

Symbols

$a \equiv a(r, \tau)$	amount of the adsorbed substance referred to the apparent volume of the adsorbent	[mole · cm^{-3}]
$c \equiv c(r, \tau)$	concentration	[mole · cm^{-3}]
c_0	constant concentration in the gas phase	[mole · cm^{-3}]
d	thickness of the diffusion boundary layer	[cm]
D	effective diffusion coefficient in the pore phase	[cm^2 · s^{-1}]
D_g	diffusion coefficient in the gas phase	[cm^2 · s^{-1}]
D_K	Knudsen diffusion coefficient	[cm^2 · s^{-1}]
F	specific surface area of the adsorbent	[m^2 · g^{-1}]
$g \equiv k_a/D$		
$h \equiv \alpha k_d/D$		
k_a	adsorption rate coefficient	[s^{-1}]
k'_a	adsorption rate coefficient	[mole · m^{-2} · s^{-1} · Torr^{-1}]
k_d	desorption rate coefficient	[s^{-1}]
k'_d	desorption rate coefficient	[mole · m^{-2} · s^{-1}]
k'_e	"theoretical" adsorption rate coefficient	[mole · m^{-2} · s^{-1} · Torr^{-1}]
$K \equiv D_g/dD$		
$M(\tau)$	amount of substance adsorbed by the particle	[mole]
M_a	molecular weight of the adsorbate	[g · mole^{-1}]
q	slope of the linear isotherm	
r	radial coordinate	[cm]
r_0	radius of the adsorbent particle	[cm]
$\bar{r}_p$	average pore radius	[cm]
R	universal gas constant	[Torr · cm^3 · mole^{-1} · deg^{-1}]

T	absolute temperature	[deg]
$\bar{v}_a$	average velocity of the adsorbate molecules	[cm · s^{-1}]
v_0	flow rate of the gas mixture	[cm^3 · s^{-1}]
$V \equiv 4/3\pi r_0^3$	volume of the particle	[cm^3]
$y_j \equiv y(\tau_j)$	the measured sorption rate, as the deflection of the pen-arm of the recorder	[mm]
y_0	corresponding deflection for the hydrocarbon flux	[mm]
α	quotient of the pore volume and the apparent volume of the adsorbent	
β	condensation coefficient	
φ	molecular cross-sectional area of the adsorbate	[m^2 · mole^{-1}]
ϱ	apparent density of the adsorbent	[g · cm^{-3}]
τ	time coordinate	[s]
χ	labyrinth factor	

REFERENCES

1. VARGA, K., FEJES, P.: Acta Chim. Acad. Sci. Hung. **71,** 387 (1972)
2. VARGA, K.: Acta Chim. Acad. Sci. Hung. **73,** 411 (1972)
3. VARGA, K., FEJES, P.: Acta Cybernetica Szegediensis (in press)
4. VARGA, K.: Chromatographia **1,** 217 (1968)
5. KIRÁLY, J.: unpublished result
6. BÖLCS, GY.: Hidrológiai Közl. **1965,** 237
7. BOYD *et al.:* J. Chem. Phys. **19,** 548 (1951)
8. FEJES, P., CZÁRÁN, E.: Acta Chim. Acad. Sci. Hung. **29,** 171 (1961)
9. MCLEAN, A. L., HARNSBERGER, H. F.: J. Coll. Int. Sci. **23,** 577 (1967)
10. GREGG, S. J., RAMSAY, J. D. F.: J. Phys. Chem. **73,** 1243 (1969)
11. SCHNEIDER, P., SCHMIDT, J. M.: Poristaya struktura katalizatorov i protsessi perenosa v geterogennom katalize (Ed.: Boreskov, G. K.) "Nauka", Novosibirsk 1970, pp. 116

Károly VARGA, Pál FEJES — Radiochemistry Department of the "József Attila" University, Szeged, Hungary.

Acta Chimica Academiae Scientiarum Hungaricae, Tomus 74 (4), pp. 439—443 (1972)

STUDY OF THE ELECTRON-EXCHANGE REACTION BETWEEN IRON(II) AND IRON(III) IN FORMAMIDE

A. VÉRTES and M. SUBA

(Department of Physical Chemistry and Radiology, Eötvös Loránd University, Budapest)

Received 18 July, 1971

The electron exchange reaction between iron(III) and iron(II) was studied by means of the Mössbauer effect. No electron exchange can be detected in anhydrous formamide solution. After the addition of water, iron ions solvated by both water and formamide are formed; the rate constant for the electron exchange between these species is greater than 2 $l \cdot mole^{-1} \cdot s^{-1}$.

The majority of models describing the mechanisms of electron transfer reactions can be divided into two main groups depending on whether they assume an *indirect* or a *direct* electron transfer. In the indirect mechanism the electron transfer is brought about by some atom, molecule, ion or radical [1–9], while in the direct mechanism the rate constant of the electron transfer reaction is affected by the Coulombic repulsion between the polar solvent and the ion taking part in the electron exchange reaction [10–19].

It can be seen from the above that in the case of given reaction partners (*e.g.* Fe(II) and Fe(III)) the variation of the solvent may be used to decide whether the electron exchange proceeds by a direct or an indirect mechanism. Taking this into consideration, RUFF *et al.* [20] studied the Fe(II)–Fe(III) exchange in formamide; both the dipole moment (>3) and the dielectric constant (117 at 25 °C) of formamide are larger than those of water, and so, in the case of a direct mechanism, the rate constant of the electron exchange reaction should be larger in formamide than in water. In contrast with this, however, it was found that the rate constant of the Fe(III)–Fe(II) electron exchange reaction was two orders of magnitude smaller in formamide than in water (in formamide at 50 °C $k \approx 5 \times 10^{-2}$ $l \cdot mole^{-1} \cdot s^{-1}$). It was concluded from this that the electron-transfer reaction takes place by an indirect mechanism.

RUFF *et al.* measured the electron exchange by an isotopic tracer technique. The great drawback of this method is that after each given reaction time the reaction components must be separated from each other, and only then can the radioactivity of the labelled component be measured. This step of the method contains several possibilities of experimental error, and so we too have studied the above electron exchange reaction in formamide, using our method based on Mössbauer spectroscopy and not requiring a separation [21].

Experimental method

The principles of the method have already been described [21].

Anhydrous $^{57}FeCl_3$ was prepared by the oxidation of iron powder containing 86% ^{57}Fe in a chlorine atmosphere. Anhydrous $FeCl_2$* was prepared by deoxygenation of hydrated $FeCl_2$ in a current of hydrogen and argon, and then by dehydration with dry hydrogen chloride at 800—850 °C. The $FeCl_2$ was prepared from natural iron. The formamide was purified by repeated vacuum distillation.

Solutions of $^{57}FeCl_3$ and of $FeCl_2$ containing 0.02 mole per 1000 g formamide were prepared in a nitrogen atmosphere. Equal volumes of these solutions were mixed to give a solution containing 0.01 mole each of $^{57}FeCl_3$ and $FeCl_2$ per 1000 g formamide.

The electron exchange reaction took place at 20 °C in an atmosphere of nitrogen.

Results and discussion

Mössbauer lines corresponding to Fe(II) did not appear for the anhydrou, formamide solution 48 hours after the mixing of the $^{57}FeCl_3$ and $FeCl_2$ solutionss and thus no measurable electron exchange could be detected under such con-

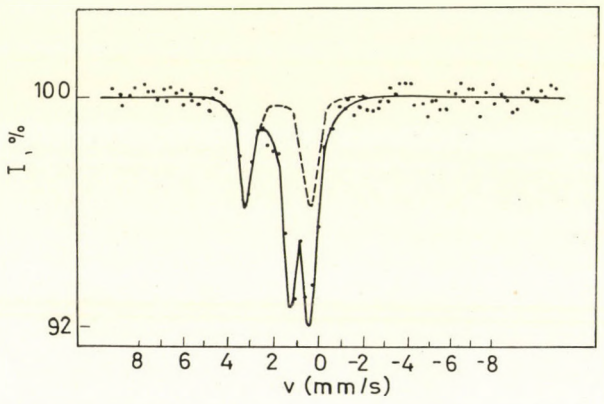

Fig. 1. Mössbauer spectrum of a formamide solution containing 0.01 mole each of $^{57}FeCl_3$ and $FeCl_2$ per 1000 g solvent, and 8 weight % H_2O (at liquid nitrogen temperature). Electron exchange reaction time, $t = 20$ seconds. (The solutions had stood for 1 week before mixing.)

ditions. The electron exchange began directly after the addition of water only when the water content was greater than ≈25 weight %. If, however, the Fe(II) and Fe(III) solutions were left to stand for some days before mixing, then a rapid electron exchange could be measured in the solution even when it contained 8% water.

Figure 1 shows the Mössbauer spectrum of a solution containing 0.01 mole each of $^{57}FeCl_3$ and $FeCl_2$ per 1000 g solvent and 8 weight % water,

* The authors acknowledge the assistance of Mrs. J. TAKÁCS, of the Central Physics Research Institute, in the preparation of the anhydrous $FeCl_2$.

after an electron exchange reaction time of 20 seconds. The Fe(II) and Fe(III) solutions had stood for a week before mixing. The iron(II) lines indicate the electron exchange. In the present case the rate constant $k > 2$ l · mole^{-1} · s^{-1}.

In the anhydrous formamide solution of $^{57}FeCl_3$ the Fe(III) exhibits a magnetic hyperfine structure, and thus the electron spin relaxation time (τ_R) and the average life time of the excited ^{57}Fe nucleus (τ) exceed the Larmor precession time (ω^{-1}): *i.e.* τ, $\tau_R > \omega^{-1}$ [22].

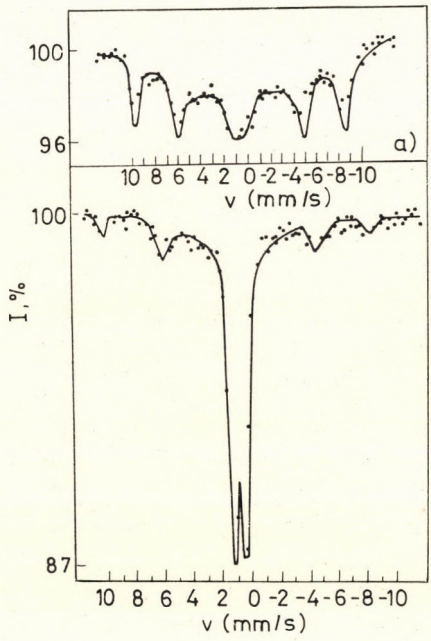

Fig. 2. Mössbauer spectrum of a formamide solution containing 0.02 mole $^{57}FeCl_3$ per 1000 g solvent, and 9.07 weight % H_2O (at liquid nitrogen temperature). (a) Fresh solution. (b) After standing for 6 days. (The value of the internal magnetic field H = 560 kOe. This value indicates that at most one chlorine occupies a place in the inner ligand-sphere of the iron [22].)

After the addition of water the magnetic hyperfine structure is gradually lost, and finally only one quadrupole line-pair is seen in the Mössbauer spectrum.* Figure 2 shows the Mössbauer spectrum of a solution containing 0.02 mole $^{57}FeCl_3$ per 1000 g formamide and 9.07 weight % water, as a function of time.

This experimental result clearly indicates that the inner ligand sphere of the iron changes after the addition of water, some of the formamide mole-

* The loss of the magnetic hyperfine structure and the decrease of the relaxation time indicate that dimerization (and possibly polymerization) occurs in the solution after the addition of water, and thus there is a large probability of spin–spin interaction (relaxation), which leads to a decrease of the relaxation time.

cules being expelled by water molecules. The electron exchange takes place between the mixed solvents of iron(III) and iron(II) so formed, whereas the rate constant for the electron exchange in anhydrous formamide solution is practically zero. On the above basis it can be clearly established that the electron exchange between Fe(II) and Fe(III) in aqueous formamide solution proceeds via an indirect mechanism.

In the measurements of RUFF *et al.* [20] the solutions contained small amounts of water and HCl, and this is why electron exchange could be detected. It must be noted, however, that, as follows from the above experimental results, the rate constant measured in water-containing formamide solutions is characteristic not of the electron exchange, but of the water-formamide ligand-exchange, and this is a relatively slow process leading to equilibrium. It may be assumed on the basis of the Frank–Condon principle and the symmetry conditions necessary for the electron exchange, that the ligand exchange must take place to identical extents in the environments of the iron(II) and iron(III) prior to the electron exchange. It is nevertheless not known whether the ligand exchange rates are the same in the environments of the two forms of the iron, or even whether only one of them is the rate-determining process.

In the present system, therefore, the method is suitable for the study of the kinetics of the ligand exchange (or the slower ligand exchange), but the electron exchange after the development of equilibrium is so fast that only a lower threshold value can be determined for this rate constant ($k > 2$ l · · mole^{-1} · s^{-1}).

As shown by the loss of the magnetic hyperfine structure, either after or parallel with the ligand exchange a process occurs (possibly a polymerization) which results in a spin–spin interaction. However, the measurements indicate that this process does not hinder the electron exchange (it does not decrease its rate). The latter result means that the rate constants for the formation and decomposition of the polynuclear species in solution are very large. Because of the conditions already mentioned, the electron exchange reaction can take place only in the case of monomers.

*

The authors wish to express their thanks to Dr. Imre RUFF and Dr. Mária KOMOR for their participation in the discussion of the results.

REFERENCES

1. DODSON, R. W.: In the discussion of W. F. Libby's paper in J. Phys. Chem. **56,** 863 (1952)
2. REYNOLDS, W. L., LUMRY, R. J.: Chem. Phys. **23,** 2560 (1955)
3. HORNE, R. A., AXELROD, E. H.: J. Chem. Phys. **40,** 1518 (1964)
4. RUFF, I.: J. Phys. Chem. **69,** 3183 (1965)
5. RUFF, I.: Acta Chim. Acad. Sci. Hung. **47,** 241 (1966)
6. RUFF, I.: *ibid.* **47,** 255 (1966)

7. RUFF, I.: *ibid.* **52,** 251 (1967)
8. RUFF, I.: J. Phys. Chem. **72,** 1792 (1968)
9. RUFF, I.: Quart. Rev. **22,** 199 (1968)
10. MARCUS, R. J., ZWOLINSKI, B. J., EYRING, H.: J. Phys. Chem. **58,** 432 (1954)
11. MARCUS, R. A.: Chem. Phys. **24,** 966 (1956)
12. MARCUS, R. A.: J. Chem. Phys. **26,** 867 (1957)
13. MARCUS, R. A.: Can. J. Chem. **37,** 155 (1959)
14. MARCUS, R. A.: Disc. Faraday Soc. **29,** 21 (1960)
15. MARCUS, R. A.: J. Phys. Chem. **67,** 853 (1963)
16. HUSH, N. S.: Trans. Faraday Soc. **57,** 557 (1961)
17. LEVICH, V. G., DOGONADZE, R. R.: Dokl. Akad. Nauk SSSR **124,** 123 (1959)
18. DOGONADZE, R. R.: Dokl. Akad. Nauk SSSR **133,** 1368 (1960)
19. DOGONADZE, R. R., CHISMADZHEV, Y. A.: Dokl. Akad. Nauk SSSR **144,** 1077 (1962)
20. RUFF, J., RENDEK, E.: Acta Chim. Acad. Sci. Hung. **60,** 57 (1969)
21. VÉRTES, A.: Radiochem. Radioanal. Letters **4,** 337 (1970)
22. VÉRTES, A., PARAH, F.: Acta Chim. Acad. Sci. Hung., to be published

Attila VÉRTES
Magdolna SUBA
} Budapest VIII., Puskin u. 11–13.

Acta Chimica Academiae Scientiarum Hungaricae, Tomus 74 (4), pp. 445—452 (1972)

DIE DISPERSITÄT DES PLATINS IN PLATIN-ALUMOSILIKAT-TRÄGERKATALYSATOREN IN ABHÄNGIGKEIT VON DEN EIGENSCHAFTEN DES TRÄGERS

E. CZÁRÁN* und K. H. SCHNABEL**

*(*Zentralforschungsinstitut für Chemie der Ungarischen Akademie der Wissenschaften, **Zentralinstitut für Physikalische Chemie der Deutschen Akademie der Wissenschaften)*

Eingegangen am 25. Juli, 1971
Durchgearbeitet am 20. September 1971

Die vorliegenden Ergebnisse zeigen, daß die Aufnahme von Platinverbindungen durch Alumosilikate je nach deren chemischen Eigenschaften sehr unterschiedlich sein kann. Die Aufnahmegeschwindigkeit ist sowohl von der Art der Platinverbindung als auch von der chemischen Zusammensetzung des verwendeten Alumosilikates und einer eventuellen chemischen Modifizierung abhängig. Von uns wurden Alumosilikate mit einem SiO_2-Gehalt von 20 und 85% untersucht, als Platinkomponenten wurden H_2PtCl_6 und $Pt(NH_3)_4Cl_2$ verwendet. Es wird vermutet, daß die Aufnahme dieser Platinverbindungen durch Alumosilikate auf einer chemischen Wechselwirkung mit der Trägeroberfläche beruht, wobei die Platinchlorwasserstoffsäure wahrscheinlich mit amphoteren Aluminiumoxidanteilen der Oberfläche reagiert, während das Platintetramminion gegen Protonen der Si-OH-Gruppen ausgetauscht wird. Dieses Ergebnis steht in Übereinstimmung mit BENESI, CURTIS und STUDER [4], die fanden, daß der Platintetramminkomplex am reinen Silicagel wesentlich stärker als am Al_2O_3 adsorbiert wird. Eine bessere Aufnahme der Platinkomponente führt meist zur Erhöhung der Metalldispersität, wobei zu beobachten ist, daß eine starke Bindung des Metallkomplexes an der Oberfläche zu einer Erschwerung ihrer Reduktion führen kann. Die von DSISKO und Mitarbeitern aufgestellte Regel, daß die erzielbare Metalldispersität bei Metall-Trägerkatalysatoren der Oberflächenkonzentration der Metallkomponente umgekehrt proportional ist, gilt nach unseren Ergebnissen nur dann, wenn gleichartige Bindung der Platinkomponente an der Oberfläche vorliegt.

Die von uns erzielten Ergebnisse dürften auch für die Herstellung von getränkten Trägerkatalysatoren von Bedeutung sein, da die von uns gefundenen Unterschiede in der Platinaufnahme bei der Verwendung verschiedener Träger bzw. Platinkomponenten gerade bei kurzer Einwirkzeit besonders groß sind.

I. Einleitung

Die Dispersität des Metalls hat bei Metall-Trägerkatalysatoren bekanntlich wesentlichen Einfluß auf Aktivität und Selektivität. Es gibt aber bisher nur wenige systematische Untersuchungen über den Zusammenhang zwischen Trägereigenschaften, Herstellungsbedingungen und der erzielbaren Metalldispersität.

SAIDMAN und Mitarbeiter [1] untersuchten die Dispersität des Platins auf Aluminiumoxidträgern mit unterschiedlicher Oberflächengröße und fanden, daß die erzielte Metalldispersität der Oberflächenkonzentration des Metalls umgekehrt proportional ist, d. h. bei gleichem Platingehalt steigt die Metalldispersität mit zunehmender Größe der Trägeroberfläche an. Diese

Gesetzmäßigkeit wurde von DSISKO und Mitarbeitern auch an anderen Metall-Träger-Systemen bestätigt.

Die von SAIDMAN und Mitarbeitern gefundene Gesetzmäßigkeit dürfte jedoch nur dann gelten, wenn bei der Aufbringung der Metallkomponente auf den Träger eine gleichmäßige oder zumindest gleichartige Verteilung der Metallverbindung über die gesamte Trägeroberfläche erzielt wird, und wenn eine gleichartige Bindung aller Metallatome bzw. -ionen an die Trägeroberfläche vorliegt.

In früheren Mitteilungen [2, 3] konnten wir bereits nachweisen, daß bei der Verwendung von mikroporösen Trägern (mit Poren, deren Durchmesser kleiner als 30 Å waren) erhebliche Abweichungen von dieser Gesetzmäßigkeit beobachtet werden.

BENESI, CURTIS und STUDER [4] wiesen darauf hin, daß bei der Ausbildung der Metalldispersität an Platin-Silicagelen die Wahl der Platin-Ausgangskomponente eine entscheidende Rolle spielt. Dabei ist offensichtlich die Wechselwirkung zwischen dem verwendeten Platinkomplex und der Trägeroberfläche von großer Bedeutung.

In einer vorangehenden Arbeit [3] konnten wir nachweisen, daß die erzielbare Metalldispersität auch beim System Pt-Aktivkohle erheblich von der Wechselwirkung zwischen Träger und Tränkkomponente abhängt.

Bei den bisher untersuchten Metall-Träger-Systemen handelte es sich jedoch durchweg um Träger mit einer chemisch einheitlichen Oberfläche.

In der vorliegenden Arbeit wird nun das — auch praktisch nicht uninteressante — System Pt-Alumosilikat untersucht. Hier haben wir es mit einem Träger zu tun, dessen Oberfläche chemisch nicht einheitlich ist, sondern aus verschiedenen oxidischen Zentren bzw. Bereichen auf der Basis von Al und Si zusammengesetzt ist. Als Platinkomponenten wurden H_2PtCl_6 (wo Platin anionisch enthalten ist) und $Pt(NH_3)_4Cl_2$ (kationisches Platin) verwendet.

II. Herstellung der Pt-Alumosilikate

Als Objekt unserer Untersuchungen wurde das bereits in [2] beschriebene Alumosilikat mit 85% SiO_2 ausgewählt. Zu Vergleichsuntersuchungen wurde das ebenfalls bereits beschriebene hydrothermal bei 40 at 2 h behandelte Alumosilikat mit 85% SiO_2, ein mit NH_4F fluoriertes Alumosilikat mit 85% SiO_2 und ein Alumosilikat mit anderem Al/Si-Verhältnis (20% SiO_2) eingesetzt. Das letztere hatte eine nach BET gemessene Oberflächengröße von 220 m^2/g, das fluorierte Alumosilikat von 26 m^2/g.

Die Katalysatoren wurden durch Adsorption der Platinkomponente am Träger, der bei 350 °C ausgeheizt wurde, aus überstehender verdünnter Lösung hergestellt, wobei jeweils 5 bzw. 50 mg Platin je Gramm Träger in der Lösung enthalten waren. Es wurden immer 10 g Träger und 50 ml Lösung verwendet.

Tabelle I

Platindispersität von Platin-Alumosilikat-Trägerkatalysatoren, hergestellt mit H_2PtCl_6, Reduktion bei 420 °C, Methode nach WEIDENBACH *und* FÜRST [5]

Träger	Platingehalt (%)	Platindispersität (m^2/g)
Alumosilikat, 85% SiO_2	0,45	48
	4,40	7
Alumosilikat, 85% SiO_2	0,72	36
mit NH_4F fluoriert	3,32	4
Alumosilikat, 85% SiO_2	0,40	52
hydrothermal behandelt	2,15	2
Alumosilikat, 20% SiO_2	0,48	37
	4,37	22

Nach Aufnahme der zur Verfügung stehenden Platinmenge bzw. nach Erreichung eines Adsorptionsgleichgewichtes wurde die überstehende Lösung abfiltriert, der Träger an der Luft getrocknet und dann bei 420 °C im Wasserstoffstrom reduziert. Danach wurde die partielle Platinoberfläche nach der Methode von WEIDENBACH und FÜRST [5] bestimmt.

Die bei der Verwendung von H_2PtCl_6 erzielten Ergebnisse zeigt Tab. I.

Diese Tabelle zeigt, daß mit H_2PtCl_6 auf Alumosilikat verhältnismäßig geringe Werte der Platindispersität erzielt werden. Besonders auffällig ist der starke Abfall bei Erhöhung des Platingehaltes. Eine Ausnahme bildet hier lediglich das Pt-Alumosilikat mit 20% SiO_2, wo auch bei einem Pt-Gehalt von 4,37% noch eine wesentlich höhere Platindispersität erzielt wird als bei den anderen Pt-Alumosilikaten mit vergleichbarem Pt-Gehalt.

Tabelle II zeigt die entsprechenden Ergebnisse bei der Verwendung von $Pt(NH_3)_4Cl_2$ als Platinkomponente.

Bei der Verwendung von Platintetramminchlorid als Platinkomponente wird also am SiO_2-reichen Träger eine wesentliche Verbesserung der Platindispersität erzielt, besonders bei hohem Platingehalt. Beim Al_2O_3-reichen Träger wird dagegen mit Platintetramminchlorid als Platinkomponente kein wesentlicher dispersitätsverbessernder Effekt erzielt. Die Fluorierung des Trägers führt bei beiden Platinkomponenten zu einer Verminderung der Platindispersität.

Tabelle II

Platindispersität von Pt-Alumosilikaten, hergestellt mit $Pt(NH_3)_4Cl_2$, Reduktion bei 420 °C, Methode nach WEIDENBACH *und* FÜRST [5]

Träger	Platingehalt (%)	Platindispersität (m^2/g)
Alumosilikat, 85% SiO_2	0,5	69
	4,86	50
Alumosilikat, 85% SiO_2 mit NH_4F fluoriert	0,34	29
Alumosilikat, 85% SiO_2 hydrothermal behandelt	0,455	44
Alumosilikat, 20% SiO_2	0,40	29
	2,98	32

III. Aufnahmegeschwindigkeit von H_2PtCl_6 und $Pt(NH_3)_4Cl_2$ an Alumosilikaten

Die unterschiedlichen Dispersitätseffekte bei unseren Versuchen deuten offensichtlich darauf hin, daß die Wechselwirkung zwischen Träger und der Tränkkomponente in den untersuchten Fällen unterschiedlich und für die Ausbildung der Metalldispersität verantwortlich ist.

Wir untersuchten daher die Aufnahmegeschwindigkeit beider Komponenten an den genannten Trägern aus wäßriger Lösung unter Tränkbedingungen, wie wir sie bei der Herstellung der Katalysatoren anwandten.

Die jeweils in der Lösung vorhandene Platinmenge wurde kolorimetrisch mit $SnCl_2$ bestimmt. Dabei stellte sich zunächst heraus, daß Alumosilikate die Platinchlorwasserstoffsäure wesentlich langsamer aufnehmen als Aktivkohlen. Während eine Aktivkohle, wie in [3] berichtet, 5% Pt etwa in einer Stunde aufnimmt, wird dieser Platingehalt bei Alumosilikaten in den meisten Fällen gar nicht erreicht. $Pt(NH_3)_4Cl_2$ nehmen Alumosilikate dagegen meist besser auf als Aktivkohlen. Abb. 1 und 2 zeigen die bei Verwendung von H_2PtCl_6 erhaltenen Aufnahmekurven.

Die Aufnahme des $Pt(NH_3)_4Cl_2$ durch verschiedene Alumosilikate ist in Abb. 3 und 4 dargestellt.

Die Betrachtung der erhaltenen Aufnahmekurven zeigt, daß sich die verwendeten Träger in bezug auf die Aufnahme der beiden Platinkomponenten erheblich unterscheiden. Im allgemeinen nehmen die mikroporösen Träger die Platinkomponenten schneller auf als grobporöse Träger. Zieht man jedoch die unterschiedlichen Oberflächengrößen in Betracht, so erkennt man, daß die

bei mikroporösen Trägern mehr adsorbierte Menge keineswegs der Oberflächenzunahme äquivalent ist. Das spricht dafür, daß bei mikroporösen Trägern nicht die gesamte Oberfläche für die Adsorption der Platinverbindungen ausgenutzt wird.

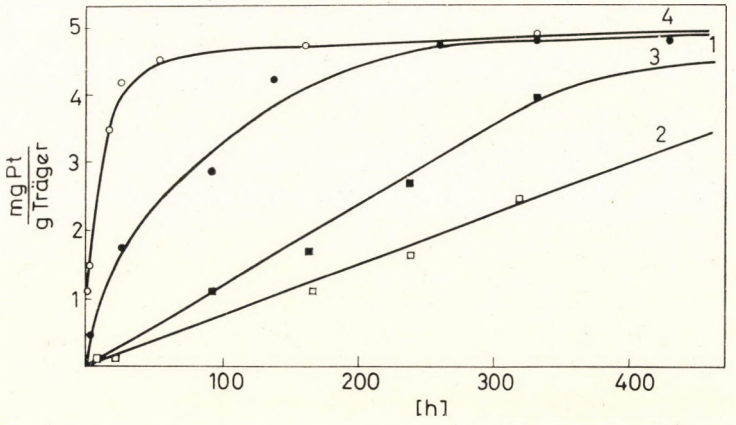

Abb. 1. H_2PtCl_6-Aufnahme durch verschiedene Alumosilikate. (Ausgangslösung: 50 mg Pt in 50 ml H_2O—10 g Träger.) 1. Alumosilikat mit 85% SiO_2; 2. Alumosilikat mit 85% SiO_2 mit NH_4F fluoriert; 3. Alumosilikat mit 85% SiO_2, hydrothermal behandelt, 4. Alumosilikat mit 20% SiO_2

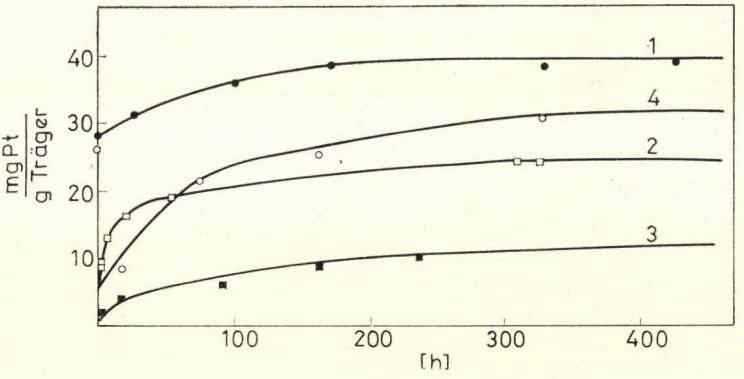

Abb. 2. H_2PtCl_6-Aufnahme durch verschiedene Alumosilikate (Ausgangslösung 500 mg Pt in 50 ml H_2O—10 g Träger.) Bezeichnungen wie Abb. 1

Ein Vergleich zwischen der Aufnahme der Platinchlorwasserstoffsäure und des Platintetramminchlorids zeigt jedoch, daß außerdem eine spezifisch chemische Wechselwirkung vorliegt. Während die Platinchlorwasserstoffsäure am schnellsten von einem Alumosilikat mit 20% SiO_2 aufgenommen wird, am Alumosilikat mit 85% SiO_2 aber eine wesentlich langsamere Aufnahme erfolgt, geht die Aufnahme des Platintetramminchlorids an diesen beiden

Trägern in umgekehrter Weise vor sich: Am Alumosilikat mit 85% SiO_2 erfolgt eine ausgesprochen schnelle Aufnahme, sie ist vergleichbar mit der Austauschgeschwindigkeit des Platintetramminions an einem NaY-Molekularsieb unter ähnlichen experimentellen Bedingungen, während die Aufnahme an

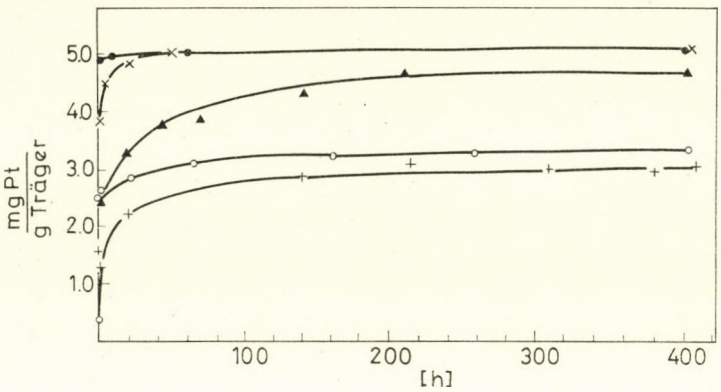

Abb. 3. Aufnahme von $Pt(NH_3)_4Cl_2$ durch verschiedene Alumosilikate. (Ausgangslösung 50 mg Pt in 50 ml H_2O—10 g Träger.) Schwarze Kreise: Molekularsieb NaY; Schrägkreuze: Alumosilikat mit 85% SiO_2; Dreiecke: Alumosilikat mit 85% SiO_2, hydrothermal behandelt; Kreuze: Alumosilikat mit 85% SiO_2, mit NH_4F fluoriert; Kreise: Alumosilikat mit 20% SiO_2

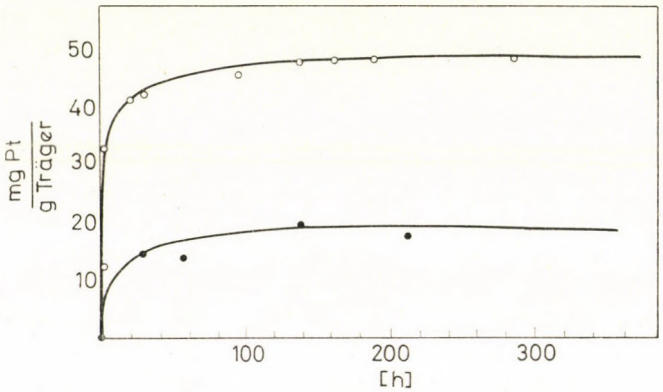

Abb. 4. Aufnahme von $Pt(NH_3)_4Cl_2$ durch verschiedene Alumosilikate. (Ausgangslösung 500 mg Pt in 50 ml H_2O—10 g Träger.) Kreise: Alumosilikat mit 85% SiO_2; schwarze Kreise: Alumosilikat mit 20% SiO_2

einem Alumosilikat mit 20% SiO_2 wesentlich verlangsamt ist und auch nicht zu einer vollständigen Adsorption der angebotenen Menge führt.

Diese Ergebnisse könnten so gedeutet werden, daß H_2PtCl_6 infolge des sauren Charakters mit amphoteren Al—OH-Gruppen der Oberfläche unter Salzbildung reagiert, während das Platintetramminion gegen Protonen in

Si—OH-Gruppen ausgetauscht wird. Zur Bestätigung einer derartigen Deutung bedarf es jedoch noch weiterer Untersuchungen.

Bei der Aufnahme größerer Mengen an H_2PtCl_6 verlieren die chemischen Faktoren offensichtlich an Bedeutung. Die aufgenommene Menge richtet sich hier hauptsächlich nach der Oberflächengröße. Dies deutet darauf hin, daß bei der Aufnahme größerer Mengen von H_2PtCl_6 hauptsächlich eine physikalische Adsorption erfolgt (Abb. 2).

IV. Diskussion der Ergebnisse

Die vorliegenden Ergebnisse sprechen dafür, daß für die Ausbildung der Dispersität des Metalls bei Metall-Trägerkatalysatoren nicht allein die Oberflächenkonzentration der auf dem Träger befindlichen Metallkomponente von Bedeutung ist. Ein ebenso wichtiger Faktor für die Ausbildung der Metalldispersität ist die chemische Wechselwirkung zwischen Metallkomponente und Träger.

Bei dem von uns untersuchten System Pt-Alumosilikat besteht offensichtlich ein Zusammenhang zwischen der Aufnahmegeschwindigkeit der Platinkomponente am Träger und der erzielten Metalldispersität. Die unterschiedliche Aufnahmegeschwindigkeit der Platinkomponenten wird vor allem bei geringen Platinmengen durch eine unterschiedlich starke chemische Wechselwirkung zwischen Metallkomponente und Trägeroberfläche bedingt. Darauf weist das unterschiedliche Verhalten der beiden Platinkomponenten sowohl bei der Veränderung der chemischen Zusammensetzung des Trägers als auch bei seiner chemischen Modifizierung hin.

Eine schnellere Aufnahme der Platinkomponente führt im allgemeinen auch zu einer Erhöhung der Metalldispersität. Eine Ausnahme bildet die Dispersität des Platins auf dem Al_2O_3-reichen Alumosilikat unter Verwendung von H_2PtCl_6 als Platinkomponente, wo trotz hoher Aufnahmegeschwindigkeit eine verhältnismäßig geringe Dispersität des Platins erzielt wurde. Hier geben jedoch einige Versuche Aufschluß, die zum Verhalten der hergestellten Katalysatoren bei verschiedenen Reduktions- bzw. Tempertemperaturen durchgeführt wurden. Tab. III zeigt einige dabei erhaltene Ergebnisse.

Bei den beiden mittleren Temperaturspalten handelt es sich um die Tempertemperatur, bei der ein bereits reduzierter Katalysator im H_2-Strom behandelt wurde.

Während also alle Katalysatoren zwischen 300 und 400 °C die höchste Platindispersität erreichen und dann zu sintern beginnen, steigt die Dispersität des Platins auf dem Al_2O_3-reichen Alumosilikat bis 520 °C noch an. Wir vermuten, daß dieser Katalysator infolge der stärkeren Bindung der H_2PtCl_6 an den Träger wesentlich schwerer reduzierbar ist und daher erst bei hohen Temperaturen vollständig reduziert wird.

Tabelle III

Platindispersität von Platin-Alumosilikat-Trägerkatalysatoren, hergestellt mit H_2PtCl_6, in Abhängigkeit von der Reduktions- bzw. Tempertemperatur, Methode WEIDENBACH *und* FÜRST [5]

Träger	Platingehalt (%)	Platindispersität (m^2/g)			
		200 °C	300 °C	400 °C	520 °C
Alumosilikat, 85% SiO_2	0,45	31	40	56	28
	4,40	16	14	14	—
Alumosilikat, 20% SiO_2	0,48	22	38	59	117
	4,37	47	25	11	—

Der starke Abfall der Platindispersität bei höherem Platingehalt, der am SiO_2-reichen Alumosilikat bei der Verwendung von H_2PtCl_6 als Platinkomponente auftritt, läßt vermuten, daß ein Teil des Platins nur locker gebunden wird und daher bei der Reduktion auf bereits gebildeten Platinkristalliten aufwächst.

Auf eine nur lockere Adsorption größerer H_2PtCl_6-Mengen deuten ja auch die H_2PtCl_6-Aufnahmekurven hin. Der wesentlich geringere Dispersitätsabfall bei größerem Platingehalt am Al_2O_3-reichen Alumosilikat spricht dafür, daß die festere Adsorption an Al—OH-Zentren oder -Bereichen erfol gt

LITERATUR

1. SAIDMAN, N. M., DSISKO, W. A., KARNAUCHOW, A. P., KRASILENKO, N. P., KOROLEWA, N. G., WISCHNIOKOWA, G. P.: Kinetika i kataliz, **9**, 863 (1968)
2. BAKARDIJEW, I., MÜLLER, H., REICHELT, J., SCHNABEL, K. H., WENCKE, K.: Mber. dtsch. Akad. Wiss. Berlin **11**, 880 (1969)
3. PARLITZ, B., SCHNABEL, K. H., SARACHOW, A. I., PLAVNIK, G. M., DUBININ, M. M.: in Vorbereitung
4. BENESI, H. A., CURTIS, R. M., STUDER, H. P.: J. Catalysis **10**, 328 (1968)
5. WEIDENBACH, G., FÜRST, H.: Chem. Techn. **15**, 589 (1963)

Elisabeth CZÁRÁN; Budapest II., Pusztaszeri út 59/67
Karl-Heinz SCHNABEL; DDR—1199, Berlin, Rudower Chaussee 5

Acta Chimica Academiae Scientiarum Hungaricae, Tomus 74 (4), pp. 453—460 (1972)

ИССЛЕДОВАНИЕ ФИЗИКО-ХИМИЧЕСКИХ СВОЙСТВ ПРИВИТЫХ СОПОЛИМЕРОВ ПОЛИВИНИЛОВОГО СПИРТА С ПОЛИВИНИЛПИРИДИНОМ

С. А. ТАШМУХАМЕДОВ, П. П. ЛАРИН, А. Ш. КАРАБАЕВ, Ш. А. АЗИЗОВ, Р. С. ТИЛЛАЕВ, Х. У. УСМАНОВ

(СССР, Ташкентский Государственный университет им. В. И. Ленина)

1971. IX. 2

Работа заслушана на Международном симпозиуме макромолекулярной химии, Будапешт, 25—30 августа 1969 г.

1. Показано, что присутствие воды или метанола в реакционной смеси изменяет соотношение компонентов в сополимере, и зависимость отношения D_{1956} ($см^{-1}$)/D_{1100} ($см^{-1}$) от дозы облучения в растворе метанола имеет более плавный ход, чем в водном растворе.

2. Показана возможность использования ИК-спектроскопии для количественного определения содержания поливинилпиридина в его сополимере с поливиниловым спиртом.

3. Исследованием растворимости, набухания и плотности привитых сополимеров поливинилового спирта с поливинилпиридином установлено, что в ходе их радиационно-химического синтеза протекают процессы структурирования макромолекул, степень которого растет с увеличением дозы облучения.

4. Показано, что плотность привитых сополимеров помимо химического состава и дозы облучения зависит также и от природы растворителя, используемого при синтезе.

В последние годы привитая сополимеризация как метод направленного изменения свойств полимеров получила настолько большое распространение при решении различных задач в полимерной химии, что к настоящему времени возникает необходимость в конкретизации изучения свойств модифицированных полимеров в зависимости от условий синтеза. Особенно это относится к радиационно-привитым полимерам, так как характер радиационно-химических эффектов, наблюдаемых в полимерах, зависит от используемого диапазона доз и мощностей излучения, в которой проводится облучение температуры, а также от химической природы составляющих компонентов, Вследствие этого привитой сополимер, полученный таким способом, отличается по свойствам от сополимеров, полученных другими путями [1, 2]. Ранее нами на примере привитых сополимеров перхлорвинила с полистиролом, поливинилацетатом и полиметилметакрилатом был обнаружен ряд закономерностей изменения свойств полученных продуктов в зависимости от условий их синтеза (3—5).

В данной работе приводятся результаты исследований физико-химических свойств привитых сополимеров поливинилового спирта (ПВС) с поливинилпиридином (ПВП).

Экспериментальная часть

Привитые сополимеры ПВС—ПВП синтезировали радиационно-химическим способом, используя γ-излучение от источника Co^{60}. Использовали промышленный образец ПВС, растворимый в горячей воде, (содержание гидроксильных групп 28,7%) с характеристической вязкостью, равной 0,58 и плотностью, равной 1,300 г/см³ при 30°С. Мономер -2- винилпиридин перед использованием очищался от ингибитора перегонкой в вакууме при 69—71°С (18 мм рт. ст., $n_D^{22} = 1{,}5490$, $d^{24} = 0{,}9827$ г/см³). Для получения привитых сополимеров применяли метод одновременного облучения смеси полимера и мономера в вакууме (при 10^{-3} мм рт. ст) в интервале доз облучения от 0,1 до 10,0 Мрад при мощности дозы 8; 19; 70 рад/сек. Ставили несколько серий опытов, в ходе которых изменяли дозу облучения и мощность дозы, а также концентрацию растворителя (вода, метанол). Подробные данные по кинетике прививки описаны в работе (6). Для выделения привитых сополимеров, продукты привитой сополимеризации подвергали экстракции бензолом для удаления гомополимера ПВП, после чего обработкой в течении трех суток дистиллированной водой при 75°С извлекали не вошедший в реакцию ПВС.

Образцы для получения спектров готорились по методу прессования с KBr (7). Запись спектров производилась на инфракрасном двухлучевом спектрофотометре IR — 10 в областях 3700—2600 $см^{-1}$ (призма из LiF), 1800—700 $см^{-1}$ (призма из NaCl) и 700—400 $см^{-1}$ (призма KBr). Для сравнения со спектрами поглощения сополимеров приведены ИК-спектры исходных веществ— поливинилпиридина и поливинилового спирта. Степень набухания, теплоту набухания, плотность и сорбционную способность полученных продуктов измеряли при 25°С, методика определения которых не отличалась от приведенной в (3—5).

Экспериментальные результаты и их обсуждение

На рис. 1 приведены ИК-спектры привитых сополимеров ПВС—ПВП, полученных при действии различных доз радиации на смесь ПВС — и ВП в растворах воды и метанола. Наличие полос поглощения, характерных для ПВП (3100, 3080, 3025, 1595, 1572, 1480, 1440, 1000, 790, 752 $см^{-1}$) и ПВС (3430, 2965, 2940, 1710, 1630, 1330, 1100, 850 $см^{-1}$) свидетельствует об образовании привитого сополимера ПВС и ПВП, причем, с увеличением дозы облучения растет интенсивность ПВП полос поглащения и соответственно уменьшается интенсивность полос поглащеиня, характерных для ПВС.

Полное отнесение частот для ПВС к соответствующим видам колебания было сделано Криммом, Лянгом, Сатерлендом (8). Наблюдаемое заметное уменьшение полосы поглощения ОН-групп, связанных водородными связями, в привитом сополимере связано о тем, что ПВС значительную часть гидрок-

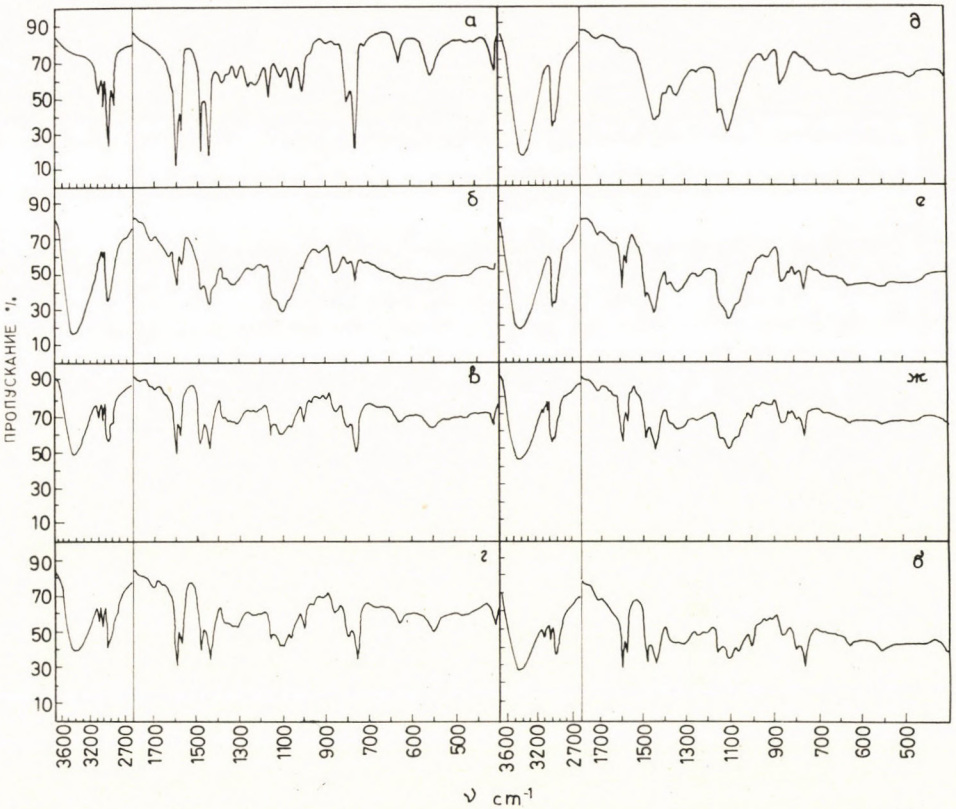

Рис. 1. ИК-спектры привитых сополимеров ПВС—ПВП: а) ПВП; Привитые сополимеры, полученные в растворе воды: б) Доза 0,25 Мрад; в) Доза 1,0 Мрад; г) Доза 2,0 Мрад; д) ПВС Привитые сополимеры, полученные в растворе метанола е) Доза 0,25 Мрад; ж) Доза 1,0 Мрад; з) Доза 2,0 Мрад

сильных групп расходует на образование привитого сополимера с поливинилпиридином. Симбатно уменьшается интенсивность полосы поглощения при 1100 $см^{-1}$, которая соответствует валентным колебаниям С—О связей ПВС. Полоса поглощения с частотой 1144 $см^{-1}$ некоторыми авторами (9) отнесена к валентным колебаниям С—О связей и в кристаллических областях ПВС. Кримом, Лянгом, Сатерлендом (8) эта полоса отнесена к валентным колебаниям С–О–С связей, образующихся в результате сшивки цепей ПВС с выделением воды. Отнесение полосы поглощения 1144 $см^{-1}$ к кристаллическим областям ПВС, сделанное (9), они считают неверным. К аналогичному выводу пришли и другие авторы (10).

В привитых сополимерах ПВС и ПВП полоса поглощения 1144 $см^{-1}$ отсутствует. Исчезновение данной полосы поглощения связано, повидимому, с тем, что в процессе прививки под действием облучения происходит разрыв эфирных связей между цепями поливинилового спирта. При сопоставлении

ИК-спектров привитых сополимеров ПВС и ПВП, полученных при одной интегральной дозе, но в разных растворителях, видно некоторое различие в интенсивностях полос поглощений. Интенсивность полос поглощений, характерных для ПВП в привитых сополимерах, полученных в случае применения в качестве растворителя воды, несколько выше, чем в привитых сополимерах, где в качестве растворителя применен метанол. Следовательно, эффективность прививки ВП и ПВС в растворе воды выше, чем в растворе метанола, то есть вода является более эффективным растворителем, чем метанол.

Аналогичная картина наблюдается и в случае привитых сополимеров, полученных при одной интегральной дозе и разных концентрациях растворителя. В этом случае ИК-спектры привитых сополимеров идентичны, однако, интенсивность полос поглощения привитого ПВП выше там, где в качестве растворителя была взята вода.

Полоса поглощения 1596 $см^{-1}$ очень чувствительна к содержанию ПВП в привитом сополимере. Поэтому эта полоса поглощения была использована нами, как аналитическая, для количественного определения привитого гомополимера по ИК-спектрам.

Зависимость отношения оптических плотностей полос поглощения 1596 $см^{-1}$ (ПВП) и 1100 $см^{-1}$ (ПВС) от общей дозы облучения приведена на рис. 2 (а, б). Как видно из рисунка, присутствие метанола в смеси дает более *плавное* увеличение содержания ПВП в сополимере, чем присутствие воды. Для получения привитого сополимера ПВС с ВП в водном растворе с содержанием привитого ПВП 75—80% достаточно общей дозы облучения 1 Мрад, в то время как в растворе метанола этот предел увеличивается до 4 Мрад.

Зависимость отношения оптических плотностей вышеуказанных полос поглощения от содержания ПВП, определенного гравиметрическим методом, дает возможность количественного определения процентного содержания ПВП в сополимере по ИК-спектрам (рис. 2, в).

Линейная закономерность данной зависимости показывает, что с увеличением содержания привитого полимера в сополимере линейно увеличивается интенсивность полос поглощения, характерных для ПВП.

Как известно, одним из характерных свойств привитого сополимера является его растворимость, на которую кроме химического строения заметное влияние оказывает метод синтеза. Оказалось, что синтезированные нами привитые сополимеры ПВС—ПВП не растворяются в воде и разбавленных водных растворах минеральных кислот, хлорированных и ароматических углеводородах, спиртах и кетонах, а также в диметилформамиде, диоксане, пиридине, бензиловом спирте и др. Подобное поведение привитых сополимеров могло быть объяснено тем обстоятельством, что компоненты сополимера резко отличаются друг от друга по растворимости. Однако использование смесей растворителей гомополимеров, составляющих основные и привитые боковые цепи, а также растворителей промежуточного типа, в частности

бензилового спирта, в молекулах которого наряду с бензольным кольцом содержатся и полярные гидроксильные группы, не привело к желаемым результатам. Эти исследования свидетельствуют о протекании под действием ионизирующего излучения процессов сшивания макромолекул привитого сополимера в ходе его синтеза с образованием структурированной трехмерной сетки.

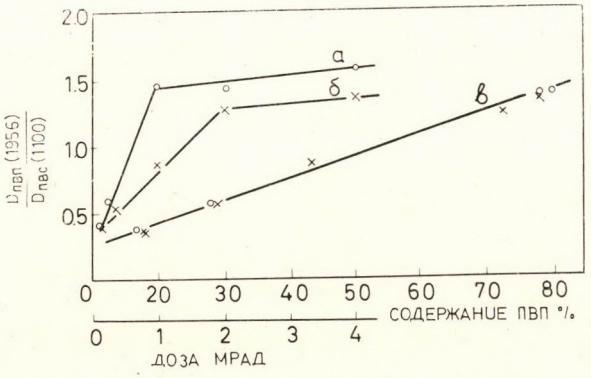

Рис. 2. Зависимость отношения оптических плотностей полос поглощения 1596 $см^{-1}$ (ПВП и 1100 $см^{-1}$ (ПВС) от общей дозы облучения (а, б) и от содержания ПВП в сополимере (в) а—в растворе воды; б—в растворе метанола; -о— в растворе воды; -х— в растворе метанола

Из литературных данных известно, что ПВП относится к сшивающимся под действием излучения полимерам (11). Относительно же ПВС имеются противоречивые сведения, когда речь идет об облучении его в твердом виде, но в присутствии воды он сшивается с образованием геля (12). В связи с этим представляло интерес исследование набухания привитых сополимеров ПВС—ПВП в различных растворителях, в качестве которых были выбраны бензол, бензиловый спирт и смесь воды и метанола в соотношении 1 : 1.

Из данных, представленных на рис. За видно, что по мере увеличения содержания ПВП в привитых сополимерах набухаемость их в вышеуказанных растворительях повышается. Причем наименьшая степень набухания наблюдается в бензоле, вследствие отсутствия его сродства к ПВС. В смеси воды и метанола, являющихся растворителями ПВС и ПВП, степень набухания больше, чем в бензоле, а в бензиловом спирте является средней между степенью набухания в бензоле и смеси воды и метанола. Это обусловлено присутствием в его молекулах бензольных ядер и гидроксильных групп, что обеспечивает сродство и к ПВС и ПВП. Но при высоком содержании ПВП в сополимере ($\sim$ 70—80%) набухание в нем резко увеличивается.

Из рисунка 3б следует, что для привитых сополимеров, составы которых близки между собой (78, 05; 78, 20; 78, 69; 79, 80% ПВП), степень набухания уменьшается с увеличением дозы облучения, при которой они синтезировались. Такая закономерность имеет место в случае всех вышеуказанных

растворителей и свидетельствует о протекании процессов сшивания макромолекул привитого сополимера при его синтезе. Причем с увеличением дозы облучения степень сшивания возрастает. Тем самым эти результаты подтверждают данные по растворимости полученных привитых сополимеров.

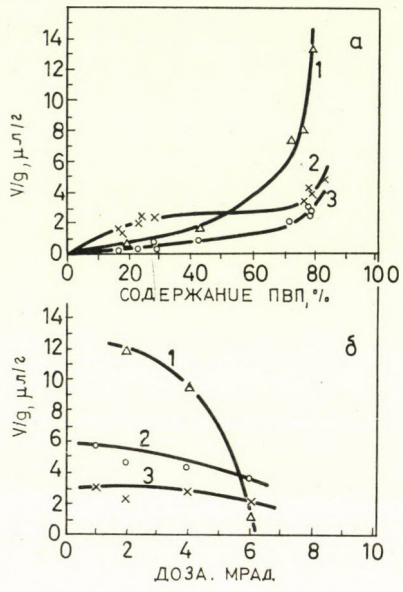

Рис. 3. Зависимость равновесной степени набухания от содержания (а) привитого сополимера и от общей дозы облучения (б): 1 — бензиловый спирт; 2 — смесь метанол-вода (1 : 1); 3 — бензол

На основании вышеизложенного следует полагать, что характер радиационно-химических эффектов будет влиять и на другие физико-химические характеристики радиационно-привитых сополимеров, и в частности на их плотность. Хорошо известно, что ПВС относится к полимерам с плотной упаковкой макромолекул, связанной с наличием межмолекулярных водородных связей. Прививка к нему ПВП, имеющего объемные боковые группы, очевидно должна привести к разрыхлению структуры исходного полимера. Действительно, данные рис. 4 а подтверждают это. В то же время, помимо химического состава, видно влияние природы растворителя, в присутствии которого проводится реакция прививки. Вода, являющаяся растворителем ПВС, по сравнению с метанолом в большей степени разрыхляет его структруру, т. е. вода в большей степени разрыхляет надмолекулярные структуры полимера, проникая не только между ними, но и внутрь структур. Очевидно, поэтому привитой сополимер, полученный в присутствии воды обладает несколько меньшей плотностью. Помимо этого данные рис. 4 б указывают на рост плотности при-

витых сополимеров, имеющих близкий состав, но синтезированных при разных дозах. Этот факт также можно интерпретировать как свидетельство увеличения степени структурирования на это свойство.

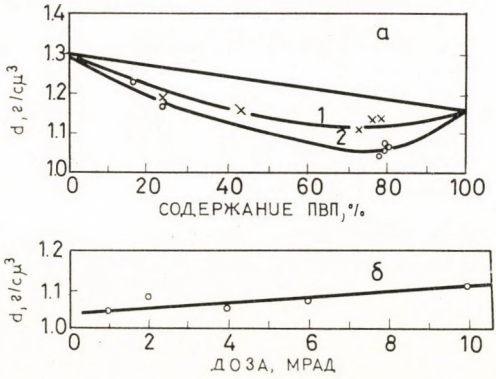

Рис. 4. Зависимость плотности привитых сополимеров от содержания (а) и от общей дозы облучения (б): 1 — образцы, полученные в растворе метанола: 2 — образцы, полученные в растворе воды



Рис. 5. Зависимость теплоты набухания от состава привитого сополимера.

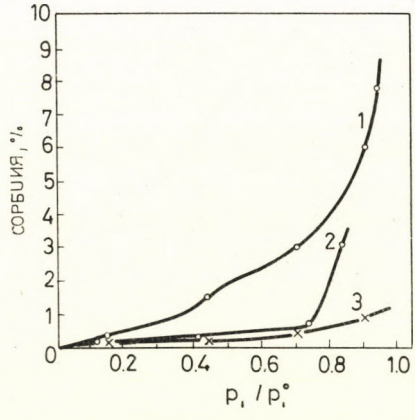

Рис. 6. Изотермы сорбции паров воды привитыми сополимерами, 1 — ПВС; 2 — 23,57% ПВП; 3 — 67,47% ПВП

Различие в теплотах набухания привитых сополимеров, имеющих близкий состав и синтезированных при разных дозах облучения, было незначительным, очевидно вследствие небольших тепловых эффектов, сопровождающих процесс набухания. В том случае, когда содержание ПВП в сополимере повышалось, теплота набухания (рис. 5) уменьшалась по сравнению с исходным ПВС. Такая же картина наблюдается и в изменении сорбции паров воды (рис. 6) привитыми сополимерами, т. е. имеет место определенная корреляция данных по теплотам набухания в воде и сорбции паров воды привитыми сополимерами.

SUMMARY

It has been shown that in the presence of water or methanol in the reaction mixture the ratio of components in the copolymer changes, and the dependence of $D_{PVP}(1596\ cm^{-1})/(D_{PVA}(1100\ cm^{-1})$ on the irradiation dose in methanol is smoother than in water.

The possibility of quantitative determination of poly(vinylpyridine) in its copolymer with poly(vinyl alcohol) by means of IR spectroscopy has been demonstrated.

Studies on the solubility, swelling and the density of PVA—PVP graft copolymers have revealed that in the course of radiation chemical copolymerization the macromolecules undergo structuration to a degree increasing with increasing irradiation dose.

It has been shown that, in addition to the chemical composition and irradiation dose, the density of graft copolymers depends also on the nature of solvent used in the synthesis.

ЛИТЕРАТУРА

1. Cordier, P.: J. chim. phys. et phys.-chim. biol. **64,** 423 (1967)
2. Jozefowicz, J., Dannon, J.: J. chim. phys. et phys.-chim. biol. **65,** 1742 (1968)
3. Ташмухамедов, С. А., Усманов, Х. У., Тиллаев, Р. С.: Высокомолек. соед., (А) **10,** 379 (1968).
4. Ташмухамедов, С. А., Усманов, Х. У., Тиллаев, Р. С.: Высокомолек. соед., (А) **10,** 1303 (1968).
5. Ташмухамедов, С. А., Усманов, Х. У., Тиллаев, Р. С.: Известия ВУЗ, Химия и хим. технология. т. 12, вып. **4,** 490 (1969).
6. Ташмухамедов, С. А., Карабаев, А. Ш., Тиллаев, Р. С., Усманов, Х. У.: Узб. хим. **4,** 78 (1969).
7. O'Connor, R. T., Du Pre, E. F., Ma Call, E. R.: Analyt. Chem. **29,** 998 (1957)
8. Krimm, S., Liang, C. Y., Sutherland, G. B. B. M.: J. Polym. Sci. **22,** 227 (1956)
9. Tadokoro, H., Seki, S., Nitta, I.: J. Chem. Phys. **23,** 1351 (1955)
10. Бондарева, Л. В., Жандарева, З. А., Михайлов, Н. В., Токарева, Л. Г., Шаблигин, М. В.: Спектроскопия полимеров. Сб. докл. Всесоюзн. симпозиум по спектроскопическим методам иссл. структ. полимеров. Киев, 1968, стр. 154.
11. David, C., Verhasselt, A., Geuskens, G.: J. Polym. Sci. **16,** 2181 (1967)
12. Химические реакции полимеров, т. 2, 1967, стр. 118, М., изд-во «Мир».

С. А. ТАШМУХАМЕДОВ
П. П. ЛАРИН
А. Ш. КАРАБАЕВ
Ш. А. АЗИЗОВ
Р. С. ТИЛЛАЕВ
Х. У. УСМАНОВ

(СССР, Ташкентский Государственный университет им. В. И. Ленина)

Acta Chimica Academiae Scientiarum Hungaricae, Tomus 74 (4), pp. 461—470 (1972)

RECHERCHES DANS LE DOMAINE DES POLYPHÉNYLACÉTYLÈNES DE POLYCONDENSATION (II)

CR. SIMIONESCU et S. VASILIU

(Inst. Polytechnique, Jassy, Roumanie)

Réçu le 14 Septembre, 1971

Une étude systématique a été effectuée sur [14] dérivés halogénures en vue d'établir leur activité catalytique dans la réaction de polycondensation du phénylacétaldéhyde donnant des polyphénylacétylènes à structure régulière.

La conversion de la phénylacétaldéhyde varie avec la nature du catalyseur, ce qui permet d'établir la série de l'activité catalytique suivante: $SnCl_4 > ZnCl_2 > BF_3 > > SbCl_5 > FeCl_3 > TiCl_4 \approx HgCl_2 > AlCl_3 > SnCl_2 > CoCl_2 > NiCl_2 > MgCl_2 > CdCl_2$.

Les polymères synthésisés possèdent des poids moléculaires élevés par rapport aux polyphénylcétylènes de polymérisation. On a envisagé aussi l'influence du catalyseur sur le degré moyen de polycondensation.

Les déterminations de la structure des polyphénylacétylènes de polycondensation ont été effectuées par voie chimique aussi que par spectroscopie IR, ce qui nous a conduit à la configuration *trans*-alcénique de ces polymères.

Les propriétés électrophysiques envisagés par des spectres RPE et par la détermination de la conductibilité électrique et celle de l'énergie d'activation situent les polyphénylacétylènes de polycondensation dans le domaine des polymères semiconducteurs de propriétés satisfaisantes (10^{15}—10^{19} spin/g, $\sigma = 10^{-15}$—10^{-12} Ω^{-1} cm^{-1}, $E_A = 0{,}98$—$2{,}1$ eV).

L'analyse thermique différentielle montre, que les polyphénylacétylènes obtenus par la polycondensation du phénylacétaldéhyde sont des polymères à stabilité thermique remarquable.

Dans une note antérieure [1], nous avons présenté quelques résultats sur la polycondensation du phénylacétaldéhyde en présence du chlorure de zinc. (et réaction a été effectuée pour obtenir des polyphénylacétylènes à structure régulière.

On continue ces recherches en vue d'envisager la possibilité d'utiliser d'autres halogénures métalliques dans la réaction de polycondensation des composés carbonyliques. Ces résultats obtenus que nous allons présenter ici permettent de tirer certaines conclusions se rapportant à l'activité catalytique de ces halogénures.

Selon V. A. KARGIN et ses collaborateurs, il est possible d'obtenir certaines polymères acétyléniques en chauffant l'acétyladéhyde, l'acétone ou l'acétophénone avec $ZnCl_2$, $BeCl_2$ et $TiCl_4$ [2, 3].

Nos recherches ont traité l'activité catalytique des halogénures suivants: $MgCl_2$, $ZnCl_2$, $CdCl_2$, $HgCl_2$, BF_3, $AlCl_3$, $SnCl_2$, $SnCl_4$, $TiCl_4$, $SbCl_5$, $FeCl_3$, $CoCl_2$ et $NiCl_2$.

Les conclusions concernant l'activité de ces halogénures dans la réaction de polycondensation du phénylacétaldéhyde ont été tirées de l'étude de la structure et des propriétés électrophysiques des polymères synthétisés.

Pour les halogénures hydratés, le procédé de déshydratation par chauffage dans l'atmosphère de chlore a été suivi, conformément aux indications des données bibliographiques. Par cette manière, on a obtenu les chlorures anhydres de magnésium [4], de cadmium [5], le chlorure stanneux [6], le chlorure de cobalt [7] et de nickel [8].

Les mêmes conditions expérimentales ont été utilisées, que dans le cas du chlorure de zinc. Les polycondensations ont été ainsi réalisées par le procédé de bloc, travaillant en tube fermé, dans l'atmosphère d'azote, dans une concentration de 0,2 mole halogénure/mole monomère, à la température de 230 °C; la durée de réaction étant 18 heures.

Pour purifier les polyphénylacétylènes synthésisés ils ont été dissous dans le benzène et précipités après par l'alcool méthylique.

Les degrés de la conversion pour la polycondensation du phénylacétaldéhyde avec plusieurs catalyseurs (même concentration, température, et durée de réaction), sont rassemblés dans le Tableau I.

Tableau I

No crt.	Catalyseur	Conversion %
1	$SnCl_4$	94,25
2	$ZnCl_2$	93,06
3	BF_3	90,74
4	$SbCl_5$	89,00
5	$FeCl_3$	80,71
6	$TiCl_4$	67,54
7	$HgCl_2$	66,97
8	$AlCl_3$	62,38
9	$SnCl_2$	53,45
10	$CoCl_2$	49,21
11	$NiCl_2$	42,00
12	$MgCl_2$	38,79
13	$CdCl_2$	12,07

Le Tableau montre l'activité catalytique suivante: $SnCl_4 > ZnCl_2 > BF_3 > SbCl_5 > FeCl_3 > TiCl_4 \approx HgCl_2 > AlCl_3 > SnCl_2 > CoCl_2 > NiCl_2 > MgCl_2 > CdCl_2$.

La polycondensation du phénylacétaldéhyde se déroule selon le mécanisme classique des réactions protoncatalysées de condensation, spécifique aux combinaisons carbonyliques. L'activité catalitique des halogénures se traduit par la formation des complexes de coordination avec les monomères

carbonyliques. Cette propriété s'ensuit de l'augmentation de la réactivité du groupe carbonyl et du détachement des hydrogènes devenus labiles du C_α. Il se forme ainsi des carbanions actifs qui initient le processus de polycondensation, avec la formation intermédiaire des composés aldoliques, d'après le schéma suivant:

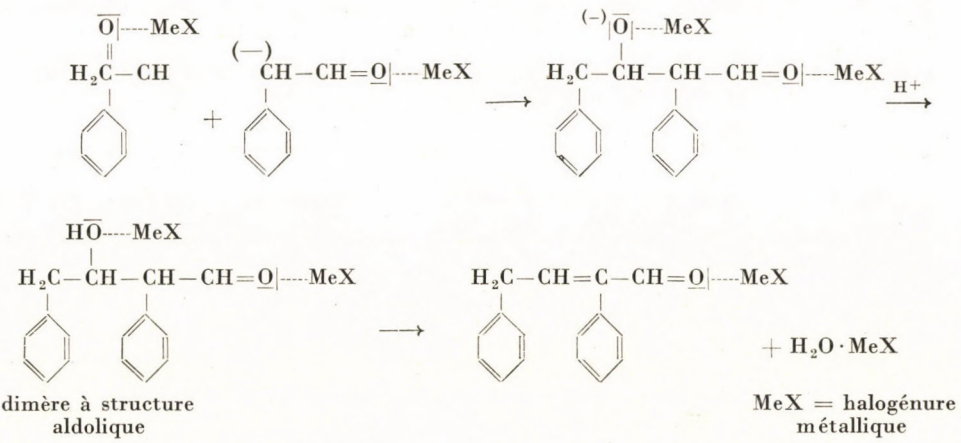

L'halogénure hydraté, qui se forme dans la réaction n'est pas stable et se décompose refaisant le sel libre, capable d'activer de nouveau le monomère. La réaction continue sur le compte des carbanions complexés en réalisant l'augmentation de la chaîne d'hydrocarbure avec une structure polyénique conjuguée.

Les résultats confirment l'efficacité des halogénures métalliques dans le processus de la polycondensation et présentent de nouvelles possibilités de l'utilisation de ces catalyseurs.

Les polyphénylacétylènes synthétisés sont complètement solubles dans les solvents organiques habituels: benzène, toluène, chloroforme, acétone, diméthylformamide et insolubles dans les alcools, pétrole éther, l'eau, les hydrocarbures normales.

Les polymères se présentent en forme de poudres. Leurs couleurs varient du jaune pâle au marron foncé, selon la nature du catalyseur. Les températures de fusion se trouvent dans l'intervalle de 78°—185 °C (Tableau II).

Afin d'établir la structure des polyphénylacétylènes de polycondensation, on a déterminé premièrement leurs poids moléculaires moyens. Par cette manière, l'influence du catalyseur sur le degré moyen de polycondensation pouvait être étudiée. Les déterminations ont été effectuées par cryoscopie, dans le benzène. Les données sont consignées dans le Tableau III.

On constate, que dans les réactions catalysées par $SnCl_4$, $HgCl_2$, $ZnCl_2$, $SbCl_2$, $CoCl_2$, BF_3, $TiCl_4$, $AlCl_3$ et $SnCl_2$ le degré moyen de polycondensation

Tableau II

Certaines caractéristiques des polyphénylacétylènes de polycondensation

No crt.	Catalyseur	Couleur du polymère	Température de fusion, °C
1	$SnCl_4$	marron foncé	185
2	$ZnCl_2$	jaune pâle	138
3	BF_3	jaune intense	126
4	$SbCl_5$	marron	135
5	$FeCl_3$	marron foncé	148
6	$TiCl_4$	jaune intense	140
7	$HgCl_2$	marron foncé	160
8	$AlCl_3$	jaune pâle	121
9	$SnCl_2$	jaune intense	137
10	$CoCl_2$	jaune	84
11	$NiCl_2$	jaune	79
12	$MgCl_2$	jaune	80
13	$CdCl_2$	jaune	78

Tableau III

No crt.	Catalyseur	Degré moyen de polycond.	Calculé %		Trouvé %			
			C	H	C		H	
1	$SnCl_4$	15	93,02	5,94	92,81	93,00	5,52	5,66
2	$HgCl_2$	15	93,02	5,94	92,47	92,87	5,33	5,17
3	$ZnCl_2$	14	92,94	5,94	91,67	92,34	5,61	5,38
4	$SbCl_5$	13	92,85	5,95	92,46	91,90	5,26	5,85
5	$CoCl_2$	10	92,48	5,97	88,94	89,37	5,50	5,56
6	BF_3	9	92,30	5,98	90,25	92,14	5,36	5,40
7	$TiCl_4$	9	92,30	5,98	91,50	92,20	5,64	5,50
8	$AlCl_3$	9	92,30	5,98	89,33	90,00	5,78	5,23
9	$SnCl_2$	9	92,30	5,98	91,33	92,10	5,66	5,82
10	$FeCl_3$	8	92,08	5,99	91,81	92,04	5,86	5,37
11	$MgCl_2$	7	91,80	6,01	90,50	90,71	5,80	5,93
12	$NiCl_2$	5	90,90	6,06	90,02	90,84	6,01	5,81
13	$CdCl_2$	5	90,90	6,06	89,42	89,98	5,61	5,87

varie entre 9 et 15, valeurs comparables à celles, obtenus par Paushkin dans la polycondensation de l'acétylferrocène [9, 10, 11].

Pour les quatre halogénures suivants: $FeCl_3$, $MgCl_2$, $NiCl_2$ et $CdCl_2$, le degré moyen de polycondensation est de même ordre de grandeur, que celui

des polymères phénylacétylèniques, obtenus dans les réactions de polymérisation [12, 13, 14].

Ces résultats, ainsi que ceux de l'analyse chimique (Tableau III) et des spectres IR sont en bonne corrélation, confirmant la structure attribuée à ces polymères. Les polyphénylacétylènes obtenus du phénylacétaldéhyde par polycondensation ont des structures régulières, ayant des groupes méthyléniques et carbonyls aux extrémités de la chaîne macromoléculaire:

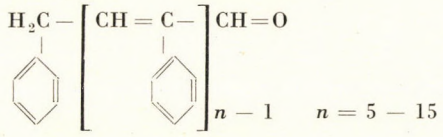

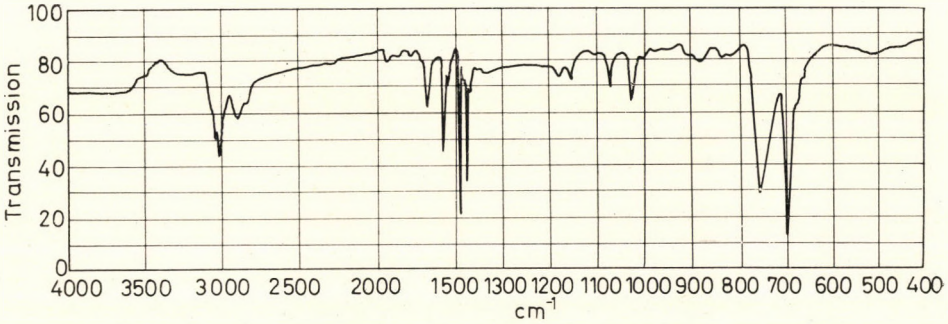

Fig. 1. Spectre infrarouge des polyphénylacétylènes de polycondensation

Les spectres IR ont été enregistrés par un spectrophotomètre de type Perkin — Elmer, en KBr.

On constate que tous les spectres sont identiques, confirmant, que la nature du catalyseur n'influence pas la structure.

Dans les spectres apparaissent toutes les absorptions caractéristiques au noyau benzènique monosubstitué. Ainsi remarque-t-on dans la région 3020 — 3080 cm^{-1} les bandes d'absorption des vibrations, ν_{AR}(C—H), la bande de 3020 cm^{-1} étant fondamentale.

Entre 690—750 cm^{-1} on remarque les bandes de ν_{AR}(C—H) correspondant aux atomes d'hydrogène, restés dans le noyau substitué.

Les bandes se trouvant entre 1440 cm^{-1} et 1590 cm^{-1} sont attribuées aux vibrations de ν_{AR}(C—C). Les absorptions de 1440 cm^{-1} et 1490 cm^{-1} sont dues à la scission de la vibration doublement dégenérée à une fréquence de 1485 cm^{-1}, spécifique au noyau benzènique. Cette scission est caractéristique aux composés monosubstitués. Elle est déterminée par la disparition de la symétrie moléculaire [15].

Les bandes de ce domaine indiquent aussi la conjugaison du noyau aromatique avec les liaisons C=C du systhème conjugué ouvert et avec le groupement C=O. Cette conjugaison entraîne l'augmentation de l'intensité de la bande située à 1570 cm^{-1} [15].

Par suite de cette conjugaison, les vibrations de valence νC=C du système conjugué aliphatique et les vibrations de la liaison =CH vinylique se superposent à celle du noyau aromatique.

Le group carbonyl qui se trouve à l'extrémité de la chaîne macromoléculaire s'identifie par la vibration νC=O (1680—1700 cm^{-1}) et par la vibration

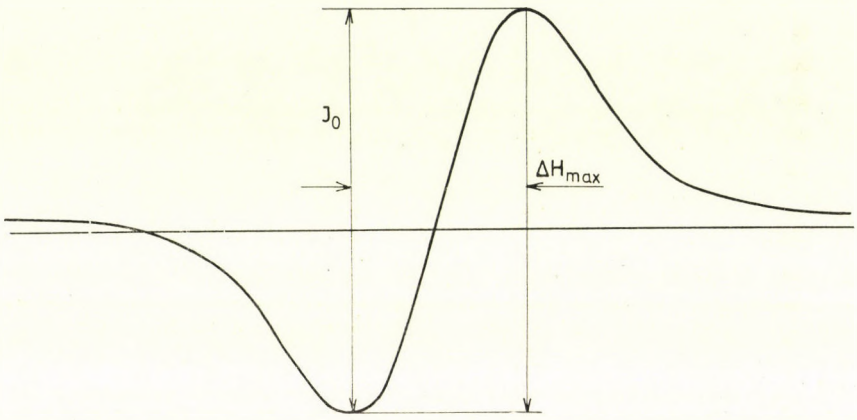

Fig. 2. Spectre RPE des polyphénylacétylènes de polycondensation

de la liaison νCH de l'aldéhyde de 2900 cm^{-1}. De même, la vibration des liaisons νCH du groupement CH_2 terminal se situe à la même fréquence (2900 cm^{-1}), les bandes respectives se superposant.

Les Spectres IR permettent aussi de tirer certaines conclusions relatives à la configuration stérique des polyphénylacétylènes de polycondensation, grâce aux bandes d'intensité moyenne de 1150—1170 cm^{-1}, caractéristiques aux vibrations de déformation dans le plan de la liaison C—H trans-alcéniques [15]. On attribue ainsi aux polyphénylacétylènes de polycondensation une structure transalcénique.

Les polyphénylacétylènes peuvent être considérés comme des polymères semiconducteurs.

Afin de caractériser *la structure électronique et les propriétés semiconductrices* on a enregistré des spectres RPE. Ils sont en corrélation avec les résultats montrant la variation de la conductibilité électrique avec la température.

Les spectres RPE ont été enregistrés par un spectromètre de type E—12 EPR VARIAN, U.S.A. Pour toutes les preuves, les spectres RPE présentent un signal étroit, symétrique, de type singlette sans structure hyperfine.

La concentration de spin a été déterminée par comparaison avec l'étalon de graphite, ayant une concentration de $3 \cdot 10^{15}$ spin/g et utilisant la méthode de la double intégration graphique des surfaces. Les données traitant du paramagnétisme des polyphénylacétylènes de polycondensation sont consignées dans le Tableau IV.

Tableau IV

Tableau synoptique des caractéristiques électrophysiques des polyphénylacétylènes de polycondensation selon la nature du catalyseur

No crt.	Catalyseur	Spectres RPE		Conductibilité spécifique ohm^{-1} cm^{-1}	Energie d'activation eV
		spin/g	ΔH_{max} (gauss)		
1	$SnCl_4$	1,631 10^{18}	8,76	2,4 10^{-13}	1.5
2	$ZnCl_2$	2,686 10^{19}	8,3	1,4 10^{-13}	1,41
3	BF_3	2,296 10^{19}	8,8	8,0 10^{-15}	1,26
4	$SbCl_5$	1,846 10^{18}	8,9	2,0 10^{-12}	1,32
5	$FeCl_3$	1,640 10^{18}	8,25	1,0 10^{-14}	1,75
6	$TiCl_4$	6,994 10^{16}	7,25	4,17 10^{-14}	1,4
7	$HgCl_2$	1,56 10^{18}	8,2	4,0 10^{-15}	2,1
8	$AlCl_3$	5,80 10^{18}	7,5	1,3 10^{-14}	1,77
9	$SnCl_2$	9,55 10^{18}	8,8	1,13 10^{-13}	1,27
10	$CoCl_2$	1,02 10^{18}	6,3	2,1 10^{-14}	1,46
11	$NiCl_2$	7,30 10^{15}	9,2	2,51 10^{-14}	1,12
12	$MgCl_2$	4,63 10^{15}	8,8	9,09 10^{-14}	0,98

On remarque, que les produits se trouvent dans le domaine des polymères semiconducteurs, pour lesquels les spectres RPE présentent un contenu de 10^{15}—10^{22} spin/g [16]. Vers la limite inférieure de ces valeurs se situent les polyphénylacétylènes obtenus avec $NiCl_2$ et $MgCl_2$.

La conductibilité électrique a été déterminée par la mesure de la résistance électrique dans l'intervalle de température 23°—149 °C sur des tablettes comprimées, faites aux pressions d'approximativement 10 t/cm^2. Les résultats obtenus indiquent que la loi exponentielle des semiconducteurs est respectée: $\sigma = \sigma_0 \cdot e^{(-\Delta E/2kT)}$.

On a déterminé dès courbes $\log \sigma = f(1/T)$. Les valeurs de l'énergie d'activation ont été comparées aux résultats obtenus par la méthode RPE, en vue d'établir la corrélation entre la concentration en spin et la conductibilité électrique du polymère. Les valeurs de la conductibilité spécifique et de l'énergie d'activation sont consignées dans le Tableau IV.

On observe en général que, aux concentrations de spin relativement faibles correspondent des énergies d'activation plus élevées et inversement, ce qui prouve qu'il y a un rapport direct entre le nombre des électrones libres et

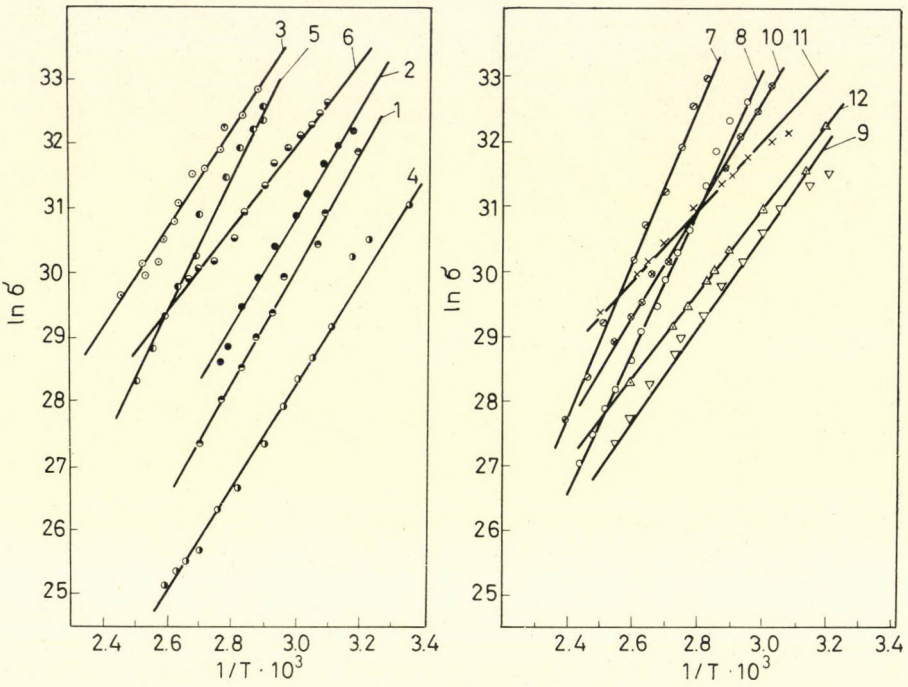

Fig. 3. Variation de la conductibilité électrique avec la température selon la nature du catalyseur 1 — $SnCl_4$; 2 — $ZnCl_2$; 3 — BF_3; 4 — $SbCl_5$; 5 — $FeCl_3$; 6 — $TiCl_4$; 7 — $HgCl_2$; 8 — $AlCl_3$; 9 — $SnCl_2$; 10 — $CoCl_2$; 11 — $NiCl_2$; 12 — $MgCl_2$

la conductibilité électrique. Selon les valeurs obtenus ($\sigma = 10^{-15}$—10^{-12} $\Omega^{-1} \cdot cm^{-1}$), les polyphénylacétylènes de polycondensation que nous avons étudiés se classent parmi les polymères semiconducteurs de caractéristiques satisfaisantes.

Pour faire la comparaison, nous présentons un tableau comprenant les caractéristiques électrophysiques de polyphénylacétylènes obtenus par divers auteurs. (Tableau V.)

Pour caractériser *les propriétés thermiques*, on a enregistré les stabilités des polymères obtenus, dans l'intervalle de température 20°—900 °C. Les en-

Tableau V

Auteur	RPE spin/g	σ ohm^{-1} cm^{-1}	E_A (eV)
Okamoto [17]	—	10^{-16}	0,48
Schantarowich [14]	10^{17}—$3 \cdot 10^{19}$	—	—
Berlin [18—20]	$2{,}4 \cdot 10^{17}$—$3{,}4 \cdot 10^{19}$	$3 \cdot 10^{-19}$—$3 \cdot 10^{-16}$	1,1—1,4
Simionescu, Cr., Dumitrescu, Sv. [12]	10^{16}—10^{17}	10^{-10}—10^{-13}	0,189—0,055
Nos propres données	10^{15}—10^{19}	$4 \cdot 10^{-15}$—$2 \cdot 10^{-12}$	0,98—2,1

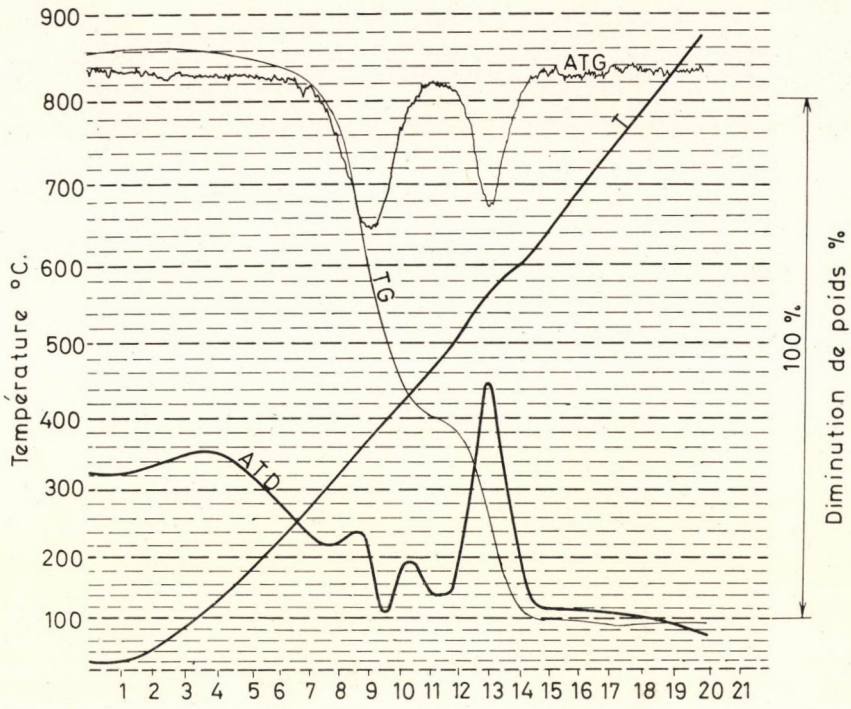

Fig. 4. Courbes d'analyse thermique differentielle du polyphénylacétylène de polycondensation

registrements ont été effectués par un appareil de type PAULIK F., PAULIK J., ERDEY L., MOM Budapest.

Les polyphénylacétylènes de polycondensations présentent une stabilité thermique remarquable, les pertes de poids ne commencent qu'à partir de 230°—320 °C.

Dans le processus de thermodestruction deux plus importantes étapes apparaisent qui se situent dans les domaines suivants:

Ire étape: 230—512 °C

IIe étape: 435—820 °C

Pour les deux étapes la cinétique de la destruction a été étudiée à l'exception des polymères obtenus en présence de $SnCl_4$ et $SbCl_5$ pour lesquels on n'a pu étudier que la deuxième phase du processus destructif. Les paramètres cinétiques ont été calculés par la méthode FREEMAN—CARROL [21].

Les données de l'analyse thermique différentielle sont consignées dans le Tableau VI.

Pour la Ire étape l'ordre de réaction est compris entre 0,4—0,9, et l'énergie d'activation entre 17—35 kcal/mole.

Pour ce qui est de la IIe étape, qui se situe dans le domaine des températures élevées, elle est caractérisée par un puissant effet exothermique.

Tableau VI

Les données de l'analyse thermique différentielle

No crt.	Catalyseur	Ire Etape				IIe Etape			
		Temp. °C	Pertes %	Ordre de réact.	Energie d'activ. (kcal/mole)	Temp. °C	Pertes %	Ordre de réact.	Energie d'activ. (kcal/mole)
1	$SnCl_4$	320—512	22,50	—	—	512—820	70	1,2	68,32
2	$ZnCl_2$	240—484	48,43	0,9	35,00	484—723	51,57	1	55,27
3	BF_3	244—440	22,84	0,7	29,38	440—700	57,36	1	44,26
4	$SbCl_5$	296—470	12,50	—	—	470—693	80,25	1	59,46
5	$FeCl_3$	260—456	20,60	0,6	22,29	456—726	75,88	1,7	37,20
6	$TiCl_4$	285—450	25,77	0,6	17,41	450—716	62,88	1	24,14
7	$HgCl_2$	264—470	23,23	0,8	21,18	470—740	70,20	1,7	32,51
8	$AlCl_3$	260—477	33,18	0,4	23,03	477—698	66,72	1,3	43,98
9	$SnCl_2$	275—435	18,46	0,8	26,11	435—730	71,75	0,9	29,38
10	$CoCl_2$	248—460	35,78	0,9	28,97	460—664	59,00	1	65,12
11	$NiCl_2$	234—480	59,47	0,9	24,11	480—540	33,63	0,8	56,74
12	$MgCl_2$	230—480	59,57	0,9	21,78	480—638	29,25	1	77,01

L'ordre de réaction varie entre 0,8—1,7 et l'énergie d'activation est de 24—77 kcal/mole.

BIBLIOGRAPHIE

1. Simionescu, Cr., Vasiliu, S.: Plaste und Kautschuk **4**, 260 (1971)
2. Kargin, V. A., Kabanov, V. A., Zubov, V. P.: Ger., **1**, 162, 080 (1960)
3. Kargin, V. A., Kabanov, V. A., Zubov, V. P., Papisov, I. M., Kurochkina, G. I.: Dokl. Akad. Nauk SSSR, **140**, 1, 122 (1961)
4. Treadwell, Zürrer: Helv. Chim. Acta **15**, 1276 (1932)
5. Pascal, P.: Traité de chimie minérale VII, 257 (1932)
6. Pascal, P.: Nouveau traité de chimie minérale VIII, 361 (1963)
7. Bose, Khundkar: J. Indian Chem. Soc. Ind. News **14**, 39 (1951)
8. Pascal, P.: Nouveau traité de chimie minérale XVII, 216 (1963)
9. Paushkin, Ya. M. et collab.: Dokl. Akad. Nauk SSSR, **149**, 856 (1963)
10. Paushkin Ya. M. et collab.: Vîsokomolek. soed., **6**, 545 (1964)
11. Paushkin Ya. M. et collab.: J. Polym. Sci., 4, 1481 (1964)
12. Simionescu, Cr., Dumitrescu, Sv.: European Polymer Journal **6**, 635 (1970)
13. Simionescu, Cr., Dumitrescu, Sv.: Die Makromolekulare Chemie **136**, 47 (1970)
14. Shantarowich, P. S.: Vîsokomolek. soed. **3**, 1495 (1961)
15. Avram, M., Mateescu, Gh.: Spectroscopia în infraroșu. Aplicații în chimia organică, Bucarest (1966)
16. Charentenay, F. X., Castel, P., Teyssié, Ph.: Rev. Inst. franç. Pétrole Ann. Combustibles liquides **13** (**9**), 1270 (1963)
17. Okamoto, J. et collab.: Chem. and Ind. 2004 (1961)
18. Berlin, A. A. et collab.: J. Polymer Sci. **55**, 621 (1961)
19. Berlin, A. A. et collab.: Vîsokomolek. soed. **1**, 1361 (1959)
20. Berlin, A. A. et collab.: Vîsokomolek. soed. **1**, 1817 (1959)
21. Freeman E. S., Carrol, B.: J. Phys. Chem. **62**, 394 (1958), J. Polymer Sci. **54**, 259 (1961),

Cr. Simionescu
S. Vasiliu
Jassy, str. Universitatii nr. 16. Roumanie.

Acta Chimica Academiae Scientiarum Hungaricae, Tomus 74 (4), pp. 471—478 (1972)

STEREOCHEMICAL STUDIES, XI*
STUDIES ON CYCLIC 2-HYDROXYCARBOXYLIC ACIDS, II**

SYNTHESIS OF *CIS*- AND *TRANS*-2-HYDROXYCYCLOPENTANECARBOXYLIC ACID AND *CIS*- AND *TRANS*-2-HYDROXYCYCLOHEPTANECARBOXYLIC ACID

G. BERNÁTH, GY. GÖNDÖS, P. MÁRAI and L. GERA

(Institute of Organic Chemistry, A. József University, Szeged)

Received September 14, 1971

Catalytic reduction of 2-carbethoxycyclopentanone (**V**) with Raney nickel catalyst in ethanol as well as reduction with sodium borohydride and subsequent fractional distillation of the resulting *cis*- and *trans*-2-carbethoxycyclopentanol (**VI, VII**) gave gas-chromatographically homogeneous products.

The analogous reductions of 2-carbethoxycycloheptanone (**XIII**) yielded a mixture of *cis*- and *trans*-2-carbethoxycycloheptanol (**XIV, XV**) as shown by gas-chromatographical and preparative evidence, contrary to a recent publication [13] according to which the product of these reactions was stereohomogeneous *cis*-2-carbethoxycycloheptanol (**XIV**). The *cis*- and *trans*-isomers (**XIV, XV**) were successfully separated by fractional distillation.

In the course of our studies [1–4] on the stereochemistry and conformational problems of common-membered alicyclic systems and aiming at the elucidation of the mechanism of some reactions of cyclic aminoalcohols and related compounds, well reproducible syntheses of *cis*- and *trans*-cyclopentanol-2-carboxylic acid (**I, II**) and of *cis*- and *trans*-cycloheptanol-2-carboxylic acid (**III, IV**) were required, suitable for the preparation of larger quantities of these compounds. The synthesis of the related *cis*- and *trans*-1-tetralol-2-carboxylic acid was reported earlier [5, 6].

The synthesis of *cis*- and *trans*-2-carbethoxycyclopentanol (**VI, VII**) and *cis*- and *trans*-cyclopentanol-2-carboxylic acid (**I, II**), as well as the determination of their configurations was achieved by PASCUAL and CASTELLS [7]. A mixture of *cis*- and *trans*-2-carbethoxycyclopentanol (**VI, VII**) obtained by catalytic reduction of 2-carbethoxycyclopentanone (**V**) with Adams PtO_2 catalyst was separated by a tedious fractional crystallization of their 3,5-dinitrobenzoates. In our experience this method, which, according to recent literature data [8] has been in current use, is time-consuming and gives very poor yields, especially of the *trans* isomer isolated from the mother liquors. Recently MÖHRLE and BAUMANN elaborated a continuous countercurrent distribution method for the separation of *cis*- and *trans*-2-carbethoxycyclo-

* Part X: BERNÁTH, G., LÁNG, K. L., KOVÁCS, K., RADICS, L.: Acta Chim. Acad. Sci. Hung. **73**, 81 (1972)

** As Part I of this Series is regarded: BERNÁTH, G., SOHÁR, P., LÁNG, K. L., TORNYAI, I., KOVÁCS, Ö. K. J.: Acta Chim. Acad. Sci. Hung. 64, 81 (1970)

pentanol [9]. For the preparation of stereohomogeneous **VI** and **VII** in larger quantities, it proved more suitable to separate the mixture of *cis*- and *trans*-2-carbethoxycyclopentanol, obtained by catalytic or sodium borohydride reduction of 2-carbethoxycyclopentanone (**V**), by means of an efficient fractionating column. Reduction with Raney nickel catalyst in ethanol solution at 60 °C and 120 atm. initial pressure gave a product containing 87.3% *cis*- and 12.7% *trans*-2-carbethoxycyclopentanol (Fig. 1). More *trans* isomer was formed in the sodium borohydride reduction of **V** at low temperatures; in

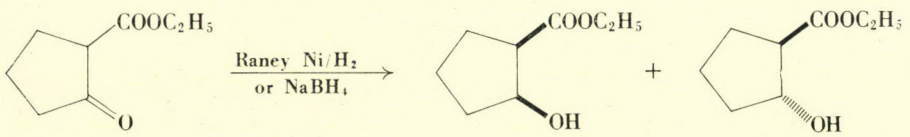

V **VI** **VII**

Fig. 1

ethanolic solution at —65 °C the **VI** : **VII** ratio was 34.7 : 65.3. We found a similar change of the *cis* : *trans* isomer ratio in the reduction of 2-carbethoxy-4-*t*-butylcyclopentanone with sodium borohydride [10]: the ratio of isomers containing the hydroxyl and carbethoxyl functions in *trans* position increased with decreasing temperature. The reduction of 2-carbethoxycyclopentanone (**V**) with sodium borohydride has also been made by LACASA and PASCUAL [11]. The reaction gave, however, mainly *trans*-2-hydroxycyclopentane carboxylic acid instead of *cis*- and *trans*-2-carbethoxycyclopentanol.

The isomer ratio of the reduction of 2-carbethoxycyclopentanone (**V**) with Raney nickel, potassium borohydride and Adams PtO_2 catalyst was studied by PASCUAL and VIÑAS [12]. The *cis* : *trans* ratio was determined by separation of the 3,5-dinitrobenzoates by fractional crystallization, or by comparing the melting points of the crude 3,5-dinitrobenzoates with a melting point diagram prepared with different mixtures of pure, authentic *cis*- and *trans*-2-carbethoxycyclopentanol dinitrobenzoates. The results obtained include, however, some uncertainties resulting from this approach.

Fractional distillation on a column of high efficiency of the mixtures of *cis*- and *trans*-2-carbethoxycyclopentanols (**VI, VII**) obtained in our reduction processes gave gas-chromatographically homogeneous *cis*- and *trans*-2-carbethoxycyclopentanol.

Interestingly, while both *cis*-cyclohexanol-2-carboxylic acid (**X**) and *cis*-cyclopentanol-2-carboxylic acid (**III**) can be isomerized by prolonged refluxing with concentrated sodium hydroxide or potassium hydroxide solution, and the *trans* isomers can be recovered from the equilibrium mixture in good yields

[13, 14], *cis*-cyclopentanol-2-carboxylic acid (**I**) undergoes dehydration under similar conditions [15] giving cyclopentene-1-carboxylic acid (**IX**) (Fig. 2). Therefore, alkaline isomerization cannot be used for the preparation of *trans*-cyclopentanol-2-carboxylic acid (**II**). Ethyl cycloheptanone-2-carboxylate (**XIII**) was obtained by PALAU, PASCUAL and RÁFOLS [16] by condensation of

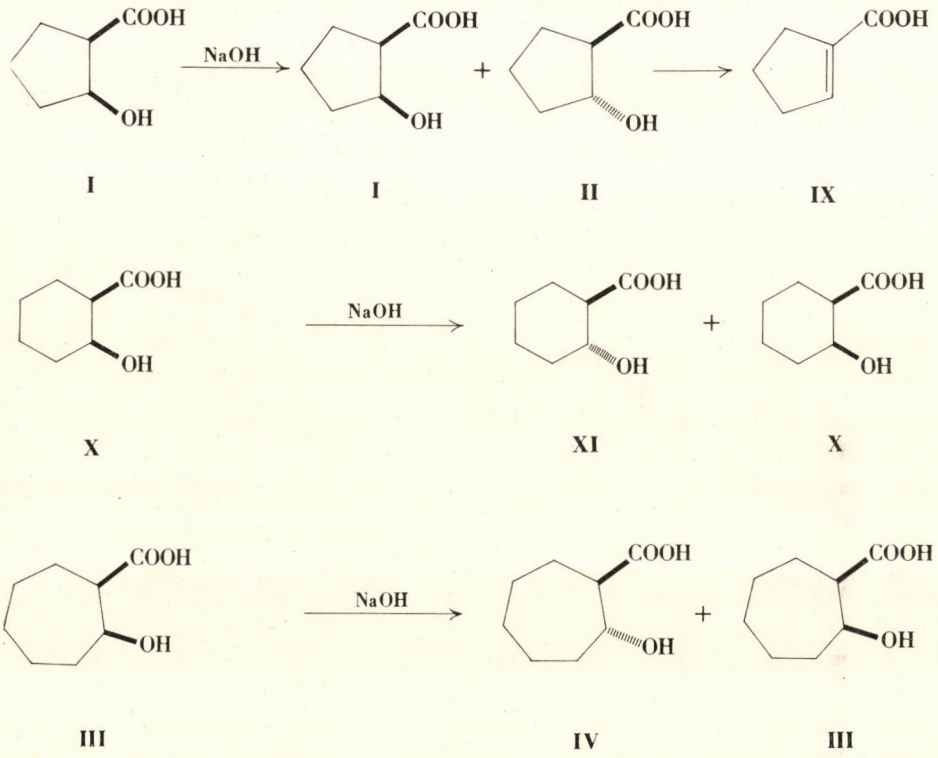

Fig. 2

cycloheptanone and diethyl oxalate in ether solution with sodium ethoxide in a yield of merely 17.4%. A better yield (73—84%) resulted from using the method of JAKOB and DEV [17, 20], condensing cycloheptanone and diethyl carbonate with sodium hydride in ethereal solution (Fig. 3). A still higher yield

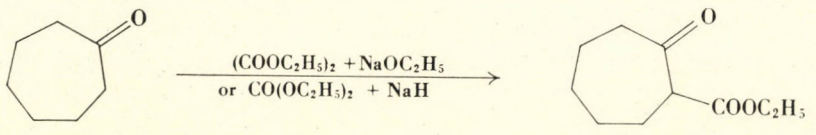

Fig. 3

(90%) was obtained by RHOADS *et al.* in 1963 [18] by condensing cycloheptanone and diethyl carbonate with sodium hydride in diethyl carbonate solution at room temperature.

We tried the condensation of cycloheptanone (**XII**) and diethyl carbonate in the presence of sodium amide as catalyst and an excess of diethyl carbonate as solvent; 61.4% 2-carbethoxycycloheptanone (**XIII**) was obtained.

Considerably higher yields than those described by PALAU, PASCUAL and RÁFOLS [16] resulted from our experiments condensing cycloheptanone and

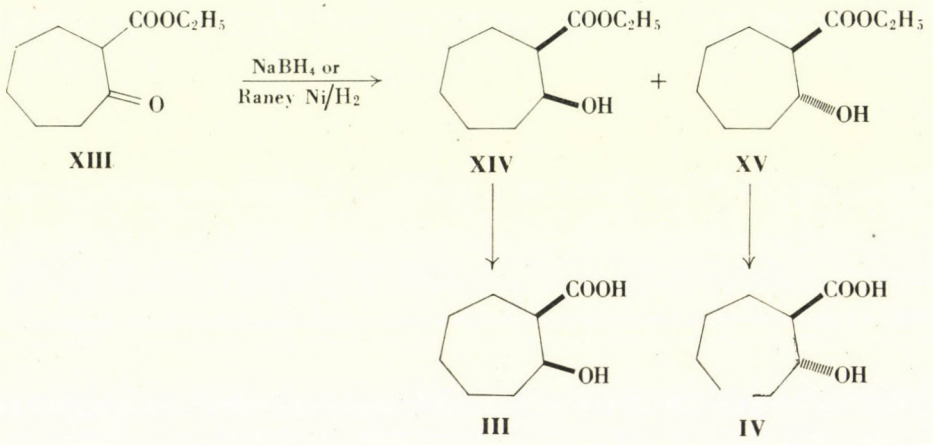

Fig. 4

diethyl oxalate in ethanolic solution with sodium ethoxide. Our yields (60.3–66.8%) slightly exceeded those obtained by a recently published and practically identical method of the Indian authors [13].

The reduction of 2-carbethoxycycloheptanone (**XIII**) was effected by PALAU, PASCUAL and RÁFOLS in ethanolic solution with PtO_2 catalyst, or in methanolic solution with sodium borohydride. The resulting mixture of *cis*- and *trans*-2-carbethoxycycloheptanol (**XIV**, **XV**) was not separated, neither was the isomer ratio determined. Pure *cis*-cycloheptanol-2-carboxylic acid (**III**) was isolated by crystallization after hydrolysis of the product of the catalytic reduction. The stereohomogeneity of the hydroxycarboxylic acids was supported by the infrared spectra. The *trans*-cycloheptanol-2-carboxylic acid (**IV**) was prepared by alkaline isomerization of the *cis*-hydroxycarboxylic acid (**III**).

In their recent paper [13], the Indian authors also deal with the synthesis of **III** and **IV** without referring to the above paper [16] of the Spanish authors. They declare the reduction product of 2-carbethoxycycloheptanone (**XIII**) obtained in ethanolic medium with sodium borohydride to be *cis*-2-

carbethoxycycloheptanol (**XIV**), but no evidence of the stereohomogeneity is given. The refractive index ($n_D^{23} = 1.4768$) of the reaction product evidently containing both *cis* and *trans* isomers (**XIV**, **XV**), is considerably higher than that found by us for ethyl *cis*- and *trans*-cycloheptanol-2-carboxylate ($n_D^{23} = 1.4705$ and $n_D^{23} = 1.4740$, respectively). They also regard the reduction product of 2-carbethoxycycloheptanone (**XIII**) made at atmospheric pressure in abs. ethanol with W–7 Raney nickel catalyst, as a homogeneous *cis* compound, affording again no proof of the stereohomogeneity.

On the analogy of the reduction of related cyclic 2-oxocarboxylates, it does not seem convincing that the catalytic or sodium borohydride reduction of 2-carbethoxycycloheptanone should result in homogeneous *cis*-2-carbethoxycycloheptanol (**XIV**). We found by gas chromatographic analysis that the reaction product of the reduction of 2-carbethoxycycloheptanone (**XIII**) in ethanolic solution with Raney nickel catalyst at 70 °C and 100 atm. starting pressure was a mixture of 85.4% *cis*- and 14.6% *trans*-2-carbethoxycycloheptanol (**XIV**, **XV**). Interestingly in this case the isomer ratio of the sodium borohydride reduction was not significantly different from that of the catalytic reduction, though with the analogous compounds having cyclopentane and cyclohexane skeleton the formation of the *trans* isomer predominated in the sodium borohydride reduction. In the reduction of 2-carbethoxycycloheptanone, the sodium borohydride method gave less *trans* isomer than the catalytic process. The same relation was observed in the reduction of 2-carbethoxycyclooctanone. Consequently, the isomer ratios in the catalytic and sodium borohydride reductions are highly dependent on the ring size.

Bhargava, Mathur and Saharia prepared *cis*-cycloheptanol-2-carboxylic acid (**III**) by the hydrolysis of the reduction product of 2-carbethoxycycloheptanone. The melting point of the acid is not given, only that of the S-benzylisothiuronium salt and of the 3,5-dinitrobenzoate was determined. They prepared the *trans*-cycloheptanol-2-carboxylic acid from the *cis* isomer by isomerization with KOH. The melting point of *trans*-cycloheptanol-2-carboxylic acid (**IV**) is 86—87 °C. This is practically in accordance with the value given earlier by Palau, Pascual and Ráfols [16] and Sanchez [21] for **IV** obtained by the same method by alkaline isomerization (87–88 °C).

By subjecting the mixture of *cis*- and *trans*-2-carbethoxycycloheptanol (**XIV**, **XV**) to fractional distillation on a column of high efficiency, we succeeded in obtaining both isomers in gas-chromatographically homogeneous purity. Mild hydrolysis of the stereohomogeneous ethyl hydroxycarboxylates gave *cis*- and *trans*-2-cycloheptanol-2-carboxylic acid (**III**, **IV**). As under the conditions of hydrolysis no isomerization can occur, the *cis*- and *trans*-cycloheptanol-2-carboxylic acids produced are undoubtedly stereohomogeneous substances (m.p. 70.5–71.0 °C and 86.5–87.5 °C, respectively).

Experimental

Cis- and *trans*-2-carbethoxycyclopentanol (VI, VII)

(*a*) 100.0 g (0.64 mole) 2-carbethoxycyclopentanone (**V**) was dissolved in 250 ml ethanol and hydrogenated in an autoclave at 60 °C in the presence of Raney nickel catalyst (35 g), washed several times with ethanol; the starting pressure was 120 atm. After the calculated quantity of hydrogen had been absorbed, the catalyst was filtered off and the solvent evaporated. According to gas chromatographic analysis, the reaction product contained 87.3% *cis-* and 12.7% *trans*-2-carbethoxycyclopentanol (**VI, VII**). (Stationary phase: polyethyleneglycol adipate 20%; column height: 2 m; diameter: 0.4 cm; temperature: 160 °C; retention time: 6 min. for **VI**, 12.5 min. for **VII**.) Three combined runs were distilled at reduced pressure. The main distillation product collected at 34–36 torr between 118–125 °C was 270.2 g (88.8%), $n_D^{24} = 1.4550$.

The separation of the *cis* and *trans* isomers was achieved using ABBEG's "Drehbandkolonne" (W. Büchi Glassware Factory, Flawil, Switzerland) of 30 theoretical plates. For separating larger quantities, a homemade column of 120 cm length, isolated by a silver-coated vacuum jacket of 10^{-3} torr, covered with asbestos string, was used. The filling of the column consisted of 0.3–0.5 mm glass filament wound up into a spiral of 5 mm diameter and broken to pieces of 1.5–2 windings. Fractions 1–18 collected at 121–124 °C and 36–37 torr (183.0 g; 67.7%; $n_D^{24} = 1.4547$–1.4551 (lit. $n_D^{25} = 1.4553$ [8])) consisted of stereohomogeneous *cis*-2-carbethoxycyclopentanol (**VI**); the combined fractions 19 and 20 (21.5 g; 7.95%) were a mixture of the *cis* and *trans* isomers (**VI, VII**) in a ratio of about 3 : 7. The distillation residue and the column washing were combined and redistillated to give 39.7 g (14.7%) stereohomogeneous *trans* isomer (**VII**). Distillation losses amounted to 26.0 g (9.65%).

(*b*) In a 2–1 three-necked round-bottomed flask equipped with a mechanical stirrer, a reflux condenser connected to a $CaCl_2$ drying tube, and a dropping funnel, 30.0 g (0.80 mole) sodium borohydride and 2 l ethanol were placed. The flask was cooled to —65 °C in a bath of acetone and solid carbon dioxide. 250 g (1.6 mole) 2-carbethoxycyclopentanone (**V**) was added dropwise to the reaction mixture, which was stirred at this temperature for further 5 hrs. and let to stand at room temperature overnight. The reaction mixture was decomposed by dropwise addition of 150 ml glacial acetic acid, diluted with water and filtered on a fluted filter paper. After evaporating the ethanol at 38–40 torr, the residue spontaneously separated to an organic and an aqueous phase. The aqueous part was extracted with 3×500 ml ether, the combined organic ethereal phases were washed twice with 5% $NaHCO_3$ solution and twice with water, then dried over anhydrous Na_2SO_4. After filtration and evaporation of the ether, the residue was fractionated at diminished pressure. The main distillation product collected between 120 and 128 °C at 36 torr was 201.1 g (79.4%) ($n_D^{25} = 1.4540$) and contained 65.3% *trans-* and 34.7 *cis*-2-carbethoxycyclopentanol (**VII, VI**).

Fractional distillation, starting with 230.0 g gave in the fractions 1 to 6 (b.p. 129–130 °C at 42 torr) 63.1 g (27.4%) stereohomogeneous *cis*-2-carbethoxycyclopentanol, $n_D^{25} = 1.4549$ (lit. $n_D^{25} = 1.4551$ [8]). Fractions 7 and 8 (36.1 g; 15.7%; b.p. 130–140 °C at 42 torr; $n_D^{25} = 1.4541$) contained the *cis* and *trans* isomers together, whereas fractions 9 to 12 (85.7 g; 37.2%; b.p. 140 °C at 42 torr, $n_D^{25} = 1.4538$; lit. $n_D^{25} = 1.4534$ [8]) consisted of stereohomogeneous *trans*-2-carbethoxycyclopentanol (**VII**). Redistillation of the combined distillation residue and column washing yielded 21.9 g (10.3%) *trans*-2-carbethoxycyclopentanol. Distillation losses amounted to 21.5 g (9.4%).

2-Carbethoxycycloheptanone (XIII)

(*a*) In a 2–1 round-bottomed flask fitted with a stirrer and reflux condenser, sodium ethoxide was prepared in 1.2 l abs. ethanol from 23.0 g (1.0 g-atom) sodium. To this ice-cool solution a mixture of 112.2 g (1 mole) cycloheptanone (**XII**) and 147.2 g (1 mole) diethyl oxalate was added dropwise in 30 min, under stirring. The mixture was stirred for 2 hrs. under ice cooling, then for further 8 hrs. at room temperature. After standing overnight and the usual [13, 19] decomposition with dil. H_2SO_4, extraction with benzene and decarbonylation, it was redistilled to obtain 110.6–123.0 g (60.3–66.8%) 2-carbethoxycycloheptanone (**XVI**), b.p. 126–128 °C at 12–13 torr (lit. 122—124 °C at 9 torr [18] and 125–126 °C at 12 torr [13]).

(*b*) 112.2 g (1 mole) cycloheptanone and 1.5 l diethyl carbonate was placed in a 4–1 three-necked round-bottomed flask provided with a stirrer and reflux condenser, and 31.0 g

(0.13 mole) sodium hydride was added cautiously, in portions, under stirring and bubbling nitrogen through the mixture. It was refluxed and stirred under a protective atmosphere of nitrogen for 3 hrs., then cooled to room temperature. 500 ml water and 1 l 18% H_2SO_4 were added dropwise under continuous stirring and cooling. The upper organic phase was separated in a separating funnel, and the excess of diethyl carbonate was distilled off at 35–40 torr. The fraction collected between 90–145 °C (142 g; 76.5%) was redistilled and the fraction boiling at 140–146 °C at 35–40 torr collected to obtain 115 g (62.1%) 2-carbethoxycycloheptanone (**XIII**), $n_D^{23} = 1.4670$ (lit. b.p. 106–107 °C at 4.5 torr, 125–126 °C at 12 torr [13] and 122–124 °C at 9 torr [18]).

$C_{10}H_{16}O_3$ (185.2). Calcd. C 65.21; H 8.69. Found C 65.56; H 9.09%.

Cis- and *trans*-2-carbethoxycycloheptanol (XIV, XV)

(*a*) 100.0 g (0.54 mole) 2-carbethoxycycloheptanone (**XIII**) in 100 ml ethanol was hydrogenated in an autoclave at 60 °C and 120 atm. initial pressure in the presence of 30 g Raney nickel catalyst washed to neutral with ethanol. After completing the hydrogenation, the catalyst was filtered off and the reaction product remaining after evaporation of the ethanol was analyzed by gas chromatography. (Column height 2 m; stationary phase: polyethyleneglycol adipate 20%; temperature 160 °C; temperature of detector 180 °C; retention times (relative to cyclohexanol): *cis*-2-carbethoxycycloheptanol (**XIV**): 8.4; *trans*-2-carbethoxycycloheptanol (**XV**): 11.3). The reaction product containing 85.4% *cis*- and 14.6% *trans*-2-carbethoxycycloheptanol was redistilled at diminished pressure. From three combined runs 232.0 g (76.5%) main product, b.p. 135–145 °C at 30 torr, was obtained (lit. b.p. 120–122 °C at 15 torr [13]). The yield, with the forerun and distillation residue, was nearly quantitative.

(*b*) 260 ml abs. ethanol was placed in a 750-ml three-necked round-bottomed flask equipped with a stirrer and reflux condenser, and 4.4 g (0.116 mole) sodium borohydride was added in portions under stirring, followed by the dropwise addition of a solution of 35.4 g (0.192 mole) 2-carbethoxycycloheptanone in 70 ml abs. ethanol while the flask was cooled with sodium chloride-ice mixture to −8 °C. After the addition of the oxoester, the reaction mixture was stirred at −8 to −10 °C for 2 hrs and at room temperature for further 15 hrs, then 16.5 ml acetic acid was added dropwise. After adding 300 ml water, the ethanol was distilled off at reduced pressure (35—40 torr) and the residue extracted with 3×200 ml ether. The combined ether solutions were washed until neutral with 5% $NaHCO_3$ solution, then with water, and dried over Na_2SO_4. The crude ester (25.1 g) left behind after the distillation of the ether, was distilled at reduced pressure (at 35–40 torr) to yield 19.6 g (54.8%) *cis*- and *trans*-2-carbethoxycycloheptanol (**XIV**, **XV**). Gas-chromatographic determination of the isomer ratio showed 90.4% *cis*- and 9.6% *trans*-2-carbethoxycycloheptanol content. The *cis* and *trans* isomers were separated by fractional distillation on a column of high efficiency at a rate of collection of 6–8 ml/hr. *Cis*-2-carbethoxycycloheptanol (**XIV**) had b.p. 150–151 °C at 39–40 torr, and $n_D^{23} = 1.4705$ (lit. b.p. 112–113 °C at 1.6 torr, $n_D^{23} = 1.4768$ [13]); *trans*-2-carbethoxycycloheptanol (**XV**) had b.p. 156–157 °C at 39–40 torr, $n_D^{23} = 1.4740$.

Cis-cycloheptanol-2-carboxylic acid (III)

8.0 g (0.043 mole) gas-chromatographically homogeneous *cis*-2-carbethoxycycloheptanol (**XIV**) was shaken with 100 ml 2 *N* NaOH solution at room temperature for 10 hrs. To remove contaminations, the alkaline solution was extracted with 2×100 ml ether and acidified by cautiously adding conc. HCl, then extracted with 5×200 ml ether. The combined ethereal solution was dried over Na_2SO_4 and evaporated to give 5.8 g (85.4%) *cis*-cycloheptanol-2-carboxylic acid (**III**). After repeated recrystallization from benzene the m.p. was 70.5–71 °C (lit. m.p. 71–72 °C [16], [21]).

Trans-cycloheptanol-2-carboxylic acid (IV)

From 4.0 g (0.0215 mole) gas-chromatographically homogeneous *trans*-2-carbethoxycycloheptanol (**XV**) 2.9 g (85.4%) *trans*-cycloheptanol-2-carboxylic acid (**IV**) was obtained by the method described for the *cis* isomer. After repeated recrystallization from benzene the m.p. was 86.6–87 °C (lit. m.p. 86.5–87 °C [16], 87—88 °C [21]).

*

The authors' thanks are due to REANAL Factory of Laboratory Chemicals for financial support of this work. We are indebted to Mrs. É. TOMORI (Pharmaceutical Research Institute, Budapest) for the gas-chromatographic analyses, to Miss O. CSAPÓ for taking part in some experiments, to Mrs. K. L. LÁNG and Mrs. G. BARTÓK for the microanalyses and to Miss A. VIGH for her valuable technical assistance.

REFERENCES

1. BERNÁTH, G., KOVÁCS, K., LÁNG, K. L.: Tetrahedron Letters **1968,** 2713
2. BERNÁTH, G., KOVÁCS, K., LÁNG, K. L.: Acta Chim. Acad. Sci. Hung. **65,** 347 (1970)
3. BERNÁTH, G., LÁNG, K. L., GÖNDÖS, GY., MÁRAI, P., KOVÁCS, K.: Tetrahedron Letters **1968,** 4441
4. BERNÁTH, G., LÁNG, K. L., GÖNDÖS, GY., MÁRAI, P., KOVÁCS, K.: Acta Chim. Acad. Sci. Hung. **74,** 479 (1972)
5. BERNÁTH, G., KOVÁCS, K., LÁNG, K. L.: Acta Chim. Acad. Sci. Hung. **64,** 183 (1970)
6. BERNÁTH, G., SOHÁR, P., LÁNG, K. L., TORNYAI, I., KOVÁCS, Ö. K. J.: Acta Chim. Acad. Sci. Hung. **64,** 81 (1970)
7. PASCUAL, J., CASTELLS, J.: J. Am. Chem. Soc. **74,** 2899 (1952)
8. BAUMANN, H., FRANKLIN, N. C., MÖHRLE, H.: Tetrahedron **23,** 4331 (1967)
9. MÖHRLE, H., BAUMANN, H.: Ann. **716,** 61 (1968)
10. BERNÁTH, G., SVOBODA, M.: Tetrahedron **28,** 3475 (1972)
11. LACASA, F., PASCUAL, J.: Anales real soc. españ. fís. y quím. (Madrid) **51B,** 551 (1955); C. A. **50,** 11.252g (1956)
12. PASCUAL, J., VIÑAS, J.: Bull. soc. chim. France **1960,** 1430
13. BHARGAVA, S. S., MATHUR, K. C., SAHARIA, G. S.: Indian J. Chem. **8,** 714 (1970)
14. PASCUAL, J., SISTARÉ, J., REGÁS, A.: J. Chem. Soc. **1949,** 1943
15. DIECKMANN, W.: Ann. **317,** 27 (1901)
16. PALAU, J., PASCUAL, J., RÁFOLS, J. M.: Bull. soc. chim. France **1964,** 269
17. JACOB, T. M., DEV, S.: Chem. Ind. (London) **1956,** 576
18. RHOADS, S. J., GILBERT, J. C., DECORA, A.W., GARLAND, T. R., SPANGLER, R. J., URBIGKIT, M. J.: Tetrahedron **19,** 1625 (1963)
19. SNYDER, H. R., BROOKS, L. A., SHAPIRO, S. H.: Org. Synth. Coll. Vol. II., p. 531. John Wiley and Sons., Inc., New York, 1946
20. *Cf.* Ref. [16], p. 273, Note 1
21. SANCHEZ, A. M.: Rev. Real. Acad. Cienc. Exactas, Fis. Natur. Madrid **61,** 71 (1967): C. A. **68,** 77824h (1968)

Gábor BERNÁTH
György GÖNDÖS
Pál MÁRAI
Lajos GERA

Szeged, Dóm tér 8, Hungary.

Acta Chimica Academiae Scientiarum Hungaricae, Tomus 74 (4), pp. 479—497 (1972)

STEREOCHEMICAL STUDIES, XII* CYCLIC AMINOALCOHOLS AND RELATED COMPOUNDS, V**

N → O ACYL MIGRATION IN N-BENZOYL DERIVATIVES OF *CIS*- AND *TRANS*-2-AMINOMETHYLCYCLOPENTANOL AND *CIS*- AND *TRANS*-2-HYDROXYMETHYLCYCLOPENTYLAMINE***

G. BERNÁTH, K. L. LÁNG, GY. GÖNDÖS, P. MÁRAI and K. KOVÁCS

(Institute of Organic Chemistry, A. József University, Szeged)

Received June 1, 1971

Cis- and *trans*-2-aminomethylcyclopentanol and *cis*- and *trans*-2-hydroxymethylcyclopentylamine were prepared from *cis*- and *trans*-2-hydroxycyclopentanecarboxamide and *cis*- and *trans*-2-aminocyclopentanecarboxylic acid, respectively, by reduction with lithium aluminium hydride. The kinetics of the N → O acyl migration reaction of *cis*- and *trans*-N-benzoyl-2-aminomethylcyclopentanol and of *cis*- and *trans*-N-benzoyl-2-hydroxymethylcyclopentylamine have been studied. The measurements were made in abs. dioxane solution in the presence of an 0.5 mole excess of hydrochloric acid. The second order rate constants for N-benzoyl-*cis*-2-aminomethylcyclohexanol at temperatures of 100.8, 110.0 and 125.0 °C were $k_2 \cdot 10^3 \cdot \text{sec}^{-1} = 2.89$, 3.37 and 5.35, respectively, the activation energy $\Delta E^{\ddagger} = 11.70$ kcal/mole, the activation entropy $\Delta S^{\ddagger} = -41.8$ e.u., whereas the corresponding values for N-benzoyl-*cis*-2-hydroxymethylcyclopentylamine were found to be $k_2 \cdot 10^3 \cdot \text{sec}^{-1} = 3.87$, 7.80 and 10.31 at 84.0, 100.4 and 110.0 °C, $\Delta E^{\ddagger} = 11.22$ kcal/mole, and $\Delta S^{\ddagger} = -36.9$ e.u. The rate of N → O acyl migration in the *trans* isomers was essentially lower than in the *cis* isomers. The rate constants of the N → O acyl migration reaction of N-benzoyl-*trans*-2-aminomethylcyclopentanol and N-benzoyl-*trans*-2-hydroxymethylcyclopentylamine at 130.2 °C were $k_2 \cdot 10^3 \cdot \text{sec}^{-1} = 0.74$ and 0.87, respectively. It has been shown that the N→O acyl migration occurs with inversion in N-benzoyl-*trans*-2-aminomethylcyclopentanol. The transition states of the N → O acyl migration reactions are discussed and compared with those of 1,3-aminoalcohols with cyclohexane skeleton, studied earlier.

Introduction

In the course of our studies to clarify the stereochemical and conformational relations of common-membered alicyclic systems as well as the mechanism of some reactions of cyclic aminoalcohols and related compounds, we described earlier [1, 2] N → O acyl migration reactions of N-benzoyl and *p*-substituted N-benzoyl derivatives of *cis*- and *trans*-2-aminomethylcyclohexanol and of *cis*- and *trans*-2-hydroxymethylcyclohexylamine. On the basis of the differences in the reaction rates of the diastereomers and the thermodynamic data of the reactions, conclusions were drawn regarding the conformational

* Part XI: BERNÁTH, G., GÖNDÖS, GY., MÁRAI, P., GERA, L.: Acta Chim. Acad. Sci. Hung. **74,** 471 (1972)

** Part IV: BERNÁTH, G., LÁNG, K. L., KOVÁCS, K., RADICS, L.: Acta Chim. Acad. Sci. Hung. **73,** 81 (1972)

*** Preliminary communication: BERNÁTH, G., LÁNG, K. L., GÖNDÖS, GY., MÁRAI, P., KOVÁCS, K.: Tetrahedron Letters **1968,** 4441.

relations of the model compounds and the part processes of the N → O acyl migration reaction.

The present paper deals with the stereospecific synthesis of the corresponding cyclopentane derivatives: *cis*- and *trans*-2-aminomethylcyclopentanol (**I, II**) and *cis*- and *trans*-2-hydroxymethylcyclopentylamine (**III, IV**) (Fig. 1). On the basis of the preparative results, of the reaction rate constants

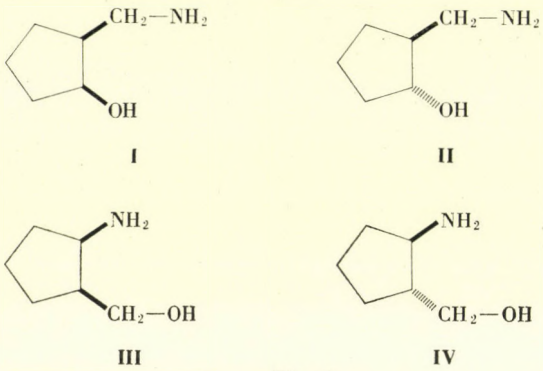

Fig. 1

and the thermodynamic data, the mechanism of the N → O acyl migration of these 1,3-aminoalcohol N-benzoyl derivatives (**XXV, XXVIII**) has been studied and compared with that of the analogous compounds (**XXIX–XXXII**) with cyclohexane skeleton, which were studied in detail by us earlier [2]. Our results, published in preliminary form [3, 4] are presented here in detail.

Numerous further N-acyl derivatives of 1,3-aminoalcohols with cyclopentane skeleton serving as model compounds for the present kinetic investigation were also prepared. These compounds, together with their analogues with cyclohexane skeleton, were used as model compounds in the investigations to elucidate the relations between chemical structure and pharmacologic effect [5]. Several compounds proved to be valuable because of their activity on the central nervous system. The description of the compounds, mainly carboxamides, is to be found elsewhere [6–8].

Synthesis of the model compounds

The stereospecific syntheses of *cis*- and *trans*-2-aminomethylcyclopentanol (**I, II**) and of *cis*- and *trans*-2-hydroxymethylcyclopentylamine (**III, IV**) were achieved by the lithium aluminium hydride reduction of *cis*- and *trans*-2-hydroxycyclopentanecarboxamide (**V, VI**) and *cis*- and *trans*-2-aminocyclopentanecarboxylic acid (**VII, VIII**), respectively.

The synthesis of 2-aminomethylcyclopentanol has been described earlier by MOUSSERON *et al.* [9]. However, the configuration of the 2-aminomethyl-

cyclopentanol obtained from 2-cyanocyclopentanol (**X**) (prepared from 2-chlorocyclopentanol (**IX**) with sodium cyanide) by reduction with sodium in boiling ethanolic solution, has not been given. It could be expected, that similarly to the 2-aminomethylcyclohexanol [2], obtained from 2-cyanocyclohexanol with the same method by MOUSSERON *et al.* this method of preparing 2-aminomethylcyclopentanol would also give a mixture of the *cis*- and *trans*-isomers **I**, **II** (Fig. 2).

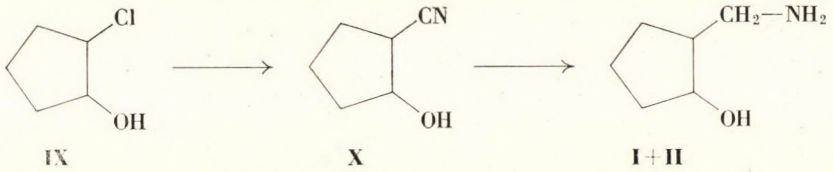

IX X I + II

Fig. 2

Similarly, the synthesis of 2-hydroxymethylcyclopentylamine described by GASSMAN and HECKERT [10] (Fig. 3) is not stereospecific either; the lithium aluminium hydride reduction of the oxime (**XII**) prepared from 2-carbethoxycyclopentanone (**XI**) yields a mixture of *cis*- and *trans*-2-hydroxymethylcyclopentylamine (**III**, **IV**).

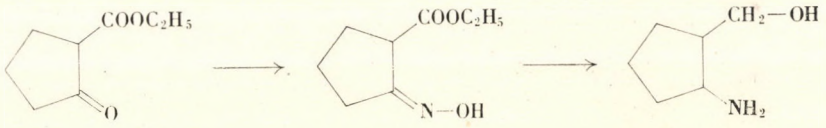

XI XII III + IV

Fig. 3

The syntheses of *cis*- and *trans*-2-hydroxycyclopentanecarboxylic acid (**XIII**, **XIV**) and *cis*- and *trans*-2-carbethoxycyclopentanol (**XV**, **XVI**) were achieved by PASCUAL *et al.* [11]. The mixture of *cis*- and *trans*-2-carbethoxycyclopentanol (**XV**, **XVI**) obtained on the reduction of 2-carbethoxycyclopentanone (**XI**) in the presence of Adams' PtO_2 catalyst, was separated by tedious fractional crystallization of the 3,5-dinitrobenzoates.

Recently MÖHRLE and BAUMANN [12] elaborated a continuous countercurrent distribution method for separating *cis*- and *trans*-2-carbethoxycyclopentanol. Though this method is excellent for separating smaller quantities, in our experiments, especially in the preparation of larger quantities, it was more convenient to use fractional distillation on a column of high efficiency for the separation of the mixture of *cis*- and *trans*-2-carbethoxycyclopentanol (**XV**, **XVI**) obtained by the reduction of 2-carbethoxycyclopentanone in the presence of Raney nickel catalyst or with sodium borohydride. The fractional distillation yielded gas-chromatographically homogeneous *cis*- and *trans*-2-carbeth-

oxycyclopentanol [3, 14], and is less time consuming than the methods mentioned above, though the method of PASCUAL *et al.* has been still in use according to the literature [13].

The *cis*- and *trans*-2-hydroxycyclopentanecarboxamides (**V, VI**) were prepared from these stereohomogeneous ethyl 2-hydroxycyclopentanecarboxylates by reaction in saturated methanolic ammonia solution at room temperature. Reduction of the 2-hydroxycyclopentanecarboxamides with lithium

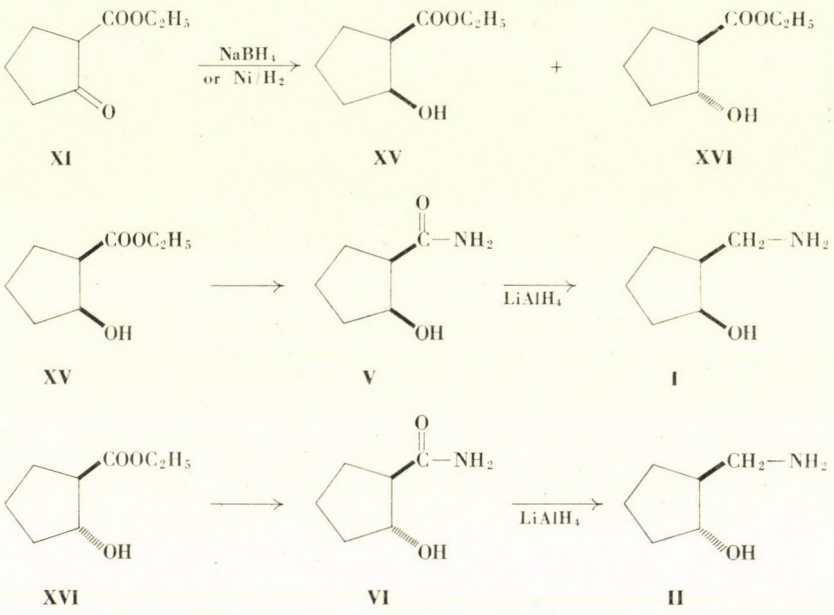

Fig. 4

aluminium hydride in abs. tetrahydrofuran at 60 °C gave *cis*- and *trans*-2-aminomethylcyclopentanol (**I, II**) in good yields (Fig. 4). The stereohomogeneity of the compounds **I, II** was proved by IR and NMR spectroscopy. A detailed analysis of the IR and NMR spectra as well as their comparison with the spectra of analogous compounds with cyclohexane and cycloheptáne skeleton, will be presented in a subsequent paper.

We prepared *cis*-aminocyclopentanecarboxylic acid (**VII**) by the method of PLIENINGER and SCHNEIDER [15], by Hofmann degradation of *cis*-2-carbamoylcyclopentanecarboxylic acid (**XX**); *trans*-aminocyclopentanecarboxylic acid (**VIII**) was obtained by ammonia addition to 1-cyclopentene-1-carboxylic acid (**XXI**) [15, 16].

For the synthesis of *cis*-cyclopentane-1,2-dicarboxylic anhydride (**XIX**), necessary for the preparation of *cis*-2-carbamoylcyclopentanecarboxylic acid (**XX**), several methods are known [17–23].

For the preparation of cyclopentane-*trans*-1,2-dicarboxylic acid (**XVIII**) we used the PERKIN method [17–19] (Fig. 5) improved by BAILEY and SORENSON [20], with some modification. We found in the decarboxylation reaction of ethyl cyclopentane-1,1,2,2-tetracarboxylate (**XVII**) that the reaction time of about three hours suggested by BAILEY and SORENSON (until the distillation of ethyl acetate has been finished) was insufficient. The reaction time necessary for the oily phase to disappear took 20 to 25 hours. The yield given by BAILEY and SORENSON was attained only with this essentially longer reaction time. The transformation of cyclopentane-*trans*-1,2-dicar-

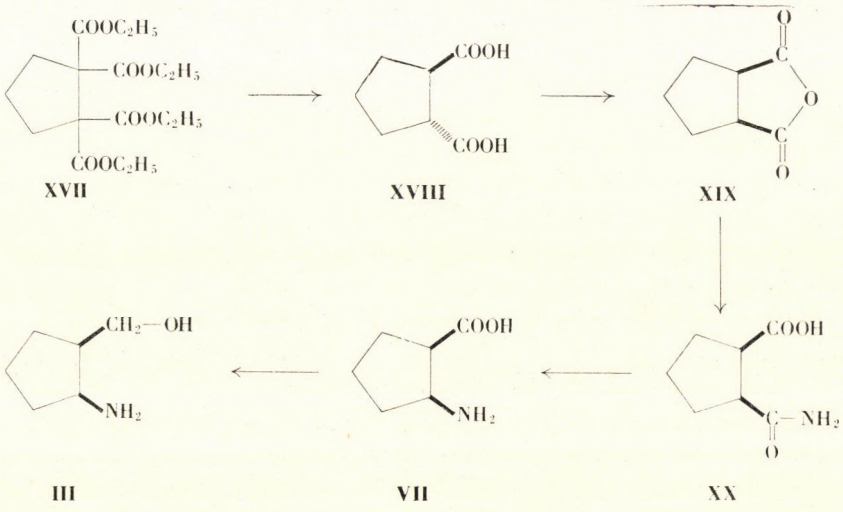

Fig. 5

boxylic acid (**XVIII**) into cyclopentane-*cis*-1,2-dicarboxylic anhydride (**XIX**) can be accomplished in an essentially better yield than that reported [15], by increasing the quantity of the acetic anhydride used.

The solid distillation residue of the cyclopentane-*cis*-1,2-dicarboxylic anhydride (**XIX**) was crystallized from benzene-petroleum ether. We found that the residue mainly consisted of cyclopentane-*trans*-1,2-dicarboxylic acid, which can be used in a subsequent reaction for preparing the anhydride. In this way the yield could be further increased.

Our method used for the preparation and Hofmann degradation of *cis*-2-carbamoylcyclopentanecarboxylic acid (**XX**) was, apart from some modifications, essentially that described by PLIENINGER and SCHNEIDER [15]; our yield, however, essentially exceeded those reported in the literature. The m.p. of *cis*-2-aminocyclopentanecarboxylic acid (**VII**) was found to be 223–224 °C instead of the reported value of 202–204 °C [15]. At the latter temperature only a transformation of the crystal form takes place and the new form melts at 223–224 °C.

COOK and LINSTEAD [24] prepared 1-cyclopentene-1-carboxylic acid by the hydrolysis of 1-cyclopentene-1-carbonitrile obtained by the dehydration of cyclopentanone cyanohydrin. SCHARF and KORTE [25] synthesized ethyl 1-cyclopentene-1-carboxylate by dehydration of the mixture of *cis*- and *trans*-2-carbethoxycyclopentanol (**XV, XVI**) with P_4O_{10}. This mixture was obtained by reducing 2-carbethoxycyclopentanone (**XI**) with Adams' PtO_2 catalyst [11]. As mainly the Δ^2-isomer formed, pure ethyl 1-cyclopentene-1-carboxylate could be obtained by isomerization with sodium ethoxide in abs. ethanol. From the fact that the dehydration process gave mainly the Δ^2-isomer olefinic acid, SCHARF and KORTE concluded that the reduction in the presence of PtO_2 led to *trans*-2-carbethoxycyclopentanol (**XVI**) as the main product.

This is consistent neither with our results obtained in reproducing the method of PASCUAL and CASTELLS [11], nor with the isomeric ratios produced in the presence of other catalysts. The main product of reduction of 2-carbethoxycyclopentanone (**XI**) in the presence of different catalysts was always *cis*-2-carbethoxycyclopentanol (**XV**). The sodium borohydride reduction of both 2-carbethoxycyclopentanone and 2-carbethoxycyclohexanone resulted in a larger amount of the *trans* isomer. By performing the sodium borohydride reduction at lower temperatures, the formation of the *trans* isomer became even more pronounced, which is in accordance with our experience in the reduction of 2-carbethoxy-4-*t*-butylcyclopentanone [26].

PROCHÁZKA and LEŠETICKÝ [27] stated in a paper published in 1966 that the earlier methods of preparing ethyl 1-cyclopentene-1-carboxylate were unsatisfactory and badly reproducible. By dehydration of *cis*-2-carbethoxycyclopentanol in abs. pyridine with thionyl chloride in chloroform they obtained ethyl 1-cyclopentene-1-carboxylate of 98% purity in 70% yield.

We found that our method used for the synthesis of 1-cyclohexene-1-carboxylic acid [28] was also suitable for the preparation of 1-cyclopentene-1-carboxylic acid (**XXII**) by the distillation of cyclopentanol-2-carboxylic acid (**XXI**) at atmospheric pressure. For this purpose we used the cyclopentanol-2-carboxylic acid (**XXI**) obtained by the hydrolysis of the fractions containing both isomers from the fractional distillation of the mixture of *cis*- and *trans*-2-carbethoxycyclopentanol (**XV, XVI**). In the course of a slow distillation at atmospheric pressure, dehydration takes place and subsequent isomerization with KOH gives 1-cyclopentene-1-carboxylic acid (**XXII**) in a good yield. From this, *trans*-2-aminocyclopentanecarboxylic acid can be prepared with the method of PLIENINGER and SCHNEIDER [15] (Fig. 6).

Reduction of ethyl *cis*- and *trans*-2-aminocyclopentanecarboxylate (**XXIII, XXIV**) with lithium aluminium hydride gave *cis*- and *trans*-2-hydroxymethylcyclopentylamine (**III, IV**). The *cis*- and *trans*-2-aminocyclopentanecarboxylic acid (**VII, VIII**) can also be reduced directly in tetrahydrofuran at 60 °C. Though the reduction takes an essentially longer time, we found this

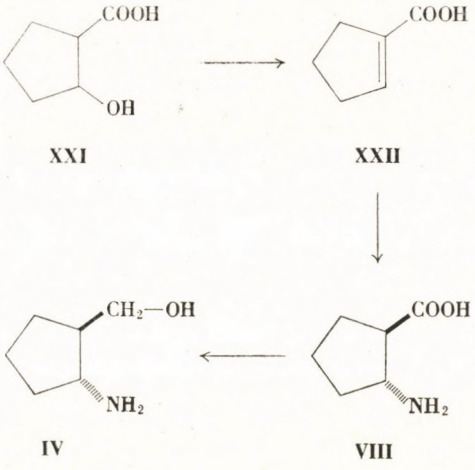

XXI XXII

IV VIII

Fig. 6

latter process more convenient, because the losses arising from the esterification and the recovery of the ester from the salt can thus be avoided.

Results and discussion

N → O acyl migration has been discussed in numerous papers [29–32]. The mechanism and kinetics, stereochemical, preparative and other applications of the process have been extensively studied. The importance of O → O, N → O and N → S acyl migrations and acyl exchange processes in biology has also been reviewed [31]. A very comprehensive review of acyl migration processes is to be found in a recent paper of PAVLOVA and RACHINSKII [32], with 228 references, comprising the work done in the field of acyl migration up to 1968.

In our paper [2], submitted for publication just before the paper of PAVLOVA and RACHINSKII appeared, we also thoroughly discussed several aspects of the N → O acyl migration reaction in 1,2-, 1,3- and 1,4-aminoalcohols, in connection with kinetic investigations on N → O acyl migrations in N-benzoyl- and *p*-substituted N-benzoyl derivatives of *cis*- and *trans*-2-aminomethylcyclohexanol and *cis*- and *trans*-2-hydroxymethylcyclohexylamine. Therefore, we shall not discuss here the literature of the N → O acyl migration.

The N → O acyl migration reactions of the N-benzoyl-*cis*-2-aminomethylcyclopentanol (**XXIV**) was studied in the temperature range 100.8 to 125 °C, and that of N-benzoyl-*cis*-2-hydroxymethylcyclopentylamine (**XXVII**) between 84.0 and 110.0 °C. Because of the essentially lower reactivity of the

corresponding *trans* isomers, the N → O acyl migration reaction of N-benzoyl-*trans*-2-aminomethylcyclopentanol (**XXVI**) and N-benzoyl-*trans*-2-hydroxymethylcyclopentylamine (**XXVIII**) was studied only at 130.2 °C. The extremely low reactivity of the *trans* isomers (**XXVI, XXVIII**) at lower temperatures and the side reactions occurring at higher temperatures did not allow to obtain well reproducible rate constants, therefore it was not possible to determine the activation energies and activation entropies of these reactions. The reaction rate constants calculated from the second order equation, the activation energies and activation entropies are listed in Table I. For comparison, the corresponding constants of the analogous cyclohexane derivatives (**XXIX–XXXII**) determined under identical conditions are given in brackets.

The data in Table I show that — in contrast with the analogous cyclohexane derivatives studied earlier — the rate of the N → O acyl migration reaction, as well as the activation energy and activation entropy of the reactions of *cis*- and *trans*-N-benzoyl-2-aminomethylcyclopentanol (**XXV, XXVI**) and *cis*- and *trans*-N-benzoyl-2-hydroxymethylcyclopentylamine (**XXVII, XXVIII**) are essentially higher for the *cis* derivatives (**XXV, XXVII**) than for the *trans* derivatives (**XXVI, XXVIII**). This result is in good agreement with that found in the N → O acyl migration reaction of *cis*- and *trans*-2-benzamidocyclopentanol and *cis*- and *trans*-2-*p*-nitrobenzamidocyclopentanol [33], where the reaction rate of the *cis* isomers also exceeds that of the *trans* isomers by orders of magnitude. It has been shown that, whereas *cis*-2-benzamidocyclopentanol gave 42.2% *cis*-O-benzoyl-2-aminocyclopentanol hydrochloride with retention and 36.4% unchanged starting material at 20 °C in 15 hours, from the reaction of the *trans* isomer under identical conditions 100% unchanged starting material was recovered. In the case of *trans*-2-benzamidocyclopentanol, remarkable N → O acyl migration could only be observed at 100 °C. The striking rate difference is due to the fact that the N → O acyl migration reaction of *trans*-2-benzamidocyclopentanol takes place with inversion.

However, the N → O acyl migration reactions of cyclic 1,2- and 1,3-aminoalcohols do not necessarily show parallelism [1, 2]; whereas the reaction rate of the N → O acyl migration of *cis*-2-benzamidocyclohexanol [34] markedly exceeds that of the *trans* isomer (302 : 76), in the case of the 1,3-cyclohexane derivatives investigated by us (the N-benzoyl- and *p*-substituted N-benzoyl derivatives of *cis*- and *trans*-2-aminomethylcyclohexanol and *cis*- and *trans*-hydroxymethylcyclohexylamine) it were the *trans* isomers which had the higher reaction rates. The ratio of the reaction rates was about the same as in the case mentioned above. This was explained by us with the reaction mechanism, with the conformations of the monoazamonooxadecalin-like transition states of the reactions.

The first step of N → O acyl migration is the protonation of the oxygen atom of the acid amide; it is known that acid amides in acidic solution are

Table I

Reaction rate constants, activation energies and activation entropies of the N → O *acyl migration reactions of cis- and trans-*N*-benzoyl-2-aminomethylcyclop ntanol* (**XXV**, **XXVI**) *and cis- and trans-*N*-benzoyl-2-hydroxymethylcyclopentylamine* (**XXVII**—**XXVIII**)

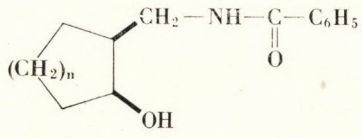

$n = 1$: **XXV**
$n = 2$: **XXIX**

t, °C	$k_2 \cdot 10^3 \cdot \text{sec}^{-1}$
100.8	2.89 (2.20)
110.0	3.37
125.0	5.33

$\Delta E^{\ddagger}$ = 11.70 (15.84) kcal/mole
$\Delta S^{\ddagger}$ = —41.8 (—30.7) e.u.

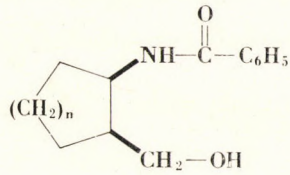

$n = 1$: **XXVII**
$n = 2$: **XXXI**

t, °C	$k_2 \cdot 10^3 \cdot \text{sec}^{-1}$
84.0	3.87
100.4	7.80 (5.15)
110.0	10.31

$\Delta E^{\ddagger}$ = 11.22 (11.66) kcal/mole
$\Delta S^{\ddagger}$ = —36.9 (—40.0) e.u.

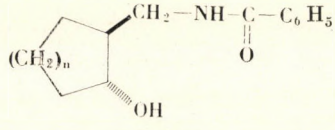

$n = 1$: **XXVI**
$n = 2$: **XXX**

t, °C	$k_2 \cdot 10^3 \cdot \text{sec}^{-1}$
100.0	— (4.80)
130.2	0.74

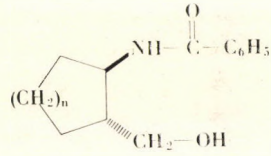

$n = 2$: **XXVIII**
$n = 2$: **XXXII**

t, °C	$k_2 \cdot 10^3 \cdot \text{sec}^{-1}$
100.0	— (20.28)
130.2	0.87

Note. The corresponding constants of the analogous cyclohexane derivatives (n = 2, **XXIX**—**XXXII**) are given in brackets. The rate constants were determined at 100.0 ± 0.3 °C [1, 2].

protonated mainly at the carbonyl oxygen [35, 36]. This is followed by a nucleophilic attack by the oxygen atom of the alcoholic hydroxyl group at the carbonyl carbon atom, resulting in the formation of the bicyclic transition state. This attack takes place on the quasi-carbonium carbon atom of the pro-

tonated acid amide, perpendicularly to the plane of the three substituents attached to it. This perpendicular attack is also the most favoured energetically, as this transition state allows the maximum overlap of the π-electron clouds of the nucleophilic part and the carboxyl group — as it is the case, *e.g.*, in acid-catalysed esterification [37].

The relative stabilities of the bicyclic transition states alone, however, insufficiently explain the relative reaction rates because the tendency to ring closure does not go parallel with the stability of the product, even if the reaction product is isolable and stable [38]. The rate difference in the N → O acyl migration reaction of *cis*- and *trans*-2-benzamidocyclohexanol cannot be explained merely on the basis of the small difference in the enthalpy of *cis*- and *trans*-hydrindane (0.74 ± 0.52 kcal/mole at 292 °K [39]). The more marked rate difference in the N → O acyl migration reaction of the *cis*- and *trans*-1,3-aminoalcohols with cyclopentane skeleton would be even more difficult to explain on this basis, because in this case the hetero ring of the mono-azamonooxahydrindane-like transition state is six-membered.

A comparison of the rates of the N → O acyl migration reactions of N-benzoyl-*cis*-2-aminomethylcyclopentanol (**XXV**) and N-benzoyl-*cis*-2-hydroxymethylcyclopentylamine (**XXVII**) shows the reaction rate of the latter to be higher — in accordance with our results on the analogous cyclohexane derivatives (**XXIX**, **XXXI**) — since the hydroxymethyl group is less shielded than the secondary hydroxyl group of N-benzoyl-*cis*-2-aminomethylcyclopentanol (**XXV**).

It is worth mentioning that the activation energies of the N → O acyl migration reactions of N-benzoyl-*cis*-2-aminomethylcyclopentanol (**XXV**) and N-benzoyl-*cis*-2-hydroxymethylcyclopentylamine (**XXVII**) do not show a marked difference ($\Delta E^{\ddagger} = 11.70$ and 11.22 kcal/mole, respectively). The reaction rates of both compounds are, however, essentially different; this can be explained by the circumstance that the activation entropy of N-benzoyl-*cis*-2-hydroxymethylcyclopentylamine (**XXVII**) has a considerably smaller negative value ($\Delta S^{\ddagger} = -36.9$ e.u.) than that of N-benzoyl-*cis*-2-aminomethylcyclopentanol (**XXV**) ($\Delta S^{\ddagger} = -41.8$ e.u.).

In the present case the reaction mechanism can be explained by the higher activation entropy of N-benzoyl-*cis*-2-aminomethylcyclopentanol (**XXV**) containing a secondary hydroxyl group. Namely, in the N → O acyl migration reactions of N-benzoyl-*cis*-2-aminomethylcyclohexanol (**XXIX**) and N-benzoyl-*cis*-2-hydroxymethylcyclohexylamine (**XXXI**) the relations between the reaction rates analogous to that of the corresponding cyclopentane derivatives (**XXV**, **XXVII**) containing a primary or secondary hydroxyl group and the approximately equal ratio of the reaction rates are due to the counteracting effects of the pronounced difference between the activation energies of the two isomers (**XXIX**, **XXXI**) (15.84 and 11.66 kcal/mole, respectively) and the

marked difference of opposite direction between the activation entropies (—30.7 and —40.0 e.u.) of the reactions.

In the N → O acyl migration of the cyclopentane derivatives (**XXV**, **XXVII**) it is the activation entropy of **XXV**, containing a secondary hydroxyl group, which is the higher, whereas in the case of the analogous cyclohexane derivatives (**XXXIX**, **XXXI**) the activation entropy of **XXXI** containing a primary hydroxyl group is higher. The three substituents attached to the carbonyl carbon atom of the acid amide involved in the formation of the bicyclic transition state from the protonated form of N-benzoyl-*cis*-2-hydroxy-

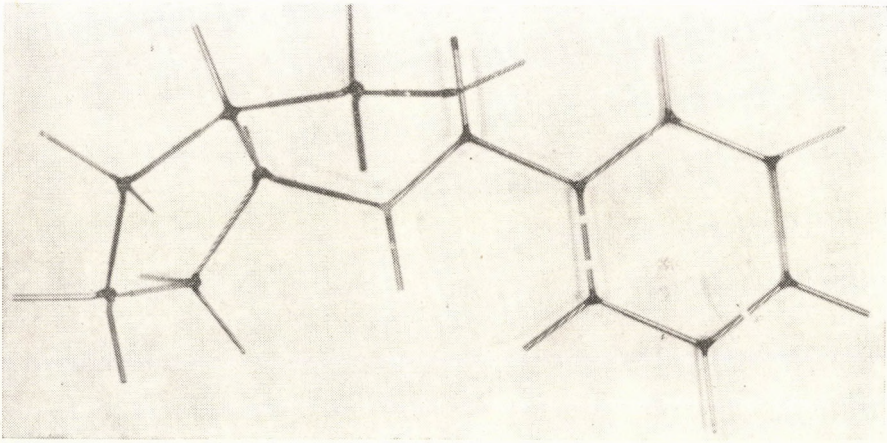

Fig. 7

methylcyclopentylamine (**XXVII**), considered to be in the half-chair conformation of the cyclopentane skeleton [13, 40–42], lie in a plane perpendicular to that of the figure. The hydroxyl group is attacking in the plane of the figure, at right angle to the plane determined by the three substituents (Fig. 7).

In the case of N-benzoyl-*cis*-2-aminomethylcyclopentanol, the formation of the bicyclic transition state is, of course, less favoured; this accounts for the very high negative activation entropy of the reaction. It is, however, to be emphasized that in the present case, contrary to the *trans* isomers, the hydrogen–hydrogen interactions do not increase during the ring conversion required for the formation of the bicyclic transition state.

The rate constants of the N → O acyl migration reactions of N-benzoyl-*trans*-2-aminomethylcyclopentanol (**XXVI**) and N-benzoyl-*trans*-2-hydroxymethylcyclopentylamine (**XXVIII**) are lower by about an order of magnitude even at 130.2 °C than those of the *cis* isomers (**XXV**, **XXVII**) determined at 100.8 and 100.4 °C, respectively (see Table I). This may seem surprising, as the bicyclic transition state of the N → O acyl migration is six-membered in 1,3-

aminoalcohols, and its formation could be expected to occur readily also in the *trans* isomers, as the energy difference between the analogous *cis* and *trans* carbocyclic compounds (*cis*- and *trans*-hydrindane) is negligible.

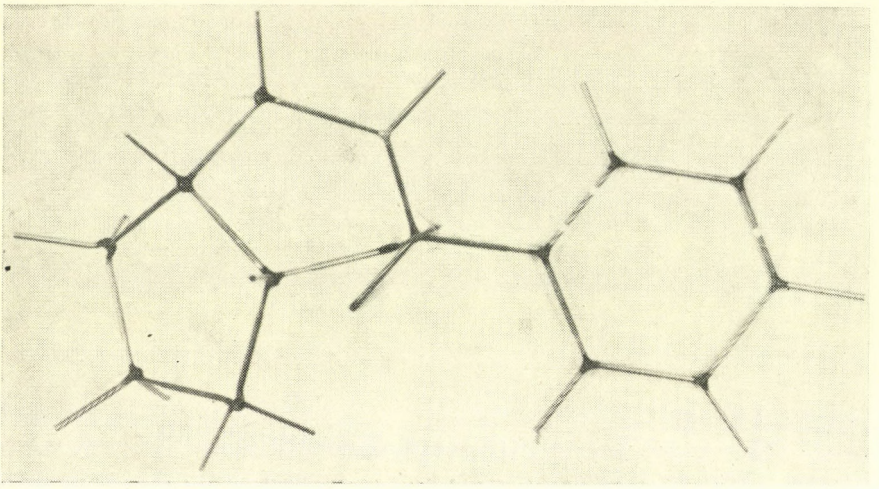

Fig. 8

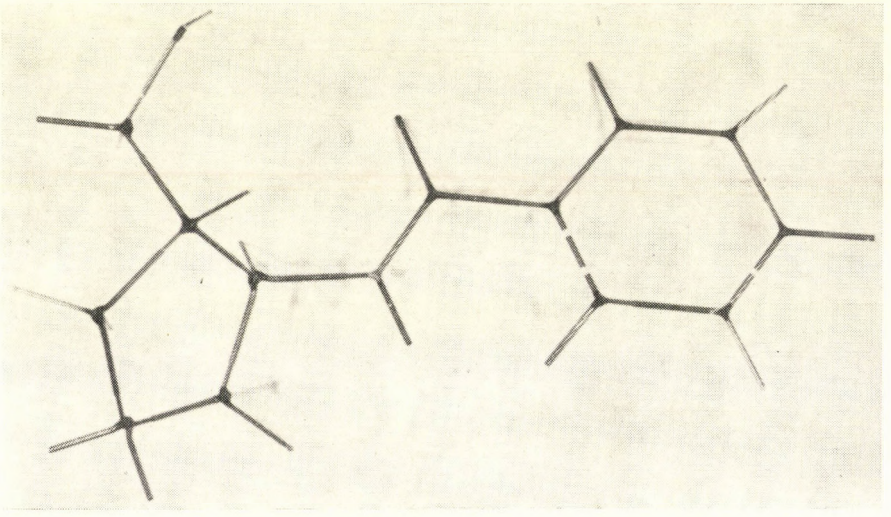

Fig. 9

However, an examination of the Dreiding models shows convincingly that whereas the attack of the alcoholic hydroxyl group on the carbonyl carbon atom of the acid amide can easily occur in the *cis* isomers because of the small distance of the atoms taking part in the reaction (Fig. 8), in the *trans* iso-

mers, owing to the rigidity of the cyclopentane skeleton, the functions are placed so far from each other that the attack of the hydroxyl group becomes incomparably more difficult, even in the case of the hydroxymethyl derivative (**XXVIII**) (Fig. 9).

N → O acyl migration in N-benzoyl-*trans*-2-aminomethylcyclopentanol can occur more favourably with the inversion mechanism because of the great distance between the secondary hydroxyl group and the carbonyl carbon

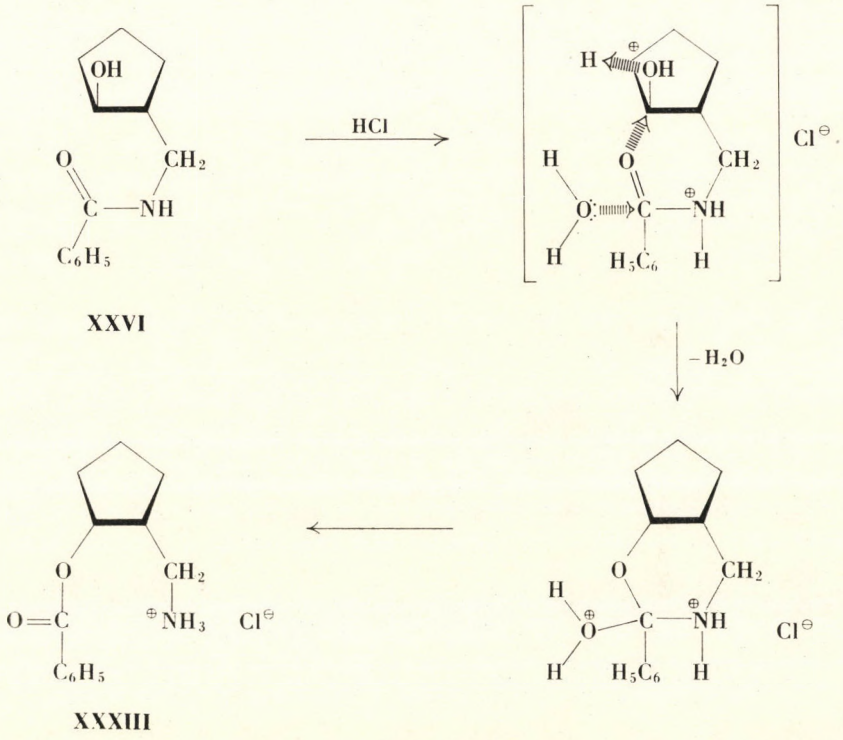

Fig. 10

atom of the acid amide. Though the inversion mechanism is energetically much less favoured than the retention mechanism, in the present case the oxygen atom of the acid amide group may assume a comparatively near position to the cyclopentane ring so that the N → O acyl migration reaction may occur with inversion (Fig. 10).

The melting point of the picrate prepared from O-benzoyl-2-aminomethylcyclopentanol hydrochloride obtained by N → O acyl migration from N-benzoyl-*trans*-2-aminomethylcyclopentanol (**XXVI**), was identical with that of the picrate prepared from O-benzoyl-*cis*-2-aminomethylcyclopentanol made by N → O acyl migration from N-benzoyl-*cis*-2-aminomethylcyclo-

pentanol (**XXV**). The *cis* configuration of **XXXIII** was also supported by the fact that the O → N acyl migration reaction of **XXXIII** effected in alkaline medium gave N-benzoyl-*cis*-2-aminomethylcyclopentanol (**XXV**) (Fig. 11). The melting point and IR spectrum of the product were identical with those of the authentic *cis* derivative (**XXV**).

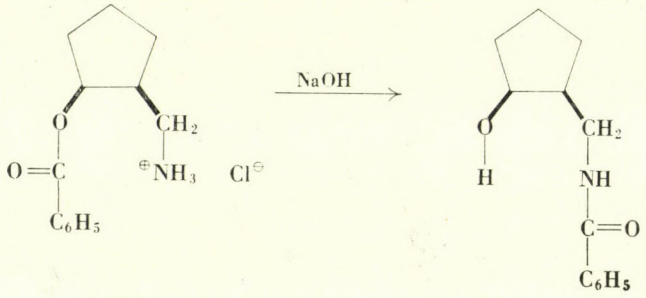

XXXIII **XXV**

Fig. 11

In view of the fact that N → O acyl migration occurs in N-benzoyl-*trans*-2-aminomethylcyclopentanol (**XXVI**) with inversion, it is not surprising that the reaction rate found is essentially lower than that of the *cis* isomer (**XXVI**. The moderate reaction rate of the N → O acyl migration reaction of N-benzoy-) *trans*-2-hydroxymethylcyclopentylamine (**XXVIII**), which seems less evident because of the presence of a primary hydroxyl group, may also be well interpreted with the aid of the Dreiding models.

A comparison of the reaction rates of the N → O acyl migration reactions of analogous cyclopentane and cyclohexane derivatives shows the rigidity of the cyclopentane ring; the rate constant of the N → O acyl migration of N-benzoyl-*cis*-2-aminomethylcyclohexanol (**XXIX**) increases to its three-fold value by rising the temperature from 80 to 100 °C and is approximately the same at 100 °C as that of the analogous cyclopentane compound (**XXV**); by contrast, in the case of N-benzoyl-*cis*-2-aminomethylcyclopentanol a rise in the temperature by 25 °C increases the rate constant only by a factor of 1.5.

Investigations on the N → O acyl migration reactions of analogous 1,3-aminoalcohols with cycloheptane skeleton are in progress.

Experimental

cis-2-Hydroxycyclopentanecarboxamide (V)

15.8 g (0.10 mole) of *cis*-2-carbethoxycyclopentanol (**XV**) [3, 14] in 90 ml of abs. methanol saturated with ammonia was allowed to stand at room temperature for 10 days. The product left after evaporation of the methanol was recrystallized twice from benzene to obtain 7.3 g (56.52%) of white crystal plates, m.p. 86.5–87.5 °C.

$C_6H_{11}NO_2$ (129.15). Calcd. C 55.79; H 8.58; N 10.85%. Found C 55.90; H 8.47; N 11.06%.

trans-2-Hydroxycyclopentanecarboxamide (VI)

From 10.0 g (0.06 mole) of *trans*-2-carbethoxycyclopentanol (**XVI**) [3, 14], similarly as described for the *cis* isomer (**V**), after recrystallization from benzene 5.6 g (68.6%) of *trans*-2-hydroxycyclopentanecarboxamide (**VI**), m.p. 101.5–102.5 °C, was obtained. Repeated recrystallizations for analysis gave m.p. 102.5–103.5 °C.

$C_6H_{11}NO_2$ (129.15). Calcd. C 55.79; H 8.58; N 10.85%. Found C 51.91; H 8.32; N 10.98%.

cis-2-Aminomethylcyclopentanol (I)

In a 1-l three-necked round-bottomed flask, equipped with a reflux condenser with $CaCl_2$ tube and with a dropping funnel, 500 ml of abs. tetrahydrofuran was placed, to which 13.3 g (0.35 mole) of lithium aluminium hydride was added in portions, under stirring. To this mixture, warmed to 60 °C, 12.9 g (0.10 mole) of *cis*-2-hydroxycyclopentane carboxamide (**V**) was given in portions during 2 hrs. The reaction mixture was stirred at 60 °C for further 20 hrs., then (according to the method of MIČOVIĆ and MIHAILOVIĆ [43] successively 13.3 ml of water, 13.3 ml of 5% NaOH solution and 40 ml of water were added. The metal hydroxide was filtered off, and the filtrate dried over Na_2SO_4. The product which remained after evaporation of the tetrahydrofuran was distilled under diminished pressure to obtain 6.6 g (57.31%) of a colourless viscous oil, b.p. 124–128 °C at 38 torr; $n_D^{24} = 1.4886$. (Lit. b.p. 122 °C at 15 torr, $n_D^{?} = 1.4886$, without indication of the configuration [9].)

N-Benzoyl-*cis*-2-aminomethylcyclopentanol (XXV)

From 1.2 g (0.01 mole) of *cis*-2-aminomethylcyclopentanol (**I**) and 1.7 g (0.012 mole) of benzoyl chloride, with the Schotten–Baumann method [44] 2.2 g (96.1%) of N-benzoyl-*cis*-2-aminomethylcyclopentanol, m.p. 97.5–98.0 °C, was obtained. Recrystallized twice from benzene, m.p. 99.0–99.5 °C.

$C_{13}H_{17}NO_2$ (219.27). Calcd. C 71.20; H 7.82; N 6.39%. Found C 71.69; H 7.89; N 6.43%.

trans-2-Aminomethylcyclopentanol (II)

From 12.9 g (0.10 mole) of *trans*-2-hydroxycyclopentanecarboxamide (**VI**), with the method described for the *cis* isomer (**I**), 9.1 g (79.01%) of a colourless viscous oil was obtained. B.p. 85–87.5 °C at 4 torr; $n_D^{24} = 1.4790$. (Lit. b.p. 122 °C at 15 torr, $n_D^{25} = 1.4886$, without indication of the configuration [9].)

N-Benzoyl-*trans*-2-aminomethylcyclopentanol (XXVIII)

From 1.75 g (0.015 mole) of *trans*-2-aminomethylcyclopentanol (**II**), similarly to the method described for the *cis* isomer, 3.20 g (95.9%) of N-benzoyl-*trans*-2-aminomethylcyclopentanol (**XXVIII**), m.p. 77.5–78.5 °C, was obtained. After repeated recrystallizations from benzene, m.p. 78.5–79.0 °C.

$C_{13}H_{17}NO_2$ (219.27). Calcd. C 71.20; H 7.82; N 6.39%. Found C 71.14; H 7.82; N 6.18%.

1-Cyclopentene-1-carboxylic acid (XXII)

A mixture of 79.1 g (0.50 mole) *cis*- and *trans*-2-carbethoxycyclopentanol (**XV**, **XVI**) and 320 ml 20% NaOH solution was shaken for 2 hrs. The unchanged starting material was extracted with 2×100 ml ether, then the aqueous phase was acidified with a 1 : 3 mixture of hydrochloric acid and water. The solution was saturated with ammonium chloride, then extracted with 5×200 ml ether. The combined ethereal extracts were dried over anhydrous Na_2SO_4 and evaporated. 54.2 g (83.3%) of a mixture of *cis*- and *trans*-cyclopentanol-2-carboxylic acid (**XIII**, **XIV**) was obtained, which was then distilled at atmospheric pressure. On heating dehydration occurred and cyclopentenecarboxylic acid distilled as a colourless liquid, which solidified in the receiver in the form of white crystals. After refluxing with 30% KOH for 20 hrs., the usual work-up gave 1-cyclopentene-1-carboxylic acid (38.2 g; 82.9%, calculated for cyclopentanol-2-carboxylic acid) suitable for further reactions without purification. By crystallizing a small part from water, white needles were obtained, m.p. 121–121.5 °C (lit. m.p. 121 °C [45]).

trans-2-Aminocyclopentanecarboxylic acid (VIII)

44.8 g (0.40 mole) of 1-cyclopentene-1-carboxylic acid (**XXII**) was shaken with 25% ammonium hydroxide solution in an autoclave at 170 °C for 64 hrs. Application of the procedure described by PLIENINGER and SCHNEIDER [15] gave 19.9 g (38.6%) of *trans*-2-aminocyclopentanecarboxylic acid (**VIII**), m.p. 239–240 °C (lit. m.p. 240 °C [15]).

trans-2-Hydroxymethylcyclopentylamine (IV)

From 15.5 g (0.12 mole) of *trans*-2-aminocyclopentanecarboxylic acid (**VIII**) in 600 ml abs. tetrahydrofuran with 15.9 g (0.42 mole) of lithium aluminium hydride, similarly as described for the preparation of *cis*-2-aminomethylcyclopentanol, 11.0 g (80.0%) of *trans*-2-hydroxymethylcyclopentylamine (**IV**) was obtained, b.p. 136–139 °C at 36 torr; $n_D^{24} = 1.4794$. (Lit. b.p. 120–125 °C at 30 torr [10], without indication of the configuration.)

$C_6H_{13}NO$ (115.18). Calcd. C 62.58; H 11.30%. Found C 62.66; H 11.03%.

The hydrochloride crystallized from ethanol–ether had m.p. 117 °C.

$C_6H_{14}ClNO$ (151.64). Calcd. C 47.52; H 9.31; Cl^- 23.38%. Found C 47.48; H 9.40; Cl^- 24.46%.

N-Benzoyl-*trans*-2-hydroxymethylcyclopentylamine (XXVIII)

Schotten–Baumann acylation of the former *trans*-2-hydroxymethylcyclopentylamine (**VI**) gave white crystals, m.p. 133.5–134.0 °C, in nearly quantitative yield. Recrystallization from ethanol–water gave m.p. 134.0–134.5 °C.

$C_{13}H_{17}NO_2$ (219.27). Calcd. C 71.20; H 7.82; N 6.39%. Found C 70.74; H 7.70; N 6.60%.

Cyclopentane-*trans*-1,2-dicarboxylic acid (XVIII)

69.8 g (69.4%) of ethyl *n*-pentane-1,1,5,5-tetracarboxylate (**XVII**) was prepared by the method of BAILEY and SORENSON [20] by condensing 972.0 g (6.0 moles) of diethyl malonate and 101.0 g (0.5 mole) of trimethylene dibromide with sodium ethoxide prepared from 23.0 g (1.0 mole) of sodium. From this 117.9 g (0.33 mole; 65.8%) of ethyl cyclopentane-1,1,2,2-tetracarboxylate (**XVII**) was obtained (the yield is not given by BAILEY and SORENSON [20]). This product was placed, without further purification, in a 2-l round-bottomed flask. After the addition of 250 ml of conc. sulfuric acid, 250 ml acetic acid and 550 ml water, the mixture was slowly distilled for about 25 hrs. applying a 40 cm long Vigreaux column (until the distillation of the ethyl acetate formed ceased). The concentrated reaction mixture was cooled, the brown crystals which separated (43.6 g; 83.8%) were filtered off, and recrystallized from water using decolourizing charcoal. 35.1 g (67.5%) of white crystals (**XVIII**) were obtained, m.p. 159.0–160.5 °C (lit. m.p. 161–162 °C [20] and 160 °C [19]).

Cyclopentane-*cis*-1,2-dicarboxylic anhydride (XIX)

35.1 g (0.22 mole) of cyclopentane-*trans*-1,2-dicarboxylic acid (**XVIII**) and 250 ml of acetic anhydride were refluxed in a 500 ml round-bottomed flask for 10 hrs., then the acetic acid formed and the excess acetic anhydride were distilled off at 38–40 torr. The remaining cyclopentane-*cis*-1,2-dicarboxylic anhydride was distilled at 3 torr and the fraction boiling between 95 and 100 °C was collected. Recrystallization of the crystalline distillation product from petroleum ether gave white crystal plates (25.2 g; 81.3%), m.p. 73–74 °C (lit. m.p. 73.5–74.0 °C [21]).

cis-2-Carbamoylcyclopentanecarboxylic acid (XX)

To 100 ml conc. ammonium hydroxide 25.2 g (0.18 mole) of cyclopentane-*cis*-1,2-dicarboxylic anhydride (**XIX**) was added in small portions, under constant shaking. The reaction mixture was allowed to stand at room temperature for half an hour, then the excess ammonia was removed at 40 torr. The remaining aqueous solution was acidified at 10 °C by adding conc. HCl. The white crystals which separated after standing at 4 °C were filtered off, washed with cold water and dried to give 25.0 g (88.45%; lit. yield 54% [15]) of *cis*-2-carbamoylcyclopentanecarboxylic acid, in suitable purity for further use; m.p. 126–128 °C (lit. m.p. 126–129 °C [15]).

cis-2-Aminocyclopentanecarboxylic acid (VII)

To an aqueous solution (125 ml) of 32.0 g (0.80 mole) sodium hydroxide, 32.0 g (0.20 mole) of bromine was added, with intense stirring, at 0 °C. The reaction mixture was cooled to 0 °C again, and in small portions 25.0 g (0.16 mole) of finely powdered *cis*-2-carbamoylcyclopentanecarboxylic acid (**XX**) was added during 1 hr. After adding 24.0 g (0.60 mole) of sodium hydroxide dissolved in 100 ml of water, the reaction mixture was warmed to 75 °C in about 15 min. and allowed to stand at this temperature for further 5 min., then cooled and neutralized with conc. HCl. 30 ml of acetic acid was added and the mixture was evaporated to dryness at 38–40 torr. The distillation residue was refluxed with 4×250 ml abs. ethanol. The combined ethanolic solutions were evaporated, the residue was dissolved in 500 ml of water, decolourized with charcoal and purified on Dowex 50 ion exchange resin. The column was washed with water and then the produced *cis*-2-aminocyclopentanecarboxylic acid (**VII**) was eluated with a 1 : 10 mixture of conc. ammonium hydroxide and water. The crude product remaining after evaporation of the water was recrystallized from aqueous acetone, to give 15.6 g (75.93%) of **VII** as colourless needles. After changing the crystal form at 202 °C, the substance had m.p. 223–224 °C [15].

cis-2-Hydroxymethylcyclopentylamine (III)

From 15.5 g (0.12 mole) of *cis*-2-aminocyclopentanecarboxylic acid (**VII**), with the method described for *trans*-2-hydroxymethylcyclopentylamine (**IV**), 11.1 g (80.68%) of a colourless viscous oil was obtained, $n_D^{25} = 1.4930$, b.p. 95–97 °C at 2 torr. (Lit. b.p. 76.5–77 °C, at 0.3 torr, without indication of the configuration [10].)

$C_6H_{13}ON$ (115.18). Calcd. C 62.57; H 11.38%. Found C 62.74; H 11.58%.

The hydrochloride of **III** separated from abs. ethanol–abs. ether in the form of hygroscopic white crystals. The hydrobromide was obtained from abs. ethanol–abs. ether as mildly hygroscopic white crystals, m.p. 82–83 °C.

$C_6H_{14}BrNO$ (196.10). Calcd. C 36.75; H 7.20; Br^- 40.75%. Found C 36.55; H 7.55; Br^- 40.47%.

N-Benzoyl-*cis*-2-hydroxymethylcyclopentylamine (XXVII)

This compound was prepared from *cis*-2-hydroxymethylcyclopentylamine (**III**) with Schotten–Baumann benzoylation, in nearly quantitative yield; m.p. 108.0–108.5 °C (from ethanol–water).

$C_{13}H_{17}NO_2$ (219.27). Calcd. C 71.20; H 7.83; N 6.39%. Found C 70.99; H 7.39; N 6.10%.

N → O acyl migration of N-benzoyl-*cis*-2-aminomethylcyclopentanol (XXV)

N-Benzoyl-*cis*-aminomethylcyclopentanol (**XXV**) (0.828 g; 0.0037 mole) was dissolved in 80 ml abs. ethanol and 9 ml of 3.9 *N* (0.035 mole) of ethanolic hydrochloric acid solution was added. The reaction mixture was heated in a sealed tube at 100 °C for 12 hrs., then evaporated to dryness and the residue extracted by refluxing twice with 7 ml of water. During the extraction 0.80 g of the material was dissolved and 0.03 g insoluble residue remained in the flask. The aqueous solution was decolourized with activated carbon and evaporated to dryness at 40 torr. The residue was crystallized from a mixture of abs. ethanol and abs. ether. The white crystals which separated on cooling liquified after filtration. The picrate (0.82 g, m.p. 205–207 °C) was recrystallized three times from ethanol to obtain yellow crystals, m.p. 217–218 °C.

$C_{19}H_{20}O_9N_4$ (448.38). Calcd. C 50.89; H 4.50; N 12.50%. Found C 50.65; H 4.80; N 12.67%.

N → O acyl migration reaction of N-benzoyl-*trans*-2-aminomethylcyclopentanol (XXVI)

N-Benzoyl-*trans*-2-aminomethylcyclopentanol (**XXVI**) (0.828 g; 0.0037 mole) was dissolved in 80 ml abs. ethanol and to this solution 9 ml of 3.9 *N* (0.035 mole) ethanolic HCl solution was added. The reaction mixture was heated in a sealed tube at 130 °C for 20 hrs., then evaporated to dryness, and the residue (0.80 g) extracted twice by refluxing with 7 ml of water. 0.2 g of the material dissolved during the extraction, and 0.6 g insoluble residue remained in the flask. The aqueous solution was decolourized with charcoal and treated as described for the *cis* isomer (**XXV**). The hydrochloride of the O-acyl derivative obtained was

hygroscopic and liquified on standing. The picrate (0.19 g, m.p. 203–206 °C) was prepared by adding an aqueous solution of sodium picrate to the aqueous solution of O-benzoyl-2-aminomethylcyclopentanol; after three recrystallizations from ethanol it weighed 0.1 g, m.p. 217 °C.

$C_{19}H_{20}O_9N_4$ (448.38). Calcd. C 50.89; H 4.50; N 12.50%. Found C 50.82; H 4.85; N 12.48%.

O → N acyl migration

0.1 g (0.004 mole) of O-benzoyl-2-aminomethylcyclopentanol hydrochloride (obtained by the N → O acyl migration reaction of N-benzoyl-*trans*-2-aminomethylcyclopentanol (**XXVI**) was dissolved in 3 ml of water. On the addition of 4 ml 1.0 *N* (0.004 mole) sodium hydroxide, the N-benzoyl-2-aminomethylcyclopentanol immediately separated. The crystals were filtered off after short standing at room temperature, washed with water and dried to obtain 83 mg of white crystals, m.p. 95–96 °C. Recrystallization from aqueous ethanol gave 50 mg of white crystals, m.p. 97–98 °C, melting without depression in admixture with an authentic sample of N-benzoyl-*cis*-2-aminomethylcyclopentanol (**XXV**). The IR spectrum was identical with that of authentic N-benzoyl-*cis*-2-aminomethylcyclopentanol.

Kinetic measurements

The kinetic measurements of the N → O acyl migration reaction were made by the method described in our earlier paper [2]. The data obtained are listed in Table I.

*

Financial support of this work by the Chemical Works of GEDEON RICHTER Ltd., Budapest, and by REANAL Factory of Laboratory Chemicals, Budapest, is acknowledged. Thanks are due to Mr. L. GERA and Miss O. CSAPÓ for taking part in some experiments, to Miss A. VIGH for technical assistance, to Mrs. G. BARTÓK-BOZÓKI and Mrs. É. GÁCS-GERGELY for the microanalyses. We wish to express our thanks to Dr. P. SOHÁR (Pharmaceutical Research Institute, Budapest) for IR and NMR spectra and to Mrs. É. TOMORI (Pharmaceutical Research Institute, Budapest) for gas-chromatographic analyses.

REFERENCES

1. BERNÁTH, G., KOVÁCS, K., LÁNG, K. L.: Tetrahedron Letters **1968,** 2713
2. BERNÁTH, G., KOVÁCS, K., LÁNG, K. L.: Acta Chim. Acad. Sci. Hung. **65,** 347 (1970)
3. BERNÁTH, G., LÁNG, K. L., GÖNDÖS, GY., MÁRAI, P., KOVÁCS, K.: Tetrahedron Letters **1968,** 4441
4. BERNÁTH, G., LÁNG, K. L., GÖNDÖS, GY., MÁRAI, P., CSÓKÁSI, E., KOVÁCS, K.: Stereochemical Studies on Cyclic 1,3-Aminoalcohols. Lecture presented before the Committee of Organic Chemistry, Hungarian Academy of Sciences, Budapest, April 30, 1968
5. SZPORNY, L. *et al.:* To be published
6. BERNÁTH, G., CSÓKÁSI, E., HEVÉR, I., GERA, L., KOVÁCS, K.: Acta Chim. Acad. Sci. Hung. **70,** 271 (1971)
7. BERNÁTH, G., KOVÁCS, K., PÁLOSI, É., GÖRÖG, P., SZPORNY, L.: Hung. Pat. 156.542, July 4, 1971
8. BERNÁTH, G., KOVÁCS, K., PÁLOSI, É., GÖRÖG, P., SZPORNY, L.: Swiss Pat. 505,786, Apr. 15, 1971
9. MOUSSERON, M., JULLIEN, J., WINTERNITZ, F.: Bull. soc. chim. France **1948,** 878
10. GASSMAN, P. G., HECKERT, D. C.: Tetrahedron **21,** 2725 (1965)
11. PASCUAL, J., CASTELLS, J.: J. Am. Chem. Soc. **74,** 2899 (1952)
12. MÖHRLE, H., BAUMANN, H.: Ann. **716,** 61 (1968)
13. BAUMANN, H., FRANKLIN, N. C., MÖHRLE, H.: Tetrahedron **23,** 4331 (1967)
14. BERNÁTH, G., GÖNDÖS, GY., MÁRAI, P., GERA, L.: Acta Chim. Acad. Sci. Hung. **74,** 471 (1972)
15. PLIENINGER, H., SCHNEIDER, K.: Chem. Ber. **92,** 1594 (1959)
16. CONNORS, T. A., ROSS, W. C. J.: J. Chem. Soc. **1960,** 2119
17. PERKIN, W. H., Jun.: Ber. **18,** 3246 (1885)
18. PERKIN, W. H., Jun.: J. Chem. Soc. **51,** 240 (1887)
19. PERKIN, W. H., Jun.: J. Chem. Soc. **65,** 572 (1894)

20. BAILEY, W. J., SORENSON, W. R.: J. Am. Chem. Soc. **76,** 5421 (1954)
21. FUSON, R. C., COLE, W.: J. Am. Chem. Soc. **60,** 1237 (1938)
22. BRENNER, J. H.: J. Org. Chem. **26,** 22 (1961)
23. EISENBRAUN, E. J., HANEL, P. G., SCHORNO, K. S., DILGEN, SR. ST. F., OSIECKI, J.: J. Org. Chem. **32,** 3010 (1967)
24. COOK, A. H., LINSTEAD, R.: J. Chem. Soc. **1934,** 956
25. SCHARF, H. D., KORTE, F.: Chem. Ber. **97,** 2425 (1964)
26. BERNÁTH, G., SVOBODA, M.: Tetrahedron **28,** 3475 (1972)
27. PROCHÁZKA, M., LEŠETICKÝ, L.: Coll. Czechoslov. Chem. Commun. **31,** 3824 (1966)
28. BERNÁTH, G., KOVÁCS, K., LÁNG, K. L.: Acta Chim. Acad. Sci. Hung. **64,** 183 (1970)
29. FODOR, G.: "New methods and recent developments of the stereochemistry of ephedrine, pyrrolizidine, granatane and tropane alkaloids", in Recent Developments in the Chemistry of Natural Carbon Compounds, Vol. 1. (Eds: BOGNÁR, R., BRUCKNER, V., FODOR, G.) Publishing House of the Hungarian Academy of Sciences, Budapest, 1965
30. CRAM, D. J.: "Intramolecular rearrangements", in Steric Effects in Organic Chemistry, pp. 290—295. (Ed.: NEWMANN, M. S.), John Wiley and Sons, New York, 1956
31. AKABORI, Y.: Kagaku Na Ryoiki **19,** 270 (1965); C. A. **63,** 16631 (1965)
32. PAVLOVA, L. V., RACHINSKII, F. YU.: Usp. Khim. **1968,** 1369
33. FODOR, G., KISS, J.: J. Chem. Soc. **1952,** 1589
34. FODOR, G., FODOR-VARGA, É., FURKA, Á.: Croatica Chim. Acta **29,** 303 (1957)
35. GILLESPIE, R. J., BIRCHALL, T.: Can. J. Chem. **41,** 188 (1963)
36. GILLESPIE, R. J., BIRCHALL, T.: Can. J. Chem. **41,** 2642 (1963)
37. BENDER, M. L.: Chem. Rev. **60,** 53 (1960)
38. ELIEL, E. L.: Stereochemie der Kohlenstoffverbindungen, pp. 245—47. Verl. Chemie, GmbH, Weinheim, 1966
39. BROWN, C. C., ROSSINI, F. D.: J. Phys. Chem. **64,** 927 (1960)
40. ELIEL, E. L., ALLINGER, N. L., ANGYAL, S. J., MORRISON, G. A.: Conformational Analysis. pp. 200—206, Interscience Publishers, New York, London, Sydney, 1965
41. HANACK, M.: Conformation Theory. pp. 72—78, Academic Press, New York and London, 1965
42. BERNÁTH, G., SOHÁR, P., LÁNG, K. L., TORNYAI, I., KOVÁCS, Ö. K. J.: Acta Chim. Acad. Sci. Hung. **64,** 81 (1970)
43. MIČOVIĆ, V. M., MIHAILOVIĆ, LJ. M.: J. Org. Chem. **18,** 1190 (1953)
44. VOGEL, A. I.: Practical Organic Chemistry, 3rd Edition, p. 582, Longmans, Green and Co. Ltd., London, 1961
45. COOK, A. H., LINSTEAD, R.: J. Chem. Soc. **1934,** 956

Gábor BERNÁTH
Kornélia L. LÁNG
György GÖNDÖS
Pál MÁRAI
Kálmán KOVÁCS
Szeged, Dóm tér 8, Hungary.

RECENSIONES

Nomenclature of Inorganic Chemistry Definitive Rules 1970 *International Union of Pure and Applied Chemistry (IUPAC)*

2nd Edition, pp. 110. Issued by the Commission on the Nomenclature of Inorganic Chemistry. Butterworth, London

The new nomenclature of inorganic chemistry is a partly revised and greatly extended version of the rules accepted by the IUPAC in 1957; it includes the nomenclature of the following classes of compounds:

1. Elements; 2. Formulae and Names of Compounds in General; 3. Names for Ions and Radicals; 4. Iso- and Heteropolyanions; 5. Acids; 6. Salts and Salt-like Compounds; 7. Coordination Compounds; 8. Addition Compounds; 9. Crystalline Phases of Variable Composition; 10. Polymorphism; 11. Boron Compounds. The correct application of the nomenclature is assisted by 5 tables.

The 1957 Rules have been subjected to major revision with special emphasis on the following points:

(*a*) In accordance with the generally accepted alphabetical principle, the components are listed, wherever possible, in alphabetical order. Thus, the earlier, complicated order of listing electropositive and electronegative components is replaced by the alphabetical order within both groups of components. Similarly, in the names of coordination compounds the ligands are listed in alphabetical order. The adoption of this principle greatly simplifies naming in a systematic manner.

Examples:	$KNaCO_3$	potassium sodium carbonate
	$Ca_5F(PO_4)_3$	pentacalcium fluoride tris(phosphate)
	K_2 $[Cr(CN)_2O_2(O_2)NH_3]$	potassium *a*mminedicyanodi*ox*o*per*oxochromate(2—)

(*b*) The use of multiplying prefixes has been clarified. As opposed to earlier practice, multiplying prefixes should be used in the abbreviated names of polyatomic anions, ending in *-ate*, if the isopolyanion of the central atom is known. The numerical prefixes are reserved for isopolyanions.

Multiplying prefixes should be used also in conjunction with trivial group names such as sulfite, thiosulfite and thiosulfate, because the Rules permit use of the trivial name disulfite for the S_2O_5 group, and the names thiosulfite and thiosulfate (instead of monothiosulfite and monothiosulfate) for the S_2O_2 and S_2O_3 groups, respectively.

Examples:	$(SO_4)_2$ group:	bis(sulfate)
	S_2O_7 group:	disulfate

(*c*) The trivial names for a few phosphorus-containing acids have been changed, because not all of the hydrogens can be substituted in these acids:

	Old name	New name
H_2PHO_3	phosphorous acid	phosphonic acid
$H_2P_2H_2O_5$	diphosphorous acid, pyrophosphorous acid	diphosphonic acid
HPH_2O_2	hypophosphorous acid	phosphinic acid

(*d*) There are new rules for indicating the proportion of constituents in addition compounds. The proportion is given by Arabic numerals separated by the solidus, in parentheses after the name.

Examples: $3CdSO_4 \cdot 8H_2O$ cadmium sulfate — water (3/8)
$Al_2(SO_4)_3 \cdot K_2SO_4 \cdot 24H_2O$ aluminium sulfate — potassium sulfate — — water (1/1/24)

In the new Nomenclature the rules for naming iso- and heteropolyacids and coordination compounds have been greatly extended, and the rules for naming boron compounds have been formulated.

The new, revised edition of the Nomenclature of Inorganic Compounds is of paramount importance in paving the road toward the general use of a unified, international nomenclature.

P. FODOR-CSÁNYI

W. KUTZELNIGG, G. DEL RE and G. BERTHIER: *σ and π Electrons in Organic Compounds*

Topics in Current Chemistry, Ed. A. Davison, M. J. S. Dewar, K. Hafner, E. Heilbronner, U. Hofmann, K. Niedenzu, Kl. Schäfer, G. Witting.

122 pp. Springer Verlag, Berlin–Heidelberg–New York, 1971

The authors who are actively working in the field of applications of quantum chemical methods to organic compounds, have written an excellent treatise about the problems of σ and π electrons.

After a short hystorical review the booklet gives a correct and modern definition of the σ and π orbitals based on natural orbitals. This is followed by the usual definition of the σ–π separation in the framework of the independent particle (HARTREE–FOCK) model and a more general one using the group function formalism. Afterwards they discuss the limits of this separation, giving some examples (e.g. the problem of hyperfine coupling constants in ESR spectra) and review the correlation effects in π electron systems.

In the next chapter specific properties of σ and π electrons are described. Here we can find the discussion of spatial distribution of σ and π electrons, the question of their binding energies and polarizabilities, the problem of localization of the σ and of the delocalization of π electrons. Finally their reactivities are discussed.

The fifth chapter of the booklet reviews the various methods for calculations on electrons and the theoretical determination of their ionization potentials and excitation energies.

The last chapter deals with σ electron theories and with the joint treatment of σ and π electrons in unsaturated molecules. It gives also a clear and concise description of population analysis. All chapters contain many references to the recent literature and well chosen illustrative examples mostly in the form of figures and tables.

By summarizing in a small booklet many results of the investigations performed in the last years this excellent work fills a gap in the literature concerned with σ and π electrons. Its clear presentation makes the book easily readable. We can only regret that the authors did not discuss in more detail the semiempirical theories of σ and π electrons, though this would necessarily have lengthened the text. The book is highly recommendable to quantum chemists, physicists, and to organic chemists who have some knowledge in theoretical chemistry.

J. LADIK

INDEX

INORGANIC AND ANALYTICAL CHEMISTRY – INORGANISCHE UND ANALYTISCHE CHEMIE – НЕОРГАНИЧЕСКАЯ И АНАЛИТИЧЕСКАЯ ХИМИЯ

KŐRÖS, E., ORBÁN, M., BURGER, M., VÖRÖS, K. and FÜSSY, É.: Iodine Exchange between Molecular Iodine and Some Iodomethylcarbonyl Compounds in Benzene 387

PANCHAL, B. R. and BHATTACHARYA, P. K.: Study of Metal Exchange in Some π-Bonded Complexes, II 399

PHYSICAL CHEMISTRY – PHYSIKALISCHE CHEMIE – ФИЗИЧЕСКАЯ ХИМИЯ

VÉRTES, G. and NAGY, F.: Oxidation on the Nickel Hydroxide Electrode, VI. Mechanism of the Oxidation of Primary Alcohols 405

VARGA, K. and FEJES, P.: Study of the Rate of Sorption on a Single Spherical Adsorbent Particle, III. Experimental Confirmation of the Rate Equation 417

VÉRTES, A. and SUBA, M.: Study of the Electron-Exchange Reaction between Iron(II) and Iron(III) in Formamide 439

CZÁRÁN, E. und SCHNABEL, K. H.: Die Dispersität des Platins in Platin-Alumosilikat-Trägerkatalysatoren in Abhängigkeit von den Eigenschaften des Trägers (Investigation of the Distribution and Dispersity of Platinum in Platinum-Alumosilicate Carrier Catalysts under the Conditions of Industrial Production) 445

Таммухамедов С. А., Ларин П. П., Карабаев А. Ш., Азизов Ш. А., Тиллаев Р. С., Усманов Х. У.: Исследование физико-химических свойств привитых сополимеров поливинилового спирта с поливинипиридином. (TASHMUKHAMEDOV, S. A., LARIN, P. P., KARABAYEV, A. SH., AZIZOV, SH. A., TILLAYEV, R. S. and USMANOV, KH. U.: Physico-Chemical Properties of Poly(vinyl Alcohol)—Poly(vinylpyridine) Graft Copolymers 453

SIMIONESCU, CR. et VASILIU, S.: Recherches dans le domaine des polyphénylacétylènes de polycondensation (II) 461

ORGANIC CHEMISTRY – ORGANISCHE CHEMIE – ОРГАНИЧЕСКАЯ ХИМИЯ

BERNÁTH, G., GÖNDÖS, GY., MÁRAI, P. and GERA, L.: Stereochemical Studies, XI. Studies on Cyclic 2-Hydroxycarboxylic Acids, II. Synthesis of *Cis*- and *Trans*-2-Hydroxycyclopentanecarboxylic Acid and *Cis*- and *Trans*-2-Hydroxycycloheptanecarboxylic Acid 471

BERNÁTH, G., LÁNG, K. L., GÖNDÖS, GY., MÁRAI, P. and KOVÁCS, K.: Stereochemical Studies, XII. Cyclic Aminoalcohols and Related Compounds, V. N → O Acyl Migration in N-Benzoyl Derivatives of *Cis*- and *Trans*-2-Aminomethylcyclopentanol and *Cis*- and *Trans*-2-Hydroxymethylcyclopentylamine 479

RECENSIONES 499

ACTA CHIMICA

ТОМ 74—ВЫП. 4

РЕЗЮМЕ

Обмен йода между молекулярным йодом и некоторыми йодометилкарбонильными соединениями в бензоле

Э. КЁРЁШ, М. ОРБАН, М. БУРГЕР, К. ВЁРЁШ и Е. ФЮШИ

Был исследован обмен йода между молекулярным йодом и 1-фенил-2,3-диметил-4-йодоацетил-пиразолоном (IAcруг), монойодоацетоном (IA), а также моной'одоуксусной кислотой (IAcOH) в бензоле. Скорость реакции соответствует следующему уравнению: $v = k_0 \cdot [RCOCH_2I]$ Были получены следующие параметры активации: для IAcруг $E_a = 21{,}2$ ккал/моль, $\lg A = 11{,}35$, $\Delta S^{\ddagger} = -9$ э. е.; для IA: $E_a = 17{,}8$ ккал/моль, $\lg A = 6{,}79$, $\Delta S^{\ddagger} = -28$ э. е.; для IAcOH: $E_a = 13{,}9$ ккал/моль, $\lg A = 6{,}14$, $\Delta S^{\ddagger} = -31$ э. е. Было исследовано влияние света, кислорода и воды. На основе экспериментальных данных полагалось, что ступенями, лимитирующими скорость реакции, являются образование возбужденных молекул $RCOCH_2I$ и, хотя и в меньшей степени, гомолитическая диссоциация молекул $RCOCH_2I$.

Исследование обмена металла в некоторых комплексах с π-связями, II

Б. Р. ПАНЧАЛ и П. К. БАТТАЧАРЯ

Константы образования хелатов тиогликолевой и тиомолочной кислот с Be(II), Zn(II) и Co(II), соответственно, были определены с помощью метода Эрвинга-Розотти, используя метод наименьших квадратов во всех случаях, где возможно. Величины констант интерпретировались на основе представлений π-взаимодействий между M и S. Замещение Zn(II) в хелатах на Cd(II), Hg(II) и Ag(I) объяснялось большей степенью B-характера в ионах последних металлов, по сравнению с Zn(II).

Окисление на окисно-никелевом электроде, VI

Возможные ступени процесса окисления спиртов

ДЬ. ВЕРТЕШ и Ф. НАДЬ

В ходе исследования окисления первичных спиртов, протекающего на окисно-никелевом электроде, были рассмотрены вероятности различных возможных путей реакции.

Было установлено, что скорость окисления не зависит от концентрации гидроксильных ионов.

Скорость окисления первичных спиртов, содержащих ароматическое кольцо, — согласно наблюдениям — превышает скорость окисления алифатических спиртов на окисно-никелевом электроде.

На основе вышеприведенных результатов, а также принимая во внимание индуктивные эффекты, обычно используемые при обсуждении механизма органических реакций, и аналогию в строении вероятных промежуточных продуктов и некоторых стабильных свободных радикалов, полагалось вероятным, что первой — и в то же время лимитирующей скорость — ступенью окисления является гомолитический отрыв атома водорода, с последующим выходом вначале протона, а затем электрона из молекулы.

Изучение скорости сорбции на единственном шарообразном зерне адсорбента, III

Экспериментальное подтверждение уравнения скорости

К. ВАРГА и П. ФЕЙЕШ

На установке, пригодной для *непосредственного* измерения скорости сорбции, были определены скорости собрции некоторых углеводородов на пористых зернах окиси алюминия, силиката алюминия и активированного угля. Результаты измерений подвергались расчету методом дигитальной оценки параметров на основе уравнения(ий) скорости сорбции, приводимого в предыдущем сообщении. Было обнаружено, что теоретически выведенное уравнение(ия) скорости справедливо для описания скорости сорбции, протекающей на пористых веществах, если степень заполнения поверхности невелика, и соответственно этому, действительная кинетика после диффузионного процесса транспорта соответствует закону Лангмюра и линейна. Величины параметров, определяющие скорость сорбции (толщина граничного слоя диффузии, эффективная константа диффузии в порах, наклон изотермы, постоянные в зависимости скорости типа Лангмюра), являются реальными с физической точки зрения. Константа скорости сорбции, например, в пределах двух порядков согласуется с газово-кинетическим числом столкновений.

Исследование реакции электронного обмена между железом(II) и железом(III) в формамиде

А. ВЕРТЕШ и М. ШУБА

Реакция электронного обмена между железом(II) и железом(III) в формамиде была изучена методом эффекта Мёссбауэра. Обмен электронов не был обнаружен в безводном формамиде. После добавления воды сольват железа, содержащий также воду, был получен; константа скорости переноса электрона $K > 2$ л · моль$^{-1}$.сек$^{-1}$.

Исследования распределения и дисперсности платины в катализаторах с платина-алюминий-силикатными носителями в условиях промышленного производства

Э. ЦАРАН и К. Х. ШНАБЕЛ

Дисперсность катализаторов с платина-алюмосиликатными носителями, была исследована в зависимости от выбора исходного соединения платины, содержащего носитель и активный компонент. Было установлено, что в случае таких носителей, которые являются однородными не с химической точки зрения — в отличие от до сих пор распространенных представлений — дисперсность, достигнутая при приготовлении катализатора, пропорциональна не обратной величине поверхностной концентрации, а, в первую очередь, зависит от химического взаимодействия носителя и исходного соединения платины.

Исследования в области поликонденсированных полифенилацетиленов, II

Ц. СИМЬОНЕСКУ и ВАСИЛИН

Была исследована каталитическая активность 13 галогенидов металлов в поликонденсации фенилацетальдегида, приводящей к полифенилацетиленам с регулярным строением.

Степень превращения фенилацетальдегида зависит от природы катализатора; галогениды располагаются в следующем ряду по активности: $SnCl_4 > ZnCl_2 > BF_3 > SbCl_3 > FeCl_3 > TiCl_4 \approx HgCl_2 > AlCl_3 > SnCl_2 > CoCl_2 > NiCl_2 > MgCl_2 > CdCl_2$.

Молекулярный вес синтезированных таким образом полимеров превышает молекулярный вес полифенилацетиленов, полученных путем полемеризации; было установлено влияние катализатора на среднюю степень поликонденсации.

Строение поликонденсированных полифенилацетиленов было исследовано как химическим путем, так и с помощью ИК спектроскопии. Было установлено, что полимеры обладают конфигурацией транс-алкенов.

Согласно электрофизическим свойствам, определенным на основе ЭПР спектров, электропроводимости и ее энергии активации, полифенилацетилены могут быть отнесены к полимерам-полупроводникам с удовлетворительными свойствами (10^{15}—10^{19} спин/г, $\sigma = 10^{-15}$ ом$^{-1}$ см$^{-1}$, $E_A = 0{,}98$—$2{,}1$ эв).

Согласно данным ДТА, полифенилацетилены, полученные путем данной поликонденсации фенилацетальдегида, представляют собой полимеры со стабильностью, достойдой внимания.

Стереохимические исследования, XI

Исследования в области циклических 2-гидроксикарбоксильных кислот, II.

Г. БЕРНАТ, ДЬ. ГЁНДЁШ, П. МАРАИ и Л. ГЕРА

При каталитическом воостановлении 2-карбетоксициклопентанена(V) в этанольной среде с помощью никеля Ренея, а также при восстановлении $NaBH_4$-ом были получены *цис*- и *транс*-2-карбетокси-циклопенатнолы (VI, VII), разделение которых с помощью фракционированной дестилляции приводит к однородным с газово-хроматографической точки зрения *цис*- и *транс*-изомерам.

Аналогичные восстановления 2-карбетокси-циклогептанона (XIII) приводят — как на основе газовохроматографических, так и препаративных доказательств — к совместному образованию *цис*- и *транс*-2-карбетоксициклогептанолов (XIV, XV), разделение которых было успешно осуществлено с помощью фракциональной дестилляции. Следует отметить, что настоящие данные опровергают те недавно опубликованные литературные данные [13], согласно которым данные реакции приводят к образованию стереооднородного *цис*-продукта.

Стереохимические исследования, XII

Циклические аминоспирты и их производные, V. N → O ацильная миграция в N-бензоильных производных *цис*- и *транс*-2-аминометил-циклопентанолов, а также *цис*- и *транс*-2-гидроксиметил-циклопентиламинов

Г. БЕРНАТ, К. Л. ЛАНГ, ДЬ. ГЁНДЁШ, П. МАРАИ и К. КОВАЧ

Восстановлением амидов *цис*- и *транс*-циклопентанол-2-карбоновых кислот, а также *цис*- и *транс*-2-аминоциклопентанкарбоновых кислот с помощью $LiAlH_4$ были получены *цис*- и *транс*-2-аминометилциклопентанолы, а также *цис*- и *транс*-2-гидроксиметилциклопентиламины, соответственно. Кинетически изучалась реакция ацильной миграции N → O в *цис*- и *транс*-N-бензоил-2-аминометилциклопентанолах, а также в *цис*- и *транс*-N-бензоил-2-гидроксиметилциклопентиламинах. Измерения проводились в среде абсолютного диоксана и с полумолярным избытком HCl. В случае N-бензоил-*цис*-2 аминометилциклогексанола при температурах 100,8, 110,0 и 125,0 °C были получены следующие константы скорости реакции второго порядка $k_2 \cdot 10^3$ [сек$^{-1}$] = 2,89, 3,37 и 5,33, соответственно; энергия активации реакции равна $\Delta E^{\ddagger} = 11{,}70$ ккал/моль, а энтропия активации $\Delta S^{\ddagger} = -41{,}8$ энтр. ед.; а в случае N-бензоил-*цис*-2-гидроксиметилциклопентиламина — следующие значения: $k_2 \cdot 10^3$ [сек$^{-1}$] = 3,87, 7,80 и 10,31 при температурах 84,0, 100,4 и 110,0 °C, соответственно, $\Delta E^{\ddagger} = 11{,}22$ ккал/моль и $\Delta S^{\ddagger} = -36{,}9$ энтр. ед. Скорость ацильной миграции N→O в случае *транс*-изомеров значительно ниже величины для *цис*-изомеров. В случае N-бензоил-*транс*-2-аминометилциклопептанола и N-бензоил-*транс*-2-гидроксиметилциклопентиламина при температуре 130,2 °C были получены следующие константы скорости реакции N → O ацильной миграции $k_2 \cdot 10^3$ [сек$^{-1}$] = 0,74 и 0,87, соответственно. Было установлено, что реакция ацильной миграции N → O в случае N-бензоил-*транс*-2-аминометилциклопентанола протекает с инверсией. Рассматривались переходные состояния реакции ацильной миграции N→O, и последняя сравнивалась для случаев циклопентанового скелета с ранее изученными 1,3-аминоспиртами с циклогексановым скелетом.

Radiation Chemistry III

PROCEEDINGS OF THE THIRD SYMPOSIUM

10—15 MAY 1971, TIHANY, HUNGARY

edited by J. DOBÓ and P. HEDVIG

This meeting provoked special world-wide interest. There were over 200 participants present and practically all important schools of radiation chemistry were represented. The main results obtained in the field of aqueous solutions, organic compounds, monomers and polymeric compounds were discussed. A novelty of this Symposium is that in addition to the results of the basic research attained in these fields, some industrially realized processes have also been presented. A general development broadening the scope of radiation chemistry could definitely be established.

In English · Approx. 960 pages · Cloth

Laboratory Manual on Crystal Growth

edited by I. TARJÁN

The book is a stand-by long since required in the international literature for laboratory practice dealing with the study of crystal growth and the processes of growing crystals. The first part is concerned with simple experiments related to the fundamental problems of crysta growth. The second part presents various processes, equipments and facilities for growing crystals. Finally, practical directions are given for the treatment and processing of crystals.

In English · 250 pages · Cloth

AKADÉMIAI KIADÓ

Publishing House of the Hungarian Academy of Sciences

B u d a p e s t

Chemical Analysis by Emission Spectroscopy Fundamentals

by J. Mika and T. Török

The first part of the work, Fundamentals, gives a detailed treatment of the theoretical and practical principles of excitation, the dispersion of light, the determination of the wavelength and intensity of spectral lines, which are indispensable for an understanding of the physical and chemical phenomena underlying spectrochemical analysis. In addition to the classical methods, modern techniques are described, such as excitation by hollow-cathode tubes, plasma burner, by laser, etc. Methods which are used rarely for special purposes are also included in the book.

In English . Approx. 580 pages . Cloth

BUTTERWORTH Ltd
London

AKADÉMIAI KIADÓ
Budapest

A co-edition — distributed in the socialist countries by Kultura, Budapest, in all other countries by Butterworth Ltd., London

Printed in Hungary

A kiadásért felel az Akadémiai Kiadó igazgatója — Műszaki szerkesztő: Zacsik Annamária

A kézirat nyomdába érkezett: 1972. V. 18. — Terjedelem: 10,50 (A/5) ív, 42 ábra

72.73596 Akadémiai Nyomda, Budapest — Felelős vezető: Bernát György